2005 Condensed Phase and Interfacial Molecular Science Research Meeting

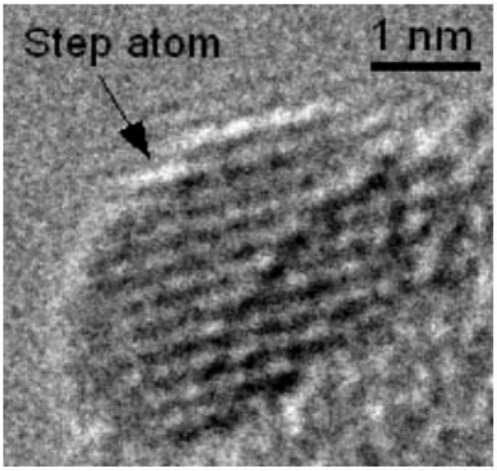

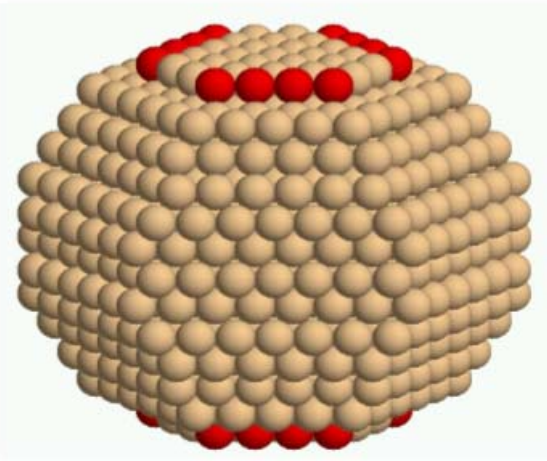

Airlie Conference Center
Warrenton, Virginia
October 23-26, 2005

Office of Basic Energy Sciences

Chemical Sciences, Geosciences & Biosciences Division

Cover

TEM image (left) and calculated model (right) of a Ru nanoparticle active in ammonia synthesis. In the model the active step sites are indicated red. From Honkala, Remediakis, Logadottir, Nørskov,

Hellmann, Dahl, Carlsson, Christensen, Science **307**,555 (2005)

Foreword

This volume summarizes the scientific content of the 2005 Research Meeting on Condensed Phase and Interfacial Molecular Science (CPIMS) sponsored by the U. S. Department of Energy (DOE), Office of Basic Energy Sciences (BES). This marks the second meeting of CPIMS and, based on the overwhelmingly positive response to the inaugural meeting last year, CPIMS has become the fourth of the regular Contractors' Meetings within the Fundamental Interactions Team. CPIMS is unique among those four in that the primary participants are principal investigators funded through two core research activities in our Division: the Chemical Physics Program and the Photochemistry and Radiation Research Program.

In keeping with the notion that CPIMS makes connections across BES research programs based on common topical interests, one of the main themes of this year's meeting will be the molecular-level understanding of chemistry relevant to heterogeneous catalysis. To emphasize this theme, five investigators who are funded under the BES Catalysis and Chemical Transformations Program will be featured on the agenda: Eric Altman (Yale), Wayne Goodman (Texas A&M), Michael Henderson (PNNL), Steven Overbury (ORNL), and Peter Stair (Northwestern/ANL). In addition, we are delighted that Jens Nørskov from the Technical University of Denmark has agreed to give the plenary talk this year. We hope that the blending of these external experts in catalysis with the CPIMS PIs who have expertise in surface and cluster science will provide an interesting and useful cross fertilization of ideas and concepts that benefits both groups. The remainder of the agenda is devoted to physical and chemical properties in the liquid phase, which is one of the more dominant themes in CPIMS.

As with last year's meeting, the cross-cutting nature of CPIMS means that the meeting is graced by the presence of a number of program managers from our Division. At the time of this writing these include Michael Casassa, Greg Fiechtner, Mary Gress, Dick Hilderbrandt, Raul Miranda, Mark Spitler, and Frank Tully. The contributions of this year's speakers for their investment of time and for their willingness to share their ideas with the meeting participants are most gratefully acknowledged. Thanks also go to Dick Hilderbrandt for assembling the book of abstracts and to Raul Miranda for consultations regarding the Catalysis and Chemical Transformations program. Finally, this meeting would not be possible without the excellent logistical support it receives from Diane Marceau from our Division, Sophia Kitts and Kellye Sliger from the Oak Ridge Institute of Science and Education, and the staff of the Airlie Conference Center.

Eric Rohlfing
Team Leader, Fundamental Interactions
Chemical Sciences, Geosciences and Biosciences Division
Office of Basic Energy Sciences
September 2005

Agenda

U. S. Department of Energy
Office of Basic Energy Sciences
2005 Meeting on Condensed Phase and Interfacial Molecular Sciences

Sunday, October 23

3:00-6:00 pm	**** Registration ****
6:00 pm	**** Reception at the Pub (No Host) ****
7:00 pm	**** Dinner ****

Monday, October 24

7:00 am	**** Breakfast ****
8:00 am	*Introductory Remarks* **Eric Rohlfing**, DOE Basic Energy Sciences
Session I	*Chair:* **Will Castleman**, Pennsylvania State University
8:15 am	*Heterogeneous Catalysis from First Principles* **Jens Nørskov**, Technical University of Denmark
9:15 am	*Cluster Deposition Studies of the Effects of Cluster Size and Support Defects on Model Catalysts* **Scott Anderson**, University of Utah
9:45 am	*Catalysis by Metal Alloys: From Single Crystals to Nanoparticles* **Wayne Goodman**, Texas A&M University
10:15 am	**** Break ****
10:45 am	*Catalyst Structures* **Peter Stair**, Northwestern University
11:15 am	*Atomistic Modeling of Cooperative Phenomena in Surface Reaction Processes* **Jim Evans**, Ames National Laboratory
11:45 am	*Photocatalysis on Single Crystal TiO_2* **Mike Henderson**, Pacific Northwest National Laboratory
12:15 pm	**** Lunch ****
5:00 pm	**** Reception on the Rooftop Terrace (No Host) ****
6:00 pm	**** Dinner ****

Session II Chair: **Mostafa El-Sayed**, Georgia Tech

7:00 pm	*Laser Induced Reactions in Solids and at Surfaces* **Wayne Hess**, Pacific Northwest National Laboratory
7:30 pm	*Optical Manipulation of Ultrafast Electron and Nuclear Motion on Metal Surfaces* **Hrvoje Petek**, University of Pittsburgh
8:00 pm	*Laser Dynamic Studies of Photoreactions on Single-Crystal and Nanostructured Surfaces* **Rick Osgood**, Columbia University

Tuesday, October 25

7:00 am	**** Breakfast ****
Session III	Chair: **Michael Duncan**, University of Georgia
8:30 am	*Catalysis at Metal Surfaces Studied by Non-Equilibrium and STM Methods* **Ian Harrison**, University of Virginia
9:00 am	*An Exploration of Catalytic Chemistry on Au/Ni(111)* **Sylvia Ceyer**, MIT
9:30 am	*Growth, Characterization, and Reactivity of Model Transition Metal Oxide Catalysts* **Eric Altman**, Yale University
10:00 am	**** Break ****
10:30 am	*Surface Chemical Dynamics* **Mike White**, Brookhaven National Laboratory
11:00 am	*Structure, Stability and Reaction Dynamics for CO Oxidation Catalysis by Au Supported on Functionalized Oxide Supports* **Steve Overbury**, Oak Ridge National Laboratory
11:30 am	*Thermochemistry and Reactivity of Transition Metal Clusters and Their Oxides* **Peter Armentrout**, University of Utah
12:00 pm	**** Lunch ****

Session IV	Chair: **Bruce Kay**, Pacific Northwest National Laboratory
4:00 pm	*Photochemistry at Interfaces* **Ken Eisenthal**, Columbia University
4:30 pm	*Solvation/Fluidity on the Nanoscale, and in the Environment* **Jim Cowin**, Pacific Northwest National Laboratory
5:00 pm	*Electronically Non-Adiabatic Interactions in Molecule Metal-Surface Scattering* **Alec Wodkte**, University of California, Santa Barbara
5:30 pm	*The Role of Electronic Excitations on Chemical Reaction Dynamics at Metal, Semiconductor, and Nanoparticle Surfaces* **John Tully**, Yale University
6:00 pm	**** Reception at the Pavilion (No Host) ****
7:00 pm	**** Banquet Dinner at the Pavilion ****

Wednesday, October 26

7:00 am	**** Breakfast ****
Session V	Chair: **Mark Johnson**, Yale University
8:30 am	*Role of Solvent: Reactions in Supercritical Fluids* **David Bartels**, Notre Dame Radiation Research Laboratory
9:00 am	*Ionic Liquids: Radiation Chemistry, Solvation Dynamics and Reactivity Patterns* **James Wishart**, Brookhaven National Laboratory
9:30 am	*Understanding Nanoscale Confinement Effects in Solvent-Driven Chemical Reactions* **Ward Thompson**, University of Kansas
10:00 am	**** Break ****
10:15 am	*Recent Advances in Computer Simulations of Molecular Processes at the Liquid Water Surface* **Liem Dang**, Pacific Northwest National Laboratory
10:45 am	*X-Ray Spectroscopy of Volatile Liquids and Their Surfaces* **Rich Saykally**, Lawrence Berkeley National Laboratory
11:15 am	*Gas Phase Investigation of Condensed Phase Phenomena* **Lai-Sheng Wang,** Pacific Northwest National Laboratory
11:45 am	*Closing Remarks* **Eric Rohlfing**, DOE Basic Energy Sciences
12:00 pm	**** Lunch **** (Optional boxed lunches available)

Table of Contents

Invited Presentations (Ordered by Agenda)

Heterogeneous Catalysis from First Principles
Jens Nørskov.....1

Cluster Deposition Studies of the Effects of Cluster Size and Support Defects on Model Catalysts
Scott Anderson.....2

Catalysis by Metal Alloys: From Single Crystals to Nanoparticles
Wayne Goodman.....6

Catalyst Structures
Peter Stair.....7

Reaction Processes at Surfaces: Non-Equilibrium Statistical Mechanics and Electronic Structure Analyses
Jim Evans.....8

Photocatalysis on Single Crystal TiO_2
Michael Henderson.....12

Laser Induced Reactions in Solids and at Surfaces
Wayne Hess.....13

Optical Manipulation of Ultrafast Electron and Nuclear Motion on Metal Surfaces
Hrvoje Petek.....17

Laser Dynamic Studies of Photoreactions on Single-Crystal and Nanostructured Surfaces
Richard Osgood.....21

Catalysis at Metal Surfaces Studied by Non-Equilibrium and STM Methods
Ian Harrison.....25

An Exploration of Catalytic Chemistry on Au/Ni(111)
Sylvia Ceyer.....29

Growth, Characterization, and Reactivity of Model Transition Metal Oxide Catalysts
Eric Altman.....32

Surface Chemical Dynamics
Michael White.....33

Structure, Stability and Reaction Dynamics for CO Oxidation Catalysis by Au Supported on Functionalized Oxide Supports
Steve Overbury.....37

Thermochemistry and Reactivity of Transition Metal Clusters and Their Oxides
Peter Armentrout.....38

Photochemistry at Interfaces
Ken Eisenthal.....42

Solvation/Fluidity on the Nanoscale and in the Environment
Jim Cowin.....46

Electronically Non-Adiabatic Interactions in Molecule Metal-Surface Scattering
Alec Wodkte.....50

The Role of Electronic Excitations on Chemical Reaction Dynamics at Metal, Semiconductor, and Nanoparticle Surfaces
John Tully.....51

Role of Solvent: Reactions in Supercritical Fluids
David Bartels.....55

Ionic Liquids: Radiation Chemistry, Solvation Dynamics and Reactivity Patterns
James Wishart.....59

Understanding Nanoscale Confinement Effects in Solvent-Driven Chemical Reactions
Ward Thompson.....63

Recent Advances in Computer Simulations of Molecular Processes at the Liquid Water Surface
Liem Dang.....67

X-Ray Spectroscopy of Volatile Liquids and Their Surfaces
Rich Saykally.....72

Gas Phase Investigation of Condensed Phase Phenomena
Lai-Sheng Wang.....75

Research Summaries (Alphabetically by First PI)

Aerosol and Nanoparticle investigations at the Chemical Dynamics Beamline of the Advanced Light Source
Musahid Ahmed.....79

Electronic Structure of Transition Metal Clusters, and Actinide Complexes, and Their Reactivities
Krishnan Balasubramanian **83**

Clusters: Unraveling Fundamental Oxygen Transfer Reaction Mechanisms Effected by Heterogeneous Catalysts
A. W. Castleman, Jr. **87**

Theory of Dynamics in Complex Systems
David Chandler **91**

Transport and Reactivity in Amorphous Solids
L. René Corrales **93**

New Ultrafast Techniques for Electron Radiolysis Studies
Robert A. Crowell **97**

Vibrational Spectroscopy at Metal Cluster Surfaces
Michael A. Duncan **101**

Electronic Structure and Reactivity Studies in Aqueous Phase Chemistry
Michel Dupuis **105**

Interfacial Oxidation of Complex Organic Molecules
G. Barney Ellison **108**

The Effect of Crystallization on the Proton Pump Function of Bacteriorhodopsin
Mostafa El-Sayed **112**

Liquid and Chemical Dynamics in Nanoscopic Environments
Michael D. Fayer **116**

Accurate Descriptions of Chemical Reactions in Aqueous Systems
Bruce C. Garrett **120**

Chemical Reaction Dynamics in Nanoscale Environments
Evelyn M. Goldfield **124**

Reactive Intermediates in the Condensed Phase: Radiation and Photochemistry
David Gosztola **128**

Computational Nanophotonics: Modeling Optical Interactions and Transport in Tailored Nanosystem Architectures
Stephen K. Gray **131**

Dynamics of Electrons at Interfaces on Ultrafast Timescales
Charles B. Harris **137**

Electronic Structure and Optical Response of Nanostructures
Martin Head-Gordon **141**

Influence of Co-Solvents and Temperature on Nanoscale Self-Assembly of Biomaterials
Teresa Head-Gordon **145**

Optical Spectroscopy at the Spatial Limit
Wilson Ho **149**

Theory of the Reaction Dynamics of Small Molecules on Metal Surfaces
Bret E. Jackson **152**

Structure and Dynamics of Chemical Processes in Water Clusters
Kenneth D. Jordan **156**

Nucleation in Solution
Shawn M. Kathmann **160**

Structure and Reactivity of Ices, Oxides, and Amorphous Materials
Bruce D. Kay **164**

Non-Thermal Reactions at Surfaces and Interfaces: Chemical Kinetics and Dynamics at Interfaces
Greg A. Kimmel **168**

Radiolysis of Water at Ceramic Oxide Interfaces
Jay A. LaVerne **172**

Fundamental Properties of Solvent Pools of Reverse Micelles Used in Nanoparticle Synthesis
Nancy E. Levinger **176**

Time-Resolved and Computational Studies of Short-Lived Molecular Excited States of Importance to Photochemistry and Photobiology
Edward C. Lim **180**

Single-Molecule Kinetics and Dynamics in the Condensed Phase and at Interfaces: Single-Molecule Interfacial Dynamics and Single-Protein Conformational Dynamics
H. Peter Lu **184**

Solvation, Spectroscopy, and Electron Transfer
Mark Maroncelli **188**

Metallic Nanoparticles under Irradiation
Dan Meisel **191**

Center for Radiation Chemistry Research
John R. Miller.....194

Spectroscopy of Organometallic Radicals
Michael D. Morse.....198

New Single- and Multi-Reference Coupled-Cluster Methods for High Accuracy Calculations of Ground and Excited States
Piotr Piecuch.....202

Radiation-Induced Dynamics in the Condensed Phase
Simon M. Pimblott.....206

Development of Statistical Mechanical Techniques for Complex Condensed-Phase Systems
Gregory K. Schenter.....210

Reactive Intermediates in High Energy Chemistry
Ilya A. Shkrob.....214

Self-Organization and Oxidative Surface Reaction Dynamics of Condensed Phase Systems
Steven J. Sibener.....218

Generation, Detection and Characterization of Gas-Phase Transition Metal Containing Molecules
Timothy C. Steimle.....222

Structural Dynamics in Complex Liquids Studied with Multidimensional Vibrational Spectroscopy
Andrei Tokmakoff.....226

Structural Studies of the Solvation Effects and Chemical Interactions in Open-Shell Systems
G. N. R. Tripathi.....229

Accurate Binding Energies and Structural Patterns of Water Clusters (n=2-21)
Sotiris S. Xantheas.....233

Studies of Protein Conformational Dynamics Via Single-Molecule Electron Transfer
Sunney Xie.....237

Invited Presentations

(ordered by agenda)

Heterogeneous catalysis from first principles

J. K. Nørskov
Center for Atomic-scale Materials Physics
Technical University of Denmark

Electronic structure methods based on density functional theory have reached a level of sophistication where they can be used to describe complete catalytic reactions on transition metal surfaces. This gives an unprecedented insight into these processes, and it allows us to pinpoint the origin of the catalytic activity of a metal in terms of its electronic structure. The ammonia synthesis is used to exemplify the approach. It will be shown that by combining density functional calculations with kinetic modelling we can now predict the catalytic activity under industrial conditions of a supported catalyst with no other information about the catalyst than the number of active sites. We can also predict the relative catalytic activities of different metals. The generality of the approach is illustrated by including a number of other catalytic reactions into a universal property-activity scheme, which identifies the surface properties that determine the catalytic activity for a whole class of reactions.

Cluster deposition studies of the effects of cluster size and support defects on model catalysts

PI: Scott L. Anderson,
Department of Chemistry, University of Utah,
315 S. 1400 E. RM Dock, Salt Lake City, UT 84112-0850
anderson@chem.utah.edu

Program Scope:

This program is aimed at improving our understanding of supported catalysts. Size- and energy-selected metal cluster ions are deposited on single crystal or thin film oxide supports and the physical and chemical behavior is studied. Sample temperature is varied over a wide range to examine diffusion and sintering effects on the size and binding site distributions, along with associated effects on the catalytic behavior.

Recent Progress:

Our effort in the reporting period started with a study of deposition dynamics, morphology, and CO adsorption behavior for Ir_n ($n \leq 15$) on TiO_2, as described in publication A, below. More recently, we have focused on gold nanocluster catalysts, with studies of deposition, agglomeration and CO-adsorption effects for $Au/TiO_2(110)$ and $Au/Al_2O_3/NiAl(110)$ reported in publications C and D. We also have completed a detailed study of room temperature CO oxidation catalysis on size-selected $Au_n/TiO_2(110)$ catalysts, reported in publications B and E. This abstract will focus on CO oxidation chemistry, and how it relates to cluster size, morphology, and adsorbate affinity.

CO oxidation on Au/TiO_2 has been extensively studied, yet it is still unclear what the active form of gold is. Haruta and co-workers[1] first showed that nanoscale gold on high surface area TiO_2 was active, and reported that CO oxidation activity peaked quite sharply for average particle size around 3 nm, as determined by transmission electron microscopy (TEM). The TEM-visible particles are nearly spherical, thus 3 nm corresponds to ~1000 atoms. Such catalysts also contain other metal species that may be active, as shown by a provocative experiment by Fu et al.[2] who studied the water gas shift reaction on Au/CeO_2. They found that activity was identical for catalysts with nanometer scale metal particles, and for catalysts where these TEM-visible metal particles had been etched away. Their conclusion was that the large TEM-visible particles are simply spectators, and the active gold is in the form of much smaller gold-support complexes. Work on planar model Au/TiO_2 catalysts in the groups of Goodman,[3] Campbell,[4] and others, has also shown substantial activity for samples containing particles of a few nanometers diameter (but containing a distribution of much smaller particles as well). Superficially, these results seem consistent with those of Haruta et al., however, the gold islands in the planar model catalysts are only a few atomic layers thick, thus they contain many fewer gold atoms than the TEM-visible particles on the high surface area catalysts. Goodman and co-workers suggested that particle thickness was the critical factor, with peak activity for two layer particles. Recently they studied CO oxidation activity on continuous overlayers of Au on TiO_x films grown on Mo(112), with bilayer structures being the most active.[5]

In contrast to this work indicating that rather large nanostructures are responsible for catalyst activity, several studies have shown non-negligible activity for much smaller Au species, in this and in related systems. For example, size-selected cluster deposition of Au_n on MgO by Heiz and co-workers[6] showed onset of CO oxidation activity at Au_8 – a size unlikely to form bilayer structures. As shown below, we see substantial activity for Au_3/TiO_2, and we can show that this cluster is a single layer structure.

Au/TiO_2 model catalysts were prepared by deposition of Au_n^+ on room temperature single crystal rutile $TiO_2(110)$, at an impact energy of 1 eV/atom. All samples contained 0.1 ML equivalent of gold. The catalysts were characterized by a combination of x-ray photoelectron spectroscopy (XPS), ion scattering spectroscopy (ISS), CO and H_2O temperature-programmed desorption (TPD), then CO oxidation activity was probed by pulsed reaction mass spectrometry. One difficulty in studying CO oxidation on Au/TiO_2 in a UHV experiment, is that the O_2 reactant has nearly zero sticking probability, leading previous researchers to use thermal or rf O atoms sources to populate the surface with the oxygen

reactant.[4] We found that exposing the samples to 600 L of $^{18}O_2$ does create a small population of reactive oxygen on the surface, and used this approach in order to include the oxygen activation step in our protocol.

The CO oxidation reaction was then carried out by exposing the oxygen pre-loaded surface to a sequence of 100 pulses of CO, each lasting ~150 msec and amounting to an integrated dose of ~0.2 L/pulse. $C^{18}O^{16}O$ product desorbing from the surface was monitored by a differentially-pumped mass spectrometer. Fig. 1 shows the CO pulse (x0.01) and CO_2 signals from the first pulse on clean TiO_2 and for TiO_2 with Au_1, Au_3, and Au_6 deposited. The inset shows the decay of CO_2 production over the 100 pulse sequence. Activity can be restored by re-exposing the samples to O_2, indicating that the decay results from depletion of the active oxygen, rather than gold sintering or other irreversible catalyst changes.

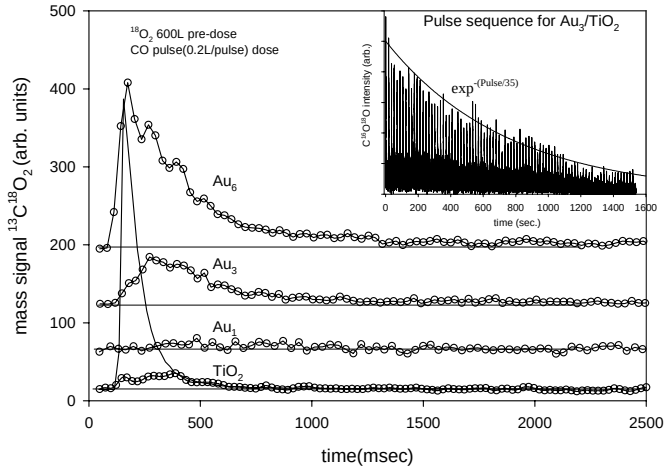

Figure 1 A single CO pulse (x0.01) and resulting CO_2 evolution for different samples. Inset: CO_2 decay over the sequence of 100 CO pulses for Au_3/TiO_2

Note that some CO oxidation occurs on the oxygen-dosed TiO_2, attributed to reaction with active oxygen generated by O_2 interaction with TiO_2 vacancy sites. This "vacancy" activity is largely suppressed by deposition of Au_1 or Au_2, suggesting that these small clusters are binding at the vacancies and poisoning them. Vacancy binding is also indicated by XPS showing electron transfer from the vacancies to gold. As noted, Au_3 is the first size where activity above the background level is observed. Results are shown for Au_6/TiO_2 to indicate that both the intensity and CO_2 evolution temporal behavior are strongly size dependent. The size dependence of the initial activity is shown in Fig. 2 (bottom frame, open triangles).

Having shown strong dependence of activity on cluster size, and substantial activity for much smaller clusters than those in previous studies of high surface area or planar model catalysts, the obvious question is what causes the size dependence. Potentially interesting properties include cluster morphology, and the affinities of different size clusters for the reactants and products of the CO oxidation reaction. ISS provides a simple approach to characterizing morphology. The samples are probed by a low intensity He^+ beam at 1 keV, and ions scattered through 135 ˚ are energy analyzed. Under these conditions the signal results almost entirely from scattering from a single surface atom, and the energy loss reflects the mass of that atom. Because of a combination of shadowing and ion survival probability (ISP) effects, only atoms in the top-most sample layer are detected with significant intensity. If we consider the ratio of signal for scattering from Au atoms, to the sum of the signals for scattering from Ti and O atoms (the Au/substrate ratio, top frame, Fig. 2), we expect that the maximum value should be found for dispersed Au atoms on top of the substrate, because all Au atoms are fully exposed to the beam, and the shadowed areas on the substrate are non-overlapping. For clusters where the gold forms 1-d or 2-d, single layer structures, modest diminution in Au/substrate ratio is expected, because there is some gold-gold shadowing, and the substrate shadows overlap to some extent. Finally, the ratio should decrease steeply for multilayer clusters, because some Au atoms are no longer in the top-most layer. As Fig. 2 shows, deposited Au atoms have the highest dispersion, as expected if sintering is minimal, and consistent with our XPS studies (publication C). Au_2 - Au_4 are single layer clusters, but starting at Au_5, there is a transition to two layer structures. The question is how well the morphology correlates to activity, and comparison with the activity trend shown in the lower frame shows that there is no one-to-one correlation. For example, Au_5, which is where we first begin to see multilayer clusters on the surface, is one of the least reactive.

The other obvious question is how the reactants bind to the catalyst, and again, ISS can be used as

a sensitive probe. The idea here is that when an adsorbate binds to the surface, the scattering signal from atoms immediately beneath and surrounding the adsorption site is attenuated by a combination of shadowing, blocking, and ISP effects. CO binding was probed by comparing ISS spectra for as-deposited $Au_n/TiO_2(110)$, before and after exposure to 5 L of CO (~1.25 ML). At room temperature, very little CO sticks to TiO_2. For Au_1/TiO_2, there is substantial (18%) attenuation of Au signal (Fig. 2, bottom frame, square symbols), and little effect on the Ti or O signals, indicating that CO is binding on top of Au (which, in turn, is bound to the vacancies), and does not bind significantly to the support. As cluster size increases, the CO-induced attenuation of Au signal rapidly decreases, indicating that CO no longer binds atop the clusters. At the same time, the attenuation of Ti and O signals increases, suggesting that CO is binding on the substrate. This attenuation is not observed in absence of gold, therefore, we conclude that CO binds on the substrate, but in association with the larger gold clusters. Comparison of CO binding affinity with CO oxidation activity indicates a general anti-correlation, but certainly not the one-to-one correlation expected if CO binding were the limiting factor.

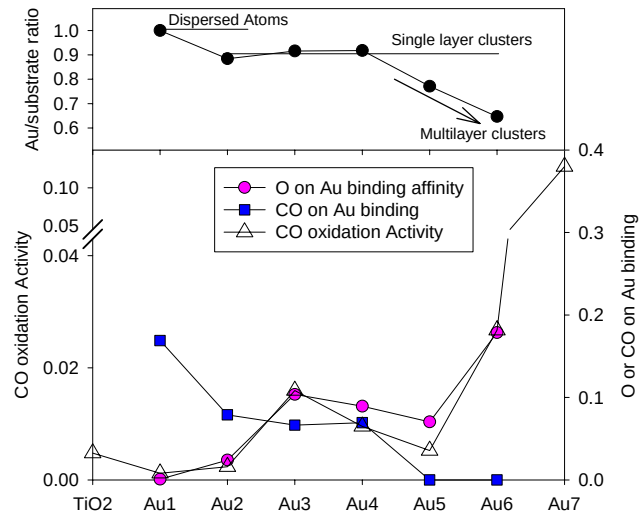

Figure 2 Top: ISS Au/substrate ratio. Bottom: Activity v.s. cluster size and CO and oxygen binding affinities.

A similar ISS study of the effects of 600 L $^{18}O_2$ exposure shows several interesting results. ^{18}O is clearly observed on the surface, and attenuates signals from ^{16}O, Ti, and Au, indicating the ^{18}O is adsorbing at sites both on top of gold, and on the substrate. The substrate binding is expected – STM and computational studies have shown O_2 binding both molecularly and dissociatively at TiO_2 vacancy sites, with binding energies in the 1.5 ~ 2 eV range. The interesting point is that the O_2-induced Au ISS attenuation (Fig. 2, bottom frame, filled circles) is almost perfectly correlated with the CO oxidation activity, indicating that the ability of the clusters to bind (and activate) O_2 is the limiting factor in the catalytic reaction. The ISS results do not directly tell us the binding motif, however, calculations by Pala and Liu for O_2 approach to Au_7/TiO_2 suggest that the oxygen dissociates, with one atom ending up on top of the gold cluster, and such a scenario is consistent with our results.

The observation that oxygen is bound both on gold and on the substrate raises another question. The strong correlation between gold-bound oxygen concentration and activity indicates that this oxygen is the oxidant. It is still possible, however, that substrate-bound oxygen might diffuse to the gold sites and thus serve as a reservoir of oxidant. We can address this question by doing some bookkeeping. If we fit the CO_2 decays during the 100 pulse sequence (Fig. 1, inset), we can estimate the total amount of CO_2 produced in the process of completely depleting the reactive oxygen. The number of CO pulses required to drop the CO_2 production to 1/e times the initial value varies from ~35 for Au_3 to ~85 for Au_5/TiO_2. We can also estimate the total amount of oxygen bound atop gold from the ISS attenuation results. The ratio of total CO_2 to Au-bound gold is unity within the experimental uncertainty, indicating that only oxygen bound atop gold during the O_2 exposure is available to react, i.e., the substantial pool of substrate-bound oxygen is inactive at room temperature.

The final interesting point concerns the kinetics of CO_2 evolution. It can be seen in the main frame of Fig. 1, that the temporal behavior of the CO_2 signal is quite different for different size clusters. In particular, Au_3, Au_4, and Au_7 all give CO_2 with an induction period of ~150 msec, while Au_5 and Au_6 both have CO_2 evolution peaking coincident with the peak of the CO reactant pulse. It should be noted that these pulse shapes do not change, within our sensitivity, from the first CO pulse to the hundredth.

The CO_2 induction period is not simply related to CO oxidation activity. The group of clusters with induction periods include both highly active (Au_7) and relatively inactive (Au_4) clusters, as does the group with no induction period. It seems clear that the activity is simply correlated with the ability of the clusters to bind and activate the oxygen reactant. The CO_2 evolution behavior depends on the actual rates of reaction, convoluted by the desorption lifetimes of the CO and CO_2. Further study over a variable temperature range should be helpful in sorting this out. At present we can say that the CO_2 desorption lifetime may account for the slow decay of CO_2 evolution, but cannot account for the induction periods.

Future Plans

Several experiments are underway to complete our study of CO oxidation on Au_n/TiO_2. We have modified our cluster source so that it now has adequate intensity to deposit Au_n up to about 15 atoms, and the first goal is simply to extend the size range. According to the two-layer hypothesis of Goodman and co-workers, we expect that clusters in the 8 - 15 atom size range should be highly active, but that may well not be the whole story. Another hypothesis about gold activation is that electron transfer from TiO_2 vacancies to gold is critical in activating the gold. In catalysts grown by sintering of Au on TiO_2, or in the layered $Au/TiO_x/Mo$ catalysts studied by Goodman and co-workers[5], the ratio of vacancies to gold is probably higher than what is expected to result from deposition of intact Au_n on near-stoichiometric TiO_2.

In addition to extending the size range, we plan to study the kinetics of CO oxidation and CO_2 evolution as a function of temperature, from cryogenic temperatures to ~350K (higher temperatures result in rapid sintering). These experiments should allow us to learn more about the mechanism, and understand the factors that separately control activity and CO_2 evolution temporal behavior.

After completing the work on Au_n/TiO_2, we plan experiments aimed at understanding bimetallic catalysts, including the Pd-Au catalysts used in vinyl acetate synthesis, and bimetallic catalysts composed of refractory metals, that nonetheless, are calculated to have activities similar to noble metal catalysts.[7-9]

Publications support by DOE, 2003 - present

A. "Deposition dynamics and chemical properties of size-selected Ir clusters on TiO_2", Masato Aizawa, Sungsik Lee, and Scott L. Anderson, Surf. Sci. 542 (2003) 253-75.

B. "CO oxidation on Au_n/TiO_2 catalysts produced by size-selected cluster deposition" Sungsik Lee, Chaoyang Fan, Tianpin Wu, and Scott L. Anderson, JACS (comm) 126 (2004) 5682-3.

C. "Agglomeration, Support Effects, and CO Adsorption on Au/TiO_2 (110) Prepared by Ion Beam Deposition" Sungsik Lee, Chaoyang Fan, Tianpin Wu, and Scott L. Anderson, Surf. Sci. 578 (2005) 5-19

D. "Agglomeration, Sputtering, and Carbon Monoxide Adsorption Behavior for Au/Al_2O_3 Prepared by Au_n^+ Deposition on Al_2O_3/NiAl(110)", Sungsik Lee, Chaoyang Fan, Tianpin Wu, and Scott L. Anderson, J. Phys. Chem. B109 (2005) 11340-11347

E. "Cluster size effects on CO oxidation activity, adsorbate affinity, and temporal behavior of model Au_n/TiO_2 catalysts", Sungsik Lee, Chaoyang Fan, Tianpin Wu, and Scott L. Anderson, J. Chem. Phys. (in press, 7/05).

Other References

[1] M. Haruta, Catal. Today **36** (1), 153 (1997).

[2] Q. Fu, H. Saltsburg, and M. Flytzani-Stephanopoulos, Science **301** (5635), 935 (2003).

[3] M. Valden, X. Lai, and D. W. Goodman, Science **281** (5383)), 1647 (1998).

[4] V. A. Bondzie, S. C. Parker, and C. T. Campbell, Catal. Lett. **63** (3-4), 143 (1999).

[5] M. S. Chen and D. W. Goodman, Science (Washington, DC, United States) **306** (5694), 252 (2004).

[6] A. Sanchez, S. Abbet, U. Heiz, W.-D. Schneider, H. Häkkinen, R. N. Barnett, and U. Landman, J. Phys. Chem. A **103**, 9573 (1999).

[7] J. Greeley and M. Mavrikakis, Journal of Physical Chemistry B **109** (8), 3460 (2005).

[8] V. Pallassana, M. Neurock, L. B. Hansen, and J. K. Norskov, Journal of Chemical Physics **112** (12), 5435 (2000).

[9] J. R. Kitchin, J. K. Norskov, M. A. Barteau, and J. G. Chen, Journal of Chemical Physics **120** (21), 10240 (2004).

Catalysis by Metal Alloys: From Single Crystals to Nanoparticles

D. W. Goodman
Department of Chemistry
Texas A&M University
College Station, TX 77842- 3012

Model mixed-metal catalysts consisting of Pd alloyed with Au, Cu, and Ag as bulk films on refractory metal single crystals and as nanoparticles supported on oxides have been characterized using an array of surface techniques including X-ray photoemission spectroscopy (XPS), low energy ion scattering spectroscopy (LEIS), Auger electron spectroscopy (AES), low energy electron diffraction (LEED), infrared reflection absorption spectroscopy (IRAS), metastable impact electron spectroscopy (MIES), scanning tunneling microscopy (STM), temperature programmed desorption (TPD), and reaction kinetics. The surface sensitivity of LEIS and IRAS has been exploited for elucidating atomic composition of the outermost surface layer. Of special interest is the composition of the surface compared to the overall composition, particularly in transitioning from planar surfaces to nanoparticles, in the presence and absence of adsorbates. The mechanistic details of the vinyl acetate synthesis reaction, used to probe the structure-function relationship of these alloy surfaces, will also be discussed.

Catalyst Structures

Peter C. Stair

Department of Chemistry
Center for Catalysis and Surface Science
Northwestern University

Chemistry Division
Argonne National Laboratory

At many length scales the structure of heterogeneous catalysts plays an important role in determining their performance. The size and shape of catalyst particles in the length scale of 0.1 mm determines the motion of the catalytic material in a reactor and the importance of reagent diffusion in catalytic chemistry. The size of supported catalytic particles in the range 1 to 100 nm influence their activity and selectivity for catalytic reactions. In the same length scale regime, the porosity of catalytic materials controls the access and duration of contact between reagents and catalytic sites. Finally, in the 0.1 to 1 nm length scale the size and shape of pores control the orientation and size of reagent molecules involved in catalytic transformations as well as the atomic arrangement at active sites. Following a brief introduction with examples at each of these length scales, this talk will review the results of synthetic, measurement and computational efforts to produce, characterize, and understand the influence catalyst structures on catalytic chemistry.

Raman spectroscopy has been employed to study the molecular structure of vanadium oxide monolayers supported on high surface area alumina and the formation of deactivating coke deposits during catalytic butane dehydrogenation. In combination with measurements of catalytic activity, selectivity, and stability, under a variety of reaction conditions, the relationship between catalyst structure and performance has been examined. We find that there is an optimum mixture of vanadia cluster sizes for the production of olefins during catalytic dehydrogenation and the avoidance of deactivating coke.

Making use of length scales in the 10 nm range, we have prepared a series of novel nanostructured membrane catalysts based on a combination of Anodic Aluminum Oxidation (AAO) and gas phase Atomic Layer Deposition (ALD). The membranes have been tested for activity and selectivity in the oxidative dehydrogenation of cyclohexane to cyclohexene and benzene. The performance of these membranes for this reaction shows a remarkable dependence on the pore dimensions which is currently under study.

Reaction Processes at Surfaces:
Non-Equilibrium Statistical Mechanics and Electronic Structure Analyses

Jim Evans and Mark Gordon
Ames Laboratory, Iowa State University, Ames, IA 50011
evans@ameslab.gov mark@si.fi.ameslab.gov

PROGRAM SCOPE:

The Chemical Physics Program at Ames Laboratory supports integrated efforts in ***electronic structure theory, non-equilibrium statistical mechanics, and multi-scale modeling***. The primary focus is on development of theoretical methods to enable system specific modeling of **heterogeneous catalysis, semiconductor surface phenomena, and clusters related to surface science**.

Electronic structure theory efforts integrate development of fundamental theory by expanding the capability for accurate treatment of large or complex systems of interest to DOE, with optimal strategies for computational implementation within GAMESS. One component of the effort involves the development and application of QM/MM methods (specifically a Surface Integrated Molecular Orbital - Molecular Mechanics or SIMOMM approach), designed to treat adsorption and reaction phenomena on semiconductor surfaces. Other components involve providing a rigorous basis for tight-binding (TB) methods and utilizing density functional theory (DFT) for studies of extended surfaces and materials. As indicated above, a general feature of our program involves interfacing of electronic structure and *non-equilibrium statistical mechanical (or multi-scale modeling) studies* of surface phenomena. The latter include Kinetic Monte Carlo (KMC) simulation of atomistic models and coarse-grained continuum formulations. One aspect of this effort relates to heterogeneous catalysis on metal surfaces, where we consider both reactions on extended single crystal surfaces (including connecting atomistic to mesoscale behavior) as well as nanoscale catalyst systems (exploring the role of fluctuations). Anther aspect focuses on reaction processes on semiconductor surfaces (including self-organization, etching and oxidation).

RECENT PROGRESS:

HETEROGENEOUS CATALYSIS

(i) Atomistic modeling of CO-oxidation on Pd(100) and other unreconstructed metal(100) surfaces. We have developed an atomistic lattice-gas model and associated efficient KMC simulation algorithm to realistically describe CO-oxidation on metal(100) surfaces under UHV conditions [8-10]. A critical prerequisite is the precise description of ordering in the CO/metal(100) and O/metal(100) systems which is controlled by weak adspecies interactions. In addition, one must reliably describe at the atomistic level the adsorption kinetics for CO and O, as well as the interaction and reaction of CO and O. Determination of key adspecies binding and interaction energies is obtained by comparing model predictions with experimental observations for adlayer ordering, temperature-programmed desorption spectra, etc. Also extensive plane-wave DFT studies are used to guide parameter selection. Primary application to date has been for CO+O/Pd(100) where we have analyzed: bistability of the steady-state mapping out the full P-T bifurcation diagram; temperature-programmed reaction kinetics; and nanoscale adlayer evolution during titration reactions.

(ii) Heterogeneous-Coupled-Lattice-Gas (HCLG) simulation approach connecting atomistic ordering to mesoscale patterns in surface reactions. A significant challenge for multiscale modeling is to describe the interplay between local ordering and reaction kinetics in catalytic reactions and development of mesoscale pattern formation. The length scale (~few microns) of the latter is controlled by rapid diffusion of species such as CO. We have further developed our HCLG

simulation approach to treat this problem [10,21]. A key challenge is to accurately and efficiently determine mesoscale surface transport of CO, which constitutes a non-trivial many-body collective diffusion problem. Various algorithms are being developed to predict both the thermodynamics and kinetic components of diffusion coefficients in mixed reactant adlayers.

(iii) Fronts and fluctuations in nanoscale reaction systems: Studies of CO-oxidation on Field Emitter Tips (FET's) provide rare insight into fluctuation effects and spatial front formation in nanoscale reaction systems. Our initial focus was on analyzing enhanced fluctuations (and their effects) near the *non-equilibrium critical point* corresponding to the loss of bistability [1,11]. Recent work has related the sharp fronts observed in FET studies to greatly reduced chemical diffusivity.

SEMICONDUCTOR SURFACE CHEMISTRY AND SURFACE SCIENCE

(i) Morphological evolution during competitive etching and oxidation of vicinal Si(100) surfaces. Exposure of *vicinal Si(100)-(2×1)* to oxygen at around 600C produces step recession associated with etching [Si + O(ads) → SiO(gas) + vacancy, where these surface vacancies diffuse to and erode steps] in competition with oxide formation [Si + 2O(ads) → SiO_2] [12,23]. The oxide islands tend to pin receding steps producing complex surface morphologies. We have performed integrated QM/MM and non-equilibrium lattice-gas modeling studies to characterize both the key reaction energetics and the development of nano- and meso-scale surface morphologies. Simulations recover the observed dramatic bending of meandering S_B steps around pinning sites, and the snap-off of stiffer S_A steps. We analyze in detail both anisotropic step recession and pinning site densities.

(ii) Self-organization of perfect atomic rows of Group III metals on Si(100). Deposition of Group III metals on Si(100) produces perfect atomic rows aligned orthogonal to the Si-dimer rows. Both this structure and the associated size or length distribution are quite unexpected for diffusion-mediated island formation on surfaces (governed by homogeneous nucleation). Again *ab-initio* studies of surface energetics together with atomistic lattice-gas modeling are used to elucidate the key factors underlying this unusual behavior [24]. Surface diffusion is highly anisotropic, but the key factor is restricted aggregation with the atomic rows, the sides being energetically unfavorable.

DEVELOPMENT OF ELECTRONIC STRUCTURE THEORY

(i) Rigorous basis for Tight-Binding Theory. We have developed molecule-deformed minimal atomic basis sets capable of reproducing full-valence space CASSCF wavefunctions. This approach was applied to analyze bonding of Si_4H_6, and Si_2-Si_{10}, and band structure in crystals [14-16].

(ii) Efficient high-level calculations. A configurational analysis, based on cluster considerations and proximities of localized orbitals, achieved considerable computational reduction for CASSSCF type MCSCF. Related work generates CI wave functions void of configurational "deadwood".

(iii) Grid-free Density Functional Theory (DFT). In order to provide an alternative to the common numerical grid-based approach to solving the DFT equations, we have developed a purely analytic approach that relies on the resolution of the identity.

FUTURE PLANS:

HETEROGENEOUS CATALYSIS

(i) CO-oxidation, NO-reduction and related reactions on surfaces of Rh, Pd, etc. We will develop further realistic atomistic models for catalytic reactions on various metal (111) and (100) surfaces, and in nanoscale systems (e.g., Field-Emitter-Tips or supported clusters). We will analyze reaction behavior primarily utilizing KMC simulation. Efforts will explore high-pressure catalysis and associated oxide formation processes. Model development will incorporate input from electronic structure studies.

(ii) Multiscale modeling of pattern formation in surface reactions. We will continue to develop efficient multiscale algorithms including implementation parallel KMC simulation as part of the HCLG approach, and efficient algorithms for on-the-fly analysis of chemical diffusion.

(iii) Atomistic modeling of STM studies of nanoscale ordering and dynamics in surface reaction systems. Through collaboration with the Salmeron group (LBL), we plan to explore surface phenomena related to ordering and dynamics in mixed adlayers on metal surfaces.

SEMICONDUCTOR SURFACE CHEMISTRY AND SURFACE SCIENCE

Atomistic and coarse-grained modeling of etching, oxidation, and other reactions on Si(100) surfaces. Our atomistic lattice-gas modeling could be further refined to incorporate a more realistic description of step, island, and pit structure on the Si(100) surface. This would enable more detailed modeling of nanoscale features of etching and reaction on imperfect or vicinal surfaces. However, separate from this approach, coarse-grained phase-field type formulations will be developed to describe morphology on a larger scale. This latter approach is potentially highly versatile, allowing efficient integration of various models for the surface chemistry with a computationally efficient framework to describe complex surface morphologies. QM/MM will be applied to provide precise and detailed information on key energetics as input to such modeling. Processes of interest will include etching by oxygen and oxidation, etching via halogens, and film growth via CVD.

DEVELOPMENT OF ELECTRONIC STRUCTURE THEORY

(i) Rigorous basis for semi-empirical approaches. Our recent work showed that bonding-related energy changes are typically dominated by the zeroth-order parts of molecular wavefunctions, and that the latter can be represented and analyzed in terms of "quasiatomic" orbitals, i.e. *minimal basis set atomic orbitals that are deformed by their molecular environments*. This approach will be extended and a variety of applications pursued for surface processes and materials systems.

(ii) Extending the QM/MM method (SIMOMM). The SIMOMM method has so far been applied to silicon, diamond, and silicon carbide surfaces. We will now develop, implement and test extensions of the SIMOMM methodology to important catalytic oxide surfaces. Of immediate interest are silica and alumina. We also plan to develop an interface between SIMOMM and our effective fragment potential (EFP) method in order to develop robust theoretical models for the surface-liquid interface.

(iii) Reliable computations on heavier elements. Electronic structure calculations on molecules containing heavy elements are traditionally performed with effective core potentials (ECP) which contain the essential scalar relativistic effects implicitly. However, the typical ECP valence orbitals do not have the correct nodal characteristics. This can cause serious problems, especially with regard to spectral properties. We plan to develop model core potentials (MCP) and their energy derivatives, and implement these into GAMESS. Unlike ECPs, MCPs have the correct nodal behavior.

DOE-SPONSORED PUBLICATIONS 2003-: (*indicates partial SciDAC support)

[1] Critical Behavior in an Atomistic Surface Reaction Model exhibiting Bistability: CO-Oxidation, N. Pavlenko, R. Imbihl, J.W. Evans, Da-Jiang Liu, Phys. Rev. E **68**, 016212 (2003).

[2] *Are both symmetric and buckled dimers on Si(100) minima?...,* Y. Jung, Y. Shao, M.S. Gordon, D.J. Doren, M. Head-Gordon, J. Chem. Phys. **119**, 10917 (2003).*

[3] *Structures and Fragmentations of Small Silicon Oxide Clusters by ab initio…* W.C. Lu, C.Z. Wang, V. Nguyen, M.W. Schmidt, M.S. Gordon, K.M. Ho, J. Phys. Chem. A **107**, 6936 (2003).

[4] *MCSCF Method for Ground and Excited States based on Full Optimizations of Successive Jacobi Rotations*, J. Ivanic, K. Ruedenberg, J. Comp. Chemistry **24**, 1250 (2003).

[5] *Split-Localized Orbitals can yield Stronger Configuration Interaction Convergence than Natural Orbitals*, L. Bytautas, J. Ivanic, K. Ruedenberg, J. Chem. Phys. **119**, 8217 (2003).
[6] *Spin-orbit Coupling in molecules: chemistry beyond the adiabatic approximation*, D.G. Federov, S. Koseki, M.W. Schmidt, M.S. Gordon, Int. Rev. Phys. Chem. **22**, 551 (2003).
[7] *The Parallel Implementation of a Full CI Program*, Z. Gan, Y. Alexeev, R.A. Kendall, M.S. Gordon, J. Chem. Phys. **119**, 47 (2003).

[8] *Lattice-Gas Modeling of CO Adlayers on Pd(100),* D.-J. Liu, J. Chem. Phys. **121**, 4352 (2004).
[9] *Lattice-Gas Modeling of the Formation and Ordering of Oxygen Adlayers on Pd(100),* D.-J. Liu, J.W. Evans, Surface Science **563**, 13-26 (2004)
[10] *From Atomic Scale Reactant Ordering to Mesoscale Reaction Front Propagation: CO Oxidation on Pd(100)*, D.-J. Liu, J.W. Evans, Phys. Rev. B **70**, 193408 (2004)
[11] *Crossover between Mean-Field and Ising Critical Behavior in a Lattice-Gas Reaction-Diffusion Model*, D.-J. Liu, N. Pavlenko, and J.W. Evans, J. Stat. Phys., **114**, 101 (2004).
[12] *Atomistic Modeling of Morphological Evolution during Simultaneous Etching and Oxidation of Si(100),* M. Albao, D.-J. Liu, C. H. Choi, M.S. Gordon, J.W. Evans, Surf. Sci. **555**, 51 (2004)*
[13] *Adsorption of Acetylene on Si(100)*, J.M. Rintelman, M.S. Gordon, J. Phys. Chem. **108**, 7820 (2004).
[14] *Theoretical Studies of Growth Reactions on Diamond Surfaces*, P. Zapol, L. A. Curtiss, H. Tamura, and M. S. Gordon, in *Comp. Materials Chemistry*, L.A. Curtiss, M.S. Gordon, Eds., pp. 266-307 (2004).
[15] *Molecule Intrinsic Minimal Basis Sets. I Ab-Initio Optimized Molecular Orbitals*, W. C. Lu, C. Wang, M. Schmidt, L. Bytautas, K. M. Ho, K. Ruedenberg, J. Chem. Phys. **120**, 2629 (2004)
[16] *Molecule Intrinsic Minimal Basis Sets. II. Bonding… for Si_4H_6 and Si_2 to Si_{10}*, W. C. Lu, C. Z.Wang, M. Schmidt, L. Bytautas, K. M. Ho, K. Ruedenberg, J. Chem. Phys. **120**, 2638 (2004).
[17] *Electronic Structures in Crystals…Highly Localized Quasiatomic Minimal Basis Orbitals*, W. C. Lu, C. Z. Wang, T.L. Chan, K. Ruedenberg, K. M. Ho, Phys. Rev. B **70**, 041101 (2004).
[18] *Spin-orbit coupling methods and applications to chemistry*, D.G. Federov, M.W. Schmidt, S. Koseki, M.S. Gordon, in *Adv. in Relativistic Molecular Theory*, Vol. 5, World Sci., Singapore, pp. 107-136, 2004.
[19] *Economical Description of Electron Correlation*, L. Bytautas, K. Ruedenberg, *Symp. Recent Advances in Electron Correlation Methodology* (A. K. Wilson, K. A. Peterson Ed.s, ACS, 2004).
[20] *Dissociation Potential Curves of Low-Lying States in Transitions Metals. II. Hydrides of Groups 3 & 5*, S. Koseki, Y. Ishihara, D.G. Fedorov, M.W. Schmidt, M.S. Gordon, J. Phys. Chem. **108**, 4707 (2004).
[21] *Correlation Energy Extrapolation through Intrinsic Scaling. I, II, III,* L. Bytautas, K. Ruedenberg, J. Chem. Phys. **121**, 10905 (2004); **121,** 10919 (2004); **121,** 10852 (2004).

[22] *Connecting-the-Length-Scales from Atomistic Ordering to Mesoscale Spatial Patterns in Surface Reactions: HCLG Algorithm*, D.-J. Liu, J.W. Evans, SIAM Multiscale Modeling **4**, in press (2005).*
[23] *Kinetic Monte Carlo Simulation of Non-Equilibrium Lattice-Gas Models: …Surface Adsorption Processes*, J.W. Evans, Handbook Mat. Modeling A, S. Yip, Ed. (Springer, Berlin, 2005), Ch.5.12.*
[24] *Competitive Etching and Oxidation of Vicinal Si(100) Surfaces*, M.A. Albao, D.-J. Liu, C.H. Choi, M.S. Gordon, J.W. Evans, MRS Proc. **859E**, JJ3.6 (2005).*
[25] *Monotonically Decreasing Size Distributions for One-Dimensional Ga Rows on Si(100)*, M.A. Albao, M. Evans, J. Nogami, D. Zorn, M.S. Gordon, J.W. Evans, Phys. Rev. B **71**, 071523 (2005).*
[26] *Correlation Energy Extrapolation Through Intrinsic Scaling. IV,* L. Bytautas, K. Ruedenberg, J. Chem. Phys. **122**, 155144 (2005).
[27] *Multi-Reference Second-Order Perturbation Theory: How Size Consistent is 'Almost Size Consistent'?* J. M. Rintelman, I. Adamovic, S. Varganov, M. S. Gordon, J. Chem. Phys., in press.
[28] *Advances in Electronic Structure Theory: GAMESS a Decade Later*, M. S. Gordon, M. W. Schmidt, THEOCHEM, in press (2005).
[29] *Potential Energy Surfaces of Si_mO_n Cluster Formation and Isomerization* P.V. Avramov, I. Adamovic, K.-M. Ho, C.Z. Wang, W.C. Lu, M.S. Gordon, J. Phys. Chem., in press.
[30] *Morphological Evolution during Epitaxial Thin Film Growth: Formation of 2D Islands and 3D Mounds*, J.W. Evans, P.A. Thiel, M.C. Bartelt, Surface Science Reports, in press (2006).

Photocatalysis on Single Crystal TiO_2

Michael A. Henderson
Institute for Interfacial Catalysis
Chemical Sciences Division
Pacific Northwest National Laboratory
Richland, WA 99352, USA
Tel. (509) 376-2192
Fax. (509) 376-5106
email ma.henderson@pnl.gov

The 1972 pioneering work of Fujishima and Honda [1] involving photoelectrochemical splitting of water on TiO_2 electrodes continues to inspire growth in the field of heterogeneous photocatalysis. The level of research involving photocatalysis at oxide semiconductor surfaces has significantly increased recently with the advent of new applications such as photo-induced hydrophilicity, indoor air purification, and bacterial disinfection, and with new hopes of improving older applications such as water purification and harvesting sunlight to split water. This increased interest in oxide-based photocatalysis is also reflected by the 2000+ patents and 6000+ publications in the last 6 years involving TiO_2 as a photocatalytic promoter. Despite the increased interest, the vast majority of research effort on oxide photocatalysis has been applied in nature. As a result, there is a growing needed for molecular-level insights into such issues as the surface and bulk structural dependences, the dynamics of charge trapping and transfer processes, the role of dopants, and the mechanistic details that intertwine excited and ground state chemistries.

In this presentation, I will give an overview of oxide photocatalysis focusing on research involving fundamental studies on well-defined single crystal oxide surfaces. Examples will concentrate on experimental work being performed at PNNL. Specifically to be discussed will be the mechanisms of acetone and trimethyl acetate photo-oxidation on the rutile TiO_2(110) surface.

1. A. Fujishima and K. Honda, "Electrochemical photolysis of water at a semiconductor electrode." Nature 238 (1972) 37.

Chemical Kinetics and Dynamics at Interfaces

Laser induced reactions in solids and at surfaces

Wayne P. Hess (PI), Kenneth M. Beck, and Alan G. Joly
Chemical Sciences Division, Pacific Northwest National Laboratory
P.O. Box 999, Mail Stop K8-88, Richland, WA 99352, USA
wayne.hess@pnl.gov

Program Scope

The elucidation of physical and dynamic processes of electronically excited solids is essential to understanding radiation chemistry of condensed matter. Radioactive decay (from waste or other sources) releases huge quanta of energy that can induce reactions in the surrounding material. The initial high energy quantum is absorbed by the host material and ionization tracks are formed along the decay vector. The high energy species thus produced, such as core holes and free electrons, relax very quickly to form electron-hole pairs, excitons, and other species. These much less energetic secondary products then induce the transformations commonly regarded as radiation damage. It is therefore possible to study much radiation chemistry using initial excitation energies in the chemically relevant range between roughly 2 and 20 eV. The lower end of this range is easily generated by table top laser sources. Photo-stimulated desorption, of atoms or molecules, provides a direct window into many important processes and is particularly indicative of electronic excited state dynamics.

Excited state chemistry in solids is inherently complex and greater understanding is gained using a combined experiment/theory approach. We collaborate with leading solid-state theorists using *ab initio* calculation and analysis to model laser desorption and photoemission experiments. The experiments are designed specifically to test hypothetical models and theoretical predictions resulting from the calculations. We have developed laser techniques to study solid-state chemistry using tunable femtosecond and nanosecond lasers to excite wide-gap materials under highly controlled conditions. We monitor particle emission using quantum-state specific laser ionization and probe surface chemical transformations using surface sensitive techniques such as x-ray photoelectron spectroscopy.

Laser control of chemical reactions has been actively pursued since the development of tunable lasers. Two-pulse, or pump dump control, has been proposed to enhance a particular reaction channel. To date we have explored mainly incoherent or passive control strategies using single pulses and pulse pairs. We have demonstrated that laser control of desorbed products and quantum states is possible by judicious choice of laser wavelength, pulse duration, and delay between femtosecond pulses. Our main goal in using a laser control approach is to verify our hypothetical models rather than pursuit of laser control as an end in itself.

Recent Progress and Future Direction

My team's laboratory studies are based on surface science and laser excitation and probe techniques. We interrogate desorbed atoms or molecules from ionic crystals using resonance enhanced multiphoton ionization and time-of-flight mass spectrometry. In single-pulse experiments, photon energies are chosen to excite specific surface structural features that lead to particular desorption reactions. In pulse pair experiments, the initial laser pulse induces formation of transient species in the near surface region. A subsequent pulse then further excites either the sample or the nascent transient species to induce specific particle emission. Our laser systems are a combination of excimer, Nd:YAG, ultrafast, and tunable solid state or dye lasers. Pump laser

output may be frequency converted using nonlinear techniques to produce photon energies ranging from 1 to 8 eV. The radiation sources are tuned to excite either bulk or surface states leading to controlled laser desorption of atoms or molecules.

The photon energy selective approach takes advantage of energetic differences between surface and bulk exciton states and probes the surface exciton directly. Application of this approach to controlling the yield and state distributions of desorbed species requires detailed knowledge of the atomic structure, optical properties, and electronic structure within a developing surface exciton desorption model. Our model indicates that it is possible to excite the surface over the bulk of ionic crystals using tunable excitation and thus induce controllable surface specific reactions. We recently demonstrated nearly exclusive surface excitation of KBr, KI, NaCl and other alkali halides. Previously, all other excitation sources (e.g. lasers, synchrotron, and electron) produced a mixture of surface and bulk excitation leading to multiple reactions. By generating the hyperthermal (surface) channel without significant thermal emission (bulk channel), we proved that a particular channel could be selected.

Direct surface excitation, in principle, allows incoherent control over product quantum state and velocity distributions. Using excitation photon energies between 5.5 and 6.5 eV we are able to control the Br atom mean kinetic energy between 0.12 and 0.37 eV. These selected kinetic energy distributions exceed the thermal mean kinetic energy (0.03 eV) expected from bulk excitation. Demonstration of controlled velocity distributions effectively confirms the theoretical model. A method for extending laser control to the particle *electronic state* (spin-orbit) distribution is also predicted from our model. Such control has been demonstrated for subset of crystals that meet specific conditions. The factors required for electronic state control are the relative size of energetic shift between the surface and bulk exciton bands and the spin-orbit energy of the desorbed halogen atom. A large shift between the surface and bulk exciton band in combination with a small relative spin orbit splitting is required for effective control. If the relative level separations are reversed laser control is not possible due to interference between the bulk and surface channels. These factors predict that electronic state control is possible for all alkali-chlorides and fluorides and no alkali- bromides and iodides.

Technological applications of alkali halides are limited compared to oxide materials. Oxides serve as dielectrics in microelectronics and form the basis for exotic semi- and super-conducting materials. Although the electronic structure of oxides differs considerably from alkali halides, it now appears possible to generalize the exciton model for laser surface reactions to these interesting new materials. We ask the question “Can an oxide surface exciton or a combination of excitons lead to controllable desorption and hence specific surface modification?” If exciton based desorption can be generalized to oxides then selective excitation of surface excitons could lead to controllable surface sculpting, on an atomic scale, for many important materials. The O-atom velocity and kinetic energy profiles for 4.7 eV photo-excitation have been obtained indicating that surface excitons can possibly combine leading to hyperthermal O-atom desorption. The O-atom KE distribution is clearly hyperthermal indicating that a surface exciton mechanism could likely be responsible.

While exciton-based desorption is plausible for MgO, we note that the higher valence may require a bi- or tri-exciton mechanism. The details of this mechanism need to be delineated and confirmed by demonstrating laser control of the various desorption processes. We have recently observed hyperthermal neutral Mg-atom desorption. This is quite a novel result as Mg-atom desorption requires that two electron transfer to a corner site Mg^{2+} ion in a very short time and then desorb prior to relaxation. The hyperthermal distribution indicates that the exciton model is extendable now to metal atom desorption processes – a previously unknown mechanism. Future

plans include femtosecond pulse-pair photo-emission electron microscopy to probe dynamics of oxide nanostructures on surfaces.

Our excitation techniques are site specific as it is possible to selectively excite terrace, step, or corner surface sites. Therefore, we have explored various sample preparation techniques that produce high concentrations of low-coordinated surface sites such as 4-coordinated steps and 3-coordinated corner or kink sites. In particular, we have employed reactive ballistic deposition (a technique developed in Bruce Kay's lab) to grow very high surface area MgO thin films. These films have been thoroughly characterized using XPS, SEM, TEM, and XRD techniques. Similarly, we have also studied laser desorption of MgO nano-powders grown by a chemical vapor deposition technique (grown by the E. Knoezinger group, Vienna). The nano-powders show cubic structure and edge lengths ranging between 3 and 10 nm (through TEM analysis). Both sample types provide unique insight into site-selective exciton-based desorption processes and are the focus of ongoing work. We plan to grow and study several other oxide surfaces in the near term including CaO, ZrO_2, and TiO_2.

References to publications of DOE BES sponsored research (2003 to present)

1. "Photon stimulated desorption from KI: Laser control of I-atom velocity distributions" M Henyk, AG Joly, KM Beck, and WP Hess, Surf. Sci. **528**, 219 (2003).

2. "Synergistic effects of exposure of surfaces of ionic crystals to radiation and water." JT Dickinson, KH Nwe, WP Hess, and SC Langford, Appl. Surf. Sci. **208**, 2 (2003).

3. "Surface excitons detected by atomic desorption." AG Joly, KM Beck, M Henyk, WP Hess, PV Sushko, and AL Shluger, Surf. Sci. **544**, L683 (2003).

4. "The origin of temperature-dependent yield of Frenkel-pairs generated by valence excitation in NaCl", K Tanimura and WP Hess, Phys. Rev. B, **69**, 155102 (2004).

5. "Laser control of product electronic state: desorption from alkali halides." KM Beck, AG Joly, N Dupuis, P Perozzo, W Hess, P Sushko, and A Shluger, J. Chem. Phys. **120**, 2456 (2004).

6. "Determination of surface exciton energies by velocity resolved atomic desorption." WP Hess, AG Joly, KM Beck, PV Sushko, and AL Shluger, Surf. Sci. **564**, 62 (2004).

7. "Interaction of wide band gap single crystals with 248 nm excimer laser irradiation: laser induced near-surface absorption in single crystal NaCl." K H Nwe, S C Langford, WP Hess, and JT Dickinson, J. Appl. Phys. **97**, 043501 (2005).

8. "Interaction of wide band gap single crystals with 248 nm excimer laser irradiation: The effect of water vapor and temperature on laser desorption of neutral atoms from sodium chloride" KH Nwe, SC Langford, WP Hess, and JT Dickinson, J. Appl. Phys. **97**, 043502 (2005).

9. "Surface electronic properties and site-specific laser desorption processes of highly structured nanoporous MgO thin films." M Henyk, KM Beck, MH Engelhard, AG Joly, WP Hess, and JT Dickinson, Surf. Sci. (in press).

10. “A mechanism of photo-induced desorption of oxygen atoms from MgO nano-crystals.” PE Trevisanutto, PVSushko, AL Shluger, K. M. Beck, M. Henyk, A. G. Joly, and W. P. Hess, Surf. Sci. (in press).

11. G. “Introduction to Photoelectron Emission Microscopy: Principles and Applications.” G Xiong, AG Joly, WP Hess, M Cai, and JT Dickinson, J. Chin. Phys. (invited article).

12. “Laser control of desorption through selective surface excitation.” W. P. Hess, A. G. Joly, KM Beck, M Henyk, DP Gerrity, NF Dupuis, P Perozzo, PV Sushko, and AL Shluger, J. Phys. Chem. (Feature Article in October 27, 2005 issue).

*Collaborators include AL Shluger, PV Sushko, DP Gerrity, JT Dickinson, and M Henyk

Optical manipulation of ultrafast electron and nuclear motion on metal surfaces

Hrvoje Petek (petek@pitt.edu)
Department of Physics and Astronomy
University of Pittsburgh
Pittsburgh, PA 15269

Since the pioneering work of Langmuir on electron emission from metals, alkali atom overlayers on metal surfaces have been central to development of theories of chemisorption.[1-4] Our research goal is to study dynamics of alkali atoms on noble metal surfaces in response to excitation by a near UV light. The photoinduced charge transfer whereby an electron is transferred from the metal to chemisorbed alkali atoms transforms their ground ionic state to a neutral excited state. This charge redistribution initiates alkali atom photodesorption.[5] This year we have taken a step back to reassess more than 70 years of theory of chemisorption of alkali atoms on metals.

According to the Gurney theory of chemisorption and its later elaborations such as the Anderson impurity theory, chemisorption occurs through the configuration interaction of the valance *n*s state of the alkali atoms with the continuum of states in the metal.[2-4, 6] The basic elements of chemisorption as described by the Gurney and Anderson theories are presented in Fig. 1. As alkali atoms are brought to a metal surface, their highest occupied *n*s states are perturbed through Coulomb interaction with electrons in the metal. The energy of the *n*s state, which is established at large distance by aligning the work function Φ of the metal with the ionization potential E_{IP} of the atom, increases on account of the Coulomb repulsion with the screening charge in the metal. Assuming that the electron and nuclear motions can be separated, the ionic alkali atom core creates a negative image charge at the metal surface, which repels the *n*s electron. As an alkali atom is brought to a surface, its *n*s state is destabilized with respect to the Fermi level E_F. It acquires density of states (DOS) above E_F and width Γ, which is proportional to the rate of charge exchange with the surface. At the chemisorption distance R, the *n*s state correlates with an unoccupied (virtual) state, to which is often ascribed a large (eV) bandwidth.[6] Within this model, the *n*s electron is delocalized within the metal and the charge remaining on the alkali atom is proportional to the DOS of the virtual *n*s state that lies below E_F.[7]

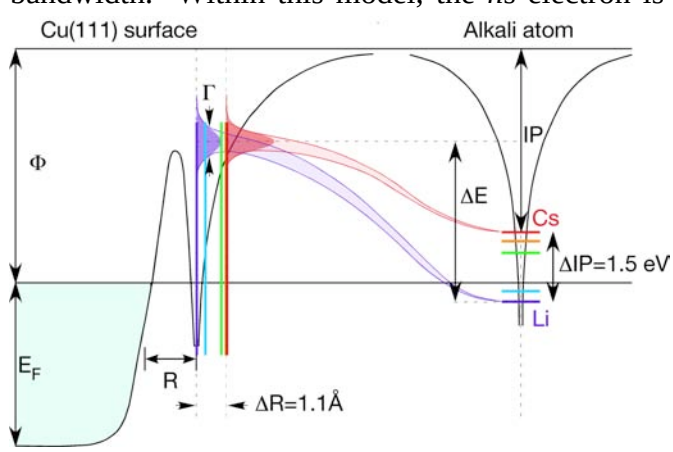

Figure 1. *Chemisorption of alkali atoms on Cu(111) combining concepts of the Anderson theory and experimental observables.*

Although the Anderson impurity model has been the basis for our understanding the chemisorption on metals for more than 35 years, the above scenario has not been tested systematically even for alkali atoms. The difficulty lies in part in the difficulty of experimentally probing the electronic structure of alkali atoms at low coverages

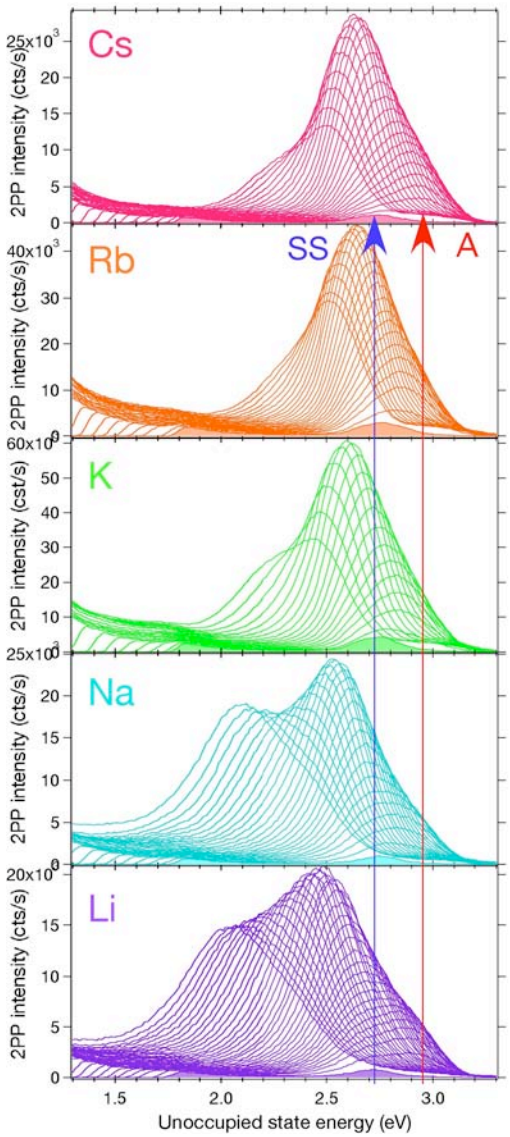

Figure 2. *Detail of 2PP spectra of the SS→A resonance as a function of alkali atom coverage for Li-Cs that shows the period independent alkali atom DOS. The main differences can be attributed to the alkali atom-dependent tuning rates of SS with coverage.*

where interadsorbate interactions do not complicate the fundamental aspects of the atom-surface interaction. Specifically, standard techniques such as photoemission do not provide evidence for the occupied DOS of the *n*s state. A weak signal near the E_F in He* metastable induced electron emission spectra, which are highly surface specific, has been attributed to the *n*s DOS.[8]

Methods that probe the unoccupied states have met more success in exploring the chemisorption properties of alkali atom/metal surfaces. In field emission, inverse photoemission, and two-photon photoemission experiments there are numerous reports of resonances 2-3 eV above E_F that have been attributed to the *n*s state.[5, 9-11] However, most of these experiments did not have sufficient energy resolution, nor were they sufficiently systematic to provide quantitative data for comparison with theory. Of particular note, however, are the experiments of Fischer et al., who measured the energy of the *n*s state for Na/Cu(111) from zero to >1 ML coverage.[11] They found that, together with the work function and image potential IP state, the *n*s state energy decreases with coverage from its low coverage limit at 2.86 eV up to the coverage of 0.4 ML. At this point the alkali overlayer becomes metallic, Φ begins to increase, and the *n*s state abruptly becomes an occupied quantum well state.

In the past year we have performed a survey two-photon photoemission (2PP) spectra of the *n*s state for all the available alkali atoms Li-Cs on Cu(111) surface (Fig. 2). The 2PP spectra excited with 3.05 eV light are limited in range of alkali atom coverage and spectral coverage by the onset of the interfering one photon photoemission when Φ decreases to ~3.4 eV. At zero coverage, the only sharp feature in the 2PP spectra is the occupied Shockley surface state (SS) -0.39 eV relative to E_F. Upon adsorption of alkali atoms a new state labeled A appears at energy just above SS for all alkali atoms. Increasing the alkali atom coverage reduces Φ, and along with it, the energy of every surface state that is confined by the image potential at the metal/vacuum interface.[11] Because states that are closer to Φ tune faster, the separation between A and SS tunes into resonance with the laser, resulting in the resonance enhancement observed in the 2PP

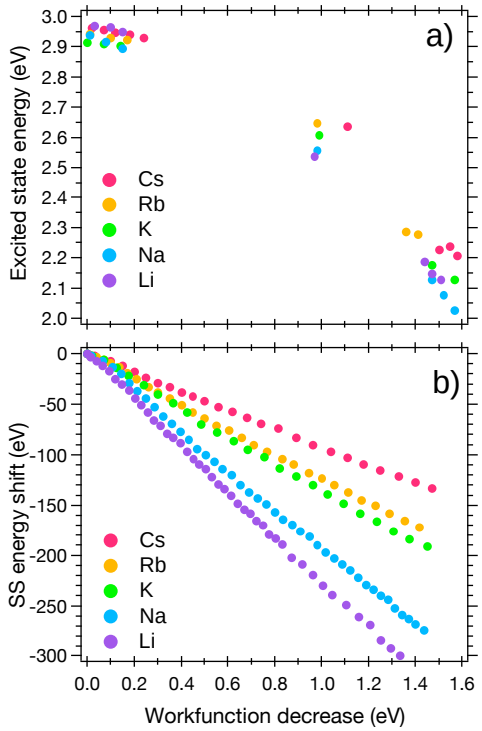

Figure 3. *The energy of* ***a)*** *alkali atom resonance and b) the energy shift of the Shockley surface state for different coverages plotted against the work function change.*

spectra of Fig. 2.[5] By extracting the energy of A in the pre-resonant, resonant, and post-resonant regions, where the peak assignment is unambiguous, we obtain the plot of the *n*s state energy vs. work function shift $\Delta\Phi$ in Fig. 3a. Remarkably, at the low coverage limit, the energy of the *n*s state for all alkali atoms is 2.95±0.05 eV independent of the period (*n*), and it tunes with an identical $\Delta\Phi^{3/2}$ dependence.

Returning to Fig. 1, it is quite remarkable that the *n*s state energy is identical for all alkali atoms considering that the leading factors that determine it, namely E_{IP} and the chemisorption distance R, differ substantially with *n*. As shown in Fig. 1, the E_{IP} decreases from 5.39 eV for Li to 3.89 eV for Cs. The difference in the E_{IP} of isolated atoms may be compensated by different chemisorption distances, which should increase the energy of *n*s states as *n* decreases. The chemisorption height R varies from 2.0 Å for Li to 3.09 Å for Cs, which should compensate for the differences in Φ. Nevertheless, it would be quite a coincidence for these two factors to compensate each other perfectly to yield the observed universal behavior.

The data in Fig. 3a suggest that the energy of *n*s states depends mainly on an entirely different factor, namely, the work function of the metal Φ. Both the period and the coverage dependence of the *n*s state energies in Figs. 2 and 3a are consistent only with the coverage dependent work function of the surface. To see how the work function may come into play, we need to examine the electronic structure of alkali atom covered surfaces from a different perspective. The *n*s electrons are bound in the surface normal direction by the crystal potential at the surface side and the image potential on the vacuum side, as are the image potential states. Thus, we can describe the *n*s states from the perspective of hybridized states of the IP potential. Borisov and Gauyacq described the states of supported by the IP potential of the Cs/Cu(111) system with the Hamiltonian:

$$H = T + V_{e-surf} + V_{e-Cs^+} + V_{e-\overline{Cs}} \,, \qquad [1]$$

where T is the kinetic energy operator, V_{e-surf} is the electron-surface interaction potential, V_{e-Cs^+} is the electron-cation pseudopotential, and $V_{e-\overline{Cs}}$ describes the interaction of the electron with the image charge of Cs^+.[12] The solutions to the Schrödinger equation yield the *n*s state, and the IP states that are perturbed by the *n*s state. The *n*s state has some IP character at the surface, but at large distances correlates with the atomic state. This model treats the IP character of the *n*s state more accurately than conventional approaches based on the density functional theory. If we adopt this perspective, than the

experimental results imply that chemisorbed alkali atoms act as structureless point dipoles independent of their period. For that to be true, the properties of the *n*s electron must be dominated by the image potential, as is expected for the unperturbed IP states.

Even though the *n*s state energy are consistent with their IP parentage, other aspects of the 2PP spectra point to the influence of the crystal potential. There is a clear distinction between the spectra of Cs, Rb, and K on one hand, and Na and Li, on the other. LEED structural studies show that large alkali atoms (Cs, Rb, and K) occupy on-top sites, while small alkali atoms (Na and Li) occupy three-fold hollow sites.[13] These tendencies are probably responsible for the characteristic differences between the 2PP spectra. The main difference between the large and small alkali atoms arises from the different tuning of the energy of SS with alkali atom coverage (Fig. 3b), which is best captured in one photon photoemission spectra (not shown). Figure 3b clearly shows that the properties of SS, which is much more strongly coupled to the surface than the IP states, strongly correlate with the chemisorption height.

The final observable of chemisorption is the *n*s state linewidth Γ. We have attempted to extract Γ from by modeling of the SS-A resonance; however, we have not been able to obtain a satisfactory fit with a three state optical Bloch equation model, despite having independent information on SS from one-photon photoemission spectra. It is clear, however, that the linewidths for all alkali atoms are much narrower than typically attributed to *n*s states, which has been attributed to the *L*-projected band gap of Cu(111).[14] The experimental linewidths are even narrower than predicted by realistic theoretical models that include the effects of the band gap and the inelastic electron scattering.[15] Perhaps this discrepancy also speaks to the substantial IP character of the *n*s states of alkali atoms.

We are proceeding to investigate the alkali atom resonance energy for substrates with different work functions (Ag(111)), to calculate the resonance energy by different theoretical approaches, and to measure the excited state electron and nuclear dynamics.

References

1. I. Langmuir, Phys. Rev. **43**, 224 (1933).
2. R. W. Gurney, Phys. Rev. **47**, 479 (1935).
3. J. W. Gadzuk, Phys. Rev. B **1**, 2110 (1970).
4. J. P. Muscat and D. M. Newns, Prog. Surf. Sci. **9**, 1 (1978).
5. H. Petek and S. Ogawa, Annu. Rev. Phys. Chem. **53**, 507 (2002).
6. P. Nordlander and J. C. Tully, Phys. Rev. B **42**, 5564 (1990).
7. G. Butti, et al., Phys. Rev. B **72**, 125402 (2005).
8. B. Woratschek, et al., Phys. Rev. Lett. **55**, 1231 (1985).
9. R. Dudde, et al., Phys. Rev. B **44**, 1198 (1991).
10. E. W. Plummer and R. D. Young, Phys. Rev. B **1**, 2088 (1970).
11. N. Fischer, et al., Surf. Sci. **314**, 89 (1994).
12. A. G. Borisov, et al., Phys. Rev. B **65**, 205414 (2002).
13. R. D. Diehl and R. McGrath, J. Phys. C **9**, 951 (1997).
14. A. G. Borisov, et al., Phys. Rev. Lett. **86**, 488 (2001).
15. A. G. Borisov, et al., Phys. Rev. B **65**, 235434 (2002).

LASER DYNAMIC STUDIES OF PHOTOREACTIONS ON SINGLE-CRYSTAL AND NANOSTRUCTURED SURFACES

Richard Osgood,
Center for Integrated Science and Engineering, Columbia University, New York, NY 10027, Osgood@columbia.edu

Program Scope or Definition:

The scope of our current research program is to examine the photon-initiated reaction mechanisms, half-collision dynamics, and other optically induced dynamics effects, which occur for adsorbates on well-characterized, semiconductor or metal-oxide surfaces. From the perspective of energy needs, photoexcitation has been of continuing interest for its importance in photocatalytic destruction of environmental pollutants, in several methods of solar-energy conversion, and for a variety of applications in nanotechnology. Our recent work in this program has yielded several new research findings regarding the basic chemical dynamics of surface photofragmentation.

The goal of the current program has been to develop a thorough understanding of the dynamics of surface photoreactions using UHV-prepared model molecular-adsorbate/ *nanostructured* surface systems. The research questions in our evolving program are as follows: What are the mechanisms for reactions on nanostructured surfaces? For substrate-electron transfer reactions, how do substrate ligands modify the chemistry? What new resonant-excitation physics are introduced by elementary excitations on a nanoobject surface? In particular, the research plan of this program is to extend our understanding of the photodynamics of molecular adsorbates by concluding our studies of heterogeneous photo-electron transfer using well characterized thiolate spacer-layers; examining fragmentation on nanostructured metal-oxide surfaces, including those with complex reconstruction and nanofaceted surfaces; and investigating dynamical processes on nanoobjects, including *in-situ*-deposited metal clusters and vapor-grown metal-oxide nanowires. Thus a major thrust of this research is examining reaction dynamics on nanostructured surfaces. Our primary dynamics probe is measurement of the kinetic energy and internal energies of the desorbed photofragments using time-of-flight (TOF) mass-spectroscopy and resonance-enhanced multiphoton ionization (REMPI) in conjunction with a pulsed tunable UV- or visible-laser system. The work has been carried out in ultrahigh vacuum, allowing the use of other surface spectroscopies such as temperature-programmed desorption, Auger, XPS, etc. Important components of this research involve collaboration or close consultation with the Surface Dynamics Group in the Chemistry Department at Brookhaven National Laboratory and the use of instrumentation at BNL's two major user facilities, the Center for Functional Nanomaterials and the National Synchrotron Light Source. The project uses synchrotron spectroscopies at the NSLS and variable-temperature STM imaging to investigate surface-bound reaction products, and appropriate E&M and chemical computational tools.

Recent Progress:

Surface Dynamics on Metal-Oxide Surface.

We have investigated the ultraviolet photochemistry of the methyl halide, CH_3I, on a small-bandgap metal-oxide surface using time-of-flight quadrupole mass spectrometry (TOF-QMS), temperature programmed desorption (TPD) and Auger electron spectroscopy (AES). Since the UV photochemistry of this same species has been previously studied on other classes of substrate crystals, our experiments provide comparative data on an additional class of substrate materials. Our results show that CH_3I has adsorbed phases, which are similar to those on other metal oxides, e.g. TiO_2, and thus displays similar thermal desorption spectra. In addition, its UV photochemical bond-cleavage mechanisms resemble those on a medium bandgap semiconductor and certain single-crystal metal surfaces; thus measurement of the flight times from time-of-flight quadrupole mass spectroscopy shows that UV bond cleavage is a result of dissociative electron attachment at low coverage and direct photodissociation at a coverage>>1 ML. In particular, in the presence of low-fluence-pulse irradiation at 248 nm, angle-resolved TOF-QMS measurements show that 1.6 eV and 0.3 eV CH_3 fragments are ejected from the adsorbate surface; these fragments originate from direct photodissociation and dissociative photoinduced electron transfer, respectively. These energetic photoejected fragments have characteristic angular distributions peaked at ~0° with respect to the surface normal showing that the adsorbate molecule is oriented with its carbon-halide bond along the surface normal. This adsorbate orientation, along with the impulsive nature of either of the two possible reaction mechanisms, is consistent with the low level of secondary-methyl-reaction products seen in the thermal desorption data and the strong signal from our ejected CH_3 fragments.

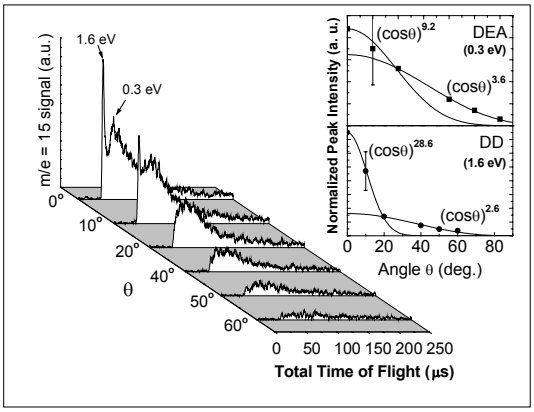

Fig. 3: Measurements of angular dependence of the TOF spectrum for a CH_3I coverage of. 1.33 ML. The inset shows the measured peak intensity versus angle and a $(\cos\theta)^n$ fitting of the data. Different mechanisms dominate at high and low coverage; at 1.33ML both direct

Formation and Characterization of Metal Oxide Nanoobjects

A major goal of the current program is to carry out surface dynamics on free-standing metal-oxide nanocrystals. The most common method of preparation of these objects is via colloidal growth. Indeed we have recently worked with the O'Brien Group at Columbia to characterize the growth of these colloidal particles (ZnO nanorods) using X-ray powder diffraction. One of the most difficult problems in investigating the UHV surface reactions on these colloidal-grown nanoobjects is the preparation of a pristine surface. For example, free-standing quantum dots are typically prepared with terminating ligands, such as TOPO for CdSe dots; removal of these ligands is extremely

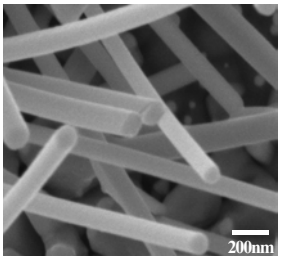

FE-SEM Mag: 80K

Fig. 2: Field-emission SEM of vapor-grown ZnO nanowires. Growth at Columbia University; micrograph taken by John Warren at the BNL CFN.

difficult under UHV conditions. One direction is to alleviate this quandary is to examine nanoobjects, which are grown *in situ*. For example we have recently investigated vapor-phase-grown single-crystal nanowires of metal oxides such as the ZnO wires grown and characterized recently in our group, which are shown in Fig. 2. We have recently characterized the bulk properties of these wires using optical, synchrotron, TEM, and electron probes.

A second approach, which we have chosen to investigate, is TiO_2 nanoparticles, which are prepared by reactive-layer-assisted deposition (RLAD), in which Ti atoms are initially deposited on a multilayer of H_2O (or NO_2) grown on a Au(111) substrate at temperature <100 K. Our initial work has been to characterize the chemical, structural and electronic properties of these oxide nanoparticles using XPS, STM and STS. To do this we have worked collaboratively with Jan Hrbek at Brookhaven National Laboratory, whose group along with that of Mike White, also at BNL, who has pioneered this method. In particular, we have shown that ~1nm diameter TiO_2 particles, formed with an H_2O reactive layer, can be obtained after raising the substrate temperature to 300K; see Fig. 3. When a NO_2 reactive layer was used, TiO_2 nanoparticles (~1nm at 300K) were grown with NO_3 radicals decorating their surfaces at temperatures bellow 500K. Further annealing induces the desorption of N-containing species and leaves behind flat TiO_2 rutile and anatase particles (~5nm after being annealed to 700K) with various facets. STS studies showed different electronic structure for different TiO_2 particle sizes. This UHV compatible method for preparing well-defined TiO_2 nanoparticles can be used in molecular-level studies of reaction mechanisms of photocatalytic processes on TiO_2 nanoparticle surfaces.

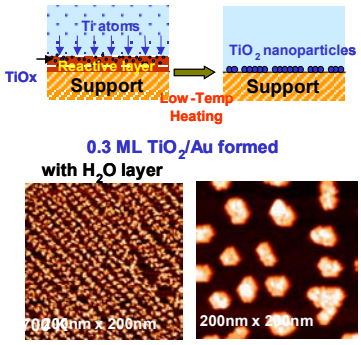

Fig. 3: TiO_2 nanoparticles formed by RLAD on a single crystal Au substrate: top, schematic of process; bottom, SEM of particles on the same substrate (Data taken by Dr. Z. Song)

Initial Chemical and Photochemical Studies on Well Characterized Nanoparticles

We have begun to look at the UHV photochemistry of these particles as well. We have begun to examine the chemical properties of uncapped TiO_2 nanoparticles prepared using RLAD approach described above. The particles appear to exhibit thermal catalytic activities, which are significantly different, that is more active, than single crystal TiO_2. For example, we have found that NO can dissociate and react with surface atomic H to form NH_3 on TiO_2 nanoparticles, while N_2O was the only dissociative product detected when NO adsorbed on a

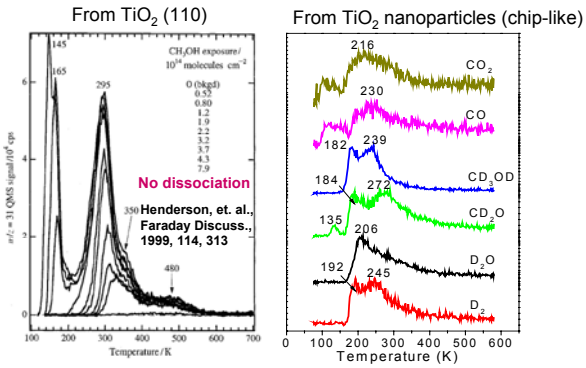

Fig. 4: Thermal desorption spectroscopy from single crystal and from our nanoparticle TiO_2. The results show that only the nanoparticle form results in thermal reactions of CH_3OH on the TiO_2

TiO_2 (110) single crystal. We have also found that CH_3OH can dissociate on TiO_2 nanparticles and form CH_2O; previously an absence of dissociation of CH_3OH was reported for single-crystal TiO_2 surfaces; see Fig. 4. More recently we have begun an investigation of the UV photochemistry of these particles as well.

Future Plans:

Our current plans are to begin studies of non-angle resolved TOF measurements using our current nanoparticle TiO_2 preparation methods. Our goal is to compare TOF velocity signatures on a well defined single-crystal sample with those obtained on nanoparticle surfaces. One area of interest will be to understand how bond cleavage mechanisms change with nanoparticle size. A second direction will be to examine the chemistry for forming nanocrystals using RLAD so as to understand the conditions for obtaining monodisperse and/or monophase nanocrystals.

Recent DOE-Sponsored Publications

1. K. Adib, G.G. Totir, J.P. Fitts, T. Miller, G.W. Flynn, S.A. Joyce and R.M. Osgood, Jr., "Chemistry of CCl_4 on Fe_3O_4(111)-(2x2) Surfaces in the Presence of Adsorbed D_2O." Surf. Sci. 537, 191 (2003).
2. Z. Zhu, A. Srivastava, and R.M. Osgood, Jr., "Reactions of Organosulfur Compounds with Si(100)," J. Phys. Chem. B 107, 13939 (2003).
3. A. Srivastava and R.M. Osgood, Jr., "State-Resolved Dynamics of 248 nm Methyl-Iodide Fragmentation on GaAs(110)." J. Chem. Phys. 119, 10298 (2003).
4. K.T. Rim, J.P. Fitts, T. Muller, K. Adib, N. Camillone III, R.M. Osgood, Jr., S.A. Joyce and G.W. Flynn, "CCl_4 Chemistry on the Reduced Selvedge of a α-Fe_2O_3(0001) Surface: A Scanning Tunneling Microscopy Study." Surf. Sci. 541, 59 (2003).
5. K.T. Rim, T. Muller, J.P. Fitts, K. Adib, N. Camillone III, R.M. Osgood, Jr., E.R. Batista, R.A. Friesner, B.J. Berne, S.A. Joyce, and G.W. Flynn, "An STM Study of Competitive Surface Reactions in the Dissociative Chemisorption of CCl_4 on Iron Oxide Surfaces," Surf. Sci. 524, 113 (2003).
6. G. G. Totir, Y. Le and R. M. Osgood, Jr., "Photoinduced-Reaction Dynamics of Halogenated Alkanes on Iron-Oxide Surfaces: CH_3I on Fe_3O_4 (111)-(2×2)," J. of Phys. Chem. B, 109, 8452 (2005).
7. Z. Zhu, T. Andelman, M. Yin, T-L. Chen, S.N. Ehrlich, S.P. O'Brien, R.M. Osgood, Jr., "Synchrotron X-ray Scattering of ZnO Nanorods: Periodic Ordering and Lattice Size," J. Mater. Res. 21, 1033 (2005).
8. Z. M. Zhu, T. Chen, Y. Gu, J. Warren and R. M. Osgood, Jr., "Zinc-oxide Nanowires Grown by Vapor-Phase Transport Using Selected Metal Catalysts: A Comparative Study," Chem. Mats., 17, 4227 (2005).
9. Z. Song, J. Hrbek, R.M. Osgood, Jr., "Formation of TiO_2 Nanoparticles by Reactive-Layer-Assisted Deposition and Characterization By XPS and STM," Nano. Letts. 5, 1357(2005)
10. G.Y. Le, G.G. Totir, G.W. Flynn and R.M. Osgood. "Chloromethane Surface Chemistry on Fe_3O_4(111)-(2×2): a Thermal Desorption Spectroscopy Comparison of CCl_4, CBr_2Cl_2, and CH_2Cl_2." Submitted to Surf. Sci. (2004)
11. N. Camillone III and T. R. Pak, K. Adib and R. M. Osgood, Jr, "Tuning molecule–surface interactions with nanometer-thick covalently-bound organic monolayers,"

Catalysis at Metal Surfaces Studied by Non-Equilibrium and STM Methods

Ian Harrison
Department of Chemistry, University of Virginia
Charlottesville, VA 22904-4319
harrison@virginia.edu

This research program employs non-equilibrium techniques to investigate the nature of the transition states for activated dissociative chemisorption of small molecules on catalytic metal surfaces. Two separate approaches/ideas are under investigation. In the first, we posit that dissociative chemisorption reactions on metal surfaces are primarily surface mediated electron transfer reactions for many hard-to-activate small molecules. Accordingly, the lowest lying affinity levels of these adsorbates, which are accessible by surface photochemistry and scanning tunneling microscopy (STM), will play a key electronic structure role in determining barrier heights for dissociative chemisorption. Electron transfer excitation into these adsorbate affinity levels followed by image potential acceleration towards the surface and rapid quenching may leave the adsorbate in the "transition state region" of the ground state potential relevant to thermal catalysis from where desorption and/or dissociation may ultimately occur. Using a low temperature scanning tunneling microscope (STM) we have been investigating the chemistry and photochemistry of CH_3Br, CO_2, and CH_4 on Pt(111). In our second approach towards probing surface transition states, we dose hot gas-phase molecules on to a cold surface and measure dissociative sticking coefficients macroscopically via Auger electron spectroscopy (AES) or microscopically (under development) by imaging chemisorbed fragments via low T_s STM. A local hot spot, microcanonical unimolecular rate theory (MURT) model of gas-surface reactivity[1,2,3] is used to extract transition state characteristics for dissociative chemisorption. An important long-range goal of our research is to microscopically characterize the different transition states for dissociative chemisorption occurring at metal terrace sites as compared to step sites – a goal of long-standing interest to the catalysis and electronic structure theory communities.[4]

Recent progress has come through improvements in tip preparation for our home-built STM and the ability to irradiate our surfaces using a 193 nm excimer laser. Our initial focus has been to microscopically characterize several photoactive small molecule systems on Pt(111) using STM with picoamp currents and low bias voltages to avoid inducing electron transfer chemistry. Methyl bromide was found to form a well-ordered (6 x 3) monolayer if multilayers were annealed to 104 K. RAIRS spectra show that molecules in the (6 x 3) monolayer stand vertically along the surface normal, while at lower coverages the molecules may tilt or lie down. The four molecules of the (6 x 3) unit cell were assigned to top and 3-fold hollow sites, in equal measure, leading to a saturation coverage of 0.22 ML. Several other ordered structures could be observed at submonolayer coverages dependent on the kinetic history of the sample. Dissociative electron attachment (DEA) to CH_3Br could be accomplished using electrons from the STM tip or photogenerated electrons from the substrate. Surprisingly, the angular distribution of the CH_3 photofragments from 193 nm photoinduced DEA of the ordered (6 x 3) CH_3Br/Pt(111) system was not sharply peaked around the surface normal but rather was quite broad (c.f., ESDIAD). We believe the broad angular distribution is due to electrostatic torquing during dissociation of the transient CH_3Br^- anions formed within the monolayer of oriented dipolar CH_3Br molecules. We've discovered that CO_2 undergoes 193 nm photoinduced DEA on Pt(111) and we are able to

image this molecule by STM as shown in Figure 1. CO_2 forms several ordered structures including (3 x 2) and (3 x 3). RAIRS indicates that most CO_2 molecules lie in the surface plane but a small fraction may stand up. We believe that vertically oriented molecules image lower than horizontally oriented molecules (0.25 Å vs. 0.50 Å high). Consequently, the relatively isolated white dots in the hex lattice in the upper left of Fig. 1(a) are assigned as vertical molecules that image as relatively dark dots when surrounded by horizontal molecules in the (3 x 3) structure shown slightly further to the upper left in Fig. 1(a), and again in Fig. 1(b). More difficult to image, but still tractable, is CH_4 on Pt(111) which desorbs from the surface at just 66 K. The CH_4 monolayer appears to form an ordered ($\sqrt{3}$ x $\sqrt{3}$) structure. Irradiating physisorbed CH_4 at 193 nm yields chemisorbed CH_3 radicals which are relatively easy to image. Several manuscripts are being written up and our immediate future work will concentrate on looking for spatial variations in photoinduced DEA of adsorbates to answer the question, "Are steps sites more photochemically active than terrace sites?".

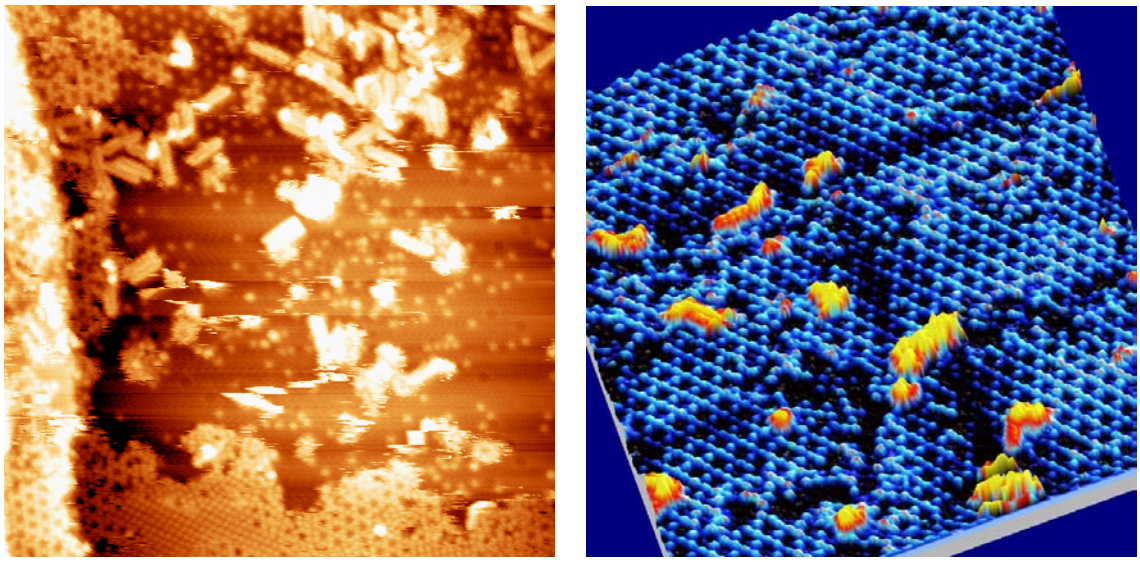

Fig. 1 STM images of CO_2 on Pt(111) at T_s = 30 K (a) Intermediate coverage following some annealing shows singleton molecules and several ordered structures [300 Å x 300 Å]. (b) CO_2 in a (3 x 3) lattice [200 Å x 200 Å].[5]

A 3-parameter formulation of the simple MURT model for activated dissociative chemisorption illustrated schematically in Fig. 2(a) has proven capable of *quantitatively* analyzing/predicting dissociative sticking coefficients for methane on Pt(111),[1,3] Ni(100),[2] Ir(111),[6] and SiH_4 on Si(100)[7] for varied thermal equilibrium and non-equilibrium experiments spanning some 8 orders of magnitude in sticking and ten orders in pressure, even at rovibrational eigenstate resolved levels of detail.[8] Fig. 2(b) demonstrates that it is possible to extract transition state characteristics based on variable (T_g, T_s) sticking coefficient measurements using a heated effusive gas doser, AES of products, and 3-parameter PC-MURT analysis. Electronic structure theory[9] and CH_4 supersonic molecular beam experiments on Pt(553)[10] suggest that Pt(111) step sites have a threshold energy for CH_4 dissociation, E_0, some 30 kJ/mol lower than on Pt(111) terraces. We plan to use a heated effusive beam of CH_4 incident on a Pt(111) surface held at $T_s \sim$ 80 K and image the CH_3 dissociation products left behind by STM. By locally measuring $S(T_g, T_s \sim 80\ K)$ as a function of T_g in combination with PC-MURT analysis we hope to directly characterize the transition states at steps and terraces. Fig. 3 provides PC-MURT simulations of some possible experimental outcomes assuming ΔE_0 = 30 kJ/mol between terraces and steps.

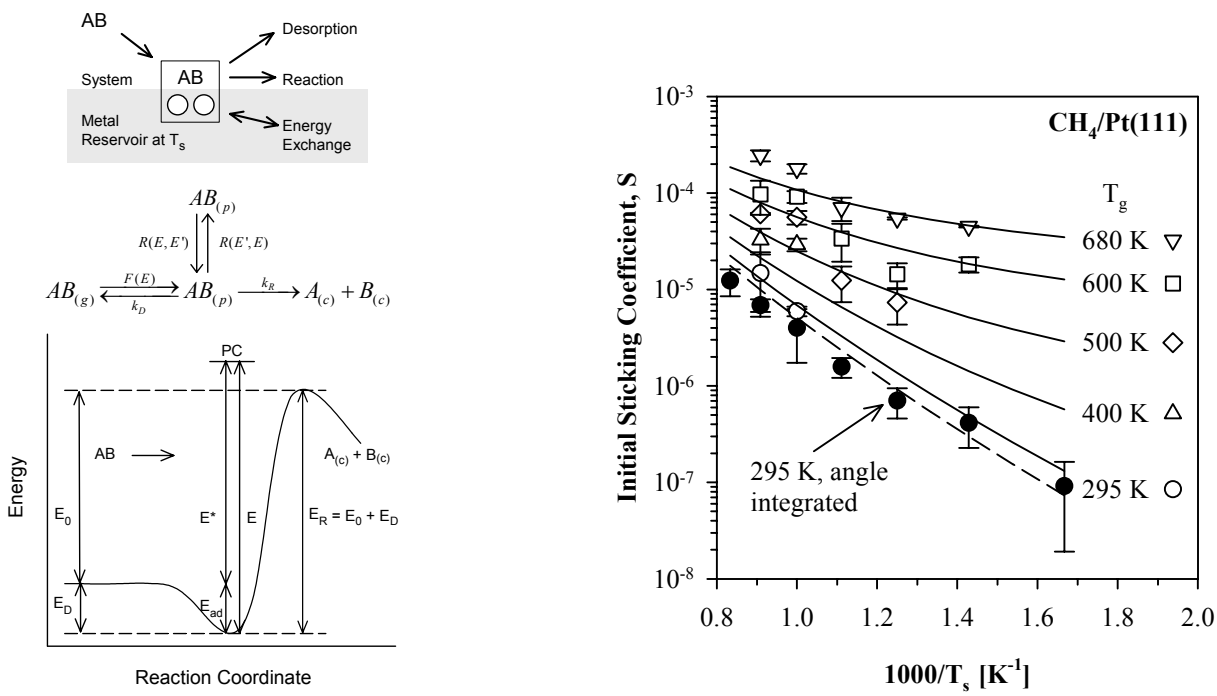

Fig. 2 (a) Schematic depiction of the MURT model for activated dissociative chemisorption. (b) PC-MURT predictions (lines) for dissociative sticking of CH_4 on Pt(111) for several gas temperatures of an effusive CH_4 beam are compared to experiment[11] (points). The PC-MURT parameters are {E_0 = 49 kJ/mol, ν_D = 335 cm^{-1}, s = 2}.

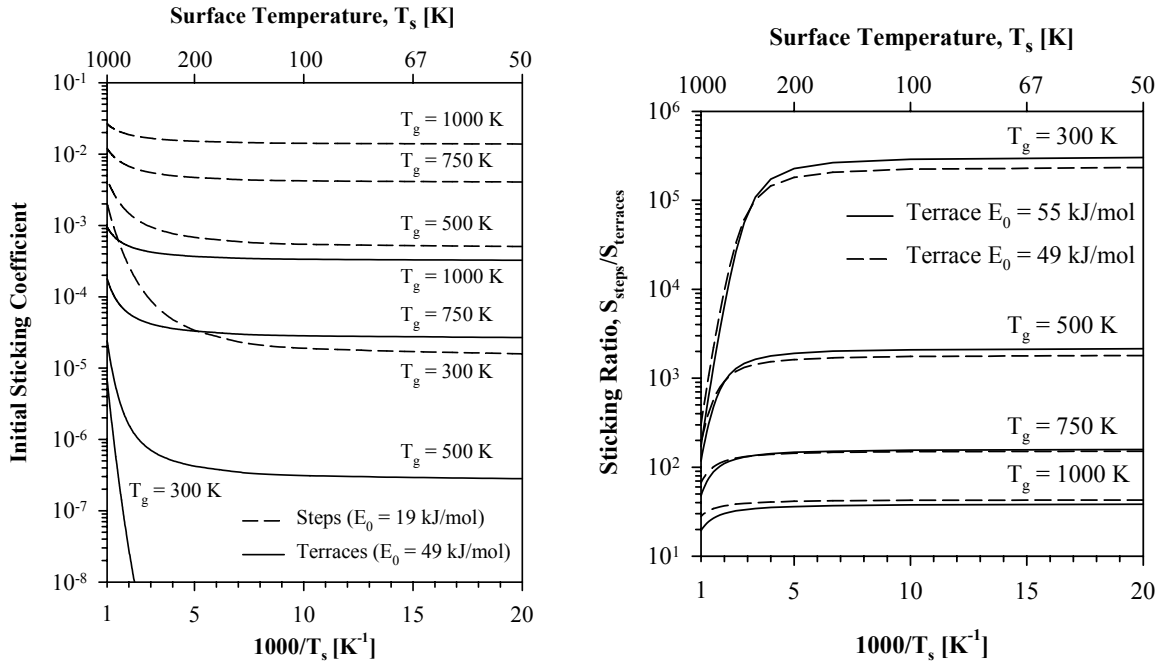

Fig. 3 (a) PC-MURT predictions of $S(T_g, T_s)$ for dissociative chemisorption of CH_4 on Pt(111) terraces and steps for several gas temperatures of a normally incident effusive CH_4 beam. The simulations assume that only the reaction threshold energy, E_0, differs at the steps. Surface temperatures above ~80 K should keep the surface free of physisorbed CH_4 during effusive beam dosing (i.e., τ_d (T_s = 80 K) < 10^{-3} s) and STM imaging of CH_3 dissociation fragments near steps or terraces could fix local $S(T_g, T_s)$ values. (b) Ratio of $S(T_g, T_s)$ values for steps versus terraces based on two reasonable PC-MURT parameter sets (i.e., terrace E_0 = 52± kJ/mol; steps 30 kJ/mol less).

DOE Publications in 2003-2005: none

References:

[1] A. Bukoski, D. Blumling, and I. Harrison, "Microcanonical unimolecular rate theory at surfaces. I. Dissociative chemisorption of methane on Pt(111)," J. Chem. Phys. **118**, 843 (2003).

[2] H. L. Abbott, A. Bukoski, and I. Harrison, "Microcanonical unimolecular rate theory at surfaces. II. Vibrational state resolved dissociative chemisorption of methane on Ni(100)," J. Chem. Phys. **121**, 3792 (2004).

[3] A. Bukoski, H. L. Abbott, and I. Harrison, "Microcanonical unimolecular rate theory at surfaces. III. Thermal dissociative chemisorption of methane on Pt(111) and detailed balance," J. Chem. Phys. **123**, 094707 (2005).

[4] F. Abild-Pedersen, O. Lytken, J. Engbaek, G. Nielsen, I. Chorkendorff, and J. K. Norskov, "Methane activation on Ni(111): Effects of poisons and step defects," Surf. Sci. **590**, 127 (2005).

[5] T. Schwendemann and I. Harrison, "manuscript in preparation," (2005).

[6] H. L. Abbott and I. Harrison, "Dissociative chemisorption and energy transfer for methane on Ir(111)," J. Phys. Chem. B **109**, 10371 (2005).

[7] D. F. Kavulak, H. L. Abbott, and I. Harrison, "Nonequilibrium activated dissociative chemisorption: SiH_4 on Si(100)," J. Phys. Chem. B **109**, 685 (2005).

[8] H. L. Abbott, A. Bukoski, D. F. Kavulak, and I. Harrison, "Dissociative chemisorption of methane on Ni(100): Threshold energy from CH_4 ($2\nu_3$) eigenstate-resolved sticking measurements," J. Chem. Phys. **119**, 6407 (2003).

[9] Z. P. Liu and P. Hu, "General rules for predicting where a catalytic reaction should occur on metal surfaces: A density functional theory study of C-H and C-O bond breaking/making on flat, stepped, and kinked metal surfaces," J. Am. Chem. Soc. **125**, 1958 (2003).

[10] A. T. Gee, B. E. Hayden, C. Mormiche, A. W. Kleyn, and B. Riedmuller, "The dynamics of the dissociative adsorption of methane on Pt(533)," J. Chem. Phys. **118**, 3334 (2003).

[11] K. M. DeWitt, L. Valadez, H. L. Abbott, K. W. Kolasinski, and I. Harrison, "Using effusive molecular beams and microcanonical unimolecular rate theory to characterize CH_4 dissociation on Pt(111)," submitted (2005).

An Exploration of Catalytic Chemistry on Au/Ni(111)

Professor S. T. Ceyer
Department of Chemistry
Massachusetts Institute of Technology
Cambridge, MA 02139
stceyer@mit.edu

Project Scope

This project explores the breadth of catalytic chemistry that can be effected on a Au/Ni(111) surface alloy. A Au/Ni(111) surface alloy is a Ni(111) surface on which 10-30% of the Ni atoms are replaced at random positions by Au atoms. That is, the vapor deposition of a small amount of Au onto Ni single crystals does not result in an epitaxial Au overlayer or the condensation of the Au into droplets. Instead, it results in a strongly bound surface alloy. Gold atoms at coverages less than 0.3 ML replace Ni atoms on a Ni(111) surface, even though Au is immiscible in bulk Ni. The two dimensional structure of the clean Ni surface is preserved. This alloy is found to stabilize an adsorbed peroxo-like O_2 species that is shown to be the critical reactant in the low temperature catalytic oxidation of CO and that is suspected to be the critical reactant in other oxidation reactions. These investigations may reveal a new, practically important catalyst for catalytic converters and for the production of some widely used chemicals.

Recent Progress

We have embarked on an ultrahigh vacuum, laboratory study of the interactions and chemistry between CO and O_2 on this Au/Ni(111) alloy. We discovered that the Au/Ni(111) surface alloy, with Au coverages up to 0.3 ML, efficiently catalyzes the oxidation of CO at 70 K.

The experiment is carried out by adsorbing the saturation coverage of molecular O_2 on the 0.24 ML Au/Ni surface alloy. The vibrational spectrum of the oxygen layer is measured by high resolution electron energy loss spectroscopy. The dominant feature, at 865 cm^{-1}, is assigned to the vibration of the O=O bond of molecular oxygen adsorbed on the alloy with its bond axis largely parallel to the surface. Molecular oxygen so adsorbed is characterized as a peroxo (O_2^{-2}) or superoxo (O_2^{-1}) species. Similar vibrational frequencies have been observed for molecular oxygen adsorbed on other metals. Shoulders at about 950 cm^{-1} and 790 cm^{-1} on the main 865 cm^{-1} feature indicate the presence of both peroxo or superoxo species at multiple sites.

The feature at 865 cm^{-1} and its shoulders attributed to molecularly adsorbed O_2

disappear after heating this layer to 280 K while two features at 580 and 435 cm^{-1} grow in. In fact, the feature at 865 cm^{-1} has already disappeared at 150 K. Given the absence of O_2 desorption, this behavior is interpreted as dissociation of molecularly adsorbed O_2 into atomically adsorbed O atoms. Two modes for atomically adsorbed O atoms are observed. A feature at 580 cm^{-1} is the same frequency as observed for O atoms bound to Ni(111) while a lower frequency feature, at 435 cm^{-1}, is attributed to O atoms bound to Ni atoms that are adjacent to the Au atoms. Note that there is no evidence for a vibrational mode around 580 cm^{-1} in the spectrum measured at 77 K, which demonstrates the absence of atomically bound oxygen. Therefore, the adsorption of O_2 on the Au/Ni(111) surface alloy at 77 K appears to be solely molecular. In contrast, O_2 dissociatively adsorbs on Ni(111) at a temperature as low as 8 K, while it adsorbs neither molecularly nor dissociatively on Au(111) at or above 100 K.

A beam of thermal energy CO is then directed at the O_2 covered Au/Ni(111) surface alloy held at 70 K. Upon introduction of the beam, CO_2 is produced in the gas phase, as measured by a quadrupole mass spectrometer. A control experiment is carried out whereby the CO beam impinges on the back of the crystal mount. In this configuration, no CO_2 is produced. This result provides clear evidence that CO reacts with molecularly adsorbed O_2 on this alloy at 70 K.

After exposure of the O_2-covered surface alloy at 70 K to CO, a vibrational spectrum is measured. Two C=O stretch vibrational modes are observed at 2170 and 2110 cm^{-1}, along with the Au/Ni-CO stretch mode at 435 cm^{-1}. The O=O mode at 865 cm^{-1} is much reduced in intensity, while the shoulder at 790 cm^{-1} has maintained its intensity. The decrease in intensity of the 865 cm^{-1} feature is interpreted to mean that some of the molecularly adsorbed O_2 has reacted with CO to form gas phase CO_2. The product remaining from this reaction is an O atom adsorbed to Au, as evidenced by the appearance of a new feature at 660 cm^{-1}. The molecularly adsorbed O_2 that gives rise to the feature at 790 cm^{-1} does not react with CO.

This alloy surface covered with CO and some molecularly adsorbed O_2 is heated at 2 K/s while the partial pressures at masses 44 and 28 are monitored. Rapid production and desorption of CO_2 is clearly observed between 105-120 K, along with desorption of CO. The production of CO_2 in this temperature range occurs at the same temperature at which O_2 dissociates. This observation suggests that the formation of CO_2 occurs between a CO and a "hot" O atom. A "hot" atom is defined as an atom, produced by bond dissociation, that has not yet equilibrated with the surface. From 120 K to about 250 K, there is slow production of CO_2, by reaction of the adsorbed O atoms represented by the vibrational mode at 660 cm^{-1} and by the adsorbed O atoms that did not react

immediately as a hot O atom upon O_2 dissociation between 105-120 K. No O_2 is observed to desorb.

After raising the temperature to 300 K, a vibrational spectrum is measured. The spectrum indicates the presence largely of CO. Some adsorbed O atoms may also be present, as evidenced by the presence of intensity between 500-580 cm^{-1}. Heating the surface to 900 K results in no additional desorption of CO_2 or any other products.

These results demonstrate that a Au/Ni(111) surface catalyzes the oxidation of CO at low temperature. Clearly, the substitution of a small number of Ni atoms on the Ni(111) surface by Au atoms has dramatically changed the chemistry of Ni. The oxidation of CO on Ni has never been observed under UHV laboratory conditions, presumably because both the oxygen atom and the CO are too strongly bound, and hence the barrier to their reaction is too large. The introduction of gold into the Ni lattice serves to weaken the bonds between oxygen and CO so as to allow the reaction to proceed. These results also imply that nanosize Au clusters are not a necessary requirement for low temperature CO oxidation in general. Rather, the interaction of the Au atoms around the perimeter of the Au nanocluster with the transition metal of the oxide support likely provides the active sites that stabilize the adsorption of molecular O_2 that is necessary for the oxidation of CO.

Future Plans

A major thrust of this project is to explore the range of reactivity of the O_2 species molecularly adsorbed on the Au/Ni(111) surface alloy. The hypothesis is that our newly observed molecular O_2 adsorbate is the crucial reactant in two oxidation reactions to be studied: the direct synthesis of H_2O_2 from H_2 and O_2 and the epoxidation of propylene to form propylene oxide. In addition, it is planned to investigate whether the Au/Ni surface alloy is also active for the reduction of NO by CO. It is possible that a molecularly adsorbed NO species with a bond order approaching one is the active species in the NO reduction reaction at low temperature on the Au/Ni(111) surface alloy.

Growth, Characterization, and Reactivity of Model Transition Metal Oxide Catalysts

Eric I. Altman
Department of Chemical Engineering
Yale University
New Haven, CT 06520

Oxides of the early transition metals are used as catalysts for the reduction of NO emitted from power plants and for a wide range of partial oxidation reactions. Detailed surface science studies of these materials and reactions have been restricted by the limited availability of the macroscopic single crystal samples required for these types of studies. To overcome this obstacle, we have been using epitaxial growth techniques to create high quality films that can then be characterized using surface science techniques such as scanning tunneling microscopy (STM), electron diffraction (RHEED and LEED), photoelectron spectroscopy (UPS and XPS), and temperature programmed desorption (TPD). Through the use of molecular beam epitaxy (MBE) we can also manipulate the locations of the transition metal cations in multi-component systems, allowing support and ligand effects to be characterized. The work has been focusing on W, V, and Ti oxides, all of which are extensively used in industry. Our work on WO_3 (100) thin films has revealed that transition metal oxides can respond to reduction in several different ways depending on the degree of reduction and the reduction temperature, creating a myriad of possible reaction sites on the surface. Initial reduction simply removes terminal oxygen atoms from the surface. At higher temperatures, continued reduction causes W^{5+} migration into the bulk creating pits that eventually organize into regular arrays of rows and troughs. Meanwhile, at lower temperatures, STM images show terminal oxygen structures persisting on the surface and the emergence of half-height steps that can be explained by a shearing of the surface plane. For the row and trough structures, STM showed that 1-propanol adsorbs solely on the tops of the rows. TPD showed that molecules adsorbed at these sites undergo dehydration to form propene, the same as on a fully oxidized surface, but that the propene forms at much lower temperatures on the reduced surface, suggesting that adsorption site structure does not affect the favored reaction pathway but does strongly affect kinetics. To investigate how oxide–oxide interactions influence reactivity, we have been studying the interaction of vanadia layers with WO_3 and TiO_2; vanadia was chosen for these studies because catalytic studies have shown that highly dispersed vanadia on reducible oxide supports is highly active and selective for a number of reactions where bulk V_2O_5 shows little reactivity. Epitaxial V_2O_5 monolayers could be grown on the (001) and (101) surfaces of the anatase TiO_2 polymorph, and WO_3 (100). Attempts to maintain the V_2O_5 stoichiometry beyond a monolayer, however, produced poorly ordered three dimensional clusters. On the other hand, it was found that epitaxial VO_2 could be grown ad infinitum on anatase (001). At high growth temperatures a c(2x2) structure was observed on the surface of these epitaxial VO_2 films that was attributed to oxygen adsorbed on top of every other surface V atom, oxidizing the surface V to 5+. For a monolayer, this oxidizes all of the V to 5+ demonstrating how the monolayer can be unique in maintaining both epitaxy and the V_2O_5 stoichiometry throughout. The bulk-terminated anatase (001) and WO_3 (100) surfaces are isostructural with the perovskite (001) surface formed by numerous materials such as $SrTiO_3$, $SrFeO_3$, and $CaVO_3$. Since vanadia has shown a tendency to form epitaxial monolayers on these materials, we are beginning to study how the electronic properties of the underlying transition metal cations affect the reactivity of the vanadia with the structure held constant.

Surface Chemical Dynamics

M. G. White, R. J. Beuhler, N. Camillone III, and A. L. Harris

Chemistry Department, Brookhaven National Laboratory, Upton, NY 11973

(mgwhite@bnl.gov, beuhler@bnl.gov, nicholas@bnl.gov, alexh@bnl.gov)

1. Project Scope

Thermal and photo-induced reactions on extended and nanostructured surfaces are being investigated with the aim of understanding the dynamics, energetics, and morphology-dependence of elementary surface reactions that play key roles in energy-related catalysis. Experimentally, laser pump-probe methods are being used to investigate the dynamics of interfacial charge and energy transfer that leads to adsorbate reaction and/or desorption on metal and metal oxide surfaces. Ultrafast laser capabilities are also being developed to initiate and probe electronic and nuclear motion with femtosecond resolution. Of particular interest are time-resolved studies on supported metal nanoparticles that will investigate the size dependence of desorption, reaction, electronic relaxation and adsorbate vibrational relaxation. Size-dependent correlations are also the focus of gas-phase studies of small transition metal and metal compound clusters (carbides, oxides, sulfides) which are being investigated in an effort to characterize their structure, composition and reactivity as a prelude to size-selected deposition onto solid supports.

2. Recent Progress

Femtosecond-Pulse Photoinduced Desorption: Major construction of the new UHV chamber, ultrafast laser system, and optical train designed for the time-resolved study of chemical reaction dynamics is complete. Preliminary experiments involving the desorption of molecular oxygen from Pd(111) under irradiation at 780 nm with a pulse width of ~ 120 fs have been performed. Single pulse photoinduced desorption measurements are consistent with what is known about this well-characterized adsorbate/substrate system [1,2]. At an estimated absorbed fluence of 2.3 mJ/cm^2, desorption is extremely efficient. As shown in the figure, a considerable fraction of a monolayer is desorbed by a single laser pulse. We estimate that approximately 0.25 ML is desorbed by the first pulse, corresponding to a single photon cross section of the order of 10^{-17}cm^2. This measurement represents reaching a major developmental milestone in building toward the time-resolved and nanocluster-size dependent dynamics experiments described below.

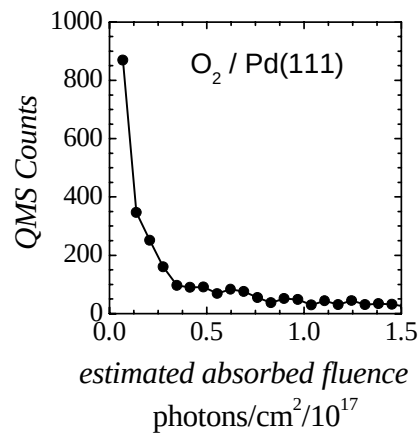

Photoinduced desorption of O_2 from Pd(111).

Photo-induced desorption and reaction of O_2 on TiO_2 surfaces: We have started a new effort to investigate photoinduced reactions on TiO_2 surfaces with the goal of understanding the excitation and energy transfer processes that lead to surface reaction. Closely connected with any photoinduced surface chemistry on TiO_2 is the interaction of O_2 with surface defects or vacancy sites at which an O^{2-} anion is missing. Adsorbed molecular oxygen is linked to the photooxidation activity of TiO_2 surfaces, however, fundamental questions remain as to the nature of the O_2 adsorption sites and the energy transfer processes that lead to desorption and reaction. Work this year focused on developing a flexible sample mount and the ability to prepare a well-characterized *p*(1x1)-TiO_2(110) surface with a reproducible concentration of surface oxygen vacancies (typically ~10%) by thermal desorption (TPD) of H_2O and CO_2 which exhibit distinct desorption features for binding at terrace and vacancy sites [3,4]. For low temperature (~105 K)

adsorption on a reduced surface, the O_2 TPD curve exhibits a sharp peak centered at ~400 K that is attributed to chemisorbed O_2 at four coordinate Ti^{4+} sites adjacent to oxygen anion vacancies [3]. The latter sites are thought to be the most photoactive towards desorption and oxidation reactions. Laser pump–probe experiments are planned that will attempt to measure the final state distributions of desorbed O_2 [5] that are sensitive to both the O_2-surface potential and mechanism for desorption.

Structure and reactivity of transition metal compound clusters: We have recently constructed a new ion-beam apparatus for the preparation of metal containing clusters, which can be mass-selected for size-dependent reactivity studies in the gas-phase and, ultimately, deposited on surfaces. Experiments are focused on the gas-phase structure and reactions of several of the early transition metal compounds (carbides, sulfides), which are known in their bulk form to be active catalysts for a wide range of heterogeneous reactions [6]. The clusters are generated by reactive sputtering in a high pressure magnetron source, mass-selected using a quadrupole filter and then guided through a hexapole scattering cell where gas-phase association and reaction with small molecules is investigated. Coupled with density functional theory (DFT), these experiments provide information on the structure and metal-center reactivity for clusters that are representative of nanostructured forms of carbide and sulfide catalytic materials. This effort complements surface science studies in our laboratory in which larger metal carbide nanoparticles can be generated by reactive metal deposition on a Au(111) substrate [P4,P6].

Initial studies focused on the gas-phase structure and reactivity of several early transition metal sulfide clusters, $M_xS_y^+$ (M = Mo, W, Nb, Ta). These materials are layered compounds (MS_2) in the bulk, and like graphite, can form fullerene and tube-like structures. The gas-phase cluster distributions for $Mo_xS_y^+$ and $W_xS_y^+$ are quite similar with a number of prominent mass peaks (x/y = 2/6, 3/7, 4/6, 5/7, 6,/8, 7/10, 8/12). The $M_4S_6^+$ cluster is the most prominent peak under a wide range of source conditions, suggesting very high stability [P5]. Gas-phase collisions with CO and NH_3 lead only to the formation of cluster adducts with up a maximum of four adsorbed molecules, e.g., $(CO)_n$ (n = 1-4). DFT calculations indicate that the most stable $M_4S_6^+$ structure is a compact cluster with the four metal atoms arranged in an internal tetrahedron surrounded by bridging S-atoms (near T_d symmetry) [P5]. Calculations of the relative adduct stability (CO and NH_3) are found to be in good agreement with the observed mass spectra and provide additional support for the proposed structure. Similar experiments have been performed for the other prominent metal sulfide clusters and DFT calculations are currently underway to obtain their lowest energy structures. In general, we find that adding the constraint of reproducing the experimentally observed relative adduct stability with CO or NH_3 is crucial for evaluating the likelihood of energetically similar structures.

3. Future Plans

Photo-induced desorption and reaction of O_2 on TiO_2 surfaces: With the ability to prepare well-characterized TiO_2(110) surfaces, laser pump-probe experiments will be initiated that probe the photoinduced dynamics of desorption and surface reaction of adsorbed O_2. The accepted mechanism for O_2 photodesorption involves electron-hole pair formation in the TiO_2 substrate and capture of the hole by adsorbed oxygen. Recent theoretical calculations suggest, however, that a direct, vertical transition between the ground state to a repulsive excited state of the O_2/TiO_2 surface bound complex may be a better description [7]. The desorption mechanism will be probed by experiments that measure the polarization dependence of the yield and final state properties of desorbed O_2 following UV laser photoexcitation above the band gap of TiO_2 (~3.1 eV). Detection of the desorbed O_2 will be accomplished by (2+1) REMPI [5] or one-photon photoionization using coherent VUV radiation. Measurements of the kinetic energy distributions, photoexcitation wavelength dependence and polarization dependence of the O_2 photodesorption yield should provide important clues as to the nature of the photodesorption mechanism and perhaps distinguish desorption channels associated with chemically distinct surface bound O_2 species, i.e., α-O_2 or β-O_2, observed in previous studies [8]. In addition, the insight into surface preparation, thermal and photochemistry garnered from these studies will provide an important foundation for the ultra-fast studies on nanoparticles supported on TiO_2 discussed below.

Time-Resolved Photoinduced Chemical Dynamics at Nanoparticle Surfaces: Our goal in these experiments is to bring together the ultra-fast and the ultra-small to understand the chemical dynamics behind the chemistry of nanostructured materials. Towards this end we aim to apply time-resolved techniques developed to probe dynamics on 2-D planar surfaces [9-12] to the study of the chemistry of molecules adsorbed on supported nanoparticles. There are several aspects of nanoscale systems that we expect to lead to significant changes in their photochemical reactivity and dynamics. For example, spatial confinement of ballistic electrons, size-dependent electronic structure [13] and the sensitivity of electron-phonon coupling to surface thermal vibrations [14] could significantly extend hot electron lifetimes in nanoparticles. Also, changes in geometric and electronic structure may lead to changes in molecule–surface coupling. Our plan is to explore the size-dependence of the photoinduced chemical dynamics as the nanoparticle size is varied through the regime spanning the non-metal to metal transition.

Initial studies will involve a two-pulse correlation method wherein the excitation pulse (800 nm, ~ 100 fs, ~ 1 mJ/cm^2) is split into two pulses and directed to impinge upon the surface separated in time by a variable delay. The photoinduced desorption yield is measured by a mass spectrometer. Because the relaxation times of the electronic temperature and the lattice temperature differ by an order of magnitude, the time delay dependence of the yield depends upon the desorption mechanism. For example, when electronic coupling dominates, the desorption yield correlation width approximates the relaxation time of the electronic temperature, showing a sub-picosecond to picosecond response. For a phonon-mediated process, desorption remains efficient for much longer delay times and shows a much longer (~ 20 ps) correlation width [11].

Given the correlation between reactivity and electronic structure proposed to explain the size-dependent reactivity of metal nanoparticles supported on TiO_2 [13], our initial experiments will focus on probing the photoinduced desorption dynamics of O_2 and CO from Pd_n/TiO_2 or Au_n/TiO_2. CO and O_2 adsorption and activation are necessary for catalytic oxidation to occur in these systems. By pumping the electrons of the CO– or O_2–(or O–)nanoparticle complex and monitoring the desorption event in real time, we will probe the coupling between the adsorbates and the nanoparticle electrons and phonons in these catalytically relevant systems.

Structure and reactivity of transition metal compound clusters: The main goal of this effort is to study the correlation of reactivity of metal and metal compound clusters with particle size (structure), chemical composition and chemical environment. The latter provide a means of modifying the catalytic properties of a bulk metal in terms of its overall activity and more importantly, its selectivity. For example, the early transition metals (e.g., Ti, Mo, W,) are very active but unselective catalysts and alloying with carbon results in carbided surfaces that behave like the Group 10 noble metals (Pt, Pd) for hydrogen transfer reactions [6]. Recent studies in our laboratory have shown that depositing MoC_x as nanoparticles on a Au(111) substrate results in further modification of the reactivity [P4,P6]. In the future, the new ion-beam cluster apparatus will be used to deposit size-selected clusters of transition metal compounds onto a solid substrate. This approach provides far more control of size and chemical composition of the individual particles, as well as the type of substrate. The latter is often dictated by the ability of the surface to facilitate particle nucleation. Having the ability to characterize the structure and reactivity of nanoclusters in the gas-phase and by theory will be key to understanding their behavior when deposited on surfaces. Initial studies will focus on the deposition of the Ti_8C_{12} Metcar and the M_4S_6 (M=Mo, W) cluster as model carbides and sulfides. Possible substrates include metals [Au(111)], graphite, or metal oxides [MgO(100) and TiO_2(110)] which will allow investigations of particle-surface interactions. Deposited particles will be characterized under UHV conditions using XPS, Auger spectroscopy and inelastic ion scattering. Temperature programmed reaction (TPR) of molecules such as CO, H_2O and SO_2 will be used to investigate reactivity and probe the active metal sites. Parallel theoretical studies will be performed through collaborations with Jim Muckerman, Jose Rodriguez and Ping Liu (Chemistry Department, BNL) who have extensive experience with modeling the interactions of molecules with metal containing clusters and extended surfaces. In addition, the apparatus has been

designed to fit on the X-24 beam line at the NSLS, which can be used to perform Mo L-edge x-ray absorption, fluorescence or total electron yield measurements (XAS, EXAFS). The latter can be used to probe the local electronic (oxidation state, coordination number) and atomic structure of Mo atoms within the supported carbide or sulfide nanoclusters.

Cited References

1. J. A. Misewich, A. Kalamarides, T. F. Heinz, et al., *J. Chem. Phys*. **100**, 736 (1993).
2. D.P. Quinn, T.F. Heinz, *J. Vac. Sci. Technol. A*, **21**, 1312 (2003).
3. M. A. Henderson, W. S. Eppling, C. L. Perkins and C.H. F. Peden, *J. Phys. Chem. B* **103**, 5328 (1999).
4. T. L. Thompson, O. Diwald and J. T. Yates, *J. Phys. Chem. B* **107**, 11700 (2003).
5. R. J. Beuhler and M. G. White, *J. Chem. Phys*. **120**, 2445 (2004).
6. H. H. Hwu, and J. G. Chen, *Chem. Rev*. **105**, 185 (2005); S. T. Oyama, *Catal. Today* **15**, 179 (1992).
7. M. P. de Laura-Castells and J. L. Krause, *J. Chem. Phys*. **118**, 5098 (2003).
8. C. N. Russu and J. T. Yates, *Langmuir* **13**, 4311 (1997); C. L. Perkins and M. A. Henderson, *J. Phys. Chem*. **105**, 3856 (2001).
9. F. Budde, T. F. Heinz, M. M. T. Loy, et al., *Phys. Rev. Lett*. **66**, 3024 (1991).
10. D. G. Busch, S. Gao, R. A. Pelak, et al., *Phys. Rev. Lett*. **75**, 673 (1995).
11. M. Bonn, S. Funk, C. Hess, et al., *Science* **285**, 1042 (1999).
12. C. Hess, S. Funk, M. Bonn, et al., *Appl. Phys*. A **71**, 477 (2000).
13. M. Valden, X. Lai, D. W. Goodman, *Science* **281**, 1647 (1998).
14. T. Valla, M. Kralj, A. Siber, et al., *J. Phys.: Condens. Matter*, **12**, L477 (2000).

DOE Supported Publications 2003-2005

P1. Gas-Phase Production of Molybdenum Carbide, Nitride and Sulfide Clusters and Nanocrystallites, J. M. Lightstone, H. Mann, M. Wu, P. M. Johnson, and M. G. White, *J Phys. Chem*. **B107,** 10359 (2003).

P2. State-Resolved Dynamics of Oxygen Atom Recombination on Polycrystalline Ag, R. J. Beuhler and M. G. White, *J. Chem. Phys.* **120**, 2445 (2004).

P3. Reactivity Studies with Gold-Supported Molybdenum Nanoparticles, D. V. Potapenko, J. M. Horn, R. J. Beuhler, Z. Song and M. G. White, *Surf. Sci*. **574**, 244-258 (2005).

P4. The Characterization of Molybdenum Carbide Nanoparticles Formed on Au(111) using Reactive-Layer Assisted Deposition, J. M. Horn, Z. Song, D. V. Potapenko, J. Hrbek and M. G. White, *J. Phys. Chem. B* (Communication) **109**, 44-47 (2005).

P5. Reactivity of the $M_4S_6^+$ (M= Mo, W) Cluster with CO and NH_3 in the Gas-Phase: An Experimental and DFT Study, J. M. Lightstone, M. J. Patterson and M. G. White, *Chem. Phys. Lett.* **413**, 429-433 (2005).

P6. The Reactions of Cyclohexene on Au(111)-Supported Molybdenum Carbide Nanoparticles, D. V. Potapenko, J. M. Horn and M. G. White, *J. Catal.*, accepted for publication.

Structure, Stability and Reaction Dynamics for CO oxidation Catalysis by Au supported on Functionalized Oxide Supports

Steven H. Overbury, Sheng Dai
WenfuYan, Bong-Kyu Chang
Chemical Sciences Division, Oak Ridge National Laboratory, Oak Ridge, TN 37831-6201
overburysh@ornl.gov

It has been widely reported that the activity of Au catalysts depends strongly upon the size of the Au nanoparticles. It is also increasingly appreciated that the activity and stability of Au catalysts is determined by preparation conditions and upon the type of support in ways which have not yet been clearly explained. For example, the support may be expected to alter or control the nucleation of nascent Au particles, the growth and diffusion of reduced Au particles, storage and transfer of reactants species, stability of reaction intermediates such as hydroxyl or carbonates, morphology of the Au particles and reactivity of interface states at the perimeter of Au particles. To learn more about support effects, we have experimented with many types of supports prepared by sol-gel techniques and impregnated with Au. The goal is to systematically tailor the Au-support interaction by rational modification of the support surface. In particular, we have applied a surface sol-gel process (SSP) as a key synthesis methodology for the layer-by-layer functionalization technique to tailor the surfaces of non-porous and mesoporous materials for catalysis applications with monolayer precision. This novel technology enables molecular-scale control of surface composition and surface layer thickness over a dispersed high surface area support. The general technique consists of two half reactions: (a) condensation of metal-alkoxide precursor molecules with surface hydroxyl groups and (b) hydrolysis of the adsorbed metal-alkoxide species to regenerate surface hydroxyls. The iteration of the above sequential condensation and hydrolysis reactions allows the layer-by-layer coating of a selected metal oxide on a hydroxyl-terminated surface. These surfaces provide new substrates for studies of the effect of support surfaces upon the activity of Au catalysts. Using this approach we have prepared libraries of modified supports by growing single or double layers of various oxides (alumina, titania, zirconia, germania) onto non-porous or mesoporous supports such as Cabosil silica, mesoporous SBA-15 silica, aluminum oxide, or various polymorphs of TiO_2 (mesoporous, anatase, P25). These materials have been used as supports for Au catalysts, in which the Au was incorporated using the method of deposition precipitation. Results of these preparations before and after various thermal and redox treatments have been analyzed by volumetric gas adsorption, NMR, x-ray diffraction, Z-contrast STEM and XANES/EXAFS to probe the structure and stability of the resulting Au catalysts and to assess the success of the synthesis for achieving the desired result. Variations in the catalytic activity before and after various thermal treatments have been probed using CO oxidation as a test reaction. Transient studies on this oxidation reaction are being performed to determine the kinetic processes and limitations of this reaction and how these vary depending upon the nature of the catalyst. Results of this approach, the key conclusions and their implications will be discussed.

Research sponsored by the Division of Chemical Sciences, Geosciences, and Biosciences, Office of Basic Energy Sciences, U.S. Department of Energy, under contract DE-AC05-00OR22725 with Oak Ridge National Laboratory, managed and operated by UT-Battelle, LLC.

THERMOCHEMISTRY AND REACTIVITY OF TRANSITION METAL CLUSTERS AND THEIR OXIDES

P. B. Armentrout
315 S. 1400 E. Rm 2020, Department of Chemistry, University of Utah,
Salt Lake City, UT 84112; armentrout@chem.utah.edu

Program Scope

The objectives of this project are to obtain quantitative information regarding the thermodynamic properties of transition metal clusters, their binding energies to various ligands, and their reactivities. Using a guided ion beam tandem mass spectrometer, we examine the reactions of size-specific transition metal cluster ions with simple molecules and measure the absolute cross sections as a function of kinetic energy for each reaction.

Since 2003, our DOE sponsored work has included studies of the kinetic energy dependences of the size-specific chemistry of Co_n^+ (n = 2 - 16) cluster ions reacting with D_2,[1] and of Ni_n^+ (n = 2 - 18) and Co_n^+ (n = 2 - 20) reacting with O_2.[2,3] Further, we have extended our studies to reactions with more complex molecules, specifically, the size-specific reactions of Fe_n^+ (n = 2 - 15) with ammonia (ND_3),[4] and Ni_n^+ (n = 2 - 16) with methane (CD_4).[5] An invited review of our recent work that emphasizes the relationship to bulk phase properties was also published.[6] The latter point is illustrated in Figure 1 for the example of cobalt clusters bound to hydrogen and oxygen where it is clear that bulk phase bond dissociation energies (BDEs) are approached for modest-sized clusters. Comparable behavior has been observed for V, Cr, Fe, and Ni clusters bound to D and O atoms.

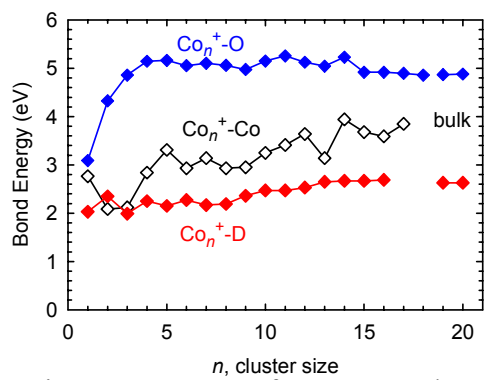

Figure 1. BDEs of D, Co, and O to Co_n^+ as a function of cluster size. Lines labeled bulk indicate the BDEs of H and O atoms to Co films.

Recent Progress

Reactions of Clusters with D_2. We have now studied V_n^+ (n = 2 - 13),[7] Cr_n^+ (n = 2 - 14),[8] Fe_n^+ (n = 2 - 15),[9] Co_n^+ (n = 2 - 16),[1] and Ni_n^+ (n = 2 - 16)[10] cluster ions reacting with D_2. For all four metal systems, the only products observed are M_nD^+ and $M_nD_2^+$. The failure to observe M_mD^+ and $M_mD_2^+$ products where $m < n$ indicates that the M_nD^+ and $M_nD_2^+$ products dissociate exclusively by D and D_2 loss, consistent with the thermochemistry derived in this work.

In the Co system, all clusters that form $Co_nD_2^+$, n = 4, 5, ≥9, do so in barrierless exothermic processes except for n = 9. Comparison of the thermal rates of reaction for cobalt clusters finds that they approach the collision limit for large clusters ($n \geq 11$) and parallel but are somewhat faster than the rates observed for neutral cobalt clusters.

Using methods developed over the past decade,[11] we analyze the kinetic energy dependence of the endothermic cross sections in order to determine threshold energies for these processes, which can then be directly related to $D_0(M_n^+\text{-D})$. The BDEs obtained are shown in

Figure 1. For smaller clusters, variations in the BDEs must be related to the geometric and electronic structures of the metal cluster ions. Values for larger clusters can be compared to values for H atom binding to bulk cobalt surfaces, between 2.60 and 2.65 eV.[12] Figure 1 shows that the largest Co_n^+-D BDEs ($n \geq 13$) equal the bulk phase value. Similar correspondences were observed in the Cr, V, Fe, and Ni systems even though the limiting values vary with the metal, which shows that the cluster bonds accurately track the variations in the bulk phase thermochemistry of different metals. Such correspondences with such small cluster sizes are somewhat surprising, but can be understood by the local nature of chemical bonding.

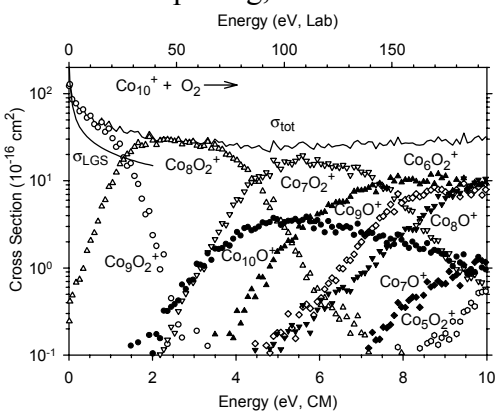

Figure 2. Reaction of Co_{10}^+ with O_2. Dioxide (open symbols) and monoxide (closed symbols) product product ions are shown.

Reactions of Clusters with O_2. Studies of the kinetic energy dependences of the V_n^+ (n = 2 - 17),[13] Cr_n^+ (n = 2 - 18),[14] Fe_n^+ (n = 2 - 18),[15] Co_n^+ (n = 2 - 20),[3] and Ni_n^+ (n = 2 - 18)[2] cluster ions reacting with O_2 have been completed. The reactions of metal cluster cations with O_2 are complicated as a large number of products are observed, e.g., the results of Figure 2 are representative of clusters larger than Co_5^+. The magnitudes of the total reaction cross sections at thermal energies are comparable to the collision cross section, indicating that the reactions are efficient and exothermic. Cluster dioxide ions are the dominant products at low energies. This work shows that metal-oxygen bonds are stronger than metal-metal bonds for all five metals, hence, primary products dissociate by sequential metal atom loss to form smaller cluster dioxide ions. Oxygen atom loss to form cluster monoxide ions, M_mO^+, is much less efficient. Analysis of the kinetic energy dependence is used to provide both $D_0(M_n^+\text{-O})$ and $D_0(M_n^+\text{-2O})$. As shown in Figure 1, the metal cluster oxygen BDEs measured in our work compare favorably to those for bulk phase surfaces.

Reactions of Clusters with CD_4. We have studied the kinetic energy dependences of reactions of Fe_n^+ (n = 2 - 16)[16] and Ni_n^+ (n = 2 - 16)[5] with CD_4. Figure 3 shows results for Ni_6^+, which are typical of most clusters. All observed reactions are endothermic. The lowest energy process for iron is dehydrogenation, whereas for nickel, double dehydrogenation is efficient enough that the $Ni_nCD_2^+$ species is not observed except for the smallest and largest clusters. These results are qualitatively consistent with reactivity observed for hydrocarbons on Fe and Ni surfaces, namely, carbide formation occurs in an activated process.

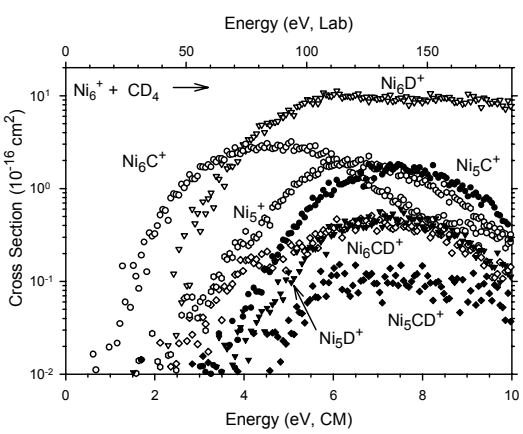

Figure 3. Reaction of Ni_6^+ with CD_4 with primary (open symbols) and secondary (closed symbols) products.

Thresholds for the various primary and secondary reactions are analyzed and BDEs for cluster bonds to C, CD, and CD_2 are determined. Importantly, the accuracy of these BDEs can be assessed because there are usually two independent routes to measure BDEs for each cluster to D, C, CD, and CD_2, e.g.,

$D_0(Ni_6^+\text{-D})$ can be measured in the primary reaction of Ni_6^+ or the secondary reaction of Ni_7^+. We find that the values obtained from the primary and secondary processes are in good agreement with one another for D (which also agrees with the results from reactions with D_2), C, and CD. For the CD_2 ligand, however, we find that the BDEs obtained from the primary reaction are generally low compared with those from the secondary reaction, which is evidence that there are barriers in excess of the endothermicity of the initial dehydrogenation reaction. For larger clusters, evidence suggests that the barrier lies in the initial dissociative chemisorption step.

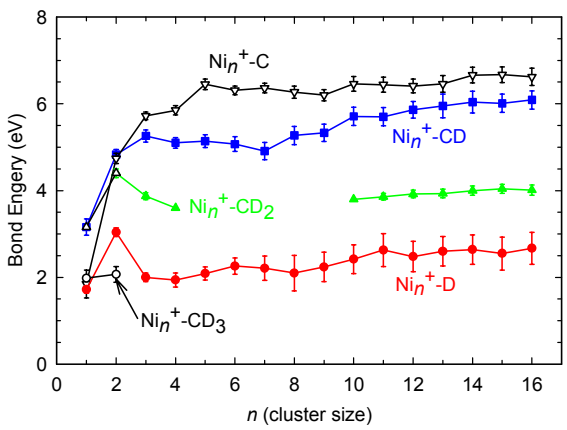

Figure 4. BDEs of D, C, CD, CD_2, and CD_3 to Ni_n^+ vs. cluster size.

Figure 4 shows the final BDEs determined in the nickel study.[5] We find that the values vary somewhat for small clusters but rapidly reach a relatively constant value with increasing cluster size. The magnitudes of these bonds are consistent with simple bond order considerations, namely, D (and CD_3) form one covalent bond, CD_2 forms two, and CD and C form three. Given the results of Figure 1, it seems reasonable that our experimental BDEs for larger clusters should provide reasonable estimates for heats of adsorption to surfaces. As little experimental information is available for *molecular* species binding to surfaces, the thermochemistry derived here for clusters bound to C, CD, and CD_2 provides some of the first experimental thermodynamic information on such molecular species.

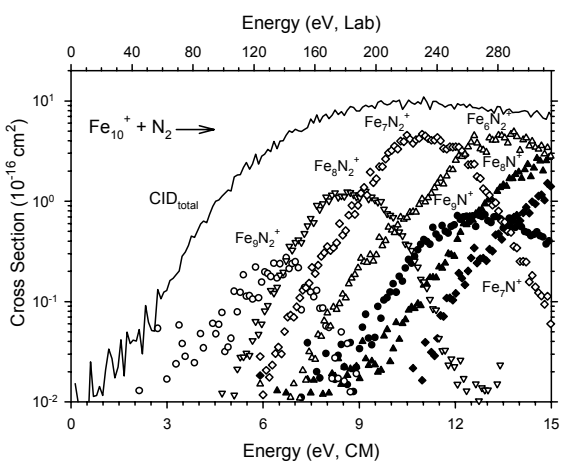

Figure 5. Reaction of Fe_{10}^+ with N_2 showing cross sections for dinitride (open symbols), mononitride (closed symbols), and the total CID products (solid line).

Reactions of Iron Clusters with N_2. This study is designed to provide insight into the rate-limiting step in the Haber process, which uses a promoted iron catalyst to manufacture ammonia from N_2 and H_2 at high pressures and temperatures. Despite the very strong N_2 bond energy of 9.76 eV, activation of this molecule on iron cluster cations, Fe_n^+ (n = 1 - 19), is observed, as illustrated in Figure 5. Both $Fe_mN_2^+$ and Fe_mN^+ product ions, where $m \leq n$, are observed and the former can be identified as a dinitride species. An energetic barrier for N_2 activation of about 0.48 eV is obtained for the largest clusters. Fe_n^+-N and Fe_n^+-2N bond energies as a function of cluster size are derived from threshold analysis of the kinetic-energy dependences of the endothermic reactions. These experimental values are somewhat smaller than bulk phase values, although this is potentially because the activation barriers for N_2 activation have been underestimated in the surface work, as previously suggested by Benziger.[17]

Future Plans

Experimental work has been completed on the reactions of Co_n^+ with N_2 and CD_4. These systems are designed to allow us to examine the periodic trends in the thermochemistry and reaction mechanisms for activation of dinitrogen and methane. We have also initiated studies of oxygenated iron clusters, $Fe_nO_m^+$, which might mimic the chemistry of metal oxide surfaces. A broad range of stoichiometries have been produced although larger clusters tend to form clusters containing nearly equal numbers of iron and oxygen atoms. Initially, our studies are focusing on characterizing the thermodynamic stabilities of these clusters by examining their dissociation behavior in collisions with Xe. Some 30 different iron oxide cluster cations (with n = 1 - 10) have been examined and the kinetic energy dependent cross sections are being analyzed to obtain both oxygen and iron bond energies for these clusters. We intend to then examine the possibility that specific oxidation states of the iron clusters might induce efficient oxidation of species like methane.

Publications resulting from DOE sponsored research in 2003 – present (1 – 6) and References

1. F. Liu and P. B. Armentrout, J. Chem. Phys. **122**, 194320-1-12 (2005).
2. D. Vardhan, R. Liyanage, and P. B. Armentrout, J. Chem. Phys. **119**, 4166 (2003).
3. F. Liu, .F.-X. Li, P. B. Armentrout, J. Chem. Phys. **123**, 064304-1-15 (2005).
4. R. Liyanage, J. B. Griffin, and P. B. Armentrout, J. Chem. Phys. **119**, 8979 (2003).
5. F. Liu, X.-G. Zhang, R. Liyanage, and P. B. Armentrout, J. Chem. Phys. **121**, 10976 (2004).
6. P. B. Armentrout, Eur. J. Mass Spectrom. **9**, 531 (2003).
7. R. Liyanage, J. Conceição, and P. B. Armentrout, P. B. J. Chem. Phys. **116**, 936 (2002).
8. J. Conceição, R. Liyanage, and P. B. Armentrout, Chem. Phys. **262**, 115 (2000).
9. J. Conceição, S. K. Loh, L. Lian, and P. B. Armentrout, J. Chem. Phys. **104**, 3976 (1996).
10. F. Liu, R. Liyanage, and P. B. Armentrout, J. Chem. Phys. **117**, 132 (2002).
11. P. B. Armentrout, *Advances in Gas Phase Ion Chemistry*, Vol. 1; N. G. Adams and L. M. Babcock, Eds.; JAI: Greenwich, 1992; pp. 83-119.
12. K. Christmann, Surf. Sci. Report, **9**, 1 (1988). M. E. Bridge, C. M. Comrie, and R. M. Lambert, J. Catal. **58**, 28 (1979). K. H. Ernst, E. Schwarz, and K. Christmann, J. Chem. Phys. **101,** 5388 (1994).
13. J. Xu, M. T. Rodgers, J. B. Griffin, and P. B. Armentrout, J. Chem. Phys. **108**, 9339 (1998).
14. J. B. Griffin and P. B. Armentrout, J. Chem. Phys. **108**, 8062 (1998).
15. J. B. Griffin and P. B. Armentrout, J. Chem. Phys. **106**, 4448 (1997).
16. R. Liyanage, X.-G. Zhang, and P. B. Armentrout, J. Chem. Phys. **115**, 9747 (2001).
17. J. B. Benziger, in *Metal-Surface Reaction Energetics*, edited by E. Shustorovich (VCH, New York, 1991), pp. 53–107.

Photochemistry at Interfaces

Kenneth B. Eisenthal
Department of Chemistry
Columbia University
New York, NY 10027
eisenth@chem.columbia.edu

The scope of the program is the development of a molecular level description of the equilibrium and time dependent chemical and physical properties of interfaces using as the primary methods the interface selective second harmonic and sum frequency spectoscopies.

Recent Progress

Electron Transfer at an organic liquid/aqueous interface

We have carried out the first time resolved electron transfer experiments at a liquid/liquid interface. A femtosecond laser pump pulse excited coumarin 314 (C314) molecules at the liquid dimethylaniline (DMA)/aqueous interface. The interfacial excited state C314* accepts an electron from an interfacial ground state DMA molecule.

$$C314 + h\nu \longrightarrow C314^*$$
$$C314^* + DMA \xrightarrow{ET} C314^{\bullet -} + DMA^{\bullet +}$$
$$C314^{\bullet -} + DMA^{\bullet +} \xrightarrow{BET} C314 + DMA$$

The use of liquid DMA as one of the bulk liquids eliminates the contribution of translational diffusion of a donor-acceptor pair to the small separation required for the short range electron transfer process. The electron transfer dynamics was followed by the increase in the second harmonic signal generated by time delayed probe pulses as C314* decays. The electron transfer time was found to be 14±2ps.

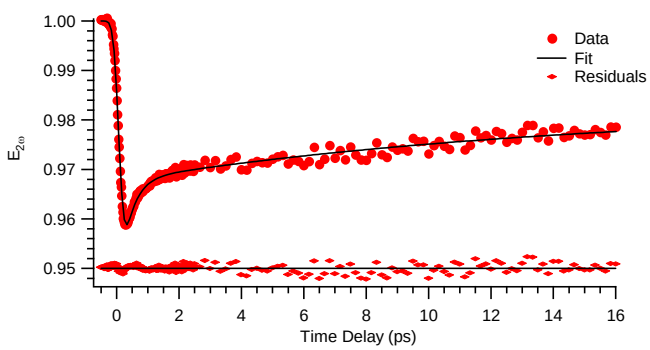

To confirm that this time constant was due to the electron transfer kinetics and not some other relaxation process, e.g. solvation, rotation, vibrational energy relaxation we changed the frequency of the probe pulse to a value which was two photon resonant with the ground to excited state transition of the product radical ion $DMA^{\bullet +}$ with a small background due to the interfacial C314, C314*, DMA and water. The formation time of $DMA^{\bullet +}$ corresponds to the electron transfer time. Its measured value, 16±3ps, is in good agreement with the 14±2ps obtained from the decay of the coumarin excited molecule. This confirms that we have correctly determined the dynamics of the interfacial electron transfer reaction.

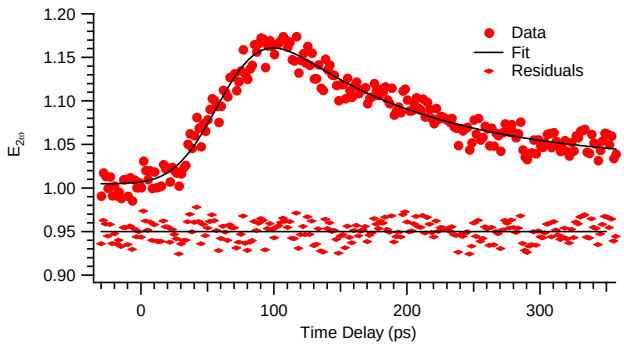

The recombination of the radical ions was found to be 163±4ps. Analysis of the dynamics using theoretical models and simulations of electron transfer at liquid/liquid interface is underway.

Interface asymmetry and rotational dynamics

Because of the inherent asymmetry of an interface in-plane intermolecular forces should differ from out of plane forces. As a consequence we anticipate that in-plane and out of plane rotational motions at a liquid interface should provide some insight into the effect of this asymmetry on time dependent interfacial phenomena. Such measurements provide a handle on frictional forces and their asymmetry at liquid interfaces which is an unexplored area at this time. In earlier studies of ultrafast molecular rotations at liquid interfaces we succeeded in establishing a method to measure the out of plane rotational motions of an organic adsorbate at air and charged aqueous interfaces. In our current research we have extended these studies to obtain interfacial in-plane rotation dynamics at an air/aqueous interface and in addition determined the effect of a negatively charged interface on rotational dynamics. For the charged interface we used a monolayer of sodium dodecylsulfate. The in-plane rotational dynamics at the air/H_2O interface was found to be 275±16ps, which is considerably slower than in bulk water, 100ps. Furthermore the in-plane (275±16ps) was faster than the out of plane (352±9ps) rotational motions at the air/water interface. At a full monolayer coverage of the anionic dodcylsulfate (100$Å^2$/dodecylsulfate interface) the in-plane rotation time constant increased to 334±13ps, which is faster than the out of plane rotations (383±9ps) at the same interface. It was surprising that the charged interface had a relatively small effect on both in and out of plane rotations considering the large effect of the surface charge on the interface orientation of C314. Although the differences in the in vs. out of plane rotational dynamics reflect the intrinsic asymmetry of the interface, the magnitude of this effect is not very large. Models are needed to understand how large an effect is to be expected and why the rotation is faster in plane. Stimulated by this work there are now simulations being carried out on rotations at aqueous interfaces.

Absolute orientation of molecules at interfaces

A method to determine the absolute orientation of molecules at liquid interfaces using sum frequency generation has been shown to be feasible. Current methods typically yield the orientation of some symmetry axis of the interfacial molecule, not its complete orientation. As a proof of method experiment we used *m*-tolunitrile, a planar molecule at the air/water interface.

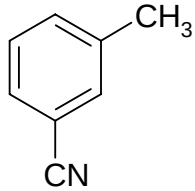

The basic idea of the method is to measure the orientation of two of the chromophores in the molecule with respect to the surface normal. Combining this with knowledge of the orientation of the two chromophores in the structure of the molecule fixes the absolute orientation of the molecule. For *m*-

tolunitrile the absolute orientation yields the twist angle of the phenyl plane with respect to the interface normal. We found that the -C≡N chromophore is at 58˚ and the C_3 axis of the-CH_3 chromophore is at 23˚, both with respect to the surface normal. The normal to the phenyl plane is then fixed at 68˚ with respect to the surface normal, i.e. the molecule is 32˚ from being totally upright. The remaining question as to whether the -C≡N projects into the water and the –CH_3 into the air is answered by the simple observation that the polar -C≡N is stabilized by hydrogen bonding with water and the –CH_3 is hydrophobic. Thus the -C≡N is expected to project into the water. In less obvious molecules the up vs. down orientation can be deteremined by measuring the phase of the generated light as we originally demonstrated for both phenol, substituted phenols and water at the air/water interfaces. The possible application of this method to almost all complex molecules is anticipated.

Charging of oxide/aqueous interfaces

We demonstrated in previous work that an optical method (second harmonic generation), which is noninvasive, can be used to determine the charge at a liquid interface, be it air/aqueous or a "buried" liquid/solid interface. The surface charge, which is determined by protonation reactions at oxide surfaces, directly impacts nanoparticle phase stability, ultrathin metal film growth on metal oxide, colloid aggregation, adsorption processes and chemical reactions (catalytic). The oxide material is often used in microparticle form to maximize the active surface area available for chemical reactions, such as excited state electron transfer in solar energy systems. Efforts to develop chemical models capable of predicting hydrated oxide properties in a wide range of natural and industrial systems require a fundamental understanding of the relation of molecular level structure and the protonation of surface hydroxyl groups. In our recent work, which seeks to connect surface properties with known surface structures we have been studying the charging behavior, due to protonation or deprotonation of surface oxygens, of single crystal faces of a number of metal oxides. We use SHG to determine and compare the charging of the (0001) and (1102) crystallographic surfaces of α-Al_2O_3. These surfaces are commonly used as models of the basal and edge type surfaces that are assumed to dominate Al-(hydr)oxide colloids and the aluminol (AlOH) layers in clays. Both of these latter materials are important in environmental issues and technology. The underlying idea of our method is based on our demonstration that when an interface is charged the second order polarization of the bulk solvent (H_2O) molecules contribute to the observed SHG. The magnitude of the interface electrostatic potential due to the net surface charge depends on the electrolyte concentration that shields the bulk water molecules from the charged surface. Thus the pH at which the SHG signal is independent of the electrolyte concentration is the pH at which the net surface charge is zero.

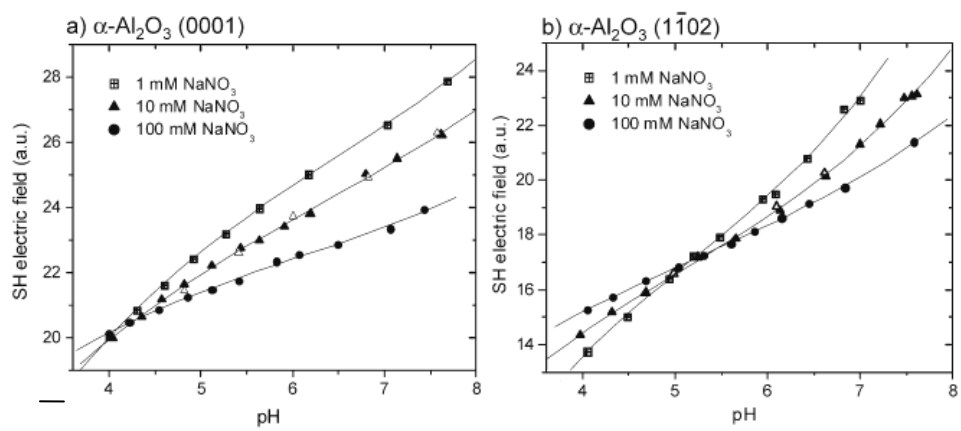

Our determinations of the pH at the point of zero charge are very different from current models of the charging of α-Al_2O_3 surfaces. For the (0001) face the model predicts little charging between pH 2 and 10, which is contrary to our findings. Similary the current model predicts that for the (1102) face the point of zero charge should be pH 8, contrary to our showing that it is 5.2. As a last significant point our results show that the acid-base chemistry of Al-(hydr)oxide particles cannot be accounted for by some combination of the acid-base chemistry of the (0001) and (1102) faces. We have collaborated with a

simulations group to obtain the detailed charging (acid-base reactions) of the rutile, TiO_2, 001 crystal face.

DOE Supported Publications

Liu, J., Shang, X.M., Pompano, R., Eisenthal, K.B., "Antibiotic assisted molecular ion transport across a membrane in real time", Faraday Discussions, 2005, 129, 291-299

Garrett, B. et.al., "Role of water in electron-initiated processes and radical chemistry: Issues and scientific advances", Chem. Rev., 2005, 105, 355-389

Fitts, J.P., Shang, X.M., Flynn, G.W., Heintz, T.F., Eisenthal, K.B., "Second-harmonic generation and theoretical studies of protonation at the water/alpha-TiO2 (110) interface", J. Phys. Chem. B., 2005, 109, 7981-7986

Fitts, J.P., Machesky, M.L., Wesolowski, D.J., Shang, X.M., Kubicki, J.D., Flynn, G.W., Heintz, T.F., Eisenthal, K.B., "Electrostatic surface charge at aqueous/alpha-Al2O3 single-crystal interfaces as probed by optical second-harmonic generation", Chem. Phys. Lett., 2005, 411, 399-403

Pompano, R.R., Liu, J., Shang, X.M., Eisenthal, K.B., "Laser study of antibiotic assisted molecular-ion transport through lipid bilayers in real time", Abstracts of Papers of the American Chemical Society, 2004, 227, U486-U486

Eisenthal, K.B., Shang, X.M., Zimdars, D., Nguyen, K., Liu, J., Pompano, R., "Molecular dynamics at aqueous interfaces", Abstracts of Papers of the American Chemical Society, 2004, U213-U213

Benderskii, A.V., Heinzie, J., Basu, S., Shang, X.M., Eisenthal, K.B., "Femtosecond aqueous solvation at a positively charged surfactant/water interface", J. Phys. Chem. B., 2004, 108, 14017-14024

Eisenthal, K.B., Benderskii, A.V., Shang, X.M., "Molecules at liquid interfaces", Abstracts of Papers of the American Chemical Society, 2003, 225, U446-U446

Eisenthal, K.B., "Solvation and rotation dynamics at liquid interfaces", Abstracts of Papers of the American Chemical Society, 2003, 226, U230-U230

Chemical Kinetics and Dynamics at Interfaces

Solvation/Fluidity on the Nanoscale, and in the Environment

James P. Cowin
Chemical Sciences Division
Pacific Northwest National Laboratory
P.O. Box 999, Mail Stop K8-88
Richland, Washington 99352
jp.cowin@pnl.gov

Program Scope

Interfaces have a unique chemistry, unlike that of any bulk phase. This is true even for liquid interfaces, where one might have (incorrectly) pre-supposed that a liquid's lack of rigidity might strongly suppress perturbations due to the interface. These interfacial effects include changes in fluidity and transport, solvation of ions, and stability of excited states. The applicability of the knowledge gained extends reactions and transport across two-phase systems (like microemulsions), electrochemical systems, and in many situations where a fluid is present in molecular-scale amounts… such as in cell membranes, enzymes and ion channels, or at environmental interfaces at normal humidities, such as the surfaces of atmospheric or soil particles. We explore these systems with several unusual methods. These include re-creating liquid-liquid interfaces using molecular beam epitaxy, and use of a molecular soft landing ion source. We also explore fundamental properties of bulk ice, that relate to such issues as proton transport, amorphous ice properties, and even the effect of ice in formation of planets.

Recent Progress

Probing Nano-Fluids: We use a unique approach to study interfacially perturbed materials: a soft-landing ion source and molecular beam epitaxy together allow us to re-create liquid-liquid interfaces with high precision. This has allowed us to probe fluidity with molecular precision near solvent interfaces, and solvation potentials for ions at or near these interfaces. As shown in Figure 1, left, we grow thin films of solvent, at cryogenic temperatures. While it is still too cold for any diffusion to occur, we add to the film, very gently, a fraction of a monolayer of molecular ions (Cs^+ in this case). These ions can be inserted at will at any precise, initial location in the solvent (3-methylpentane) film. We then warm the film, and follow the ion's motion with great precision, using an electrostatic Kelvin probe.

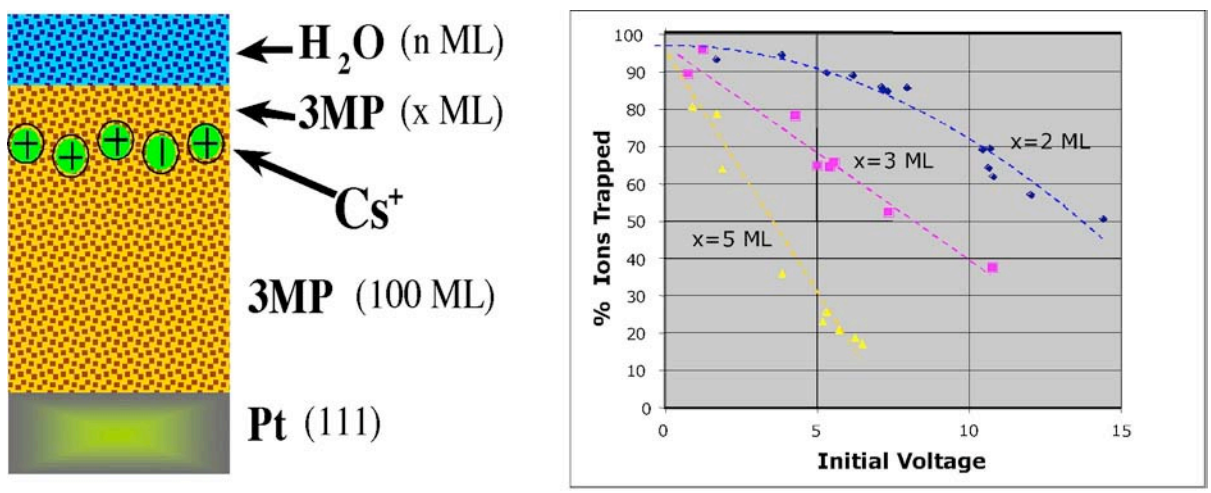

Figure 1. Probe ions placed at a distance x-monolayers (ML) away from an embedded water layer can either escape or get trapped when system is warmed (left). At right shows percent of ions that are trapped vs starting voltage

We used this approach to measure the nanometer dependence of the fluidity of 3 methyl pentane (3MP) at the 3MP-Pt, 3MP-vacuum, and 3MP-water interfaces. We were able to show that the film is orders of magnitude less viscous at the top of the film compared to the bulk material, and orders of magnitude more viscous at the bottom. (Bell et Al. 2003).

We then applied this precision ion-doping methods to map the solvation potential near the oil-water interface. Only a portion of the data is published from the first of many studies showing how we could determine the solvation potential minimum, and its maximum slope. (Wu et Al. 1999, 2001). Our most recent results include work where we gave ions a choice… by placing them x monolayers (ML) away from water interface, with a water thickness of n ML (Figure 1, right). The ions can either follow the collective ion-Pt induce potential gradient (V_f = 1 to 15 V across the 100 ML of 3MP), or fall backwards toward the water interface. We find that for n to many monolayers, the outcome is independent of n. But the fraction being trapped (Figure 1, right) varies strongly with V_f, and the distance away from the water interface. This provides information on the detailed shape of the solvation potential.

Atmospheric Dust Aging (with Alex Laskin): Dust in our atmosphere degrades our view, can make us sick, and influences climate and chemistry of the atmosphere. The dust's chemical properties that determine these effects constantly evolve, from the particle's birth until its removal from the atmosphere, typically days later. We explore atmospheric aging mechanisms of particles and their implications. These often involve solid particles with only monolayers of adsorbed water present, thus limited solvation (see "Nano-fluids" section). Analysis in the lab of samples of dust are done for each individual particles using computer controlled scanning electron microscopy with elemental analysis via emitted x-rays, and time of flight secondary ion mass spectrometry. The "Environmental" electron microscope permits imaging the particles at up to 100 % relative humidity, or several Torr of reactive gases present.

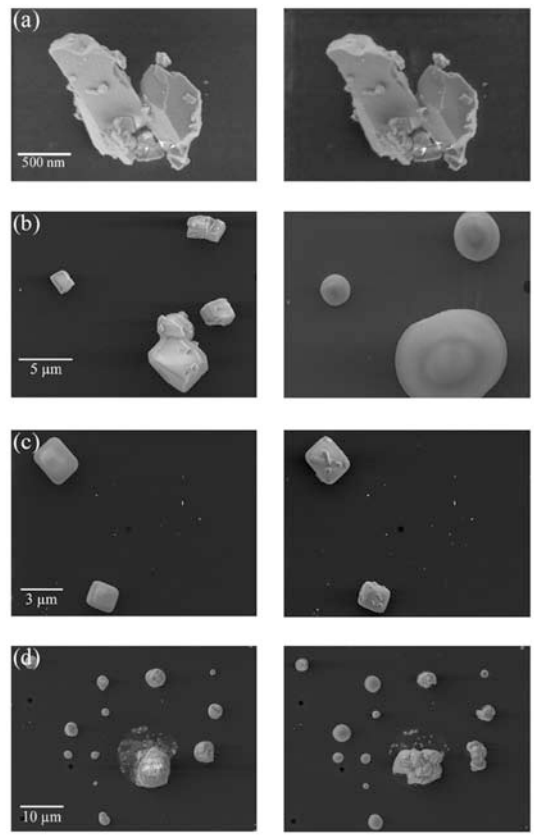

Figure 2. Single particle reaction with HNO_3 and water vapor: (a) SiO_2 before/after exposure to 1 Torr HNO_3 and ~25% RH for 20 minutes, (b) $CaCO_3$ before/exposure to 20 µTorr HNO_3 and 41% RH for 4 hours, (c) NaCl before/after exposure to 20 µTorr HNO_3 and 17% RH for 5 hours and (d) sea salt before/after exposure to 20 µTorr HNO_3 and 17% RH for 5 hours.

Collaborating with Prof. V.H. Grassian's group (U. of Iowa), we studied particles reacting with nitric acid, a pervasive trace pollution gas. Figure 1 shows changes observed for SiO_2, $CaCO_3$, NaCl and sea salt particles. Figure 2(a) shows a SiO_2 particle before and after exposure to nitric acid: no reaction is seen. Image (b) shows $CaCO_3$ dust reacting rapidly: its x-ray emission (not shown) confirms transformation to calcium nitrate (Krueger et al, 2003b). Images (c) and (d) show NaCl and sea salt particles. The NaCl particles showed only small amounts of $NaNO_3$ crystallites on the particle surfaces while sea salt particles reacted nearly completely. These transformations, accelerated by the hydroscopic nature of the products (especially Ca- and Mg- nitrate), may greatly alter common dust's lifetime and ability to seed clouds (Krueger, *et al.* 2003a; 2003b).

In a collaborative study with the group of Prof. B.J. Finlayson-Pitts (U. of California, Irvine) we probed the composition of NaCl particles reacted with hydroxyl radicals (Laskin, *et al.* 2003b). We showed that hydroxyl

radicals transformed sea salt dust into both hypochlorites/perchlorates and hydroxides, via reactions with interfacial chloride ions. In the marine boundary layer, this increases particle alkalinity, increasing the uptake and oxidation of SO_2 to sulfate in sea salt particles. This may have an important impact on global warming. Other ongoing collaborative projects include; aging of diesel exhaust particles (Prof. M.J. Molina and L.T. Molina, Massachusetts Inst. of Technology) and biomass burning particles (with W.C. Malm and J.L. Hand, Nat. Park Service and Colorado State U.).

Bulk Water Ice: Two projects involving bulk water ice (amorphous and crystalline) were done recently, one on "nano-planets", another on the pryo- and piezo-electric properties.

Probing Nano-Planets: What is a nano-planet? A nano-planet is just a fanciful way to describe the micron-sized dust in a nebula around a newborn star, that may some day agglomerate to form planets. May form planets is emphasized, as the new star's stellar wind also begins to slowly strip the nebula of this dust. A planet must form within 1 million years, or the dust supply will be gone. The problem is, scientists have a hard time understanding how the dust can stick together fast enough, to reach gravitationally bound "planetesimals" (10's of meters of size). Our studies of the properties of low temperature water ices gave us insight into that process.

Most dust grains in the outer parts of the nebulae will be heavily coated or largely composed of water ice. Most of this ice forms amorphously via condensation from the vapor at from 10 to 100 K. At these temperatures, the water dipoles tend to slightly align, creating strong electrostatic fields within or around the ice grains (see Figure 3). Even in the presence of neutralizing charges, collisions and temperature changes re-expose these electric fields, which then greatly enhances the sticking rate of the ice grains. We also measured the elastic properties of the low temperature ice. As shown in Figure 3, it is very inelastic, which also makes it much easier for two colliding icy grains to stick together. (Wang et al. 2004)

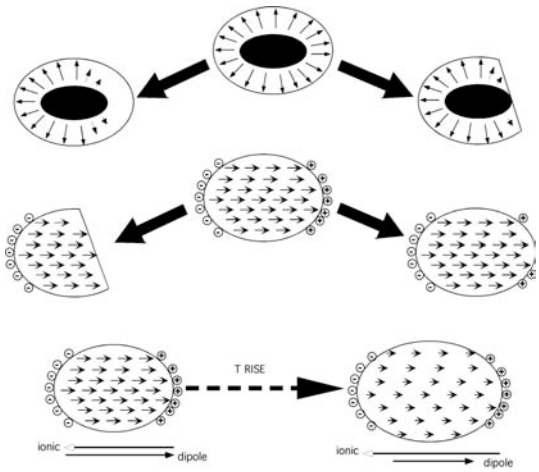

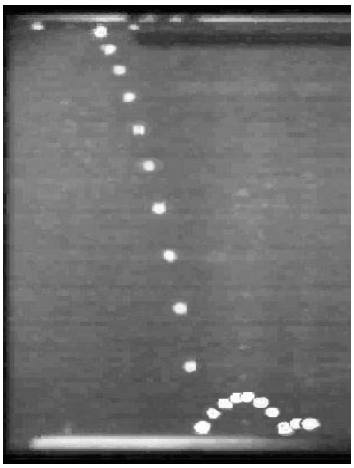

Figure 3. Left: Icy grains in pre-planetary nebula acquire electrostatic dipoles due to low temperature ice's spontaneous polarization (top). They spew charged fragments after collisions (middle), or polarize via subtle T-induced charge imbalances (bottom). Right: Time-lapse photo of a ball bouncing from an amorphous ice slab, shows how inelastic this low temperature ice is.

Pyro-and Piezo-electric Water Ice: We measured, for the first time, the pyro- and piezo-electric properties of water ice. These describe, respectively, how temperature and strain cause water ice to polarize. These properties are only non-zero for substances which possess no inversion symmetry, and most had supposed for water ice I, that it should be uniquely zero. However water ice that is slightly proton-aligned lacks inversion symmetry. So this does possess non-zero coefficients. Our soft-landed ions allow us to make water ice that is around 10% percent proton-aligned. It has strongly non-zero piezo- and pyroelectric coefficients. This has implications for the "nano-plane" work, and also can be very important in any study that attempts to probe low temperature water ice (<150 K) with electrical measurements. This work is written up, and will be submitted soon for publication.

Transport Properties in Water Ice: We measured, in 1999, to our surprise, that hydronium ions do not move in water ice, at least between 50 and 190 K. This resulted in a Science article .(Tsekouras 1999) We also showed

that D defects (Fig. 5) moved at 124 K, similar to the standard model, but that this also showed a remarkably strong electric field dependence to this motion, shifting downward to 40 K by 1.1 x 10^8 V/m. The voltage of 1.1 x 10^8 V/m is only about 40 mV across a single water molecule, and is similar to that 12 Å away from a single ion, or that across a voltage-gated proton transport channel in a cell.

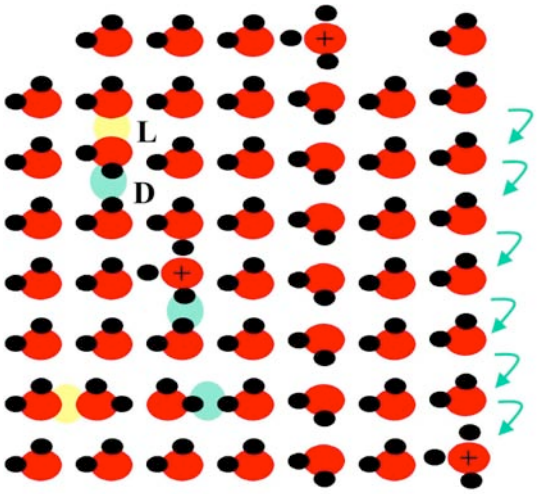

Figure 4. Water L and D defects, and proton hopping/transport

Future Plans

A major ongoing effort is now finishing the publication of several papers related to solvation at the oil water interface, and a paper on ion motion in bulk 3 methyl pentane. We are also ananlyzing results from the water defect translation work, some to be presented at this meeting.

New experiments are in planning to re-create buried interfaces, included neutrals and imbedded ions, to look at their photochemistry with FTIR, and time-resolved optical probes. This involves a special small mobile ultrahigh vacuum system that can deliver our custom tailored films to optical probes located in other PNNL labs, and at synchrotrons. One important new goal of this work will be to understand the transport of excited state and electron-driven chemistry, under the influence of intense gradient s in electric field and solvation asymmetry.

References

Bell, R. (2003a), H-F Wang, K. Wu, M. J. Iedema, and J. P. Cowin, "Nanometer-Resolved Interfacial Fluidity." *J. Amer. Chem. Soc.* 125: 5176-5185

Bell, R.C. (2003 b) H.-F. Wang, M.J. Iedema, J.P. Cowin , Sculpting Nanoscale Liquid Interfaces, in "ACS Symposium Series 861: Mesoscale Phenomena in Fluid Systems" ed. F. Case and P. Alexandridis, Amer. Chem. Soc. , Chapter 12, pp. 191-203

Gallagher, M. C. (2003), M. S. Fyfield , L. A. Bumm, J. P. Cowin and S. A. Joyce Structure of Ultrathin MgO films on Mo(001), Thin Solid Films 445, 96

Krueger, B. J.(2003a), V. H. Grassian, M. J. Iedema, J. P. Cowin and A. Laskin "Probing Heterogeneous Chemistry of Individual Atmospheric Particles Using Scanning Electron Microscopy and Energy Dispersive X-ray Analysis. " *Anal. Chem.*, 75: 5170-5179 .

Krueger, B.J. (2003b), V.H. Grassian, A. Laskin and J.P. Cowin "Laboratory Insights Into the Processing of Calcium Containing Mineral Dust Aerosol in the Troposphere." *Geophysical Research Letters* 30: 1148-1151 .

Laskin, A., (2003a), M. J. Iedema and J.P. Cowin "Time-Resolved Aerosol Collector for CCSEM/EDX Single-Particle Analysis." *Aerosol Sci. Technol*, 37: 246-260 .

Laskin, A.(2003b), D. J. Gaspar, W.-H. Wang, S.W. Hunt, J. P. Cowin, S. D. Colson, and B. J. Finlayson-Pitts "Reactions at Interfaces As a Source of Sulfate Formation in Sea-Salt Particles." *Science*, 301: 340-344 .

Laskin, A. (2004), D. J. Gaspar, W.-H. Wang, S.W. Hunt, J. P. Cowin, S. D. Colson, and B. J. Finlayson-Pitts, "Response to Comments on "Reactions at Interfaces As a Source of Sulfate Formation in Sea Salt Particles", Science 303, 628

Tsekouras, A (1999), MJ Iedema, K. Wu, GB Ellison, JP Cowin, Immobility of Protons in Ice, Nature 398 (1999) 405

Wang, H.-F. (2004), RC Bell, MJ. Iedema, AA. Tsekouras, JP Cowin, "Sticky Ice Grains Aid Planet Formation". , The Astrophysical Journal, 620, 1027-1032 (2005).

Wu , K. (1999), M.J. Iedema, J.P. Cowin, Ion Penetration of the Oil-Water Interface, Science 286, 2482

Wu, K (2001), M.J. Iedema, G.K. Schenter, J.P. Cowin Invited Feature Article: Sculpting the Oil-Water Interface to Probe Ion Solvation, J. Phys Chem. B 105, 2483

Electronically Non-Adiabatic Interactions in Molecule Metal-Surface Scattering

Alec M. Wodtke, Dept. of Chemistry and Biochemistry, University of California Santa Barbara, Santa Barbara, CA 93106 (wodtke@chem.ucsb.edu)

Abstract

Our group has been increasingly interested in developing a better understanding of the degree to which chemical reactions at solid interfaces can be accurately viewed through the "standard model of chemical reactivity" involving nuclear dynamics calculations on electronically adiabatic potential energy surfaces. This talk will present experimental observations, which suggest that excitation of electrons during energetic chemical events at metal interfaces needs to be better characterized and understood before we can be confident that our approach to heterogeneous catalysis rests on a firm theoretical foundation. The talk will emphasize recent attempts to make quantitative comparisons between experimental scattering experiments involving vibrationally excited molecules and high level *ab initio* simulations relying on density functional theory. While such attempts at experiment/theory interactions are still at an early stage, some of the difficulties that need to be overcome can already be seen; for example the well known over-binding problem in DFT can make comparisons between experiment and theory problematic as the influence of trapping may be overemphasized by theory. Some speculation about how the manipulation of electrons in solids might be used to influence reactivity at interfaces by making use of electronically non-adiabatic chemical interactions will also be presented in the hopes of stimulating discussion.

Related References

1. *Observation of orientational influences on vibrational energy transfer at metal surfaces: Rotational Cooling Associated with Vibrational Relaxation at a Metal Surface*, Alec M. Wodtke, Daniel J. Auerbach, Huang Yuhui, Chem. Phys. Lett. (in press)

2. *Insensitivity of molecular trapping at surfaces to vibration.* Alec M. Wodtke, Daniel J. Auerbach, Huang Yuhui, Chem. Phys. Lett. **413** 326-330 (2005)

3. *Conversion of large amplitude vibration to electron excitation at a metal surface*, J. White, J. Chen, D. Matsiev, D.J. Auerbach and A.M. Wodtke, Nature **433**(7025),503-505, (2005).

Other relevant literature

1. Behler, J., Lorenz, S., Reuter, K., Scheffler, M. and Delley, B., 2004

2. Y. Huang, S.J. Gulding, C.T. Rettner, D.J. Auerbach A.M. Wodtke, Science **290**, 111 (2000)

3. A.M. Wodtke and Y. Huang, D.J. Auerbach, J. Chem. Phys. **118**(17) 8033-41 (2003)

4. J. White, J. Chen, D. Matsiev, D.J. Auerbach and A.M. Wodtke, J.V.S.T. 23, 1085-1089 (2005).

5. B.R. Trenhaile et al., Surface Science 583 (2005) L135–L141

The Role of Electronic Excitations on Chemical Reaction Dynamics at Metal, Semiconductor and Nanoparticle Surfaces

John C. Tully

Department of Chemistry, Yale University, P. O. Box 208107, New Haven, CT, USA

john.tully@yale.edu

Program Scope

Achieving enhanced control of the rates and molecular pathways of chemical reactions at the surfaces of metals, semiconductors and nanoparticles will have impact in many fields of science and engineering, including heterogeneous catalysis, photocatalysis, materials processing, corrosion, solar energy conversion and nanoscience. However, our current atomic-level understanding of chemical reactions at surfaces is incomplete and flawed. Conventional theories of chemical dynamics are based on the Born-Oppenheimer separation of electronic and nuclear motion. Even when describing dynamics at metal surfaces where it has long been recognized that the Born-Oppenheimer approximation is not valid, the conventional approach is still used, perhaps patched up by introducing friction to account for electron-hole pair excitations or curve crossings to account for electron transfer. There is growing experimental evidence that this is not adequate. We are examining the influence of electronic transitions on chemical reaction dynamics at metal and semiconductor surfaces. Our program includes the development of new theoretical and computational methods for nonadiabatic dynamics at surfaces, as well as the application of these methods to specific chemical systems of experimental attention. Our objective is not only to advance our ability to simulate experiments quantitatively, but also to construct the theoretical framework for understanding the underlying factors that govern molecular motion at surfaces and to aid in the conception of new experiments that most directly probe the critical issues.

Recent Progress

Our initial focus is on the scattering of the nitric oxide molecule from the (111) face of a gold crystal. The motivation for choosing this system is the very revealing series of experiments currently being carried out by Wodtke and coworkers. They scatter highly vibrationally excited NO molecules from a gold surface and state-selectively detect the scattered molecules. They have observed very large amounts of vibrational energy loss, of order 8 quanta or more, in apparent conflict with the gradual dissipation predicted by the electronic friction model. The sudden electron jump (Franck-Condon) model also does not appear to be adequate here, as discussed below. Recently, by lowering the work function with co-adsorbed cesium, Wodtke, et al. have observed electron emission from the surface, presumably produced by direct vibration-to-electronic energy transfer. This is also in conflict with the current theoretical framework.

We have carried out BLYP, 6-311+g(d), density functional theory (DFT) calculations of the potential energy surface of a NO molecule interacting with a cluster of 20 gold atoms, using a pseudopotential that replaces all but one electron of each gold atom. The ionization energy of the bare cluster, computed in this way, fortuitously matches the experimental work function of gold. It is important to reproduce the correct work function in order to accurately describe electron transfer from the metal to the molecule. We have mapped out *ab initio* energies for a large number of NO internuclear separations, NO-surface distances, lateral positions (bridge,on-top, etc.), and orientations of the NO axis. In addition to tabulating the energy at each point, we have also computed the Lowdin charge on the NO molecule. An example of the computed charge on NO as a function of N—O separation and NO-surface distance is shown in the figure.

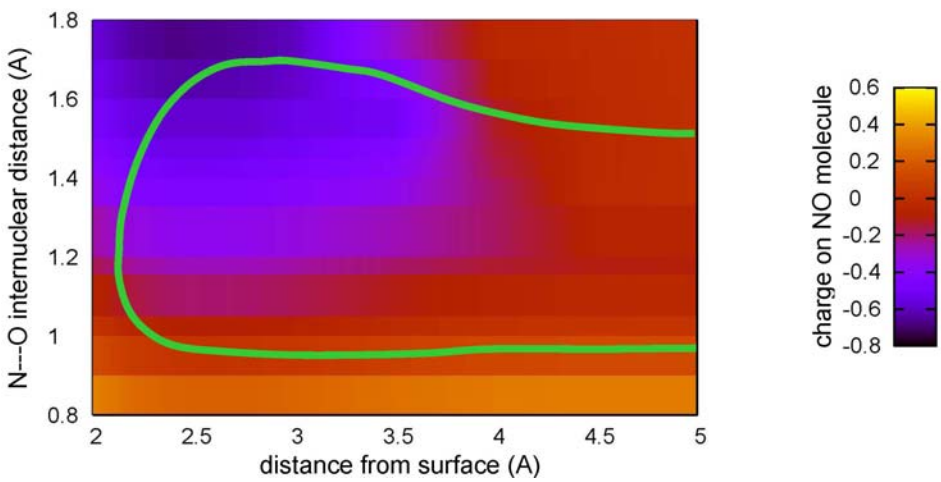

Lowdin charge on the NO molecule as a function of N—O bond length and the distance of the center of mass of NO from the surface plane. NO is oriented along the surface normal over a 3-fold site with the nitrogen end towards the surface. The interior of the light green curve is the classically allowed region for a NO molecule with infinitesimal translational energy and classical vibrational energy corresponding to the v=12 quantum state.

The figure shows that the transition between neutral and negative ion states is only partial and occurs relatively gradually as the NO molecule approaches the surface. This calls into question the Franck-Condon model which assumes a sudden electron hop.

In order to use the calculated *ab initio* points as the basis for dynamics simulations, we have constructed an analytical approximation to the potential energy surface. Because we wish to examine nonadiabatic effects in this system, we have chosen to represent the potential energy surface as the lower eigenvalue of a 2x2 Hamiltonian matrix. The diagonal elements of the 2x2 matrix are the "diabatic" neutral and ionic potential energy surfaces. These are coupled by an off-diagonal potential surface such that the ground state becomes a mixture of ionic and neutral configurations. In order to uniquely define the 2x2 symmetric matrix, we need three independent pieces of information at each nuclear configuration. We have computed only two, the ground state energy and the Lowdin charge on the NO molecule, which we assign to be the square of the coefficient of the ionic configuration in the ground state. We supplied the missing piece of information by prescribing a form for the off-diagonal coupling, a

simple exponential function of the distance of the molecule from the surface, and we then chose the two parameters in the exponential so that the resulting diabatic surfaces were optimally smooth. The analytic forms of the two diabatic surfaces were chosen to be similar to a previously used molecule-surface interaction potential, with the ionic surface modified to incorporate the image potential.

Our first step toward understanding the role of nonadiabatic electronic transitions was to carry out simulations on the ground state only, i.e., to neglect nonadiabatic transitions. Note that the Franck-Condon charge transfer mechanism is operative, in principle, even within the adiabatic approximation, since the molecule moves between neutral and ionic regions of configuration space. We have carried out classical trajectory simulations on the ground state potential energy surface, with the initial NO vibrational energy corresponding to v=15 and other conditions chosen to match the experiments of Wodtke et al. Surprisingly, with motion on the ground state only, we find large amounts of vibrational energy loss in the scattered NO molecules, in rough accord with the Wodtke results. A major contribution to this vibrational inelasticity is repeated entrances into and exits from the ionic region as the molecule vibrates; it is not a single electron hop as pictured in the Franck-Condon model. There is a serious problem, however, that casts doubt on the validity of our preliminary results: our calculated probabilities for trapping of the molecule on the surface (sticking) are much too high compared with experiment. The source of this error is likely attributable, at least in part, to an over-estimation of the binding energy of the molecule in the *ab initio* calculations, a well-known deficiency of standard density functional theory. A consequence of this is that trajectories remain in the vicinity of the surface too long, likely resulting in an overestimate of vibrational energy transfer. This deficiency must be corrected before any reliable mechanistic conclusions can be drawn.

Future Plans

The goals of our research program include both specific aspects of the NO-Au system and more general investigations of nonadiabatic behavior at surfaces. With regard to the former, we plan to address NO-Au in the following stages:

1. Carry out plane wave DFT calculations (using the VASP code) of the NO-gold interaction, as well as higher level cluster calculations to obtain more reliable *ab initio* energies.
2. Re-parameterize the 2x2 matrix representation to fit the improved *ab initio* data.
3. Carry out adiabatic molecular dynamics simulations to assess the importance of nonadiabatic transitions.
4. Introduce nonadiabatic electron-hole pair excitations via electronic frictions.
5. Carry out mixed quantum-classical dynamics (Ehrenfest and surface hopping) using the course-grained representation of the conduction band continuum as described below.
6. Through analysis of the results of application of this hierarchy of theoretical methods, draw conclusions about the importance and nature of nonadiabatic electronic transitions both in the NO-Au system and more generally.

While the NO-Au system is a valuable starting point, our goal is to develop the theoretical tools required to describe the dynamics of a wide variety of nonadiabatic molecule-surface processes. Theoretical methods to describe the interplay between

discrete electronic states of adsorbates and the continuum of conduction band states, and their influence on nuclear motion, are incomplete. A number of relevant parts of the picture exist such as the Anderson-Newns model of a bound state in a continuum, the formulation of electron-hole pair dissipation as a friction, and the stochastic wave-packet approach for solving the Liouville-von Neumann equation. But progress will require more than assembling existing parts. We propose to develop improved *ab initio* methods for computing the energies and widths of lifetime-broadened electronic states, through extension of the "constrained density functional theory". These are the properties that determine the rate and extent of electron transfer as a molecule approaches the surface. In parallel, following related work in our group, we will attempt to extend current mixed quantum-classical dynamics methods such as Ehrenfest and surface hopping to multiple lifetime-broadened potential energy surfaces.

We will carry out *ab initio* calculations of energies, charge distributions and level widths as input to constructing valence-bond type Hamiltonians for a number of chemical systems beyond NO-Au. Among these are the interaction of hydrogen atoms and hydrogen molecules with metal surfaces, including the dynamics of dissociation, and the interaction of oxygen atoms and oxygen molecules with metal and semiconductor surfaces. Both the oxygen atom and molecule are ground state triplets with low-lying singlets, and both accept an electron when approaching a metal surface, so there may be several mechanisms of nonadiabaticity in play. For example, in gas phase reactions of the oxygen molecule, the ground $O_2(^3\Sigma_g^-)$ state is generally much less reactive than the excited $O_2(^1\Delta_g)$ of the oxygen molecule. As the reactants approach, the potential energy surfaces that correlate asymptotically with $O_2(^3\Sigma_g^-)$ and $O_2(^1\Delta_g)$ usually cross each other However, because they correspond to different total spin and because spin-orbit coupling is weak, there is a negligible probability of a transition; the dynamics can be assumed to evolve on a single potential energy surface. At a metal surface, however, as the O_2 molecule reaches the crossing point, a near-resonant 2-electron exchange can convert the molecule from the triplet to the singlet; spin-orbit or magnetic interactions are not required. This is related to the "Kondo effect" that is of current interest in the condensed matter theory community. This argument suggests that the triplet ground state of oxygen may have nearly the same reactivity as the excited singlet state at metal surfaces. However, for the one case studied experimentally, dissociation of O_2 on Al(111), this does not appear to be the case; $O_2(^3\Sigma_g^-)$ has a small reaction probability in spite of a low reaction barrier on the ground state surface. Addressing this type of process properly by theory is an important challenge; it is likely that these considerations will require us to re-evaluate many chemical reaction pathways involving radical reactants or intermediates on metal surfaces. In addition, similar behavior can be expected for above band gap excited state dynamics at semiconductor surfaces. Finally, chemistry at the surfaces of metallic or semiconductor nanoparticles may display new features resulting from the discretization of the valence and conduction bands due to finite size.

Role of Solvent: Reactions in Supercritical Fluids

David M. Bartels and Daniel M. Chipman
Notre Dame Radiation Laboratory
Notre Dame, IN 46556
e-mail: bartels.5@nd.edu; chipman.1@nd.edu

Program definition

For a number of years this project has pursued the use of radiolysis as a tool in the investigation of solvent effects in chemical reactions. The project has now evolved toward the particular study of solvent effects on reaction rates in supercritical (sc-)fluids. Even more specifically, radical reactions in supercritical water are targeted because of interest to use sc-water as a coolant in future (GEN-IV) nuclear power plants. This has proven very fruitful from the basic science standpoint, as virtually any reaction we investigate exhibits behavior best characterized as "weird".

An anthropomorphic way to think about near-critical phenomena, is that the fluid is trying to decide whether it is a liquid or a gas. The cohesive forces between molecules that tend to form a liquid are just being balanced by the thermal entropic forces that cause vaporization. The result, on a microscopic scale, is the highly dynamic formation and dissipation of clusters and larger aggregates. The fluid is extremely heterogeneous on the microscopic scale. A solute in a supercritical fluid can be classified as either attractive or repulsive, depending on the average pair potential between the solute and solvent. If the solute-solvent pair potential is more attractive than the solvent-solvent potential, the solute will tend to form the nucleus of a cluster. A local density enhancement will prevail around the solute, which might have implications for various spectroscopies or for reaction rates. When the solute-solvent forces are repulsive, one might expect the solute to remain in a void in the fluid as the solvent molecules cluster together. Extremely large partial molal volumes are known for hydrophobic molecules in near-critical water. This effective phase separation should have significant implications for the chemical reactions in sc-fluids.

Our purpose in this work is to determine free radical reaction rates in supercritical fluids to develop an understanding of the important solvent effects. Among these will be the effect of local density enhancements (or depletions) on the solvation of reactants and transition states, potential of mean force in the relative diffusion (caging effects), and possible nonequilibrium energy and momentum transfer issues. Relatively few studies of free radical reactions have been carried out under supercritical conditions. We do not propose to extensively review the literature on this subject: an issue of Chemical Reviews [Chemical Reviews, 99, (1999)] contains several useful reviews of work up to 1999.

The ultimate goal of our study is the development of a predictive capability for free radical reaction rates, even in the complex microheterogeneous critical regime. No such capability now exists. The calculation of transition state geometries for free radical reactions by ab initio methods in the gas phase is still not completely reliable, though very good progress has been made. The calculation of condensed phase transition states is a much more difficult task because of the large number of configurations that must be considered, and the perturbation of the reaction energetics by the solvent.

The immediate goal of this work is to determine representative free radical reaction rates in sc-fluid and develop an understanding of the important variables to guide development and use of predictive tools. Electron beam radiolysis of water (and other fluids) is an excellent experimental tool with which to address these questions. The primary free radicals generated by radiolysis of water, $(e^-)_{aq}$, OH, and H, are respectively ionic, dipolar, and hydrophobic in nature. Their recombination and scavenging reactions can be expected to highlight the effects of clustering (i.e. local density enhancements) and solvent microheterogeneity both in terms of relative diffusion and in terms of static or dynamic solvent effects on the reaction rates. We already have transient absorption data for several of these species that highlights interesting and unexpected reaction rate behavior. A major thrust of the next several years will be to push time-resolved EPR detection of H atoms in sc-water. The Chemically Induced Dynamic Electron Polarization (CIDEP) generated in H atom recombination reactions is amenable to theoretical simulations, and provides another unique probe of the cage dynamics and potential of mean force. How different will be the potential of mean force between H atoms and between $(e\text{-})_{aq}$ and H? How easily will H atoms penetrate into water clusters?

Recent Progress

Nearly every reaction we have investigated in high temperature water has given unexpected results. Several reactions of the hydrated electron in supercritical water at 380°C have shown a minimum in reaction rate as a function of the density—at around 0.45 g/cc. This behavior remains to be explained. A most surprising result was obtained for the textbook reaction $H_2 + OH \rightarrow H + H_2O$. Arrhenius behavior was found up to 225°C, but then the reaction rate went *down*. We were unable to measure the lower reaction rate above 350°C. The reaction $H + OH\text{-} \rightarrow H_2O + (e\text{-})_{aq}$ was carefully measured up to 350°C. This reaction is very unusual in that the entropy of activation seems to suddenly change sign at about 100°C. These reaction rate results have been reported in the papers listed at the end of this report.

A large amount of transient absorption data is in process of analysis and write-up. Several thousand kinetics traces for the hydrated electron in H_2-saturated alkaline water up to 350°C are being analyzed to extract rate constants for (a) $(e\text{-})_{aq} + (e\text{-})_{aq} \rightarrow H_2 + 2OH\text{-}$; (b) $(e\text{-})_{aq} + H \rightarrow H_2 + OH\text{-}$; (c) $(e\text{-})_{aq} + H_2O_2 \rightarrow OH + OH\text{-}$; and (d) the equilibrium $(e\text{-})_{aq} + H_2O \leftrightarrow H + OH\text{-}$. The unusual reaction (a) of two hydrated electrons is diffusion limited up to 150°C, but by 250°C the reaction has essentially "turned off". Above this temperature the recombination is dominated by reaction (b). A large amount of kinetic data for the OH radical absorption at 250nm is also in process of analysis. The target is the second order recombination $OH + OH \rightarrow H_2O_2$. Unavoidably we obtain information on the $OH + H_2O_2$ reaction as well. The UV absorption of these species changes significantly with temperature, making this system a very difficult challenge. The result seems to be that OH + OH recombination rate hardly changes at all at 250bar pressure above 250°C, until the low density supercritical regime is reached at about 375°C. Then the recombination rate drops dramatically and becomes too slow to measure easily. It is very unclear why recombination reactions of the OH radical should become so much less than diffusion limited at high temperature. Most surprisingly, the simple reaction of H atoms with O_2 to give HO_2 product is found to decrease in rate above 250°C, reach a minimum at 325°C, and then suddenly increase again. It begins to appear that minima in these radical reaction rates between 300 and 350°C in water is a general feature, which still requires a general explanation.

The atomic oxygen anion is an important nucleophilic component of irradiated basic aqueous solutions, with chemistry quite different from that of its conjugate base, the electrophilic and weakly acidic hydroxyl radical. In an effort to help clarify the poorly understood solvation of O^- we have characterized with computational electronic structure methods the clusters $(O^-)(H_2O)_n$ of oxygen anion with n = 1-5 water molecules along with the related proton-transferred clusters $(OH^-)(OH)(H_2O)_{n-1}$, thereby finding unique hydrogen bonding motifs. The $(O^-)(H_2O)_n$ family, which provides the lowest energy structures in all cases, strongly prefers planar hydrogen bonding arrangements with the O^- doubly occupied p electrons, while leaving the remaining unpaired p electron free for chemical interaction with any available solutes. In the $(OH^-)(OH)(H_2O)_{n-1}$ family, on the other hand, nonplanar hydrogen bonding arrangements are the rule about the anionic center, with the OH^- moiety acting only as a hydrogen bond acceptor, never as a donor. In both families the first-shell water molecule OH bonds that are involved in making strong hydrogen bonds to the anionic center are significantly stretched by an amount that correlates quantitatively with the associated O–O distance.

Future Plans

Immediate plans are to continue the optical transient absorption measurements of OH radical and hydrated electron reaction rates. Calculations are in progress to characterize the nature of the OH absorption at 250nm in water, with a view toward understanding why this absorption seems to disappear in supercritical water. In the case of OH reactions, the transient absorption experiments will be complemented by measurements of product yields to infer reaction rates by competition. A most important target is the reaction H_2 + OH in supercritical water. Mechanisms of prototypical radiolytic reactions in aqueous solution such as H + OH → H_2O, H_2 + OH → H + H_2O, H_2 + O- → H + OH-, OH + OH → H_2O_2 and OH + OH- → O- + H_2O , as well as the OH/O- equilibrium, will be characterized by ab initio methods as initial steps toward the ultimate goal of understanding their unusual temperature dependences.

A major new effort will involve direct EPR measurements of free radicals in supercritical water. The primary target of this experiment is the hydrogen atom. The hydrogen atom is the prototypical free radical, and its reactions in condensed phase are naturally a subject of great theoretical interest. Moreover, extensive isotope effect information can be generated by comparison of D atom and muonium atom reactions. H (and D) atoms are readily generated in acidic water by electron beam radiolysis. Time-resolved EPR is found to be a convenient and specific technique for H atom detection. The large hyperfine coupling of H or D atoms make their signals unambiguous. Virtually always, time-resolved H atom signals are found to be polarized by Chemically Induced Dynamic Electron Polarization (CIDEP) in the radical recombination reactions.

The most exciting aspect of EPR detection of H and D atoms in sc-water is the potential to measure CIDEP in the H+H and D+D recombination reactions. One can calculate an average polarization enhancement per diffusional encounter, from a stochastic Liouville equation description of the combined spin and spatial diffusion. The enhancements depend upon the time-integrated spin exchange between the radicals of a pair during a diffusive encounter, and the degree of singlet triplet mixing (proportional to the difference in Larmor frequencies of the two radicals). Because spin exchange is typically very short-ranged and singlet-triplet mixing is slow, the phenomenon is sensitive to re-encounters and the full diffusional dynamics. Polarization enhancements have been calculated for the simple case of spherical radicals freely diffusing in a continuum. H atoms in liquid water may come close to this idealization, but

quantitative measurements on this system have never been successfully carried out even at room temperature. Diffusion is never fully free, and forces between the radicals will affect the size of the polarization enhancements. The size of polarization generated in these encounters can readily be estimated via the stochastic Liouville equation, assuming some relative diffusion governed by a potential of mean force. Will the mean force of the solvent in sc-water effectively keep H atoms apart or hold them together? How sensitive will the CIDEP be to the solvent density? Will the H + H recombination remain in the diffusion limit or become "third-body" limited?

Publications, 2003-2005

Bartels, D. M., K. Takahashi, et al. (2005). "Pulse radiolysis of supercritical water. 3. Spectrum and thermodynamics of the hydrated electron." Journal of Physical Chemistry A 109(7): 1299-1307.

Chipman, D. M. and J. Bentley (2005). "Structures and Energetics of Hydrated Oxygen Anion Clusters." J. Phys. Chem. A 109: 7418.

Garrett, B. C., D. A. Dixon, et al. (2005). "Role of water in electron-initiated processes and radical chemistry: Issues and scientific advances." Chemical Reviews 105(1): 355-389.

Marin, T. W., D. M. Bartels, et al. (2004). "Evaluation of silica-coated tubing for the measurement of hydrogen peroxide in hot water." Industrial & Engineering Chemistry Research 43(8): 1888-1889.

Marin, T. W., C. D. Jonah, et al. (2004). "Erratum: Reaction of OH Radicals with H_2 in Subcritical Water(vol 371, pg 144, 2002)." Chemical Physics Letters 373: 228.

Mezyk, S. P., W. J. Cooper, et al. (2004). "Free radical destruction of N-nitrosodimethylamine in water." Environmental Science & Technology 38(11): 3161-3167.

Mezyk, S. P., J. Jones, et al. (2004). "Radiation chemistry of methyl tert-butyl ether in aqueous solution." Environmental Science & Technology 38(14): 3994-4001.

Takahashi, K. J., S. Ohgami, et al. (2004). "Reaction rates of the hydrated electron with N2O in high temperature water and potential surface of the N2O- anion." Chemical Physics Letters 383(5-6): 445-450.

Marin, T. W., C. D. Jonah, et al. (2003). "Reaction of $OH^{\cdot}$ radicals with H_2 in sub-critical water." Chemical Physics Letters 371(1-2): 144-149.

Ionic Liquids: Radiation Chemistry, Solvation Dynamics and Reactivity Patterns

James F. Wishart
Chemistry Department, Brookhaven National Laboratory, Upton, NY 11973-5000
wishart@bnl.gov

Program Definition

Ionic liquids (ILs) are a rapidly expanding family of condensed-phase media with important applications in energy production, nuclear fuel and waste processing, improving the efficiency and safety of industrial chemical processes, and pollution prevention. ILs are nonvolatile, noncombustible, highly conductive, recyclable and capable of dissolving a wide variety of materials. They are finding new uses in chemical synthesis, catalysis, separations chemistry, electrochemistry and other areas. Ionic liquids have dramatically different properties compared to conventional molecular solvents, and they provide a new and unusual environment to test our theoretical understanding of charge transfer and other reactions. We are interested in how IL properties influence physical and dynamical processes that determine the stability and lifetimes of reactive intermediates and thereby affect the courses of chemical reactions and product distributions.

Successful use of ionic liquids in radiation-filled environments, where their safety advantages could be significant, requires an understanding of ionic liquid radiation chemistry. For example, characterizing the primary steps of IL radiolysis will reveal radiolytic degradation pathways and suggest ways to prevent them or mitigate their effects on the properties of the material. An understanding of ionic liquid radiation chemistry will also facilitate pulse radiolysis studies of general chemical reactivity in ILs, which will aid in the development of applications listed above. Very early in our radiolysis studies it became evident that slow solvation dynamics of the excess electron in ILs (which vary over a wide viscosity range) increases the importance of pre-solvated electron reactivity and consequently alters product distributions. Parallel studies of IL solvation phenomena using coumarin-153 dynamic Stokes shifts and polarization anisotropy decay rates are done to compare with electron solvation studies and to evaluate the influence of ILs on charge transport processes.

Methods. Picosecond pulse radiolysis studies at BNL's Laser-Electron Accelerator Facility (LEAF) are used to identify reactive species in ionic liquids and measure their solvation and reaction rates. IL solvation and rotational dynamics are measured by TCSPC and fluorescence upconversion measurements in the laboratory of E. W. Castner at Rutgers Univ. Diffusion rates are obtained by PGSE NMR in S. Greenbaum's lab at Hunter College, CUNY. We and our collaborators (R. Engel (Queens College, CUNY) and S. Lall-Ramnarine, (Queensborough CC, CUNY)) develop and characterize new ionic liquids specifically designed for our radiolysis and solvation dynamics studies. Professor Mark Kobrak of CUNY Brooklyn College performs molecular dynamics simulations of solvation processes.

Recent Progress

Solvated Electrons. Experiments performed at LEAF demonstrated for the first time that radiolysis of $[R_4N][NTf_2]$ $[R_4N][N(CN)_2]$, and $[R_4P][N(CN)_2]$ ionic liquids produces solvated electrons that absorb over a broad range in the near infrared and persisting for hundreds of nanoseconds [1,3,5]. The e_{solv}^- spectra of NTf_2^- salts of the *N*-methyl,*N*-butylpyrrolidinium (P_{14}^+) and hexyltributylammonium ($HxBu_3N^+$) cations are shown at right. (Each spectrum is representative of four examples of liquids with similar structures.) The differences in band shape and position indicate different distributions of electron solvation cavity sizes and shapes as a function of cation structure, the nature of which may be revealed by future MD simulations.

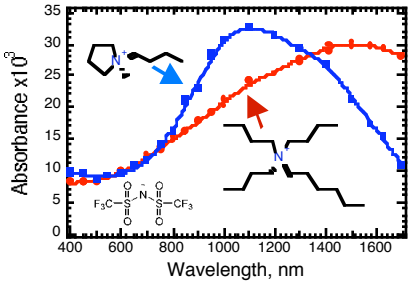

Pre-solvated electron reactivity and solvation dynamics in ILs. In the course of kinetic measurements described below it was found that relatively low scavenger concentrations substantially reduced the initial yield of solvated electrons [1]. Direct scavenging of pre-solvated ("dry") electrons competes effectively with the slower electron solvation processes in ionic liquids. For example, a pyrene concentration of only 63 mM reduces the solvated electron yield to 37% of the scavenger-free value. This finding has major implications for processing of

radioactive materials, where seemingly innocuous quantities of solutes may scavenge electrons very effectively. Conversely, dry electron scavenging facilitates the use of pulse radiolysis in electron transfer studies by providing a way to circumvent diffusion-limited precursor formation rates. Measurements of excess electron solvation processes and emission dynamics (Stokes shift and polarization anisotropy decay) of solvatochromic coumarin-153 show that the reorganization dynamics of ionic liquids occur on much longer timescales (nanoseconds) than in conventional polar solvents (picoseconds). The slow solvation dynamics would also be expected to significantly alter transition state dynamics and provide a potential means to control product distribution. This becomes particularly important for transition states with a very different polarity from the reactants and/or products.

To look at electron solvation with higher time resolution, we used low-viscosity pyrrolidinium salts and developed novel ionic liquids with even lower melting points and viscosities, based on ether-substituted pyrrolidinium cations [5]. These liquids have RT viscosities low enough (65-95 cP) to flow through the picosecond pulse-probe transient absorption system at LEAF, which requires sample exchange to avoid cumulative radiation effects. Consequently, the electron solvation process was directly observed in three ILs by monitoring the decay of pre-solvated electrons at multiple wavelengths (to yield a solvated electron spectrum similar to the blue curve above). In *N*-methyl,*N*-butyl-pyrrolidinium NTf_2^- the electron solvation lifetime $<\tau_{solv}>$ is 260 ps, while $<\tau_{solv}>$ obtained from coumarin 153 Stokes shift measurements is 220 ps.

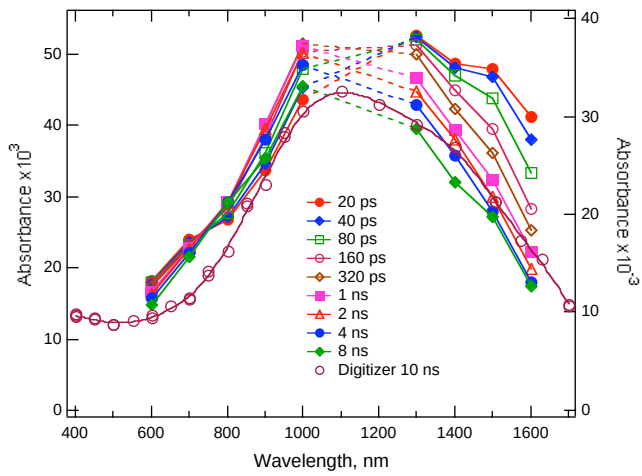

Even slower solvation processes were observed in pulse radiolysis studies of ionic liquids containing ether-, alcohol- and alkyl-functionalized quaternary ammonium dications $(CH_3)_2(R)N^+(CH_2)_nN^+(R)(CH_3)_2\ (NTf_2^-)_2$, where R = $(CH_2)_3OH$, $(CH_2)_2OCH_2CH_3$, or $(CH_2)_3CH_3$ and n = 3–8. Spectra on nanosecond timescales revealed that solvation of the excess electron is particularly slow in the case of the alcohol-derivatized ionic liquids. The blue shift of the electron spectrum to the customary 650 nm peak takes 25-40 nanoseconds at RT (viscosities ~4500-6800 cP). Comparison with the ~1 ns electron solvation time observed in similarly viscous 1,2,6-trihydroxyhexane (2500 cP) reveals the hindering effect of the ionic liquid lattice on hydroxypropyl side chain reorientation [4].

Reaction rates. Electron reactions with several aromatic acceptors, acids, and oxygen were measured in $(MeBu_3N^+)(NTf_2^-)$. Rate constants for solvated electron capture by benzophenone, pyrene and phenanthrene were on the order of $1.6 \times 10^8\ M^{-1}\ s^{-1}$, typically 100 times slower than observed in conventional polar solvents [1]. The reactions of hydrogen atoms with several of the same reactants were measured in the same ionic liquid. H-atoms react very rapidly with pyrene and phenanthrene ($\sim 3 \times 10^9\ L\ mol^{-1}\ s^{-1}$) to form H-adduct radicals [2]. The H-atom rate constants are similar to the values measured or estimated for the same reactions in aqueous solutions. The H-atom reactions with the aromatic hydrocarbons must be diffusion-controlled. but are faster than diffusion-controlled reactions for solvated electrons in the same ionic liquid.

The results indicate that the diffusion rate for the solvated electron in ionic liquids can be significantly lower than those of small neutral molecules or radicals such as the H-atom, in contrast to the situation in molecular solvents. These results support the contention that the diffusion constants of charged and neutral reactants differ considerably in ionic liquids, which could lead to a means of controlling reactivity and transport phenomena through rational selection of ionic liquid properties.

Future Plans

Electron solvation and reactivity. The validity of proposed pre-solvated electron scavenging mechanisms will be tested by exploring the competition between the electron solvation and electron capture processes in ionic liquids. Electron solvation dynamics in several families of low-viscosity ILs will be measured by pulse-probe radiolysis. Subsequently, scavengers will be added to measure the kinetics of pre-solvated electron capture. It is well

known from work in molecular solvents that many scavengers, for example SeO_4^{2-}, have widely different reactivity profiles towards pre-solvated and solvated electrons. By quantitative measurement of the scavenging profiles of many reactants, we hope to explain such conundrums mechanistically.

Many ionic liquids with slow electron solvation rates are too viscous to be flowed for pulse-probe experiments. Detailed studies of electron solvation in these ILs will be possible upon installation of the "ultrafast single-shot" detection system at LEAF. In the meantime, C-153 solvation dynamics studies will serve as proxies for the electron results to aid the study of pre-solvated electron scavenging mechanisms as measured by "time-zero" radiolytic product yields.

Charge transport in ionic liquids. Pulse radiolysis will be used to study how ionic liquids affect charge-transport reactions related to solar energy photoconversion systems, where their characteristics may prove valuable. IL-based photoelectrochemical cells have already been reported. Focus areas will be the combined effects of ionic solvation and slow solvent relaxation on the energy landscape of charge transport, including specific counterion effects depending on the ionic liquid, and the influence of the lattice-like structure of ionic liquids on the distance dependence of electron transport reactions.

Non-classical diffusion in ionic liquids. Ionic liquids contain considerable void space due to the poor packing that makes them liquids instead of solids. The combination of voids and the ionic lattice result in unusual diffusion rate trends reported in the literature. Kinetic and high-pressure pulsed-gradient spin echo NMR studies of diffusion rates of charged and neutral species will examine how ionic liquids modulate diffusion as a function of size and charge.

Publications on ionic liquids

1. *Spectrum and Reactivity of the Solvated Electron in the Ionic Liquid Methyltributylammonium Bis(trifluoromethylsulfonyl)imide* J. F. Wishart and P. Neta *J. Phys. Chem. B* **107,** 7261-7267 (2003).
2. *Pulse Radiolysis Study of the Reactions of Hydrogen Atoms in the Ionic Liquid Methyltributylammonium Bis(trifluoromethylsulfonyl)imide* J. Grodkowski, P. Neta and J. F. Wishart *J. Phys. Chem. A*, **107,** 9794-9799 (2003).
3. *Radiation Chemistry of Ionic Liquids: Reactivity of Primary Species* J. F. Wishart in "Ionic Liquids as Green Solvents: Progress and Prospects" Rogers, R. D. and Seddon, K. R., Eds.; *ACS Symp. Ser*. **856**, Ch. 31, pp. 381-396, American Chemical Society, Washington, DC, 2003.
4. *Effects of Functional Group Substitution on Electron Spectra and Solvation Dynamics in a Family of Ionic Liquids* J. F. Wishart, S. I. Lall-Ramnarine, R. Raju, A. Scumpia, S. Bellevue, R. Ragbir, and R. Engel *Radiat. Phys. Chem.* **72**, 99-104 (2005).
5. *Dynamics of Fast Reactions in Ionic Liquids* A. M. Funston and J. F. Wishart in "Ionic Liquids IIIA: Fundamentals, Progress, Challenges and Opportunities" Rogers, R. D. and Seddon, K. R., Eds.; *ACS Symp. Ser*. **901**, Ch. 8, American Chemical Society, Washington, DC, 2005. (ISBN 0-84123-893-6).
6. *Ultrafast Dynamics of Pyrrolidinium Cation Ionic Liquids* H. Shirota, A. M. Funston, J. F. Wishart, E. W. Castner, Jr. *J. Chem. Phys.* **122**, 184512 (2005), selected for the *Virtual Journal of Ultrafast Science* (6/05).
7. *Radiation Chemistry of Ionic Liquids* J. F. Wishart, A. M. Funston, and T. Szreder in "Molten Salts XIV, Proceedings of the 2004 Joint International Meeting of the Electrochemical Society, Honolulu, HI, 2004", R. A. Mantz and P. Trulove, Eds. The Electrochemical Society, Inc., Pennington, NJ, 2005.

Publications on other subjects

8. *Reactions of Charged Species in Supercritical Xenon as Studied by Pulse Radiolysis* R. A. Holroyd, J. F. Wishart, M. Nishikawa, and K. Itoh *J. Phys. Chem. B* **107,** 7281-7287 (2003).
9. *Do Main Chain Hydrogen Bonds Create Dominant Electron Transfer Pathways? An Investigation in Designed Proteins* Y. Zheng, M. A. Case, J. F. Wishart, and G. L. McLendon *J. Phys. Chem. B* **107,** 7288-7292 (2003).
10. *Radiation Chemistry of Methyl*-tert-*Butyl Ether (MTBE) in Aqueous Solution* S. P. Mezyk, J. Jones, W. J. Cooper, T. Tobien, M. G. Nickelsen, J. W. Adams, K. E. O'Shea, D. M. Bartels, J. F. Wishart, P. M. Tornatore, K. S. Newman, K. Gregoire, and D. J. Weidman *Envir. Sci. Tech.*, **38**, 3994-4001 (2004).

11. *Long-Range Electron Transfer across Peptide Bridges: the Transition from Electron Superexchange to Hopping* R. Abdel Malak, Z. Gao, J. F. Wishart, and S. S. Isied, *J. Am. Chem. Soc.* **126**, 13888-13889 (2004).
12. *Convergence of Spectroscopic and Kinetic Electron Transfer Parameters for Mixed-Valence Binuclear Dipyridylamide Ruthenium Ammine Complexes* A. J. Distefano, J. F. Wishart, and S. S. Isied *Coord. Chem. Rev.*, **249**, 507-516 (2005).
13. *The LEAF Picosecond Pulse Radiolysis Facility at Brookhaven National Laboratory* J. F. Wishart, A. R. Cook, and J. R. Miller *Rev. Sci. Inst.* **75**, 4359-4366 (2004), selected for the *Virtual Journal of Ultrafast Science* (12/04).
14. *Search for the 3-body Photodisintegration of Be* D. E. Alburger, R. E. Chrien, R. J. Sutter, and J. F. Wishart, *Phys. Rev. C* **70**, 064611 (2004).
15. *Radiolysis with RF Photoinjectors: Supercritical Xenon Chemistry* J. F. Wishart in "Femtosecond Beam Science" Uesaka, M., Ed.; Imperial College Press, London, in press.

Understanding Nanoscale Confinement Effects in Solvent-Driven Chemical Reactions

Ward H. Thompson
Department of Chemistry, University of Kansas, Lawrence, KS 66045
Email: *wthompson@ku.edu*

Program Scope

It is now possible to synthesize nanostructured porous materials with a tremendous variety of properties including sol-gels, zeolites, organic and inorganic supramolecular assemblies, reverse micelles, vesicles, and even proteins. The interest in these materials derives from their potential for carrying out useful chemistry (*e.g.*, as microporous and mesoporous catalysts with critical specificity, fuel cell electrodes and membranes, molecular sieves, and chemical sensors) and for understanding the chemistry in similar systems found in nature. Despite the advances in synthetic techniques, our understanding of chemistry in solvents confined in nanoscale cavities and pores is still relatively limited. Ultimately, one would like to design nanostructured materials adapted for specific chemical purposes, *e.g.*, catalysis or sensing, by controlling the cavity/pore size, geometry, and surface chemistry. To develop guidelines for this design, we must first understand how the characteristics of the confining framework affect the chemistry. Thus, we are addressing the fundamental question *How does a chemical reaction occur differently in a nano-confined solvent than in a bulk solvent?*

Solvent-driven reactions, typically those involving charge transfer, should be most affected by confinement of the solvent. The limited number of solvent molecules, geometric constraints of the nanoscale confinement, and solvent-wall interactions can have dramatic effects on both the reaction energetics and dynamics. Our primary focus is on proton transfer – a key class of solvent-driven reactions of widespread importance in chemistry and biology – and related processes. A fundamental understanding of proton transfer reactions in nano-confined solvents will impact many areas of chemistry in addition to providing important insights into the larger class of solvent-driven reactions. The diversity among nanocavities (*e.g.*, in their size, shape, flexibility, and interactions with the solvent and/or reactants) makes it difficult to translate studies of one system into predictions for another. Thus, we are focusing on developing a unified understanding of reaction dynamics in the diverse set of confinement frameworks.

Recent Progress

Proton Transfer. A model intramolecular phenol-amine proton transfer system in a CH_3Cl solvent confined in a smooth, hydrophobic spherical cavity has been investigated. We have developed a valence bond description for the reaction complex based loosely on a widely applied model.[1] Monte Carlo and mixed quantum-classical molecular dynamics

simulations have been used to investigate complex position distributions, free energy curves, and proton transfer reaction dynamics.

The key results of Monte Carlo simulations[2] in spherical, hydrophobic nanocavities are 1) The reactant proton transfer complex is located near the cavity wall while the product complex is found primarily in the interior (analogous to the case of charge transfer chromophores[3–5]). 2) The reaction free energy depends strongly on the reaction complex position varying from endothermic (by $\sim$ 1 kcal/mol) near the cavity wall to exothermic (by $\sim$ 5 kcal/mol) deep in the cavity interior. Together these demonstrate that the reaction coordinate must involve motion of the reaction complex from near the cavity wall to the interior (analogous to previous time-dependent fluorescence results[4]). We observe small, but not dramatic, cavity size effects on the position distributions and free energy curves for fixed complex position.

That the reaction complex position is part of the reaction coordinate for proton transfer in these nanoconfined solvents is confirmed by mixed quantum-classical molecular dynamics simulations in which the proton is treated quantum mechanically while all the other coordinates are described classically. Specifically, we have used vibrationally adiabatic simulations (based on nonequilibrium trajectories initiated as reactants) to a first-order look at the rate constants and reaction mechanism.[6] The results show that the reaction becomes more exothermic and the rate constants increase as the cavity is made larger. This is attributed to an increase in the effective solvent polarity as the cavity size is increased. It is also found that the reaction free energies decrease and the rate constants increase as the O-N hydrogen bond distance is lengthened. This is attributed to the increased dipole moment of the ion pair product complex as R_{O-N} is elongated. This leads to better solvation of the products compared to the reactants, thereby decreasing ΔG_{rxn}.

On the basis of the Monte Carlo results[2] it was expected that three possible mechanisms might be observed. Specifically, the reaction must involve both solvent reorganization (as in a proton transfer reaction in bulk solvent) and motion of the reaction complex from near the wall (where reactants are favored) to the cavity interior (where products are favored). These can occur with solvent reorganization preceding the complex motion, reactant complex motion into the cavity interior preceding solvent reorganization, or concerted complex motion and solvent reorganization. In the mixed quantum-classical molecular dynamics simulations, all three mechanisms are observed. The concerted pathway occurs relatively rarely. The dominant pathway involves solvent reorganization followed by diffusion of the nascent products into the cavity interior. However, the relative contribution of the two major pathways depends on both cavity size and O-N distance. Specifically, the mechanism in which reactant complex motion into the cavity interior precedes solvent reorganization becomes more prevalent as the cavity size is increased. This is attributed to the changes in the layered solvent density. This same mechanism becomes less prevalent as the heavy atom distance is increased for fixed cavity size. This is attributed to better solvation of the product complex as R_{O-N} is increased in the polar methyl chloride solvent. The effect of

including vibrationally nonadiabatic transitions in the rate constants, kinetic isotope effects, and mechanism is an important issue that is being addressed by surface hopping simulations.

Conformational Equilibria. We have also investigated conformational energetics in nanoconfined solvents. This is an important issue in the rational design of microporous and mesoporous catalysts where conformational dynamics and energetics can affect both catalyst activity and selectivity. To address this issue we have used Monte Carlo simulations with umbrella sampling to calculate two-dimensional free energy surfaces of 1,2-dichloroethane (DCE) in nanoconfined methanol.[7] Specifically, the free energy has been obtained as a function of the solute position and DCE dihedral angle in spherical hydrophobic cavities. The free energy surfaces obtained from the simulations are somewhat complex with several local minima. The structure of the free energy surfaces is strongly influenced by the solvent radial density (*i.e.*, how the methanol solvent packs in the nanocavity), which shows significant layering. Both the *trans* and *gauche* conformers have local minima corresponding to the DCE molecule lying in each of the solvent layers. In addition, the *trans* conformer has additional minima at (center-of-mass) positions between solvent layers in which the DCE molecule is aligned perpendicular to the cavity wall with a CH_2-Cl moiety in each layer. This perpendicular orientation is primarily due to packing effects and is only weakly affected by the DCE electrostatic interactions. These features of the free energy surfaces indicate that the most stable conformer depends strongly on the position of the DCE molecule in the cavity. We are currently investigating the conformational dynamics for this system.

Future Plans

We are currently pursuing a number of extensions of the work described above. We are investigating the effects of solvent flexibility and polarizability on energetics and dynamics in nanoconfinement. We are extending the mixed quantum-classical molecular dynamics simulations to include quantization of the hydrogen bond, *e.g.*, O-N, coordinate. In addition, we are developing valence bond models for more realistic phenol-amine proton transfer systems (both intermolecular and intramolecular). Finally, we are systematically investigating the effect of surface chemistry on reactivity in confined solvents as is now described.

Chemistry in Silica Pores. Atomically smooth confining frameworks are convenient for exploring many of the fundamental effects of nanoscale confinement on chemistry (and display interesting and complex dynamics). However, these models lack two critical features: molecular-scale roughness and site-specific chemical functionality (*e.g.*, hydrogen bonding). Atomistic cavity and pore models alleviate these problems but at the expense of computational efficiency. We have developed hybrid amorphous silica pore models that provide the critical features missing in atomically smooth frameworks but at a reasonable computational effort. Specifically, the system is divided into a several Ångstroms thick atomistic region that defines the pore surface and an exterior region that contains all the remaining wall atoms that are treated implicitly as an external potential.

These models will be used to investigate the critical question *How does the surface chem-*

istry of the confining framework affect reactivity in a nanoconfined solvent? Specifically, we have developed an approach for systematically varying the surface chemistry of these silica pores from hydrophilic to hydrophobic. Starting from the unterminated amorphous silica a hierarchy of stressed Si-O bonds that would be readily cleaved by hydrolysis is determined and used to introduce surface silanol moieties. Altering the stress cutoff for the hydrolysis event leads to various silanol surface densities. Alternatively, hydrophobic modification to the surface can be achieved though replacement of the silanol moieties with other functional groups (*e.g.*, -OCH_3). We are currently validating these silica pore models by investigating the conformational equilibria of ethylene glycol in pores of varying size and surface chemistry; these results can be directly compared with previous experimental measurements of the *trans-gauche* equilibrium in sol-gel pores.[8] Subsequently, we will investigate (intramolecular, intermolecular, and surface) proton transfer reactions in these pores as a function of the surface chemistry.

References

[1] H. Azzouz and D. Borgis, *J. Chem. Phys.* **98**, 7361-7375 (1993).

[2] †S. Li and W.H. Thompson, *J. Phys. Chem. B* **109**, 4941-4946 (2005). "Proton Transfer in Nano-confined Polar Solvents. I. Free Energies and Solute Position "

[3] W.H. Thompson, *J. Chem. Phys.* **117**, 6618-6628 (2002).

[4] †W.H. Thompson, *J. Chem. Phys.* **120**, 8125-8133 (2004). "Simulations of Time-Dependent Fluorescence in Nano-Confined Solvents"

[5] †J.A. Gomez and W.H. Thompson, *J. Phys. Chem. B* **108**, 20144-20154 (2004). "Monte Carlo Simulations of Absorption and Fluorescence Spectra in Ellipsoidal Nanocavities"

[6] †W.H. Thompson, *J. Phys. Chem. B* ASAP, (2005). "Proton Transfer in Nano-confined Polar Solvents. II. Adiabatic Proton Transfer Dynamics"

[7] †J.A. Gomez, A.K. Tucker, T.D. Shepherd, and W.H. Thompson, *J. Phys. Chem. B* **109**, 17479-17487 (2005). "Conformational Free Energies of 1,2-Dichloroethane in Nanoconfined Methanol"

[8] R.-S. Luo and J. Jonas, *J. Raman. Spectrosc.* **32**, 975-978 (2001).

[9] †S. Li, T.D. Shepherd, and W.H. Thompson, *J. Phys. Chem. A* **108**, 7347-7355 (2004). "Simulations of the Vibrational Relaxation of a Model Diatomic Molecule in a Nanoconfined Polar Solvent"

[10] †S. Li and W.H. Thompson, *Chem. Phys. Lett.* **405**, 304-309 (2005). "How Accurate is Time-Independent Perturbation Theory for Calculating Frequency Shifts of Diatomic Molecules in Rare Gas Fluids?"

†DOE-sponsored publication.

Molecular Theory & Modeling

Recent advances in computer simulations of molecular processes at liquid water surface

Liem X. Dang and Collin Wick
Chemical Sciences Division
Pacific Northwest National Laboratory
902 Battelle Blvd., Mail Stop K1-83
Richland, WA 99352
liem.dang@pnl.gov

Summary. The adsorption and distribution of ions at aqueous liquid interfaces are fundamental processes encountered in a wide range of chemical and biological systems. In particular, the manner in which solvent molecules solvate ions is relevant to problems in chemical and physical processes. For example, solvation of ions affects chemical reactions at interfaces and the distribution of ions and/or counter-ions influences the structure and stability of large molecules and membranes. The focus of research on this project is the characterization of solvation processes at aqueous liquid interfaces using molecular dynamics (MD) computer simulation techniques. We develop fundamental, molecular-scale information about the interactions of ions and molecules in solvent phases and across aqueous liquid interfaces. We focus special effort on understanding the precise mechanism and dynamics of the transfer process, and on learning the role of many-body effects on the transfer mechanism of solutes across the aqueous liquid interface. We use MD simulations to compute potentials of mean force for dilute solutions and density profiles in concentrated solutions. In addition, research on chemical separation science involves the development of methods and potential models for use in the simulation of crown ether molecules mediating ion transport across water-organic liquid interfaces. Results of this research further our understanding of ion transport across liquid-liquid interfaces, which in turn, provides basic knowledge needed to address DOE's environmental restoration issues.

Hydroxyl radical at the air-water interface. In order to assess the OH solvation behavior on a long time scale, a free energy profile for transfer of an OH radical across the air/water interface was calculated using a constrained molecular dynamics technique. The radical was transferred along the normal to the interface (z). The free energy profile is defined up to an arbitrary additive constant corresponding to the free energy of a reference state, which was chosen to be the water slab with the hydroxyl radical located in the gas phase. The resulting free energy profile as well as the density profile are shown in Figure1 and 2. Our calculated value of the free energy of solvation, $\Delta G_s = -3.0$ kcal/mol, agrees well with the experimental value of $\Delta G_s = -3.9 \pm 0.3$ kcal/mol. This results provides a validation of our revised OH force field employed in this work. The present OH parametrization represents a refinement of the force field used in our previous study, which underestimated the OH–water binding as well as the OH hydration free energy. Due to its radical character, it is rather difficult to accurately describe the hydroxyl by a simple empirical force field. Yet, the fact that with the revised OH force field it was possible to reach a reasonable agreement between the calculated and experimental free energy of solvation indicates that MD simulations with empirical potentials can provide a very useful insight into the processes at the air/water interface involving radicals. The future work is to look at how the presence of ions influences the OH that include the calculations of free energy profiles of OH for NaCl, NaBr, and NaI solutions to compare it with pure water.

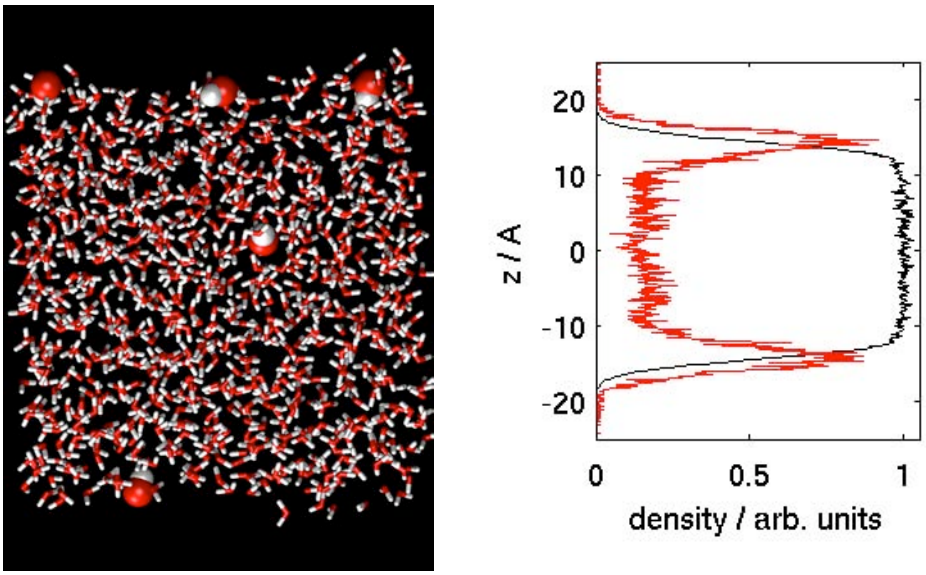

Figure 1. (a) A snapshot from the simulation of five OH radicals in the water slab. (b) Density profiles of OH (in red) and H_2O (in black) indicating the propensity of OH for the air/water interface.

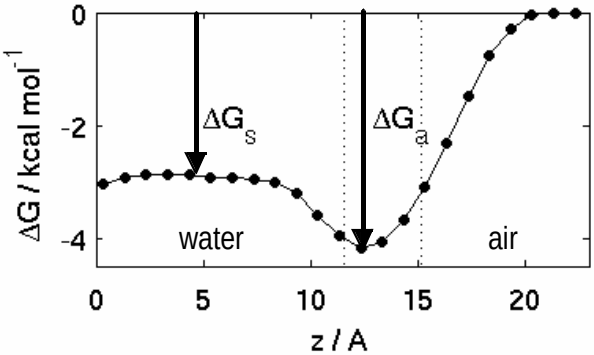

Figure 2. Free energy profile for transfer of a OH radical across the air/water interface. The interfacial region is indicated by the dotted lines. ΔG_s denotes the free energy of bulk solvation, and ΔG_a the free energy of adsorption on the water surface.

Cesium and iodide ion distributions at H_2O-vapor and H_2O-CCl_4 interfaces. Molecular dynamics simulations of H_2O-CCl_4 and H_2O-vapor interfaces were carried out at different cesium and iodide ion concentrations to compare ion distribution, interfacial orientational and structural properties, and dynamics. It was found that cesium was repelled by both interfaces, but iodide was active at both interfaces, but to a much greater degree at the H_2Ovapor interface as demonstrated in Figure 3. The Iodide induced dipole was found to increase at the interface, and orient perpendicular to the interface for both systems, leading to stronger hydrogen bonds with water. For the H_2O-CCl_4, though, there was a compensation between these strong hydrogen bonds and short to moderate ranged repulsion between iodide and CCl_4. Ion pairing was found to be higher at the H_2O-CCl_4 interface than at the H_2O-vapor interface, and the lowest in the water bulk. Hydrogen bond distance and angular distributions showed weaker water-water hydrogen bonds at both interfaces, but generally stronger water-iodide hydrogen bonds at them. Both translational and rotational dynamics of water were faster at the interface, while for CCl_4, its

translational dynamics was slower, but rotational dynamics faster at the interface. For many of the studied systems and species, translational diffusion was found to be anisotropic at both interfacial and bulk regions.

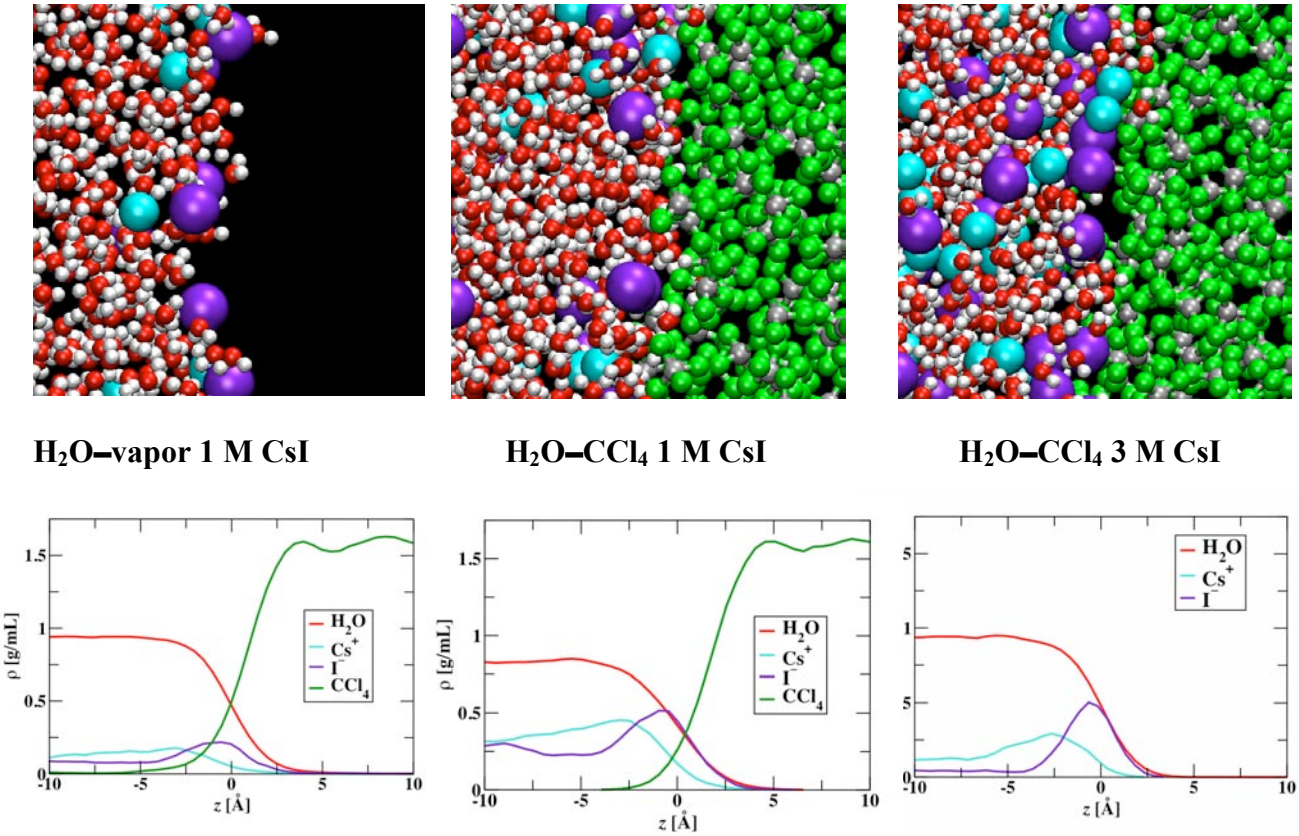

Figure 3. Snapshots from the simulations of CsI ions in the water slab. (b) Density profiles of CsI ions indicating the propensity of CsI for the water interfaces.

HI at the water liquid/vapor interface. We carried out simulations to characterize solvation properties of hydronium-iodide (HI) salt at the water liquid/vapor interface. In Figure 4, we present the density profiles for water center-of-mass, oxygen atoms in H_3O^+ ions, and I^- ions obtained from a MD simulation. Upon examining these density profiles as well as the MD simulation snapshots, we can make the following observations. 1) A significant number of iodide anions are present near the Gibbs dividing surface (GDS) and form well-defined maximum, and the H_3O^+ molecules are found to have enhanced concentration near the interface with significant population at the interface. 2) These results differ from the results of NaI salt at the water

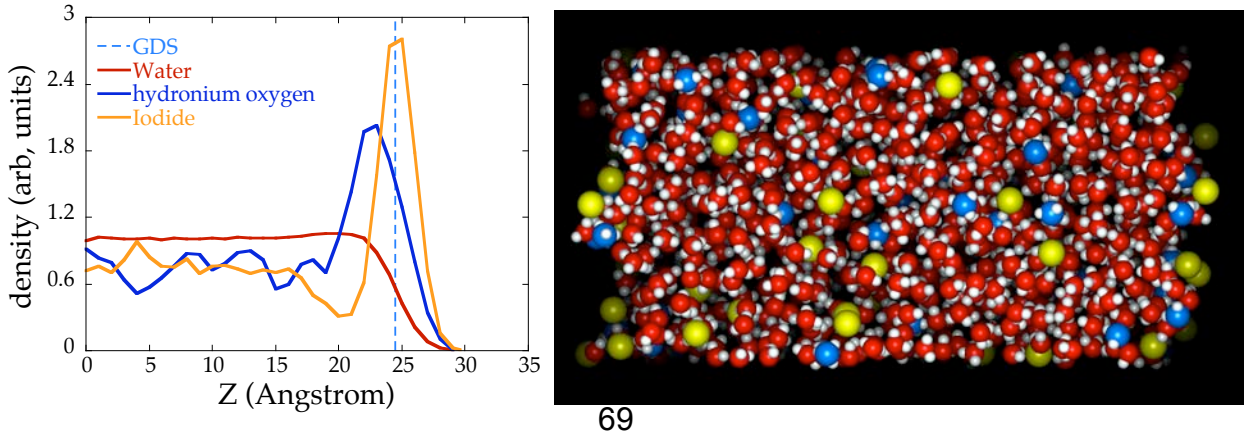

Figure 4. Computed density profiles of HI and a molecular dynamics snapshot of HI at the liquid/vapor interface water. The Gibbs dividing surface (GDS) is the location where the solvent density is half its bulk value. At the right, O atoms in H_3O^+ and I^- ions are indicated by blue and yellow spheres, respectively. Interfaces are at the left and right of the right image.

liquid/vapor interface, in which the width of the electric double layer is smaller. The new results are supported by our earlier studies on the potential of mean force for the transport mechanism of an ion (Na^+ and H_3O^+) across the water liquid/vapor interface. In the previous studies, the computed H_3O^+ potential of mean force indicates that H_3O^+ is found closer to the dividing surface than the Na^+, and the computed free energy for H_3O^+ is lower (about 6 kcal/mol) at the dividing surface. 3) It is interesting to point out that the hydration energies of H_3O^+ and Na^+ are nearly identical; therefore, the different behavior of these ions at the aqueous interface can be attributed to the differences in the shape, charges distribution, as well as the polarizability of the ion used in our classical simulations.

The mechanism of proton transport in liquid water is quantum mechanical in nature; therefore, our classical polarizable model for H_3O^+ (*i.e.*, fixed charge) may not accurately capture the H_3O^+ - H_2O interaction. It is well known that the proton diffusion mechanism in water will strongly influence the results and this mechanism is also known to have non-negligible quantum effects. An accurate study of the proton transport mechanism requires quantum statistical treatment of the hydrogen motion in liquid water. Thus, extension of our study to include quantum effects and comparison of the results to the results presented in this paper will be a worthwhile next step. It remains to be seen whether the mechanism of proton transport will have a significant effect on the distribution of H_3O^+ at the interface. Finally, the present study may also contribute to the understanding of ion-induced nucleation of water vapor, which is thought to be an importance in many atmospheric processes

Collaborators on this project include Tsun-Mei Chang, Collin Wick, Bruce C. Garrett, Gregory Schenter, John Fulton, Matina Roeselova, Pavel Jungwirth and Douglas J. Tobias (UC, Irvine).

<u>References to publications of DOE sponsored research (2003-present)</u>

1. L. X. Dang, "Solvation of the Hydronium Ion at the Water Liquid/Vapor Interface," *Journal of Chemical Physics* **11**9, 6351 (2003).

2. T. M. Chang and L. X. Dang, "On Rotational Dynamics of an NH_4^+ Ion in Water," *Journal of Chemical Physics* **11**8, 8813 (2003).

3. L. X Dang and T. M. Chang, "Many-Body Interactions in Liquid Methanol and its Liquid/Vapor Interface: A Molecular Dynamics Study," *Journal of Chemical Physics* **11**9, 9851 (2003).

4. L. X. Dang, G. K. Schenter and J. L. Fulton "EXAFS Spectra of Dilute Solutions of Ca^{2+} and Sr^{2+} in Water and Methanol," *Journal Phys. Chem*. **B 107**, 14119 (2003).

5. L. X. Dang and B. C. Garrett. "Molecular Mechanism of Water and Ammonia Uptake by the Liquid/Vapor Interface of Water" *Chemical Physics Letters 385, 309 (2004).*

6. L. X. Dang, "Ions at the Liquid/Vapor Interface of Methanol" *Journal of Physical Chemistry* **A 108**, 9014 (2004). **Featured on Journal Cover**

7. M. Roeselova, J. S. Vieceli, L. X. Dang, B. C. Garrett and D. J. Tobias "Hydroxyl radical at the air-water interface" *Journal of American Chemical Society* **126**, 16308 (2004).

8. T.-M. Chang and L. X, Dang "Liquid/Vapor Interface of Methanol-Water Mixtures: A Molecular Dynamics Study" *Journal of Physical Chemistry* **B 109**, 5759 (2005).

9. M. M., T. Frigato, L. Levering, H. C. Allen, D. J. Tobias, L. X. Dang,and P. Jungwirth "A unified molecular picture of the surfaces of aqueous acid, base, and salt solutions" *Journal of Physical Chemistry* **B 109**, 7617 (2005). **Featured on Journal Cover**

10. V. –A. Glezakou, Y. C. Chen, J. L. Fulton, G. K. Schenter and L. X. Dang "Electronic Structure, Statistical Mechanical Simulations, and EXAFS Spectroscopy of Aqueous Potassium" *Theoretical Chemistry Accounts* (in press 2005, Invited paper).

11. L. X. Dang and T. M. Chang, "Recent advances in molecular simulations of ion solvation at liquid interfaces" *Chemical Review* (2005, Invited paper).

X-ray Spectroscopy of Volatile Liquids and their Surfaces

Richard J. Saykally
Department of Chemistry
University of California
and
Chemical Sciences Division
Lawrence Berkeley National Laboratory
Berkeley, CA 94720-1460
saykally@berkeley.edu

Program Scope or Definition

The goal of this project is to explore and develop novel methodologies for probing the nature of volatile liquids and solutions and their surfaces, employing combinations of liquid microjet technology, with synchrotron X-ray and Raman spectroscopies.

Recent Progress

Utilizing the intense monochromatic soft X-Rays available at the LBNL Advanced Light Source (ALS), we have investigated the temperature dependence of the bulk structure of deeply supercooled liquid water by X-ray absorption spectroscopy[1]. It was recently suggested that the hydrogen bond network of liquid water comprised rings and chains, rather than the traditionally accepted disordered tetrahedral network. Our temperature- dependent measurements indicate that this interpretation greatly overestimates geometric distortions within the hydrogen bond network. Using an experimentally determined "energetic criterion" for a hydrogen bond, we find that the NEXAFS spectrum of liquid water is actually in good agreement with the traditional view of water as a locally tetrahedral liquid.

Using liquid microjets to avoid the problem of radiation damage to fragile solutes, we have measured the pH-dependent NEXAFS spectra of several amino acids, including glycine, proline, lysine, and the dipeptide diglycine[2,3]. We find that the nitrogen terminus of primary amino acids is sterically shielded at high pH, and exists in an "acceptor-only" state, wherein neither amine proton is involved in hydrogen bonding to the surrounding solvent. The diglycine study characterized a similar behavior in this first study of the peptide bond hydration.

We have carried out a systematic study of the perturbative effect of a variety of inorganic salts on the unoccupied water orbitals. We conclude that monovalent cations have a very small effect on the local electronic structure, whereas simple anions are strongly perturbative[4][Plus 2 new papers submitted to *J. Phys. Chem. B*].

We have recently addressed the long standing controversy over whether continuum or a multi-component ("intact" or "broken bond," etc.) models best describe the hydrogen bond interactions in liquid water. The temperature dependence of water's Raman spectrum has long been considered to be among the strongest evidence for a multi-component distribution. However, we have shown, using a combined experimental and theoretical approach, that many of

the features of the Raman spectrum considered to be hallmarks of a multi-state system, including the asymmetric band profile, the isosbestic (temperature invariant) point, and van't Hoff behavior, actually result from a continuous distribution[5]. This work complements the study of the structure of pure liquids by X-ray absorption spectroscopy that has been ongoing. We have published a joint theory/experiment study of liquid methanol that characterized the nature of H-bonded domains[6,7].

Future Plans

In forthcoming scheduled runs at the Berkeley ALS, we plan to focus on the following problems:

1. Measure NEXAFS spectra for pure liquid water, alcohols, and hydrocarbons, seeking to achieve deep supercooling via controlled evaporation. In conjunction with theoretical modeling, we will seek a coherent description of these systems.

2. Extend the study of amino and hydration vs. pH to all natural amino acids. Use the same approach to study hydration of the peptide bonds in small polypeptides.

3. Complete the study of ionic perturbation of local water structure, such that the entire Hofmeister series is addressed. We seek a comprehensive picture of the effects of both cations and anions on the water structure.

4. Raman spectroscopy measurements will also be performed on these systems, the data from which provide complementary insights and aid in the theoretical modeling.

5. In the course of our studies of liquid jets, we have recognized that we have a unique capability to study the detailed physics of the evaporation process for water, which remains a serious limitation in geological modeling. We plan to utilize small microjets to characterize the isotope fractionation in evaporation, free from the complications caused by the reverse process of condensation.

6. Finally, we will continue to explore and compare ion and electron detection of NEXAFS spectra, seeking to reproduce earlier measurements of surface phenomena obtained with ion detection. Thus far, we have not been able to reproduce the original measurements with our newly-designed X-ray spectrometer.

References (DOE supported papers 2003-present)

1. J.D. Smith, C.D. Cappa, K.R. Wilson, B.M. Messer, R.C. Cohen, and R.J. Saykally, "Energetics of Hydrogen Bond Network Rearrangements in Liquid Water," *Science* **306**, 851-853 (2004). LBNL-56349
2. B.M. Messer, C.D. Cappa, J.D. Smith, K.R. Wilson, M.K. Gilles, R.C. Cohen, and R.J. Saykally, "pH Dependence of the Electronic Structure of Glycine," *J. Phys. Chem. B* **109**, 5375-5382 (2005). LBNL-56348
**Cover Article*.

3. B.M. Messer, C.D. Cappa, J.D. Smith, W.S. Drisdell, C.P. Schwartz, R.C. Cohen, R.J. Saykally, "Local Hydration Environments of Amino Acids and Dipeptides Studied by X-Ray Spectroscopy of Liquid Microjets," *J. Phys. Chem. B* (accepted 2005).
4. C.D. Cappa, J.D. Smith, K.R. Wilson, B.M. Messer, M.K. Gilles, R.C. Cohen, and R.J. Saykally, "Effects of Alkali Metal Halide Salts on the Hydrogen Bond Network of Liquid Water,"*J. Phys. Chem. B* **109**, 7046-7052 (2005). LBNL-56812
**Cover Article*.
5. J.D. Smith, C.D. Cappa, K.R. Wilson, R.C. Cohen, P.L. Geissler, and R.J. Saykally, "Unified description of temperature-dependent hydrogen-bond rearrangements in liquid water," *PNAS* (accepted 2005). LBNL-58789
6. K.R. Wilson, M. Cavalleri, B.S. Rude, R.D. Schaller, T. Catalano, A. Nilsson, L.G.M. Pettersson, and R.J. Saykally, "X-ray Absorption Spectroscopy of Liquid Methanol Microjets: Bulk Electronic Structure and Hydrogen Bonding Network," *J. Phys. Chem. B* **109**, 10194-10203 (2005). LBNL-56350
**Cover Article*.
7. K.R. Wilson, B.S. Rude, J. Smith, C.D. Cappa, D.T. Co, R.D. Schaller, M. Larsson, T. Catalano, and R.J. Saykally, "Investigation of volatile liquid surfaces by synchrotron x-ray spectroscopy of liquid microjets," *Review of Scientific Instruments* **75**, 725-736 (2004). LBNL-56347

Chemical Kinetics and Dynamics at Interfaces

Gas Phase Investigation of Condensed Phase Phenomena [1]

Lai-Sheng Wang (PI)
Department of Physics, Washington State University, 2710 University Drive, Richland, WA, 99354 and the Chemical Sciences Division, Pacific Northwest National Laboratory, P.O. Box 999, MS K8-88, Richland, WA 99352. E-mail: ls.wang@pnl.gov

Program Scope

This program is aimed at obtaining a microscopic understanding of environmental materials and solution chemistry in the gas phase using a variety of cluster models. Our primary experimental technique is photoelectron spectroscopy (PES) coupled with electrospray ionization (ESI), which is used to produce solvated clusters from solution samples. Experiment and ab initio calculations are combined to:

- obtain a molecular-level understanding of the solvation of complex anions (both singly and multiply charged) important in condensed phases
- understand the molecular processes and initial steps of dissolution of salt molecules by polar solvents
- probe the structure and dynamics of solutions and air/solution interfaces

Complexes anions, in particular multiply charged anions, are ubiquitous in nature, often found in solutions and solids. However, few complex anions have been studied in the gas phase due to the difficulty in generating them and their intrinsic instability as a result of strong intramolecular Coulomb repulsion in the case of multiply charged anions. Microscopic information on the solvation and stabilization of these anions is important for the understanding of solution chemistry and properties of inorganic materials or atmospheric aerosols involving these species. Gas phase studies with controlled solvent numbers and molecular specificity are ideal to provide such microscopic information. We have developed a new experimental technique to investigate multiply charged anions and solvated species directly from solution samples and probe their electronic structures, intramolecular Coulomb repulsion, stability, and energetics using electrospray and PES. A central theme of this research program lies at obtaining a fundamental understanding of environmental materials and solution chemistry. These are important to waste storage, subsurface and atmospheric contaminant transport, and other primary DOE missions.

Recent Progress (2003-2005)

Observation of Solvent-Mediated Folding of a Linear Doubly Charged Anion and Bulk vs. Interfacial Aqueous Solvation of Dicarboxylate Dianions: The dicarboxylate dianions provide an interesting set of systems with two well-separated and localized charges. Stepwise solvation of these anions by water is expected to lead to a competition between Coulomb repulsion and water-water interactions. In addition, carboxylate is an important negative charge carrier in proteins, present in the C-terminal of polypeptides and the side chains of aspartic and glutamic acids. Linear dicarboxylate dianions $^{-}O_2C\text{-}(CH_2)_n\text{-}CO_2^{-}$ have two distinct charged groups ($-CO_2^{-}$) linked by a flexible aliphatic chain and can be viewed as simple models for peptides. We studied the microsolvation of the suberate dianion, $^{-}O_2C\text{-}(CH_2)_6\text{-}CO_2^{-}$ by water and observed a solvent-mediated folding as a function of solvent number. We showed that water molecules solvate the two negative charges in the linear suberate alternately at the two ends, but not the middle hydrophobic aliphatic chain. As the solvent number increases, a folding occurs at about 16 waters, where the cooperative hydrogen bonding of water is large enough to overcome the Coulomb repulsion

[1] Collaborators on these projects include X. B. Wang, H. K. Woo, and P. Jungwirth.

and pull the two negative charges closer through a water bridge. This conformation change, revealed both from the PES data and molecular dynamics simulation is a manifestation of the hydrophilic and hydrophobic forces at the molecular level. This work provides a simple and clean model system to study the hydrophilic and hydrophobic effects and may be relevant to understanding the hydration and conformation changes of biological molecules.

We further expanded such study to a series of dicarboxylate dianions with different aliphatic chain lengths both in water clusters and in extended aqueous slabs using PES and molecular dynamics simulations. Photoelectron spectra of hydrated succinate, adipate, and tetradecandioic dianions with up to 20 water molecules were obtained. Even-odd effects were observed as a result of the alternate solvation mode of the two negative charges with increasing solvent numbers. The competition between hydrophilic interactions of the charged carboxylate groups and hydrophobic interactions of the aliphatic chain leads to conformation changes in large water clusters containing dicarboxylates bigger than adipate. It also leads to a transition from bulk aqueous solvation of small dicarboxylates to solvation at the water/vapor interface of the larger ones. While oxalate to adipate solvate in the inner parts of the aqueous slab, suberate and longer dicarboxylate dianions have a strong propensity to the surface. This transition also has consequences for the folding of the flexible aliphatic chain and for the structure of aqueous solvation shells around the dianions.

Vibrational Cooling in A Cold Ion Trap: Vibrationally Resolved PES of Cold C_{60}^-: We demonstrated vibrational cooling of anions via collisions with a background gas in an ion trap attached to a cryogenically controlled cold head (10 – 400 K). Photoelectron spectra of vibrationally cold C_{60}^- anions, produced by ESI and cooled in the cold ion trap, were obtained. Relative to spectra taken at room temperature, vibrational hot bands were completely eliminated, yielding well resolved vibrational structures and a more accurate electron affinity for neutral C_{60}. The electron affinity of C_{60} was measured to be 2.683 ± 0.008 eV. The cold spectra revealed complicated vibrational structures for the transition to the C_{60} ground state due to the Jahn-Teller effect in the ground state of C_{60}^-. Vibrational excitations in the two A_g modes and eight H_g modes were observed, providing ideal data to assess the vibronic couplings in C_{60}^-.

Observation of Weak C-H···O Hydrogen-Bonding by Unactivated Alkanes: Weak C-H···O hydrogen bonding has been recognized to play a major role in biological molecular structures and functions. Using the newly developed low-temperature PES apparatus we studied the C-H···O hydrogen bonding between unactivated alkanes and the carboxylate functional group. We observed that gaseous linear carboxylates, $CH_3(CH_2)_nCO_2^-$, assume folded structures at low temperatures due to weak C-H···O hydrogen bonding between the terminal CH_3 and CO_2^- groups for $n \geq 5$. Temperature-dependent studies showed that the folding transition depends on both the temperature and the aliphatic chain length. Theoretical calculations revealed that for n = 3-8, the folded conformations are more stable than the linear structures, but C-H···O hydrogen bonding only forms for species with $n \geq 5$ due to steric constraint in the smaller species. One C-H···O hydrogen bond is formed in the n = 5 and 6 species, whereas two C-H···O hydrogen bonds are formed for n = 7 and 8. Comparison of the photoelectron spectral shifts for the folded relative to the linear conformations yielded lower limits for the strength of the C-H···O hydrogen bonds in $CH_3(CH_2)_nCO_2^-$, ranging from 1.2 kcal/mol for n = 5 to 4.4 kcal/mol for n = 8.

Solvation of the Azide Anion (N_3^-) in Water Clusters and Aqueous Interfaces: As a classic example of a strong nucleophile, the azide anion is of considerable importance in organic and inorganic chemistry. We obtained the PES spectra of $N_3^-(H_2O)_n$ (n = 0-16) clusters and performed computational studies on these hydrated N_3^- clusters. PES spectra of the solvated azide anions were observed to consist of a single peak, similar to that of the bare N_3^-, but the spectral width was observed to broaden as a function of cluster size due to solvent relaxation upon electron detachment. The adiabatic and vertical electron detachment energies were measured as a function of solvent number. The measured electron binding energies indicate that the first four solvent molecules have much stronger interactions with the solute anion, forming the

first solvation shell. The spectral width levels off at $n = 7$, suggesting that three waters in the second solvation shell are sufficient to capture the second shell effect in the solvent relaxation. Density functional calculations were carried out for N_3^- solvated by one to five waters and showed that the first four waters interact directly with N_3^- and form the first solvation shell on one side of the solute. The fifth water does not directly solvate N_3^- and begins the second solvation shell, consistent with the observed PES data. Molecular dynamics simulations on both solvated clusters and bulk interface revealed that the asymmetric solvation state in small clusters persist for larger systems and that N_3^- prefers interfacial solvation on water clusters and at the extended vacuum/water interface.

***Direct Experimental Observation of the Low Ionization Potentials of Guanine in Free Oligonucleotides*:** PES was used to probe the electronic structure of mono-, di-, and trinucleotide anions in the gas phase. A weak and well-defined threshold band was observed in the photoelectron spectrum of 2'-deoxyguanosine 5'-monophosphate ($dGMP^-$) at a much lower ionization energy than the other three mononucleotides. Density function theory calculations revealed that this unique spectral feature is due to electron detachment from a π orbital of the guanine base on $dGMP^-$, whereas the lowest ionization channel for the other three mononucleotides takes place from the phosphate group. This low energy feature was shown to be a "fingerprint" in all the spectra of di- and trinucleotides that contain the guanine base. The experiment provides direct spectroscopic evidence that the guanine base is the site with the lowest ionization potential in oligonucleotides and DNA and is consistent with the fact that guanine is most susceptible to oxidation to give the guanine cation in DNA damages.

Future Plans

The main thrust of our BES program will continue to focus on cluster model studies of condensed phase phenomena in the gas phase. The experimental capabilities developed provide us with opportunities to examine fundamental chemical physics issues in complex anion solvation and solution chemistry. The work planned for the Chemical Physics Program for the immediate future is briefly outlined below.

Continued Development of the Second Generation ESI-PES Apparatus — Controlling the Cluster Temperatures: The ESI-PES apparatus developed in our laboratory has proven to be a powerful technique to study multiply charged anions and solvated species. It has allowed a wide range of solution-phase species to be investigated in the gas phase. Over the past several years, we have gained considerable experience in operating this apparatus and recognized several of its limitations. A critical feature of this apparatus is its ability to trap ions and accumulate number density from the continuous ESI source for subsequent time-of-flight mass analysis. The current trap is operated at room temperature. A second generation ESI-PES apparatus, which is aimed at controlling the cluster temperature, is being developed in our laboratory. A cryogenic ion trap is being constructed to produce cold anions, which will be essential to suppress thermal broadening in the PES spectra. Furthermore, the current ion trap stores all incoming ions, which reduces the trapping efficiency due to space charge effect. A quadrupole mass filter will be added to pre-select the ions of interest for storage and accumulation. This is particularly important for large clusters and weakly populated species. Preliminary results have already been obtained and we have demonstrated the cooling effect on the trapped anions. In the coming year, we will continue to develop the apparatus to enhance its flexibility and efficiency. In particular, we plan to install an ion funnel in the ESI source, which is expected to increase the ion signals by a factor of five. This improvement will be important to study solvated species and weakly populated anions.

Confirmation Change vs. Temperature: the Effect of Entropy: We anticipate that this second generation ESI-PES apparatus will significantly expand our capability and flexibility to study solvated species in the gas phase. A good example is to reexamine the microsolvation of dicarboxylate dianions, discussed above. The previous experiment on solvated dicarboxylate was done at room temperature, but the real temperature of the cluster was unknown. However, theoretical calculations indicate that the folding

transition is not only dependent on the solvent number, but also on the cluster temperature due to the effect of entropy. In the new apparatus, the ion trap temperature can be controlled and varied from 17 to 400 K. Systematic studies of the folding conformation change as a function of temperature will be performed and compared with MD simulations.

Gas Phase Studies of Free and Solvated Oligonucleotides: The ionization of nucleotides plays very important roles in the chemistry of DNA. Induced by electrophiles or ionizing radiation, the electron deficient site (hole) on the nucleotide and its migration directly leads to DNA damages. In most cases, the initial oxidation site or the electron-loss center ultimately moves via the DNA π stack to end up at a guanine base, resulting in a guanine cation. This is attributed to the low ionization potential of guanine relative to the other DNA bases. Thus the electronic structure of nucleotides and their ionization properties are essential for understanding the mechanism of DNA damages. Gas phase PES studies probe the intrinsic electronic properties of the nucleotides and provide important experimental data to compare with and verify theoretical methods. We have already studied nucleotide anions in the gas phase and observed that nucleotides with guanine bases possess low ionization potentials, consistent with the fact that guanine is most susceptible to oxidation to give the guanine cation in DNA damages. We plan to study the gas phase formation of the Watson-Crick base pairs, as well as solvent and counter-ion stabilization on the structure and energetics of DNA nucleotides in the gas phase.

References to Publications of DOE Sponsored Research (FY 2003-2005)

1. "Probing Solution Phase Species and Chemistry in the Gas Phase" (X. B. Wang, X. Yang, and L. S. Wang), *Int. Rev. Phys. Chem.* **21**, 473-498 (2002). (**invited review**)
2. "Photodetachment of Hydrated Oxalate Dianions in the Gas Phase, $C_2O_4^{2-}(H_2O)_n$ (n = 3-40) – From Solvated Clusters to Nano Droplet" (X. B. Wang, X. Yang, J. B. Nicholas, and L. S. Wang), *J. Chem. Phys.* **119**, 3631-3640 (2003).
3. "Solvent-Mediated Folding of A Doubly Charged Anion" (X. Yang, Y. J. Fu, X. B. Wang, P. Slavicek, M. Mucha, P. Jungwirth, and L. S. Wang), *J. Am. Chem. Soc.* **126**, 876-883 (2004).
4. "Solvation of the Azide Anion (N_3^-) in Water Clusters and Aqueous Interfaces: A Combined Investigation by Photoelectron Spectroscopy, Density Functional Calculations, and Molecular Dynamics Simulations" (X. Yang, B. Kiran, X. B. Wang, L. S. Wang, M. Mucha, and P. Jungwirth), *J. Phys. Chem. A* **108**, 7820-7826 (2004).
5. "Bulk vs. Interfacial Aqueous Solvation of Dicarboxylate Dianions" (B. Minofar, M. Mucha, P. Jungwirth, X. Yang, Y. J. Fu, X. B. Wang, and L. S. Wang), *J. Am. Chem. Soc.* **126**, 11691 (2004).
6. "Direct Experimental Observation of the Low Ionization Potentials of Guanine in Free Oligonucleotides Using Photoelectron Spectroscopy" (X. Yang, X. B. Wang, E. R. Vorpagel, and L. S. Wang), *Proc. Natl. Acad. Sci.* (USA) **101**, 17588-17592 (2004).
7. "The Role of Water on Electron-Initiated Processes and Radical Chemistry: Issues and Scientific Advances" (B. C. Garrett, *et al.*), *Chem. Rev.* **105**, 355-389 (2005).
8. "Interior and Interfacial Aqueous Solvation of Benzene Dicarboxylate Dianions and Their Methylated Analogues: A Combined Molecular Dynamics and Photoelectron Spectroscopy Study" (B. Minofar, L. Vrbka, M. Mucha, P. Jungwirth, X. Yang, X. B. Wang, F. J. Fu, and L. S. Wang), *J. Phys. Chem. A* **109**, 5042-5049 (2005).
9. "Observation of Weak C-H···O Hydrogen-Bonding by Unactivated Alkanes" (X. B. Wang, H. K. Woo, B. Kiran, and L. S. Wang), *Angew. Chem. Int. Ed.* **44**, 4968-4972 (2005). *Angew. Chem.* **117**, 5048-5052 (2005).
10. "Vibrational Cooling in A Cold Ion Trap: Vibrationally Resolved Photoelectron Spectroscopy of Cold C_{60}^- Anions" (X. B. Wang, H. K. Woo, and L. S. Wang), *J. Chem. Phys.* **123**, 051106 (2005).
11. "Temperatures Dependent Photoelectron Spectroscopy of Methyl-Benzoate Anions: Observation of Steric Effect in *Ortho*-Methyl-Benzoate" (H. K. Woo, X. B. Wang, B. Kiran, and L. S. Wang), *J. Phys. Chem. A* , in press (2005).

Research Summaries
(by PI)

"Aerosol and Nanoparticle investigations at the Chemical Dynamics Beamline of the Advanced Light Source"

Musahid Ahmed and Stephen R. Leone
Chemical Dynamics Beamline
Lawrence Berkeley National Laboratory
University of California, Berkeley, CA 94720
mahmed@lbl.gov and srleone@lbl.gov

Scope

Nanoscience in the 21st century is thriving – aerosols and nanoparticles are being studied in unprecedented detail across a broad spectrum of disciplines. Applications for the particles have been found in fields varying from medicine to computers, and the particles themselves are integral to studies ranging from spectral emissions in interstellar space to climate changes in our own environment.

Systematic studies with vacuum ultraviolet light (VUV) and soft x-ray radiation can contribute to the study of aerosol chemistry and nanoparticle physics in new and important ways. We have initiated a major program in the study of these species at the Chemical Dynamics Beamline at the Advanced Light Source (ALS)[1]. The project encompasses novel studies of the production, detection, size measurement and selection, and chemical interactions of nanoparticles. The combination of size-selected particle beams and tunable VUV light affords the opportunity to study the optical and electronic properties of these ultra fine particles in regimes not accessible earlier.

Under the aegis of this program we have designed and constructed a novel experimental apparatus coupled to the tunable VUV light source at a synchrotron. The main features of the apparatus are an aerodynamic lens system to generate focused particle beams and provisions to detect scattered photons, image photoelectrons and perform time of flight mass spectrometry on volatile species desorbed from aerosols and nanoparticles. To date we have performed VUV light scattering of ultrafine silica particles, photoelectron imaging of insulating and metallic particles, developed a novel source for biological mass spectrometry and made forays into studying aerosol chemistry with tunable VUV light. Below we detail these results and highlight our capabilities at the chemical dynamics beamline.

VUV light scattering of nanoparticles

We have undertaken a fundamental study of the optical properties of aerosol particles using VUV radiation. Traditionally, Mie theory combined with visible scattering experiments have been used to understand the interaction of visible light with particles ranging in size from 0.2 to 10 microns. However, the scattering cross section at visible wavelengths decreases rapidly for particles smaller than 200 nm making these approaches difficult to implement for ultrafine particles. We have extended these fundamental studies to vacuum ultraviolet (VUV) wavelengths in an effort to examine the scattering properties of particles smaller than 200 nm. Furthermore, few studies in this wavelength region have explored the complex interplay between scattering and absorption.

Silica particles, chemically synthesized online, are size-selected by a differential mobility analyzer, and introduced into vacuum through a set of aerodynamic lenses. The resulting focused particle beam is crossed at 90 degrees with the VUV radiation. These silica particles were previously determined to be spheres (SEM) and therefore the VUV scattering results are amenable to standard Mie Theory analysis. The scattered photons from the crossing area of the VUV synchrotron beam and particle beam are detected with a rotatable VUV photon detector. The angular distributions of scattered photons (ADSP) originating from 70, 100, 200 nm diameter silica particles are measured with 145.9 and 118.1 nm synchrotron radiation. As predicted by Mie theory, these angular distributions show strong forward scattering. Using Mie theory to analyze our experimental results, the refractive

indices of these chemically synthesized silica particles are determined to be 2.6 + 1.1i and 1.6 + 0.0001i for 118.1 nm and 145.9 nm wavelengths, respectively. A careful comparison of scattered fluxes at visible and VUV wavelengths clearly shows enhanced size sensitivity at shorter wavelengths. The smallest particle size detected in this way using visible illumination was 250 nm. Conversely, our VUV studies exhibited a small size detection limit of 70 nm, which is presently limited by the particle transmission efficiency our aerosol endstation. As anticipated, VUV scattering is a more sensitive probe for ultrafine particles and their optical properties[2].

We also performed elastic light scattering with free, spherical silica nanoparticles prepared by approaches from colloidal chemistry, with diameters between 100 nm and 240 nm. The colloidal nanoparticles of defined size are transferred from an aqueous solution into the gas phase using the particle beam apparatus. There is evidence for modulations in the scattered light intensity as a function of scattering angle, which is clearly distinguished from the forward scattering component. The experimental results are compared to Mie scattering simulations for isolated particles, yielding good agreement with the experimental results. Deviations from Mie simulations are observed for samples consisting of significant amounts of aggregates. The present results indicate that the optical properties of free nanoparticles and aggregates are sensitively probed by vacuum ultraviolet radiation[3].

Aerosol Chemistry

We implemented the capability of studying aerosol composition and chemistry using VUV photoionization. This "soft" ionization technique has been shown to yield near "fragment free" mass spectra of a variety of organic molecules. In this way, VUV photoionization is ideally suited for compositional analysis of complex organic mixtures associated with aerosol particles. In general, aerosol particles are generated *in situ* and focused into the aerosol endstation using an aerodynamic lens. The particles are then flash vaporized (50-500^{0}C) and the resulting molecules are photoionized near threshold and then analyzed using time of flight (TOF) mass spectrometry. In this way, the chemical composition of aerosol particles can be monitored in the course of a chemical reaction.

The first studies of aerosol chemistry using this technique were conducted in collaboration with Prof. Tom Baer (University of North Carolina). Oleic acid aerosol particles are generated in urban areas as a by-product of meat grilling in the fast food industry. In addition, oleic acid aerosols have been extensively characterized by many other laboratories and provide a nice benchmark for the new technique. Oleic acid particles were generated in situ and introduced into the aerosol endstation. The resulting mass spectrum (at 9 eV) obtained after the oleic acid aerosol was vaporized contained a single dominant parent peak at 284 amu.[4] In contrast, electron impact ionization mass spectra obtained by other groups under identical conditions yield a complicated mixture of peaks arising from extensive fragmentation of the oleic acid molecule. This extensive fragmentation prohibits the detailed investigation of more complex aerosol chemistry due to interference between reactant and product fragmentation peaks in the electron impact mass spectrum.

To further explore this point, oleic acid aerosols were reacted with O_3 (a ubiquitous atmospheric oxidant). The VUV photoionization mass spectrum showed a decrease of the parent ion with O_3 addition as well as an increase in the particle phase products located at lower masses. In previous electron impact studies, these lower mass products were obscured by the extensive fragmentation of the reacting oleic acid. Therefore, VUV photoionization allows products of heterogeneous aerosol chemistry to be identified with high accuracy. In addition, tunable VUV light can be used to separate isomers and overlapping masses, as has been demonstrated recently in the case of flame chemistry[5].

We have also constructed a 130 L aerosol reaction chamber to be used in conjunction with the aerosol endstation and the commercial particle sizing instruments currently operational at the Chemical Dynamic Beamline. The reaction chamber was designed for measuring the kinetics of secondary aerosol formation. The goal of these experiments is to examine both the size and chemical evolution of particles generated by the gas phase reaction of aerosols with ozone and OH radicals. We are able to follow in real time both the particle size evolution as well as the chemistry. As expected from the previous oleic acid experiments, VUV photoionization allowed us to

monitor in real time, with less fragmentation, how the particle composition evolved as a function of reaction time. Although, analysis of these results are currently underway, we have observed the evolution of pinonic acid in the particle phase, a major product previously identified by other groups. However, unlike previous studies by other groups who conduct post analysis of products using GC-MS techniques, we were able to follow the pinonic acid concentration in the aerosol particle in real time. These experiments have recently been extended using a movable injector flow apparatus coupled to the aerosol endstation.

Photoelectron Imaging of Nanoparticles

Vacuum ultraviolet (VUV) light offers an opportunity to study the optical properties of particles in difficult to access spectral regions. There are at present no molecularly incisive methods for spectroscopically probing the surfaces of free nano-aerosol particles. Optical methods, based upon infrared spectroscopy or Raman scattering, have been developed to investigate micron-sized particles. These techniques are difficult to extend to submicron particles due to poor signal to noise ratios. Additionally, these spectroscopic techniques lack the sensitivity to examine the surface structure of nanoparticles. Due to the shallow escape depth of electrons, valence band VUV photoelectron spectroscopy is well suited to the study of the electronic structure of nanoparticles.

The technique of velocity-mapped imaging photoelectron spectroscopy coupled to synchrotron radiation allows simultaneous measurement of angular and energy release from ionization events with 4π steradian collection efficiency[6]. This technique coupled with beams of free nanoparticles allows for detailed investigations of the ionization and relaxation dynamics in these systems. The kinetic energy release suggests that these ultra fine particles (50-300 nm) show bulk-like behavior. A remarkable size dependent asymmetry in the angular distributions of the released photoelectrons is observed for insulating nanoparticles. A model utilizing optical absorption and electron emission is invoked to explain the asymmetry. Typically at our VUV photon energies, the absorption depth and escape probability of a low energy electron is a few nanometers. It is therefore not surprising that when the particle radius approaches the size of both the photoabsorption length and electron escape depth that homogenous photoelectron emission is expected. Conversely, as the particle size exceeds both the photoabsorption and electron escape depths the images become more asymmetric, suggesting that only a fraction of the total particle volume is emitting photoelectrons. This technique offers a means of measuring surface specific chemical properties and in addition, the valence bands of nanoparticles can be mapped free of substrate effects.

The ionization energies of biological nanoparticles have been determined using the same photoelectron imaging technique. Biological nanoparticles produced by aerosol methods are photoionized with VUV light. The ionization energy of the nanoparticles is derived from a plot of the photoelectron spectrum versus incident photon energy. The nanophase results are compared to ionization energies determined theoretically and other surface science experiments.

Biological Mass Spectrometry

Using the aerosol apparatus we have developed a novel method to introduce fragile biomolecules into the gas phase via formation of aerosol nanoparticles, followed by thermal vaporization and detection by VUV photoionization mass spectrometry. The general strategy is to synthesize dry nanoparticles comprised of biomolecules that are then thermally vaporized in high vacuum. The resulting vapor, containing free neutral biomolecules, can be “softly” ionized with tunable VUV synchrotron radiation producing nearly fragmentation-free mass spectra. In fact, the degree of fragmentation can be finely controlled via the thermal or photon energy, yielding greater insight into the role of internal energy in the photoionization mass spectra of amino acids and other bio-molecules.

To first demonstrate the general utility of this approach and to illustrate how internal energy affects single photon ionization mass spectra, we examined the amino acid tryptophan in detail. In addition, we measured the ionization

energies of a number of biomolecules; for some, these are the first reported measurements. Finally erythromycin (733 amu) is the largest molecule that has been detected completely fragment free with this technique[7].

Future work

To date, our results on nanoparticle VUV scattering are really "proof of principle." The fundamental studies of spherical particles will be extended to sub-70 nm particles with the incorporation of a nano-nozzle to access sub-70 nm particles. Future studies will be also extended to non-spherical particles requiring more sophisticated theoretical techniques. In addition, we will employ more advanced detection techniques, which would allow VUV scattering to be measured in concert with the various other particle probes (velocity map imaging, VUV TOF + particle impact vaporization) currently in use or in development here are the Chemical Dynamics Beamline. Specifically, imaging detectors would allow us to measure many scattering angles simultaneously, improving the S/N ratio over the current single angle detection scheme. Such a detector has been recently acquired along with the capabilities of performing timing and coupling to a Echelle spectrometer. This allows the study of fluorescence from VUV irradiated nanoparticles. By making these detection improvements the optical properties of more complex aerosols can be simultaneously correlated with size and chemical composition. These improvements will be particularly important for simulating aerosol formation in planetary atmospheres where the optical properties of laboratory aerosols can be correlated with remote sensing measurements of planetary albedo.

We plan to extend our velocity map imaging studies to higher photon energies and smaller particles. Studies will be conducted at higher photon energies to explore in detail the angular asymmetry produced by electrons at higher kinetic energies (5-10 eV). Concurrently, efforts will be dedicated to transferring nanoparticles (1- 10 nm) into the endstation for photoelectron imaging experiments. 1-10 nm particles would be an important size region to study the transition from small clusters, exhibiting quantum size effects, to the bulk electronic structure in solids.

Initial results obtained to date all suggest that VUV photoionization + impact particle vaporization is a powerful technique for probing complex heterogeneous organic chemistry in laboratory simulated aerosol particles. We anticipate this technique will be of great interest to the aerosol community affording them the ability to tackle more complex chemical problems by reducing the analysis problems associated with electron impact particle analysis.

Efforts are currently underway to improve the sensitivity of the TOF, as well as to extend the transmission efficiency of the instrument to sub 70 nm particles. If successful an entirely new class of problems can be addressed with the chemical specificity of VUV photoionization.

---

1. D. S. Peterka and M. Ahmed, "Atoms to Aerosols – The Chemical Dynamics Beamline," *Syn. Rad. News.*, **18**, 35 (2005).
2. J. Shu, K. R. Wilson, A. N. Arrowsmith, M. Ahmed, and S. R. Leone, "Light scattering of ultrafine silica particles by VUV synchrotron radiation," *Nano Lett.* ***6,*** *1009* (2005*)*
3. J. Shu, K. R. Wilson, M. Ahmed, S. R. Leone, C. E. Graf, and E. Ruhl, "Elastic light scattering from nanoparticles by monochromatic vacuum-ultraviolet radiation," *J. Chem. Phys*. (submitted).
4. E. R. Mysak, K. R. Wilson, M. Jimenez-Cruz, M. Ahmed, and T. Baer. "Synchrotron Radiation Based Aerosol Time-of-Flight Mass Spectrometry for Organic Constituents" *Anal. Chem.* (ASAP DOI: 10.1021/ac050440e).
5. T. A. Cool, K. Nakajima, T. A. Mostefaoui, F. Qi, A. McIlroy, P. R. Westmoreland, M. E.Law, L. Poisson, D. S. Peterka, and M. Ahmed, "Selective detection of isomers with photoionization mass spectrometry for studies of hydrocarbon flame," *J. Chem. Phys.*, ***119****, 8356, (2003).*
6. D. S. Peterka, A. Lindinger, L. Poisson, M. Ahmed, D. M. Neumark, "Photoelectron imaging of helium droplets," *Phys. Rev. Lett.* **91**, 043401, (2003)
7. K. R. Wilson, M. Jimenez-Cruz, C. Nicolas, L. Belau, S. R. Leone, and M. Ahmed, "Fragment-free VUV photoionization mass spectra of biomolecules by thermal vaporization of aerosol nanoparticles: application to tryptophan, phenylalanine-glycine-glycine and β-carotene," *J. Phys. Chem. A* (submitted).

"Electronic Structure of Transition Metal Clusters, and Actinide Complexes, and Their Reactivities"

K. Balasubramanian

Institute of Data Analysis and Visualization, University of California, Davis, Livermore, California 94550; Chemistry and Material Science Directorate, Lawrence Livermore National Laboratory, University of California, Livermore, California 94550; Glenn T. Seaborg Center, Lawrence Berkeley National Laboratory, Berkeley, California 94720; Dept of Mathematics, computer science and physics, California State University East Bay, Hayward CA

balu@csueastbay.edu

Program Scope

Our research funded by DOE Chemical sciences division deals with computational chemistry of transition metal clusters and actinide complexes. Gas-phase spectroscopic studies on these clusters are benefited by our computations. Computations of actinide complexes are important to understanding of the complexes found in geochemical and biochemical environment and are thus critical to management of high-level nuclear wastes. We are carrying out computational studies ton these species. The geometrical and electronic properties such as ionization potentials, electron affinities, and binding energies of transition metal clusters vary dramatically with cluster sizes. Especially thrid and second row transition metal clusters transition metal carbides and silicides are considered. Uranyl and plutonyl complexes of environmental importance are being studied. These studies are made with relativistic complete active space multi-configuration self-consistent-field (CASSCF) followed by large-scale CI computations and relativistic CI (RCI) computations up to 60 million configurations.

Recent Progress

Our recent progress in this area is described extensively in publications[1-20], which contain all the details of the results, tables and figures. Here we briefly outline the major highlights, in each of the categories. For this purpose the clusters and complexes that we have studied were grouped into the various categories and each of them is briefly described below.

Electronic Structure of Transition Metal Species.

The transition metal-containing species studied included ruthenium carbide, RuC[1], gold dihydride[2], AuH_2, niobium clusters[4], and the niobium carbide[9]. The RuC molecule has been a challenging species due to the open-shell nature of Ru resulting in a number of low-lying electronic states for this molecule. We have carried out state-of-the-art complete active space multi-configuration self-consistent field followed by multireference configuration interaction methods that included up 18 million configurations, in conjunction with relativistic effects. We have computed 29 low-lying electronic states of RuC with different spin multiplicities and spatial symmetries with energy separations less than 38 000 cm^{-1}. We find two very closely lying electronic states for RuC, viz., $^1\Sigma^+$ and $^3\Delta$ with the $^1\Sigma^+$ being stabilized at higher levels of theory. Our computed spectroscopic constants and dipole moments are in good agreement with experiment although we have reported more electronic states than those that have been observed experimentally. Our computations reveal a strongly bound $X^1\Sigma^+$ state with a large dipole moment and an energetically close $^3\Delta$ state with a smaller dipole moment. Overall our computed energy separations of the excited states with energy separations less than 18000 cm^{-1} agree quite well.

In collaboration with Prof Lester Andrews, AuH_2 molecule was formed in solid hydrogen by reactions of excited gold atoms from laser ablation and irradiation after thermal evaporation. The X^2B_2 ground state of the AuH_2 molecule is separated by a 53 kcal/mol barrier from the $Au(^2D) + H_2$ decomposition products and it is 27 kcal/mole more stable than $Au(^2D) + H_2$. The bending modes of AuH_2, AuHD, and AuD_2 have been observed at 638.1, 570.6, and 457.0 cm^{-1}. These frequencies and the lack of infrared intensity in the stretching modes are in agreement with the results of relativistic ECP DFT, MP2 and CCD calculations. The computed bending potential energy surfaces of three electronic states of AuH2 using CASSCF/MRSDCI methods reveal that there is a barrier for conversion of the X^2B_2 ground state to $Au(^2S) + H_2$.

Geometries and energy separations of the various low-lying electronic states of Nb_n and Nb_n^- (n = 4, 5) clusters with various structural arrangements have been investigated. The complete active space multi-configuration self-consistent field (CASMCSCF) method followed by multi-reference singles and doubles configuration interaction (MRSDCI) calculations that included up to 52 million configuration spin functions have been used to compute several electronic states of these clusters. The ground states of both Nb_4 ($^1A'$, pyramidal) and Nb_4^- ($^2B_{3g}$, rhombus) are low-spin states at the MRSDCI level. The ground state of Nb_5 cluster is a doublet with a distorted trigonal bipyramid (DTB) structure. The anionic cluster of Nb_5 has two competitive ground states with singlet and triplet multiplicities (DTB). The low-lying electronic states of these clusters have been found to be distorted due to *Jahn-Teller* effect. The electron affinity, ionization potential, dissociation and atomization energies of Nb_4 and Nb_5 have been calculated and the results have been found to be in excellent agreement with the experiment.

We have studied the potential energy curves and spectroscopic constants of the ground and low-lying excited states of NbC[9] the complete active space multi-configuration self-consistent field (CASSCF) followed by multireference configuration interaction (MRCI) methods, in conjunction with relativistic effects and 5s3p3d1f, 3s3p1d basis sets con Nb and C respectively. For comparative purposes we performed comparative B3LYP and CCSD(T) calculations. We have identified 26 low-lying electronic states of NbC with different spin multiplicities and spatial symmetries within 40000cm^{-1}. At the MRSDCI level of theory the $^2\sum^+$ and $^2\Delta$ states are nearly degenerated, with the $^2\Delta$ 172 cm^{-1} lower than the $^2\sum^+$ state. However after spin-orbit splitting the $^2\Delta$ state becomes lower by 646 cm^{-1}, in reasonable agreement with the experimental result 831 $cm^{-1.}$ Our computed spectroscopic constants and dipole moments are in good agreement with experiment. On the other hand our results for the excited sates of NbC are different from previous density functional calculation, mainly due to the strong multiconfigurational character of NbC that cannot be handled properly at this level of theory. We have reported more electronic states than those that have been observed experimentally.

Electronic Structure of Actinide Complexes.

We have carried out extensive ab initio calculations on the structure and spectra of $H_2UO_2SiO_4.3H_2O$, $HUO_2PO_4.3H_2O$, and $HUO_2AsO_4.3H_2O$. The calculated structures and vibrational spectra have been compared with the available experimental data.The silicate, phosphate and arsenate minerals are quite abundant in nature and their structural and bonding studies are important to the understanding of the mobility of uranium in natural systems and in soils contaminated by actinides. The theoretical studies of these model molecules are thus quite important for the basic understanding of the uranyl-silicate, uranyl-phosphate, and uranyl-arsenate bondings of naturally occurring uranyl minerals.

The USi3W molecule has been studied very recently in solid form through EXAFS technique. The phosphate and the arsenate molecules are studied as the simplest forms of the corresponding uranyl compounds $(UO_2)_3(PO_4)_2(H_2O)_4$, and $(UO_2)[(UO_2)(AsO_4)]_2(H_2O)_4$. The geometry optimization of USi3W, UP3W, and UAs3W at both the DFT/B3LYP and MP2 levels show that the water molecules in these tri-hydrated complexes lie in a plane containing the uranium and the silicate, phosphate or arsenate group, and thus forming pentagonal bi-pyramid structures. We have compared the calculated geometries with the available crystal structure data

and the agreement is quite satisfactory at both the DFT/B3LYP and MP2 levels. Our calculated vibrational spectra of USi3W compare quite well with the observed vibrational spectra of $(UO_2)_2SiO_4.2H_2O$. We have compared the calculated U-O_3 and U-O_4 distances of these molecules. They show that the uranyl-silicate and uranyl-phosphate interactions would be similar and the uranyl-arsenate interaction would be less than both of them.

We have studied the electronic and spectroscopic properties of plutonyl carbonate complexes of the types PuO_2CO_3 and the hydrated forms, $PuO_2CO_3.nH_2O$, (n=1,2). Our computed equilibrium geometries and vibrational spectra of these species agree quite well with the EXAFS and Raman data available on related complexes. We have reported the results of ab initio quantum chemical computations on the plutonyl carbonate complex and its hydrated forms, viz., PuO_2CO_3, $PuO_2CO_3.H_2O$ and $PuO_2CO_3.2H_2O$. The results of our computations at the DFT, MP2 and CCSD levels show that the computed geometries and vibrational frequencies are in reasonable agreement among these theoretical levels. Our computed geometries for the various interatomic distances at both MP2 and DFT levels agree quite well with the experimental EXAFS results of Clark et al. at Los Alamos in solution for the limiting Pu(VI)O_2-carbonate complex. Our predicted equatorial carbonate vibrational mode frequency of 754 cm^{-1} at the MP2 level is consistent with the observed Raman band at 755 cm^{-1} in solution form of plutonyl carbonate complex..

Extensive ab initio calculations have been carried out on the structure and bonding characteristics of $UO_2(CO_3)_2^{2-}$ and $M_2UO_2(CO_3)_2$ (M= Li^+, and Na^+) both in the gas phase and in solution using coupled cluster doubles (CCD), Møller-Plesset second order perturbation theory (MP2) and density functional (DFT) theory. The calculated structure and vibrational spectra have been compared with the available experimental data. The nature of the boding in these species is discussed. The formation of uranyl carbonate formation is one of the most important processes governing the actinide migration from geo-repositories. The uranyl carbonato complexes are known to form water-soluble metal salts. In order to understand the nature of metal binding with carbonato complexes, we have studied here the structure and bonding of $UO_2(CO_3)_2^{2-}$ and $M_2UO_2(CO_3)_2$ (M= Li^+, and Na^+). The gas phase calculations on $UO_2(CO_3)_2^{2-}$ at the DFT/B3LYP, MP2, and CCD levels reveal that, analogous to higher uranyl carbonate complexes, the gas-phase structure $UO_2(CO_3)_2^{2-}$ is a D_{2h} structure with the carbonates in the equatorial position and the uranyl forming the axial linear bonds.

Future Plan

We are continuing to investigate second, third row transition metal clusters, carbides and other complexes of transition metals and actinides. There are many challenges as we attempt to study these species. Both relativistic effects including spin-orbit effects and electron correlation effects must be considered accurately. We have also been investigation actinide complexes of environmental importance and their salvation phenomena. We have been looking at methods to consider aquous complexes of uranyl, plutonyl an dneputnyl species. Theoretical spectroscopy of transition metal carbides particularly MoC and ZrC are being studied.

References to Publications of DOE-sponsored work in 2003-2005

1. R. Guo and K. Balasubramanian, "Theoretical study of the low-lying electronic states of ruthenium trimer (Ru_3)", *J. Chem. Phys.* **118**, 142-148 (2003)

2. S. Roszak and K. Balasubramanian, **"**Electronic structure and spectroscopic properties of electronic states of VC_2, VC_2^-, and VC_2^+", *J. Chem. Phys.* **118** 130-141 (2003).

3. D. Majumdar, S. Roszak K. Balasubramanian, and H. Nitsche" Theoretical study of aqueous uranyl carbonate (UO_2CO_3) and its hydrated complexes: $UO_2CO_3.nH_2O$ (n = 1 - 3)", *Chemical Physics Letters* **372**, 231-238 (2003).

4. V. Wheaton, D. Majumdar, K. Balasubramanian, L. Chauffe, and P. G. Allen, "A Comparative Theoretical Study of Uranyl Silicate Complexes", *Chemical Physics Letters* **371**, 349-356 (2003).

5. D. Majumdar and K. Balasubramanian, "A theoretical Study of Potential Energy Curves and Specroscopic Constants of VC", *Molecular Physics* **101**, 1369-1376 (2003).

6. R. Guo, K. Balasubramanian and H. F. Schaefer III, "The Treacherous Potential Energy hypersurface of AgSiO", *J. Chem. Phys.* **118**, 10623-10630(2003).

7. K. Balasubramanian, W. Siekhaus and W. McLean II, "Potential Energy Surfaces for the Uranium Hydridng and UH_3 Catalysis", *J. Chem. Phys.* **119**, 5879-5900(2003).

8. D. Majumdar and K. Balasubramanian, "Theoretical study of the electronic states of Niobium Trimer (Nb_3) and its anion (Nb_3^-)", *J. Chem. Phys.* **119**, 12866-12877 (2003).

9. R. Guo and K. Balasubramanian, "Spectroscopic Constants and Potential Energy Curves of Ruthenium Carbide: RuC", *J. Chem. Phys.* **120**, 7418-7425(2004).

10. Lester Andrews, Xuefeng Wang, and K. Balasubramanian, "The Gold Dihydride Molecule, AuH_2: Calculations of Structure, Stability and Frequencies, and the Infrared Spectrum in Solid Hydrogen", *J. Phys. Chem A.* **108**, 2936-2940 (2004).

11. K. Balasubramanian, "Relativity and the Periodic Table", (D. Rouvary & R. B. King, editors), Periodic Table into the 21st Century, 2004

12. K. Balasubramanian, "Relativistic Double Group Spinor Representations of Non-rigid Molecules", *J. Chem. Phys.* **120**, 5524-5535(2004).

13. D. Majumdar and K. Balasubramanian, "Theoretical Study of the Electronic States of Nb_4, Nb_5 clusters and their anions (Nb_4^-, Nb_5^-), *J. Chem. Phys.* **121,** 4014-4032 (2004).

14. K. Balasubramanian, "Mathematical Basis of Periodicity in Atomic and Molecular Spectrsocopy", Mathematics of the Periodic Table, Editors: R. B. King and D. H. Rouvray, Nova Press, NJ 2004

15. D. Chaudhuri and K. Balasubramanian, "Electronic Structure and Spectra of Plutonyl Complexes and their hydrated forms: PuO_2CO_3 and PuO_2CO_3.nH2O (n=1,2)", *Chemical Physics Letters*, 399, 67-72 (2004)

16. D. Majumdar and K. Balasubramanian, "Theoretical studies on uranyl–silicate, uranyl–phosphate and uranyl–arsenate interactions in the model $H_2UO_2SiO4 \cdot 3H_2O$, $HUO_2PO_4 \cdot 3H_2O$, and $HUO_2AsO_4 \cdot 3H_2O$ molecules", *Chemical Physics Letters*, **397**, 26-33 (2004).

17. D. Majumdar and K. Balasubramanian, "Theoretical studies on the electronic structures of $UO_2(CO_3)_2^{2-}$ and its metal salts: $M_2UO_2(CO_3)_2$ (M = Li^+, and Na^+)", *Molecular Physics*, **103**, 931 – 938(2005)

18. P. A. Denis and K. Balasubramanian, "Spectroscopic Constants and Potential Energy Curves of low-lying electronic states of NbC", J. Chem. Phys. **123**, 054318 (2005) –Published online 9Aug 2005.

19. Z. Cao and K. Balasubramanian, "Theoretical Studies of hydrated complexes of uranyl, neptunyl and plutonyl in aqueous solution: $UO_2^{2+}(H_2O)_n$, $NpO_2^{2+}(H_2O)_n$, and $PuO_2^{2+}(H_2O)_n$", J. Chem. Phys. In press

20. K. Balasubramanian, "Applications of Enumerative Combinatorics to Chemistry and Spectrosocpy", *Advances in Quantum Chemistry*, in press

Clusters: Unraveling Fundamental Oxygen Transfer Reaction Mechanisms Effected by Heterogeneous Catalysts

A. W. Castleman, Jr.
Penn State University
Departments of Chemistry and Physics
104 Chemistry Building
University Park, PA 16802
awc@psu.edu

Program Scope:

It would be difficult to overstate the importance of catalysis in maintaining the economic competitiveness of the nation, with its role in effecting industrially and environmentally significant reactions, as well as ones involved in energy production. Developing an understanding of the basic principles that govern catalytic reactions is crucial for the tailoring of catalysts with desired efficiency and selectivity. Unraveling the details of various catalytic processes and providing information on the physical and chemical principles requires endeavors which span a wide range of investigations from empirical observations of catalytic processes to fundamental surface science. Our program is designed to elucidate selected aspects of the basic principles needed to realize the nature of selected sites of oxygen transfer reactions involving transition metal oxides and noble metal clusters. These studies serve to shed light on some of the fundamental mechanisms involved.

In recent years, there has been a growing acceptance of the use of gas phase clusters to model metal oxide surfaces and to study industrially and environmentally significant reactions, providing a valuable *complementary* method for probing the active sites responsible for selected classes of reactions. Our continuing program is designed to investigate the roles of charge state, oxidation state, geometrical and surface effects, and stoichiometry. These studies of gas phase clusters offer the opportunity to probe complicated catalytic reactions on the nanoscale and avoid common problems such as elucidating effects which can arise due to various methods of catalyst preparation. Through these studies, information necessary to further understand the processes and fundamental mechanisms which take place in catalytic reactions may be identified. Such findings will find use in guiding the production of customized catalysts with desired selectivity and turn over rates.

Recent Progress:

During the recent grant period, we have continued our program aimed at uncovering the characteristics and mechanistic details of oxygen transfer reactions. In this context, we have probed reactions utilizing transition metal and noble metal oxides to study the fundamental steps of various industrially and environmentally significant reactions. Through our recent studies, we have revealed some new and significant findings regarding oxygen transfer reactions involving ethylene and vanadium oxide clusters and for the oxidation of CO in the presence of oxidized gold clusters. Furthermore, we have gained more insight into the mechanisms of these reactions through a collaboration with the theoretical group of Professor Vlasta Bonačić-Koutecký at the Humboldt University in Berlin.

Through previous experimental investigations and theoretical findings, we revealed the presence of an oxygen centered radical structure and have proposed a facile oxygen transfer mechanism involving $V_2O_5^+$ and $V_4O_{10}^+$ clusters and ethylene, which is in direct analogy to mechanisms believed to occur on vanadia surfaces. In order to provide a more complete understanding of the factors influencing the dynamics of this observed oxygen atom transfer reaction, detailed energetic studies of $V_2O_5^+$ and $V_4O_{10}^+$ clusters were undertaken during the past year. We have found the Langevin equation to serve as a kinetic model that fully accounts for our experimental findings. We discovered that not every cluster-molecule collision is effective in leading to a reaction product. This is revealed by the observation of a reaction rate constant

lower than the expected collision frequency of $1x10^{-9}$ cm^3s^{-1} if every collision were effective. This is evidence that the ion-molecule association is the rate-determining step, with subsequent steps proceeding without significant barriers. Valuable new information about cluster reactivity is gained from this kinetic model which allows, from experimental data on the energy dependence of the reaction cross section, a determination of the magnitude of reaction barriers which would influence the course of a reaction. These findings have provided insight into the general mechanism of this reaction that is of considerable interest in the area of fundamental catalysis, as well as in the industrial production of acetaldehyde. Our work establishes that the barrier for H-atom transfer plays little role despite statements in the literature to the contrary.

Other recent studies have focused on reactions responsible for CO oxidation on gold clusters. During the year, we have investigated gold oxides of varying stoichiometry for the monomer and dimer cations and for gold cluster anions with one to 16 gold atoms. Particular attention has been focused on determining whether the sole role of the cluster surface is to effect oxygen atom production, and most importantly, whether the dissociation of the oxygen molecule is sufficient to induce the oxidation reaction. Utilizing a fast-flow reactor mass spectrometer, we have investigated the oxidation of CO in the presence of a variety of preoxidized gold cluster ions. Our experiments are unique in the fact that we introduce the oxygen at the source in order to produce gold species that contain both molecular and atomized oxygen. This enables us to avoid the rate-limiting activation of the oxygen molecule and examine the role of atomic oxygen for the oxidation reaction. From these studies, along with the theoretical investigation of various structural features, we have found that the presence of a peripheral oxygen atom is necessary for the production of CO_2; however, it is not sufficient. It is more a synergistic effect between the presence of a peripheral oxygen atom and surmountable reaction barriers that governs the reaction. To our knowledge, this fact has not been previously revealed and is of fundamental value in tailoring the design of more efficient and selective catalysts.

Preliminary studies of the cations have revealed products of the form $Au_nO_m(CO)_x^+$. These species could be the products of either an association reaction, replacement of oxygen atoms or dioxygen with carbon monoxide, or the oxidation of CO. For the anions, we did not observe any products containing both CO and oxygen for the monomer or dimer species. However, with those anionic clusters containing three or more gold atoms, species of the form $Au_nO_m(CO)_x^-$ began to emerge. Through density functional calculations performed for the dimer and trimer anion clusters, it was realized that there is a relationship between the lowest unoccupied molecular orbital (LUMO) of the gold oxide species and the binding energy of CO to produce the $Au_nO_mCO^-$ species. Moreover, this relationship predicts the favorable association of CO onto Au_3O^-, in agreement with our experimental results in which we only observe association for this species.

Another interesting difference between the cations and anions was found in studies in which the concentration of CO reactant gas was varied widely. With the anion studies, one series of experiments was conducted in which pure CO was added at the reactant gas inlet located downstream of cluster production. The addition of pure CO to the gold oxide cations resulted in the disappearance of all species present following cluster production. With a lower concentration of CO added to the gold oxide clusters, we observed products of the form $Au_nO_m(CO)_x^+$, which could be association, replacement, or oxidation products, as discussed above. With further study, and via comparison with the findings for the anions, these results could offer valuable insight into the effect of charge state on the efficiency of the CO oxidation reaction.

At present we are probing the reactions between gold oxide anions and CO utilizing a guided ion beam mass spectrometer. These studies offer the opportunity for mass selection so that we may definitively determine parent/product relationships. Furthermore, we have the ability to gain further structural information via collision induce dissociation studies. These further studies, along with previous experimental and theoretical investigations, provide further evidence for the lack of reactivity of oxygen atoms at bridging sites. As these and our previous measurements have shown, the peripheral oxygen atoms do display reactive oxidation of CO, but only in cases with appropriately low reaction barriers.

Future Studies:

In order to further understand the effect of charge state on the oxidation of CO in the presence of gold, we will employ the guided ion beam apparatus to study the larger anion species as well as cations of similar size. This affords the opportunity for mass selection of individual gold oxide reactants prior to interaction with the CO reactant gas. Not only will these studies allow for more information regarding the role of charge state, they will also provide information on the parent/product branching ratios. In addition, collision induced dissociation, as well as theoretical calculations, will be performed on the gold oxide cations and larger anion species ($Au_nO_m^-$, $n \geq 4$) in order to uncover structural information. Through these studies, information of the reaction pathways may be realized in order to provide further insight into the processes occurring on gold catalysts.

To further our program in contributing to a greater knowledge of condensed phase catalysis, we plan to move toward investigating the effect of the support on the oxidation of CO in the gas phase. In the context of fuel cell development, we plan to study the effects of $Au_nM_xO_y^{+/-}$ (M = Ti, Cs, Fe) on the oxidation of CO. For these studies, we will employ the guided ion beam mass spectrometer in order to study mass selected species and perform collision induced dissociation. Rate constants will be determined using the fast-flow reactor technique. These studies will commence with investigation of the efficiency of $M_xO_y^{+/-}$ clusters for the oxidation of CO as a prelude to a detailed study of the reactions between CO and bimetallic oxide cluster ions comprised of gold and other metals of varying stoichiometry and electronegativity. The individual metal oxide work will allow for the effect of the surface material to be determined prior to studying the bimetallic clusters.

We also plan to continue our collaboration with the theoretical group of Professor Vlasta Bonačić-Koutecký in order to gain further insight into the interactions and reaction pathways that are involved in the oxidation of CO in the presence of gold. Subsequently, related studies of the chemistry of nitrogen oxides will be undertaken. The information gained from the combined experimental and theoretical studies will allow us to obtain valuable insight into the fundamental processes and mechanistic details that govern catalytic reactions in the presence of gold and other metals.

Publications Resulting from this Grant:

527. "Calculation to Determine the Mass of Daughter Ions in Metastable Decay," J. R. Stairs, T. E. Dermota, E. S. Wisniewski, and A. W. Castleman, Jr., *Int. J. Mass Spectrom.* **213**, 81 (2002).
530. "NH_3 Adsorption Around Ni_n ($n \leq 4$) Clusters," B. Chen, A. W. Castleman, Jr., C. Ashman, and S. N. Khanna, *Int. J. Mass Spectrom.* **220/2**, 171 (2002).
532. "Studies of Metal Oxide Clusters: Elucidating Reactive Sites Responsible for the Activity of Transition Metal Oxide Catalysts," (invited feature article) K. A. Zemski, D. R. Justes, and A. W. Castleman, Jr., *J. Phys. Chem. B* **106**, 6136 (2002).
534. "Dynamics of Gas Phase Clusters: Insights into Size and Solvation Effects on Electronic Relaxation and Hydrogen Transfer," E. S. Wisniewski, B. D. Leskiw, S. M. Hurley, T. E. Dermota, D. P. Hydutsky, K. L. Knappenberger, Jr., M. A. Hershberger, and A. W. Castleman, Jr., In *Femtochemistry and Femtobiology: Ultrafast Dynamics in Molecular Science* (A. Douhal and J. Santamaria, Eds.) World Scientific: Singapore, New Jersey, London, 21-41 (2002).
537. "Solvation Effects on Electronic Excited States of Methanol: A Study of Neat and Mixed Methanol/Water Clusters," E. S. Wisniewski, M. A. Hershberger, and A. W. Castleman, Jr., *J. Chem. Phys.* **116**, 5738 (2002).
538. "Cluster Dynamics: Influences of Solvation and Aggregation," Q. Zhong and A. W. Castleman, Jr., *Quantum Phenomena in Clusters and Nanostructures* (S. N. Khanna and A. W. Castleman, Jr., Eds.) Springer: Berlin, Heidelberg, New York, Hong Kong, London, Milan, Paris, Tokyo, (2003).
540. "Femtosecond Photodissociation Dynamics of Excited State SO_2," E. S. Wisniewski and A. W. Castleman, Jr., *J. Phys. Chem. A* (R. S. Berry Issue) **106**,10843 (2002).

544. "Comparison of Methyl and Hydroxyl Protons Generated in a Coulomb Explosion Event: Application of a Time-of-Flight Gating Technique to Methanol Clusters," E. S. Wisniewski and A. W. Castleman, Jr., special issue of *Int. J. Mass Spectrom.* devoted to Gaseous Ion Thermochemistry and Solvation **227**, 577 (2003).

551. "$V_2O_5^+$ Reactions with C_2H_4 and C_2H_6: Theoretical Considerations of Experimental Findings," D. R. Justes, A. W. Castleman, Jr., R. Mitrić, and V. Bonačić-Koutecký, *Eur. Phys. J. D* **24**, 331 (2003).

559. "Photodissociation of Sulfur Dioxide: The Ẽ State Revisited," K. L. Knappenberger and A. W. Castleman, Jr., *J. Phys. Chem.A*, **108**, 9-14 (2004).

560. "Probing the Dynamics of Ionization Processes in Clusters", A. W. Castleman, Jr. and T. E. Dermota, *Latest Advances in Atomic Cluster Collisions* (A. Solov'yov and J.-P. Connerade, Eds.) World Scientific: Singapore, New Jersey, London, 253-269 (2004).

561. "Ultrafast dynamics in cluster systems", T. E. Dermota, Q. Zhong, and A. W. Castleman, Jr., *Chemical Reviews*, **104**, 1861-1886 (2004)

563. "Reactivity of Atomic Gold Anions Toward Oxygen and the Oxidation of CO: Experiment and Theory," M. L. Kimble, A. W. Castleman, Jr., R. Mitrić, C. Bürgel, and V. Bonačić-Koutecký, *J. Am. Chem. Soc.*, **126**, 2526-2535 (2004).

564. "Probing the Oxidation of Carbon Monoxide Utilizing Au_n^-," M. L. Kimble and A. W. Castleman, Jr., *Proceedings of Gold 2003: New Industrial Applications for Gold Conference* Vancouver, Canada, September 28 – October 1, 2003.

565. "Gas phase Studies of Au_n^+ for the Oxidation of Carbon Monoxide," M. L. Kimble and A. W. Castleman, Jr., Special Issue of the *Int. J. Mass Spectrom.*, in Honor of Professor Tilmann D. Märk. **233**, 99-101 (2004).

568. "Reactions of Vanadium and Niobium Oxides with Methanol," D. R. Justes, N. A. Moore, and A. W. Castleman, Jr., *J. Phys. Chem. B*, **108**, 3855-3862 (2004).

570. "Elucidating Mechanistic Details of Catalytic Reactions Utilizing Gas Phase Clusters," M. L. Kimble, D. R. Justes, N. A. Moore, and A. W. Castleman, Jr., *Clusters and Nano-Assemblies: Physical and Biological Systems* (P. Jena, S. N. Khanna, B. K. Rao, Eds.) World Scientific: Singapore, New Jersey, London, 127-134 (2005).

572. "The Influence of Cluster Formation on the Photodissociation of Sulfur Dioxide: Excitation to the E State", K. L. Knappenberger, Jr., and A. W. Castleman, Jr., *J. Chem. Phys*., **121**, 3540-3549 (2004).

573. "A Kinetic Analysis of the Reaction between $(V_2O_5)_{n=1,2}^+$ and Ethylene", N. A. Moore, R. Mitrić, D. R. Justes, V. Bonačić-Koutecký, and A. W. Castleman, Jr., *J. Chem. Phys*., (submitted).

575. "Joint Experimental and Theoretical Investigations of the Reactivity of $Au_2O_n^-$ and $Au_3O_n^-$ with Carbon Monoxide", Michele L. Kimble, Nelly A. Moore, A. Welford Castleman, Jr., Christian Bürgel, Roland Mitrić, and Vlasta Bonačić-Koutecký, (in prep.).

585. "Is O_2 Dissociation Sufficient to Effect the Oxidation of CO on Anionic Gold Clusters?", M. L. Kimble, N. A. Moore, A. W. Castleman, Jr., C. Bürgel, R. Mitrić, and V. Bonačić-Koutecký, (in prep.).

586. "Interactions of CO with $Au_nO_m^-$ ($n \geq 4$)", M. L. Kimble, A. W. Castleman, Jr., C. Bürgel, R. Mitrić, and V. Bonačić-Koutecký, (in prep).

Theory of Dynamics in Complex Systems

David Chandler

Chemical Sciences Division
Lawrence Berkeley National Laboratory
And
Department of Chemistry
University of California, Berkeley
Berkeley, California 94720

My DOE sponsored research is devoted to developing and applying theoretical treatments of complex systems. The specific systems currently under investigation are disordered dielectrics, and super-cooled liquids and glasses. To treat the phenomena exhibited by such materials, my coworkers and I have considered models based upon a coarse grained picture of space and time, for which Ref. [1] is illustrative. We have shown that these models can be used to intepret thermal properties, such as the percipitous growth of relaxation times as temperature is lowered towards a glass transition, and we have uncovered an unsuspected crossover, where the relaxation of a glass former evolves from hierarchical dynamics at low temperatures to diffusive dynamics yet lower temperatures. We have recently shown how this crossover is manifested experimentally [2]. This particular manifestation focuses on so-called "decoupling," where viscosity growth, for example, is not proportional to a diffusion constant inverse. We have also succeeded at explaining decoupling [3] and demonstrated its connection to distributions of exchange and persistence processes in glass forming materials [4].

Decoupling is a fluctuation effect, and when such effects are present, one expects the presence of growing length scales as with a phase transition, and also non-linear response. In our work, we have demonstrated that growing length scales are found in d+1 dimensions, where d is the physical dimension, and 1 refers to time [1,5]. Dynamical arrest of glass formers is an order-disorder phenomenon in space-time, namely an entropy crisis in trajectory space. Others before us have ventured the view that the dynamical arrest of glass formers is related to an entropy crisis. This view has in the past suffered from inconsistencies. It had before been suggested that this collective phenomenon would occur in state space, By showing it occurs in trajectory space, we have avoided the inconsistencies of prior treatments.

Among topics for the future, I am focusing on non-linear effects. Two illustrations are noteworthy. First, on applying a dc force field, the resulting drag velocity of a probe molecule in a super cooled material is less per unit force at high force strength than it is at low force strength. As such, the response to a sufficiently strong ac field will cause amplification, akin to the action of a ratchet. Second, a super cooled material under shear will produce a shear banding of mobility. In the presence of this banding, the macroscopic mobility of a probe molecule will vanish in directions transverse to the

shear. Therefore, the action of shear leads to a dynamic switch – current is halted by shaking. While not yet observed experimentally, the theoretical principals from which we have found these effects seem entirely sound, and I believe experimental verification will soon follow.

We have also recently completed our nascent studies of virus capsid assemblies [6]. Nature's ability to engineer the fabrication of these nanoscale objects is truly remarkable. We have created a class of mesoscopic models obeying Newtonian dynamics that can exhibit assembly, used transition path sampling to examine the assembly, and mapped out ranges of conditions over which kinetically trapped glassy configurations are avoided and self-assembly occurs.

References:

1. Pan, A.C., J.P. Garrahan and D. Chandler, "Heterogeneity, growing lengthscales, and universality in the dynamics of kinetically constrained lattice gases in two dimensions", cond-mat/0410525, *Phys Rev. E.* in press, (2005).

2. Pan, A.C., J.P. Garrahan and D. Chandler, "Decoupling of self-diffusion and structural relaxation during a fragile-to-strong cross-over in a kinetically constrained lattice gas" *ChemPhysChem* **6** 1783-1785 (2005).

3. Jung, Y., J.P. Garrahan and D. Chandler. "Excitation lines and the breakdown of Stokes-Einstein relations in super-cooled liquids," Phys. Rev. E, 69, 061205.1-061205.7 (2004).

4. Jung, Y.J., J.P. Garrahan and D. Chandler, "Dynamical exchanges in facilitated models of supercooled liquids", *J Chem. Phys.* **123**, 084509 (2005).

5. Merolle, M., J.P. Garrahan and D. Chandler, "Space-time thermodynamics of the glass transition", *PNAS* **102**, 10837-10840, (2005)

6. Hagan, M.F., and D. Chandler, "Dynamics of virus capsid assembly," manuscript in preparation.

Molecular Theory & Modeling

Transport and reactivity in amorphous solids

L. René Corrales
Chemical Sciences Division
Pacific Northwest National Laboratory
902 Battelle Blvd.
Mail Stop K1-83
Richland, WA 99352
rene.corrales@pnl.gov

The objectives of this work are to understand the factors that control the interactions and transformations of nuclear waste glasses, optical and micro-electronic devices, and bioactive materials caused by chemical reaction, ion transport and irradiation processes that can compromise their fabrication and performance lifetime. Underlying the extent to which a material will undergo physical and chemical transformations are the molecular level structural characteristics, and the collective response to the operational environment. The former has a strong dependence on processing history and the latter depends on the particular composition, such as the concentration of radionuclides embedded into a glass, and physical state of the material that can include phase separated states or introduction of heterogeneous environments such as aqueous solid interfaces. **There is a great interest to DOE in networked oxide glasses, such as silicates and phosphates, because they are well suited for use in entombing nuclear waste and they form the basis of optical fibers, photonic devices, scintillators for radiation detection, and bio-inorganic composites for modern nanotechnology.**

The structure of networked oxide glass forming systems is rigorously examined using molecular dynamics (MD) simulation methods. Underlying the confidence that simulations can provide a concise and accurate picture of the atomic and molecular structure is the ability to compare experimentally measured quantities with MD results. Our emphasis has been in comparing MD data with neutron and X-ray diffraction, EXAFS, and NMR results. Challenges remain in the ability to calculate IR and Raman spectra as well as to determine NMR shifts, because they require electronic structure methods. An important factor in employing electronic structure methods for glass systems is that the system size is limited and, therefore, structural features and their distributions may not be well represented. Nonetheless, it remains the only means to acquire certain information to compare with experiment and to quantify predictions of structure – property relationships. We have been focusing on developing a systematic approach in which simulated glasses are first produced and structures validated using classical molecular dynamics, and then employing a strategy of making a series of smaller sized samples that as an averaged group are statistically identical to the large glass structures that can be used for electronic structure simulations.[1] Alternatively, the small glass structures are created from first principle based MD methods and the resulting structures carefully analyzed and compared to larger simulated structures. In this way, it is possible to provide a complete analysis of the simulated structure with measured quantities that can be directly compared to experiment.

Having built confidence that our simulated structures are in fact related to real glass systems we can proceed to extract structural details that are not accessible to experiment. Simulations can also be used to decisively determine sources of anomalies, and to determine the factors that control phase behavior and structural reorganization. The role of the structural response to chemical reactions of silica with water have shown the significance of the "quality" of the glass network in providing stability as well as instability towards chemical reactions.[2] Below, we describe in more detail two examples of how MD simulations are used to examine ion segregation near a melt surface,[3] and to ascertain the source of the anomalous shift of the first sharp diffraction peak (FSDP) in alkali silicate glasses and the extent to which the FSDP is correlated with intermediate range glass structure.[4] In a key collaboration with a BES Materials Science program, our research aims at understanding damage formation and corresponding evolution of recoil ions cascades in oxide ceramics.[5,6] In this collaboration, my work focuses on determining the factors that control energy dissipation in MD simulations in support of improving simulation methodologies to study systems taken far from equilibrium.[7,8]

The volatility of alkali ions from an oxide melt has been a topic of interest for some time,[9,10,11] and remains a technological issue and of great scientific interest. The rate at which a melt of a glass forming system achieves equilibrium is of interest and so is the resulting near surface structure. The factors that drive the enrichment and reconstruction of the surface must be characterized as a means of gaining control of the surface states. A molecular level understanding of the structure of viscous melts can be obtained using atomic level classical molecular dynamics (MD) computer simulations. In this work, MD simulations are used to determine the free energy profile near the surface of melts at thermodynamic equilibrium. The results provide insight into the cause of ion migration observed in cleaved glass surfaces and provide insight into observed volatilization processes.

The reconstruction of a glass surface depends significantly on kinetic processes such as the diffusion of ions to the surface. In contrast, in a melt the thermodynamic equilibrium state is independent of the path(s) it took to get there and establishes a clear picture of the preferred thermodynamic state. Thus, by determining the free energy profile or landscape of the melt, the preferred ion distribution is identified. The free energy then provides details of the chemical potential driving force for ion migration to the surface in the melt or the glass phase.

The net conclusions found are that the surface state of sodium calcium aluminosilicate glass melts reveal that the thermodynamic equilibrium state near the surface leads to an enrichment of NBO and sodium ions. The chemical equilibrium condition of the surface is likely the driving force for alkali ions to enrich the surface of a cleaved glass, but does so significantly slower than in the melt state. Surface exposure drives the NBO atoms to the surface so as to drive the network forming cations, with higher charge, into the bulk of the system and the network modifiers to the surface with the sodium ion being the dominant surface cation species.

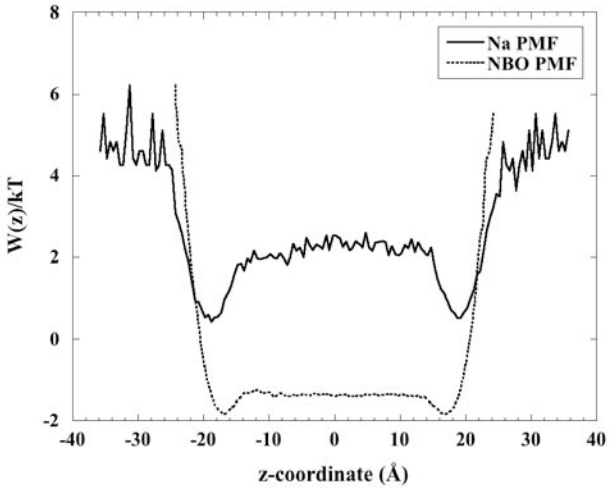

Figure 1. The potential of mean force of the density profile going across both interfaces into the center of the simulation cell for the sodium ions (top) and the NBO ions (bottom). Near the surface there is a significant decrease in the free energy for both of the systems.

The first sharp diffraction peak (FSDP), or prepeak, observed in a number of network-forming glasses is considered to be an indication of the medium range order.[12,13] The origin of the FSDP and its relation to real space structural features in a network glass remain highly controversial.[14] The intensity and position of the FSDP changes with temperature, pressure, composition, and neutron irradiation doses. The composition dependence of the FSDP in silicate glasses reveals a trend in the lithium silicate glasses inconsistent with other alkali silicate glasses. The origin of this anomaly has been suggested to come from the negative scattering length of lithium.[15]

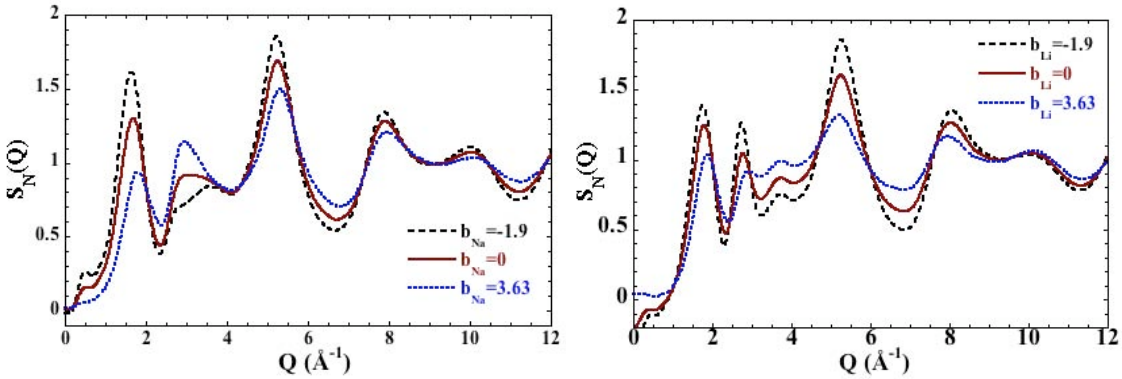

Figure 2. Influence of the neutron scattering length on the total structure factors in sodium disilicate (left) and lithium disilicate glasses (right). The decrease in the peak height as the scattering length goes from negative to positive is seen for both the Na and Li containing glasses. Hence, the scattering length clearly dictates the peak height.

In our work the source of the experimentally observed anomalous behavior of the First Sharp Diffraction Peak (FSDP) in lithium silicate glasses was determined using classical molecular dynamics simulations. Partial structure factors obtained from simulations were used to investigate the sensitivity of the total structure factor to the scattering length of

alkali ions. The result clearly establishes that the major difference of the FSDP between lithium and sodium disilicate glasses is due to the negative scattering length of lithium ions. Additionally, it was determined that the unusual intense FSDP in lithium silicate glass has little to do with differences of the medium range structure in these glasses.

Our research goals are targeted towards exploring the response of networked oxide materials to radiation sources that includes high-energy ion implantation, recoil cascades, electronic excitations, and thermal spikes. For crystalline systems the initial configurations are complicated by the presence of defects and dopants. The need to determine the role of initial configurations, i.e. the distribution of defects and impurities, has a significant affect on the results and, thus, a means to collect significant statistics must be considered. Similarly, the quality of a glass structure must also be considered prior to carrying out the simulations. An excellent example is provided by ice and glassy water (a.k.a amorphous solid water) that are known to support electronic excitations. Future research is planned to study by first principle molecular dynamics the differences in how the two "extreme" systems support low-lying electronic excitations as well as high-energy species that can be formed from irradiation processes. The comparison of bulk-type structures with structures formed on metal surfaces will be made. Charge transfer between different phases and between distinct materials will be explored.

Collaborators: J. Du (PNNL), R. Devanathan (PNNL), W. J. Weber (PNNL), H. Jónsson (UW), A. Chartier (CEA-Saclay), C. Meis (CEA-Saclay)

This work was supported by the Office of Basic Energy Science, U.S. Department of Energy. Battelle operates the Pacific Northwest National Laboratory for US DOE.

---

[1] R. M. Van Ginhoven, H. Jonsson, L. R. Corrales, Phys. Rev. B 71, 024208 (2005)
[2] R. M. Van Ginhoven, H. Jonsson, L. R. Corrales J. Phys. Chem. B 109, 10936 (2005)
[3] L. R. Corrales, J. Du, J. Amer. Cer. Society, in press (2005)
[4] J. Du, L. R. Corrales, Phys. Rev. B in press (2005)
[5] A. Chartier, C. Meis, J.-P. Crocombette, W. J. Weber, L. R. Corrales, Phys. Rev. Letters 94, 025505 (2005)
[6] R. Devanathan, L. R. Corrales, W. J. Weber, A. Chartier, C. Meis, Nucl. Inst. Meth. B 228, 299 (2005).
[7] L. R. Corrales, A. Chartier, R. Devanathan, Nucl. Instr. Meth. Phys. B 228, 274 (2005).
[8] L. R. Corrales, J. Du, Phys. Chem. Glasses, in press (2005).
[9] É. Preston, W. W. S. Turner, J. Soc. Glass Technol. 16, 219, 331 (1932).
[10] L. E. Oldfield, R. B. Wright, Glass Technology 3, 59 (1962).
[11] M. Holá, J. Matousek, J Hlavác, Dep. Technol. Silic., Inst. Chem. Technol., Prague, Czech. Silikaty (Prague) (1974), 18(3), 209-15.
[12] S.R. Elliott, Nature 354, 445 (1991) .
[13] S.R. Elliott, Phys. Rev. Lett. 67, 711 (1991).
[14] C. Massobrio, A. Pasquarello, J. Chem. Phys. 114, 7976 (2001).
[15] S.R. Elliott, J. Phys.: Condens. Matter 4, 7661 (1992).

New Ultrafast Techniques for Electron Radiolysis Studies

Robert A. Crowell, David Gosztola, and Ilya A. Shkrob
Chemistry Division
Argonne National Laboratory
9700 S. Cass Ave.
Argonne, IL 60439
rob_crowell@anl.gov

Program:

Reaction Intermediates in Condensed Phase: Radiation and Photochemistry

Scope:

It is the goal of this project to develop ultrafast techniques for electron pulse radiolysis. Ultrafast ($<10^{-11}$ps) physical processes play a pivotal role in all chemical reactions. Detailed knowledge of primary events such as energy (charge) transfer, thermalization, solvation and the chemistry of pre-thermalized electrons is essential in order to produce a complete picture of reactivity. Due to the lack of a suitable femtosecond source of ionizing radiation, experimental studies on the primary events in radiation induced chemical reactions are virtually nonexistent. Understanding of these ultrafast processes will be beneficial to areas as diverse as photochemistry, materials processing, device fabrication, catalysis, astro and environmental chemistry and radiation processing. It is the ultimate goal of this project to provide such information so that we can gain a full understanding of radiation chemistry. Achievement of this goal requires the implementation of ultrafast laser, radiolytic and x-ray spectroscopic techniques, techniques that currently do not collectively exist for this purpose. Recent advances in super-intense ultrashort laser technology have led to the ability to generate subpicosecond electron, proton and x-ray pulses *without* the use of a traditional electron accelerator. The objective of our current efforts is to develop a state-of-the-art table-top 5-20 TW terawatt laser system (T^3) that will produce these types of pulses for chemical physics studies. Utilized in conjunction with our ultrafast laser system the electron pulses will provide unprecedented insight into many of the contemporary issues concerning the primary processes of radiation induced chemical reactions.

Recent Progress:

The Terawatt Ultrafast High Field Facility (TUHFF) has been constructed in the Chemistry Division. The first version of a 20 TW laser has been competed and routinely generates subpicosecond electron pulses. The most significant accomplishment over the last year has been the observation of solvated electrons generated in water using the electron pulses from the T^3 system. The solvated electrons have been observed using two different methods, electron pump/ fs optical probe (picosecond resolution measurements, Figure 1) and electron pump/ CW optical probe (nanosecond to microsecond resolution, Figure 2). Another major advancement has been the ability to reproducibly generate electron pulses with charges as high as 3.0 nC with MeV energies (Figure 3). The

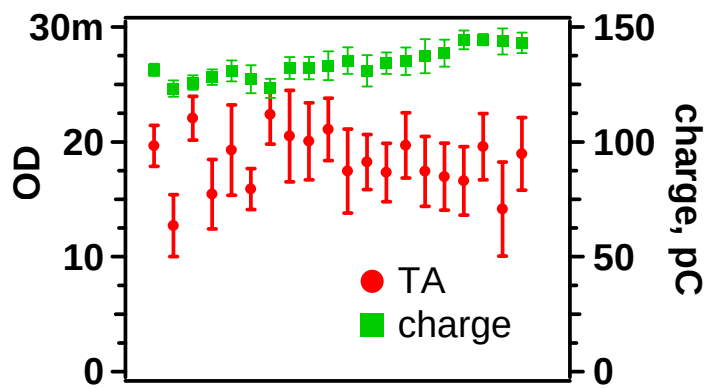

Figure 1. Electron pulse optical probe TA signal of the solvated electron in water taken at a delay time of 670 ps. Each point is an average of ten shots and the error bars represent 95% confidence limits. Note the lack of correlation between the TA signal (red) and the transmitted electron charge (green).

electron pulse charge is typically in the range of 1.5-2.0 nC. The main focus over the last six months has been placed on the optimization of pump-probe techniques on the T^3 system and characterization of the electron beam. Additionally, significant progress has been made in the areas of development of adaptive optics, electro-optic measurement of the electron pulse longitudinal profile, and measurement of the electron energy spectrum (Figure 3).

Due to large shot-to-shot variations in the yield of high-energy electrons (200 ± 100 pC at 10 TW and 2.0 ± 0.3 nC at 20 TW) and low repetition rate of the setup (10 Hz), the standard pump-probe detection of transient absorption kinetics is not an efficient approach for ultrafast measurements at TUHFF. For these reasons, high priority was put on the development of a robust single-shot detection methodology that provides an alternative way to sample ultrafast kinetics. Our current solution is ultrafast Frequency Domain Single-Shot (FDSS) transient absorption (see publication 10). Additional improvements (by almost an order of magnitude) in the signal to noise have been realized by normalizing the ps pump probe signal (Figure 1) by the CW signal (Figure 2).

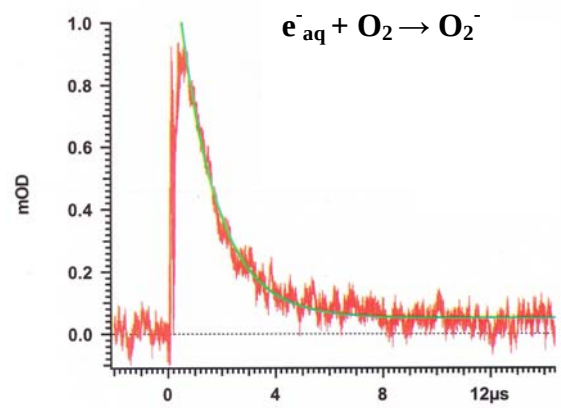

Figure 2. Dynamics of the solvated electron in water using the CW probe technique. The signal strength corresponds to a charge of 75pC. The decay is due to the reaction of the solvated electron with impurities, mainly oxygen.

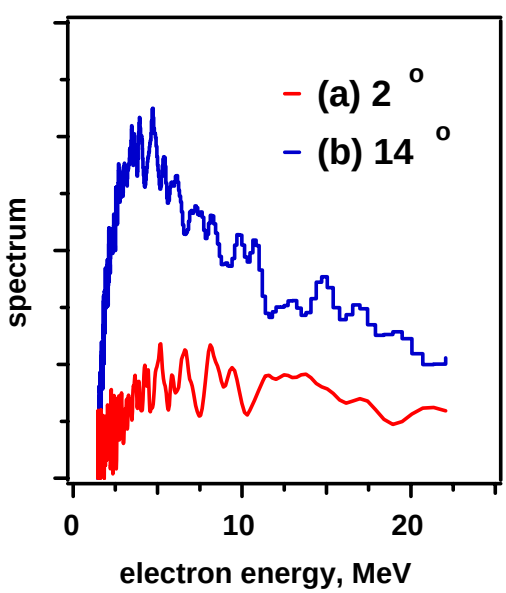

Figure 3. Energy spectrum of the electron beam measured with a 2° and 14° skimmer

Future Plans. The main focus of our current effort is directed towards using TUHFF to perform our first time-resolved measurements. It is expected that our first measurements will have a time resolution of ~5ps, limited by the electron pulse charge and energy dispersion. As the pulse charges increases the experimental time resolution will also improve. Recently our group has carried out several femtosecond photoionization studies of liquid water (see abstract of Shkrob et. al and references therein). This work has provided a significant amount of insight into the dynamics of solvation and thermalization for above-the-gap ionization of liquids. We will use this knowledge as the starting point for our first radiolysis experiments. The first studies will focus on thermalization and solvation dynamics of electrons that are generated in water radiolysis. This work will be followed by studies of the reactivity of electron precursors (i.e., chemistry that occurs before thermalization). An upgraded version of the TUHFF laser system has been designed and will be implemented in the future. This upgrade will include a deformable mirror and improvements in the stretcher/compressor system. Other future projects which are already in progress include development of ultrasensitive electro-optic sampling methods to characterize the longitudinal (temporal) characteristics of the electron pulses and the generation of hard x-rays via Thompson scattering.

Recent Publications

1. D. A. Oulianov, R. A. Crowell, D. J. Gosztola, and Y. Li "Ultrafast time-resolved x-ray absorption spectroscopy of solvent-solute transient structures," Nucl. Instr. and Meth. in Phys. Res. B. (in press)

2. R. A. Crowell, I. A. Shkrob, D. A. Oulianov, O. Korovyanko, D. J. Gosztola, Y. Li and R. Rey-Castro, "Motivation and development of ultrafast laser based accelerator techniques for chemical physics research," Nucl. Instr. and Meth. in Phys. Res. B (in press)

3. M. C. Sauer Jr., I. A Shkrob**,** R. Lian, R. A. Crowell, D. M. Bartels, X. Chen, D. Suffren, and S. E. Bradforth, "Electron photo-detachment from aqueous anions. II. Ionic strength effect on geminate recombination dynamics and quantum yield for hydrated electron," J. Phys. Chem. A. 108, 10414 (2004).

4. R. Lian, R. A. Crowell, and I. A. Shkrob "Solvation of electrons generated by two 200nm photon ionization of liquid H_2O and D_2O," J. Phys. Chem. A. 109, 1510 (2005).

5. R. Lian, R. A. Crowell, I. A. Shkrob, D. M. Bartels, D. A. Oulianov, and D. J. Gosztola, “Recombination of Geminate ($OH:e^-$) Pairs in Concentrated Alkaline Solutions: Lack of Evidence for Hydroxyl Radical Deprotonation,” Chem. Phys. Lett. 389, 379 (2004).

6. M. C. Sauer Jr., I. A. Shkrob, and R. A. Crowell "Electron Photodetatchment from Aqueous Anions. I. Quantum Yields for Generation of Hydrated

Electron by 193 and 248nm Laser Photoexcitation of Sundry Inorganic Anions," J. Phys. Chem A, 108, 5490 (2004).

7. R. A. Crowell, R. Lian, I. A. Shkrob, J. Qian, D. A. Oulianov, and S. Pommeret, "Light-induced temperature jump causes power-dependent ultrafast kinetics of electrons generated in multiphoton ionization of liquid water," J. Phys. Chem. A 108, 9105 (2004).

8. R. Lian, D. A. Oulianov, I. A. Shkrob and R. A. Crowell, "Geminate recombination of electrons generated by above the gap (12.4eV) photoionization of liquid water," Chem. Phys. Lett., 398, 102.

9. R. Lian, R. A. Crowell, I. A. Shkrob, D. M. Bartels, X. Chen, and S. E. Bradforth, “Ultrafast Dynamics for the Electron Photodetachment of Aqueous Hydroxide,” J. Chem. Phys. 120, 11712 (2004).

10. I. A. Shkrob, D. A. Oulianov, R. A. Crowell, and S. Pommeret “Frequency Domain single-shot (FDSS) ultrafast transient absorption spectroscopy” J. Appl. Phys. 96, 25 (2004).

11. R. A. Crowell, R. Lian, D. A. Oulianov, and I. A. Shkrob “Geminate recombination of the hydroxyl radicals generated from the 200nm photodissociation of hydrogen peroxide,” Chem. Phys. Lett. 383, 481 (2004).

12. R. A. Crowell, D. J. Gosztola, I. A. Shkrob, D. Oulianov, C. D. Jonah, and T. Rajh “Ultrafast Processes in Radiation Chemistry,” Radiat. Phys. Chem. 70, 501 (2004)

13. L. Zhao, R. Lian, I. A. Shkrob, R. A. Crow ell, S. Pommeret, E. L. Chronister, A. D. Liu, and A. D. Trifunac,, “Ultrafast studies on the photophysics of matrix-isolated radical cations of polycyclic aromatic hydrocarbons,” J. Phys. Chem. A 108, 25 (2004).

Vibrational Spectroscopy at Metal Cluster Surfaces

DE-FG02-96ER14658

Michael A. Duncan

Department of Chemistry, University of Georgia, Athens, GA 30602-2556

maduncan@uga.edu

Program Scope

The focus of our research program is the study of gas phase metal clusters to evaluate their potential as models for the fundamental interactions present on heterogeneous catalytic surfaces. These clusters are molecular sized aggregates of metals or metal compounds (oxides, carbides). We focus specifically on the bonding exhibited by "physisorption" on cluster surfaces. Complexes containing one or more metal atoms bound to small molecules provide the models for physisorption. Infrared spectroscopy in various forms is employed to measure the vibrational spectroscopy of the metal clusters themselves and, in particular, the spectra of physisorbed molecules. These studies investigate the nature of the metal-adsorbate interaction and how it varies with metal composition and cluster size. The vibrational frequencies measured are compared with the predictions of theory to reveal the electronic state and geometric structure of the system. Neutral clusters are studied with infrared multiphoton ionization spectroscopy, while ionic clusters are studied with mass-selected infrared photodissociation spectroscopy.

Recent Progress

The main focus of our work over the last two years has been infrared spectroscopy of mass-selected cation-molecular complexes, e.g., $V^+(CO_2)_n$, $Ni^+(C_2H_2)_n$, $Ni^+(H_2O)_n$, $Nb^+(N_2)_n$. These species are produced by laser vaporization in a pulsed-nozzle cluster source, mass-selected with a specially designed reflectron time-of-flight mass spectrometer and studied with infrared photodissociation spectroscopy using an IR optical parametric oscillator laser system (IR-OPO; wavelength coverage: 2000-4500 cm^{-1}). We have studied the infrared spectroscopy of various transition metal ions in complexes with CO_2, acetylene, water and molecular nitrogen. In each system, we examine the shift in the frequency for selected vibrational modes in the adsorbate molecule that occur upon binding to the metal. The number and frequencies of IR-active modes in multi-ligand complexes reveals the structures of these systems, while sudden changes in vibrational spectra or IR dissociation yields are used to determine the coordination number for the metal ion in these complexes. In some systems, new vibrational bands are found beginning at a certain complex size that correspond to intra-cluster reaction products. In small complexes with strong bonding, we use the method of “rare gas tagging” with argon or neon to enhance dissociation yields. In all of these systems, we employ a close interaction with theory to investigate the details of the metal-molecular interactions that best explain the spectroscopy data obtained. We perform our own density functional theory (DFT) or MP2 calculations (using Gaussian 03W) and when higher level methods are required (e.g., CCSD), we collaborate with local theorists (P.v.R. Schleyer, H.F.

Schaefer). Our infrared data on these transition metal ion-molecule complexes is the first available, and it provides many examples of unanticipated structural and dynamic information.

Studies of metal-CO_2 clusters have investigated Fe^+, Ni^+ and V^+ metal ions with from one up to 10-14 CO_2 ligands attached. In all of these systems, the CO_2 asymmetric stretch (2349 cm^{-1} in the isolated molecule) is studied and found to shift 30-50 cm^{-1} to higher frequency when the ligand is attached directly to the metal. Ligands are found to bind in a linear configuration with the metal, i.e., M^+-OCO, with high symmetry configurations for multiple ligands. When external ligands are present, a second band is measured at 2350 cm^{-1}. Its proximity to the isolated molecule band establishes that this represents molecules bound externally on the surface of the cluster that experience only a small perturbation. In the iron system, the coordination number is not clearly evident from the onset of the surface band, but this appears gradually in the n=4-6 size range. For nickel and vanadium, however, the surface band appears sharply at a cluster size of n=5, and this is also the cluster size at which the overall dissociation yield abruptly increases. The coordination in these systems is therefore four ligands. In both vanadium and nickel clusters with CO_2, another new vibrational band strongly shifted further to the blue emerges at much larger cluster sizes in the n=8-10 size range. This is assigned as a CO_2 ligand bound to a metal *oxide* core ion of the form $MO^+(CO)$, i.e., an oxide carbonyl species that results from an intracluster oxidation reaction.

$M^+(C_2H_2)$ clusters have been studied for the metals vanadium, iron, cobalt and nickel in the region of the symmetric and asymmetric stretching modes of acetylene. Although the symmetric stretch is not IR active for the isolated molecule, distortion of the ligand in these complexes induces IR activity for this mode. The C-H stretches in these systems are shifted to the red by 30-50 cm^{-1} from the corresponding modes in the isolated acetylene molecule, consistent with predictions for π-complexes. However, the magnitude of the red-shift is different for the different metals, consistent with the relative amounts of sigma donation and π-back bonding. Fe^+, Co^+ and Ni^+ all form π-complexes with acetylene, while V^+ forms a three-membered ring metallacycle. Multiple acetylene complexes have been studied for Ni^+ and Co^+. Coordination numbers are established as four acetylenes for nickel and three for cobalt. New vibrational bands emerge that are shifted even further to the red, but these are only seen after the coordination is exceeded by one ligand. These bands are assigned to the presence of a cyclobutadiene ligand that results from an intracluster cyclization reaction. Prof. P.v.R. Schleyer has collaborated with us on the theory of these systems.

$M^+(H_2O)_n$ complexes and those tagged with argon have been studied for iron, nickel and vanadium complexes. In the vanadium system, partial rotationally resolved spectra have been obtained. In the iron system, complexes with one or two water molecules (argon tagged) exhibit isomeric structures for both argon and water binding sites. Nickel complexes have been studied for up to 30 water molecules, providing a detailed probe of the dynamics of solvation. Hydrogen bonded structures appear for the first time at a cluster size of n=4-5, and the free-OH symmetric stretch disappears at n=8 indicating that most external water molecules are bound within a hydrogen bonding network after this size. The IR signature that we have recently identified for clathrate structures in protonated water clusters, $H^+(H_2O)_n$, is a single peak for the free-OH asymmetric stretch, but this signature is not found for the $Ni^+(H_2O)_n$ complexes.

$M^+(N_2)_n$ complexes have been studied in the N-N stretch region for Fe^+, V^+ and Nb^+ complexes. Again, binding to metal makes this mode IR active even though it is forbidden in the isolated molecule. Theory shows that most metals prefer end-on binding configurations, but some (e.g., cobalt) prefer to bind side-on as in a π-complex. The N-N stretch is red shifted for these

metals, and coordination numbers are six for the V^+ and Nb^+ complexes. $M^+(N_2)_4$ complexes for both of these metals are found to have a square-planar structure. In Nb^+, addition of the fifth ligand induces a spin change on the metal ion from quintet to triplet.

Future Plans

Future plans for this work include the extension of these IR spectroscopy studies to more ligands, to complexes with multiple metal atoms and to a more extended region of the IR spectrum. In the vanadium-water system, we have already measured spectra in the water bending mode region for complexes containing up to 15 metal atoms, using a free electron laser. This work establishes the feasibility of studies on larger metal systems. We want to study more reactive metals with hydrocarbons such as ethylene or methane that might produce carbenes, vinylidene or ethylidyne species. These systems should exhibit characteristic IR spectra, and will allow us to make better contact with IR spectroscopy on metal surfaces. Studies of carbon monoxide have been limited so far because the tuning range of our present laser system only extends down to 2000 cm^{-1}. However, new crystals have just become available (silver-gallium-selenide) to extend the range of OPO systems like ours down to the 1000-2000 cm^{-1} range. We recently obtained one of these crystals, which will allow us to study ligands like CO and to probe other adsorbate molecules in additional vibrational modes (C-C stretch of acetylene, water bending mode, etc.).

In all of these studies, we have focused on the qualitative effects of metal-adsorbate interactions and trends for different transition metals interacting with the same ligand. Our collaboration with theory has revealed that density functional theory has serious limitations for these metal-ligand complexes that were not previously recognized. This is particularly evident in metals such as vanadium and iron, where two spin states of the metal lie at low energy. DFT has difficulty identifying the correct relative energies of these spin states. Further examinations of this issue are planned, as it has significant consequences for the applications of DFT.

Publications (2003-2005) for this Project

1. M.A. Duncan, "Infrared Spectroscopy to Probe Structure and Dynamics in Metal Ion-Molecule Complexes," *Intl. Rev. Phys. Chem.* **22**, 407 (2003).

2. N.R. Walker, G.A. Grieves, R.S. Walters and M.A. Duncan, "The Metal Coordination in $Ni^+(CO_2)_n$ and $NiO_2^+(CO_2)_m$ Complexes," *Chem. Phys. Lett.* **380**, 230 (2003).

3. R.S. Walters, N.R. Walker, D. Pillai and M.A. Duncan, "Infrared Spectroscopy of $V^+(H_2O)$ and $V^+(D_2O)$ Complexes: Ligand Deformation and an Incipient Reaction," *J. Chem. Phys.* **119**, 10471 (2003).

4. N.R. Walker, R.S. Walters and M.A. Duncan, "Infrared Photodissociation Spectroscopy of $V^+(CO_2)_n$ and $V^+(CO_2)_nAr$ Complexes," *J. Chem. Phys.* **120**, 10037 (2004).

5. T.D. Jaeger, A. Fielicke, G. von Helden, G. Meijer and M.A. Duncan, “Infrared Spectroscopy of Water Adsorption on Vanadium Cluster Cations (V_x^+; x=3-15),” *Chem. Phys. Lett.* **392**, 409 (2004).

6. R.S. Walters and M.A. Duncan, “Infrared Spectroscopy of Solvation and Isomers in $Fe^+(H_2O)_{1,2}Ar_m$ Complexes,” *Austr. J. Chem.* **57**, 1145 (2004).

7. N.R. Walker, G.A. Grieves, R.S. Walters and M.A. Duncan, “Growth Dynamics and Intracluster Reactions in $Ni^+(CO_2)_n$ Complexes via Infrared Spectroscopy,” *J. Chem. Phys.* **121**, 10498 (2004).

8. R.S. Walters, P.v.R. Schleyer, C. Corminboeuf and M.A. Duncan, “Structural Trends in Transition Metal Cation-Acetylene Complexes Revealed Through the C-H Stretch Fundamentals,” *J. Am. Chem. Soc.* **127**, 1100 (2005).

9. T.D. Jaeger and M.A. Duncan, "Infrared Photodissociation Spectroscopy of $Ni^+(benzene)_x$ Complexes," *J. Phys. Chem. A* **109**, 3311 (2005).

10. E.D. Pillai, T.D. Jaeger and M.A. Duncan, "Infrared spectroscopy and density functional theory of small $V^+(N_2)_n$ clusters," *J. Phys. Chem. A* **109**, 3521 (2005).

11. R.S. Walters and M.A. Duncan, “Solvation Processes in $Ni^+(H_2O)_n$ Complexes Revealed by Infrared Photodissociation Spectroscopy,” *J. Am. Chem. Soc.*, in press.

12. R.S. Walters, E.D. Pillai, P.v.R. Schleyer and M.A. Duncan, “Vibrational spectroscopy of $Ni^+(C_2H_2)_n$ (n=1-4) complexes,” *J. Am. Chem. Soc.*, in press.

13. N.R. Walker, R.S. Walters and M.A. Duncan, "Frontiers in the Infrared Spectroscopy of Gas Phase Metal Ion Complexes," *New Journal of Chemistry*, in press.

Molecular Theory & Modeling

Electronic Structure and Reactivity Studies in Aqueous Phase Chemistry

Michel Dupuis
Chemical Sciences Division
Pacific Northwest National Laboratory
902 Battelle Blvd.
Mail Stop K1-83
Richland, WA 99352
michel.dupuis@pnl.gov

Summary.[#] We are interested in the theoretical characterization of molecular properties and reactivity of clusters and molecules, in particular in the condensed phase. One focus of our research involves the initial molecular processes that follow the primary energy deposition in radiolysis of water as observed in various applied technologies. We aim to characterize: i) the mechanisms and dynamics of the intrinsic reactions; ii) the effects of medium on the dynamics; iii) the mechanism of energy transfer within the solute and into the solvent; iv) the mechanism of (vibrational) energy transfer and/or secondary reactions in the locally-heated medium in the vicinity of the initial energy release. *Direct ab initio molecular dynamics* (MD) calculations are been carried out to investigate the ionization dynamics of the $(H_2O)_{17}$ cluster which is the first water cluster that includes a four-fold coordinated water. A second focus of our research involves the determination of vibrational spectra that account for anharmonicities and mode coupling. These effects are known to be particularly large in strongly interacting ion-water clusters. We are calculating spectra for several ion-water clusters for which high resolution spectroscopic data have recently become available. To this end we use the direct *ab initio* MD method combined with quasi-classical initial conditions. A third focus involves the theoretical characterization of organic radicals and radical ions in solution, including the calculation of reduction potentials, acidities, bond dissociation energies, and activation energies, all data relevant to thermochemical kinetic models, such as those in DOE programs in environmental management sciences and that can not be easily measured. This research is done in collaboration with Don Camaioni (PNNL). For this we use *continuum models* of solvation in the context of DFT calculations. Important limitations in the accuracy of continuum models of solvation for describing organic radical ions have been traced to the definition of molecular cavities. This finding is leading us to propose novel semi-empirical and *ab initio* definitions of molecular cavities for the accurate predictions of molecular properties.

Direct Dynamics Study of Chemical Reactions (*Dupuis with Furuhama, JSPS, Tokyo)*

Motivation: We have undertaken a computational characterization of the primary processes induced by ionizing radiation of aqueous systems. We aim to elucidate the initial reaction immediately following the ionization of $(H_2O)_{17}$, to estimate the reaction time, and to quantify the vibrational energy transfer from the reactive subsystem to the medium.

Approach: Direct *ab initio* MD calculations at the RHF/3-21+G* level of the theory (that has been benchmarked to be of semi-quantitative accuracy) are being carried out to investigate the ionization dynamics of the cluster $(H_2O)_{17}$ which is the first water cluster that includes a four-fold coordinated water. A quasi-classical MD trajectory is calculated starting on the $(H_2O)_{17}$ potential surface and switching to the

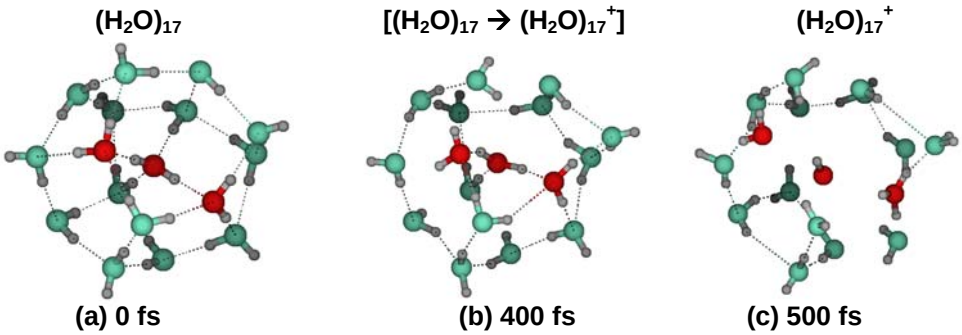

$(H_2O)_{17}^+$ at a given time. It was observed that two neighboring water molecules to the ionized molecule interact strongly with the ionized molecule to form what we call a "reactive trimer (cluster)". The other 14 water molecules constitute the "medium".

Results: Within less than 50 fs after ionization a proton transfers from the ionized molecule to a neighboring molecule, and H_3O^+ and OH are formed. We characterize the distribution of vibrational energy before and after ionization by calculating the kinetic energy in the instantaneous intra-molecular vibrational internal coordinates of the reactive cluster and of the "medium" cluster. Upon ionization it is observed that two "strongly" interacting water molecules move to closer contact the ionized water. One of the bonded OH acquires slower oscillations that ultimately end in one H^+ atom being transferred to one of the two interacting water molecules within ~ 35 fs to form the hydronium ion and the OH radical. Following the proton transfer the hydronium ion and the third water molecule diffuse away from the OH radical. Upon ionization of $(H_2O)_{17}$, the total kinetic energy of the total 17-mer cluster increases. A kinetic energy increase is seen in all the low frequency inter-molecular modes of the "medium" 14-mer. These low-frequency modes act as the locally-heated bath. The increase in kinetic energy in the modes of the 14-mer is consistent with a reorganization of the "solvent" molecules upon creation of the ionized center to adopt a configuration more energetically favorable.

<u>Quasi-Classical Direct ab Initio Dynamics for Vibrational Spectroscopy</u> *<u>(Dupuis with Aida, Hiroshima)</u>*

Motivation: Fundamental insights about the forces involved in hydrogen bonds, proton transfer, and ionic solvation can be obtained from measured cluster properties. Recent high resolution spectroscopic studies of water clusters and ion-water clusters are proviting data in need of "fresh theoretical treatments, both to refine assignments and elucidate structures."[W.H. Robertson *et al.*, Science 299, 1367 (2003); K.R. Amis *et al.*, Science 299, 1375 (2003); C. Chaudhuri *et al.* Molec. Phys. 99, 1161 (2001)].

Approach: We apply the method of direct dynamics to generate quasi-classical trajectories with forces calculated 'on the fly' at the quantum chemical MP2/aug-cc-pVDZ level of theory to account for anharmonicities and mode couplings. We calculate the density of vibrational states from the velocity autocorrelation function (ACF), the IR intensities from the dipole ACF, and the Raman intensities from the molecular polarizability ACF. Initial atomic velocities are defined consistent with the harmonic vibrations. The analysis can be performed on a subset of internal coordinates to assign DOS peaks to selected internal coordinates, akin to traditional FG analyses.

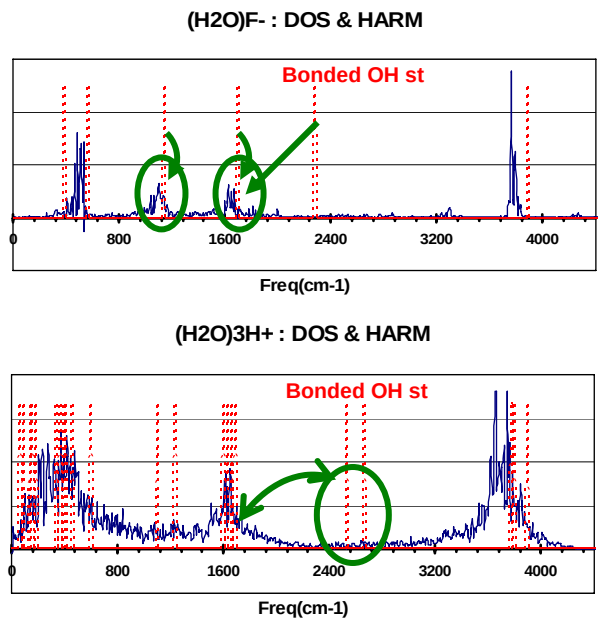

Results: Spectra for $(H_2O)F^-$ and for $(H2O)_3H^+$ are shown. The simulation data are in accord with the VSCF results of Chaban *et al.* [J. Phys. Chem. A 107, 4952 (2003)] for $(H_2O)F^-$, in particular showing the large shift of the H-bonded stretch (harmonic ~ 2400 cm^{-1} and anharmonic ~ 1500 cm^{-1}). Thus the methodology is found to account well for anharmonicities and mode couplings, as well as to capture the most significant quantum effects of zero point vibrations. Our calculations suggest that a similar shift exist for the H-bonded stretches in the protonated water trimer.

<u>Ab Initio</u>*<u>-based Characterization of Aqueous Solvation of Organics (</u><u>*Dupuis with Camaioni, PNNL*</u>**<u>)</u>**

Motivation: After extensive experimental characterization of tank wastes during the 1990s (Mecham et al. 1998; Camaioni et al. 1998; Meisel et al. 1993, Meisel et al. 1991), theoretical input, based on *ab initio* theories, is needed to obtain an improved understanding of chemical reactions in aqueous phase and to provide fundamental data (thermochemical, spectroscopic, and reactivity data of organic radical ions) that cannot be easily measured and yet is needed for the development of reliable thermochemical kinetic models.

Approach: We apply existing solvation models (e.g., COSMO, and Chipman's SS(V)P) with MO and DFT theories using large basis sets with the solute residing in a molecular shaped cavity embedded in a dielectric continuum.

Results: Continuum solvation models provide a practical way to characterize solvation effects on the energetics of many chemical reactions; however, they are unable to yield **consistently** chemical accuracy for many systems outside the type of molecules used to calibrate the models. Systematic investigations have shown that current cavity definition models do not reproduce well the detailed solute-solvent interactions. We are developing more accurate and consistent chemical functionality-based schemes of defining cavities involving atomic radii dependent on atomic charges that capture specific solute-solvent interactions. The protocol was initially defined for oxoanions and is currently being extended to other organic functional groups.

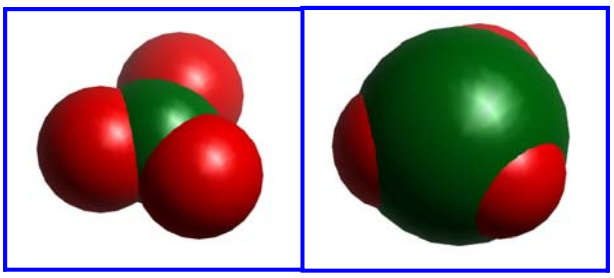

Two Cavity models based on Van der Waals radii (left) and atomic charges-dependent radii (right). The later model captures well the specific interactions of the solute with the first solvation shell.

References to publications of DOE Chemical Physics sponsored research (2003-present)

1. S. Ammal, H. Yamataka, M. Aida, and **M. Dupuis**, "Dynamics-Driven Reaction Pathway in an Intramolecular Rearrangement," *Science* **299**, 1555 (2003).
2. M. Aida and **M. Dupuis**, "IR and Raman Intensities in Vibrational Spectra from Direct Ab Initio Molecular Dynamics: D_2O as an Illustration," *Journal of Molecular Structure (Theochem*) **633**, 247 (2003).
3. D. Camaioni, **M. Dupuis**, and J. Bentley, "Theoretical Characterization of Oxoanions XO_m^{n-} Solvation," *Journal of Physical Chemistry A* **107**, 5778 (2003).
4. **M. Dupuis**, G. K Schenter, B. G. Garrett, and E. E. Arcia, "Potentials of Mean Force With Ab Initio Mixed Hamiltonian Models of Solvation," *Journal of Molecular Structure (Theochem*) **632**, 173 (2003).
5. T. Autrey, A. K. Brown, D. M. Camaioni, **M. Dupuis**, N. S. Foster, and A. Getty, "Thermochemistry of Aqueous Hydroxyl Radical from Advances in Photoacoustic Calorimetry and ab initio Continuum Solvation Theory", J. Am. Chem. Soc. (Communication), **126**, 3680 (2004).
6. **M. Dupuis** and M. Aida, "Vibrational Spectra from Quasiclassical Direct ab Initio Dynamics", Electronic Encyclopedia of Computational Chemistry, Wiley & Sons, (2004).
7. M. Aida and **M. Dupuis**, "Fundamental Absorption Frequency from Quasi-classical Direct ab initio Molecular Dynamics: Diatomic Molecule", Chem. Phys. Lett. 401, 170 (2005).
8. B. C. Garrett, D. A. Dixon, D. M. Camaioni, D. M. Chipman, M. A. Johnson, C. D. Jonah, G. A. Kimmel, J. H. Miller, T. N. Rescigno, P. J. Rossky, S. S. Xantheas, St. D. Colson, A. H. Laufer, D. Ray, P. F. Barbara, D. M. Bartels, K. H. Becker, K. H. Bowen, Jr., S. E. Bradforth, I. Carmichael, J. V. Coe, L. R. Corrales, J. P. Cowin, **M. Dupuis**, K. B. Eisenthal, J. A. Franz, M. S. Gutowski, K. D. Jordan, B. D. Kay, J. A. LaVerne, S. V. Lymar, T. E. Madey, C. W. McCurdy, D. Meisel, S. Mukamel, A. R. Nilsson, T. M. Orlando, N. G. Petrik, S. M. Pimblott, J. R. Rustad, G. K. Schenter, S. J. Singer, A. Tokmakoff, L. S. Wang, C. Wittig, and T. S. Zwier, "The Role of Water on Electron-Initiated Processes and Radical Chemistry: Issues and Scientific Advances", Chem. Rev. 105, 355 (2005).
9. J.D. Watts and **M. Dupuis**, "A Coupled-Cluster Analysis of the Photoelectron Spectrum of $FeCl_3^-$", Molec. Phys. 103, 2223 (2005).
10. S. Hirata, M. Valiev, **M. Dupuis**, S.S. Xantheas, S. Sugiki, and H. Sekino, "Fast electron correlation methods for molecular clusters in the ground and excited states". Molec. Phys. 103 2255 (2005).

[#] This research was performed in part using the Molecular Science Computing Facility in the William R. Wiley Environmental Molecular Sciences Laboratory (EMSL) at the Pacific Northwest National Laboratory (PNNL). The EMSL is funded by DOE's Office of Biological and Environmental Research. PNNL is operated by Battelle for DOE.

Interfacial Oxidation of Complex Organic Molecules

G. Barney Ellison — (Grant DE-FG02-93ER14364)

We propose to build a new experiment to study the oxidation of surfactants coating water droplets. We plan to produce a stream of organic aerosols, size-select them and inject them into an atmospheric flow tube where they will be dosed with OH radicals. The resultant oxidized particles will be analyzed with a novel aerosol mass spectrometer.

All clouds and ice particles nucleate on aerosols.[1] In 1999 Ellison *et al.* published a model[2] that proposed a chemical structure for marine aerosols, accounted for their organic content, and described the chemical evolution or atmospheric processing of the organic material. This model was further extended into biology.[3]

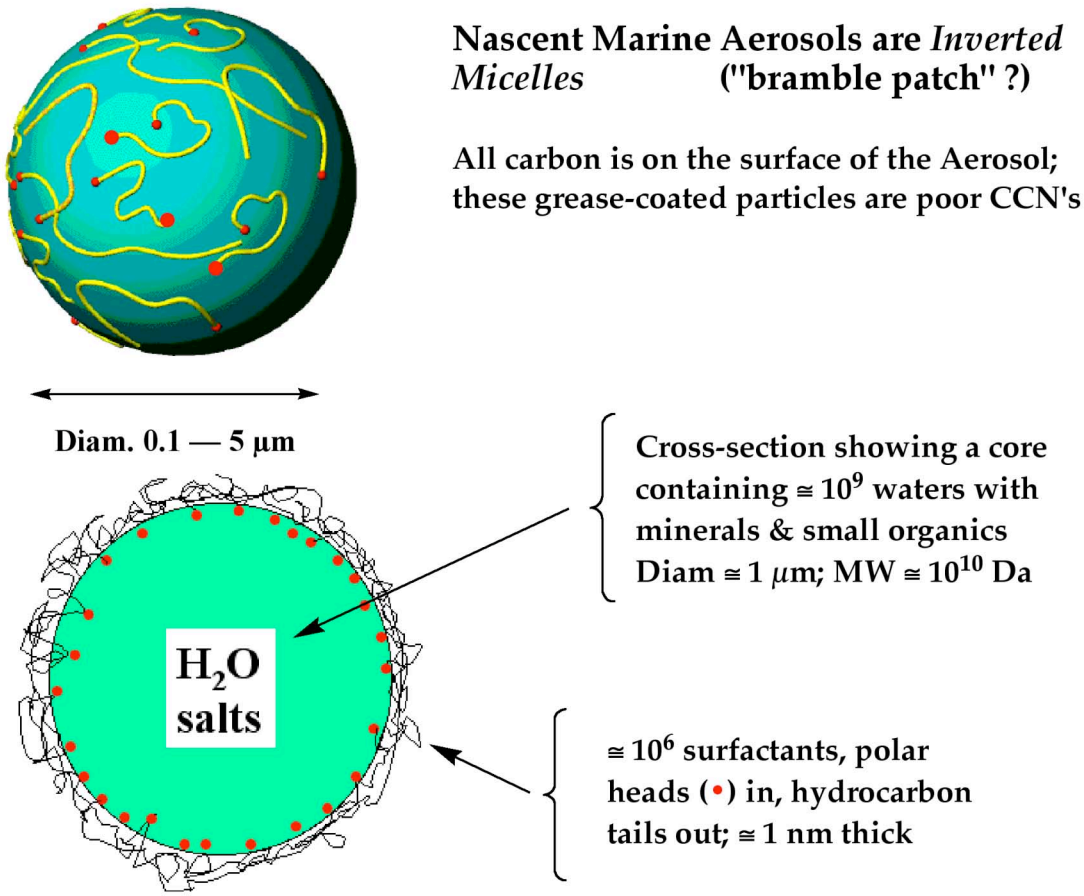

Fig. 1

Fig. 1 shows the model for organic aerosols as inverted micelles. Hydrophobic surfactants are carried up from the ocean's surface and born into the atmosphere on the surface of the drop. The surfactants will be bound to the aqueous drop by several polar groups (such as $—N(CH_3)_3^+$, $—CO_2^-$, *etc*); in Fig. 1 these polar groups are indicated by a red dot, (•).The inverted micelle model predicted[2] that the aerosol's organic surfactants would be steadily oxidized in the atmosphere. Based on the density[4] of OH radicals, $\rho(OH) = 10^6$ cm^{-3}, it was conjectured that the processing time would be 3–8 hours. This processing by atmospheric radical chemistry will transform the organic film into a **hydrophilic layer**. Consequently the oxidized aerosols are much better cloud condensation nuclei (CCN's) than the nascent particles; this transformation is shown in (1).

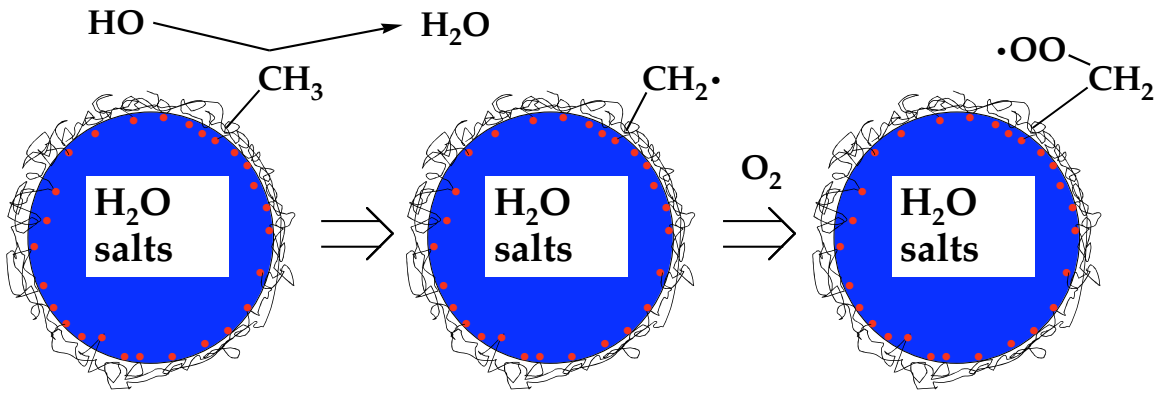

(1)

As the surfactants are oxidized by atmospheric oxidants such as OH, O_3, O_2, or NO_3, the hydrophobic alkyl groups are transformed into alcohols, aldehydes, carboxylic acids, *etc.* A surface sprinkled with polar groups (such as alcohols, aldehydes, and carboxylic acids) is easy[5] to "wet" and will be an excellent CCN. The fundamental molecular reactions driving the chemical transformations in eq. (1) are poorly understood. Initially we choose to concentrate on the OH-mediated oxidation of organic films. Because of the large bond energy[6] of water [DH_{298}(H-OH) = 118.82 ± 0.07 kcal mol^{-1}] OH radicals will abstract H atoms when they strike a film of saturated organics. The bond energies[7,8] of all alkanes are less than 100 kcal mol^{-1} so it is exothermic by almost 1 eV for an OH radical to abstract a H atom.

We propose to build a new experiment to a) produce a stream of organic aerosols in a flow tube, b) oxidize them with OH/O_2 radicals, and c) to analyze these particles with a novel aerosol mass spectrometer. A schematic outline of our new apparatus is shown in Fig. 2. A stream of synthetic air sweeps through a bubbler charged with a dilute solution of $NH_4^+HSO_4^-$ and the ammonium salt of an alkanoic acid such as lauric acid, $CH_3(CH_2)_{10}CO_2^-NH_4^+$. The stream of air emerging from the bubbler is entrained with a population of aqueous droplets that are coated with a single organic surfactant, $CH_3(CH_2)_{10}CO_2^-$. We desire a stream of particles of a constant, nominal diam. of 1 — 10 μm. A 10 μm organic aerosol (see top of Fig. 2), it contains roughly 10^{13} waters in the core and carries about 10^9 surfactant $CH_3(CH_2)_{10}CO_2^-$ ions. The heat of vaporization of water is 40.7 kJ mol^{-1}; therefore it takes roughly 1.2 μJ to vaporize a 10 μm drop. If we use a 50 W CO_2 laser that is focused to a 100 μm spot, then an aerosol traveling at 10^4 cm sec^{-1} will be irradiated for approximately 1 μsec. Consequently the coated water droplet can be steadily heated up to 50 μJ. The surfactant-coated droplet will completely dissociate and release the carboxylates for analysis by a quadrupole mass filter. [We may require a drift region to break up RCO_2^-(water clusters)$_n$].

Photodissociation of a 10 μm droplet in Fig. 2 will release 10^9 ions and a gentle extraction lens (200 V cm^{-1}) should collect approximately 10^{-5} of the resultant RCO_2^- ions into quadrupole. If the particle density in the flow tube is 10^4 aerosols cm^{-3}, then a 25 cm^2 flow tube with buffer gas flowing at 10 cm sec^{-1} will pass 2.5 x 10^6 aerosols sec^{-1}. If the aerodynamic lens has a 1 mm diam entrance, then the lens will transmit 3 x 10^3 aerosols sec^{-1}. Consequently a quadrupole mass filter should monitor 5 x 10^7 ions sec^{-1}. If the OH/O_2 chemistry oxidizes only 0.1 % of the surfactants, we should have oxidation product [OO-RCO_2^-] count rates of 5 x 10^4 sec^{-1}. The quadrupole mass filter in Fig. 5 must be able to monitor about 10^7 [$CH_3(CH_2)_{10}CO_2^-$] ions sec^{-1} at m/z 199 Da and

simultaneously detect roughly 10^4 [•OO-$C_{11}H_{22}CO_2^-$] ions sec^{-1} at m/z 230 Da. This should be a straightforward task for a quadrupole mass filter.

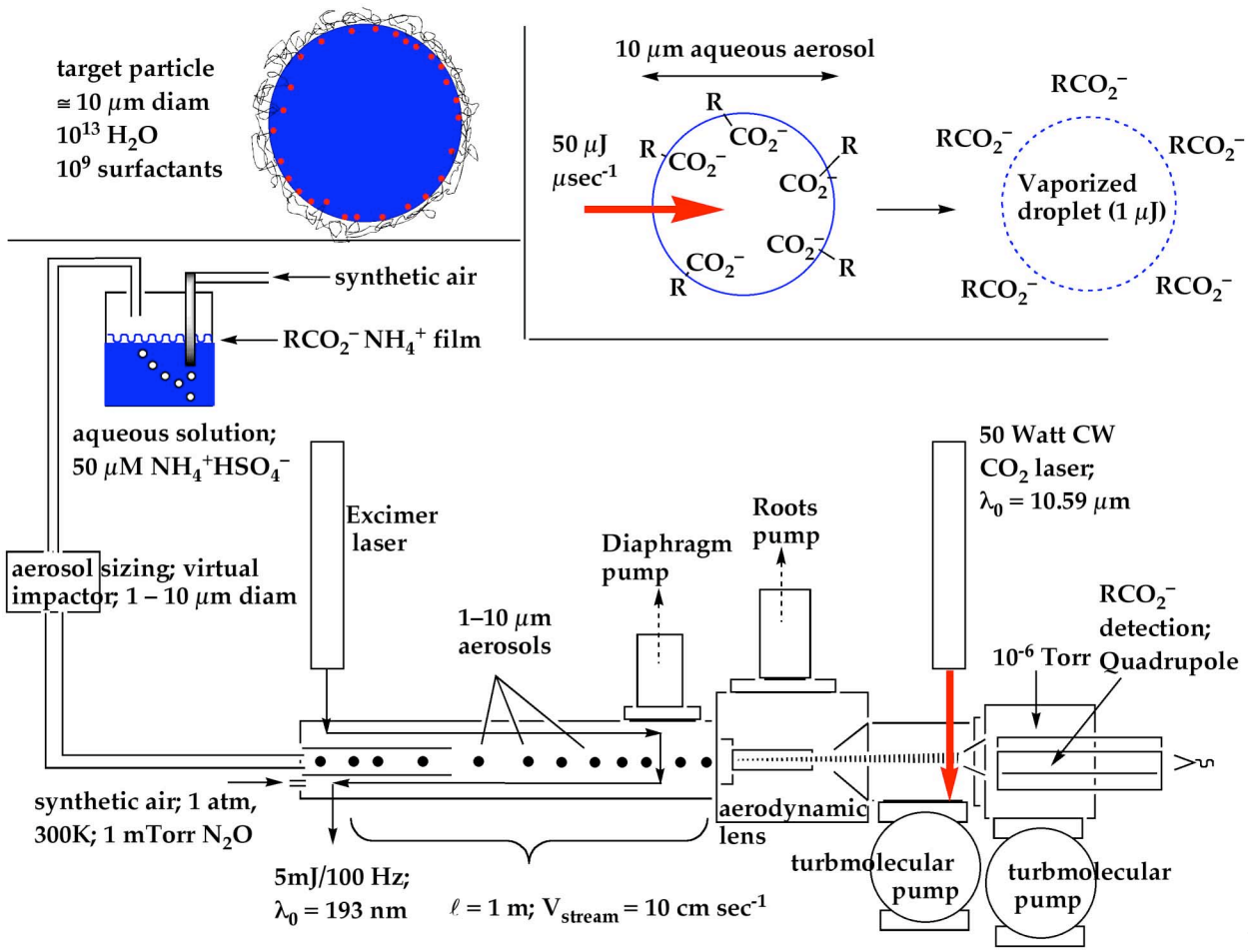

Fig.2

An uncertain part of the experiment in Fig. 2 is the CW IR photodissociation of the surfactant-coated droplets with concomitant release of the NH_4^+ and RCO_2^- ions. It is essential that we disintegrate the aerosol into its constituent monomers without molecular fragmentation. There is a recent, relevant study of this problem.[9] A pulsed IR laser-induced thermal ablation of aerosol particles resulted in the ejection of desolvated ions into the gas phase. Dessiaterik *et al*. carried out studies of ethylene glycol droplets containing 10^{-6} and 10^{-1} M RbCℓ. A high-power infrared CO_2 laser pulse vaporized the aerosol particles, and the resulting ions were detected by time-of-flight mass spectrometry and by total current measurements. The results show that, at low concentrations, the ion signal was directly proportional to the ion concentration, whereas the signal saturates above 10^{-4} M RbCℓ. By comparing the TOF signal to the total current measured on the ion repeller plate, it was demonstrated[9] that ion-ion recombination was the major cause of signal saturation. A 10 μm organic aerosol will carry 10^9 surfactants on the surface; this corresponds to a carboxylate "concentration" of 5×10^{-6} mole L^{-1}.

There has been a huge effort to design and build aerosol mass spectrometers.[10] As far as we are aware, no one has been able to detect organic radicals on aerosol particles. Consequently a major, initial goal of this program will be to design and build

the experiment in Fig. 2. In particular, we must be able to use a mass spectrometer to detect ions without fragmentation. We plan to explore the mass spectrometry of organic aerosols with different coatings. With a lauric acid coating, we should detect a single negative ion at m/z 199. As we vary the surfactant from lauric to myristic to palmitic to stearic, m/z of the ion should shift from 199 to 227 to 255 to 283.

Surfactant coating aerosol		RCO_2^- m/z (Da)	$\bullet OO\text{-}RCO_2^-$ m/z (Da)
lauric acid	$CH_3(CH_2)_{10}CO_2^-$	199	230
myristic acid	$CH_3(CH_2)_{12}CO_2^-$	227	258
palmitic acid	$CH_3(CH_2)_{14}CO_2^-$	255	286
stearic acid,	$CH_3(CH_2)_{16}CO_2^-$	283	314

As we oxidize these surfactants with OH/O_2 the m/z of the resulting oxidant, $\bullet OORCO_2^-$, should shift from 230 to 258 to 286 to 314.

Negative ion detection of carboxylate ions should be straightforward since they are robust[11] anions; $EA(RCO_2) \cong 3.5$ eV. The oxidation products, $\bullet OO\text{-}RCO_2^-$, are radical/anions and are called distonic ions.[12] Typical R-OO bond energies are roughly[8,13] 1.5 eV; consequently we must fragment the aerosols very gently to detect the $\bullet OO\text{-}RCO_2^-$ ions intact. Of course working with negative ions has the advantage that our detection scheme is blind to the huge amounts of H_2O or N_2 in the flow tube. If traces of pump oil contaminate the aerosols, we might not detect them because they will not be charged. But they will interfere with reactions of OH at the atmosphere/aerosol interface.

1 H. R. Pruppacher and J. D. Klett, Microphysics of Clouds and Precipitation, 2nd Ed. ed. (Kluwer Academic Publishing, Dordrecht: Holland, 1997).

2 G. B. Ellison, A. F. Tuck, and V. Vaida, J. Geophys. Res.-Atmos. **104**, 11633 (1999).

3 C. M. Dobson, G. B. Ellison, A. F. Tuck, and V. Vaida, Proc. Natl. Acad. Sci. U. S. A. **97**, 11864 (2000); V. Vaida, A. F. Tuck, and G. B. Ellison, Phys. Chem. Earth **25**, 195 (2000).

4 J. H. Seinfeld and S. N. Pandis, *Atmospheric Chemistry and Physics: From Air Pollution to Climate Change*. (John Wiley & Sons, New York City, 1998).

5 Y. Rudich, I. Benjamin, R. Naaman, E. Thomas, S. Trakhtenberg, and R. Ussyshkin, J. Phys. Chem. A **104**, 5238 (2000).

6 B. Ruscic, D. Feller, D. A. Dixon, K. A. Peterson, L. B. Harding, R. L. Asher, and A. F. Wagner, J. Phys. Chem. A **105**, 1 (2001).

7 J. Berkowitz, G. B. Ellison, and D. Gutman, J. Phys. Chem. **98**, 2744 (1994).

8 S. J. Blanksby and G. B. Ellison, Acc. Chem. Res. **36**, 255 (2003).

9 Y. Dessiaterik, T. Nguyen, T. Baer, and R. E. Miller, J. Phys. Chem. A **107**, 11245 (2003).

10 D. T. Suess and K. A. Prather, Chem. Rev. **99**, 3007 (1999); C. A. Noble and K. A. Prather, Mass Spectrom. Rev. **19**, 248 (2000).

11 J. C. Rienstra-Kiracofe, G. S. Tschumper, H. F. Schaefer III, S. Nandi, and G. B. Ellison, Chem. Revs. **102**, 231 (2002).

12 H. I. Kenttämaa, in The Encyclopedia of Mass Spectroscopy, edited by P. B. Armentrout (Elsevier, Amsterdam, 2003), Vol. 1: **Theory and Ion Chemistry**, pp. 619.

13 S. J. Blanksby, T. M. Ramond, G. E. Davico, M. R. Nimlos, S. Kato, V. M. Bierbaum, W. C. Lineberger, G. B. Ellison, and M. Okumura, J. Am. Chem. Soc. **123**, 9585 (2001).

The Effect of Crystallization on the Proton Pump Function

Of Bacteriorhodopsin

Laurie Sanii and Mostafa El-Sayed

Laser Dynamics Lab., Georgia Tech, Atlanta, Georgia

Bacteriorhodopsin ("bR") , the other photosynthetic system in nature besides chlorophyll, is a retinal protein with 248-amino acid, 26 kDa transmembrane protein first discovered in the purple membrane (cell membrane) of the salt-marsh bacterium *Halobacterium salinarium* by Oesterhelt and Stoeckenius in 1971.Upon light absorption, retinal isomerizes. This is followed a dark cycle of intermediates resulting in the deprotination of the its Schiff base (to form the M-intermedite)and the proton pump to the surface of the cell membrane. This created proton gradient is latter used to make the ATP of the bacteria (the fuel of its life processes),

Our program is focused on using spectroscopic tools to study the photo cycle of bR and its perturbed forms in order to understand the mechanism of the proto pump process.. We tried to answer questions regarding the relationship between the protein packing structure of bacteriorhodopsin (bR) and its function as a proton pump.

In 2002, a novel crystallization method published by Bowie and Farham[2] resulted in an unusual antiparallel monomeric packing structure of bicelle bacteriorhodopsin (bcbR) crystals the spectroscopic properties of which had not been studied..Last year, tew investigated these bcbR crystals to better understand how the changes in the protein tertiary structure affect the function. Specifically: Does the retinal Schiff base retain its ability to isomerize in this unusual protein packing structure of bR? How is the hydration of its binding pocket affected? Does the protein retain the ability to undergo the photocycle and pump protons? If so, how are the rates of the deprotonation/reprotonation of the Schiff base affected by the antiparallel monomer packing structure of the protein? Is Asp_{85} still the proton acceptor during the deprotonation process of the photocycle? In this work, visible, Raman, FTIR, and single-wavelength transient absorption spectroscopy (flash photolysis) have been used to answer these questions.

Diamond-shaped bcbR crystals approximately 100 x 200 µm in size were synthesized by the hanging-drop crystallization method published by Farham *et al*.[2] and are shown in Figure 1. .

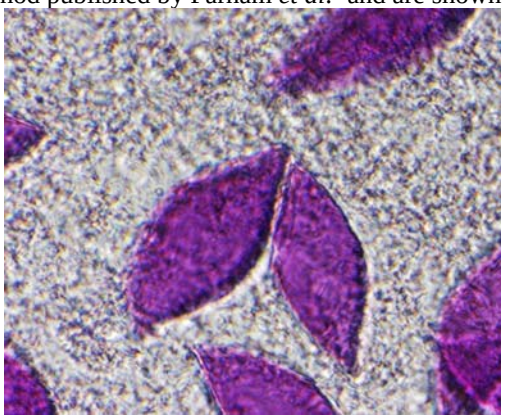

Figure 1: Typical diamond-shaped bcbR crystals within their DMPC:Chapso detergent matrix.

A mass of hydrated bcbR crystals still within their detergent matrix was investigated by visible spectroscopy. Reversible changes in the absorption maximum upon exposure to light illustrate that the photo-isomerization of the retinal Schiff base is still possible in the bcbR crystals. The visible absorption spectrum of hydrated, light-adapted single bcbR crystals is compared to that of hydrated, light-adapted native bR to better understand the hydration environment of the retinal Schiff base binding pocket within the bcbR crystals. From these studies, it was concluded that the band broadening in single bcbR crystals relative to native bR is due to a difference in hydration environments among the various retinal binding

pockets within the bcbR crystals, a characteristic shared in the cbR crystals. In both single-crystal visible and single-crystal Raman spectroscopy experiments, it was shown that it is possible to 'trap' the deprotonated retinal Schiff base if the bcbR crystals are dried under exposure to either broad band light, or 514 nm laser excitation. Raman and visible spectroscopy performed on bcbR crystals that are dehydrated in the dark do not result in the previously-observed deprotonated Schiff base, thereby confirming that retinal Schiff base deprotonation is a photochemical process, not simply the product of a thermal deprotonation of the parent species.

Single-crystal Raman spectroscopy using the 514 nm incident wavelength was used to detect bands belonging to the M intermediate in single hydrated bcbR crystals. Raman bands belonging to both the parent and the M intermediate were observed in the hydrated bcbR crystals. To demonstrate that the new bands appearing are actually due to the photochemical formation of the M intermediate and not simply due to resonance enhancement of a thermally formed M analogue, Raman band intensities were monitored as a function of 514 nm laser power. In these studies the intensities of the Raman bands increased nonlinearly with the increasing laser power, confirming that in the hydrated bcbR crystals the M intermediate is being formed photochemically (Figure 2). Single-wavelength transient absorption spectroscopy (flash photolysis) was used to monitor the rise and decay kinetics of the M intermediate in bcbR crystals in both H_2O and D_2O. In these studies, the M intermediate rise time in bcbR crystals in H_2O was found to be three times faster compared to that of native bR and cbR crystals,, with a decay time that was seven times slower than in either native bR or the previously-published *in-cubo* (cbR) crystals[3].

The kinetic isotope effect for M rise in bcbR crystals was found to be nearly 9, in contrast with the published value of 5.5 for the KIE in native bR. The KIE for M decay in bcbR crystals was found to be 2.0, in contrast with the published value of 1.7 for the KIE in native bR. Possible explanations for these observations are given.

Finally, FTIR difference spectroscopy was used to monitor both the changes in the protein *and* the surrounding amino acids during the proton transfer time scale. It was found that Asp_{85} was the proton acceptor during the formation of the M intermediate in bcbR crystals, indicated by the appearance of a positive band at 1760 cm^{-1}. In addition, the C=C stretch region of the deprotonated retinal Schiff base in the bcbR crystals in either H_2O or D_2O (Figures 3 and 4) was found to be more broad than in native and in the previously-observed cbR crystals. The possibility of our ability to resolved the C=C stretch in the two M states in bcbR crystals was discussed.

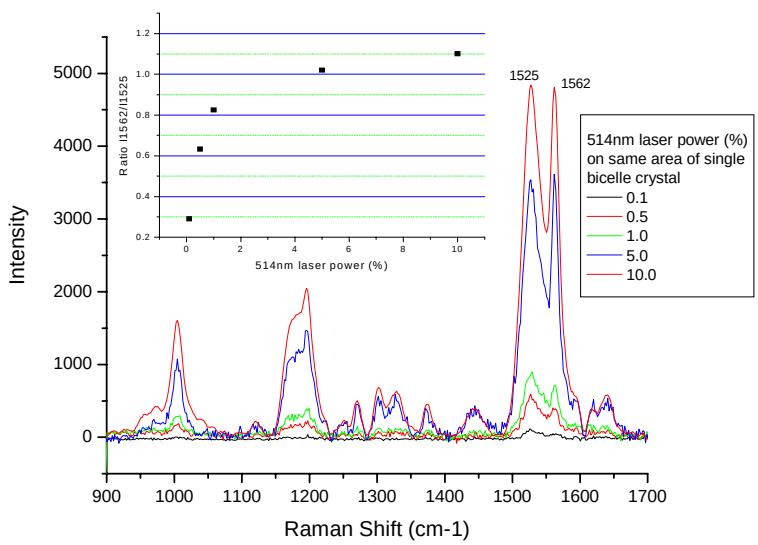

Figure 2: Increasing the power of the 514 nm Raman laser on a hydrated single bcbR crystal increases the intensity ratio (inset) between the 1562 nm band (M intermediate) and the 1525 nm band (parent) nonlinearly. This is the first indication that the bcbR crystals are capable of making the M intermediate

photochemically, and that the deprotonated Schiff base is caused by photochemical formation of the M intermediate and not by thermal dehydration of the parent.

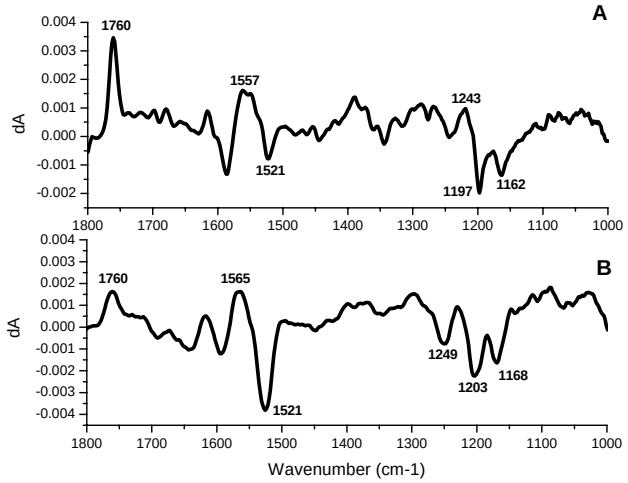

Figure 3: Changes in the FTIR spectrum upon irradiation with 514 nm laser for a mass of bcbR crystals (A) and native bR (B) in H_2O. The presence of the 1760 cm^{-1} band in the bcbR crystal spectrum indicates protonation of the Asp_{85} residue upon the formation of M. The more broad absorption of the positive band at 1557 cm^{-1} in the bcbR crystals relative to the same band at 1565 cm^{-1} for the native suggests that in the bcbR crystals there is heterogeneity in the M state population.

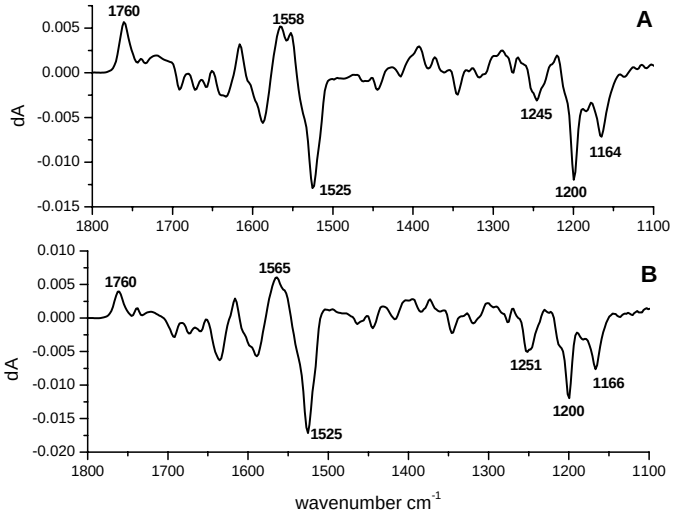

Figure 4: Changes in the FTIR spectrum upon irradiation with 514 nm laser for a mass of bcbR crystals (A) and native bR (B) in D_2O. The presence of the 1760 cm^{-1} band in the bcbR crystal spectrum again indicates protonation of the Asp_{85} residue upon the formation of M. The broad, somewhat forked absorption of the positive band centered at 1558 cm^{-1} in the bcbR crystals relative to the same band at 1565 cm^{-1} for the native again suggests that in the bcbR crystals there is heterogeneity in the M state population.

Future work on this project involves the use of microsecond and millisecond time-resolved FTIR spectroscopy to better understand the origin of the broad deprotonated retinal Schiff base region described

above. Time-resolved FTIR spectroscopy would capture the changing FTIR spectrum during the M rise and decay processes to determine that if in these bcbR crystals the origin of the broad band is due to two simultaneously forming M populations (parallel photocycles) or is actually due to an equilibrium between the M1 (extracellular trajectory) and M2 (cytoplasmic trajectory) populations.

References:

(1) Oesterhelt, D.; Stoeckenius, W. *Nature (London), New Biology* **1971**, *233*, 149. **71**, *233*, 152.

(2) Bowie, J.; Farham, S. *Journal of Molecular Biology* **2002**, *316*, 1. Farham, S.; Yang, D.; Bare, E.; Yohannan, S.; Whitelegge, J. P.; Bowie, J. U. *Journal of Molecular Biology* **2004**, *335*, 297.

(3) Heberle, J.; Buldt, G.; Koglin, E.; Rosenbusch, J. P.; Landau, E. M. *Journal of molecular biology* **1998**, *281*, 587. le Coutre, J.; Gerwert, K. *FEBS letters* **1996**, *398*, 333.

Publications in 2003-2004

1. El-Sayed, Ivan; Huang, Xiaohua; El-Sayed, Mostafa A., "Surface Plasmon Resonance Scattering and Absorption of anti-EGFR Antibody Conjugated Gold Nanoparticles in Cancer Diagnostics; Applications in Oral Cancer," Nano Letters **4(5)**, 829-834, (2005).

2. Sanii, Laurie S.; Schill, Alex W.; and Moran, Cristin E.; and El-Sayed, Mostafa A., "The Protonation-Deprotonation Kinetics of the Protonated Schiff Base in Bicelle Bacteriorhodopsin Crystals", Biophysical Journal (2005), 89, 444-451.

3. Sanii, Laurie S.; and Mostafa A. El-Sayed, "Partial Dehydration of the Retinal Binding Pocket and Proof for Photochemical Deprotonation of the Retinal Schiff base in Bicelle Bacteriorhodopsin Crystals." Photochemistry and Photobiology, accepted.

4. Sanii, Laurie S.; and El-Sayed, Mostafa A., "Determination of the Role of Aspartate Residue in the Function of bcbR Crystals by FTIR Difference Spectroscopy". Manuscript in preparation.

5. Heyes, Colin D.; Reynolds, Keith B.; El-Sayed, Mostafa A., "Eu^{3+} Binding to Europium-Regenerated Bacteriorhodopsin upon Delipidation and Monomerization", FEBS Letters, **562(1-3),** 207-210, (2004).

Liquid and Chemical Dynamics in Nanoscopic Environments

Michael D. Fayer
Department of Chemistry, Stanford University, Stanford, CA 94305
email: fayer@stanford.edu

The goal of this research project is to greatly increase understanding of the influences on the properties of liquids and chemical processes caused by the confinement of liquids in systems in which the size scale is approaching molecular dimensions. For very small systems, interfacial affects as well as structural confinement will play an important role in system properties. We are initially focusing on water, but we will examine other liquids as well. Over the last year, the bulk of the experiments and theory have focused on reverse micelle, but other nanoscopic structures, in particular experiments on water channels in Nafion membranes and in sol gel glasses have been initiated. Chemical processes are intimately tied into the properties and dynamics of the solvent in which they occur. In addition to investigating the influence of nanoconfinement on liquid properties, we are investigating the resulting modification of chemical processes. Electron transfer is a basic chemical process, and it is sensitive to its environment. Understanding and control of photoinduced electron transfer and geminate recombination is an important problem that has significant implications for solar energy conversion. Photoinduced electron transfer experiments in nanoscopic media, such as the water nanopools of reverse micelles, offer the opportunity to explore the impact of nanoscopic environments on a fundamental chemical process.

The main tools that we are employing for the investigation of liquid dynamics are ultrafast infrared vibrational experiments that can directly probe structural evolution of water or other liquids in nanoscopic environments. Several types of experiments are of particular importance and can provide very detailed understanding of the relationships between size, structure, and dynamics. They are ultrafast infrared multidimensional vibrational echo experiments and ultrafast infrared spectrally resolved and polarization selective transient absorption experiments. Photoinduced electron transfer and geminate recombination are being studied using transient absorption and stimulated emission that enables us to monitor both forward electron transfer and geminate recombination. We will also employ new ultrafast 2D vibrational echo chemical exchange experiments to study electron transfer under ground state thermal equilibrium conditions. In addition to experiments, several theoretical studies are being conducted, some in collaboration with outside theoretical groups. Of particular importance are collaborative efforts to perform molecular dynamics simulations that permit calculation of our experimental observables.

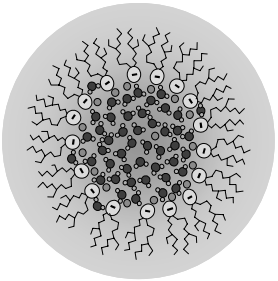

The dynamics of water in nanoscopic pools 1.7 – 28 nm in diameter in AOT reverse micelles were studied with ultrafast infrared spectrally resolved stimulated vibrational echo and pump-probe spectroscopies. The figure is a schematic of an AOT reverse micelle. Iso-octane surrounds surfactants with negatively charged head groups that have associated Na^+ counter ions. The interior is the water nanopool. The experiments were conducted on the OD hydroxyl stretch of low concentration HOD in

the H_2O, providing a direct examination of the hydrogen bond network dynamics. The dilute OD stretch is used to avoid excitation transfer. The vibrational echo experiments are sensitive to hydrogen bond dissociation and reformation dynamics, which are observed to change with reverse micelle size. Vibrational echo decays were obtained at the peak of the absorption spectrum for each size reverse micelle as a function of T_w, the time between the second and third pulses in the vibrational echo pulse sequence. The data are fit using time dependent diagrammatic perturbation theory to obtain the frequency-frequency correlation function (FFCF) for each micelle. The results are compared to the FFCF of water. In bulk water, the slowest time scale dynamics are caused by global structural evolution of the hydrogen bond network that involves making and breaking of hydrogen bonds.

To simplify the data display, the figure shows the peak shifts of the vibrational echo decay curves as a function of T_w. As T_w is increased there is more time for structural evolution of the hydrogen bond network, which results in more spectral diffusion, and hence, a faster vibrational echo decay with a reduced peak shift. When the peak shift becomes zero, structural evolution is complete in the sense that all configurations have been sampled. The water dynamics occur on a variety of time scales. The greatest difference between bulk water and nanoconfined water occurs on the longest time scale, τ_2 in the table. As the size of the water nanopool is decreased there is a dramatic slowing of the hydrogen bond network evolution. When the nanopool size is 28 nm (w_0 = 60), the data (not shown) are indistinguishable from bulk water. For the smallest nanopools, the longest time scale component of the water dynamics is ~15 times longer than dynamics in bulk water. In collaboration with the group of Professor James Skinner, University of Wisconsin at Madison, molecular dynamics simulations of the vibrational echo experiments are in progress.

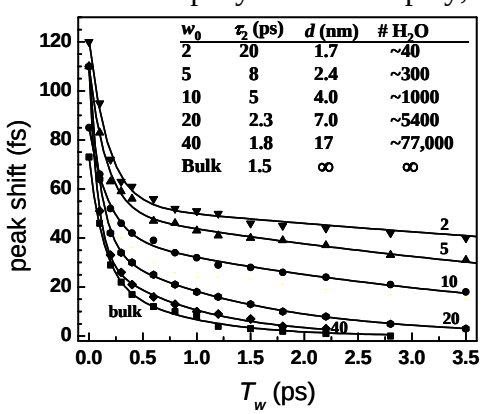

The time resolved orientational anisotropies of water in AOT reverse micelles were also studied using ultrafast infrared polarization and spectrally resolved pump-probe spectroscopy, and the results were compared to the same experiments on bulk water. Nanopool sizes were studied from w_0 = 2 to 60 (1.7 nm to 28 nm).The orientational anisotropy data. for three smallest water nanopool sizes (4 nm, 2.4 nm, and 1.7 nm) and bulk water are shown in the figure. The nanowater orientational relaxation can be fit well with bi-exponential decays for these small sizes. The bi-exponential decays were analyzed using a wobbling-in-a-cone model that involves fast orientational diffusion within a cone followed by slower, full orientational relaxation. The data provide the cone angles, the diffusion constants for motion within the cones, and the final diffusion constants as a function of the nanopool size. The two processes can be

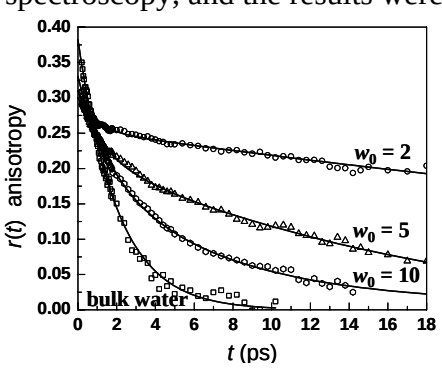

interpreted as a local angular fluctuation of the OD and a global hydrogen bond network rearrangement process. The trend in the long decay constants indicates a longer hydrogen bond network rearrangement time with decreasing reverse micelle size. This observation is consistent with the results from the vibrational echo experiments. Comparisons of the data to the molecular dynamics simulations of Professor Branka Ladanyi, Colorado State University, show semiquantitative agreement. Above ~7 nm in diameter, the anisotropy decay becomes single exponential. As the diameter of the nanopool becomes greater than 7 nm, the orientational relaxation rapidly approaches that of bulk water. For 28 nm diameter, the nanopool and bulk water anisotropy decays are identical, 2.04 ps.

The change from bi-exponent decay to single exponential decay of the anisotropy happens suddenly between 4 nm and 7 nm diameter nanopools. This change can be understood by comparing the time scales for the diffusion in the cone component to the slowest decay component of the FFCF measured with the vibrational echo experiments. As the nanopool becomes larger, the time to sample the full cone becomes longer and the time for global hydrogen bond rearrangement (slowest component of the FFCF, τ_2 in the table above) becomes faster. The cone is produced because the orientational relation can only sample a limited range of angles until the network globally rearranges, which permits all angles to be sampled. When the time scale for global rearrangement becomes faster than the time to "hit the cone angular limit," then orientational relaxation is not restricted by a "fixed" network structure, and single exponential orientational diffusion occurs. The combined anisotropy data and vibrational echo data supports this picture.

In addition to the ultrafast IR experiments described briefly above, we have begun similar experiments on non-ionic head group reverse micelles, water nanopools in sol gel glasses, and water channels in Nafion hydrogen ion exchange membranes. Nafion is a membrane composed of Teflon with side chains terminated by sulfonate head groups, the same head groups as in AOT reverse micelles. The polymer chains form bundles with the head groups on the outside. Between the bundles are water channels that serve as hydrogen ion conduction channels in fuel cell applications. Proton transfer through the channels is controlled by the water hydrogen bond rearrangement dynamics. The size of the channels is determined by the water content of the membrane. We have recently obtained the first orientational relaxation data in Nafion, and we are studying the anisotropy decay as a function of membrane hydration. Vibrational echo experiments will also be performed. We have also conducted photoinduced electron transfer and geminate recombination experiments between donors and acceptors in liquids and micelles. These experiments are the first to examine radical recombination following forward electron transfer from subps to ns time scales. The results are being analyzed with a statistical mechanics theory that include important factors such as diffusion with the hydrodynamic effect, the radial distribution function, and for the micelles the influence of a spatially non-homogeneous dielectric constant. Future electron transfer and proton transfer experiments will be conducted in water nanopools of reverse micelles as a function of the nanopool size to examine the influences of nanoscopic confinement on chemical processes.

Publication Supported by DOE

"Dynamics of Water Confined on a Nanometer Length Scale in Reverse Micelles: Ultrafast Infrared Vibrational Echo Spectroscopy," Howe-Siang Tan, Ivan R. Piletic, Ruth E. Riter, Nancy E. Levinger and M. D. Fayer, Phys. Rev. Lett. 94, 057405(4) (2005).

"Photoinduced Electron Transfer in the Head Group Region of Sodium Dodecyl Sulfate Micelles," J. Nanda, P. K. Behera, H. L. Tavernier and M. D. Fayer, J. Lumin. 115, 138-146 (2005).

"Orientational Dynamics of Water Confined on a Nanometer Length Scale in Reverse Micelles," Howe-Siang Tan, Ivan R. Piletic, and M. D. Fayer, J. Chem. Phys. 122, 174501(9) (2005).

"Polarization Selective Spectroscopy Experiments: Methodology and Pitfalls," Howe-Siang Tan, Ivan R. Piletic and M. D. Fayer, J.O.S.A. B 22, 2009-2017 (2005).

"The Dynamics of Nanoscopic Water: Vibrational Echo and IR Pump-probe Studies of Reverse Micelles," Ivan R. Piletic, Howe-Siang Tan and M. D. Fayer, J. Phys. Chem. B accepted (2005).

"Dynamics of Water Confined on Nanometer Length Scales: Orientational Relaxation and Spectral Diffusion in Small to Large Reverse Micelles," Ivan R. Piletic, Howe-Siang Tan and M. D. Fayer, in preparation (2005).

"Photoinduced Electron Transfer and Geminate Recombination in Liquids," Alexei Goun, Ksenija Glusac, and M. D. Fayer, in preparation (2005).

"Photoinduced Electron Transfer and Geminate Recombination in the Group Head Region of Micelles," Ksenija Glusac, Alexei Goun, and M. D. Fayer, in preparation (2005).

Molecular Theory & Modeling

Accurate Descriptions of Chemical Reactions in Aqueous Systems

Bruce C. Garrett
Chemical Sciences Division
Pacific Northwest National Laboratory
902 Battelle Blvd.
Mail Stop K9-90
Richland, WA 99352
bruce.garrett@pnl.gov

The long-term objective of this project is to understand the factors that control the chemical reactivity of atomic and molecular species in aqueous environments. Chemical reactions in condensed phase environments play crucial roles in a wide variety of problems important to the Department of Energy (DOE), for example:

- Corrosion in nuclear reactors promoted by reactive radical species, such as OH.
- Release of hydrogen from chemically-bound hydrogen for use as a fuel.
- Chemical production using catalysis to provide efficient energy use.
- Contaminant degradation in the environment by natural and remedial processes.
- Degradation of materials used for nuclear waste entombment.
- Destruction of hazardous waste by supercritical oxidation.

The need in all of these areas is to control chemical reactions to eliminate unwanted reactions and/or to produce desired products. The control of transport and reactivity in these complex systems demands knowledge of the factors that drive the chemical reactions and requires understanding how the driving factors of the systems can be manipulated to affect the reaction rates. The goals of this research are the development of theoretical methods for describing reactions in condensed phases (primary aqueous liquids) and the application of these methods to prototypical problems of interest to DOE.

The calculation of accurate rate constants for reactions in condensed phases remains a major challenge. Electronic structure calculations of molecular interaction energies for extended systems are necessarily approximate. Accurate dynamical calculations require a quantum mechanical treat and for extended systems they are also necessarily approximate - variety of approximations but few benchmark studies. A wide variety of approximate methods for both energetics and dynamics exist with little or no accurate benchmarks to validate their performance for extended systems. Our approach builds upon the success of variational transition state theory (VTST) for predicting rate constants of gas-phase reactions. VTST provides a systematically improvable framework for computing rate constants of liquid-phase reactions, including both nonequilibrium solvation and quantum mechanical effects. The reaction energetics are treated by a hierarchical approach (from accurate first principles calculations on model systems to approximate treatment of solvation energies by QM/MM and continuum solvation models), in which in which higher accuracy calculations on model systems provide benchmarks for more approximate methods that can be applied to more realistic models of the reactive system. In the VTST approach to condensed-phase reactions the solvent influence on reaction energetics is computed from equilibrium averages over solvent configurations to give a potential of mean force (PMF). A cluster model of the reactive system is treated explicitly, so the PMF is

multidimensional. The coupling of solvent dynamics to the reactive system is included by a generalized Langevin model of solvent friction.

One focus of the research in the past year has been on understanding the factors controlling radical reactions in aqueous systems. An important factor is the effect of the open-shell nature of the radical on the solvation structure around the radical, since solvation and solvent reorganization can play an important role in chemical reactivity. Towards this end, we have initiated a study of OH radicals with water to understand how the unpaired orbital in OH can affect the interaction energy. For geometries with C_s symmetry the two lowest electronic states have different symmetries (A' and A") and their energies can be calculated accurately using the CCSD(T)/aug-c-pVTZ level of theory. We also performed full valence Multi-Configuration-Self-Consistent Field (MCSCF) followed by Multi-reference Configuration Interaction (MRCI) calculations as benchmarks for these calculations.

The global minima for both the A' and A" state are for configurations in which water is the proton donor. The interaction energy at the global minimum for the A" state is 3.5 kcal/mol with an OO separation of 3.05 Å while the energy at the global minimum for the A' state is 5.6 kcal/mol with an OO separation of 3.2 Å. These values are in good agreement with previous calculations. We also performed calculations along scans for different intermolecular coordinates to systematically study the potential energy surfaces. Examples of energy scans for two configurations are shown as a function of OO separations in figure 1. The figure shows that the splitting between the two states is small, ranging from about 2.5 kcal/mol at the global minimum (H_2O is the proton donor) to less than 0.5 kcal/mol at the minimum where OH is the proton donor. Figure 2 shows the interaction energies as a function of angular coordinates for rotation the OH radical relative to the water molecule for the cases where water and OH are proton donors. Once again it is seen that the splitting between the two states is small over larger variations of the rotational coordinates. We note that we have also observed a crossing of the two states for a geometry with C_1 symmetry.

The next step in this project is to determine the behavior of the splitting between the two states as more water molecules are added to the cluster. In addition, we are interested in understanding the importance of many-body interaction in these systems. Xantheas has shown

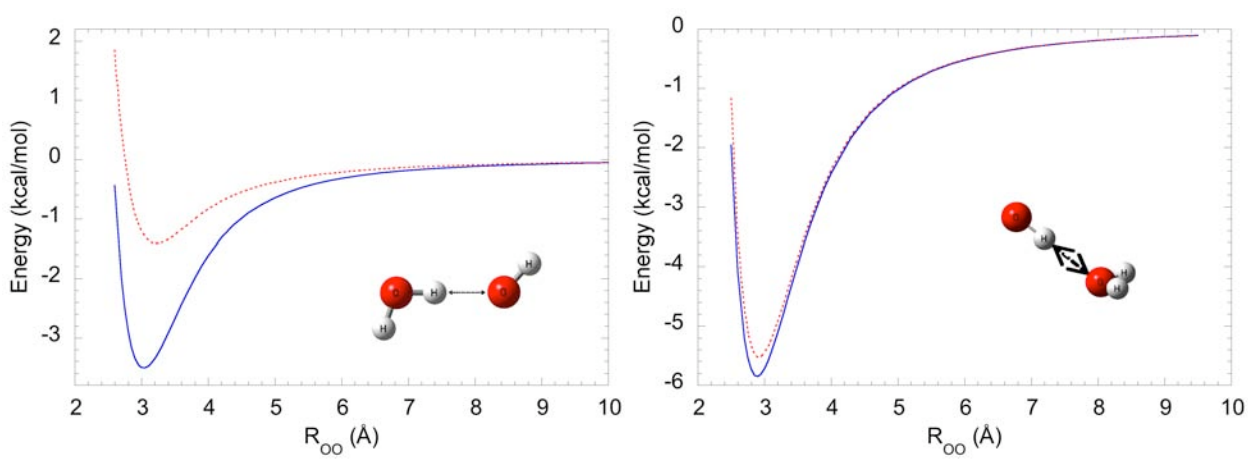

Figure 1. Energies for the A" state (higher curve) and A' state (lower curve) for OH interacting with water as a function of OO separation for two orientations of OH relative to the water molecule: H_2O as proton donor (left) and OH as proton donor (right)

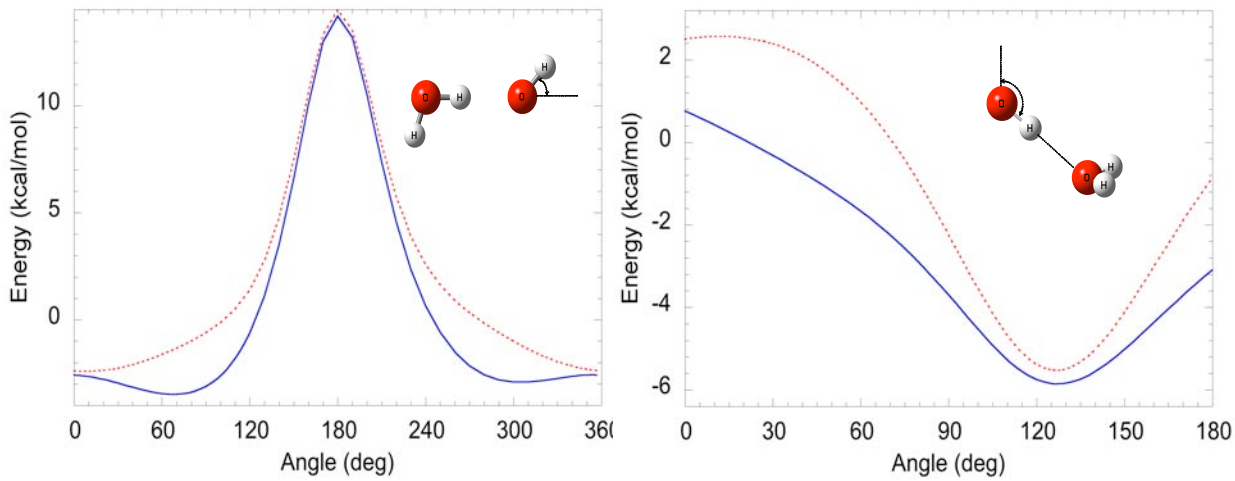

Figure 2. Energies for the A" state (higher curve) and A' state (lower curve) for OH interacting with water as a OH rotational angle for two orientations of OH relative to the water molecule: H_2O as proton donor (left) and OH as proton donor (right)

that the energetics of water clusters are dominated by pair interactions, with three-body interactions contributing around 20% to the binding energies at local minima and the sum of higher order terms contributing less than a few percent. Our preliminary studies of OH with two water molecules indicate that the three-body terms contribute up to 40% of the binding energy. Future work will quantify these effects and study the importance higher order terms. In addition have also fitted analytical potential energy surfaces for OH interacting with water and future work will extend this potential to allow studies of OH in bulk water.

Collaborators on this project include G. K. Schenter, M. Dupuis, T. Iordanov, S. S. Xantheas, J. Li, S. Du, and J. Francisco. Battelle operates Pacific Northwest National Laboratory for the U. S. Department of Energy.

References to publications of DOE sponsored research (2003-present)

1. B. C. Garrett, S. M. Kathmann, and G. K. Schenter, "Thermochemistry and Kinetics of Evaporation and Condensation for Small Water Clusters," in Water in Confining Geometries, edited by V. Buch and J. P. Devlin (Springer, Berlin, 2003), p. 25-51.
2. D. G. Truhlar and B. C. Garrett, "Reduced Mass in the One-Dimensional Treatment of Tunneling," *Journal of Physical Chemistry A* **107,** 4006-4007 (2003).
3. G. K. Schenter, B. C. Garrett, and D. G. Truhlar, "Generalized Transition State Theory in Terms of the Potential of Mean Force," *Journal of Chemical Physics* **119,** 5828-5833 (2003).
4. S. L. Mielke, K. A. Peterson, D. W. Schwenke, B. C. Garrett, D. G. Truhlar, J. V. Michael, M.-C. Su, and J. W. Sutherland, "H + H_2 Thermal Reaction: A Convergence of Theory and Experiment," *Physical Review Letters* **91,** 063201 (2003).
5. M. Dupuis, G. K. Schenter, B. G. Garrett, and E. E. Arcia, "Potentials of Mean Force with Ab Initio Mixed Hamiltonian Models of Solvation," *Journal of Molecular Structure-Theochem* **632,** 173-183 (2003).

6. Y. A. Borisov, B. C. Garrett, Y. A. Kolbanovskii, I. V. Bilera, and N. N. Buravtsev, "On the Relationship between the Enthalpy of Formation of Carbenes Upon Cleavage of the Double Bond in Fluoroolefins and the Electron Density on the Pi Bond: An Ab Initio Study," *Doklady Physical Chemistry* **392,** 212-216 (2003).
7. Y. A. Borisov, B. C. Garrett, Y. A. Kolbanovskii, I. V. Bilera, and N. N. Buravtsev, "On the Relationship between the Enthalpy of Formation of Carbenes Upon Cleavage of the Double Bond in Fluoroolefins and the Electron Density on the Pi Bond: An Ab Initio Study," *Doklady Physical Chemistry* **392,** 212-216 (2003).
8. L. X. Dang and B. C. Garrett, "Molecular Mechanism of Water and Ammonia Uptake by the Liquid/Vapor Interface of Water," *Chemical Physics Letters* **385,** 309-313 (2004).
9. B. C. Garrett, "Ions at the Air/Water Interface," *Science* **303,** 1146-1147 (2004).
10. S. M. Kathmann, G. K. Schenter, and B. C. Garrett, "Multicomponent Dynamical Nucleation Theory and Sensitivity Analysis," *Journal of Chemical Physics* **120,** 9133-9141 (2004).
11. S. M. Kathmann, G. K. Schenter, and B. C. Garrett, "Dynamical Nucleation Theory: Understanding the Role of Aqueous Contaminants," in Proceedings of the 16th International Conference on Nucleation and Atmospheric Aerosols, edited by M. Kulmala and M. Kasahara (Kyoto University Press, 2004), p. 243-246.
12. M. Roeselova, J. Vieceli, L. X. Dang, B. C. Garrett, and D. J. Tobias, "Hydroxyl Radical at the Air-Water Interface," *Journal of the American Chemical Society* **126,** 16308-16309 (2004).
13. B. C. Garrett, D. A. Dixon, D. M. Camaioni, D. M. Chipman, M. A. Johnson, C. D. Jonah, G. A. Kimmel, J. H. Miller, T. N. Rescigno, P. J. Rossky, S. S. Xantheas, S. D. Colson, A. H. Laufer, D. Ray, P. F. Barbara, D. M. Bartels, K. H. Becker, H. Bowen, S. E. Bradforth, I. Carmichael, J. V. Coe, L. R. Corrales, J. P. Cowin, M. Dupuis, K. B. Eisenthal, J. A. Franz, M. S. Gutowski, K. D. Jordan, B. D. Kay, J. A. LaVerne, S. V. Lymar, T. E. Madey, C. W. McCurdy, D. Meisel, S. Mukamel, A. R. Nilsson, T. M. Orlando, N. G. Petrik, S. M. Pimblott, J. R. Rustad, G. K. Schenter, S. J. Singer, A. Tokmakoff, L. S. Wang, C. Wittig, and T. S. Zwier, "Role of Water in Electron-Initiated Processes and Radical Chemistry: Issues and Scientific Advances," *Chemical Reviews* **105,** 355-389 (2005).
14. S. M. Kathmann, G. K. Schenter, and B. C. Garrett, "Ion-Induced Nucleation: The Importance of Chemistry," *Physical Review Letters* **94,** 116104 (2005).
15. B. C. Garrett and D. G. Truhlar, "Variational Transition State Theory," in Theory and Applications of Computational Chemistry: The First 40 Years, edited by C. E. Dykstra, K. S. Kim, G. Frenking, and G. E. Scuseria (Elsevier, in press).

Abstract

Program Title: **Chemical Reaction Dynamics in Nanoscale Environments**

DOE Grant No. DE-FG02-01ER15212

Principle Investigator:
Evelyn M. Goldfield, (PI), H. Bernhard Schlegel and William L. Hase (co-PI's)
Department of Chemistry
Wayne State University
Detroit, MI 48202
evi@sun.science.wayne.edu

Program Scope:

The major focus of the research in this program is the study of the behavior of molecular systems confined in nanoscale environments. The goal is to develop a theoretical framework for predicting how chemical reactions occur in nanoscale environments. To achieve this goal we have employed ab initio quantum chemistry, classical dynamics and quantum dynamics methods. Much of the research has focused on the behavior of molecules confined within single-walled carbon nanotubes (SWCNTs). We have also studied interactions of small molecules with the exterior surface of SWCNTs. Nonequilibrium molecular dynamics of interfaces of sliding surface interfaces have also been performed.

Recent Progress:

We (Goldfield group) have continued our research into the behavior of hydrogen molecules confined within SWCNTs of various shapes and sizes. Recently we completed a new study of the discrete energy levels of H2 and its isotopes confined within single-walled carbon nanotubes (SWCNTs) of various shapes and sizes. As in our previous studies, we explicitly treat the rotational and translational motion, solving the problem of a confined rigid rotor. Our previous studies were the first to treat translation and rotation together. Quantum mechanical energy levels are computed for the hydrogen molecule and its homonuclear isotopes confined within nanotubes of various sizes and structures using three different interaction potentials. We study the dependence on the interaction potential and the size of the nanotube of several quantities including zero-pressure quantum sieving selectivities for both isotopes and neutron spin states, ortho-para energy splittings and characteristics of the energy levels. We show that large quantum sieving selectivities as well as large deviations from gas phase ortho-para splittings occur only under the condition of extreme two dimensional (X2d) confinement, when the characteristic length of the hydrogen-carbon interaction potential is nearly equal to the radius of the nanotube. Under these conditions, we see very dramatic effects on rotational structure. The results of this research have been written up and submitted to the Journal of Physical Chemistry B: T. Lu, E. M. Goldfield and S. K. Gray, " Quantum states of hydrogen and its isotopes confined in single walled carbon nanotubes: dependence on interaction potential and extreme two dimensional confinement"

Current work is focused on the calculation of the interaction of H + H_2 within SWCNTs.. Because the transition state of this reaction is collinear, it is possible that the restriction of impact parameters that may occur will enhance the probability of reaction. However, this may depend quite strongly on the diameter of the nanotube. It is also the case that hydrogen atoms that are close to the walls of the nanotube will react strongly with carbons. Therefore, we ran wavepacket calculations to see whether H atoms at one end of a nanotube with momenta directed along the central tube axis were capable of traveling through to the other end of the tube. Portions of the wavepacket that were attracted to the walls were absorbed. We computed the distance traveled as a function of tube diameter and initial wavepacket momentum. Not surprisingly, the larger the tube, the more wavepacket density reached the other end. But, except for the smallest tubes studied, a large portion of the hydrogen did emerge on the other end of the tube.

The H + H_2 quantum calculations have been computed using a simplified model for the reaction that focuses on the most important degrees of freedom .We explicitly treat the there internal degrees of freedom of H_3. Motion relative to the nanotube is modeled with one rotational and one translational coordinate. This model should allow us to explore effects of confinement on reactivity for systems this and similar systems. Wavepackets have been propagated using this model and we are currently analyzing the results.

The Goldfield and Schlegel groups are currently studying the binding of small molecules such as NO_2 to the outer and to the inner walls of semi-conducting SWCNTs. This work is in conjunction with a member of our computer and electrical engineering department who is developing a nanotube based chemical sensor. The current project studies binding of NO_2 to a (10,0) SWCNT which is 20 Å in length. We are trying to understand experimental results that seem to indicate that this binding is quite strong. The interaction between NO_2 and a finite length semi-conducting (10,0) carbon nanotube ($C_{200}H_{20}$) has been studied at PM3, Hartree-Fock and density functional levels of theory. Semi-empirical calculations show that NO_2 adsorbs on the carbon nanotube; however, the spin unrestricted calculations have a very large spin contamination and therefore quantitatively give wrong values for band gap after NO_2 adsorption. Spin restricted open shell Hartree-Fock (ROHF) calculations give more reasonable energetics and charge distributions. We have used naphthalene and pyrene as "models" for SWCNTs and studied the interaction of two NO_2 molecules with these molecules at the B3LYP level of theory in chemisorbed as well as physisorbed configurations A mechanism for formation of NO_3 on the small molecules is also investigated at B3LYP level, which will be subsequently investigated on the (10,0) finite sized nanotube.

The dissociation of formaldehyde confined in a carbon nanotube has been studied in the Schlegel group using QM/MM methods. The nanotube was treated with the UFF molecular mechanics force field and the H_2CO was treated quantum mechanically (HF/3-21G level of theory). The results from about 100 trajectories show that both CO and H_2 fragments are formed with more vibrational excitation compared to the gas phase dissociation. CO is produced with 66% in v=0, 31% in v=1 and 3% in v=2. Vibrational levels up to v=5 are populated in case of H_2. The average vibrational quantum number for

H_2 is calculated to be 1.6 compared to ⟨v⟩=1.16 in the gas phase. Most of the available energy resides in product translation and the CO translational energy is found to be greater for dissociation within the tube. The average rotational quantum numbers are ⟨J⟩=24 for CO and ⟨J⟩= 8.9 for H_2. Compared to the gas phase dissociation, the CO rotational distribution occurs at lower values of J and at higher values of J for H_2. The CO fragment receives about 7% energy in rotation compared to 13% in the gas phase. More trajectories need to be integrated in order to get better statistics. It will also be interesting to see if a tube with a smaller diameter (such as a (5,5) tube) would cause significant changes in the dynamics. A manuscript is in preparation: S. Anand, E. M. Goldfield and H. B. Schlegel; "Dissociation of formaldehyde (H_2CO □ H_2 + CO) confined within a single walled carbon nanotube"

A current focus of the Schlegel group is the study of ionization potential (IP) and electron affinity (EA) of molecules within SWNT's. Whether the molecule or the tube will gain or loose an electron depends on the relative IP's and EA's of the molecule and the carbon nanotube, and on the stabilization resulting from their interaction. Because carbon nanotubes are highly polarizable, they stabilize cations and anions more than neutrals. Thus, when a neutral molecule is placed inside a carbon nanotube, or in close proximity to one, its ionization potential will be lowered and its electron affinity will be increased by as much as 1 eV. A series (7,7) armchair nanotubes ranging in length from 13-30 Å as well as (8,8) and (9,0) nanotubes of ca 15 Å length were calculated at the B3PW91/3-21G level of theory and the molecules within them were calculated at the B3PW91/6-311++G(d,p) level. The IP's and EA's of carbon nanotubes vary with length more than with diameter and can be understood in terms of simple Hückel theory. Five categories can be identified for the ionization of a molecule + carbon nanotube system: (i) the molecule always ionizes but the nanotube does not, (ii) the nanotube always ionizes but the molecule does not, (iii) the molecule ionizes spontaneously as soon as it is placed inside the nanotube, (iv) the nanotube ionizes spontaneously as soon as the molecule is placed inside, and (v) either the molecule or the nanotube ionizes, depending on the length of the tube. Most neutral molecules with high IP's and low EA's fall into case (ii). Atoms and molecules with very low IP's, such as alkali metals, are examples of case (iii). Halogens and molecules with high EA's can serve as examples for case (iv). Because the nanotubes have low IP's and high EA's, and because nanotubes strongly stabilize molecules within them, no example could be found for case (i) for the nanotubes in the present study. The CN radical is an intriguing example of case (v). Because the IP oscillates by more than 0.5 eV as the length is incremented, the electron is removed from CN for some lengths and from the nanotube for other lengths. This work will be submitted for publication in the very near future: J. E. Knox, M. D. Halls and H. B. Schlegel, "Carbon Nanotube Inner Phase Effects on Guest Ionization", (to be submitted to the journal *Small*, October 2005).

Nonequilibrium molecular dynamics simulations were performed in the Hase research group to study the dynamics of energy transfer at the interface of a small nanoscale hydroxylated alpha-alumina surface sliding across a much larger surface of the same material . Nonequilibrium energy distributions were found at the interface for each of the conditions studied. The velocity distribution P(v) for the atoms in a sublayer of the

smaller surface oscillates during the sliding, reflecting the periodicity of the interfacial intermolecular potential. When averaged over the sliding, this P(v) for each of the sublayers is bimodal with Boltzmann and non-Boltzmann components. The non-Boltzmann component, with temperatures in excess of 1000 K and as high as 2500 K, is most important for the interfacial H-atom sublayer and becomes less important in moving to a sublayer further from the interface. Similarly, the temperature of the Boltzmann component decreases for sublayers further from the interface and approaches the 300 K temperature of the boundary. The temperature of the Boltzmann component decreases, but the importance of the non-Boltzmann component increases, as the sliding velocity is decreased. The temperature of the non-Boltzmann component is relatively insensitive to the sliding velocity. Friction forces are determined by calculating the energy dissipation during the sliding, and different regimes are found for variation in the friction force versus sliding velocity v(s) and applied load.

Future Work:

Work in the near future will focus completing quantum study of the H + H_2 reaction confined to a nanotube. We plan to follow this up with a classical molecular dynamics study of this system, treating the motion of all atoms. Goldfield and Schlegel also plan to continue to study the interactions of other small molecules, including NO_3, with SWCNTs and map out reaction pathways that may occur on the surfaces of carbon nanotubes that may be relevant to CNT sensors.

Publications of DOE Sponsored-Research (2003-2005)

1. O. A. Mazyar, H. Xie and W. L. Hase, "Nonequilibrium energy dissipation at the interface of sliding model hydroxylated α-aluminar surfaces", J. Chem. Phys. **122**, 094713 (2005)
2. T. Lu, E. M. Goldfield and S. K. Gray, " The equilibrium constants for molecular hydrogen in carbon nanotubes based on iteratively determined nano-confined bound states", Journal of Theoretical and Computational Chemistry, special issue on Iterative Methods in Quantum Mechanics and Applications to Chemical Problems" **2**, 621 (2003)
3. T. Lu, E. M. Goldfield and S. K. Gray, "Quantum states of molecular hydrogen and its isotopes in single-walled carbon nanotubes ",J Phys Chem B **107,** 12989 (2003)

Reactive Intermediates in the Condensed Phase: Radiation and Photochemistry

David Gosztola*, Robert A. Crowell, and Ilya A. Shkrob

Radiation and Photochemistry Group, Argonne National Laboratory, Chemistry Division
9700 S. Cass Avenue, Argonne, IL 60439 TEL: (630)252-3541, FAX: (630)252-4993,
e-mail: gosztola@anl.gov

Scope:

The Radiation and Photochemistry program at Argonne National Laboratory primarily studies the initial events and ensuing chemistry that follow energetic excitations. The fundamental mechanisms of internal energy conversion, charge trapping or solvation, and charge relaxation following energetic excitation can be studied by probing both the chemical and physical dynamics of the system. Although the primary goal of the Group this past year has been to finalize construction of our wholly laser-based electron accelerator — the Terawatt Ultrafast High-Field Facility (TUHFF), and to begin making measurements of spur kinetics in water, we continue to conduct our related research using the wide range of instruments at our disposal such as our femtosecond laser system, LINAC and Van de Graaff accelerators, and the Advanced Photon Source (APS). Our research into the dynamics of structural changes in condensed phase materials caused by charge trapping complements our core program which primarily utilizes non-structural specific techniques such as transient absorption and transient DC conductivity.

During the inception of the TUHFF laser system design, it was realized that a laser system that was powerful enough to produce an ultrafast pulsed relativistic electron beam could also be used to produce ultrafast pulses of X-rays using a gas, liquid, or metal target. Since our priority has been to bring TUHFF to full operational status, we have been carrying out initial X-ray structural studies using the APS. This work will initially be focused on the following two areas: Firstly, we are currently investigating the structural nature of trap sites in nanocrystalline metal oxide semiconductor films which is the focus of the work described below. Secondly, we hope to soon begin to make dynamic X-ray absorption measurements of solvent reorganization following charge transfer to solvent (CTTS) processes.

Recent progress:

The efficiency of metal oxide semiconductor assisted radio- and photo-catalysis is often determined by energy loss pathways such as charge recombination and charge trapping. Nanoparticulate wide band gap semiconductors can behave as miniature electrochemical cells in which the electrochemical potential arises from either radiolytic or photoinduced charge separation. It is for this reason that it is important to understand the complex interplay between structure and electronic properties and how they effect both the lifetime and chemical potential of charge carriers. We have chosen to begin with nanocrystalline TiO_2 films for these experiments because of the ease in which charge carriers can be introduced through electrochemical means as well as by direct band-gap optical excitation and radiolysis.

Using a specially designed electrochemical cell, we have recently been able to simultaneously measure both the X-ray absorption (near edge: XANES, extended: EXAFS) and the optical absorption spectrum (400 nm-900 nm) of a nanocrystalline TiO_2 film while controlling its

potential. We have coupled spectroelectrochemical and X-ray absorption spectroscopies in order to begin to reveal the electronic nature of injected charge carriers and the structural changes due to their localization. In particular, localization of charge carriers may be manifested by changes in local oxidation state, local structure and symmetry, as well as in the appearance of new optical absorption transitions.

Figure 1 shows the simultaneously recorded visible absorption and XANES spectra of a nanocrystalline TiO_2 film at various potentials. The nanocrystalline film was deposited on a conductive, optically transparent electrode supported on a thin piece of Mylar. The Mylar substrate formed one window of an optically transparent cell which held a 1 mm thick layer of electrolyte solution (acetonitrile/ 0.2 M $LiClO_4$). The optical layout was such that the X-ray fluorescence could be collected without having to transverse the 1 mm of solvent. The visible absorption spectra shown in Figure 1A were recorded as the potential of the TiO_2 film was made more negative and are fully consistent with previously published nonaqueous results from other labs. Briefly, an increase in absorption throughout the visible-NIR region was observed which has been attributed to the accumulation of electrons in the film. At potentials negative of -1.3 V, electrons should begin populating the conduction band giving rise to a weak broad band centered around 1030 nm (not observable). At potentials negative of -1.8 V, a stronger absorption band appeared at 750-800 nm which has been attributed to shallow surface inter-band trapped electrons. Slowly growing in at potentials negative of -2.6V is a band at 500nm which has been attributed deep surface state traps.

The X-ray absorption spectra in the near edge region (XANES) recorded simultaneously with the absorption spectra are shown in Figure 1B. Upon reduction, the X-ray absorption edge shifted to lower energies, consistent with a reduction in the formal oxidation state of Ti^{4+}, and a decrease in the fine structure was observed, consistent with a decrease in symmetry around Ti. One possibility is the formation of Ti^{3+} since Ti_2O_3 has a D3d symmetry which is significantly different from the D2d symmetry of anatase TiO_2. It is also known that at potentials negative of -1.8V, Li^+ ions are intercalated into the porous film which may also perturb the symmetry of TiO_2.

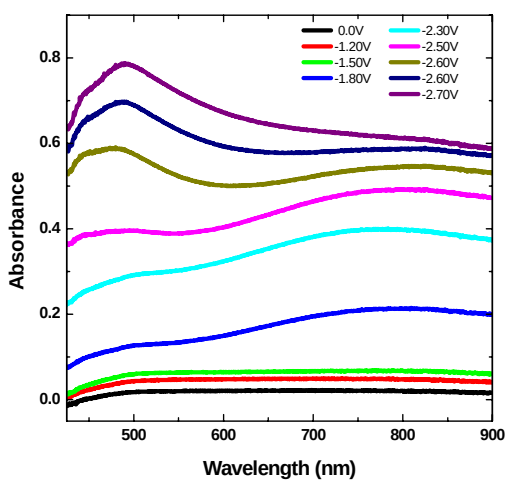

Figure 1A: Absorption spectra of TiO_2 nanocrystalline film in acetonitrile/$LiClO_4$ at various potentials. Substrate: ITO coated Mylar. Potentials are versus $Ag/AgNO_2$.

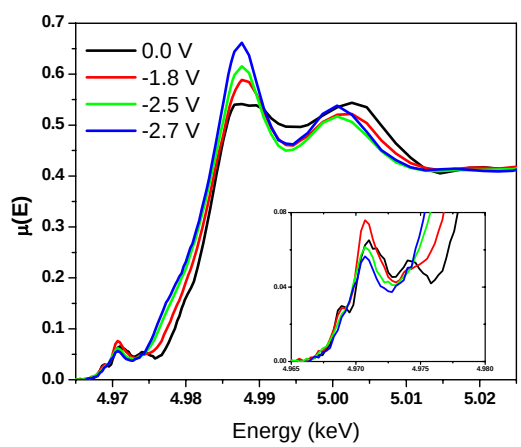

Figure 1B: X-Ray absorption spectra of TiO_2 nanocrystalline film in acetonitrile/$LiClO_4$ at various potentials recorded simultaneously with 1A.

Future plans:

We will continue with our investigations into the structural and electronic changes that accompany charge localization in nanoparticulate wide band gap metal oxide semiconductor films. In addition to the data discussed above we have already collected and are beginning to analyze extensive data sets from films in solutions lacking Li^+ ions which show marked differences. Continuing with TiO_2 films in particular, we will begin dynamic studies of the time evolution of the trapping/detrapping process itself including time-resolved measurements from photo-ejected, pre-filled trap sites to better understand charge mobility in the near absence of available trap sites. We would also like to broaden the investigation to other metal oxide semiconductor films such as ZnO which has many similar optical and electrochemical properties to TiO_2.

We intend to extend the X-ray measurements to begin studying the structural dynamics of trapped charges in liquids. We will begin with EXAFS measurements of solvent reorganization following photo-induced CCTS to be carried out at the APS.

Acknowledgment: This work was supported by the U.S. DOE, Office of BES, Division of Chemical Sciences, under contract W-31-109-Eng-38.

Publications 2003 – 2005:

Motivation and Development of Ultrafast Laser-Based Accelerator Techniques for Chemical Physics Research.
R. A. Crowell, I. A. Shkrob, D. A. Oulianov, O. Korovyanko, D. J. Gosztola, Y. Li, R. C. Rey-de-Castro, *Nucl. Instr. and Meth. In Phys. Res. B.*, In Press, (2005).

Femtosecond Thomson Scattering X-Ray Source based on Laser Wakefield Accelerator for Ultrafast X-ray Absorption Spectroscopy.
D. A. Oulianov, R. A. Crowell, D. J. Gosztola, Y. Li,
Nucl. Instr. And Meth. In Phys. Res. B., In Press, (2005).

Toward Electronically Coupled Bio-Inorganic Conjugates.
D. Gosztola, Z. Saponjic, L. Chen, L. De La Garza, N. Dimitrijevic, and T. Rajh,
Proceedings of the Electrochemical Society 205th Meeting, (2004).

Efficient, Rapid One-Electron Photooxidation of Chemisorbed Polyhydroxyl Alcohols and Carbohydrates by TiO_2 Nanoparticles in an Aqueous Solution.
M. C. Sauer, Jr., I. A. Shkrob, and D. Gosztola, *J. Phys. Chem B*, 108, 12512-12517, (2004).

Recombination of Geminate (OH,E_{aq}^-) Pairs in Concentrated Alkaline Solutions: Lack of Evidence for Hydroxyl Radical Deprotonation.
R. Lian, R. A. Crowell, I. A. Shkrob, D. M. Bartels, D. A. Oulianov, and D. Gosztola,
Chem. Phys. Lett., 389(4-6), 379-384, (2004).

Ultrafast Processes in Radiation Chemistry.
R. A. Crowell, D. J. Gosztola, I. A. Shkrob, D. A. Oulianov, C. D. Jonah, and T. Rajh,
Radiation Physics and Chemistry, 70(4-5), 501-509, (2004).

COMPUTATIONAL NANOPHOTONICS: MODELING OPTICAL INTERACTIONS AND TRANSPORT IN TAILORED NANOSYSTEM ARCHITECTURES

Stephen K. Gray (gray@tcg.anl.gov),[1] Julius Jellinek (jellinek@anl.gov),[1] George C. Schatz (schatz@chem.northwestern.edu),[2] Mark S. Ratner (ratner@chem.northwestern.edu),[2] Mark I. Stockman (mstockman@gsu.edu),[3] Koblar A. Jackson (jackson@phy.cmich.edu),[4] Serdar Ogut (ogut@uic.edu)[5]

[1]Chemistry Division, Argonne National Laboratory, Argonne, IL 60439; [2]Department of Chemistry, Northwestern University, Evanston, IL 60208; [3]Department of Physics and Astronomy, Georgia State University, Atlanta, GA 30303; [4]Department of Physics, Central Michigan University, Mt. Pleasant, MI 48859; [5]Department of Physics, University of Illinois at Chicago, Chicago, IL 60607

PROGRAM SCOPE

We carry out modeling and simulations relevant to light interacting with metal nanoparticle (MNP), nanohole and other nanostructured systems. The work includes microscopic studies of electronic, structural and optical properties, and continuum-level electrodynamics studies. A major goal is to learn how to confine and manipulate electromagnetic energy on the nanoscale. A broad range of theoretical methods is needed, and another goal is to develop a corresponding suite of nanophotonics simulation tools. We also work with applied mathematicians and computer scientists in developing optimal algorithms and software with high-performance capabilities.

At a microscopic level, we must understand the mechanisms underlying the assembly of atoms into clusters and clusters into larger systems. Understanding these mechanisms and the parameters they depend on is essential for designing cluster-based architectures with desired nanophotonics properties. The atomic-level mechanisms are ultimately defined by interatomic interactions. Accurate, but computationally efficient descriptions of these interactions are sought in order to uncover correct mechanisms. Our microscopic work also provides optical information, e.g. static and dynamic polarizabilities, for the estimation of size-dependent dielectric properties of relevance to our electrodynamics work.

Maxwell's equations, assuming certain frequency-dependent dielectric properties, describe how light interacts with nanosystem architectures. We use several computational electrodynamics methods to solve these equations numerically. These solutions allow us to develop an understanding of the physical phenomena that can occur, such as surface plasmons (SP's). SP's are collective electronic excitations near the surfaces of metallic structures. The high intensity and localization of SP's make them very relevant to chemical and biological sensing, nanoscale optics and optoelectronics.

RECENT PROGRESS

Microscopic Studies of Electronic, Structural and Optical Properties: We continued work on the construction and evaluation of new, more accurate semiempirical many-body potentials for metals. In collaboration with M. J. Lopez, we used a new, five-parameter form of the Gupta-type potential and performed extensive evaluation of the size-specific structural and dynamical properties of clusters of nickel and silver with up to ~ 2000 atoms (~ 4.4 nm). The results obtained were contrasted with those derived using other available potentials. The differences in the structural properties are explained in terms of the different effective ranges of the potentials. The predicted changes in the preferred structural motifs of silver clusters as they grow in size are

yet to be verified experimentally. We also constructed a new potential for gold using both bulk and dimer properties as fitting data and are currently evaluating it.

Large-scale molecular dynamics simulations of cluster nanoparticles deposited on substrates were initiated. Our aim is to understand the mechanisms of particle-substrate interactions as defined by the material and size of the particles, and the material, morphology, and temperature of the substrates. The ultimate goal is to acquire knowledge that will allow for rational design of cluster-assembled nanosystems with desired structural and optical characteristics. We considered silver clusters on a silica surface. We are in the process of evaluating different force fields and the effects of the surface. To elucidate the effects of particle/substrate interactions, we concomitantly perform high-level density functional theory (DFT) studies of structural forms and electronic properties of gas phase silver clusters. In collaboration with J. Wang and others we are performing DFT studies of structural and electronic properties of small and medium sized gold clusters. An intriguing finding, in press as a cover article in *J. Chem. Phys A* [9], is that medium sized gold clusters (e.g., Au_{50}) may form hollow cage structures, which are energetically competitive with their three-dimensional space-filling conformations. We also determined that filled fullerene cage structures are energetically favorable for certain medium-sized silicon clusters, including Si_{40}, Si_{45}, and Si_{50} [10].

We expanded our investigation of the static polarizabilities of Cu_n and found that the calculated values are much smaller than the reported experimental values. The central result is that, if the measured polarizabilities are assumed to be correct, they must include contributions beyond the response of the electronic charge to applied fields. One such possible contribution is the permanent dipole in the clusters [11].

The dipole moments are very sensitive to the details of cluster structure, but reliable ground state conformations for Cu_n were not available beyond n = 8. We combined the new "big bang" algorithm [1, 12] with high-level density functional theory computations to determine optimal structures of Cu_n, n = 8 – 20. We found that the published idea that Cu clusters follow the icosahedral growth pattern over these sizes needs revision [Jackson, Jellinek and coworkers, *J. Chem. Phys.* submitted]. For example, we found that icosahedral Cu_{13} is nearly 1 eV less stable than the true ground state. The preferred structures for $n \leq 16$ are layered, with increasingly oblate, platelet-like shapes. For n = 17 and beyond, more spherical structures are optimal. We showed that the size-driven shape changes in Cu_n are due to electronic factors and they closely mirror similar changes in Na_n clusters. Static electric dipole polarizabilities provide significant insight into the physical character of atomic clusters [13]. To gain a insight into the static response of clusters to external fields, we initiated work on the development of a general scheme for determination of local, or position-dependent, polarizabilities which ultimately make up the total polarizability of a finite system.

We studied the optical properties for Ag_n, n = 2-8, clusters, characterizing the absorption spectra and static dipole polarizabilities [14]. The computations were carried out using time-dependent (TD) DFT and finite-field methods within a real-space *ab initio* pseudopotential framework. The treatment represents the state-of-the art in the field. The computed spectra are in good agreement with the available quantum chemical (CI) and measured results. Very recently an experimental group informed us that of all the available theoretical results ours [14] fit best their recent, yet unpublished measured data. The central findings of our study are: 1) The static dipole polarizabilities of Ag_n exhibit even-odd alternation in the range $n \leq 6$. There is a decrease in polarizability for n = 7 and 8. We correlated this decrease with the transition from 2-D to 3-D structures at n = 7; 2) The *d* electrons play an important role in the optical spectra of Ag_n. They both quench the oscillator strength through screening the *s* electrons, and they can be directly involved in the optical transitions; 3) Determination of static dipole polarizabilities from low-

energy optical absorption data may lead to substantial errors. Other aspects of our work in progress include exploration of structural, electronic, and optical properties of Au_n clusters, investigation of the isomer specificity of optical properties of Ag_n clusters, comparative evaluation of the TD DFT/LDA and the GW-Bethe-Salpeter approaches to computation of optical spectra (in collaboration with J. R. Chelikowsky), and extension of studies to larger silver and gold clusters.

Electrodynamics Studies: This work involves realistic and model computational electrodynamics studies, as well as analytical analysis. Two kinds of rigorous computational electrodynamics theory are employed: the discrete dipole approximation (DDA) and the finite-difference time-domain (FDTD) method. DDA is a frequency-domain method while FDTD is a time-domain method. Both methods provide the ability to realistically model light interacting with nanostructured systems with overall dimensions up to microns. The methods have overlapping capabilities, but in specific applications it is often the case that one will be more convenient or more accurate. Also, we are developing an interface between classical electrodynamics and quantum chemistry so that we can study the coupling of molecules to enhanced electromagnetic fields on metal particle surfaces.

Our recent DDA studies have been concerned with triangular prisms, cubes and other anisotropic MNP structures. In joint work with Mirkin's experimental group, we studied a new class of gold triangular prisms that have been synthesized with wet chemistry methods, leading to the first observation of quadrupole resonance effects for this particle shape [15]. In addition, we characterized the properties of higher multipole resonances for such systems [16].

Motivated by earlier quasistatic limit calculations [5], we carried out FDTD studies of chirped laser pulses, with durations ranging from femtoseconds to picoseconds, interacting with 2-D nanowires and 3-D cone-shaped MNP's [17]. We showed how localized SP hot spots could be created on one region of a MNP and driven, in a controlled, spatiotemporal manner, to another region, with possible implications for chemical sensing. Two-dimensional arrays of MNP's or nanoholes are also interest for chemical sensing and other purposes. We carried out FDTD studies of MNP arrays covered by a photo-sensitive polymer, providing an interpretation of corresponding experimental results of Wiederrecht and coworkers, and pointing to an exciting new near-field imaging technique [18]. We extended our earlier FDTD work on isolated nanoholes [4] to 2-D arrays of nanoholes in metal films and the mechanism of enhanced transmission of light through such arrays was carefully analyzed [19]. Also, we characterized hole array structures fabricated by Odom's experimental group, showing that near-field microscopy measurements are sensitive to interference effects associated with SP polariton scattering [20]. Nanoscale thick metal films are also very relevant to nanophotonics. We carried out FDTD calculations to demonstrate how very intense and long-range SP polaritons could be created in such films by forcing natural radiation loss to be reflected back up to the propagation surface, thereby regenerating SP polaritons [21]. Further examples and features of the spatiotemporal control and hole problems were discussed [22].

Accurate nanophotonics simulations of metallic nanostructures are computationally challenging owing to their multiscale character: strong field variations can occur in 5-10 nm regions near metal surfaces, but overall system dimensions of a micron or more are often of interest. The use of Fourier methods to evaluate spatial derivatives should, in principle, lead to greater efficiencies in the numerical solution of Maxwell's equations. However, the abrupt material property variations often present leads to solutions with artificial oscillations known as Gibbs oscillations. In collaboration with members of Argonne's Mathematics and Computer Science (MCS) Division, significant progress was made in eliminating such errors via a reconstruction technique

[23]. Progress was also made on a different approach to the multiscale problem involving adaptive mesh refinement of the simplest form of the FDTD method. A parallel, working 2-D code has been developed that allows arbitrary 2-D cross-sectional nanowires and nanowire array structures to be studied.

Based on numerical and analytical electrodynamics work, we proposed a possible solution to one of the most important nanophotonics problems: efficient delivery of optical energy to nanoscale [8]. This solution includes adiabatic transformation of optical radiation into nano-localized SP's in graded plasmonic waveguides, and was based on an Eikonal (or WKB) approximation analysis. Employing analytical theory and numerical studies of a 1-D time-dependent Schrödinger equation, we found an efficient mechanism of laser energy deposition in dielectrics for ultrashort pulses and moderate intensities that do not cause an electron avalanche [24]. This mechanism invokes a "forest fire" where an ionized atom facilitates ionization of its neighbors. We have numerically examined a surface plasmon laser (spaser) consisting of self-similar chain of silver nanospheres in an active medium and found conditions for efficient generation [25]. We discussed the fundamental limitations of the use of thin metal slabs as perfect lens, with implications for nano-imaging, lithography and spectroscopy [26]. Numerically, on the basis of a quasistatic-limit Green's function method, we found giant fluctuations and scaling of the local second-harmonic fields in metal nanostructures [27].

FUTURE PLANS

The work on construction of more accurate, computationally efficient semiempirical potentials will be extended to other metallic systems, including bimetallic ones. These potentials will then be used in large-scale dynamical simulations of cluster-based nanoassembly. The assembly mechanisms will be studied as a function of cluster size and composition as well as the characteristics of the supports. The first system we will explore in detail is silver particles deposited on silica surfaces. As a means of achieving assembly of nanostructures with desired photonic properties, we will study the role of patterning of the supports. An important aspect of the studies will be exploration of the thermal stability of the assembled nanosystems.

The studies of Ag_n particles, both gas phase and deposited, will be extended to larger sizes and complemented by similar explorations of gold particles. The structural data obtained will be used as input in explorations of the optical properties of these systems. Among the issues addressed will be the isomer specificity of both the polarizabilities and the spectra. We will investigate the added potential particles with cage structures may have in nanophotonic applications. In particular, we will explore the possibility of tuning the optical properties of these particles by “filling” them with atoms of other elements.

We will continue the development of the scheme for characterization of position-dependent polarizabilities. The scheme will include specification of atomic contributions to the particle polarizability The atomic contributions will be further partitioned into local dipole and charge-transfer terms, which will be used to gauge the degree of non-metallic and metallic responses. Contributions from surface and interior atoms will be analyzed to probe the screening effect in metallic clusters.

As part of the methodological developments, we will continue the comparative evaluation of the TD DFT/LDA and the GW-Bethe-Salpeter approaches. In addition, we will apply our recently formulated new way of computing the full (wavevector and frequency-dependent) dielectric function. The results will be analyzed with the purpose of arriving at an understanding of the fundamental aspects of the size-evolution of the dielectric function. Such an understanding will allow for formulation of an efficient model that will link the dielectric properties of discrete finite

systems with the continuum description used in the bulk limit. This model will be used in some of our electrodynamics work.

We will use the DDA method to study a new class of nanoparticles from the Odom group at Northwestern in which multiple layers of metals are fabricated into a pyramidal shape. We will also study, in collaboration with Mirkin's experimental group, gold nanorods that support multipolar plasmon modes. In a new direction, we will begin a study of forces acting on metallic nanoparticles interacting with strong radiation fields. There are significant issues here both at the fundamental level (e.g., the relative importance of the three terms that act on the particles, arising from different terms in the Maxwell equations, the importance of conservative and nonconservative forces, and the magnitudes and directions of the forces on two neighboring nanoparticles) and for applications (e.g., how can these radiation forces be used to form particular geometric patterns).

The FDTD method will be used to examine light propagation in metal films with nanoscale slits. Preliminary work we have done suggests that sub-wavelength bending of light can be achieved with surprising efficiency in such structures. In another application of the FDTD method, we will study enhanced transmission through hole structures in which we use groove structures to enhance the coupling of light into propagating plasmons. We will also study multilayered films, in which dielectric materials and silver films are combined to create both plasmonic and photonic resonance effects that can be coupled to light using hole array structures. The use of the FDTD method in combination with the time-dependent Schrödinger equation to model various SP-enhanced spectroscopies, will be investigated. Our collaborative work with Argonne's MCS division will continue, including a 3-D generalization of the adjustable-mesh FDTD code.

Further electrodynamics plans include model studies of attosecond optical responses of metal nanostructures. Another project will be computational theory of a plasmonic laser or spaser built of a ~10 nm thick silver layer surrounded by quantum dots. Also, we will carry out a more rigorous computational investigation of the adiabatic energy concentration in graded plasmonic waveguides.

PUBLICATIONS OF DOE SPONSORED RESEARCH (2003-2005)

1. Unraveling the shape transformation in silicon clusters, K. A. Jackson, M. Horoi, I. Chaudhuri, Th. Frauenheim and A. A. Shvartsburg, *Phys. Rev. Lett.* **83**, 013401 (2004).
2. Dipolar emitters at nanoscale proximity of metal surfaces: Giant enhancement of relaxation, I. A. Larkin, M. I. Stockman, M. Achermann, and V. I. Klimov, *Phys. Rev. B* (Rapid Comm.) **69**, 121403(R) (2004).
3. Optical scattering from isolated metal nanoparticles and arrays, G. A. Wurtz, J. S. Im, S. K. Gray, and G. P. Wiederrecht, *J. Phys. Chem. B* **107**, 14191 (2003).
4. Surface plasmons at single nanoholes in Au-films," L. Yin, V. K. Vlasko-Vlasov, A. Rydh, J. Pearson, U. Welp, S.-H. Chang, S. K. Gray, G. C. Schatz, D. E. Brown, and C. W. Kimball, *Appl. Phys. Lett.* **85**, 467 (2004).
5. Coherent control of nanoscale localization of ultrafast optical excitation in nanosystems, M. I. Stockman, D. J. Bergman, and T. Kobayashi, *Phys. Rev. B* **69**, 054202 (2004).
6. Self-similar chain of metal nanospheres as efficient nanolens, K. Li, M. I. Stockman, and D. J. Bergman, *Phys. Rev. Lett.* **91**, 227402 (2003).
7. Plasmon hybridization in nanoparticle dimers, P. Nordlander, C. Oubre, E. Prodan, K. Li, and M. I. Stockman, *Nano Letters* **4**, 899 (2004).
8. Nanofocusing of optical energy in tapered plasmonic waveguides, M. I. Stockman, *Phys. Rev. Lett. 93*, 137404 (2004).

9. Hollow cages versus space-filling structures for medium-Sized gold clusters: The spherical aromaticity of the Au_{50} cage, J. Wang, J. Jellinek, J. Zhao, Z. Chen, R. B. King and P. v. R. Schleyer, *J. Phys. Chem. A*, **109**, XXX (2005).
10. Stuffed fullerene structures for medium-sized silicon clusters, J. Zhao, J. Wang, J. Jellinek, S. Yoo, and X. C. Zeng, *Eur. Phys. J. D* **34**, 35 (2005).
11. First-principles investigations of the polarizability of small and intermediate-sized Cu clusters, M. Yang and K. Jackson, *J. Chem. Phys.* **122**, 184317 (2005).
12. Statistical evaluation of the big bang search algorithm, K.A. Jackson, M. Horoi, I. Chaudhuri, Th. Frauenheim, and A. A. Shvartsburg, *Comp. Mater. Sci., in press* (2005).
13. Shape, polarizability and metallicity in Si clusters, K. A. Jackson, I. Chaudhuri, M. Yang, and Th. Frauenheim, *Phys. Rev. A* **71**, 033205 (2005).
14. Size dependence of static polarizabilities and optical absorption spectra of Ag_n (n = 2 – 8) clusters from first principles, J. C. Idrobo, S. Ogut, and J. Jellinek, *Phys. Rev. B* **72**, 085445 (2005).
15. Observation of the quadrupole plasmon mode for a colloidal solution of gold nanoprisms, J. E. Millstone, S. Park, K. L. Shuford, L. Qin, G. C. Schatz and C. A. Mirkin, *J. Am. Chem. Soc.* **127**, 5312 (2005).
16. Multipolar excitation in triangular nanoprisms, Kevin L. Shuford, Mark. A. Ratner and G. C. Schatz, *J. Chem. Phys., in press* (2005).
17. Controlled spatiotemporal excitation of metal nanoparticles with chirped optical pulses, T.-W. Lee and S. K. Gray, *Phys. Rev. B*, **71**, 035423 (2005).
18. Near-field photochemical imaging of noble metal nanostructures, C. Hubert, A. Rumyantsev, G. Lerondel, J. Grand, S. Kostcheev, L. Billot, A. Vial, R. Bachelot, P. Royer, S.-H. Chang, S. K. Gray, G. P. Wiederrecht, and G. C. Schatz, *Nano Letters* **5**, 615 (2005).
19. Surface plasmon generation and light transmission by isolated nanoholes and arrays of nanoholes in thin metal films, S.-H. Chang, S. K. Gray and G. C. Schatz, *Optics Express* **13**, 3151 (2005).
20. Surface plasmon waves in large-area subwavelength hole arrays, E.-S. Kwak, J. Henzie, S.-H. Chang, S. K. Gray, G. C. Schatz, and T. W. Odom, *Nano Letters, in press* (2005).
21. Regenerated surface plasmon polaritons, T.-W. Lee and S. K. Gray, *Appl. Phys. Lett.* **86**, 141105 (2005).
22. Electrodynamics simulations of surface plasmon behavior in metallic nanostructures, S. K. Gray. T.–W. Lee, S.–H. Chang and G. C. Schatz, *Proc. SPIE Int. Soc. Opt. Eng.* **5927**, 96 (2005).
23. Fourier spectral simulations and Gegenbauer reconstructions for electromagnetic waves in the presence of a metal nanoparticle, M. S. Min, T.-W. Lee, P. F. Fischer, and S. K. Gray, *J. Comp. Phys., in press* (2005).
24. Hole-assisted energy deposition in dielectrics and clusters in the multiphoton regime, L. N. Gaier, M. Lein, M. I. Stockman, G. L. Yudin, P. B. Corkum, M. Y. Ivanov, and P. L. Knight, *J. Mod. Optics* **52**, 1019 (2005).
25. Surface plasmon amplification by stimulated emission in nanolenses, K. Li, Xiangting Li, M. I. Stockman, and D. J. Bergman, *Phys. Rev. B* **71**, 115409 (2005).
26. Imperfect perfect lens, I. A. Larkin and M. I. Stockman, *Nano Letters* **5**(2), 339 (2005).
27. Giant fluctuations of second harmonic generation on nanostructured surfaces, M. I. Stockman, *Chem. Phys*. (invited paper), *in press* (2005).

Acknowledgment: Work at Argonne National Laboratory was supported by the U.S. Department of Energy, Office of Basic Energy Sciences, Division of Chemical Sciences, Geosciences, and Biosciences under DOE Contract No. W-31-109-ENG.

Dynamics of Electrons at Interfaces on Ultrafast Timescales

Charles B. Harris, P.I.
Chemical Sciences Division,
Lawrence Berkeley National Lab
1 Cyclotron Road, Mail Stop Latimer,
Berkeley, CA 94720
CBHarris@lbl.gov

Program scope

This is a comprehensive program to study the properties of electrons at molecule/metal interfaces on the femtosecond timescale and the nanometer lengthscale. We examine a broad variety of systems (examples include atomic adsorbates, polymer oligomers, and model solvents) and phenomena (electron solvation and localization, the band structure of interfaces, and the electronic coupling of adsorbates to a metal substrate) with both experiment and theory.

Our primary experimental technique is angle-resolved two-photon photoemission (2PPE). Briefly, a femtosecond laser pulse excites electrons from the valence band of a Ag(111) substrate to the interface with an adsorbed molecular film (typically 1–3 monolayers thick). Some delay time later, Δt, a second laser pulse photoemits the electron, sending it to a time-of-flight detector. From the kinetic energy of the electron and the photon energy of the probe pulse, we can deduce the binding energy of the electronic state. The wavelength dependence of the photoemission spectrum tells whether the state is initially occupied, unoccupied, or a final state resonance.

This technique also gives us access to a wealth of information about the electron's dynamics. The kinetics of population decay and dynamical energy shifts (two-dimensional electron solvation) are determined with < 35 meV energy resolution and ~ 100 fs time resolution. An additional experimental degree of freedom is the angle between the surface normal and the detector. Only electrons with a specific amount of momentum parallel to the surface will reach the detector. The energy versus parallel momentum (the dispersion) gives the effective mass of the electron, m^*. For localized electrons ($m^* \gg 1$) the amplitude of the signal versus parallel momentum can give an estimate of the spatial extent of localization in two dimensions.

Two-photon photoemission accesses both electronic states of the molecular film, such as the highest occupied molecular orbital (HOMO) and the lowest unoccupied molecular orbital (LUMO), as well as states intrinsic to the surface. Image-potential states (IPS) are an important example of the latter. The IPS electrons are bound a few angstroms from the metal surface, making them sensitive probes of the electronic structure and dynamics of monolayer adsorbate films. In the direction parallel to the surface, however, the IPS electrons are free-electron-like, in most cases. Interactions with any disorder of the surface or with the dynamic motions of adsorbates can localize the electron in the plane of the surface.

Recent progress

Electron solvation and localization at interfaces : Time- and angle-resolved two-photon photoemission has been used to probe the dynamics of an electron excited into an image-potential state at an interface between a metal and a polar, aprotic organic film. Interactions between the electron and one or more layers of linear nitrile molecules result in a dynamic binding energy (electron solvation) on the femtosecond timescale. The overall solvation dynamics for multilayer systems are multiphasic, with the majority of the energy relaxation occurring during the first 500 fs. Essentially, this is a two-dimensional analogue of electron solvation in

liquids, in which the system response is typically separated into a Gaussian, representing a rapid inertial response and one or more exponentials representing diffusion on multiple time scales. In our systems, the longer-lived components are relatively weak, which is consistent with studies in liquid acetonitrile, but may also reflect the fact that physisorbed molecules at cryogenic temperatures have greatly reduced translational degrees of freedom.

Rapid localization of the electron in these films is also observed, with the rate depending critically on the energetic disorder of the film, ranging from small polaron-like localization in the most ordered films to Anderson-like in the least ordered films. The spatial extent of the localized electrons parallel to the interface is estimated through their angle-dependent photoemission intensities. Unlike the solvation dynamics, however, the spatial extent shows no clear dependence on the alkyl chain length, indicating that the electrons are perhaps localized to sites primarily in the vicinity of the functional group of the molecule.

Intraband relaxation : Intraband relaxation of delocalized IPS electrons is omnipresent in 2PPE. The kinetics of population decay as a function of parallel momentum show that electrons quickly relax to the bottom of the IPS band in many different adsorbate systems. Nevertheless, the process is not well understood. The simplest organizing principle to understand these many observations is friction, and this concept explains complications that arose in previous analyses as direct consequences of the fluctuation-dissipation theorem. We have developed a theory based on Smoluchowski's equation for overdamped harmonic motion to describe the motion of electrons down an IPS band. This theory has a coefficient of friction as its only free parameter, and we find that the friction extracted from the model is equivalent to the friction one would expect for that due to electron-electron scattering between the IPS electron and the electrons in the substrate. Further work is underway to examine the friction as a function of thin film material in an effort to see if it may be tuned by, for example, attempting to decouple the IPS electron from the substrate. Finally, these methods will be extended to further elucidate the mechanism of electron localization, which may be concomittant with intraband relaxation or even provide a channel for it.

C_{60}/Ag(111) : In addition to probing image potential states, 2PPE can be used to study electronic states of molecular films. Because this technique is a two-photon process, we can examine both initially occupied (HOMO) and initially unoccupied (LUMO) states. Furthermore, through the use of angle-resolved spectra, we can directly measure the effective masses of these states when they are incorporated into electronic bands in a thin film. These band masses are important quantities in modelling electronic transport, and techniques that can extract them for both occupied and unoccupied states are few and far between. In the case of C_{60}/Ag(111), we have experimentally determined the effective masses of the HOMO, LUMO, LUMO+1, and LUMO+2-derived bands. These results were then examined from a theoretical standpoint through the use of both quantum chemical calculations and group theory (Figure 1). Further work will focus on exploring the differences between excitonic and anionic transport in this and related systems.

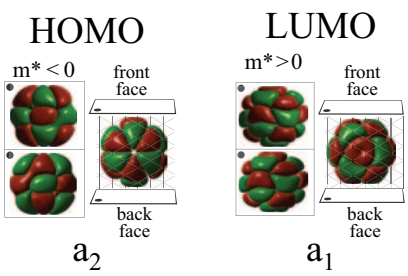

Figure 1: The C_{60} orbitals may be studied both through direct calculation of their wavefunctions or by the use of group theory. Shown are one of the five degenerate orbitals of the HOMO and one of the three degenerate orbitals of the LUMO. The HOMO state has a_2 symmetry on the surface and a negative effective mass, whereas the LUMO state has a_1 symmetry on the surface and a positive effective mass.

Continuing and Future work

Molecular electronics — PTCDA and fluorene oligomers : PTCDA is a model system for the burgeoning field of molecular electronics. It has a truly epitaxial growth on Ag(111), and the occupied electronic structure is fairly well understood. The unoccupied electronic structure and, especially, the dynamics, on the other hand, have not been explored. 2PPE may shed light on the the mechanism(s) of optical excitation (intramolecular or metal-to-molecule) and the nature of the molecular excited states of these films as a function of the layer thickness.

Polyfluorenes are blue-emitting polymers for organic light emitting diodes (OLEDs), but the nature of charge injection from the cathode into these systems is somewhat mysterious. 2PPE of films of fluorene oligomers as a function of oligomer chain length and the side-group functionalization may give details of optical charge injection in this promising technological system.

DMSO/Ag(111) : Our solvation results for nitriles can be extended by comparing them with DMSO. Acetonitrile and DMSO have very similar dipole moments and dielectric constants, yet they behave very differently as electrochemical solvents. Preliminary 2PPE results of one monolayer of DMSO/Ag(111) show that the DMSO monolayer does not solvate the IPS electrons, but the multilayer solvates a great deal and dynamically localizes the electrons. This is an important contrast to nitriles, which solvate and localize IPS electrons at all coverages. This is a direct, molecular scale probe of the contrasting differential capacitance of these two molecules as measured in electrochemistry.

Biphasic Thin Films : One area in which we plan to extend our investigations is to develop further comparisons between the systems we currently study and systems of more relevance to electrochemistry. Many electrochemical processes, however, take place in mixed environments, and so we are beginning to explore the behavior of electrons in multi-component thin films. The electron dynamics in these films are not necessarily related to any one of the components. For example, thin films containing a 1:1 mixture of meta- and para-xylene display electron localization dynamics different from those of either of the pure molecules on their own, and it is not yet entirely clear why this is the case. We have also recently started studying mixed systems of water and small organic molecules. Small amounts of water impurities have been seen to affect electron localization, and in some instances we have observed features with dramatically increased lifetimes at these interfaces. A full exploration of these systems should greatly aid in making further connections between the properties of individual electrons at interfaces and the behavior of large numbers of electrons in electrochemical cells or devices.

Articles supported by DOE funding 2002–2005

[1] S. Garrett-Roe, S. T. Shipman, P. Szymanski, M. L. Strader, A. Yang, and C. B. Harris. "Ultrafast electron dynamics at metal interfaces: Intraband relaxation of image state electrons as friction." *J. Phys. Chem. B*, **accepted** (2005).

[2] P. Szymanski, S. Garrett-Roe, and C. B. Harris. "Time- and angle-resolved two-photon photoemission studies of electron localization and solvation at interfaces." *Prog. Surf. Sci.*, **78**, 1 (2005).

[3] I. Bezel, K. J. Gaffney, S. Garrett-Roe, S. H. Liu, A. D. Miller, P. Szymanski, and C. B. Harris. "Measurement and dynamics of the spatial distribution of an electron localized at a metal–dielectric interface." *J. Chem. Phys.*, **120**, 845 (2004).

[4] C. B. Harris, P. Szymanski, S. Garrett-Roe, A. D. Miller, K. J. Gaffney, S. H. Liu, and I. Bezel. “Electron solvation and localization at interfaces.” In “Proc. SPIE,” volume 5223, pages 159–168 (2003).

[5] P. T. Snee, S. Garrett-Roe, and C. B. Harris. “Dynamics of an excess electron at metal/polar interfaces.” *J. Phys. Chem. B*, **107**, 13608 (2003).

[6] I. Bezel, K. J. Gaffney, S. Garrett-Roe, S. Liu, A. D. Miller, P. Szymanski, and C. B. Harris. “The size of a localized electron at a metal/adsorbate interface.” In “Thirteenth International Conference on Ultrafast Phenomena,” volume 72, pages 430–431. Opt. Soc. America (2002).

[7] S. H. Liu, A. D. Miller, K. J. Gaffney, P. Szymanski, S. Garrett-Roe, I. Bezel, and C. B. Harris. “Direct observation of two-dimensional electron solvation at alcohol/Ag(111) interfaces.” *J. Phys. Chem. B*, **106**, 12908 (2002).

[8] A. D. Miller, I. Bezel, K. J. Gaffney, S. Garrett-Roe, S. H. Liu, P. Szymanski, and C. B. Harris. “Electron solvation in two dimensions.” *Science*, **297**, 1163 (2002).

[9] A. D. Miller, K. J. Gaffney, S. H. Liu, P. Szymanski, S. Garrett-Roe, C. M. Wong, and C. B. Harris. “Evolution of a two-dimensional band structure at a self-assembling interface.” *J. Phys. Chem. A*, **106**, 7636 (2002).

ELECTRONIC STRUCTURE AND OPTICAL RESPONSE OF NANOSTRUCTURES

Martin Head-Gordon (m_headgordon@berkeley.edu) [1],
Steven G. Louie (sglouie@berkeley.edu) [2],
Lin-Wang Wang (lwwang@lbl.gov) [3],
Emily A. Carter (eac@princeton.edu) [4],
James R. Chelikowsky (jrc@ices.utexas.edu) [5],

[1]Department of Chemistry, University of California, and Chemical Sciences Division, Lawrence Berkeley National Laboratory, Berkeley, CA 94720; [2] Department of Physics, University of California, and Materials Sciences Division, Lawrence Berkeley National Laboratory, Berkeley, CA 94720; [3] Computational Research Division, Lawrence Berkeley National Laboratory, Berkeley, CA 94720; [4] Department of Mechanical & Aerospace Engineering, Princeton University, Princeton, NJ 08544; [5] Departments of Physics and Chemical Engineering, Institute for Computational Engineering and Sciences, University of Texas, Austin, TX 78712

1. Scope of Project.

There has been much progress in the synthesis, characterization and theoretical studies of various nanostructures such as nanotubes, nanocrystals, atomic wires, organic and biological nanostructures, and molecular junctions. However, there remain immense challenges to obtain a basic understanding of the properties of these structures and their interactions with external probes to realize their potential for applications. Some exciting frontiers in nanoscience include molecular electronics, nanoscale opto-electronic devices, nanomechanics (nanomotors), light harvesting and emitting nanostructures. The ground and electronic excited properties of the nanostructures and how they are coupled to the external stimulations/probes are crucial issues.

Since nanostructures are neither at the molecular nor the bulk limits, the calculations of their electronic and optical properties are subject to severe computational bottlenecks. The present program therefore focuses on the electronic structure theory and modeling of nanostructures, including their electronic excited-state and optical properties, with applications to topics of current interest. We are attacking the rate-determining steps in these approaches in collaboration with computational scientists and applied mathematicians, by seeking novel reformulations of the underlying physical theories.

2. Summary of Recent Progress.

As this is a multi-investigator program, space precludes us summarizing all projects that are underway. Below, we highlight a selection of recent accomplishments in slightly more detail.

Many-body methods for large systems. We are examining ways to make the proven electron correlation methods of molecular quantum chemistry applicable to systems on the nanoscale. Significant progress has been made with the development of a modification [4,8] of second order many-body perturbation theory that is both computationally less expensive, and more accurate than the standard approach. Already this approach can be applied to systems in the regime of 100 atoms, and work is underway to develop low-scaling implementations [6] that will be applicable to significantly larger systems by exploiting spatial locality. With the aid of new

developments in the theory of localized orbitals [2], early progress is also being made on formulations of coupled cluster theory [9] that have the potential for application to nanoscale systems.

Optical Response and Temperature and Pressure Effects on the Properties of Carbon Nanotubes. We carried out *ab initio* calculations (based on the GW-BSE approach) to investigate the optical response and the temperature and pressure effects on the electronic properties of carbon nanotubes. We showed that, because of the reduced dimensionality of the nanotubes, many-electron effects are very important, and they change qualitatively the optical spectrum of both metallic and semiconductor tubes. This has led us to several new discoveries -- giant exciton binding energy in semiconducting nanotubes, the existence of bound excitons in metal tubes, and net repulsive electron-hole interaction in some metallic tubes, etc. [10,11] We also computed the temperature and pressure dependences of the band gap (E_g) of the carbon nanotubes. [1,12,13] These are two of the most fundamental properties of any semiconductor. Understanding of these shifts provides important information about the nature of the band-edge electronic states and their coupling with static and dynamic lattice distortions. The family behavior in both phenomena is elucidated in terms of the structural dependent orientation of the bonding and antibonding characters of the band edge states of the nanotubes. Many of the above theoretical predictions have been verified by recent experiments.

A new method for calculating quantum transport. Current methods for calculating quantum transport properties tend to be computationally more expensive than highly optimized methods for the computation of molecular and bulk ground states. Furthermore, no simple and efficient method exists which can use the plane-wave non-local pseudopotential Hamiltonian that is so successful for ground state calculations. To address these issues, an efficient new method [14] has been developed to calculate the elastic (coherent) quantum transports using auxiliary periodic boundary conditions. This method allows the use of conventional ground state *ab initio* programs (e.g., planewave pseudopotential programs) with some relatively small changes. The scattering states of the transport problem are solved exactly in a fast and numerically stable procedure. The total computational time of this method is similar to a conventional ground state calculation, which makes it possible to calculate elastic quantum transport for large systems.

Developments in screened exchange density functional theory. One potentially efficient way of improving upon the standard density functional theory (DFT) description of properties such as semiconductor gaps is screened exchange DFT. With a new implementation of the sX model, we have begun investigating a number of interesting issues. One question is, in semiconductor systems, whether the screening should be short range (e.g., Thomas-Fermi-like) or long range (e.g. like the semiconductor dielectric function). To investigate this, we have compared the self-energy term in the sX-LDA formalism with the self-energy term in the GW approximation and the exchange-correlation hole of variational quantum Monte Carlo simulations. Calculations using sX-DFT has also been performed for the calcium hexaboride crystal structure and electron band structure. The band structure of this system is very sensitive to its crystal structure. We have also performed sX calculations on $Al_xGa_{(1-x)}N$ semiconductor alloys, that give a very different bowing parameter (E_g(x)) than LDA results.

Spintronic Materials: Bulk and Nanoscale Properties Dilute magnetic semiconductors (DMS) are semiconductors into which a magnetic impurity has been intentionally introduced, and exhibit unique magnetic, magneto-optical, and magneto-electrical effects. They hold the promise of using electron spin, in addition to charge, for creating a new class of "spintronic" semiconductor devices with unprecedented functionality. We expect that nano-crystalline DMS should exhibit intriguing magnetic properties, which are different from those of the bulk, because quantum confinement is known to enhance spin-spin interactions.

We performed calculations for the electronic structure and magnetic properties of Mn-containing Ge, GaAs, and ZnSe nanoparticles [2,15,16]. We determined the electronic structure of these systems from pseudopotentials constructed from density functional theory. Our analysis for these nanocrystals indicates that the qualitative level splitting and magnetic moment picture is similar to that of the bulk. This is due to the short-range interaction of Mn with its neighbors. However, there are also significant differences between the electronic structure of the bulk and the nanocrystals. So, while the ferromagnetism and half-metallicity trends found in the bulk are preserved in the nanocrystals, the localized Mn states are less affected by quantum confinement than are the delocalized host states. As a consequence, in nanocrystals the Mn-related impurity states become much deeper in the gap with decreasing size. The ferromagnetic stabilization in the nanocrystals is dominated by double exchange via localized holes, rather than by free holes (as in bulk GaAs:Mn) or by a Rudderman-Kittel-Kasuya-Yosida (RKKY) mechanism (an alternative to the free-hole mechanism for bulk Ge:Mn). This is a novel quantum size effect.

Development of a linear scaling orbital-free density functional theory. Development of a linear scaling density functional theory (DFT) for metallic systems will allow the study of metallic nanostructures of realistic width and length, containing thousands of atoms. We are in the final stages of implementing linear scaling orbital-free DFT (OF-DFT) [17] with arbitrary boundary conditions in real space using the Multigrid method, which employs grids on several different length scales to accelerate convergence. We first implemented periodic Multigrid OF-DFT, so as to compare with FFT-based OFDFT. We reformulated the ion-electron, Hartree repulsion, exchange-correlation, and several kinetic energy density functional (KEDF) terms via finite discretization in real space up to sixth order, and wrote and validated all required periodic Multigrid machinery against FFT-based codes. We then implemented real-space boundary conditions by changing the finite discretization algorithm, how the ion-electron potential was calculated and how the new boundary conditions are handled within Multigrid.

The Kondo effect for Co on Cu(111) We are studying the Kondo effect seen by STM for Co/Cu(111), using our first-principles embedded configuration interaction (ECI) theory. Here bulk Cu conduction electrons align their spins to screen out the Co magnetic moment, reducing low T Cu conductivity. ECI theory begins with periodic KS-DFT on the total system. Then a sub-region is treated with *ab initio* CASSCF or CI in the presence of an embedding potential based on the total DFT density. Along with implementing ECI in MOLCAS, two technical advances are: (i) use of ultrasoft pseudopotentials [18] in a consistent manner across all levels (periodic DFT, CASSCF, and CI) and (ii) elimination of approximate KEDFs in the embedding operator, instead using orbital-based KED potentials. Periodic DFT for Co/Cu(111) unphysically predict a net non-zero magnetic moment localized on the Co adatom. By contrast, ECI theory yields a singlet ground state, in agreement with experiment. Low-lying spin excitations are also outcomes of the theory, including a triplet 0.34 eV above the ground state.

3. Summary of Research Plans.

- Development of low-scaling coupled cluster theory for nanoscale systems
- Study carbon nanotubes of different diameters and chiralities, and wide bandgap BN nanotubes for which we expect even more dominant excitonic effects.
- Joint development of new eigensolvers for electronic structure calculations
- Complete orbital-free DFT implementation, modifying our Poisson solver to use boundary conditions at infinity to obtain correct Hartree potentials throughout.

4. Publications from DOE Sponsored Work, 2003-present.

[1] R.B. Capaz, C.D. Spataru, P. Tangney, M.L. Cohen, and S.G. Louie, "Hydrostatic Pressure Effects on the Structural and Electronic Properties of Carbon Nanotubes," Phys. Status Solidi (b) **241**, 3352 (2004).

[2] J.E. Subotnik, Y. Shao, W. Liang and M. Head-Gordon, "An efficient method for calculating maxima of homogeneous functions of orthogonal matrices: Applications to localized occupied orbitals", J. Chem. Phys. 121, 9220-9229 (2004).

[3] L. Kronik, M. Jain, and J.R. Chelikowsky: "Electronic structure and spin-polarization of MnGaP," Applied Phys. Lett. **85**, 2014 (2004).

[4] Y. Jung, R. Lochan, A.D. Dutoi, and M. Head-Gordon, "Scaled opposite spin second order correlation energy: An economical electronic structure method", J. Chem. Phys. 121, 9793-9802 (2004).

[5] "A localized basis that allows fast and accurate second order Moller-Plesset calculations", J.E. Subotnik and M. Head-Gordon, J. Chem. Phys. 122, 034109 (2005) (9 pages).

[6] Y. Jung, A. Sodt, P.M.W. Gill and M. Head-Gordon, "Auxiliary basis expansions for large-scale electronic structure calculations", Proc. Nat. Acad. USA 102, 6692-6697 (2005).

[7] P.M.W. Gill, A.T.B. Gilbert, S.W. Taylor, G. Friesecke, and M. Head-Gordon, "Decay behavior of least-squares expansion coefficients", J. Chem. Phys. 123, 061101 (2005)

[8] R.C. Lochan, Y. Jung, and M. Head-Gordon, "Scaled opposite spin second order Moller-Plesset theory with improved physical description of long-range dispersion interactions", J. Phys. Chem. A 109, 7598-7605 (2005).

[9] J.E. Subotnik and M. Head-Gordon, "A local correlation model that yields intrinsically smooth potential energy surfaces", J. Chem. Phys. 123, 064108 (2005).

[10] C.D. Spataru, S. Ismail-Beigi, L.X. Benedict, and S.G. Louie, "Excitonic Effects and Optical Spectra of Single-Walled Carbon Nanotubes," 27th Conference on the Physics of Semiconductors, *AIP Conference Proceedings* **772,** 1061 (2005).

[11] J. B. Neaton, K. H. Khoo, C. D. Spataru, and S. G. Louie, "Electron Transport and Optical Properties of Carbon Nanostructures from First Principles," Computer Phys. Comm. **169**, 1 (2005).

[12] R.B. Capaz, C.D. Spataru, P. Tangney, M.L. Cohen, and S.G. Louie, "Temperature Dependence of the Band Gap of Semiconducting Carbon Nanotubes," Phys. Rev. Lett. **94**, 036801 (2005).

[13] R.B. Capaz, C.D. Spataru, P. Tangney, M.L. Cohen, and S.G. Louie, "Temperature and hydrostatic pressure effects on the band gap of semiconducting carbon nanotubes," 27th Conference on the Physics of Semiconductors, *AIP Conference Proceedings* **772,** 1047 (2005).

[14] L.W. Wang, "Elastic quantum transport calculations using auxiliary periodic boundary conditions", Phys. Rev. B 72, 45417(2005).

[15] X. Huang, A. Makmal, J. R. Chelikowsky, and L. Kronik: "Size dependent spintronic properties of dilute magnetic semiconductor nanocrystals," Phys. Rev. Lett. **94**, 236801 (2005).

[16] X. Huang, Eric Lindgren and J.R. Chelikowsky: ``Surface passivation method for semiconductor nanostructures," Phys. Rev. B **71**, 165328 (2005).

[17] V. Lignères and E. A. Carter, "Introduction to Orbital-Free Density Theory," in Handbook of Materials Modeling, S.Yip (Ed.), (2005).

[18] V. Cocula, C. J. Pickard, and E. A. Carter, "Ultrasoft Spin-Dependent Pseudopotentials," J. Chem. Phys., in press (2005).

Influence of Co-Solvents and Temperature on Nanoscale Self-Assembly of Biomaterials

Teresa Head-Gordon
Department of Bioengineering, UC Berkeley
Physical Biosciences Division, Lawrence Berkeley National Laboratory
TLHead-Gordon@lbl.gov

Program Scope

Synthesis of tailor-made biomaterials requires a detailed understanding of the effect of solvent on structure, stability, and dynamics. How these physical quantities develop during self-assembly will be affected by the nature of the solvent, as evidenced by the fact that biopolymers such as proteins can be denatured or stabilized by various additives. Anfinsen's experiments on ribonuclease-A [1] showed that most proteins self-assemble in vitro without aid of other proteins or the need for specific cellular conditions to fold. In vitro protein folding is a vibrant field both experimentally and theoretically, and both seek to define how amino acid sequence translates into orchestrated fundamental forces that guide protein self-assembly. This view of protein folding as a physical process (as opposed to a biological process that seeks to determine protein function through protein structure) equates with our considering proteins as biomaterials whose properties we would like to control and design [2].

Proteins are designed to fold in nature in aqueous environments and the relative contributions of hydrophobic and hydrophilic interactions are essential to this process. Changing conditions through temperature, pressure, or solvent composition can alter the folding kinetics or relative free energies of folded and unfolded states. Non-aqueous solvents such as guanadinium hydrochloride and urea are used to denature proteins.[3,4] Additions of trifluoro-ethanol or methanol can lead to specific stabilization of certain structural motifs, [5] whereas other organic solvents such as acetone, formamide, and DMSO are known to destabilize protein native states. The formulation of effective co-solvents is important in biopharmaceutical production of peptide and proteins to improve their long-term storage and delivery.[6] In principle, molecular switches can be created by control over protein function and reactivity through their solvent environment; such a possibility was recently demonstrated by embedding hemoglobin in a glassy solid of low water content trehalose solutions to reduce the protein conformational transitions and thereby turn off function [7]. Clearly, solvent interactions mediate the thermodynamics and kinetics of protein conformations that in turn influence their self-assembly and co-assembly properties. Understanding solvent environmental influences may lead to the ability to exploit not only differences in monomer composition but solvent composition, to create polymers, both biological and non-biological, with desired properties.

Timasheff and co-workers [8] have reported that the addition of osmolytes results in preferentially hydrated protein molecules that they attribute to changes in surface tension around the protein, thereby stabilizing the protein structure in solution. However it is also observed that while osmolytes such as sugars may function as cryoprotectants, they can also exhibit a more complicated role as a destabilizing agent under conditions that may depend on the protein, on the water content, on temperature, or some combination of all variables. A definitive explanation for these competing roles that co-solvents can play as stabilizers and destabilizers, and complications due to conditions such as water content or temperature is not available. We note that the dynamics of these solutions, and relative timescales of motion of the constituents of solution are much more poorly characterized and understood than structure.

Recent Progress

The complexity of protein systems has led to consideration of simplified representations that might serve as reduced models of the protein folding process. My group has focused on understanding hydration environment through the study of individual blocked amino acids as a function of their concentration in water.[9-10] The role of hydration in the earlier steps of folding are mimicked when the local concentration of amino acids is relatively dilute, while more concentrated solutions describe the consequences of hydration in later folding stages when the local concentration of amino acids is high and driving toward the formation of a collapsed state or hydrophobic core. This can be viewed as a model systems approach for the characterization of *hydration or environmental* influence on protein self-assembly or co-assembly. It invokes the zeroth-order concept that polymers can be modeled by increasing the effective local concentration of monomers, giving rise to a situation resembling a much denser liquid of monomers in the local vicinity of the chain. We will perform liquid diffraction, quasi-elastic scattering, and molecular dynamics simulations on our model biopolymer system, N-acetyl-amino-acid-methylamide in solution with a variety of co-solvents. These combined approaches will determine how changing solvent environment that arise from perturbations in temperature, salts, osmolytes, and denaturants influences biomolecular self-assembly or co-assembly.

Future Plans

Structure of Aqueous Monomer Solutions with Chaotropes and Kosmotropes. Overall the structural view of chaotrope and kosmotrope buffers in aqueous solution of amino acids, and a breakdown of these thermodynamic stabilizing or destabilizing forces into the specifics of monomer-solvent systems, is not known or not well understood. We hope to provide a more comprehensive picture of molecular liquid structure using x-ray scattering (wide and small angle) of aqueous solutions of N-acetyl-amino acid-methylamides over a solute concentration range of 0.1-2.0M for five different amino acid types (glycine, glutamine, leucine, phenylalanine, and arginine), and with various co-solvent kosmotropic and chaotropic types. We will also investigate these solutions as a function of temperature (over the biologically relevant temperature range from 2-77C) for

which we can enhance or mitigate the net surface tension of water. We chose glycine as a model of the polypeptide backbone, glutamine and leucine as the prototypical hydrophilic and hydrophobic amino acids, respectively, and phenyalanine as the representative aromatic side chain. Arginine's guanidinium moiety allows us to characterize the chaotropic character of the sidechain itself, or paired with a kosmotropic co-solvent. X-ray scattering intensities for pure water and aqueous solutions will be measured at the Advanced Light Source (ALS) at UC Berkeley on BL 8.2.1 and 8.2.2; these beamlines are routinely used for protein crystallographic experiments, but we have adapted to them for our solution diffraction studies.

Dynamics of Aqueous Monomer Solutions with Chaotropes and Kosmotropes. Disordered materials such as the solutions we propose to investigate here offer a rich venue for materials characterization, not only through liquid state crystallography, but through timescales of motion of these weakly interacting species susceptible to thermal perturbation. There is little information available on the dynamics of the basic protypical protein-solvent interaction except for our recent published work, and virtually no information on dynamics of these systems and their solvent additives, and how dynamics might effect solution assembly or association. One hypothesis we will explore is that recognition and association of the constituents requires "timescale matching", i.e. that the behavior of kosmotropes and chaotropes on proteins not only has a thermodynamic origin, but perhaps a kinetic origin as well. We will perform quasi-elastic incoherent neutron scattering by protons at both high- and low-resolution for H_2O concentrated solutions (0.5M–2.0M) of completely deuterated single amino acids, and D_2O solutions with hydrogenated samples over the same concentration range, as a function of different co-solvent additives. Our first tests will be with urea, guanidinium hydrochloride, and glucose, since the deuterated forms of these co-solvents are relatively inexpensive. The quasi-elastic neutron scattering (QENS) experiment will likely be performed at NIST Center for Neutron Research, using the disk chopper time of flight spectrometer (DCS) where we have completed past work. All experimental analysis procedures will be carried out as done in [9].

Theoretical analysis and MD simulations of neutron and x-ray solution scattering data. It is conventional in the analysis of diffraction from molecular liquids to separate the intensity into contributions from individual molecules (self-scattering), and that arising from intermolecular correlations defined by the structure factor, *H(Q).*

$$I(Q) = \sum_{ij} x_i x_j f_i(Q) f_j(Q) \frac{\sin Qr_{ij}}{Qr_{ij}} + \sum_{i \le j} x_i x_j f_i(Q) f_j(Q) H_{ij}(Q) \qquad (1)$$

where the sums are over the atom types present in the sample, x_i is the atomic fraction and $f_i(Q)$ the Q-dependent atomic scattering factor, for atom type i. In the case of x-rays the assumption is commonly made that the scattering can be represented as arising from independent neutral atoms, each with a spherical electron density distribution. We have recently introduced a modification of the atomic scattering factors for liquid water which rescales them properly at low Q where chemical bonding effects are known to be significant, while retaining their values at large Q where chemical bonding effects on the core electron distribution should be negligible[10]. Similar types of modified atomic

scattering factors for solutes and co-solvents will be derived from high-level quantum mechanical calculations.

For the analysis of the dynamics in these aqueous solutions, we will perform simulations of solute configurations consistent with our structural experiment. Basic dynamic analysis of the data will use the Einstein relation to derive the translational self-diffusion coefficients from the mean square displacement of center of mass positions, the rotational dynamics of water using the orientational autocorrelation function, and the intermediate scattering function in order to reproduce the neutron experimental observable directly, after which we can analyze the dynamics with greater confidence.

With the advent of completely *ab initio* simulations of liquid water[11-13], it is now possible to predict the x-ray scattering from the distribution of electron density, $\rho(\mathbf{r})$, generated from the condensed phase simulation trajectory [14] using Eq. (1)

$$I(Q) = \left\langle \left| F(\mathbf{q}) \right|^2 \right\rangle \qquad \text{with } F(\mathbf{q}) = \int_0^\infty \rho(\mathbf{r}) \exp(i\mathbf{q}\mathbf{r}) d\mathbf{r} \tag{2}$$

This allows for the straight simulation of the true experimental observable, the intensity, without requiring the process of extracting radial distribution functions from intensity data over a finite Q-range. If the simulated intensity curve using Eq. (2) agrees well with experiment (with only moderately large Q-ranges), then we can analyze the corresponding real-space trajectory to ascertain the pair distribution function(s). Due to the current expense of simulating the full *ab initio* trajectory, the effective integration step in Eq. (2) will be the generation of snapshots along the classical trajectory [15].

1. C. B. Anfinsen, E. Haber, and F.H. White (1961). *Proc. Natl. Acad. Sci*., 47, 1309.
2. J. G. Tirrell & D.A. Tirrell (1996). *Curr.Opin. Solid State & Mats. Sci.* 1, 407.
3. C. N. Pace (1986). *Methods in Enzymology* 131, 266.
4. G. I. Makhatadze (1999). *J. Phys. Chem. B,* 103, 4781.
5. M. Buck (1998). *Quarterly Reviews of Biophysics* 31, 297.
6. L. N. Bell (1997). *Biotechnology Progress* 13, 342.
7. D. S. Gottfried (1996). *J. Phys. Chem.* 100, 12034.
8. S. N. Timasheff (1993). *Ann. Rev.of Biophys. & Biomol. Struct.* 22, 67.
9. D. Russo, R. K. Murakra, J. R.D. Copley, T. Head-Gordon (2005). *J.Phys.Chem.B* 109; 12966; D. Russo, R. K. Murarka, et al (2004). *J.Phys.Chem.B* 108, 19885*;* D. Russo, G. Hura, & T. Head-Gordon (2004) *Biophys. J.* 86, 1852.
10. T. Head-Gordon & G. Hura (2002). *Chemical Reviews* 102, 2651; G. Hura, J. Sorenson, R.M. Glaeser & T. Head-Gordon (2000). *J. Chem. Phys*. 113, 9140; J. Sorenson, G. Hura, R.M. Glaeser & T. Head-Gordon (2000). *J. Chem. Phys* 113, 9149; A. Pertsemlidis, A. K. Soper, J. M. Sorenson & T. Head-Gordon (1999). *Proc. Natl. Acad. Sci.* 96, 481; J. M. Sorenson, G. Hura, et al (1999). *J. Phys. Chem. B,* 103 5413; T. Head-Gordon, et al (1997). *Biophys. J.* 73, 2106-2115; A. Pertsemlidis et al (1996). *Proc. Natl. Acad. Sci.* 93, 10769.
11. E. Schwegler, G. Galli, and F. Gygi (2000) *Phys. Rev. Lett.* 84, 2429.
12. R. Car and M. Parrinello (1985). *Phys. Rev. Lett.* 55, 2471
13. M. Sprik, J. Hutter, and M. Parrinello (1996). *J. Chem. Phys.* 105, 1142.
14. M. Krack, A. Gambirasio, and M. Parrinello (2002). *J. Chem. Phys*. 117, 9409.
15. G. Hura, D. Russo, et al (2003). *Phys. Chem. Chem. Phys.* 5, 1981.

Optical Spectroscopy at the Spatial Limit

Wilson Ho

Department of Physics & Astronomy and Department of Chemistry
University of California, Irvine
Irvine, CA 92697-4575 USA

wilsonho@uci.edu

Program Scope:

This project is concerned with the experimental challenge of reaching single molecule sensitivity with sub-molecular spatial resolution in optical spectroscopy and photochemistry. These experiments would lead to an understanding of the inner machinery of single molecules that are not possible with other approaches. Results from these studies will provide the scientific basis for understanding the unusual properties, processes, and phenomena in chemical and physical systems at the nanoscale. The experiments rely on the combination of the unique properties of lasers and scanning tunneling microscopes (STM).

Recent Progress:

The phenomenon reported in a number of the papers published in the past year is concerned with a newly discovered mechanism of conductance through a single molecule – that we named "bipolar conduction" [Publications 7, 8, 10, 12, 13]. This conduction mechanism is observed only if the molecule is sandwiched between two tunnel barriers, and in our case between the vacuum barrier (tip-molecule tunnel junction) and an ultrathin oxide (molecule-substrate tunnel junction). Bipolar conduction refers to the electron flow through a molecule that involves the same electronic state at both positive and negative bias voltages. This is unusual since conventionally the highest occupied molecular orbital (HOMO) is involved in the conduction at negative bias, while the lowest unoccupied molecular orbital (LUMO) is involved in the conduction at positive bias.

Vibronic states of single molecules were observed for the first time by the STM. A necessary condition for the observation is the reduced coupling of the molecule to its environment, achieved in our experiments by adsorbing the molecule on an ultrathin (5 Å) Al_2O_3 film grown on a NiAl(110) metallic substrate [Publications 7, 8, 10, 11, 12]. The adsorption of C_{60} on such an isolating substrate led to the formation of a two-dimensional organic crystal, and the vibrational states associated with single impurities in this crystal were measured by the STM [Publications 6, 12]. There are two other publications during the past year that are concerned with the conformational changes in single molecules induced by tunneling electrons [Publication 9], and the dissociation pathways of a single molecule controlled by injecting or removing electrons from the molecule [Publication 14]. The vibronic states and conformational changes are involved in light emission from single molecules induced by tunneling electrons and are also expected to be important in other optical phenomena that are currently under investigation.

Future Plans:

The focus of the research will be on the coupling of lasers to the STM and to the determination of the conditions for achieving optical effects with sub-molecular resolution. How can sub-molecular processes be induced by photons with near-IR, visible, and near-UV wavelengths? Recently, we have succeeded in observing photon induced electron transfer to and from a single molecule with sub-molecular resolution. This observation depends on several factors: 1. stable STM, 2. stable laser power, 3. appropriately chosen system for first demonstration. These initial results open up new opportunities that we will explore in the coming year.

References to Publications of DOE Sponsored Research (2003-present):

[1] X.H. Qiu, G.V. Nazin, and W. Ho, "*Vibrationally Resolved Fluorescence Excited with Submolecular Precision*", Science **299**, 542-546 (2003).

*** "*Lighting Up Single Molecules*", Physics World **16**, 3 (2003).

*** "*Imaging Fluorescence with Submolecular Precision*", Micro/Nano **8**, 6 (2003).

*** News Item, "*Tunneling Electrons Stimulate Individual Molecules*", D.S. Burgess, Photonics Spectra, March 2003, p. 34.

[2] N. Nilius, T.M. Wallis, and W. Ho, "*Influence of a Heterogeneous Al_2O_3 Surface on the Electronic Properties of Single Pd Atoms*", Phys. Rev. Lett. **90**, 046808 (2003).

*** Figure from paper appeared on cover of this issue of Phys. Rev. Lett.

[3] G.V. Nazin, X.H. Qiu, and W. Ho, "*Atomic Engineering of Photon Emission with a Scanning Tunneling Microscope*", Phys. Rev. Lett. **90**, 216110 (2003).

[4] G.V. Nazin, X.H. Qiu, and W. Ho, "*Visualization and Spectroscopy of a Metal-Molecule-Metal Bridge*", Science **302**, 77-81 (2003). Published online 4 September 2003; 10.1126/science.1088971.

*** Perspectives, "*How to Assemble a Molecular Junction*", A.C. Kummel, Science **302**, 69 (2003).

*** La Chronologie 2003 de La Recherche, "*Pont Moléculaire*", La Recherche, Janvier 2004, p. 40.

*** Nanoelectronics, "*Irvine Team Images Single-Molecule Junction*", R. Alexander, Business Communications Company Electronic Materials Update, October 2003.

*** News of the Week, "*Molecular Electronics, Seeing is Believing, STM technique lets single-molecule junction be prepared and imaged*", Mitch Jacoby, Chemical & Engineering News, September 8, 2003, p. 16.

[5] S. Gao, J.R. Hahn, and W. Ho, "*Adsorption Induced Hydrogen Bonding by CH Group*", J. Chem. Phys. **119**, 6232-6236 (2003).

[6] C. Silien, N.A. Pradhan, W. Ho, and P.A. Thiry, "*Influence of Adsorbate-Substrate Interaction on the Local Electronic Structure of C_{60} Studied by Low-Temperature STM*", Phys. Rev. B **69**, 115434-1-5 (2004).

[7] X.H. Qiu, G.V. Nazin, and W. Ho, "*Vibronic States in Single Molecule Electron Transport*", Phys. Rev. Lett. **92**, 206102-1-4 (2004).

[8] N. Liu, N.A. Pradhan, and W. Ho, "*Vibronic States in Single Molecules: C_{60} and C_{70} on Ultrathin Al_2O_3 Films*", J. Chem. Phys. **120**, 11371-11375 (2004).

[9] X.H. Qiu, G.V. Nazin, and W. Ho, "*Mechanisms of Reversible Conformational Transitions in a Single Molecule*", Phys. Rev. Lett. 93, 196806-1-4 (2004).

[10] S.W. Wu, G.V. Nazin, X. Chen, X.H. Qiu, and W. Ho, *"Control of Ralative Tunneling Rates in Single Molecule Bipolar Electron Transport"*, Phys. Rev. Lett. **93**, 236802-1-4 (2004).

[11] H..J. Lee, J.H. Lee, and W. Ho, *"Vibronic Transitions in Single Metalloporphyrins"*, ChemPhysChem **6**, 971-975 (2005).

[12] G.V. Nazin, X.H. Qiu, and W. Ho, *"Vibrational Spectroscopy of Individual Doping Centers in a Monolayer Organic Crystal"*, J. Chem. Phys. **122**, 181105-1-4 (2005).

[13] G.V. Naxin, S.W. Wu, and W. Ho, *"Tunneling Rates in Electron Transport Through Double-Barrier Molecular Junctions in a Scanning Tunneling Microscope"*, Proc. Nat. Acad. Sci. **102**, 8832-8837 (2005).

[14] J.R. Hahn and W. Ho, *"Orbital Specific Chemistry: Controlling the Pathway in Single-Molecular Dissociation"*, J. Chem. Phys. **122**, 244704-1-3 (2005).

THEORY OF THE REACTION DYNAMICS OF SMALL MOLECULES ON METAL SURFACES

Bret E. Jackson

Department of Chemistry
701 LGRT
University of Massachusetts
Amherst, MA 01003
jackson@chem.umass.edu

Program Scope

Our objective is to develop realistic theoretical models for molecule-metal interactions important in catalysis and other surface processes. The dissociative adsorption of diatomics on metals, Eley-Rideal and Langmuir-Hinshelwood reactions, recombinative desorption and sticking on surfaces are all of interest. To help elucidate the UHV-molecular beam experiments that study these processes, we examine how they depend upon the nature of the molecule-metal interaction, and experimental variables such as substrate temperature, beam energy, angle of impact, and the internal states of the molecules. Electronic structure methods based on Density Functional Theory are used to compute the molecule-metal interaction potentials. Both time-dependent quantum scattering techniques and quasi-classical methods are used to examine the reaction dynamics. Some effort is directed towards developing improved quantum scattering methods that can adequately describe reactions on surfaces, as well as include the effects of temperature (lattice vibration) in quantum dynamical studies.

Recent Progress

We have continued our studies of Eley-Rideal (ER) and hot atom reactions. In an ER reaction, a gas-phase particle combines directly with another particle adsorbed onto a substrate. These reactions are often very exothermic. Extensive studies of the reactions of H atom beams with H-covered metal surfaces demonstrated that the cross sections for his ER reaction are small, on the order of 0.1 – 0.2 $Å^2$, even though this is a strongly exothermic and barrier-less reaction. Studies of the reaction dynamics showed why the cross section is small, and showed that the incident H atoms prefer to trap onto the surface without reacting, even at relatively high H atom coverages. These trapped "hot" atoms initially have 2 or more eV of excess energy, and are highly mobile on the surface for several 100's of fs. If they react with an adsorbate before dissipating this excess energy into the substrate, the molecular hydrogen formed can be highly excited, as in a more direct ER process. Our dynamical and kinetic models for ER and HA reactions are in excellent agreement with experiment, and demonstrate that these hot atom (HA) reactions dominate molecular hydrogen formation on metal surfaces. A textbook chapter summarizing these DOE-funded ER and HA studies has appeared in "The Chemical Physics of Solid Surfaces" [2].

We have concluded our studies of the H(g) + Cl/Au(111) reaction, which have been motivated primarily by two detailed experimental studies of this system. These experiments observe strong H atom trapping and a thermal Langmuir-Hinshelwood channel for HCl formation, as well as ER and HA channels. One of our findings is that the ER reaction cross section is much larger than for H(g) + H/metal reactions, roughly 1 –2 $Å^2$. This is due to a steering mechanism [1], and arises from the relatively large distance of the adsorbed Cl above the metal. The incoming H atom is strongly attracted to both the Cl and

the metal, but it encounters the layer of adsorbed Cl atoms first, and steers towards them. Thus there is no competition between ER reaction and trapping of the H atom onto the surface. There are also some interesting variations of ER reactivity with the Cl vibrational state, and an exchange pathway is observed (for the first time), in which the H remains bound while the Cl desorbs. More than two years have been spent using quasi-classical trajectories to study this reaction for the case of large Cl coverages, and with dissipation of the trapped hot atoms' energy into the lattice [6]. The ER and HA reaction pathways for HCl formation are a bit more complicated than for molecular Hydrogen formation. We find that HA reactions dominate the formation of HCl. We also find that there must be significant energy loss into the substrate excitations, from either the trapped hot H atoms, or the excited product HCl, in order to agree with experiment.

In an earlier study of H atom recombination on Ni(100), we allowed the lattice atoms to move, which required that we construct a potential energy surface based upon the instantaneous positions of the lattice atoms and the adsorbates. We avoided the usual problems associated with pairwise potentials by using a potential based upon ideas from embedded atom and effective medium theory, but instead of using the isolated atom electron densities, we fit the one and two-body terms to reproduce the results of our high-level electronic structure calculations. More recently we have used the part of this potential describing the Ni-Ni interactions to study the sputtering of Ni surfaces by Ar beams, in order to further test the utility of these potentials [4]. We find that this form for the potential very accurately describes the energy required to severely distort the lattice or to remove one or more Ni atoms form the lattice. Agreement of sputtering yields and threshold energies with experiments is greatly improved over earlier models.

We continued our studies of H-graphite interactions. These reactions are believed to play an important role in the formation of molecular Hydrogen on graphitic dust grains in interstellar space, as well as in the etching of the graphite walls of fusion reactors. Using electronic structure methods, we demonstrated that an H atom could chemisorb onto a graphite terrace carbon, with the bonding C atom puckering out of the surface plane by several tenths of an Å. We computed the potential energy surface for the ER reaction of an incident H atom with this chemisorbed H atom, and suggested that the reaction cross sections should be very large – on the order of 10 $Å^2$. Motivated by our studies, the group of Küppers (Bayreuth) demonstrated experimentally that H could indeed chemisorb, and that the lattice did pucker. Our computed adsorbate vibrational frequencies and (recombinative) thermal desorption temperatures were found to be in excellent agreement with experiment. Küppers and co-workers then measured the cross sections for the H(g) + D/graphite ER reaction to form HD(g), and again, theory and experiment were in excellent agreement. We demonstrated that the H_2 formed in these ER reactions should be very highly excited, vibrationally. It has been suggested that vibrationally excited H_2 might be responsible for some of the unique chemistry that occurs in interstellar clouds.

More recently, both our efforts and the efforts of the experimental groups have been focused on graphite edges. Real graphite surfaces are rough in the sense that a sizable fraction of the exposed carbon atoms can be on the edges of graphite planes, as opposed to the terraces. We have performed total energy electronic structure calculations to examine how H atoms react with edge vs terrace carbons. We found that the hydrogenation of an edge carbon proceeded with no barrier, and that the barrier for addition of a second hydrogen to the edge carbons was small [3]. These studies of graphite are also relevant to a sizable body of work examining molecular hydrogen adsorption in and on nano-crystalline graphite. We have examined how molecular hydrogen can chemisorb onto such structures, and have found two low energy pathways where H_2 dissociatively adsorbs over one or two edge carbons, resulting in a doubly-hydrogenated edge carbon, or two neighboring singly-

hydrogenated edge carbons, respectively [3]. The doubly-hydrogenated structure gives rise to a peak that has been observed (but not explained) in the radial distribution functions extracted from neutron scattering studies of graphitic nano-structures exposed to H_2. We have demonstrated that the vapor pressure of H_2 in equilibrium with these hydrogenated structures is too small to be useful for hydrogen storage, due to the strength of the bonds.

The experiments of the Küppers group have shown that the sticking probabilities of H on the graphite terrace are large. Given the significant lattice distortion required for chemisorption, this is surprising. We have used electronic structure methods to map out the H-graphite interaction as a function of the position of the bonding carbon. We find a barrier to chemisorption of about 0.2 eV, in excellent agreement with recent experiments. We have used these studies to construct a potential energy surface for trapping and sticking, and have implemented a low-dimensional collinear study of the trapping process [5]. We find that the bonding carbon can reconstruct in 50 fs, and that trapping probabilities can be 5-20%. Our results suggest that sticking proceeds via a trapping resonance, which relaxes by dissipating energy into the substrate over a ps or so. More recently we have computed the full three-dimensional potential, and have used classical mechanics to compute the sticking cross sections, which are on the order of 0.1 $Å^2$, giving sticking probabilities consistent with experiment.

We have long been interested in the dissociative adsorption of methane on metals, and have begun to compute barriers to methane dissociation on a Ni surfaces. A problem that is not well understood is how and why methane reactivity varies with the temperature of the metal. To explore this we have started to examine how these barriers change due to lattice distortion. We have recently seen that when a Ni atom puckers out of the plane of the surface, the barrier to dissociation over this Ni atom decreases. This should lead to interesting thermal effects.

Future Plans

We are finishing our fully 3D studies of H atom trapping and sticking on graphite. As in our collinear study, some additional lattice degrees of freedom are necessary to help carry energy away from the newly formed bond, and how these are included can affect the sticking probability. We have adopted an accurate potential energy surface describing the motion of the atoms in a graphite lattice, and are using this in our studies to examine the dissipation of energy into the lattice. We expect to finish this project this fall.

We are continuing our studies of H atom reactions at graphite edge sites, since much of the current experimental work is focusing on these sites. It is possible that the formation of molecular hydrogen on interstellar dust grains occurs at these edge sites, since the barrier to H adsorption on the terrace carbons is relatively large. We are examining the pathways and computing the barriers for H(g) reacting with H atoms adsorbed on the edges. We see that while singly-hydrogentaed edge carbons are relatively unreactive with respect to ER abstraction, doubly-hydrogenated structures are more reactive. We are also examining barriers to and the dynamics of H atom diffusion and recombinative desorption on the terrace, near the edge, and at the edge.

We expect to make much progress this year on the problem of methane dissociation on metals. We have demonstrated that lattice motion can significantly modify the barriers to methane dissociation. Our work also clearly shows that the standard model for including lattice motion in these problems, in which the barrier simply moves back and forth with the vibrating metal atom, are incorrect. Our calculations are being used to construct a potential energy surface for methane dissociation that explicitly includes the position of the Ni atom.

The dissociation probability as a function of incident energy, surface temperature, and molecular vibrational state will be computed using a 5 degree-of-freedom quantum model. We hope to compare the thermal effects of the terrace sites on Ni and Pt, as well as the defect sites on these metals.

References

[1]. J. Quattrucci, B. Jackson, and D. Lemoine "Eley-Rideal reactions of H atoms with Cl adsorbed on Au(111): Quantum and quasiclassical studies, J. Chem. Phys. 118, 2357-2366 (2003).

[2]. B. Jackson, "Eley-Rideal and hot atom reactions between H atoms on metal and graphite surfaces," in "The Chemical Physics of Solid Surfaces," vol. 11, D. P. Woodruff, ed., pp 51-77, Elsevier Science B. V. (2003).

[3]. X. Sha and B. Jackson,"The Location of Adsorbed Hydrogen in Graphite Nanostructures," J. Am. Chem. Soc. 126, 13095-13099 (2004).

[4]. Z. B. Guvenc, R. Hippler and B. Jackson, “Bombardment of Ni(100) surface with low-energy argons: molecular dynamics simulations, Thin Solid Films 474, 346-357 (2005).

[5]. X. Sha, B. Jackson, D. Lemoine and B. Lepetit,"Quantum studies of H Atom Trapping on a graphite surface," J. Chem. Phys. 122, 014709, 1-8 (2005).

[6]. J. Quattrucci and B. Jackson, "Quasi-classical study of Eley-Rideal and Hot Atom reactions of H atoms with Cl adsorbed on a Au(111) surface, J. Chem. Phys. 122, 074705, 1-13 (2005).

Structure and dynamics of chemical processes in water clusters: DE-FG02-00ER15066

K. D. Jordan (jordan@pitt.edu), Dept. of Chemistry, University of Pittsburgh, Pittsburgh, PA 15260
And M. A. Johnson (mark.johnson@yale.edu), Dept. of Chemistry, Yale University, New Haven, CT 06520

Our project integrates theory and experiment to reveal molecular aspects of aqueous chemistry using size-selected clusters as model systems. Because of the ubiquitous role played by the hydrated electron, e_{aq}^- ,(*1*) as a primary intermediate in biological radiation damage,(*2*) we have concentrated much of our effort on the structure and dynamics of the $(H_2O)_n^-$ clusters as microscopic analogues of e_{aq}^- .(*3-14*) In fact, there has been a resurgence of interest in these species,(*15-19*) in large part because of the difficulty in achieving a consensus description of the bulk properties of e_{aq}^- . The impact of our activity in this endeavor is evidenced by the fact that we contributed three(*13, 15, 20*) of the 14 papers cited by the Editors of Science Magazine that were collectively acknowledged as the #8 "breakthrough of the year" for 2004. Papers already published(*12-14, 20-29*) or submitted (*30, 31*)under our present DOE grant, which ends in July, 2006, are indicated by * in the reference list attached.

We have focused on unraveling the mechanism of electron attachment to well-defined water networks by analyzing a series of measurements obtained from specifically designed experiments.(*13, 29, 31*) Recent results include the determination of the local H-bonding motifs that accommodate an excess electron as well as the mode-specific rates for energy exchange between vibrations of the supporting water network and the excess electron. Our experimental approach involves coordinating anion photoelectron spectroscopy with size-selected vibrational predissociation spectra using double focusing, tandem time-of-flight methods developed at Yale.(*32*) Of particular importance to our experimental progress has been the introduction of argon-mediated cluster synthesis methodology:(*33*)

$$A + (H_2O)_n^- \cdot Ar_m \rightarrow A \cdot (H_2O)_n^- \cdot Ar_p + (m\text{-}p)\ Ar$$

which enables rational preparation of key water cluster anions (e.g., $((H_2O)_4^-)$ in abundance. Because this synthetic method naturally incorporates argon atoms into the product ions, it is ideally suited for the application of "messenger" predissociation spectroscopy:(*34*)

$$(H_2O)_n^- \cdot Ar_p + h\nu \rightarrow (H_2O)_n^- \cdot Ar_q + (p\text{-}q)\ Ar$$

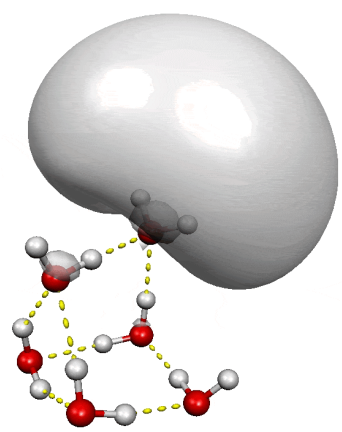

Fig. 1. Structure of the water hexamer anion illustrating the special role of the double H-bond acceptor (AA) water molecule. Note that both AA hydrogen atoms point directly into the electron cloud.

This technique has the dual advantages of cooling the complexes into their minimum energy structures and enabling one-photon (i.e., linear) action spectra that are readily compared with theory. We now have essentially complete spectral coverage from 600 cm^{-1} in the infrared to 250 nm in UV. This capability has proven remarkably powerful in that it provides both electronic and vibrational spectroscopic characterization of a wide range of solute species with a precisely controlled number of attached solvent molecules.

A. Discovery of the local electron binding site in the anionic water clusters: Spectroscopic characterization of the "AA" motif.

One of the major breakthroughs resulting from this program has been the elucidation of the structures of the small $(H_2O)_{3\text{-}6}^-$ clusters, which reveal the molecular character of the electron binding site.(*13, 14, 30*) Fig. 1 presents the structure of the hexamer anion, for example, where one molecule dominates the interaction with the excess electron cloud. This water molecule is attached to the network by accepting two H-bonds, an arrangement that enables it to orient both of its hydrogen atoms directly into the excess electron wavefunction. Note that this configuration also provides a "doorway" for the excess electron to partially penetrate into the valence orbital network.

An important consequence of the AA arrangement is that the symmetric ($?_s$) and asymmetric ($?_a$) OH stretching vibrations of this unique water molecule dominate the vibrational spectrum of the clusters in the mid infrared. This enhancement occurs because displacement of the nuclei along the $?_a$ and $?_s$ normal coordinates result in strong modulation of the excess electron wavefunction.(*7*) We have also characterized the vibrational-mode dependence of the coupling to the electron cloud by analysis of the "Fano" type lineshapes that occur when the upper levels of the vibrational transitions occur above the cluster vertical detachment energies (VDE).(*13, 35*) The resulting autodetachment rates, extracted from this treatment, reveal that the coupling strengths differ by at least an order of magnitude according to the nature of the vibrations.

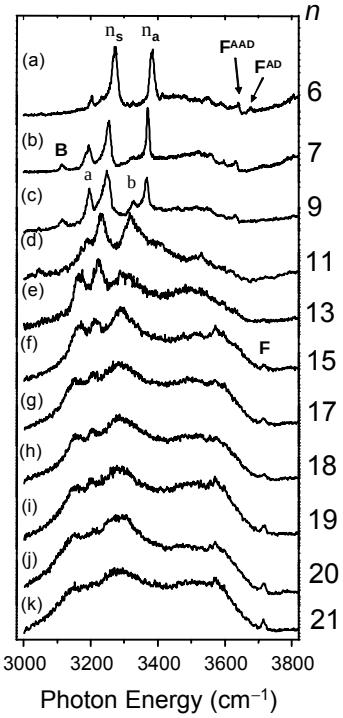

Fig. 2. Vibrational spectra of the $(H_2O)_{6\text{-}21}^-$ clusters illustrating the evolution strong doublet ($?_a$ and $?_s$) assigned to the AA water molecule. F^{AAD} and F^{AD} denote the free OH stretch vibrations associated with AAD and AD water molecules, respectively, in the hexamer anion structure (Fig. 1).

This vibronic enhancement of the transitions associated with the AA molecule leads to a favorable situation where the presence of the AA motif in the binding site is readily apparent in the more complicated spectra of the larger clusters.(*31*) Fig. 2 presents a survey of the OH stretching spectra for the $(H_2O)_n^-$ clusters over the range n = 6-21, where it is evident that the AA binding site is retained intact up to n = 9 before a modified motif emerges above n = 13. Defining the nature of the new form is now a major thrust of our work, requiring the calculation of vibrational spectra for rather large systems. We have anticipated this situation, and have already developed a computational method that can treat the subtleties of the diffuse, excess electron cloud in the context of a one-electron model.(*36*) This method involves the introduction of fictitious "Drude" oscillators on the water molecules that are optimized to recover the high order effects (dispersion, correlation) that are found to be important in ab initio treatments of small water clusters. In the past year, we have tested the level of theory required to address the binding of an excess electron through an extensive study of the trimer anion, $(H_2O)_3^-$.(*30*) This is the smallest of the water clusters that yield sharp vibrational bands, in this case the DOD bending vibrations, which lie just below the VDE (130 meV).(*9, 30*)

B. Local binding motifs and the nature of the isomers

Very recent work from the Neumark group(*17*) has identified the extension of a weak binding isomer class to much larger clusters (n = 20 - 200) than originally reported by Bowen and

co-workers.(*37*) When combined with all earlier measurements,(*9*) we now have three distinguishable isomers that evolve with cluster size as indicated in Fig. 3. One possibility advanced by Neumark is that the isomers differ primarily according to whether the excess electron resides on the surface or in the interior of the clusters. Our earlier vibrational spectroscopic studies (Fig. 2) were carried out on the high binding, class I isomers that featured the AA binding motif, and it was therefore of interest to obtain the infrared spectra of the class II

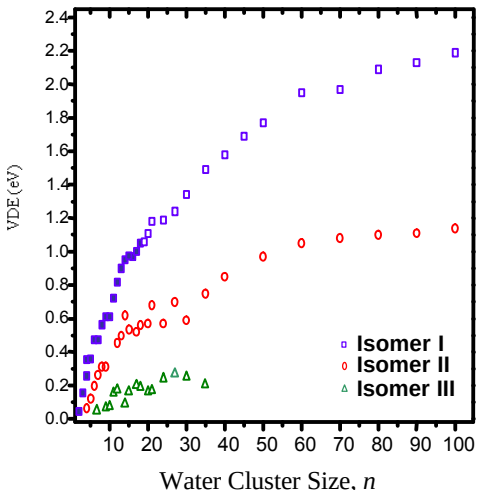

Fig. 3. Evolution of the vertical electron binding energies for the three $(H_2O)_n^-$ isomer classes. The data represent a composite of the Bowen,(*37*) Neumark,(*17*) and Johnson data.(*9*)

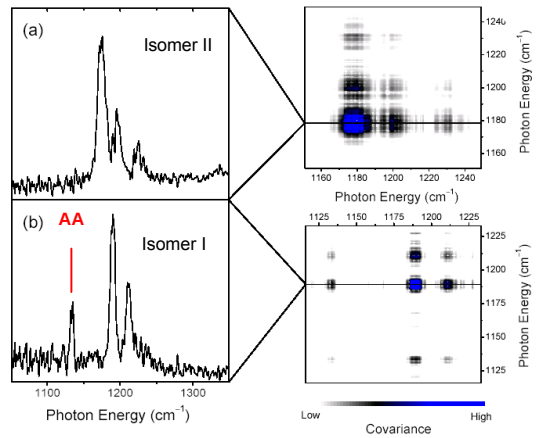

Fig. 4. Independent vibrational spectra in the bending region of the two $(D_2O)_6^-$ isomers, deconvoluted using covariance maps shown on right. The absence of the characteristic band from the AA water molecule in the weak binding isomer (II) reveals that it adopts a different local binding motif.

isomers to identify whether the more weakly bound isomer has a different local electron binding motif. We were able to isolate the spectrum of the class II form of the hexamer anion using the strong dependence of the isomer distribution on the number of attached argon atoms in the $(D_2O)_6^- \cdot Ar_m$ clusters.(*29*) This yielded spectra with systematically varying contributions of overlapping patterns from two isomers, that we were able to disentangle with a covariance mapping technique.(*38*) The two independent spectra are displayed in Fig. 4. Most importantly, the spectrum of the more weakly binding isomer does *not* display the telltale red-shifted bending vibration of the AA water molecule,(*13*) thus establishing that it indeed has a different local binding motif. Note that the two isomers of the hexamer anion both accommodate the excess electron on the surface of the cluster, but differ according to the local, molecular level binding motif. This observation raises the question of whether the binding energy differences associated with the two isomers at larger clusters, previously thought to be due to surface vs. internal electron solvation, are instead both surface states with the different local binding motif identified at $n = 6$. Spectra of the $n = 6$ - 24 clusters in both the stretch and bend region have already been obtained and indicate that the AA motif is indeed present over this entire size range. We are now engaging isomer-selective spectroscopic and associated theoretical studies of these larger clusters to determine if the spectral signature of the weak binding $n = 6$ isomer is preserved in the larger clusters as well.

References:

1. E. J. Hart, J. W. Boag, *J. Am. Chem. Soc.* **84**, 4090 (1962).

2. Farhataziz, M. A. J. Rodgers, Eds., *Radiation Chemistry* (VCH Publishers, Inc., New York, 1987).
3. L. A. Posey, M. A. Johnson, *J. Chem. Phys.* **89**, 4807 (1988).
4. P. J. Campagnola, D. M. Cyr, M. A. Johnson, *Chem. Phys. Lett.* **181**, 206 (1991).
5. P. J. Campagnola, D. J. Lavrich, M. J. DeLuca, M. A. Johnson, *J. Chem. Phys.* **94**, 5240 (1991).
6. P. J. Campagnola, D. J. Lavrich, M. A. Johnson, *J. Phys. IV* **1**, C5 (1991).
7. C. G. Bailey, J. Kim, M. A. Johnson, *J. Phys. Chem.* **100**, 16782 (1996).
8. P. Ayotte, C. G. Bailey, J. Kim, M. A. Johnson, *J. Chem. Phys.* **108**, 444 (1998).
9. J. Kim, I. Becker, O. Cheshnovsky, M. A. Johnson, *Chem. Phys. Lett.* **297**, 90 (1998).
10. J. M. Weber *et al.*, *Chem. Phys. Lett.* **339**, 337 (2001).
11. J. A. Kelley, G. H. Weddle, W. H. Robertson, M. A. Johnson, *J. Chem. Phys.* **116**, 1201 (2002).
*12. E. G. Diken, W. H. Robertson, M. A. Johnson, *J. Phys. Chem. A* **108**, 64 (2004).
*13. N. I. Hammer *et al.*, *Science* **306**, 675 (2004).
*14. J.-W. Shin, N. I. Hammer, J. M. Headrick, M. A. Johnson, *Chem. Phys. Lett.* **399**, 349 (2004).
15. K. D. Jordan, *Science* **306**, 618 (OCT 22, 2004).
16. A. E. Bragg, J. R. R. Verlet, A. Kammrath, O. Cheshnovsky, D. M. Neumark, *Science* **306**, 669 (2004).
17. J. R. R. Verlet, A. E. Bragg, A. Kammrath, O. Cheshnovsky, D. M. Neumark, *Science* **307**, 93 (2005).
18. D. H. Paik, I.-R. Lee, D.-S. Yang, J. S. Baskin, A. H. Zewail, *Science* **306**, 672 (2004).
19. L. Turi, W.-S. Sheu, P. J. Rossky, *Science* **309**, 914 (2005).
*20. J.-W. Shin *et al.*, *Science* **304**, 1137 (2004).
*21. W. H. Robertson, M. A. Johnson, E. M. Myshakin, K. D. Jordan, *Journal of Physical Chemistry A* **106**, 10010 (OCT 24, 2002).
*22. E. M. Myshakin, K. D. Jordan, W. H. Robertson, G. H. Weddle, M. A. Johnson, *J. Chem. Phys.* **118**, 4945 (2003).
*23. W. H. Robertson, M. A. Johnson, *Ann. Rev. Phys. Chem.* **54**, 173 (2003).
*24. W. H. Robertson, E. G. Diken, E. A. Price, J.-W. Shin, M. A. Johnson, *Science* **299**, 1367 (2003).
*25. E. M. Myshakin, E. L. Sibert. III, M. A. Johnson, K. D. Jordan, *J. Chem. Phys.* **119**, 10138 (2003).
*26. B. C. Garrett *et al.*, *Chem. Rev.* **105**, 355 (2005).
*27. E. M. Myshakin, K. Diri, K. D. Jordan, *J. Phys. Chem. A* **108**, 6758 (2004).
*28. J.-W. Shin *et al.*, *J. Phys. Chem. A* **109**, 3146 (2005).
*29. N. I. Hammer, J. R. Roscioli, M. A. Johnson, *J. Phys. Chem. A* **109**, 7896 (2005).
*30. J. R. Roscioli N. I. Hammer, M. A. Johnson, E. M. Myshakin, and K. D. Jordan, *J. Phys. Chem. A* **Accepted** (2005).
*31. N. I. Hammer, J. R. Roscioli, J. C. Bopp, J. M. Headrick, M. A. Johnson, *J. Chem. Phys.* **Submitted**.
32. M. A. Johnson, W. C. Lineberger, in *Techniques for the Study of Ion-Molecule Reactions* J. J. M. Farrar and W. H. Saunders, Ed. (Wiley, New York, 1988), vol. XX, pp. 591.
33. P. Ayotte, G. H. Weddle, J. Kim, M. A. Johnson, *J. Am. Chem. Soc.* **120**, 12361 (1998).
34. M. Okumura, L. I. Yeh, J. D. Myers, Y. T. Lee, *J. Chem. Phys.* **85**, 2328 (1986).
35. U. Fano, *Phys. Rev.* **124**, 1866 (1961).
36. F. Wang, K. D. Jordan, *J. Chem. Phys.* **116**, 6973 (2002).
37. J. V. Coe *et al.*, *J. Chem. Phys.* **92**, 3980 (1990).
38. L. J. Frasinski, K. Codling, P. A. Hatherly, *Science* **246**, 1029 (1989).

Molecular Theory & Modeling

Nucleation in Solution

Shawn M. Kathmann
Chemical Sciences Division
Pacific Northwest National Laboratory
902 Battelle Blvd.
Mail Stop K1-83
Richland, WA 99352
shawn.kathmann@pnl.gov

Program Scope

The focus of this project is to develop a fundamental understanding of the chemical physics governing nucleation of nano-sized salt crystals in solution. DOE has underscored the importance of nucleation by stating [http://www.sc.doe.gov/production/bes/nanoscale.html], "Since most phase transitions involving nanostructured materials occur under conditions far from equilibrium, *the kinetic pathways available to these systems are numerous and not well understood. ... It will be important for making progress in the areas of synthesis and processing, therefore, to develop our understanding of nanochemistry and the broader general issues of nucleation and growth.*" Nanostructured materials are currently of great technological interest because their properties depend strongly on size, shape, and composition that differ significantly from either bulk or isolated molecules. This complex dependence of properties is precisely the reason there is so much interest, demand, and potential for exploiting nano-sized systems. The physical, electronic, and optical properties, in principle, can be "tuned" to create new materials with desired characteristics. However, the desire of "materials by design" has been replaced by a "cook and look" approach simply because there are too many degrees of freedom in the relevant systems and appropriate molecular-level insight is needed to bridge the gap.

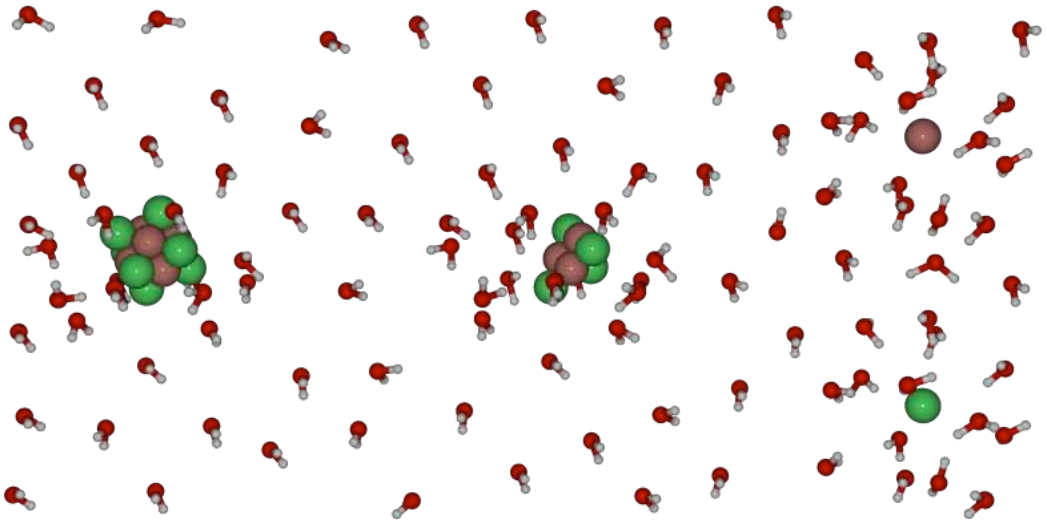

Figure 1. Illustration of salt crystallization and dissolution processes in aqueous NaCl.

The physical reason why nucleation is so sensitive can be understood intuitively. Since the nucleation process involves many mechanistic steps (typically 10's to 100's), small changes in each step can be amplified over the total number required to reach the critical cluster – defined as the cluster at the top of the nucleation barrier. The sensitivity of nucleation to subtle variations in the interaction potentials,

nuclear degrees of freedom, etc., motivates the search for relative effects on nucleation in solution with and without various seeds (ions, impurities, contaminants, etc.).

Recent Progress

Crystallization in solution is one of the most challenging problems in chemical physics. At a given temperature and pressure, solubility is defined as the concentration of a saturated salt solution in equilibrium with the salt precipitate – when this concentration is achieved the chemical potentials of the solute in solution and the pure salt crystallites are equivalent. The driving force for salt crystallization in solution occurs when the actual solute concentration exceeds the solution solubility (sometimes referred to as supersaturation). Salts having large solubilities require larger salt concentrations to crystallize than salts with lower solubilities. The relevant timescale for the nucleation event in solution is dictated by the potentials of mean force between the newly forming clusters and solvated ions. Nucleation is inherently a rare occurrence and trying to observe it directly via molecular simulation at realistic conditions is very computationally demanding – the majority of time is spent searching irrelevant regions of the solution configuration space.

Recently, we showed how various seed ions have a profound influence on the ion-induced nucleation of water from the vapor and how radically a molecular-level description departs from a continuum treatment. This work also addressed the century-old controversy concerning water's sign preference showing that the ion's chemical identity plays an essential role in addition to the sign in determining cluster thermodynamics.

Using the statistical mechanical framework of Dynamical Nucleation Theory (DNT), a molecular-level model of cluster formation is being developed for nucleation in solution. The extension of DNT to solution phase crystallization requires a cluster definition. This is equivalent to choosing a dividing surface separating reactants (clusters) from products (not clusters) in the solution configuration space (see Figure 1). A kinetic formalism can be constructed utilizing variational transition state theory (VTST) to relate the variation in the cluster Helmholtz free energy with respect to the relevant dividing surface for cluster dissolution. The cluster dissolution rate constants (α_i) and equilibrium constants K^{EQ} allow determination of association rate constants (β_{i-1}). Given these dynamical parameters the nucleation rates for crystallization can be calculated and compared with experiment for consistency/validation and/or refinement of the interaction potentials and/or formalism. We present here a simple connection between DNT and Chandler's transition state theory (TST) rate expression in solution to calculate salt dimer dissolution rate. We can define the configurational partition function of the NaCl dimer by

$$\exp[-A_{\text{Na-Cl}}(r_{\text{cut}},T)/k_{\text{B}}T] = Q(r_{\text{cut}},T) = \int_0^{r_{\text{cut}}} dr\, r^2 \exp[-W(r)/k_{\text{B}}T],$$

where $W(r)$ is the Na-Cl PMF in water, $r = R_{\text{Na-Cl}}$ is the distance between the two ions, and $A_{\text{Na-Cl}}(r_{\text{cut}},T)$ is the Helmholtz free energy of the aqueous NaCl dimer. In this expression r_{cut} is relevant coordinate used to describe the DNT dividing surface, defined as the radius of a spherical constraining volume whose center is coincident with the dimer center-of-mass. Using DNT, the NaCl dissolution rate can be expressed as

$$\alpha_{\text{Na-Cl}}(T) = -\frac{1}{\sqrt{2\pi\mu k_{\text{B}}T}} \left.\frac{dA_{\text{Na-Cl}}}{dr}\right|_{r_{\text{DNT}}} = \sqrt{\frac{k_{\text{B}}T}{2\pi\mu}} \frac{r_{\text{DNT}}^2 \exp[-W(r_{\text{DNT}})/k_{\text{B}}T]}{\int_0^{r_{\text{DNT}}} dr\, r^2 \exp[-W(r)/k_{\text{B}}T]},$$

where μ is the reduced mass of NaCl. This result shows the equivalence between DNT and Chandler's transition state theory rate expression for a reaction in solution for the special case of the NaCl dimer. The results of Smith and Dang [*JCP 100: 3757(1994)*] for the potential of mean force (PMF) between Na^+ and Cl^- atoms in SPC/E water at 300 K find that the first minimum at 2.9Å is the Contact-Ion Pair (CIP) and the second minimum at 4.9Å is the Solvent-Separated-Ion Pair (SSIP). The DNT dissolution rate for the CIP is $\alpha_{\text{CIP}} \approx 0.3$ ps^{-1} with a PMF barrier of 1.9 kcal/mol and $\alpha_{\text{SSIP}} \approx 1.7$ ps^{-1} with a PMF barrier of 0.6 kcal/mol. The result for the CIP dissolution rate agrees with the Smith and Dang result of 0.29 ps^{-1}, as it

should. It should be noted that Smith and Dang found that solvent induced re-crossing effects were important and reduced the dissolution rate for the CIP by a factor of six. We also anticipate re-crossing to be important explicit dynamical corrections will be needed to correct the DNT dissolution rate constants. This simple example demonstrates that DNT can be extended to salt crystallization in aqueous solution, however, more general dividing surfaces are required to capture the multi-component dissolution channels. For example, monomer loss channels from NaCl would require two dividing surfaces, one for each ion dissolving from the crystal cluster.

Future Plans

Nucleation of salt from concentrated solution presents several challenges not present in the dilute limit. A supersaturated solution generates clusters (or nuclei) of the new phase. These clusters can form homogeneously within the mother phase or heterogeneously on seeds, impurities, dust, or other irregularities that provide local regions of stability (e.g., defects, steps, edges, or other imperfections). The PMFs between ion pairs depends on the degree of saturation. In the subsaturated state, you have ionic hydration shells well separated from other ionic hydration shells another allowing ionic transport as evidenced by an increase in conductivity as the solution becomes more dilute. In the supersaturated solution, the PMFs favor compact salt structures and/or tightly packed ionic hydration shells that hinder transport – sometimes referred to as ion atmosphere friction. In an effort to understand these effects, we will calculate the relevant PMFs covering dilute to supersaturated concentrations of $CaCl_2$, NaCl, and AgCl. The choice of these salts is threefold: (1) atomistic simulations have been performed on several of these systems, and (2) they represent simple chemical salts of alkali halides and metal halides, and (3) display solubilities differing by many orders of magnitude.

To calculate the rates of salt cluster dissolution using DNT, simulations of the salt clusters must be performed. This will be done using interaction potentials benchmarked against accurate electronic structure calculations, Molecular Dynamics, and Monte Carlo simulations performed within our group. Monte Carlo simulations will be used to determine the Helmholtz free energies and dissolution rate constants. The interactions between the various species will incorporate polarization of both ions and water molecules using the Ewald summation technique with periodic boundary conditions for the solvent. The typical simulation cell will contain 1000 molecules to minimize correlation effects between periodic images. It must be noted that since nucleation requires describing interactions spanning from monomers to critical clusters in solution, the justification of those interactions must be verified. EXAFS experiments performed by researchers at PNNL will be utilized to validate the description of the interaction potentials since it yields concentration dependent information on the structural behavior of the ions and water molecules in solution. Radial distribution functions will be monitored for various solution concentrations to investigate the signatures leading to crystallization. The solvents for the alkali halide and metal halide salts will be chosen such that the solute concentrations to achieve crystallization are consistent with the DNT dividing surface defining the monomer reaction channels - solvents in which the salts have low solubilities meet this criteria. Additionally, various seeds will be placed within the clusters to assess their influence on cluster stability.

Simulations are also in progress to obtain concentration dependent PMFs for Ca-O, Ca-Ca, Ca-Cl, O-O, Cl-O, and Cl-Cl PMFs for aqueous $CaCl_2$ to compare with EXAFS experiments for validation of the potentials and statistical mechanical sampling. The relevant solution concentrations range from 1 to 9m $CaCl_2$. Our initial simulation results on 6m $CaCl_2$ suggest that the ions become trapped in long-lived glassy states, making it more difficult to converge the radial distribution functions. Figure 2 shows an equilibrium snapshot taken from a Monte Carlo simulation of bulk 6m $CaCl_2$ at 300K.

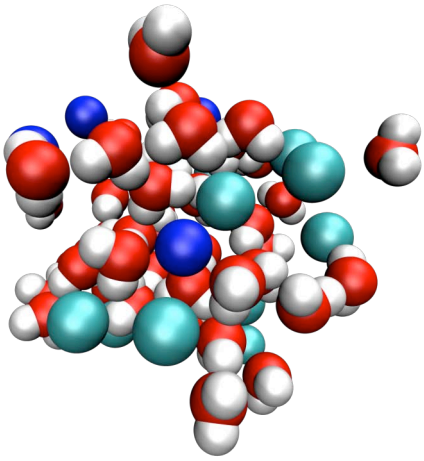

Figure 2. An equilibrium configuration from bulk 6m $CaCl_2$ at 300K showing the presence of contact as well as solvent separated ion pairs. Ca^{2+} is shown in dark blue and Cl^- in light blue.

Project Collaborators and Acknowledgements: G.K. Schenter, L.R. Corrales, L.X. Dang, B.C. Garrett, S.S. Xantheas, and John Fulton. Battelle operates Pacific Northwest National Laboratory for the U. S. Department of Energy. This research was performed in part using the Molecular Sciences Computing Facility in the William R. Wiley Environmental Molecular Sciences Laboratory.

Publications of DOE Sponsored Research (2003-present)

1. "Thermochemistry and Kinetics of Evaporation and Condensation for Small Water Clusters" B.C. Garrett, S.M. Kathmann, and G.K. Schenter in *Water in Confining Geometries*, Eds. V. Buch and J.P. Devlin (2003 Springer-Verlag Berlin Heidelberg NewYork).
2. Multi-Component Dynamical Nucleation Theory And Sensitivity Analysis, S.M. Kathmann, G.K. Schenter, and B.C. Garrett, *J. Chem. Phys.*, **120**, 9133 (2004).
3. Dynamical Nucleation Theory: Understanding the Role of Aqueous Contaminants, S.M. Kathmann, G.K. Schenter, and B.C. Garrett, Proceedings of the 16th International Conference on Nucleation and Atmospheric Aerosols, Eds. M. Kasahara and M. Kulmala, (2004 Kyoto University Press).
4. Ion-Induced Nucleation: The Importance of Chemistry, S.M. Kathmann, G.K. Schenter, and B.C. Garrett, *Physical Review Letters*, **94**, 116104 (2005).
5. **Invited Article:** Understanding the Chemical Physics of Nucleation, A Special Issue of: *Theoretical Chemistry Accounts*, S.M. Kathmann, **in press** (2005).

Chemical Kinetics and Dynamics at Interfaces

Structure and Reactivity of Ices, Oxides, and Amorphous Materials

Bruce D. Kay (PI), R. Scott Smith, Zdenek Dohnalek and John L. Daschbach

Chemical Sciences Division
Pacific Northwest National Laboratory
P.O. Box 999, Mail Stop K8-88
Richland, Washington 99352
bruce.kay@pnl.gov

Additional collaborators on these projects include G. K. Schenter, G. A. Kimmel, P. Ayotte, J. Kim, and T. Zubkov

Program Scope

The objective of this program is to examine physiochemical phenomena occurring at the surface and within the bulk of ices, oxides, and amorphous materials. The microscopic details of physisorption, chemisorption, and reactivity of these materials are important to unravel the kinetics and dynamic mechanisms involved in heterogeneous (i.e., gas/liquid) processes. This fundamental research is relevant to solvation and liquid solutions, glasses and deeply supercooled liquids, heterogeneous catalysis, environmental chemistry, and astrochemistry. Our research provides a quantitative understanding of elementary kinetic processes in these complex systems. For example, the reactivity and solvation of polar molecules on ice surfaces play an important role in complicated reaction processes that occur in the environment. These same molecular processes are germane to understanding dissolution, precipitation, and crystallization kinetics in multiphase, multicomponent, complex systems. Amorphous solid water (ASW) is of special importance for many reasons, including the open question over its applicability as a model for liquid water, and fundamental interest in the properties of glassy materials. In addition to the properties of ASW itself, understanding the intermolecular interactions between ASW and an adsorbate is important in such diverse areas as solvation in aqueous solutions, cryobiology, and desorption phenomena in cometary and interstellar ices. Metal oxides are often used as catalysts or as supports for catalysts, making the interaction of adsorbates with their surfaces of much interest. Additionally, oxide interfaces are important in the subsurface environment; specifically, molecular-level interactions at mineral surfaces are responsible for the transport and reactivity of subsurface contaminants. Thus, detailed molecular-level studies are germane to DOE programs in environmental restoration, waste processing, and contaminant fate and transport.

Our approach is to use molecular beams to synthesize “chemically tailored” nanoscale films as model systems to study ices, amorphous materials, supercooled liquids, and metal oxides. In addition to their utility as a synthetic tool, molecular beams are ideally suited for investigating the heterogeneous chemical properties of these novel films. Modulated molecular beam techniques enable us to determine the adsorption, diffusion, sequestration, reaction, and desorption kinetics in real-time. In support of the experimental studies, kinetic modeling and Monte Carlo simulation techniques are used to analyze and interpret the experimental data.

Recent Progress and Future Directions

Dynamics and Kinetics of Adsorbate/Substrate Interactions The interactions of an adsorbate with a substrate, be it a metal, an oxide, or an ice, determine the ultimate fate of that molecule, i.e. whether the molecule scatters, traps, adsorbs, or reacts. Understanding these complex

interactions at a fundamental level may eventually lead to our ability to control the reactivity and selectivity of gas/surface reactions. Understanding the effect that the nanometer scale confinement of matter has on catalytic properties is one of the current scientific challenges. Detailed analysis at the nanoscale allows us to probe the atomic scale interactions of the adsorbed metals and their oxide supports, with each other and with other adsorbed species.

We have used molecular beam scattering and temperature programmed desorption at low temperatures to study the adsorption and dissociation of alkanes (methane, ethane, propane, etc.) on MgO(100) thin films. Highly collimated molecular beams of the small alkane molecules are impinged on the sample and the adsorption dynamics and desorption kinetics are studied. The coverage dependent desorption energy and desorption prefactor for a series of normal (straight chain) alkanes adsorbed on MgO(100) are extracted from a TPD analysis technique that allows the coverage-dependent desorption energy to be accurately determined by mathematical inversion of a TPD spectrum, assuming only that the prefactor is coverage-independent. A variational method is used to determine the prefactor that minimizes the difference between a set of simulated TPD spectra and corresponding experimental data. The data show that the prefactor for desorption increases dramatically with chain length. The observed increase can be physically justified by considering the increase in rotational entropy available to the molecules in the gas-like transition state for desorption. Prior experimental work on alkane adsorption on metals indicated that the prefactor was independent of chain length. However, preliminary studies in our laboratory also indicate a significant chain length dependence for the desorption prefactor on metals which is in agreement with a recent theoretical study. Clearly, this topic requires additional research.

The interaction of water with a substrate is also of considerable interest in numerous scientific disciplines including surface science, electrochemistry, environmental science, atmospheric science, and biology. Thus, understanding the water/substrate interaction at a fundamental level will have a wide range of applications. In a recent paper we investigated the adsorption, desorption, and clustering behavior of H_2O on Pt(111) using specular He scattering. The time dependence of the scattering intensity depends on the adsorbed water structure. At low substrate temperature the exponential line shape indicates that the water is randomly adsorbed, whereas at higher temperature, the linear time dependence indicates a clustered island structure. These data show that water adsorbed on a clean Pt(111) surface undergoes a structural transition from a random distribution to clustered islands near 60 K. The water desorption kinetics can also reveal information about the water layer structure. Surprisingly, the linear time dependence of the helium signal indicates that the desorption kinetics for submonolayer water are zero-order. The zero-order desorption kinetics are consistent with a two-dimensional, two-phase coexistence between a high density H_2O condensed phase (islands) and a low density two dimensional gas-like phase on the Pt surface. Future studies will examine the effect co-adsorbates have on the water-substrate interaction.

The Effect of the Incident Beam Energy on the Properties of Amorphous Solid Water and Crystalline Ice Films. Water vapor deposited on a cold substrate (T<~130 K) forms an amorphous soild known as amorphous solid water (ASW). In general, whether a vapor deposited material grows as an amorphous or crystalline solid depends on the ability of an incident molecule to explore the entire energy landscape. The energy and time needed to find the minimum free energy crystalline configuration will depend on the incident flux, incident energy, incident angle, substrate temperature, and other factors related to the dynamics of energy transfer between the incoming molecule and the substrate. Molecular beam techniques provide a method to study these dynamic processes.

We have recently studied the effect of the incident beam energy on the phase, crystallization kinetics, and the porosity of vapor deposited water films. We find that for films deposited at 20 K and 0° incident angle on Pt (111) the collision energy (up to 205 kJ/mole) has no effect on the initial phase of the deposited film or its subsequent crystallization kinetics. The substrate temperture does affect the phase and crystallization kinetics of the deposited films but this result is independent of the incident collision energy. These results suggest that the crystallization of amorphous solid water requires cooperative motion of the water molecules in order for crystallization to occur. On the other hand, the incident beam energy does affect the porosity of the deposited films. At low beam energy (0.05 eV), the porosity of the vapor deposited film depends strongly on the incident growth angle. Films with structures from non-porous to highly porous can be grown by increasing the angle of incidence of the impinging molecules. The porosity of the ASW films decrease with increasing beam energy. Future studies will extend these measurements to other amorphous molecular solids.

Synthesis, Characterization, and Reactivity of Nanoporous Thin Films. Highly nanoporous materials can have useful applications in a variety of areas including catalysis and chemical sensors. The fundamental interaction of gases and fluids with these nanoporous films will determine the performance characteristics of such devices. Understanding these interactions is therefore essential for the rational design and synthesis of materials for particular applications.

We have previously shown that morphology of vapor deposited ASW films is strongly dependent on the incident growth angle. A simple physical mechanism, ballistic deposition, can be used to understand the dependence of morphology on the growth angle. The basic premise of ballistic deposition is that molecules incident from the gas phase stick at the first site they encounter at the surface of the solid without subsequent diffusion. Ballistic deposition at or near normal incidence results in rough surfaces due to the stochastic nature of the deposition process. At grazing incidence, deposition can not occur in regions behind high points on the surface due to simple shadowing, resulting in the formation of columnar, porous materials.

Based on ballistic deposition and shadowing concepts, we have developed a new technique, reactive ballistic deposition (RBD), to grow compositionally and structurally tailored nanoporous MgO films with extremely high porosities and surface areas. These films consist of arrays of highly oriented, predominantly independent, columnar filaments tethered to the underlying substrate. These thin films have been characterized by N_2 adsorption and electron microscopy and have surface areas as high exceeding 1000 m^2/g. The films are thermally robust, retaining their surface area up to 1200 K. We speculate that the largely independent filaments are responsible for the observed high-temperature stability and will give rise to facile transport of reagents within the film. Additionally, low energy electron diffraction (LEED) and X-ray diffraction (XRD) reveal that the films are crystalline. The feather-like structure of the individual filaments indicates that porous MgO has a very high surface area desirable for possible chemical applications.

Recently, as a first step in the chemical characterization, we have studied the physisorption of N_2 by the nanoporous MgO films. In general, physisorption is a very sensitive probe of the interaction between the substrate and the adsorbate and is thus a good probe of the distribution of binding sites on the surface where the relevant chemistry will occur. Physisorption also allows us to measure the adsorption capacity of the porous films, i.e. to measure the total number of adsorption sites. The surface area information obtained is analogous to that from N_2 Brunauer-Emmett-Teller (BET) isotherm measurements. Preliminary studies on porous films show that the percentage of defect sites is greatly increased compared to smooth dense films.

Given that the mechanism is based on a simple shadowing picture, the approach should be applicable to a wide range of nanoporous materials including metals. We have recently used the ballistic deposition technique to grow nanoporous Pd metal films. The images of the Pd films are reminiscent of the MgO films having the same filament like structure. In the future we plan to characterize the catalytic properties of these films. We have also been developing other strategies to create highly porous nanomaterials. One approach we call "Reactive Layer Desposition", involves vapor depositing Mg metal atoms onto O_2 ice multilayers. We have shown that this approach can also create MgO films with surface areas as high as 700 m^2/g. We plan to further exploit this approach to create other highly porous materials. We expect to learn how to control the reactivity of the nanoporous materials through control of the morphology and chemical composition using multiple molecular beams. Future research in this area will focus on characterizing the chemical reactivity and reaction kinetics and dynamics in these novel materials.

References to Publications of DOE sponsored Research (CY 2003- present)

1. "The deposition angle-dependent density of amorphous solid water films", Z. Dohnalek, G. A. Kimmel, P. Ayotte, R. S. Smith and B. D. Kay, Journal of Chemical Physics, 2003. **118**, 364.
2. R. S. Smith, Z. Dohnalek, G. A. Kimmel, G. Teeter, P. Ayotte, J. Daschbach and B. D. Kay. Molecular Beam Studies of Nanoscale Films of Amorphous Solid Water. In *Water in Confining Geometries*; V. Buch and J. P. Devlin, Eds.; Springer, 2003; pp 337.
3. "Temperature independent physisorption kinetics and adsorbate layer compression for Ar adsorbed on Pt(111)", G. A. Kimmel, M. Persson, Z. Dohnalek and B. D. Kay, Journal of Chemical Physics, 2003. **119**, 6776.
4. "Adsorption, desorption, and clustering of H_2O on Pt(111)", J. L. Daschbach, B. M. Peden, R. S. Smith and B. D. Kay, Journal of Chemical Physics, 2004. **120**, 1516.
5. "Helium diffusion through H_2O and D_2O amorphous ice: Observation of a lattice inverse isotope effect", J. L. Daschbach, G. K. Schenter, P. Ayotte, R. S. Smith and B. D. Kay, Physical Review Letters, 2004. 92, 198306.
6. "Reactive growth of nanoscale MgO films by Mg atom deposition onto O_2 multilayers", J. Kim, Z. Dohnalek, J. M. White and B. D. Kay, Journal of Physical Chemistry B, 2004. **108**, 11666.
7. "Role of water in electron-initiated processes and radical chemistry: Issues and scientific advances", B. C. Garrett, et al. Chemical Reviews, 2005. **105**, 355.
8. "Influence of surface morphology on D_2 desorption kinetics from amorphous solid water", L. Hornekaer, A. Baurichter, V. V. Petrunin, A. C. Luntz, B. D. Kay and A. Al-Halabi, Journal of Chemical Physics, 2005. **122**, 124701.
9. "n-Alkanes on MgO(100). I. Coverage-dependent desorption kinetics of n-butane", S. L. Tait, Z. Dohnalek, C. T. Campbell and B. D. Kay, Journal of Chemical Physics, 2005. **122**, 164707.
10. "n-Alkanes on MgO(100). II. Chain length dependence of kinetic desorption parameters for small n-alkanes", S. L. Tait, Z. Dohnalek, C. T. Campbell and B. D. Kay, Journal of Chemical Physics, 2005. **122**, 164708.
11. "Structural characterization of nanoporous Pd films grown via ballistic deposition", J. Kim, Z. Dohnalek and B. D. Kay, Surface Science, 2005. **586**, 137.
12. "Adsorption and Desoprtion of HCl on Pt(111)", JL Daschbach, J Kim, P Ayotte, RS Smith and BD Kay, Journal of Physical Chemistry B, 2005, **109**, 15506.

Non-Thermal Reactions at Surfaces and Interfaces

Chemical Kinetics and Dynamics at Interfaces

Greg A. Kimmel and Nikolay G. Petrik
Fundamental Science Directorate
Pacific Northwest National Laboratory
P.O. Box 999, Mail Stop K8-88
Richland, WA 99352
gregory.kimmel@pnl.gov

Program Scope

The objective of this program is to investigate non-thermal reactions at surfaces and interfaces using ultra-high vacuum, surface science techniques. The fundamental mechanisms of radiation damage to molecules in the condensed phase are of considerable interest to a number of scientific fields ranging from radiation biology to astrophysics. In nuclear reactor design, waste processing, radiation therapy, and many other situations, the non-thermal reactions in aqueous systems are of particular interest. Since the interaction of high-energy radiation (gamma-rays, alpha particles, etc.) with water produces copious amounts of low-energy secondary electrons, the subsequent reactions of these low-energy electrons are particularly important. The general mechanisms of electron-driven processes in homogeneous, dilute aqueous systems have been characterized in research over the last several decades. More recently, the structure of condensed water and its interactions with electrons, photons, and ions have been extensively studied and a variety of non-thermal reaction mechanisms identified. However, the complexity of the electron-driven processes, which occur over multiple length and time scales, has made it difficult to develop a detailed molecular-level understanding of the relevant physical and chemical processes.

We are focusing on low-energy, electron-stimulated reactions in thin water films. Our approach is to use a molecular beam dosing system to create precisely controlled thin films of amorphous solid water (ASW) and crystalline ice. Using isotopically layered films of D_2O and H_2O allows us to explore the spatial relationship between where the incident electrons deposit energy and where the electron-stimulated reactions subsequently occur within the films. Furthermore, working with thin films allows us to explore the role of the substrate in the various electron-stimulated reactions.

Recent Progress and Future Directions:

Electron-stimulated sputtering of amorphous solid water films on Pt(111)

For condensed gases (e.g. water ice, CO_2, etc.) the sputtering by high-energy ions is related to the *electronic* stopping power of the target material, which is the energy lost per unit path length due to electronic excitations and ionizations. Here we investigate the sputtering of thin amorphous solid water (ASW) films adsorbed on Pt(111) by 87 eV electrons. The sputtering appears to be dominated by two processes: 1) ESD of water molecules, and 2) electron-stimulated reactions leading to the production of molecular hydrogen and molecular oxygen. The sputtering yield as a function of thickness for thin films suggests that erosion of the film occurs due to reactions at both the water/vacuum interface *and* the Pt/water interface. Experiments with layered films of D_2O and H_2O demonstrate significant loss of hydrogen due to reactions at the Pt/water interface. The current results are supported by previous research that has shown that the electron-stimulated reactions leading to molecular hydrogen occur at the water/vacuum and Pt/water interfaces.

Electron irradiation results in significant desorption of water molecules from ASW films. Figure 1 shows the integrated D_2O ESD versus D_2O coverage (open circles). The fact that D_2O desorption increases until the film is thicker than the penetration depth of the incident electrons (~25 ML) indicates that energy transfer from the subsurface regions to the vacuum interface drives the D_2O desorption. Since the only product seen in any appreciable amount in post-irradiation TPD is D_2O, the total sputtering versus the initial coverage can be measured by comparing the integrated post-irradiation water TPD (i.e. the post-irradiation coverage, θ_f) to the initial coverage, θ (figure 1, solid circles).[35] The total sputtering is small for thin films and increases rapidly until reaching a maximum at ~25 ML, then decreases to a constant value for coverages greater than ~50 ML. The total sputtering versus coverage is similar to the O_2 ESD (figure 1, diamonds) and H_2 ESD yields (not shown). For H_2 ESD, we have previously shown that the prominent maximum in the yield at ~25 ML is due reactions at the buried water/Pt interface. Therefore, the results suggest that the peak in the total sputtering is also related to reactions at the buried interface, and that the partitioning of the absorbed energy between the two interfaces of thin ASW films influences the total sputtering rate.

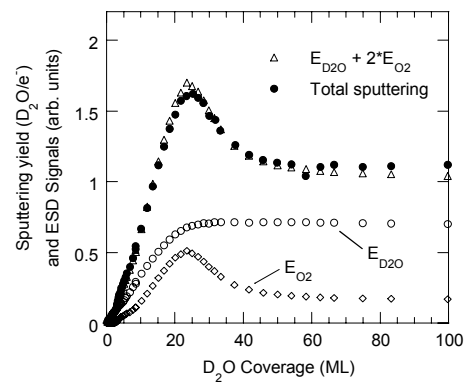

Fig. 1. D_2O and O_2 ESD, and total sputtering versus D_2O coverage.

We have used isotopically layered films to investigate the spatial profile of the sputtering by placing a fixed amount of D_2O at various locations within an H_2O film of constant thickness and measuring the post-irradiation TPD spectra of both D_2O and HDO (to account for all of the D atoms remaining in the film). Figure 2 shows the D atom mass loss from 3 ML of D_2O due to electron-stimulated reactions versus the coverage of the H_2O cap layer in an $H_2O/D_2O/H_2O$ "sandwich" with a total coverage of 25 ML. Not surprisingly, when the 3 ML D_2O layer is at or near the vacuum interface, a substantial amount of it is sputtered away during the irradiation and the D atom mass loss decreases when the D_2O layer is deposited in the middle of the film. However, when the D_2O layer is positioned near the Pt/water interface, the D atom mass loss increases again showing that significant sputtering of the film occurs from reactions forming D_2 and other products near the Pt/water interface.

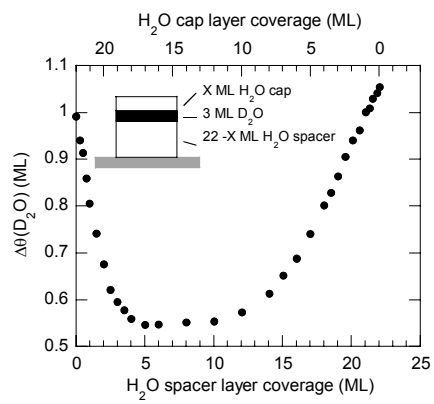

Fig. 2. Sputtered D_2O vs H_2O spacer layer coverage.

If we assume that D_2O ESD, and the electron-stimulated reactions leading to O_2 and D_2, dominate the total sputtering of the film, then we can qualitatively account for the total sputtering as a function of coverage. Since the concentration of reaction intermediates is low, each O_2 that desorbs should be correlated with the destruction of 2 D_2O, and the loss of approximately 4 D atoms, primarily through D_2 and D ESD. Therefore in mass-loss weighted units, the O_2 ESD signal versus coverage should be multiplied by 2 when compared with the D_2O ESD. Figure 1 shows the total sputtering (Y_S), as well as the integrated D_2O (E_{D2O}) and O_2 (E_{O2}) ESD signals, and the sum $E_{D2O} + 2*E_{O2}$ versus θ. The sum of twice the O_2 ESD plus the D_2O ESD semi-quantitatively reproduces the coverage dependence of the total sputtering yield. Future work will examine the role of the substrate in these electron-stimulated reactions by using different substrates such as Ru(0001) and ZrO_2.

Electron-Stimulated Production of O_2 in Thin Amorphous Solid Water Films

We have investigated the low-energy, electron-stimulated production of molecular oxygen from pure amorphous solid water (ASW) films and ASW films co-dosed with H_2O_2. Layered films of $H_2{}^{16}O$ and $H_2{}^{18}O$ are used to determine the spatial profile of the reactions in the films leading to O_2. The O_2 yield is dose-dependent, indicating that precursors are involved in the O_2 production. For temperatures below ~80 K, the O_2 yield at steady state is relatively low and nearly independent of temperature. At higher temperatures, the yield increases rapidly. The O_2 yield is enhanced from H_2O_2-dosed water films, but the experiments show that H_2O_2 is not the final precursor in the reactions leading to O_2. Instead, a stable precursor for O_2 is produced through a multi-step reaction sequence probably involving the reaction of OH radicals to produce H_2O_2 and then HO_2. The O_2 is produced in a non-thermal reaction from the HO_2. The reactions leading to O_2 occur at or near the ASW/vacuum interface. However, the ionizations and electronic excitations which initiate the reactions primarily occur deeper in the film. A kinetic model which qualitatively accounts for all of the observations is presented.

At all temperatures, the O_2 ESD signal is initially approximately zero and then increases until reaching a steady state value. At the end of the electron-irradiation, the O_2 ESD signal promptly decays to zero. Since the initial O_2 ESD yield is zero, increases with electron dose, and promptly recovers after an interruption of the electron irradiation, the O_2 is produced from a stable precursor which accumulates in the film with increasing electron dose. However, the dose dependence of the ESD yield at lower temperatures (e.g. 40 K, fig. 3) suggests that the O_2 precursor is not produced directly by a non-thermal reaction, but is itself the product of a reaction (or reactions) between some other precursors.

Using isotopically layered films of $H_2{}^{16}O$ and $H_2{}^{18}O$ allows us to profile the spatial distribution of the electron-stimulated reactions leading to O_2. For $H_2{}^{16}O$ films that have been subsequently "capped" with various amounts of $H_2{}^{18}O$, the $^{16}O_2$ ESD decreases exponentially as the coverage of the $H_2{}^{18}O$ cap layer is increased (*1/e* ~ 1.5 ML), indicating that the O_2 is made at or near the vacuum interface.

To test H_2O_2 as a possible precursor, we investigated the O_2 ESD from water films dosed with H_2O_2. Figure 3 shows the O_2 ESD versus irradiation time for relatively thick H_2O films that are capped with H_2O + H_2O_2 mixtures and irradiated at 40 K and 100 K. For comparison, the O_2 ESD from neat H_2O films is also shown. A significant enhancement of O_2 ESD for the H_2O_2 -dosed samples is observed suggesting H_2O_2 is a precursor to O_2. However, the experiments indicate that H_2O_2 is not the *final* precursor. In particular, the O_2 ESD signal from H_2O_2-dosed films is initially zero and increases as $\sim(1-e^{-\alpha t})$ at early times for all temperatures, indicating that further reactions that produce HO_2, are required prior to the electron-stimulated production of O_2.

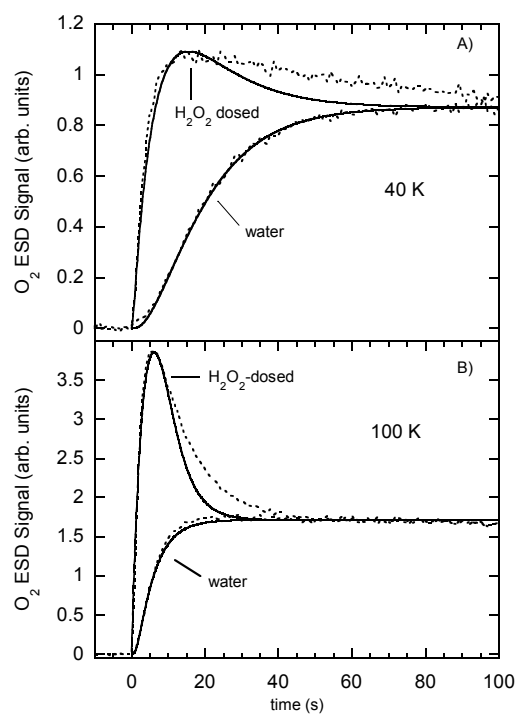

Fig. 3. O_2 ESD vs. time for pure and H_2O_2-dosed water films.

Based on the experiments, we have developed a kinetic model of the O_2 ESD in which OH is produced by the dissociation of electronically excited water molecules at the vacuum interface. The OH radicals then react to produce H_2O_2 and HO_2. The O_2 results from an electron-stimulated reaction involving the HO_2. Figure 3 compares the model (solid lines) to the data (dotted lines) for neat water films and H_2O_2-dosed films irradiated at 40 K and 100 K. The model qualitatively reproduces the results. In the future, we plan to use FTIR spectroscopy to better characterize the

electron-stimulated reaction products and precursors in the thin films, and to investigate these processes at lower electron energies (i.e. closer to the ionization threshold for water).

References to publications of DOE sponsored research (FY 2003 – present)

1. Z. Dohnálek, Greg A. Kimmel, Patrick Ayotte, R. Scott Smith, and Bruce D. Kay, "The deposition angle-dependent density of amorphous solid water films," *J. Chem. Phys.* **118**, 364 (2003).
2. Nikolay G. Petrik and Greg A. Kimmel, "Electron-Stimulated Reactions at the Interfaces of Amorphous Solid Water Films Driven by Long-Range Energy Transfer from the Bulk," *Phys. Rev. Lett.*, **90**, 166102 (2003).
3. Greg A. Kimmel, Mats Persson, Z. Dohnálek, and Bruce D. Kay, "Temperature independent physisorption kinetics and adsorbate layer compression for Ar adsorbed on Pt(111)," *J. Chem. Phys.* **119**, 6776 (2003).
4. R. S. Smith, Z. Dohnálek, G.A. Kimmel, G. Teeter, P. Ayotte, J. Daschbach and B. D. Kay. 2003. "Molecular Beam Studies of Nanoscale Films of Amorphous Solid Water". Water in Confining Geometries. V. Buch and J. P. Devlin, Springer. 337.
5. Nikolay G. Petrik and Greg A. Kimmel, "Electron-stimulated reactions in thin D_2O films on Pt(111) mediated by electron trapping," *J. Chem. Phys.* **121**, 3727 (2004).
6. Nikolay G. Petrik and Greg A. Kimmel, "Electron-stimulated production of molecular hydrogen at the interfaces of amorphous solid water films on Pt(111)," *J. Chem. Phys.* **121**, 3736 (2004).
7. Nikolay G. Petrik and Greg A. Kimmel, "Electron-stimulated sputtering of thin amorphous solid water films on Pt(111)," *J. Chem. Phys.* **123**, 054702 (2005).
8. Bruce C. Garrett, et al., "Role of Water in Electron-Initiated Processes and Radical Chemistry: Issues and Scientific Advances," *Chem. Rev.* **105**, 355 (2005).
9. Greg A. Kimmel, Nikolay G. Petrik, Z. Dohnálek, and Bruce D. Kay, "Crystalline ice growth on Pt(111): Observation of a hydrophobic water monolayer," *Phys. Rev. Lett.*, accepted.

Radiolysis of Water at Ceramic Oxide Interfaces

Jay A. LaVerne, Dan Meisel, Simon M. Pimblott, and Ian Carmichael
laverne.1@nd.edu; meisel.1@nd.edu, pimblott.1@nd.edu, carmichael.1@nd.edu
Radiation Laboratory, University of Notre Dame, Notre Dame, IN 46556

Program Scope

Radiation chemistry techniques are used to probe the influence of solid ceramic oxide interfaces on the decomposition of water and aqueous solutions. Experimental examination of systems ranging from aqueous dispersions of nanoparticles to hydroxide monolayers are coupled with model calculations on the distribution of energy deposition and species migration to give a complete description of the radiolytic processes. Interfaces provide the opportunity for the transfer of energy and charge between two phases. Adsorbed species may have completely different decomposition mechanisms than in the bulk since the surface can stabilize otherwise reactive intermediates. Understanding the radiation effects at an interface is relevant to many practical technological problems of importance to the Department of Energy. Heterogeneous systems are frequently encountered in the management of nuclear materials and nuclear waste, and in nuclear power plant infra-structure. Examples include sludge and slurries in storage facilities, and the metal oxide surfaces of the primary circuit in a nuclear reactor.

The major experimental thrust is to examine the influence of oxide interfaces on the stable products in the radiolysis of water. Aqueous suspensions or slurries are used to determine the effect of different oxide interfaces on the radiolytic production or destruction of H_2 and H_2O_2. Variation in surface bound species such as hydroxides and other oxides are being examined using FTIR and Raman reflection techniques. The focus is to identify and quantify the species escaping from the interface as well as those absorbed on it following radiolysis. Important contributions to this program include atomistic level characterization of the interface and the stochastic modeling of energy deposition across interfaces. Initial energy deposition and the subsequent migration of energy, charge or other carriers are vitally important to understanding the ultimate radiolytic outcome in heterogeneous systems.

Recent Progress

Molecular hydrogen production from water adsorbed on various ceramic oxide particles has been shown to be significantly greater than can be accounted from energy directly absorbed by the water layer. (1-3) Further studies have found similar effects in aqueous oxide slurries. (4) Energy initially deposited in the bulk oxide is transferred to the surface to initiate water decomposition, presumably by excited states like excitons. (1) Particle type, size and other parameters will have significant influence on the nature of the carriers and the probability of reaching the surface. The smaller particle sizes are thought to facilitate migration of the energy carriers to the surface. Pulse radiolysis studies on the reduction of methyl viologen ions adsorbed on the surface of silica nanoparticles suggest that the diffusion distance for reducing equivalents to reach the surface is about 15 nm. (5) Monte Carlo track calculations on the energy deposition by high-energy electrons suggest that average spur sizes in silica are larger than in water and that the 15 nm limit may just reflect the spur size. (5) Experiments on different sized zirconia particles in combination with previous results of Petrik et al. (1) suggest a

diffusion distance of 21 nm. The results indicate that energy migration occurs on the tens of nanometer scale. More in-depth calculations and experiments with other oxides will help determine the nature and range of energy migration to the particle interface.

Zirconia normally has a monoclinic crystalline structure at room temperature and is converted to the tetragonal form at about 1100 C. A recent study shows that the tetragonal volume fraction is equal to unity with increasing particle size up to about 20 nm diameter followed by a sigmoidal decrease to zero at particle diameters of greater than 200 nm. (6) In other words, small ZrO_2 particles tend to have a tetragonal structure even though that is not the stable form of the bulk oxide. Excess surface energy due to the small particle size is given as the reason for this observation. Experiments on aqueous zirconia slurries suggest that the tetragonal crystal structure is more efficient for the formation of H_2 than the monoclinic. (7) Unfortunately, these studies could not rule out surface contamination because extreme heating to remove surface contaminants also leads to the annealing from tetragonal to monoclinic form. This annealing has been shown to occur from the outer surface inward (8) so even short times at high temperatures can affect chemistry at the surface.

The energy transport within ZrO_2 particles is thought to be due to excitons based in part on scavenging studies in which Nb is added in various concentrations as an exciton trap. (1) Defects within the ZrO_2 can also trap excitons leading to a decrease in H_2 yields. Experiments were performed in which two ZrO_2 samples from the same lot were treated identically except that one was preirradiated with gamma rays to a dose of almost 900 kGy. The H_2 yield decreased by almost 30% in the preirradiated sample due to the radiolytic formation of centers capable of trapping energy carriers. Further experiments will examine H_2 formation from samples preirradiated with heavier proton or helium ions. The argon ion bombardment of ZrO_2 films was found to lead to a conversion from the monoclinic to tetragonal structure. Such a change may lead to an increase in H_2 yields rather than a decrease. These results will be especially important in understanding radiolytic aging effects on nuclear power plants.

Several of the experiments on H_2 production also sampled the gaseous products for the formation of O_2. The gaseous yield of O_2 was always at least an order of magnitude smaller than that of H_2. The stable oxidizing species in the radiolysis of water is H_2O_2. An initial speculation was that this compound can be stabilized on the oxide surface. Several experiments examining the stability of H_2O_2 in aqueous slurries of oxide particles found that the H_2O_2 decomposed to give stoichiometrically one half molecule of O_2. This decomposition was found to be extremely fast on ZrO_2 and to occur on the particle surface. Obviously, H_2O_2 is not the oxygen containing species remaining on the particle surface following radiolysis.

Previous studies have suggested that most water decomposition occurs at the particle surface, (2) although the formation of excess hydrated electrons in aqueous SiO_2 suspensions suggests that species definitely can migrate from one phase to another. (9) The surface of the oxide is covered with hydroxide groups formed from the dissociation of water. (10) Physisorbed water normally dominates the IR spectra of wet oxides, but high temperature can be used to expose the hydroxide surface as shown in Figure 1. Hydrogen formation from the surface may result in the depletion or modification of one of the hydroxide peaks and possibly to the formation of reactive oxygen species such as peroxides.

Dipole oscillator strength distributions have been constructed for SiO_2, Al_2O_3, and ZrO_2. Small but significant differences in the distributions suggest that energy deposition characteristics will be different for each of these compounds and that of liquid water. Monte Carlo track structure calculations performed using inelastic cross sections derived from the differential dipole oscillator strength distributions show that the most probable energy transfer event shifts are 22.5, 25.5, and 28 eV for H_2O, Al_2O_3, and SiO_2 , respectively. These shifts will have a significant influence on the mean spur sizes in these media. Further calculations with other oxide materials are in progress.

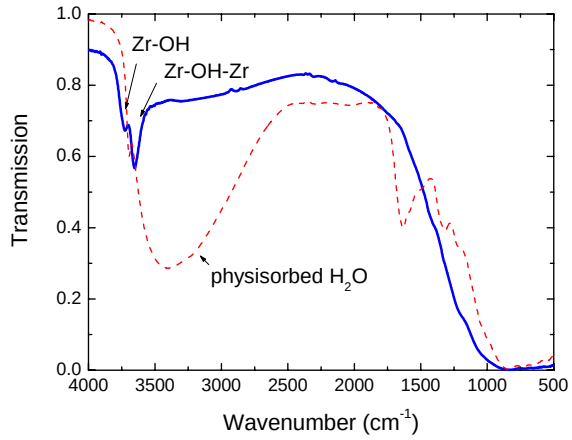

Figure 1. IR transmission of physisorbed H_2O on ZrO_2 (dashed line) and chemisorbed H_2O on ZrO_2 baked at 400 C (solid line).

Future Plans

Radiolysis studies of wet SiO_2 and ZrO_2 suggest that energy deposited directly in the oxide can lead to formation of excess production of H_2. Other oxides of technical importance, such as Al_2O_3, and TiO_2, and metal/metal-oxide composites, will be examined. In addition, a significant effort will be made to examine the effects of particle band gap energy on H_2 formation by incorporating dopants to change the energy levels. These studies may prove to be useful in the commercial production of H_2. Variation in particle size is especially important in determining the transport of energy or material through the interface and will be explored. Mixtures of similar weight percent but different particle sizes will give information on the efficiency of charge or mass transport, since the relative surface areas determine transport through the interface. Another method to determine the identity of transients is to induce defects in the solid so that trapping at these defects then competes with transient migration to the surface. Defect sites will be radiolytically produced in the solid oxide followed by the adsorption of water and further irradiation and the measurement of the radiolytic formation of H_2. The storage of energy in defect sites and the eventual manifestation of this energy in hazardous gas formation may have important implications in the long term storage of sealed containers of radioactive materials.

The radiolysis of adsorbed water can produce copious quantities of H_2, but no corresponding oxidizing species are observed to evolve from the surface. Peroxides or other oxygen species must be adsorbed on the surface or absorbed into the oxide. Water adsorbed on SiO_2, Al_2O_3, and ZrO_2 will be irradiated and the surface examined with FT-IR and Raman techniques. The presence of peroxides and several other oxygen species should be readily observable if they are radiolytically produced.

Monte Carlo track calculations will complement all the experimental studies by examining the migration of energy and charge through the interface. Special attention

will be made to determine the migration distances of different energy carriers in the oxides of interest. Electronic structure calculations will be designed to deliver accurate predictions of surface structure and coverage for the water-oxide interfaces and to characterize, at the atomistic level, the observed radiolytic transformations.

References

(1) N. G. Pretrik, A. B. Alexandrov, and A. I. Vall, *J. Phys. Chem. B* **2001**, *105*, 5935.
(2) J. A. LaVerne and L. Tandon, *J. Phys. Chem. B* **2002**, *106*, 380.
(3) J. A. La Verne and L. Tandon, *J. Phys. Chem. B* **2003**, *107*, 13623.
(4) J. A. LaVerne and S. E. Tonnies, *J. Phys. Chem. B* **2003**, *107*, 7277.
(5) B. H. Milosavljevic, S. M. Pimblott and D. Meisel, *J. Phys. Chem. B* **2004**, *108*, 6996.
(6) G. Baldinozzi, D. Simeone, D. Gosset, and M. Dutheil *Phys. Rev. Lett.* **2003**, *90*, 216103.
(7) J. A. La Verne, *J. Phys. Chem. B* **2005**, *109*, 5395.
(8) C. Li and M. Li, M. *J. Raman Spect.* **2002**, *33*, 301.
(9) T. Schatz, A. R. Cook, and D. Meisel *J. Phys. Chem. B* **1998**, *102*, 7225.
(10) H. P. Boehm, *Disc. Faraday Soc*. **1971**, *52*, 264.

DOE Sponsored Publications in 2003-2005

A. Hiroki and J. A. La Verne "Decomposition of Hydrogen Peroxide at Water-Ceramic Oxide Interfaces", *J. Phys. Chem. B*, **2005**, *109*, 3364.

J. A. La Verne "H_2 Formation from the Radiolysis of Liquid Water with Zirconia" *J. Phys. Chem. B*, **2005**, *109*, 5395.

D. Meisel "Radiation Effects in Nanoparticles", Proceedings of the International Atomic Energy Agency Panel on "Emerging Applications of Radiation in Nanotechnology", IAEA Press, Vienna, ISSN 1011-4289, ISBN 92-0-100605-5, pp. 130-141, **2005**.

B. H. Milosavljevic, S. M. Pimblott and D. Meisel, "Yields and Migration Distances of Reducing Equivalents in the Radiolysis of Silica Nanoparticles", *J. Phys. Chem. B*, **2004**, *108*, 6996-7001.

B. H. Milosavljevic and D. Meisel, "Kinetic and Thermodynamic Aspects of Adsorption on Silica Nanoparticles. A Pulse Radiolysis Study", *J. Phys. Chem. B*, **2004**, *108*, 1827-1830.

D. Meisel "Basics of Radiation Chemistry in the Real World: Nanoparticles in Aqueous Suspensions", Proceedings of the International Atomic Energy Agency Workshop on "Advances in Radiation Chemistry of Polymers", IAEA Press, Vienna, ISSN 1011-4289, ISBN 92-0-112504-6, pp. 5-14, **2004**.

J. LaVerne "Hydrogen Generation in Transuranic Waste Storage Containers", Proceedings of the International Atomic Energy Agency Workshop on "Advances in Radiation Chemistry of Polymers", IAEA Press, Vienna, ISSN 1011-4289, ISBN 92-0-112504-6, pp. 15-20, **2004**.

J. A. La Verne and L. Tandon, "H_2 Production in the Radiolysis of Water on UO_2 and Other Oxides", *J. Phys. Chem. B* **2003**, *107*, 13623-13628.

J. A. La Verne and S. E. Tonnies, "H_2 Production in the Radiolysis of Aqueous SiO_2 Suspensions and Slurries", *J. Phys. Chem. B* **2003**, *107*, 7277-7280.

Fundamental Properties of Solvent Pools of Reverse Micelles Used in Nanoparticle Synthesis

Nancy E. Levinger and Branka M. Ladanyi, Principal Investigators
Department of Chemistry, Colorado State University, Fort Collins, CO 80523-1872
Email: Nancy.Levinger@ColoState.edu, Branka.Ladanyi@ColoState.edu

With funding from this grant, we are investigating fundamental properties of the solvent pool in reverse micelles that could be used as templates for nanoparticle synthesis. The program utilizes a two-pronged approach, both experimental and theoretical, to explore basic structure and dynamics of water inside the nanoconfines of reverse micelles (RMs). We are also investigating the properties of the surfactant that surrounds the water pool. RMs are nanostructured macromolecular assemblies that form in ternary or higher order systems of polar, nonpolar and amphiphilic molecules. The reverse micellar phase occurs in an excess of the nonpolar component and corresponds to surfactant-coated polar nanodroplets dispersed in the continuous nonpolar phase. When the RM is spherical, its diameter is proportional to w_0 = [polar molecules]/[surfactant]. Four publications [1-4] have resulted from our DOE-supported research during the past year.

Experimentally, we have used quasielastic neutron scattering (QENS) to explore water motion inside the RMs. QENS is a powerful technique for investigating the dynamics of hydrogen-containing species in view of the fact that the ^{1}H isotope has a larger incoherent cross section than other nuclei. Selective deuteration of the sample can enhance signals from different portions of the RMs. We have used this procedure to enhance either the signals from H_2O or from the alkyl chain portion of the alcohol cosurfactant. Our experiments were carried out using the QENS spectrometer at the Intense Pulsed Neutron Source (IPNS) at Argonne National Laboratory and the disk chopper spectrometer (DCS) at NIST.

Our investigations have included the effects of surfactant headgroup charge, counterion type, cosurfactant and the nonpolar phase on the properties of RM systems in which water is the polar phase. An anionic surfactant, Aerosol-OT (sodium bis(2-ethylhexyl) sulfosuccinate, AOT) and a cationic surfactant, cetyltrimethylammonium bromide (CTAB), have so far been used. In the case of AOT, the effects of substituting other monovalent (K^+) and divalent counterions (Ca^{2+} and Cu^{2+}) for Na^+ are under investigation. In the case of CTAB, the role of the n-pentanol cosurfactant, which is necessary to form stable RMs in this case, is under study. In all cases, the effects of RM size, w_0, are being varied to determine its effects water mobility. Two nonpolar phases, isooctane and cyclohexane, have been used as the RM oil component.

Experiments both at IPNS and NIST explored water motion in ion exchanged AOT RMs in two different nonpolar continuous phases. The high resolution available for the DCS instruments makes it better for measuring slower translational motion while the substantial range of the QENS instrument allows measurement of shorter-time rotational motion. Experimental QENS data were analyzed using either a jump-diffusion/isotropic rotation model or bounded jump-diffusion/isotropic rotation model. The results of our QENS study of H_2O/AOT-d34/perdeuteroisooctane in the size range w_0 = 1 – 5 were described in last year's report and have since been published [1]. As noted in that report, a parallel MD study of the water hydrogen self-intermediate scattering function, $F_S(\mathbf{Q},t)$, where $\mathbf{Q}$ is the momentum transfer vector, was car-

ried out to aid in the interpretation of these results and provide additional information on water dynamics in RMs [1].

Our experimental QENS results show that water motion in RMs formed in cyclohexane is more restricted than that for water in RMs in isooctane. We attribute this to the smaller size of the RMs in cyclohexane. Replacing the standard Na^+ counterion for AOT with K^+ appears to allow freer water motion in the RMs.

In CTAB RM samples, we explored motion of both water and *n*-pentanol cosurfactant through selective deuteration, either $H_2O/C_5D_{11}OH$/deuterated CTAB/C_6D_{12} or $D_2O/C_5H_{11}OD$/deuterated CTAB/C_6D_{12} on DCS at NIST. Experimental traces required multiple Lorentzian lineshapes to fit the data, which were subsequently analyzed using a jump-diffusion-isotropic rotation model, shown in Fig. 1. Results for $D_2O/C_5H_{11}OD$/deuterated CTAB/C_6D_{12} show substantial mobility for the pentanol cosurfactant, which may signify a substantial concentration of the cosurfactant in the cyclohexane phase. Interpretation of the data from $H_2O/C_5D_{11}OH$/deuterated CTAB/C_6D_{12} RMs is somewhat more complicated as OH groups on *n*-pentanol comprise one third of the signal. Using data from the literature (Palazzo et al. *J. Phys. Chem B* **2003** *107* 1924), we can separate the contribution to the observed diffusion coefficient, $D_{obs,OH}$ from water and *n*-pentanol. Specifically, for the relative mole fractions f_{water} and f_{ROH},

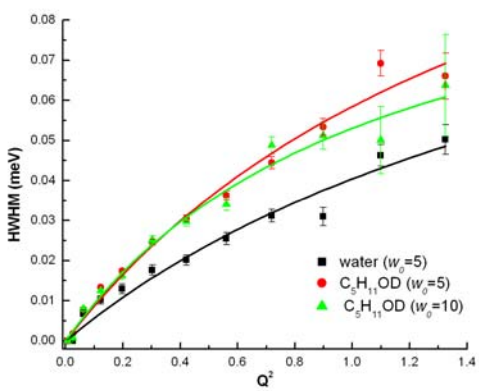

Fig. 1. Analysis of the low-*Q* QENS spectral lineshape for water/n-pentanol/CTAB/C_6D_{12} RMs in terms of the jump-diffusion model.

$$D_{obs,OH} = f_{water}D_{water} + f_{ROH}D_{ROH} = \frac{1}{3}D_{water} + \frac{2}{3}D_{ROH}$$

where D_{water} and D_{ROH} are the diffusion coefficients of water and *n*-pentanol. From this analysis, we find D_{water}=7x10^{-6} cm^2/s, about a third that for bulk water and similar to results for water in AOT RMs [1]. Furthermore, using the literature data, we can gauge the fraction of *n*-pentanol partitioned into the micellar interface:

$$D_{obs,C_5H_{11}OD} = f_{RM}D_{RM} + \left(1 - f_{RM}\right)D_{bulk},$$

where D_{bulk} and D_{RM} are the diffusion coefficients of n-pentanol and the RM in the continuous nonpolar phase. This analysis shows only ~30% of the pentanol is assembled into the RMs.

As noted above, we are using QENS to study counterion effects on water mobility within RMs. In order to gain additional insight into counterion effects, we have performed MD simulations of $w_0 = 5$ RMs in which we have compared water hydrogen $F_S(\mathbf{Q},t)$ for different alkali ions (Na^+, K^+ and Cs^+) serving as AOT counterions. In this work, we have used the e Faeder/Ladanyi model (*J. Phys. Chem. B* **104**, 1033 (2000)) of reverse micellar interior, which provided an accurate description

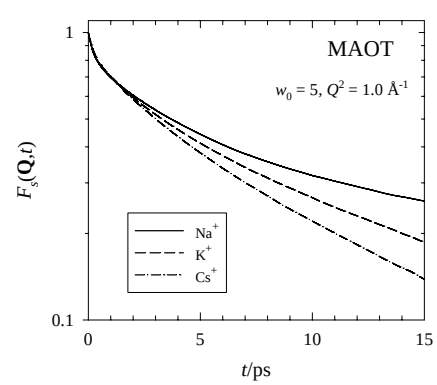

Fig. 2. Counterion effects on the self-intermediate scattering functions, $F_S(\mathbf{Q},t)$, for water hydrogens in model RMs. Depicted are the results for the AOT surfactant and counterions $M^+ = Na^+$, K^+ and Cs^+

of QENS in water/AOT/isooctane over a range of w_0 values [1]. We found strong counterion-dependence on the water mobility, as is illustrated in Fig. 2. Separation of $F_S(\mathbf{Q},t)$ into contributions from interfacial and core regions showed that it is mainly water near the interface that is affected by the counterion type. We were further able to correlate differences in water interfacial mobility with structural features, especially ion-water coordination, and the extent of disruption by the counterions of the water hydrogen bond network.

Using MD simulation, we investigated the effects of chromophore-headgroup interactions on chromophore location and solvation dynamics in RMs [3]. We focused on the electrostatic aspects of this interaction by examining how the solvation energy response, $S(t)$, differs for ionic chromophores that differ only in the charge sign. Specifically, we compared solvation responses for charge localization of two chromophores, I_2^- and "I_2^+", that differ only in charge sign. The latter chromophore is electrostatically attracted to the AOT surfactant SO_3^- headgroup and has a much higher probability of residing in the interfacial region. We found dramatically different behavior of $S(t)$ for the two chromophores, as illustrated in Fig. 3. As can be seen from the figure, the longer-time solvation response is slower and much more strongly w_0-dependent for the "I_2^+" than for the I_2^-. Further mechanistic study showed that the slow portion of the response is due not only to the fact that the "I_2^+" solute is initially in the region of low water mobility, but also to the slow motion of the solute to a different location relative to the interface.

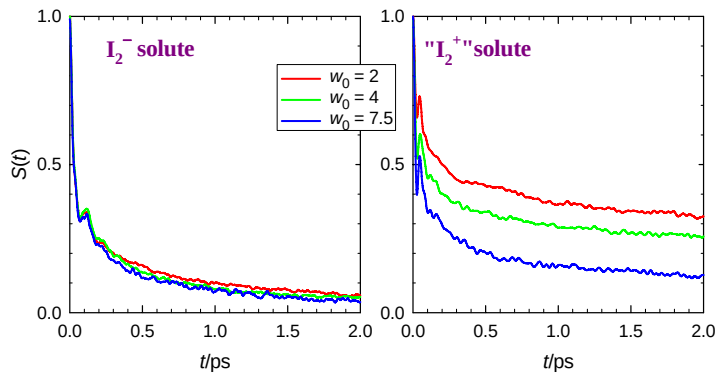

Fig. 3. Solvation response $S(t)$ for charge localization in diatomic chromophores in a AOT-like RMs of different size, w_0. Left panel: the I_2^- solute; right panel: the "I_2^+" solute.

In collaboration with the group of Professor Michael D. Fayer, one of us (N.E.L.) studied the dynamics of water in AOT reverse micelles in the w_0 range 2 – 10 using frequency-resolved infrared vibrational echo experiments [4]. The data for confined water were compared to bulk water and salt solution data. The experimentally determined frequency-frequency correlation functions showed that the confined water dynamics is substantially slower than bulk water dynamics and is size dependent. The fastest dynamics (~ 50 fs) is more similar to bulk water, while the slowest time scale dynamics is much slower than water, and, in analogy to bulk water, reflects the making and breaking of hydrogen bonds.

Work in progress involves atomistic MD simulation studies of aqueous interfaces with hydrocarbons and with ionic surfactants. Extension of these to RM systems is planned. We are continuing our investigations via QENS of the counterion effects on RM properties. Future plans include studies, using QENS and MD, of nonaqueous RMs.

Publications acknowledging DOE grant support:

1. M.R. Harpham, B.M. Ladanyi, N.E. Levinger, and K.W. Herwig, *Water motion in reverse micelles studied by quasielastic neutron scattering and molecular dynamics simulations*, J. Chem. Phys. **121,** 7855-68 (2004).

2. M.R. Harpham, B.M. Ladanyi, and N.E. Levinger, *The Effect of the Counterion on Water Mobility in Reverse Micelles Studied by Molecular Dynamics Simulations*, J. Phys. Chem. B **109,** 16891-900 (2005).

3. J. Faeder and B.M. Ladanyi, *Solvation dynamics in reverse micelles: The role of headgroup-solute interactions*, J. Phys. Chem. B **109,** 6732-40 (2005).

4. H.S. Tan, I.R. Piletic, R.E. Riter, N.E. Levinger, and M.D. Fayer, *Dynamics of water confined on a nanometer length scale in reverse micelles: Ultrafast infrared vibrational echo spectroscopy*, Phys. Rev. Lett. **94,** Art. No. 057405 (2005).

TIME-RESOLVED AND COMPUTATIONAL STUDIES OF SHORT-LIVED MOLECULAR EXCITED STATES OF IMPORTANCE TO PHOTOCHEMISTRY AND PHOTOBIOLOGY

Edward C. Lim
Department of Chemistry and The Center for Laser and Optical Spectroscopy
The University of Akron, Akron, OH 44325-3601

Phone number: (330) 972-5297
Fax number: (330) 972-6407
E-mail address: elim@uakron,edu

PROGRAM SCOPE:

The goal of this research program is to understand the role the intermoiety interactions (charge transer, van der Waals and H-bonding) play in the charge/energy transfer processes of fundamental importance to photochemistry and photobiology. Our major effort during the reporting period was directed to the origin of the ultrafast internal conversion of pyrimidine bases and $\pi\sigma^*$-mediated Intramolecular charge transfer in aminobenzonitriles and aminobenzethynes.

RECENT PROGRESS

Short-lived excited states play crucial functions in several molecular systems of importance to photochemistry and photobiology. Perhaps the two best known examples of the molecular systems displaying very short excited-state lifetimes are the nucleic acid bases that are building blocks of DNA, and 4-dimethylaminobenzonittrile (DMABN) and related molecules, which are the prototype of electron donor-acceptor molecules exhibiting Intramolecular charge transfer. Despite the great many studies that have been carried out for these molecules,[1,2] neither the origin of the ultrashort lifetimes of the DNA bases nor the mechanism of the photoinduced charge transfer in DMABN is known with any certainty. We have very recently initiated a concerted experimental and theoretical study that seeks to refine our understanding of the excited-state dynamics of these important molecular systems. The progress to date is summarized below.

DNA Bases

The hallmarks of the photophysical property of DNA bases are the ultrafast radiationless decay to the ground state, leading to the very short excited-state lifetime (subpicoseconds), and the dramatic lifetime lengthening that results from simple chemical modifications.[3] In cytosine, for which the substituent dependence of the lifetime has been most extensively studied, the ~720 fs lifetime of the unmodified base increases to ~73 ps by replacement of the C5 hydrogen by fluorine (5-fluorocytosine), and to ~280 ps by acetylation of a hydrogen atom in the amino group attached to the C4 carbon (N^4-acetylcytosine).[1,3] These observations are key to understanding the ultrafast S_1 radiationless decay of the unmodified pyrimidine bases. Although there are a number of theoretical studies that address the ultrafast nonradiative decay of nucleic acid components, none of the existing models is able to provide a rational explanation of the observed substituent effects on S_1 lifetime.

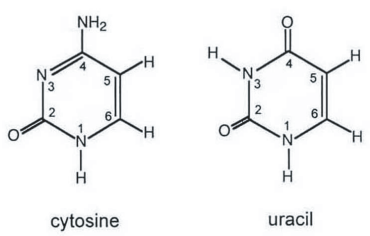

Very recently, we have presented a theoretical model for the ultrafast $S_1 \rightarrow S_0$ internal conversion of cytosine in which a state switch from the initially prepared $^1\pi\pi^*$ state to the out-of-plane deformed excited state of biradical character (I) controls the rate of the $S_1(\pi\pi^*)$ decays,[4] Fig. 1. The calculations,

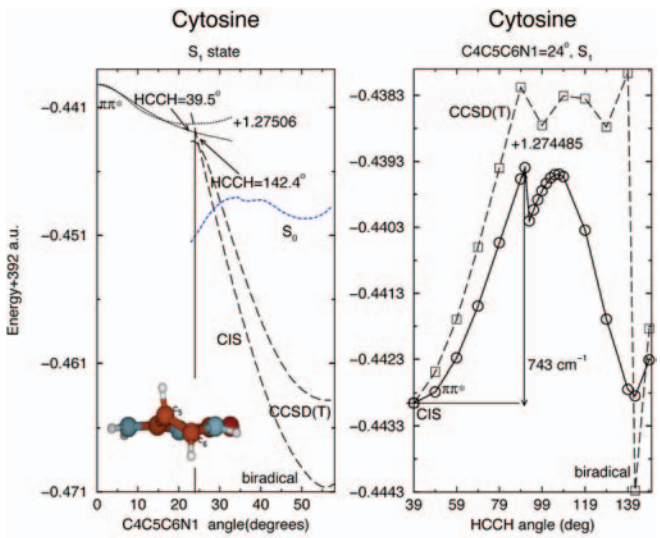

Figure 1. The energy of the S_1 state as a function of the *C4C5C6N1* dihedral angle (left panel), and of the *HC5C6H* angle (right angle). The results of the EOM-CCSD(T) calculations are shifted uniformly up by the amount of energy indicated in the figure. The insert shows the side-view of the structure of the minimum of the biradical state. The dotted line indicates the energy of the ground state at biradical configuration geometries.

based on CIS and completely renormalized equation of motion coupled cluster (CR-EOM-CCSD(r) calculations, show that the state switch from the $^1\pi\pi^*$ to the biradical sate (which intersects the ground state) is barrierless in cytosine, but has substantial energy barriers in 5-fluorocytosine and N^4-acetylcytosine.[4] This difference accounts for the dramatically longer S_1 lifetimes of the modified bases relative to the unmodified bases. The replacement of the C5 hydrogen atom by a methyl group is predicted to lead to a substantial, but not dramatic, increase in the S_1 lifetime, also consistent with experiment.

Extension of the study to uracil and thymine shows that the same mechanism applies to these pyrimidine bases as well.[5] Moreover, the three-state nonradiative decay mechanism ($S_1 \rightarrow I \rightarrow S_0$) predicts that the replacement of the C6 hydrogen by fluorine does not introduce a barrier for state switch. Consistent with this prediction, the experimentally-deduced S_1 nonradiative decay rate of 6-fluorocytosine is more than two orders of magnitude greater than that of 5-fluorocytosine. The nonradiative decay rate of 6-fluorouracil is also dramatically greater than that of 5-fluorocuracil.

Photophysics of guanine-cytosine and adenine-thymine base pairs are presently under investigation.

DMABN

The $\pi\sigma^*$-state-mediated ICT model ($^1\pi\pi^* \rightarrow {}^1\pi\sigma^* \rightarrow$ ICT) we have proposed a year ago[6] (see 2004 CPIMS Abstract), has been put to a direct experimental test through time-resolved laser spectroscopy.

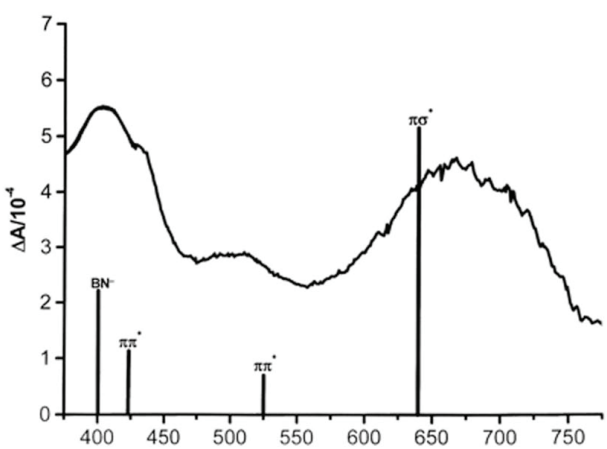

Figure 2. Transient absorption spectra of DMABN in acetonitrile recorded at 2 ps delay time, following excitation with a 305 nm, 130 fs laser pulse. Vertical lines represent the calculated (TDDFT BP86/cc-pVDZ) vertical excitation energies, with relative oscillator strengths indicated by their length.

Figure 2 shows the transient absorption spectra of DMABN in acetonitrile recorded at 2 ps delay time. Four major picosecond transients, with intensity maxima at about 670 nm, 500 nm, 430 nm and 410 nm, are apparent in the spectra. Comparison of these four transitions with the calculated (TDDFT) vertical excitation energies (and oscillator strengths),[7,8] also shown in Fig. 3, allows the assignments of the picosecond transients to specific electronic transitions. Thus, the 670-nm transient can be assigned to the $\pi\sigma^*$ state, 500-nm and 430-nm transients to the $\pi\pi^*$ state, and the 410-nm transient to the ICT state.

Figure 3 shows the time profiles of the 410 nm ICT absorption, 680 nm $\pi\sigma^*$ absorption, and 460 nm $\pi\pi^*$ absorption in the range of 0 – 30 ps. Although a detailed analysis of the excited-state dynamics is made difficult by the multi-exponential

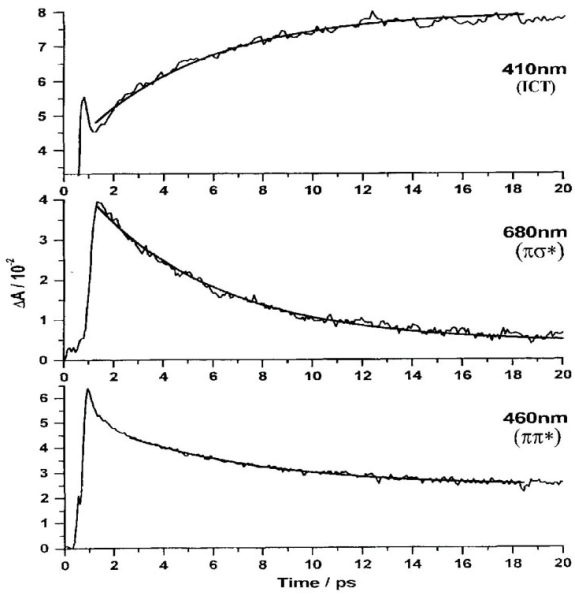

Figure 3. Time dependence of the ICT-state, πσ*-state and ππ*-state absorptions in acetonitrile. The solid lines are the results of a global fit.

character of the decay profiles, the precursor-successor relationship between the πσ* state and the ICT state is evident from the comparison of the temporal characteristics of the 410 nm and 680 nm transients. This comparison shows that the rise time (~ 3.6 ps) of the ICT-state absorption at 410 nm is identical to the decay time of the dominant, short-lived component of the πσ*-state absorption at 680 nm, within the experimental uncertainty (0.2 ps). The result is consistent with the reaction scheme, $\pi\pi^* \xrightarrow{k_1} \pi\sigma^* \xrightarrow{k_2} \text{ICT}$, in which k_1 is significantly greater than k_2. The magnitude of k_1 can be estimated from the rise time of the πσ*-state absorption, which is about 600 ± 200 fs. Interestingly, the time profile of the ππ*-state absorption at 460 nm shows a fast-decaying component of similar time scale, Fig. 2. We therefore interpret 600 fs to be the reciprocal of the rate constant (k_1) for the $^1\pi\pi^* \rightarrow {}^1\pi\sigma^*$ state switch. It is instructive to estimate the time required for the πσ*-state absorption to attain its maximum intensity (t_{max}) using these estimated rate constants (k_1 = 1/600 fs, k_2 = 1/3.6 ps) and the equation $t_{max} = \ln (k_2/k_1)/k_2 - k_1)$. The value of t_{max} so obtained is about 1.2 ps, which is close to the observed t_{max} of about 1.5 ps. For the ππ*-state absorption at 460 nm, the rise time is instrument limited. These results strongly support the occurrence of the consecutive ICT mechanism, ππ* → πσ* → ICT, in which the πσ* state, formed from the state switch by the initially excited ππ* state, plays a central role in the formation of the fully charge-separated ICT state in polar solvents.

The sequential ICT mechanism is also supported by the observation that the lifetime of the πσ* state is very short for aminobenzonitriles and aminobenzethynes that exhibit ICT, and very long for those that do not. Time-resolved resonance Raman study, which probe the CN stretches of DMABN in the three states (ππ*, πσ* and ICT), will be carried out to further test the validity of the sequential ICT model.

References

1. C. E. Crespo-Hernández, B. Cohen, P. M. Hare, and B. Kohler, *Chem. Rev.* (Washington, D.C.) **104**, 1977 (2004), and references therein.
2. Z. R. Grabowski, K. Rotkiewicz, and W. Rettig, *Chem. Rev.* (Washington, D.C.) **103**, 3899 (2003), and references therein.
3. J.-M. L. Pecour, J. Peon, and B. Kohler, *J. Am. Chem. Soc.* **122**, 9348 (2000).
4. M. Z. Zgiersi, S. Patchkovskii, and E. C. Lim, *J. Chem. Phys.* **123**, 081101 (2005).
5. M. Z. Zgerski, S. Patchkovskii, T. Fujiwara, and E. C. Lim, *J. Phys. Chem. A*, in press (October 27, 2005 issue).
6. M. Z. Zgierski and E. C. Lim, *J. Chem. Phys.* **121**, 2462 (2004).
7. M. Z. Zgierski and E. C. Lim, *Chem. Phys. Lett.* **393**, 143 (2004).
8. M. Z. Zgierski and E. C. Lim, *J. Chem. Phys.*, **122**, 111103-111106 (2005).

DOE Sponsored Publications (2005):

1. D. C. Moule, T. Fujiwara, and E. C. Lim, "Thiophosgene: A Tailor-Made Molecule for Photochemical and Photophysical Studies" in Advances in Photochemistry, Vol. 28, D. C. Neckers, W.S. Jenks, and T. Wolff, Eds. (John Wiley & Sons, Inc., 2005), pp. 27-79.
2. M. Z. Zgierski and E. C. Lim, "Electronic and Vibrational Spectra of the Low-lying $\pi\sigma^*$ State of 4-dimethylaminobenzonitrile: Comparison of Theoretical Predictions with Experiment", *J. Chem. Phys*., **122**, 111103-111106 (2005).
3. M. Z. Zgierski, T. Fujiwara and E. C. Lim, "Photophysics of Aromatics Molecules with Low-lying $\pi\sigma^*$ States: Fluorinated Benzenes," *J. Chem. Phys*., **122**, 144312-144318 (2005).
4. H. K. Kang, D. E. Kang, B. H. Boo, J. K. Lee and E. C. Lim, "Existence of Intramolecular Triplet Excimer of Bis(9-fluorenyl)methane: Phosphorescence and Delayed Fluorescence Spectroscopic and *Ab Initio* Studies", *J. Phys. Chem. A*, **109**, 6799-6804 (2005).
5. T. Fujiwara, E. C. Lim, J. Kodet, R. H. Judge, and D. C. Moule, "The Isotopic Dependence of Axes Switching in Thiophosgene Induced by $\tilde{A}\ ^1A_2$ ($n\pi^*$) ← $\tilde{N}\ ^1A_1$ Electronic Excitation", *J. Mol. Spec*., **232**, 331-340 (2005).
6. R. Campos Ramos, T. Fujiwara, M. Z. Zgierski, and E. C. Lim, "Photophysics of Aromatic Molecules with Low-Lying $\pi\sigma^*$ States: Excitation-Energy Dependence of Fluorescence in Jet-Cooled Aromatic Nitriles", *J. Phys. Chem. A* **109**, 7121-7126 (2005).
7. M. Z. Zgierski, S. Patchkovskii, and E. C. Lim, "*Ab Initio* Study of a Biradical Radiationless Decay Channel of the Lowest Excited Electronic State of Cytosine and Its Derivatives", *Chem. Phys*., **123**, 081101 (2005).
8. M. Z. Zgerski, S. Patchkovskii, T. Fujiwara, and E. C. Lim, "On the Origin of the Ultrafast Internal Conversion of Electronically Excited Pyrimidine Bases", *J. Phys. Chem. A*, in press (October 27, 2005 issue).

Single-Molecule Kinetics and Dynamics in the Condensed Phase and at Interfaces

Single-Molecule Interfacial Dynamics and Single-Protein Conformational Dynamics[1]

H. Peter Lu
Chemical Sciences Division
Pacific Northwest National Laboratory
P.O.Box 999, MSIN K8-88
Richland, WA 99352
Peter.lu@pnl.gov

Program Scope

Our research is focused on the use of single-molecule techniques to understand molecular dynamics in condensed phase and at interfaces. Single-molecule approaches are unique for heterogeneous and complex systems because the static and dynamic inhomogeneities can be identified, characterized, and/or removed by studying one molecule at a time. Single-molecule spectroscopy reveals statistical distributions correlated with microscopic parameters and their fluctuations, which are often hidden in ensemble-averaged measurements. Single molecules (and molecular complexes) are observed in real time as they traverse a range of energy states, and the effect of this ever-changing "system configuration" on chemical reactions and other dynamical processes can be mapped. We selected two system classes for our molecular dynamics research: 1) electron transfer reactions on solid surfaces (interfaces) and 2) reactions and dynamics in proteins and protein complexes. The selection of biomolecules in studying condensed-phase chemical dynamics reflects both relevance and advantages. The proteins have been engineered by years of evolution to perform interesting dynamics (large-scale conformational motion, cooperativity, selective chemistry, etc.). Many of them have been studied at length by other methods at the ensemble level providing a sound basis for interpretation of new data that are not obtainable in ensemble-averaged experiments.

Single-molecule photon stamping spectroscopy, time-resolved single-molecule anisotropy, single-molecule fluctuation and fluorescence resonance energy transfer (FRET) spectroscopy, near-field and atomic force microscopy-enhanced confocal imaging microscopes, and surface enhanced Raman spectroscopy have been applied to the study of single-protein conformation and reaction dynamics and interfacial electron transfer dynamics.

Recent Progress and Future Plans

Single-Molecule Electron Transfer Dynamics. Transition metal complexes such as ruthenium complexes, having metal-to-ligand charge (MLCT) transfer states, are being extensively investigated for their involvement in solar energy conversion, interfacial electron transfer, and electron transfer in biological systems. The dynamics of this process can be highly complex and inhomogeneous, especially when molecules are involved in interactions and perturbations with heterogeneous local environments such as at interfaces or in covalent interactions with electron-transfer proteins. Single molecule spectroscopy has been shown to be a powerful approach to studying such complex photophysical dynamics in inhomogeneous systems. However, there are only a few studies involving single molecule detection of transition metal complexes, typically due to low quantum yields and low emission rates. We have demonstrated the use of

[1] Collaborators on these projects include D. Hu, G. K. Schenter, and E. R. Vorpagel from PNNL

photon antibunching to measure triplet-state lifetimes at room temperature on a microsecond timescale. Using photon antibunching measurements under CW laser excitation, non-classical photon statistics, and excitation power dependent measurements, we were able to selectively measure the single-molecule MLCT state lifetime. We apply this approach to the studies of the MLCT state dynamics of a ruthenium complex, with the potential application of probing MLCT ground state recovering dynamics and electron transfer rates. This ruthenium complex may have a wide utilization in solar energy conversion systems and contribute to a fundamental understanding of protein redox systems.

Interfacial electron transfer (ET) dynamics is important for environmental and catalytic reaction systems. Extensive ensemble-averaged studies of the electron transfer kinetics in the dye-sensitized TiO_2 nanoparticle (NP) systems on different time scales have been reported. Their results show large discrepancies in the observed rates of electron transfer dynamics, which indicates broad inhomogeneity in the kinetics of interfacial redox reactions. To examine interfacial electron transfer inhomogeneity, we have studied the dynamics of the single-molecule interfacial electron transfer process of cresyl violet and coumarin 343 adsorbed at the surface of TiO_2 NPs. Conducting single-molecule spectroscopy experiments can avoid molecular aggregation, multiple electron injection to a single particle, and multiple electron-cation recombination at a single particle. Fluorescence intensity trajectories of individual dye molecules adsorbed on a TiO_2 NP surface show fluorescence fluctuations and blinking, with time constants distributed from milliseconds to seconds. We demonstrated that the fluorescence fluctuations are due to the interfacial ET reaction rate fluctuations, associating redox reactivity intermittency with the fluctuations of molecule-TiO_2 electronic and Franck-Condon coupling. Intermittent interfacial ET dynamics of individual molecules could be characteristic of a surface chemical reaction strongly involved with, and regulated by, molecule-surface interactions.

Currently, combining site-specific Raman spectroscopy, time-dependent wave packet scattering spectral analyses, and single-molecule fluorescence spectroscopy, we have been working on characterizing the molecular properties that control the ET processes, including donor-acceptor electronic coupling, the redox reaction driving force, the Franck-Condon factor, and nuclear relaxation energies. We have also been studying conformation-gated electron transfer dynamics of cytochrome proteins. The long-term goal of this project is to develop a noninvasive, vibration-selective, single-molecule sensitive spectroscopic methodology to study single-molecule dynamics and energetics in chemical and environmental reaction systems.

Single-molecule protein conformational dynamics under protein-protein interactions. There is increasingly more evidence showing biomolecular recognition and function are determined not only by structures but also by dynamics or flexibilities. We have combined single-molecule spectroscopy experiments and molecular dynamics (MD) simulations to examine the dynamics of flexible binding protein-protein interactions. A Wiskott-Aldrich Syndrome Protein (WASP) fragment CBD that binds only the activated intracellular signaling protein Cdc42 was labeled with a solvatochromic dye and used to probe hydrophobic interactions significant to Cdc42/CBD recognition. The single-molecule experimental study show static and dynamic inhomogeneous conformational fluctuations of the protein complex that involve bound and loosely bound states. Using MD simulation, we investigated the origin of these conformational states and associated conformational fluctuations by exploring the underlying energy landscape of the binding process. Our MD simulation revealed the double-well two-state cooperative binding-folding surface potentials of the protein-protein interactions, which shed light on characterizing the nature of the protein-protein recognition dynamics. The combined study provides a novel test ground for the theoretical study on the fundamental mechanisms of flexible binding and insights for future experimental exploration on recognition binding with large conformational changes. In principle, by using multi-color fluorescence single molecule spectroscopy, one should be able to monitor several degrees of freedom (protein folding and binding) simultaneously; although the cross-talk between the detection channels for different dyes may complicate the data analysis. Nevertheless, a full picture of cooperative binding-folding dynamics and the

structure of the underlying binding free energy landscape remain elusive. Our ongoing and future studies will employ FRET, polarization spectroscopy, and dye labeling methods to interrogate the complexity of the energy landscape.

Single-Molecule Biological Solar Energy Conversion Dynamics: Electron and Energy Transfer Dynamics and Mechanism in Photosynthetic Pigment-Protein Complexes. In nature, bacterial (*Rhodopseudomonas acidophila*) photosynthetic complexes, light-harvesting (LH1 and LH2) complexes and reaction center (RC), are a nanoscale condensed-phase system that requires a single-molecule approach to obtain a molecular-level understanding of the mechanism and dynamics. Static structure and ensemble-averaged analyses have provided significant understanding of the interactions and the reaction pathways of the photosynthetic system. It has been known that the photosynthetic process initiated by photon excitation of the LH1 and LH2, and followed by energy transfer to RC and electron separation in RC to covert solar energy to chemical energy. Based on the static structure analysis, LH1 directly surrounds the RC, and LH2 is not in direct contact with RC but transfer energy to RC through LH1. The light-absorbing pigments in LH1 and LH2 are primary bacteriochlorin (BChl) molecules in a highly symmetric ring (18 closly packed BChl in a ring) structures. The whole photosynthetic system, like a nano-machine, is embedded in the cell membrane. Our initial effort has focused on the study of LH2 complexes to evaluate the spectral fluctuations, excited state dynamics, dipolar coupling, and conformational fluctuations in membranes at room temperature.

Revealing inhomogeneous vibrational reorganization energy barriers of interfacial electron transfer: To identify and characterize inhomogeneous interfacial chemical reaction dynamics, it is highly advantageous to obtain both topographic and spectroscopic characterization of surfaces and interfacial systems. For example, the site-to-site variations in the geometries and interactions at the molecule-surface interface result in an inhomogeneous distribution of electron transfer rates that can be effectively evaluated with single-molecule methods. Vibrational-mode resolved single-molecule dynamics should be highly informative and powerful to decipher inhomogeneous chemical dynamics at interfaces and in the condensed phase. In recent years, there have been tremendous advances in applying SERS to study nanoparticles and nanostructures at the single-molecule level. Applying microscopic AFM-Raman characterization and analysis, we have found that for alizarin/TiO_2 interfaces, the vibrational reorganization energy barriers of interfacial electron transfer are inhomogeneous at a sub-mesoscale (~250 nm). We determined that (1) the total vibrational reorganization energy was inhomogeneous from site to site; (2) the alizarin/TiO_2 bridging normal modes were the primary contributor to the total vibrational reorganization energy and its inhomogeneity; (3) the mode-specific analyses indicated that the energy distributions were inhomogeneous for bridging normal modes and less inhomogeneous or homogeneous for nonbridging normal modes, especially for modes far away from the alizarin-TiO_2 coupling hydroxyl modes; and (4) the vibrational reorganization energy inhomogeneity was closely associated with the local environmental heterogeneity of the alizarin/TiO_2 interface. It is most likely that the vibrational reorganization energy inhomogeneities contributed to the inhomogeneous dynamics of the interfacial electron transfer processes. However, it remains a challenge to identify a detailed mechanism of the contribution of the inhomogeneity to both forward and backward electron transfer processes in the alizarin/TiO_2 system. Although the topographic and spectroscopic detection limits reported here have not yet reached single-molecule, single-semiconductor nanoparticle, or even nanoscale-specific sites, our results demonstrate that correlated AFM-confocal Raman microscopy is a promising approach for gaining a quantitative understanding of inhomogeneous interfacial charge transfer. Our future work includes AFM-tip enhanced near-field Raman spectroscopy to study electron transfer vibrational reorganization energy analysis at the single-nanoparticle level.

References to publications of DOE sponsored research (FY2003–present)

1. Dehong Hu, Miodrag Micic, Nicholas Klymyshyn, Yung Doug Suh, and H. Peter Lu "Correlated Topographic and Spectroscopic Imaging Beyond Diffraction Limit by Atomic Force Microscopy Metallic Tip-Enhanced Near-Field Fluorescence Lifetime Microscopy," *Rev. Sci. Inst.*, ***74****, 3347 (2003)*.
2. Yu Chen, Dehong Hu, Erich R. Vorpagel, and H. Peter Lu, "Probing Single-Molecule T4 Lysozyme Conformational Dynamics by Intramolecular Fluorescence Energy Transfer," *J. Phys. Chem. B*, **107**, 7947 (2003).
3. Dehong Hu and H. Peter Lu, "Single-Molecule Nanosecond Anisotropy Dynamics of Tethered Protein Motions," *J. Phys. Chem. B*, **107**, 618 (2003).
4. Yung Doug Suh, Gregory K. Schenter, Leyun Zhu, and H. Peter Lu, "Probing Nano-Surface Enhanced Raman Scattering Fluctuation Dynamics using Correlated AFM and Confocal Ultramicroscopy," *Ultramicroscopy*, **97**, 89 (2003).
5. Miodrag Micic, Nicholas Klymyshyn, Yung Doug Suh, H. Peter Lu, "Finite Element Method Simulation of the Field Distribution for AFM Tip-Enhanced Surface Enhanced Raman Scanning Microscopy," *J. Phys. Chem. B*, **107**, 1574 (2003).
6. V. Biju, Miodrag Micic, Dehong Hu, and H. Peter Lu, "Intermittent Single-Molecule Interfacial Electron Transfer Dynamics," *J. Am. Chem. Soc.* **126**, 9374-9381 (2004).
7. Xin Tan, Dehong Hu, Thomas C. Squier, and H. Peter Lu, "Probing Nanosecond Protein Motions of Calmodulin by Single-Molecule Fluorescence Anisotropy," *Applied Phys. Lett.*, **85**, 2420-2422 (2004).
8. H. Peter Lu, invited review, "Single-molecule spectroscopy studies of conformational change dynamics in enzymatic reactions," a special issue of *Curr Pharm Biotech* (The way down from single genes, and proteins to single molecules.), **5**, 261-269 (2004).
9. Dehong Hu, H. Peter Lu, "Single Molecule Implanting of T4 Lysozyme on Bacterial Cell Surface: Towards Study Single Molecule Enzymatic Reaction in Living Cells," *Biophys. J.*, **87**, 656-661 (2004).
10. D. Hu, M. Micic, N. Klymyshyn, Y. D. Suh, H. Peter Lu, "Correlated topographic and spectroscopic imaging by combined atomic force microscopy and optical microscopy," *J. Luminescence*, **107**, 4-12 (2004).
11. G. Harms, G. Orr, H. Peter Lu, "Probing ion channel conformational dynamics using simultaneous single-molecule ultrafast spectroscopy and patch-clamp electric recording," *Appl. Phys. Lett.*, **84**, 1792-1794 (2004).
12. Miodrag Micic, Nicholas Klymyshyn, H. Peter Lu, "Finite Element Method Simulations of the Near-Field Enhancement at the vicinity of Fractal Rough Metallic Surfaces," *J. Phys. Chem. B.*, **108**, 2939 (2004).
13. Duohai Pan, Dehong Hu, and H. Peter Lu, "Probing Inhomogeneous Vibrational Reorganization Energy Barriers of Interfacial Electron Transfer," *J. Phys. Chem.* B, **109**, 16390-16395 (2005).
14. Dehong Hu and H. Peter Lu, "Single-Molecule Triplet-State Photon Antibunching at Room Temperature," *J. Phys. Chem. B*, **109**, 9861-9864 (2005).
15. H. Peter Lu, invited review article, "Probing Single-Molecule Protein Conformational Dynamics," *Acc. Chem. Res.* **38**, 557-565 (2005).
16. H. Peter Lu, "Single-Molecule Study of Protein-Protein and Protein-DNA Interaction Dynamics," an invited book chapter in *Protein-Ligand Interactions*, edited by Uli Nienhaus, The Humana Press Inc., 2005.
17. H. Peter Lu, invited review article, "Site-Specific Raman Spectroscopy and Chemical Dynamics of Nanoscale Interstitial Systems," *J. Physics: Condensed Matter*, **17**, R333-R355 (2005).

Solvation, Spectroscopy, and Electron Transfer

Mark Maroncelli

Department of Chemistry 104 Chemistry Building,
Penn State University, University Park, PA 16802
maroncelli@psu.edu

Our DOE sponsored work focuses on understanding solvation, especially dynamical aspects of solvation, and its influence on charge transfer processes. Over the past few years our emphasis has been in two areas: i) exploring the distinctive features of solvation and charge transfer in ionic liquids and ii) using time-dependent emission spectroscopy to learn about dynamical solvent control of charge transfer reactions. Some of our recent work and future directions are summarized below.

1) Kerr-Gated Emission (KGE) Spectroscopy: We have completed construction of a versatile spectrometer for measuring time-resolved emission spectra of typical fluorophores with sub-picosecond time resolution. Although we continue to make improvements to the design, the instrument now fully functional and is described in detail in Ref. [9]. During the past year we have used it for several of the studies described below. In the near future we will extend these measurements to studies of intramolecular charge-transfer in several old and new model compounds.

2) Charge Transfer Spectroscopy: We recently completed an extensive survey of the steady-state and time-resolved emission spectroscopy of a series of molecules that undergo twisted intramolecular charge transfer (TICT) reaction in the excited state [7]. We showed that the TICT reaction rates in these systems are influenced by polar solvation dynamics and that in some cases the spectral evolution reveals a complex interplay between the two parts of the reaction coordinate, twisting and solvation. Attempts to model the steady-state spectra and their dependence on solvent reported in Ref. [7] were only partially successful. We are continuing to pursue modeling studies in order to better describe this complex spectral dynamics.

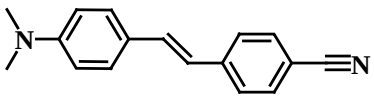

Although the KGE instrument is capable of measuring solutes with multi-nanosecond lifetimes, probes with ~1 ns lifetimes afford better spectra with signal-to-noise. One molecule that proved to be particularly well suited to the KGE experiment is 4-dimethyamino-4'-cyanostilbene or "DCS", shown above. Over the past year we have examined the spectroscopy and photophysics of this solute and have just submitted a manuscript describing these studies [11]. Measurements of steady-state spectra, transition moments, and time-resolved emission spectra as functions of solvent provided a fairly compete picture of this molecule in the S_1 state. In contrast to many conflicting and complicated interpretations of the spectral dynamics of DCS in the literature, we find that only a single excited state of strong charge-transfer character is responsible for emission in all solvents. Dynamic Stokes shifts observed with DCS are well correlated to those of the standard solvation dynamics probe C153, showing that this solute should be considered a useful new addition to the arsenal of polar solvation probes.

3) Ionic Liquids: Ionic liquids are a new category of room-temperature solvents being vigorously studied for potential use a variety of applications. A number of groups, ourselves included, have been examining fundamental aspects of solvation and reaction in these liquids, in order to learn the similarities and differences between these liquids and conventional organic solvents. Thus far we have mainly measured solvation energies and the time-dependence of solvation and solute rotation in a variety ionic liquids using steady-state spectroscopy and time-correlated single photon counting (TCSPC) [1,4-6]. We have uncovered several correlations between the observed solvation energies and dynamics and liquid characteristics such as ion size, solvent viscosity, and ion diffusion rates. But at present our understanding is purely phenomenological. We have initiated molecular dynamics studies which we hope will help provide the insight needed to construct theories of solvation in these systems.

Through the course of our TCSPC work, we found that although the observed solvent relaxation is relatively slow (~1 ns) in many instances up to half of the solvation dynamics is faster than could be detected by such experiments (< 5ps). We recently examined several ionic liquids based on the 1-butyl-3-methylimazolium cation (Im_{41}^+) using a combination of the KGE and TCSPC methods in order to examine the nature of the fast response [10]. Figures 1 and 2 display some of the results of this work. Figure 1 shows the quality of the KGE emission spectra we now regularly obtain. Figure 2 illustrates the remarkably distributed nature of the solvation response in ionic liquids. Note that significant relaxation occurs on time scales ranging between 100 fs to >1 ns. In some cases, for example $[Im_{41}^+][PF_6^-]$, we observe a distinct fast (~300 fs) component to the solvent response which resembles the inertial dynamics recently observed in some computer simulations. In other cases, for example $[Im_{41}^+][Tf_3C^-]$, fast dynamics occur at times <10 ps but it is not clear that these dynamics are distinct from those occurring at longer times. These differences appear to be correlated to (in this case) the relative size of the anion involved PF_6^- < Tf_2N^-<Tf_3C^-, but more work is needed to definitively establish the ion dependence of the fast response.

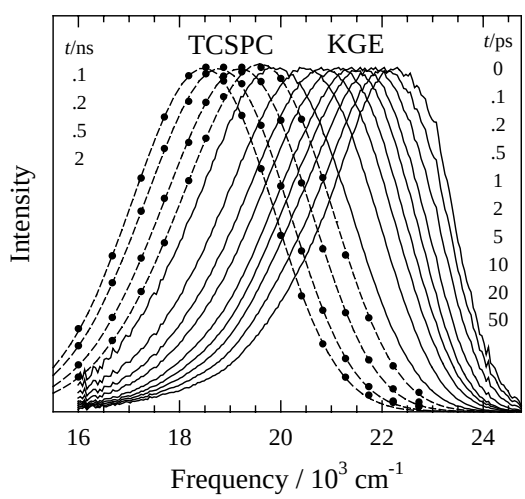

Fig. 1 (above): Time-resolved fluorescence spectra of DCS in $[Im_{41}^+][Tf_2N^-]$ at 25 ºC.

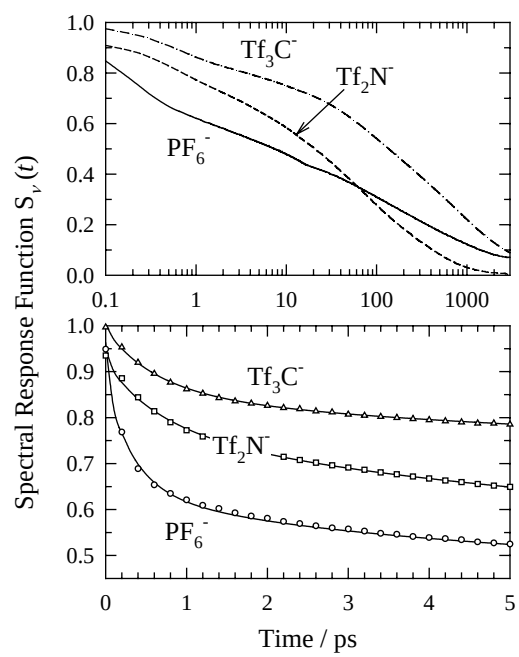

Fig. 2 (right): Spectral response functions $S_\nu(t)$ of $[Im_{41}^+][PF_6^-]$, $[Im_{41}^+][Tf_2N^-]$, and $[Im_{41}^+][Tf_3C^-]$ at 25 ºC.

Our current and future work in ionic liquids involves characterizing several series of new liquids prepared by Gary Baker (Oak Ridge NL), searching for clear signatures of dynamic heterogeneity, beginning studies of electron transfer reactions in ionic liquids, and pursuing computer simulations on simple model systems.

DOE Sponsored Publications 2003-Present:

1. J. A. Ingram, R. S. Moog, N. Ito, R. Biswas, and M. Maroncelli, "Solute Rotation and Solvation Dynamics in a Room-Temperature Ionic Liquid," *J. Phys. Chem. B* **107,** 5926-5932 (2003).
2. K. Dahl, R. Biswas, and M. Maroncelli, "Photophysics and Dynamics of Diphenylbutadiene in Alkane and Perfluoroalkane Solvents," *J. Phys. Chem. B* **107,** 7838-7853 (2003).
3. W. Song, M. Maroncelli, and P. J. Rossky, "Simulations of Alkane - Perfluoroalkane Mixing Behavior using All-Atom Potentials, Failure of the Usual Combining Rules," *J. Chem. Phys.* (2003).
4. S. Arzhantsev, N. Ito, M. Heitz, and M. Maroncelli, "Solvation dynamics of coumarin 153 in several classes of ionic liquids: cation dependence of the ultrafast component," *Chem. Phys. Lett.* **381,** 278-286 (2003).
5. N. Ito, S. Arzhantsev, M. Heitz, and M. Maroncelli, "Solvation Dynamics and Rotation of Coumarin 153 in Alkylphosphonium Ionic Liquids," *J. Phys. Chem. B* **108,** 5771-5777 (2004).
6. N. Ito, S. Arzhantsev, and M. Maroncelli, "The probe dependence of solvation dynamics and rotation in the ionic liquid 1-butyl-3-methyl-imidazolium hexafluorophosphate," *Chem. Phys. Lett.* **396,** 83-91 (2004).
7. K. Dahl, R. Biswas, N. Ito, and M. Maroncelli, “Solvent Dependence of the Spectra and Kinetics of the LE→CT Reaction in Three Alkylaminobenzonitriles,” *J. Phys. Chem. B* **109**, 1563-1585 (2005).
8. S. Arzhantsev and M. Maroncelli, “Design and Characterization of a Femtosecond Spectrometer Based on Optical Kerr Gating,” *Appl. Spectrosc*. **59**, 206-220 (2005).
9. M. Liu, N. Ito, M. Maroncelli, D. H. Waldeck, A. M. Oliver, and M. N. Paddon-Row, “Solvent Friction Effect on Intramolecular Electron Transfer,” J. Am. Chem. Soc., submitted (8/05).
10. S. Arzhantsev, H. Jin, N. Ito, and M. Maroncelli, “Observing the Complete Solvation Response of DCS in Imidazolium Ionic Liquids, from the Femtosecond to the Nanosecond Regimes,” *Chem. Phys. Lett*., submitted (9/05).
11. S. Arzhantsev, K. A. Zachariasse, and M. Maroncelli, “The Photophysics of trans-4-Dimethylamino-4’-Cyanostilbene and its use as a Solvation Probe,” *J. Phys. Chem. B*, submitted (9/05).

METALLIC NANOPARTICLES UNDER IRRADIATION

Dan Meisel
The Radiation Laboratory, University of Notre Dame
Notre Dame, IN 46556 dani@nd.edu

Program Scope

The goal of this program is to explore the effects of metallic particles at the nano-scale dimensions on radiolysis of various media, in particular water. Using radiation chemical techniques we probe the interaction of radicals generated radiolytically in the aqueous phase with the metallic interface and the possible escape of charge carriers from the metallic particles to the liquid phase.

The exchange of energy and charge-carriers between the solid and liquid phases following irradiation of a biphasic system is of interest as a fundamental phenomenon but is also relevant to a multitude of applications of technological signifcance. From energy productions to environmental remediation and from managing nuclear materials to radiotherapy, these interfaces are frequently encountered and they affect the outcome of the irradiation. Metal-water interfaces are of catalytic utility in H_2 production from water but they may also contribute to preferential localization of radiation damage in a desired tissue. Our on-going studies focus on these two mirror-image areas of the interface. We produce the radicals in the aqueous phase and study the course of their reaction in the presence of metallic particles, on one hand, but we also attempt to produce charge carriers in the metallic particle and capture them at the water-metal interface. The latter aspect is especially intriguing because the absorption of ionizing radiation by matter is proportional to its electron density, and thus, the energy is preferentially absotbed by the solid particles, most pronounced in metallic particles. For example, for Au or Pt, density of approximately 20 g cm^{-3} implies that the energy absorbed by the particle is some 20 times higher than by the same volume of water. If that energy can be funneled to the interface it may offer a method to target radiation effects, including biological damage, to the vicinity of the particle. Furthermore, the wealth of currently evolving methodologies to specifically bind biomolecules to the metallic interface allows *a-priori* selection of the identity of the targeted species at the particle interface.

Recent Progress

We have recently shown that radicals from the aqueous phase strongly adsorb on gold nanoparticles and determined the relative adsorption constants of few groups on the radical (amines, ketones ethers and directbinding via the nitrogen center of nitroxy radicals) in these radicals.(1) Other radicals were shown to adsorb to the surface of oxides and their cross-sections on the surface were determined.(2) We have shown that when the unpaired electrons are close to the metallic, but not the oxide, surface they rapidly exchange with conduction-band electrons (<20 ns; epr time scale) and thus lose their identity and memory of the radical origin (in the epr sense). Efforts to observe these and many other radicals (including nitroxides, viologens and and various aromatic conjugated derivatives of theirs) at the surface of gold and silver particles using surface enhanced Raman spectroscopy were unsuccessful. On the other hand, using the same technique, several groups have shown that adsorption of the molecular species to particles of these two metals often result with structures that resemble those of the corresponding one-

electron reduced radicals. At present we are trying to identify if electron transfer from the radical to the metallic particle has occurred, which prevents detection of the radicals.

Our recent work on the fate of radiolytically generated charge carriers in silica nanoparticle suspensions established the distance that electrons (and excitons) can migrate in this solid before localization in traps and electron-hole annihilation occurs.[3] Similar information for metallic particles, lifetime and migration distances of the carriers are not known. We, therefore, try to determine whether electrons or holes from the metal can be captured at the metal/water interface by determining the yield of water specific species from irradiation of aqueous suspensions heavily loaded with metallic particles. We choose production of H_2 as a probe reaction since ultra-fast formation of hydrogen is a potential indication of energy and early-precursor escape from the solid to the water. On the other hand, any increase in the yield of hydrogen generation by radicals from solutes in the water is an indication of a catalytic rather than a "direct" effect.

Suspensions containing up to 65% by weight of relatively large gold particles ($r \approx 0.5$ μm) show large increase in the yield of H_2. We have shown that this is not a result of charge-carriers escape from the particles but rather catalytic conversion of the radicals produced by the radiolysis to molecular hydrogen. The efficiency of carriers escape from the particles is expected to be dependent on the particles size. Therefore, we developed a method to generate metallic particle suspensions of high particle concentrations and yet at systematically increased sizes. This provides silver particles of clean surfaces, "naked" of foreign stabilizers, but highly stable even at large concentrations. Their spectroscopy, surface potential, and identity of species at the surface were determined and their behavior under irradiation is now studied. Initial results show that the yield of H_2 from these suspensions is suppressed at low radiation doses but increases dramatically at high doses. Several sources for the low-dose suppression, "conditioning" of the particles, were identified; these include the presence of residual parent ions at the particles surface (unexpectedly, complexed to hydroxide ions and thus generating negative surface potential), accumulation of electrons on the particles to generate the overpotential required for hydrogen evolution, and in some metals, adsorption of molecular hydrogen. The contribution from each of these sources is now being quantified.

Less is known in general on the fate of holes generated in nanoparticles than the fate of their counter-part electrons, partially because of difficulties associated with their optical properties. We have shown that excess holes can accumulate in silica particles and determined a lower limit for the redox potential of these scavengeable carriers. Early results suggest that seeding oxide particles with metallic particles on their surface, either as core-shell structures or as islands at the surface, enhances the ability of scavengers to react with the holes.

Future Plans

We will pursue our studies of radiolytic effects in size controlled silver particles. No report on escape of charge carriers from metallic systems has appeared so far. Because of the significance and far reaching implications of such a process we will attempt to demonstrate it in the recently developed size controlled suspensions of siver particles that were described above. The relatively broad range of sizes available (10-200 nm), and yet the reasonably narrow size distribution (±10%), also suggets experiments to identify the optimal particle size for surface enhanced Raman spectroscopy. We, therefore, will revisit our efforts to identify radicals of decreasing lifetime at the surface of these particles using surface enhanced Raman.

Because of the difficulties associated with the chemistry of the metallic systems we will need to resort to bi-component systems including the much more stable oxide particle. We envision deposition of metallic particles on silica (or other oxides) particles using well-established literature techniques. Silver, gold and platinum on silica and titania were already been prepared in our laboratory, albeit at lower concetrations than needed in our experiments. These can be produced either as core-shell or as islands-on-the-core morphologies. We will develop these approaches and study the effects of these particles on both, the catalytic reactions of radicals from the aqueous phase and on possible ejection of electron/holes from the metallic particle. Preliminary results from hybride SiO_2@Ag silica particles suggest that charge carriers migrate to the metal where they can react with a variety of scavenger molecules. In the absence of the metal the carriers remain trapped in the particle. We will study the effect of the hybrid particles on the fate of charge carriers in the solid material.

Publications Sponsored by this DOE Prgram, 2003-2005

(1) Z. Zhang, A. Berg, H. Levanon, R. W. Fessenden, and D. Meisel, "On the Interactions of Free Radicals with Gold Nanoparticles", J. Am. Chem. Soc., 125, 7959-63 (2003).
(2) Bratoljub H. Milosavljevic and Dan Meisel, "Kinetic and Thermodynamic Aspects of Adsorption on Silica Nanoparticles. A Pulse Radiolysis Study", J. Phys. Chem. B, 108, 1827-30 (2004).
(3) Bratoljub H. Milosavljevic, Simon M. Pimblott and Dan Meisel, "Yields And Migration Distances of Reducing Equivalents in the Radiolysis Of Silica Nanoparticles", J. Phys. Chem. B 108, 6996-7001, (2004).
(4) Dan Meisel, "Radiation Effects In Nanoparticle Suspensions", in "Nanoscale Materials", Ed. L. Liz-Marzan and P. Kamat, Kluwer Publishers, 119-134 (2003).
(5) Prashant V. Kamat and Dan Meisel, "Nanoparticles In Advanced Oxidation Processes", Current Opinion in Colloid & Interfacial Sci. 7, 282-7 (2003).
(6) P. V. Kamat and D. Meisel, "Nanoscience Opportunities in Environmental Remediation", Compte Remdus Chimie, 6, 999-1007 (2003).
(7) Dan Meisel, "Basics of Radiation Chemistry in the Real World: Nanoparticles in Aqueous Suspensions", Proceedings of the International Atomic Energy Agency Workshop on "Advances in Radiation Chemistry of Polymers", IAEA Press, Vienna, ISSN 1011-4289, ISBN 92-0-112504-6, pp. 5-14 (2004).
(8) Dan Meisel, "Radiation Effects on Nanoparticles", Proceedings of the International Atomic Energy Agency Panel on "Emerging Applications of Radiation in Nanotechnology," IAEA Press, Vienna, ISSN 1011-4289, ISBN 92-0-100605-5, pp. 130-141 (2005).
(9) Bruce C. Garrett, et al., "The Role of Water in Electron-Initiated Processes and Radical Chemistry: Issues and Scientific Advances", Chem. Rev. 105, 355-390, 2005.

Center for Radiation Chemistry Research

Principal Investigators: Andrew Cook, Sergei Lymar and John R. Miller,

jrmiller@bnl.gov Chemistry Department, Brookhaven National Laboratory

Scope: This program examines charged or radical species and develops tools to create and probe these species. Principal among these tools is the Laser Electron Accelerator Facility (LEAF) at Brookhaven that produces 7 ps electron pulses and detection systems. We encourage use of LEAF's present and planned capabilities by a broad range of scientists including members of this CPIMS meeting: See Facilities at http://www.cfn.bnl.gov/default.asp for a description. An example of science at LEAF is given in the talk by Jim Wishart at this conference. This poster will list some other research in our group and will describe results in two areas.

Dissociation of Aryl Halides Anions: Electronic Effects on Barriers Charge transfer to organic molecules can result in scission of chemical bonds. An important class of such reactions is a one-electron reduction of organic halides in solution leading to dissociation of the carbon-halogen (C-X) bond to produce a carbon-centered radical and a halide anion. This reaction has been studied intensely because it is a basic element of important chemical processes such as nucleophilic substitution reactions and Grignard reagent formation, but there has been little information on rates faster than 10^8 s^{-1}. Results shown at left illustrate transient absorption measurement at LEAF that obtains much shorter time resolution. The results of such measurements on several molecules correlated well (shown above right) with computed energy barriers, although this series of fast dissociation reactions showed poor correlation with overall reaction energetics. Overall energetics misses the important influence of *electronic effects* on the activation barriers for these fast reactions. These electronic effects reduce the energy for crossings of σ* and π* states, but only if bonds bend to enable the necessary interactions, leading to conical intersections (left).

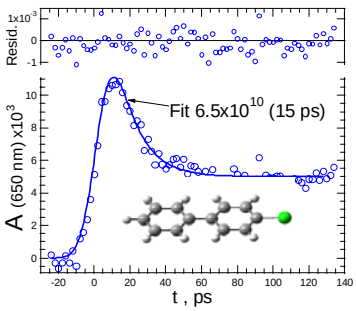

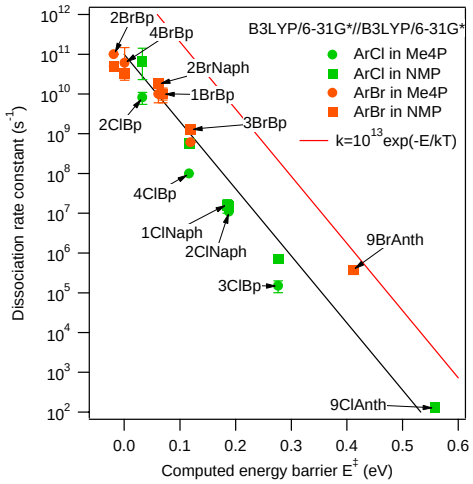

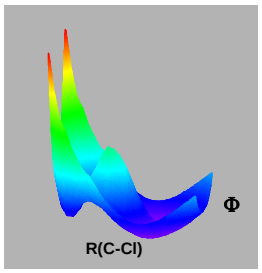

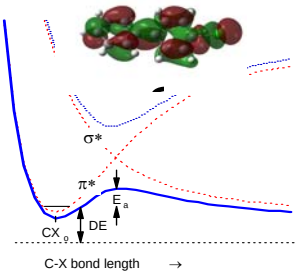

Earlier work had frequently framed the question of sequential vs. concerted reaction mechanisms. These experiments show that electron addition and bond scission occur in two distinct consecutive steps; as often occurs the idea of concerted reactions slips away as better time resolution becomes available. Further work on these reactions, if pursued, would attempt to illuminate the possibility of "concerted" reactions.

Electronic Effects in Charge Transfer by Excited Anions Solvated electrons are readily attached to benzoquinone (BQ) in pulse radiolysis experiments to create the radical anion and even its excited state (BQ^{-*}), energies of which have been established. In weakly polar fluids (e.g. THF and isooctane) the excited state is created at near- diffusion-controlled rates and is strongly preferred over the ground state in reactions that proceed, almost certainly via the 2nd excited state, BQ^{-**}.

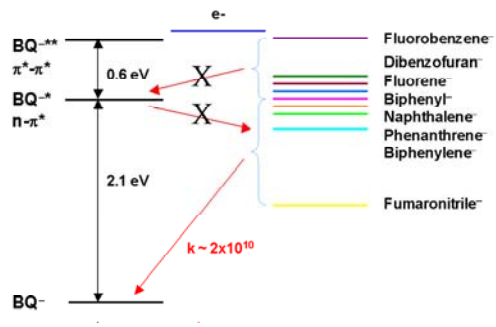

The fast rates of these bimolecular electron transfer (ET) reactions are typical and expected when for ET reactions exoergic by 50 meV or more. In contrast ET reactions directly to or from BQ^{-*} are unexpectedly slow. Reductants having sufficient redox energy to produce BQ^{-*}, but not BQ^{-**}, fail to produce either as indicated by the upper arrow with an X though it, ↛ in the figure. Similarly BQ^{-*} fails to react with a series of molecules such as naphthalene in the expected near-difusion-controlled reactions although energetics are sufficient to produce those radical anions (lower ↛). The results tell us that fast ET does not occur either to or from BQ^{-*}, although all of these reactions are energetically favorable, and the excited state lifetime of BQ- is sufficiently long. Present data shows these reactions are slower than the expected diffusion-controlled rates, but competing reactions prevent determination of how slow they are.

Future studies of quinone radical ions by a mixture of chemical reduction and pulse radiolysis experiments will be aimed at answering a few key questions:

- How serious in the apparent prohibition against ET to or from BQ^{-*}, and is it due to nuclear (Franck-Condon) of to electronic barriers?
- Can we observe excited state electron transfer involving the higher π^*- π * state in BQ-? ET from this state may be difficult due to its expected short lifetime.
- Anions of quinones are important participants in energy storage in photosynthesis. Can their excited states be used in new energy storage mechanisms?

Other Scientific Topics Include:

- Reactivity of Nitrogen Oxides including "spin-forbidden acids"
- Photodissociation of ion-pairs
- Energetics of strongly-reducing species including carboranes
- Excited states of radical ions

- Proton transfer reactions

Experimental Tools A principal component of our effort seeks to create increasingly better tools for the study for fast chemical processes. Recent efforts • obtained ~100 ps time resolution in single-shot experiments with the incorporation of a fast transient digitizer, • extended pulse-probe experiments (~10 ps resolution) to the near infrared region integrating an OPA into the system, • Developed a LabView-based control system for digitizer based experiments that provides a user-friendly interface and will simplify planned improvements. • A more stable, but lower rep-rate (10 Hz) pump laser has substantially improved system reliably and reduced effort toward laser maintenance.

Future plans for experimental systems include: • Automated collection of spectra from visible through near IR, • A fast single-shot detection system for transient absorption • Two types of pulse-pump-probe experiments that will combine excitation by electron and laser pulses • A wide range of continuous improvements to obtain improved stability, reliability and signal/noise ratios.

The experimental improvements will enable measurements of fast intramolecular electron transfer reactions. Essential here will be the single-shot experiment that will obtain high time resolution on custom-synthesized molecules not available in gram quantities. The same techniques will be applied to examination of charge transport in "molecular wires." Rates of proton transfer will be measured and correlated with free energies. Energies of conjugated carboranes will be examined. The limits of electron transfer with two-electron changes will be probed as will the boundary of concerted reactions.

Publications

The Role of Water in Electron-Initiated Processes and Radical Chemistry: Issues and Scientific Advances
B. C. Garrett, D. A. Dixon, D. M. Camaioni, *et. al.*.
Chem. Rev., 105, 355-389 (2005)

Faster Dissociation: Measured Rates and Computed Effects on Barriers in Aryl Halide Radical Anions
N. Takeda, P. V. Poliakov, A. R. Cook, and J. R. Miller
J. Am. Chem. Soc. 126, 4301-4309 (2004).

The LEAF Picosecond Pulse Radiolysis Facility at Brookhaven National Laboratory
J. F. Wishart, A. R. Cook and J. R. Miller
Rev. Sci. Inst. 75, 4359-4366 (2004).
Also selected for the December 2004 issue of the Virtual Journal of Ultrafast Science.

Electron Attachment to C_{60} in Nonpolar Solvents
R. A. Holroyd
Radiat. Phys. Chem., 72, 79-84 (2005).

Increased Yields of Radical Cations by Arene Addition to Irradiated 1,2-Dichloroethane
A. M. Funston and J. R. Miller
Radiat. Phys. Chem., 72, 601-611 (2005).

Density Inhomogeneities and Electron Mobility in Supercritical Xenon, R. A. Holroyd, K. Itoh and M. Nishikawa, *J. Chem. Phys.* 118, 706-710 (2003).

Benzene Radical Ion in Equilibrium with Solvated Electrons, R. A. Marasas, T. Iyoda, and J. R. Miller, *J. Phys. Chem. A* 107, 2033-2038 (2003).

Reactions of Charged Species in Supercritical Xenon as Studied by Pulse Radiolysis
R. A. Holroyd, J. F. Wishart, M. Nishikawa and K. Itoh, *J. Phys. Chem. B* 107, 7281-7287 (2003).

Rate of ON-OO$^-$ Bond Homolysis and the Gibbs Energy of Formation of Peroxynitrite, S. V. Lymar, G. A. Poskrebyshev, *J. Phys. Chem. A.* 107, 7991-7996 (2003).

Hydroxyl Radical Formation by O-O Bond Homolysis in Peroxynitrous Acid
S. V. Lymar, R. F. Khairutdinov and J. K. Hurst, *Inorg. Chem.* 42, 5259-5266 (2003).

Spin-Forbidden Deprotonation of Aqueous Nitroxyl (HNO), V. Shafirovich and S. V. Lymar, *J. Am. Chem. Soc.* 125, 6547-6552 (2003).

Charged Particle and Photon Interactions with Matter: Chemical, Physicochemical, and Biological Consequences with Applications
R. A. Holroyd, in *Electrons in Nonpolar Liquids* A. Mozumder and Y. Hatano, (Eds.), Marcel Dekker, New York, NY, (2004) Ch. 8, pp.175-206.

Hyponitrite Radical, a Stable Adduct of Nitric Oxide and Nitroxyl
G. A. Poskrebyshev, V. Shafirovich, S. V. Lymar, *J. Am. Chem. Soc.* 126, 891-899 (2004).

Charge Transfer Through Terthiophene End-Capped Poly(arylene ethynylene)S Funston, A. M.; Silverman, E. E.; Miller, J. R.; Schanze, K. S. *J. Phys. Chem. B* **2004**,

One-Electron Reduction of an Extended Viologen, Alison Funston, James P. Kirby, John Miller, Lubos and Josef Michl, J. Phys. Chem. *In press*

Spectroscopy of Organometallic Radicals

Michael D. Morse
Department of Chemistry
University of Utah
315 S. 1400 East, Room 2020
Salt Lake City, UT 84112-0850
morse@chem.utah.edu

I. Program Scope:

In this project, we seek to obtain fundamental physical information about unsaturated, highly reactive organometallic radicals containing open *d* subshell transition metal atoms. Gas phase electronic spectroscopy of jet-cooled transition metal molecules is used to obtain fundamental information about ground and excited electronic states of such species as the transition metal carbides and organometallic radicals such as CrC_2H, $CrCH_3$, and $NiCH_3$. High resolution infrared spectroscopy is applied to the unsaturated transition metal carbonyls, MCO, $M(CO)_2$, $M(CO)_3$, *etc*.

II. Recent Progress:

A. Optical spectroscopy of RuC, CrC_2H, $CrCH_3$, and $NiCH_3$

During the past two years, we have carried out resonant two-photon ionization (R2PI) and dispersed fluorescence (DF) spectroscopic studies of the transition metal carbide, RuC,[1] and of the polyatomic transition metal radicals CrC_2H, $CrCH_3$, and $NiCH_3$.[2] Our work on RuC has included rotationally resolved studies of the 0-0, 1-0, 2-0, 3-0, and 4-0 bands of the $[18.1]^1\Pi$ – $X^1\Sigma^+$ system, which has allowed an RKR potential curve to be generated for the $[18.1]^1\Pi$ state. In addition, the $[21.4]0^+$, [21.6]2, and $[23.2]^3\Delta_3$ states have now been identified in RuC. Excited state lifetimes have been measured for all of these states, and rotationally resolved measurements of the line positions have been made, allowing bond lengths to be determined for all of these states. Ruthenium carbide is now the best-known of all of the diatomic transition metal carbides, having 16 different electronic states (as defined by S, Λ, and Ω) identified and characterized. The fact that RuC has the greatest bond energy of all of the 3*d* and 4*d* carbides is not at all accidental to this result. The molecules with smaller bond energies have larger densities of states, and the resulting state mixing makes interpretation of the spectra much more problematic.

Our studies of the vibrationally resolved resonant two-photon ionization and dispersed fluorescence spectra of CrC_2H, $CrCH_3$, and $NiCH_3$, have been recently published in the Journal of Chemical Physics.[2] These molecules are among the most complicated open *d*-subshell molecules yet known for which optical spectra have been obtained in the gas phase. The vibronically resolved spectra that have been recorded for CrC_2H and $NiCH_3$ have allowed metal-carbon vibrational frequencies and anharmonicities to be measured for these species in their excited states. For $NiCH_3$, values of ω_e and $\omega_e x_e$ were also obtained for the ground state. For $CrCH_3$ and CrC_2H, values of $\Delta G_{1/2}$ for the Cr-C stretching vibration were also obtained for the ground state. Rotationally resolved scans over all three molecules have been accomplished, but these have not yet yielded to analysis. The $NiCH_3$ scans show obvious perturbations, since the different vibrational levels of the upper state and the scans over the ^{58}Ni and ^{60}Ni species are

all very different in appearance. In contrast, the rotationally resolved spectra of CrC_2H and $CrCH_3$ are a forest of lines.

Finally, during the collection of data on CrC_2H, we also recorded the spectrum of the minor isotopomer of chromium hydride, $^{50}Cr^1H$. We measured the excited state lifetime of this species, which is currently of considerable interest in astrophysics. This paper has now been published in the Astrophysical Journal.[3]

B. Infrared Spectroscopy of unsaturated transition metal carbonyls

We have completed the development of a slit-jet discharge source diode laser spectrometer for high-resolution investigations of unsaturated transition metal carbonyls. The device uses a slit orifice with a width of 200 μm and a length of 15 mm. A Teflon insulator separates the slit aperture from a pair of stainless steel discharge electrodes. During the operation of the pulsed valve, the discharge electrodes are biased to a negative potential, inducing a discharge in which electrons are accelerated into the slit channel, completing the circuit at the grounded slit nozzle body. Volatile organometallic molecules such as $Cr(CO)_6$, $Fe(CO)_5$, and $Ni(CO)_4$ seeded in the argon carrier gas, are exposed to the discharge, producing fragment species such as CrCO, $Cr(CO)_2$, $Cr(CO)_3$, etc.

Following supersonic expansion into vacuum, the beam of molecular fragments is crossed with the output of a lead-salt diode laser that is multipassed across the length of the slit jet expansion (currently 15 times) using a Perry cell. The transmitted laser intensity is detected using a HgCdTe detector. In order to increase the detection efficiency and discriminate against precursor molecule absorptions and noise, the discharge is pulsed at 15 kHz and the preamplified signal is detected using a lock-in detector.

In addition to the main IR laser beam, partial reflections are used to record (1) fringes from a 0.048 cm^{-1} free spectral range germanium étalon, and (2) the spectrum of a reference gas, typically OCS, N2O, or allene. These are used for absolute calibration of the instrument.

One year ago we reported that this system had been successfully tested using $Fe(CO)_5$, and that the CO stretching vibrations of FeCO and $Fe(CO)_2$, which had previously been reported, were readily detected. Since that time, we have succeeded in recording the spectrum of the ν_1 mode (CO stretch) of NiCO. The spectrum is displayed in Figure 1 below. Although the band origin portion of this spectrum could not be recorded, due to mode hops in all three diode lasers in our possession that cover this range, the band could still be assigned and fitted, using rotational constants recently obtained by a pure rotational spectroscopic study. The fitted constants from our study provide band origins of 2010.692 89(34) and 2010.645 28(23) cm^{-1} for $^{58}NiCO$ and $^{60}NiCO$, respectively. Rotational constants and bond lengths determined from the spectra are consistent with values reported from the millimeter wave spectroscopic study that was published in 2004.

In the course of collecting the NiCO spectrum, we also observed the spectrum of a molecule that depleted when the discharge was turned on. This was surprising, since the parent molecule, $Ni(CO)_4$ has no known transitions in this region. After some investigation, the

spectrum was determined to arise from the isotopically substituted species, $Ni(CO)_3(^{13}CO)$, which constitutes only 4% of the molecules in the sample. The ^{13}CO stretch of this isotopomer is shifted to lower frequencies, where it shows up as a parallel band, as displayed in Figure 2.

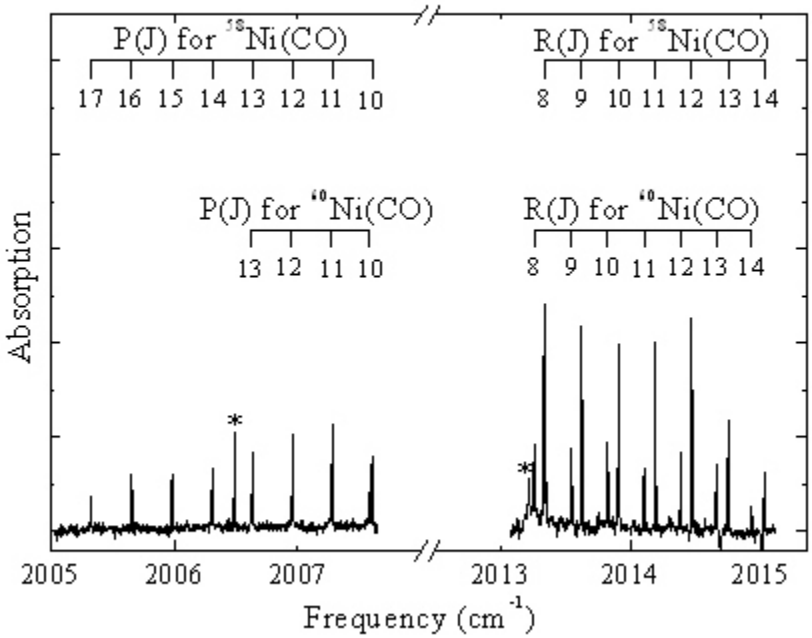

Figure 1. Rotationally resolved and assigned spectra of $^{58}NiCO$ and $^{60}NiCO$, in the CO stretching region.

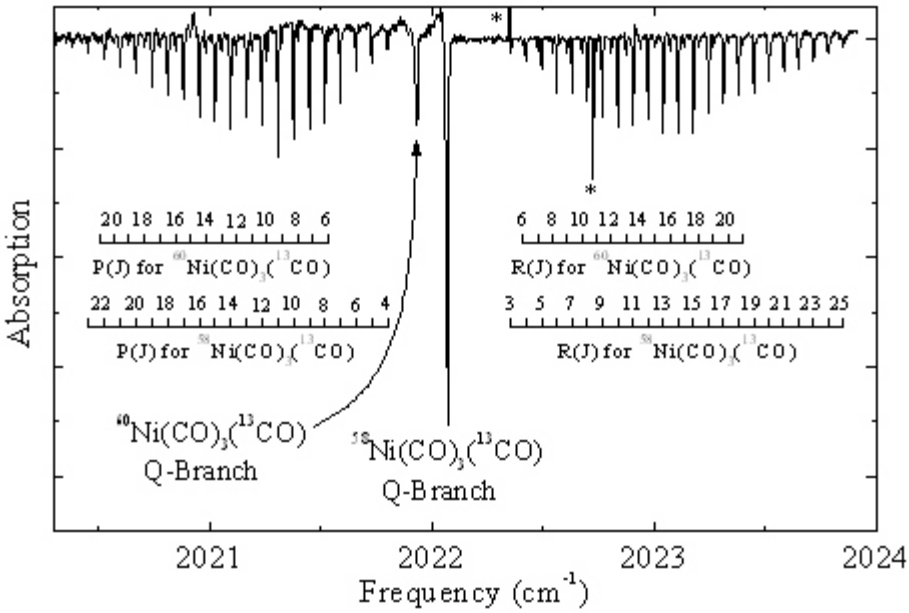

Figure 2. Rotationally resolved and assigned spectra of $^{58}Ni(CO)_3(^{13}CO)$ and $^{60}Ni(CO)_3(^{13}CO)$, in the ^{13}CO stretching region.

III. Future Plans

A. R2PI and DF spectroscopy of transition metal carbides and radicals

During the past year we have recorded spectra of a new band system of MoC, which we hope to rotationally resolve and report. We have recorded intense spectra of TiC, at high rotational temperatures, which are too complex to analyze readily. During the coming year, we plan to use dispersed single rovibronic level fluorescence to assign the rotational quantum numbers, thereby measuring the ground and excited state symmetries and rotational constants. This molecule is important for understanding the growth processes leading to formation of metallocarbohedrenes (met-cars). We also plan to study transition metal carbides that have high ionization energies, which have previously been inaccessible to studies employing the R2PI method. These molecules, which include CuC, AgC, AuC, OsC, and IrC, will now be accessible for study using the F_2 excimer laser for photoionization. We hope to obtain a satisfactory rotational analysis of the more complicated transition metal radicals CrC_2H and $NiCH_3$ as well

B. IR spectroscopy of unsaturated transition metal carbonyls

Having successfully recorded IR spectra of FeCO, $Fe(CO)_2$, and NiCO, we now plan to search for the spectra of other partially carbonylated metals. Luckily, the locations of strong IR absorptions are known from matrix isolation and some low-resolution gas phase studies. Target molecules to be sought are listed below, along with the expected IR frequencies:

Metal Monocarbonyl	Wavenumber	Metal Dicarbonyl	Wavenumber	Metal Tricarbonyl	Wavenumber
				$Fe(CO)_3$	1950 cm^{-1}
		$Ni(CO)_2$	1990 cm^{-1}	$Ni(CO)_3$	2030 cm^{-1}
CrCO	2010 cm^{-1}	$Cr(CO)_2$	1990 cm^{-1}	$Cr(CO)_3$	2000; 1880 cm^{-1}
MoCO	1890 cm^{-1}	$Mo(CO)_2$	1900 cm^{-1}	$Mo(CO)_3$	2000; 1888 cm^{-1}
WCO	1870 cm^{-1}	$W(CO)_2$	1890 cm^{-1}	$W(CO)_3$	1890 cm^{-1}

The aim of this work will be to establish the vibrational frequencies, rotational constants, geometries, bond lengths, and electronic symmetries of these molecules. After success on several of these molecules, we will move on to metal nitrosyls, such as CrNO, and NiNO.

IV. Publications from DOE Sponsored Research 2003-present:

1. N. F. Lindholm, D. A. Hales, L. A. Ober and M. D. Morse, "Optical spectroscopy of RuC: 18 000 - 24 000 cm-1," J. Chem. Phys. **121**, 6855-60 (2004).
2. D. J. Brugh, R. S. DaBell and M. D. Morse, "Vibronic spectroscopy of unsaturated transition metal complexes: CrC_2H, $CrCH_3$, and $NiCH_3$," J. Chem. Phys. **121**, 12379-85 (2004).
3. S. Shin, D. J. Brugh, and M. D. Morse, "Radiative lifetime of the v=0,1 levels of the $A^6\Sigma^+$ state of CrH," Astrophys. J. **619**, 407-11, (2004).
4. A. Martinez and Michael D. Morse, "Infrared Diode Laser Spectroscopy of Jet-Cooled NiCO and $Ni(CO)_3(^{13}CO)$," J. Chem. Phys., submitted.

New Single- and Multi-Reference Coupled-Cluster Methods for High Accuracy Calculations of Ground and Excited States

Piotr Piecuch
Department of Chemistry, Michigan State University, East Lansing MI 48824
E-mail: piecuch@cem.msu.edu

Program Scope

This research program focuses on new generations of predictive *ab initio* electronic structure methods and efficient general-purpose computer codes, exploiting coupled-cluster wave function ansatz, which can provide an accurate description of chemical reactions pathways, radicals, biradicals, and other reaction intermediates, molecular potential energy surfaces and properties other than energy, and electronic excitations in molecules. The goal is to develop accurate and affordable methods that enable precise modeling of processes and properties relevant to combustion, catalysis, and photochemistry, and important reaction mechanisms in areas such as organic chemistry. The main focus is on balancing high accuracy of the results, expected from predictive *ab initio* methods, with the ease of use and the relatively low computer cost of the proposed new approaches, so that applications do not have to be limited to small, few electron systems or small basis sets. The most promising methods developed in this research program include *renormalized coupled-cluster approaches* and other approximations employing the *method of moments of coupled-cluster equations* (MMCC), as well as *multi-reference coupled-cluster theories*. Renormalized coupled-cluster methods extend standard quantum-chemical approaches to potential energy surfaces involving biradicals, bond breaking, and excited states with an ease of a black-box calculation. Multi-reference coupled-cluster methods developed in this program are easy to use as well and have the flexibility that enables accurate calculations for all kinds of closed- and open-shell molecular systems with manageable computer costs.

Recent Progress

Background information. *Ab initio* electronic structure calculations, followed by dynamical and other types of molecular simulations, are nowadays recognized as a cornerstone for the in-depth understanding and successful modeling of chemical processes and properties. Novel quantum chemical approaches, which can accurately describe many-electron correlation effects, are critical for these studies. It is generally acknowledged that the theory that provides the best compromise between an accurate treatment of electron correlation effects and relatively low computer costs is coupled-cluster theory. The problem is that standard coupled-cluster methods, such as CCSD, CCSD(T), and EOMCCSD, work well only for non-degenerate systems and excited states dominated by one-electron transitions. One of the biggest challenges is to extend coupled-cluster methods to electronic quasi-degeneracies that occur when bond breaking, excited states dominated by two-electron transitions, and radicals, biradicals, and other open-shell systems are examined.

Recent results (2003-present). The renormalized coupled-cluster methods, such as CR-CCSD(T) , and other methods based on the aforementioned MMCC formalism, which we discovered in 2000 and incorporated in the GAMESS package in 2002, were initially developed for the ground electronic states only and most applications focused on bond breaking in singlet electronic states. Thus, we have extended the CR-CCSD(T) and other renormalized coupled-cluster methods to open-shell and excited states. One of the most promising methods that has resulted from this effort is CR-EOMCCSD(T). A few variants of the CR-EOMCCSD(T) theory for singlet excited states have been incorporated in GAMESS in 2004 and the efficient computer codes for the open-shell extension of the CR-EOMCCSD(T) method have already been developed. All of these new codes were used in various benchmark studies, including ground and excited states of the CH and OH radicals, ozone, C_2 and N_2 molecules, Be, BeH_2, Be_3, CH_2, and SiH_2, to mention a few examples, showing the ability of the inexpensive black-box CR-EOMCCSD(T) approach to describe excited states dominated by two-electron excitations with accuracies on the order of 0.1 eV, which cannot be achieved by other coupled-cluster methods characterized by the similarly low computer costs. The CR-CCSD(T) codes have also been extended to higher-order excitations, resulting in efficient CR-CCSD(TQ) approach (also included in GAMESS), which describes the combined effects of triply and quadruply excited clusters with computer costs that are only a few times larger than those characterizing the standard (and failing) CCSD(T) and CCSD(TQ) methods. The CR-CCSD(TQ) and other higher-order variants of the MMCC theory enable one to obtain very good results for multiple bond breaking and more severe cases of electronic near-degeneracies within a straightforward single-reference formalism. In particular, we found a formal way to merge the renormalized coupled-cluster methods with the extended CCSD method of Arponen and Bishop

and its analog developed by the PI and Bartlett, which provide better values of cluster amplitudes in cases of severe quasi-degeneracies characterizing multiple bond breaking. The resulting ECCSD(TQ) approach is capable of providing an accurate and effectively variational description of single- and multiple bond breaking with an ease of a single-reference calculation. We have also developed efficient coupled-cluster codes for the first-order reduced density matrices and properties of ground and excited states other than energy, including dipole and transition dipole moments, and integrated these codes in the most recent version of GAMESS.

The original renormalized coupled-cluster methods, such as CR-CCSD(T), provide great improvements in the description of biradicals and bond breaking compared to standard coupled-cluster methods of the CCSD(T) type, but they do it at the expense of slightly violating size extensivity. Since these methods will eventually be applied to systems with hundreds of electrons and thousands of basis functions (we have already successfully applied them to systems as big as Au_8 or $\{(NH_3)_3Cu\}_2O_2)^{2+}$, both of interest in catalysis), it is important to develop the rigorously size extensive extensions of the renormalized coupled-cluster methods. We have proposed two ideas in this regard. The first idea is that of the locally renormalized coupled-cluster methods, such as LR-CCSD(T), which are based on the numerator-denominator connected MMCC expansion and which lead to a size extensive description when local orbitals are employed. The LR-CCSD(T) and similar methods break chemical bonds as efficiently as the original CR-CCSD(T) and CR-CCSD(TQ) approaches, while eliminating small size extensivity errors from the CR-CCSD(T) and CR-CCSD(TQ) calculations. The second idea, which seems even more promising and which may lead to a new standard in coupled-cluster theory, is that of the biorthogonal MMCC expansion. Our preliminary analysis indicates that the resulting methods, such as CR-CCSD$(T)_L$, are not only rigorously size extensive and practical (i.e., applicable to larger many-electron systems), but they are also as accurate in studies of bond breaking as the prohibitively expensive full CCSDT (coupled-cluster singles, doubles, and triples) approach. The CR-CCSD$(T)_L$ and other methods based on the biorthogonal MMCC theory can also be extended to excited states, providing great improvements in calculations of states dominated by two-electron transitions.

The renormalized coupled-cluster methods have been applied to solve important chemical problems. In particular, in our most recent study of the mechanism of the [2+2] cycloaddition reaction of cyclopentyne to ethylene, which has remained unexplained for about 20 years, we demonstrated that unlike the previously used *ab initio* methods, the CR-CCSD(T) approach favors the concerted pathway involving a [2+1] transition state. Our findings agree with the experimentally observed stereochemistry. The popular CCSD(T) method, which is often regarded as the "gold standard" of electronic structure theory, and low-order multi-reference methods, such as CASSCF or CASMP2, support the less probable biradical mechanism which contradicts the observed stereochemistry. We have also demonstrated that in agreement with multi-reference perturbation theory and experiment, the CR-CCSD(T) method favors the concerted mechanism of the Cope rearrangement of 1,5-hexadiene involving an aromatic transition state. Again, the standard CCSD(T) approach fails in this case, favoring incorrect pathways through biradical structures. We have successfully resolved a controversy related to the discovery of a new, previously unknown, molecular species, HNOO, by accurately simulating its anharmonic vibrational spectrum which was incorrectly interpreted by one of the groups that claimed the discovery of HNOO (in collaboration with Professors Roger DeKock, Wesley Allen, and Henry F. Schaefer). We have performed unprecedented coupled-cluster calculations to address an issue of the relative stability of the clusters of up to eight gold atoms (in collaboration with Professors Mark Gordon, Horia Metiu, and co-workers), showing that the most stable structures of Au_n are planar for n=4,6 and non-planar for n=8, in sharp contrast with the results of calculations using density function theory, which predicts all three clusters to favor the planar configuration. We have carried our highly accurate calculations of the entire potential energy surface for the Be+HF reaction, including the Be+HF$\rightarrow$ BeF+H, BeH+F, and H-Be-F (bond insertion) channels using CR-CCSD(T) approach. We demonstrated that the resulting potential energy surface is as accurate as the potential surface resulting from the very expensive multi-reference configuration interaction calculations. We also demonstrated that the CR-CCSD(T) approach eliminates the failures of the CCSD(T) approach, which produces errors on the order of several eV in some regions of the BeFH potential energy surface. Our CR-EOMCCSD(T) codes for excited states have been used by us to explain the experiment by Roubin and collaborators, in which the UV radiation was used to photoisomerize acetyloacetone trapped in a nitrogen matrix. This experiment could not be understood before because of the lack of good calculations that would be consistent with the observed spectra.

In addition to the renormalized coupled-cluster methods, which can be viewed as single-reference computational black boxes that can be used by experts as well as non-experts, we have developed a few new ideas in the area of multi-reference coupled-cluster theory. In particular, after proposing the successful active-space coupled-cluster methods for excited electronic states, such as EOMCCSDt, we have extended these methods to excited states of radicals by combining the EOMCCSDt approach with the electron attached (EA) and ionized (IP) equation of motion coupled-cluster methods. The preliminary results for the ground and excited states of the CH and OH radicals are very promising. The new EA-EOMCCSDt and IP-EOMCCSDt methods provide the 0.1 eV or better accuracies for the electronic spectra of radicals with a computational effort similar to that of a standard CCSD calculation. We have also developed new classes of noniterative corrections to multi-reference coupled-cluster energies. The resulting methods can be viewed as extensions of the popular CCSD(T) approach to a genuine multi-reference formalism. They offer significant improvements in the results of multi-reference coupled-cluster calculations, particularly in the regions of potential energy surfaces plagued by intruders. We have also developed a pilot version of the new *ab initio* theory which combines the low-order multi-reference perturbation theory with the noniterative MMCC corrections to the CCSD energies. We have explored novel coding techniques. This effort has resulted in the automated implementation of parallel computer codes for CR-CCSD(T) and active-space CC methods, which were interfaced with the NWChem suite.

Finally, we have carried out the unprecedented, microscopic, and converged *ab initio* calculations for ground and excited states, and properties of closed- and open-shell nuclei, including the A=15-17 isotopes of oxygen, using new coupled-cluster methods developed in this research program for molecules and modern nucleon-nucleon interactions derived from effective field theory (in collaboration with Dr. David Dean). This shows that the highly accurate and relatively inexpensive quantum many-body methods developed by us are not limited to atoms and molecules. They have a range of applicability that crosses the boundaries between chemistry/biochemistry and physics, enabling us to study systems as small and as strongly bound as atomic nucleus and as large and as weakly bound as molecules and van der Waals species.

Future Plans

We will focus on the development of new, rigorously size extensive, renormalized coupled-cluster methods, which may set a new standard for high-level electronic structure calculations, since they are as accurate as the popular CCSD(T) approach, while eliminating the failures of CCSD(T) for biradicals and bond breaking. We will develop open-shell extensions of the size extensive renormalized coupled-cluster methods and work toward the development of analytic gradients for them. We will develop the electron-attached and ionized active-space coupled-cluster methods, which provide promising results for the electronic states of radicals with a small computer effort. We will develop new classes of multi-reference coupled-cluster methods, including perturbative and noniterative multi-reference coupled-cluster approaches. As in the past, the most practical and successful approaches will be incorporated in GAMESS. We will apply the resulting computer codes to challenging reaction mechanisms (e.g., the optical, geometrical, and structural isomerizations of cyclopropane, reactions involving OH radicals, Bergmann cyclizations, etc.), catalysis (e.g., structures of gold particles, oxygen activation by copper metalloenzymes), and molecular electronic spectra.

References (2003-present)

1. P. Piecuch, I.S.O. Pimienta, P.-F. Fan, and K. Kowalski, "New Alternatives for Electronic Structure Calculations: Renormalized, Extended, and Generalized Coupled-Cluster Theories," in: *Progress in Theoretical Chemistry and Physics*, Vol. 12, edited by J. Maruani, R. Lefebvre, and E. Brändas (Kluwer, Dordrecht, 2003), pp. 119-206.
2. P. Piecuch, K. Kowalski, P.-D. Fan, and K. Jedziniak, "Exactness of Two-Body Cluster Expansions in Many-Body Quantum Theory," *Phys. Rev. Lett.* **90**, 113001-1 - 113001-4 (2003).
3. I.S.O. Pimienta, K. Kowalski, and P. Piecuch, "Method of Moments of Coupled-Cluster Equations: The Quasi-Variational and Quadratic Approximations," *J. Chem. Phys*. **119**, 2951-2962 (2003).
4. K. Kowalski and P. Piecuch, "New Coupled-Cluster Methods with Singles, Doubles, and Noniterative Triples for High Accuracy Calculations of Excited Electronic States," *J. Chem. Phys.* **120**, 1715-1738 (2004).
5. R.L. DeKock, M.J. McGuire, P. Piecuch, W.D. Allen, H.F. Schaefer III, K. Kowalski, S.A. Kucharski, M. Musiał, A.R. Bonner, S.A. Spronk, D.B. Lawson, and S.L. Laursen, "The Electronic Structure and Vibrational Spectrum of Trans-HNOO," *J. Phys. Chem. A* **108**, 2893-2903 (2004).
6. P. Piecuch, K. Kowalski, I.S.O. Pimienta, P.-D. Fan, M. Lodriguito, M.J. McGuire, S.A. Kucharski, T. Kuś, and M. Musiał, "Method of Moments of Coupled-Cluster Equations: A New Formalism for Designing Accurate Electronic Structure Methods for Ground and Excited States," *Theor. Chem. Acc.* **112**, 349-393 (2004).
7. K. Kowalski, D.J. Dean, M. Hjorth-Jensen, T. Pappenbrock, and P. Piecuch, "Coupled-Cluster Calculations of Ground and Excited States of Nuclei," *Phys. Rev. Lett*. **92**, 132501-1 - 132501-4 (2004).

8. M.J. McGuire, P. Piecuch,K. Kowalski, S.A. Kucharski, and M. Musiał, "Renormalized Coupled-Cluster Calculations of Reactive Potential Energy Surfaces: The BeFH System," *J. Phys. Chem. A* **108**, 8878-8893 (2004).
9. K. Kowalski and P. Piecuch, "New Classes of Noniterative Energy Corrections to Multi-Reference Coupled-Cluster Energies," *Mol. Phys* .**102**, 2425-2449 (2004).
10. S. Hirata, P.-D. Fan, A.A. Auer, M. Nooijen, and P. Piecuch, "Combined Coupled-Cluster and Many-Body Perturbation Theories," *J. Chem. Phys*. **121**, 12197-12207 (2004).
11. R.M. Olson, S. Varganov, M.S. Gordon, S. Chretien, H. Metiu, P. Piecuch, K. Kowalski, S.A. Kucharski, and M. Musiał, "Where Does the Planar-to-Nonplanar Turnover Occur in Small Gold Clusters?," *J. Am. Chem. Soc.* **127**, 1049-1052 (2005).
12. M.J. McGuire and P. Piecuch, "Balancing Dynamic and Non-Dynamic Correlation for Diradical and Aromatic Transition States: A Renormalized Coupled-Cluster Study of the Cope Rearrangement of 1,5-Hexadiene," *J. Am. Chem. Soc.* **127**, 2608-2614 (2005).
13. K. Kowalski and P. Piecuch, "Extensive Generalization of Renormalized Coupled-Cluster Methods," *J. Chem. Phys.* **122**, 074107-1 - 074107-12 (2005).
14. C.D. Sherrill and P. Piecuch, "The X $^1\Sigma_g^+$, B $^1\Delta_g$, and B' $^1\Sigma_g^+$ States of C_2: A Comparison of Renormalized Coupled-Cluster and Multireference Methods with Full Configuration Interaction Benchmarks," *J. Chem. Phys.* **122**, 124104-1 - 124104-17 (2005).
15. R.K. Chaudhuri, K.F. Freed, G. Hose, P. Piecuch, K. Kowalski, M. Włoch, S. Chattopadhyay, D. Mukherjee, Z. Rolik, A. Szabados, G. Tóth, and P.R. Surján, "Comparison of Low-Order Multireference Many-Body Perturbation Theories," *J. Chem. Phys.* **122**, 134105-1 -134105-9 (2005).
16. D.J. Dean, J.R. Gour, G. Hagen, M. Hjorth-Jensen, K. Kowalski, T. Papenbrock, P. Piecuch, and M. Włoch, "Nuclear Structure Calculations with Coupled Cluster Methods from Quantum Chemistry," *Nucl. Phys. A* **752**, 299-308 (2005).
17. P.-D. Fan, K. Kowalski, and P. Piecuch, "Noniterative Corrections to Extended Coupled-Cluster Energies Employing the Generalized Method of Moments of Coupled-Cluster Equations," *Mol. Phys*. **103**, 2191-2213 (2005).
18. M. Włoch, J.R. Gour, K. Kowalski, and P. Piecuch, "Extension of Renormalized Coupled-Cluster Methods Including Triple Excitations to Excited Electronic States of Open-Shell Molecules," *J. Chem. Phys.* **122**, 214107-1 - 214107-15 (2005).
19. M. Włoch, D.J. Dean, J.R. Gour, P. Piecuch, M. Hjorth-Jensen, T. Papenbrock, and K. Kowalski, Ab Initio Coupled-Cluster Calculations for Nuclei Using Methods of Quantum Chemistry," *Eur. Phys. J. A Direct*; DOI: 10.1140/epjad/i2005-06-062-8.
20. M. Włoch, J.R. Gour, P. Piecuch, D.J. Dean, M. Hjorth-Jensen, and T. Papenbrock, "Coupled-Cluster Calculations for Ground and Excited States of Closed- and Open-Shell Nuclei Using Methods of Quantum Chemistry," *J. Phys. G: Nucl. Part. Phys.* **31**, S1291-S1299 (2005).
21. M. Włoch, D.J. Dean, J.R. Gour, M. Hjorth-Jensen, K. Kowalski, T. Papenbrock, and P. Piecuch, "Ab Initio Coupled-Cluster Study of ^{16}O," *Phys. Rev. Lett.* **94**, 212501-1 - 212501-4 (2005).
22. A. Kinal and P. Piecuch, "Is the Mechanism of the [2+2] Cycloaddition of Cyclopentyne to Ethylene Concerted or Biradical? A Completely Renormalized Coupled Cluster Study," *J. Phys. Chem. A*, Web Release Date: 22-Jun-2005; (Article) DOI: 10.1021/jp0513216.
23. K. Kowalski, S. Hirata, M. Włoch, P. Piecuch, and T.L. Windus, "Active-Space Coupled-Cluster Study of Electronic States of Be_3 Using Computer Generated Programs," *J. Chem. Phys.* **123**, 074319-1 - 074319-6 (2005).
24. D.J. Dean, M. Hjorth-Jensen, K. Kowalski, T. Papenbrock, M. Włoch, and P. Piecuch, "Coupled Cluster Approaches to Nuclei, Ground States and Excited States," in: Key Topics in Nuclear Structure, Proceedings of the 8th International Spring Seminar on Nuclear Physics, edited by A. Covello (World Scientific, Singapore, 2005), pp. 147-157.
25. P. Piecuch, M. Włoch, J.R. Gour, D.J. Dean, M. Hjorth-Jensen, and T. Papenbrock, "Bridging Quantum Chemistry and Nuclear Structure Theory: Coupled-Cluster Calculations for Closed- and Open-Shell Nuclei," in: *Nuclei and Mesoscopic Physics: Workshop on Nuclei and Mesoscopic Physics WNMP 2004, AIP Conference Proceedings*, Vol. 777, edited by V. Zelevinsky (AIP Press, 2005), pp. 28-45.
26. M.D. Lodriguito, K. Kowalski, M. W{\l}och, and P. Piecuch, "Non-Iterative Coupled-Cluster Methods Employing Multi-Reference Perturbation Theory Wave Functions," *J. Mol. Struct: THEOCHEM*, in press.
27. P. Piecuch, S. Hirata, K. Kowalski, P.-D. Fan, and T.L. Windus, "Automated Derivation and Parallel Computer Implementation of Renormalized and Active-Space Coupled-Cluster Methods," *Int. J. Quantum Chem*., in press.
28. J.R. Gour, P. Piecuch, and M. Włoch, "Active-Space Equation-of-Motion Coupled-Cluster Methods for Excited States of Radicals and Other Open-Shell Systems: EA-EOMCCSDt and IP-EOMCCSDt," *J. Chem. Phys.*, in press.
29. D.J. Dean, M. Hjorth-Jensen, K. Kowalski, P. Piecuch, and M. Włoch, "Coupled-Cluster Theory for Nuclei," in: *Condensed Matter Theories*, edited by J. Clark and R. Panoff (Nova Science Publishers, 2005), pp. XX-XXX, in press.
30. P. Piecuch, M. Włoch, M. Lodriguito, and J.R. Gour, "Noniterative Coupled-Cluster Methods for Excited Electronic States," in: *Progress in Theoretical Chemistry and Physics*, Vol. XXX, edited by S. Wilson, J.-P. Julien, J. Maruani, E. Brändas, and G. Delgado-Barrio (Springer, Berlin, 2005), in press.
31. P. Piecuch, I.S.O. Pimienta, P.-D. Fan, and K. Kowalski, "New Alternatives for Accurate Electronic Structure Calculations of Potential Energy Surfaces Involving Bond Breaking," in: *Recent Progress in Electron Correlation Methodology, ACS Symposium Series*, Vol. XXX, edited by A.K. Wilson (American Chemican Society, Washington, D.C., 2006), in press.
32. J.R. Gour, P. Piecuch, M. Hjorth-Jensen, M. Włoch, and D.J. Dean, "Coupled-Cluster Calculations for Valence Systems around ^{16}O, Phys. Rev. C, submitted (in revision).
33. J.R. Gour, P. Piecuch, and M. Włoch, "Extension of the Active-Space Equation-of-Motion Coupled-Cluster Methods to Radical Systems: The EA-EOMCCSDt and IP-EOMCCSDt Approaches," Int. J. Quantum Chem., submitted.
34. P. Piecuch and M. Włoch, "Renormalized Coupled-Cluster Methods Exploiting the left Eigenstates of the Similarity-Transformed Hamiltonian," *J. Chem. Phys*., submitted.

Radiation-induced Dynamics in the Condensed Phase

Simon M. Pimblott, Jay A. LaVerne, Daniel M. Chipman and Ian Carmichael
pimblott.1@nd.edu, laverne.1@nd.edu, chipman.1@nd.edu, carmichael.1@nd.edu
Radiation Laboratory, University of Notre Dame, Notre Dame, IN 46556

Program Scope

Fundamental processes of radiation chemistry are investigated from their earliest stages using a multi-facetted approach employing experiments in conjunction with Monte Carlo track chemistry modeling and electronic structure calculations. The goal is to determine mechanisms, kinetics, and yields in the radiolysis of aqueous and hydrocarbon based systems. Challenges associated with these types of chemical systems are found throughout the DOE portfolio. For instance, radiation effects due to the mixed radiation fields of nuclear reactors or to the self-radiolysis by α-particles from transuranic waste materials are different from those induced by γ-rays and fast electrons, because of fundamental chemical processes.

Recent Progress

Experimental measurements in coordination with Monte Carlo track chemistry calculations have examined the yield of the hydrated electron in the radiolysis of water with protons, helium ions and carbon ions. Glycylglycine, in concentrations ranging from 10^{-4} to 1 M, was employed as a scavenger for e_{aq}^-. (1)

$$^+NH_3CH_2CONHCH_2CO_2^- + e_{aq}^- + H_2O \rightarrow {}^\bullet CH_2CONHCH_2CO_2^- + NH_4^+ + OH^-$$

The inverse Laplace transform of the scavenging capacity dependence gives a reasonably accurate description of the time dependence of the transient species for heavy ion radiolysis. (2) Therefore, the quantitative production of the ammonium cation is a probe of hydrated electron yields from about 2 ns to 20 μs. Monte Carlo track chemistry simulations of product yields reproduce experimental observations, providing detailed information used to elucidate the heavy ion track physics and chemistry. Comparison of the heavy ion results with those found in γ radiolysis shows intra-track reactions are significant on the nanosecond to microsecond time scale as the ion track relaxes, and that a constant (escape) yield is not attained on this time scale. Numerical interpolation techniques gave both track average and track segment yields for use in practical applications or for comparison with other models. The model results also gave the first hints that initial (~ 5 ps) hydrated electron yields, and possibly other water decomposition products, are dependent on the type and energy of the incident radiation.

Heavy ion tracks have a very different structure from the tracks of low-LET ^{60}Co γ and fast electron radiation. As a radiation particle passes through liquid, it produces a track of highly reactive radicals and ions in a nonhomogeneous spatial distribution. These species undergo fast diffusion limited chemistry, which depends critically on the type and energy of the ionizing radiation. (3) The nonhomogeneous kinetics reflect the competition between the diffusive relaxation of the spatial distribution and the chemical reactions of the radicals and ions and give the most direct experimental information about the transfer of energy from the radiation particle to the liquid. The figure on the following page shows the evolution of a ^{3}H β track in water. The snapshots are from calculations using stochastic simulation techniques to investigate the physical and chemical factors observed to influence experimental radiation chemistry. Track structure studies provide a detailed description of ion tracks as a function of both incident particle type and velocity, specifically:

- the dependence of the spatial distribution of the energy deposition – local dose – upon the properties of the primary radiation particle, e.g. energy, charge, LET, etc.;

- the influence of the resulting spatial non-homogeneity on the chemistry of the radiation-induced radicals and molecular products; and
- the effect of track structure on the radiation chemistry of scavenging in concentrated aqueous systems.

These techniques are being used to analyze experimental radiation chemical data.

A better understanding of the ultrafast fragmentation phenomena occurring prior to solvent re-equilibration or diffusion is necessary for truly realistic stochastic modeling of radiation effects. Calculations showed that the first electronically excited state of water, which in the gas phase is dissociative along an OH coordinate, changes its nature when the OH is involved in a hydrogen bond with another water molecule in an ice-like arrangement. The previous finding that the excited potential energy curve becomes insensitive to small extensions of the OH bond has been generalized in two directions. Using higher level calculations, it was established that for larger extensions of the OH bond there is a barrier to dissociation. It was also demonstrated that this behavior is the rule rather than the exception for a large set of distorted geometries representative of liquid water configurations. This work implies that an exciton may exist with long enough lifetime to allow for migration of energy over substantial distances as has been postulated following recent experiments with water ice. (4)

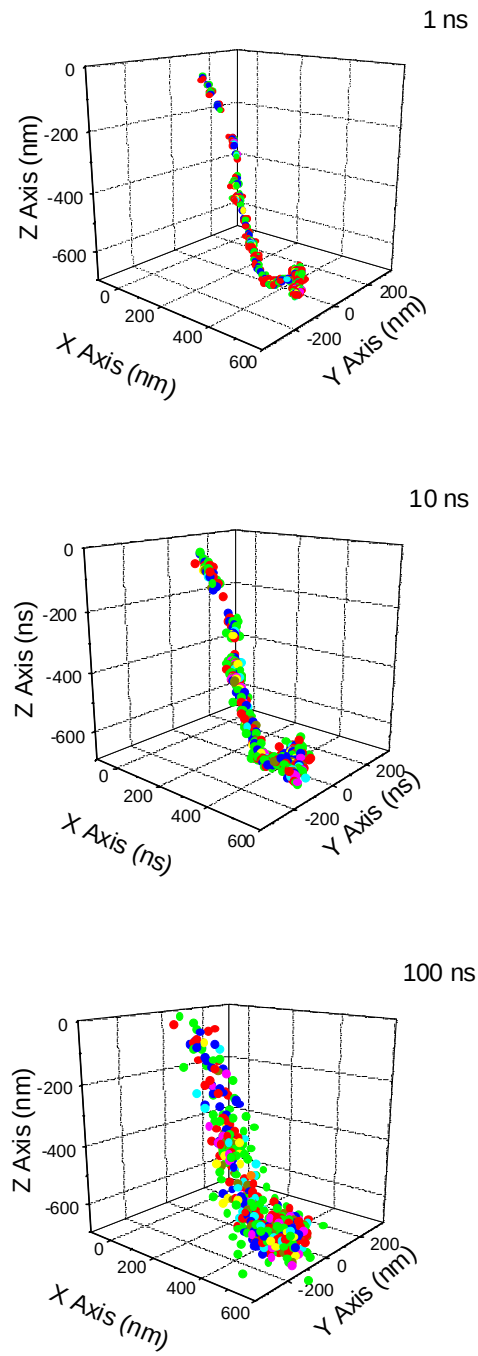

Evolution of a ^{3}H β track in water:
(•) e_{aq}^-; (•) H_3O^+; (•) OH; (•) H; (•) H_2; (•) OH^-; (•) H_2O_2; (•) $O(^1D)$ and $O(^3P)$

A combined experimental and theoretical approach was used to probe the radiolytic decomposition of liquid pyridine. The major single condensed phase product in the γ-radiolysis of pyridine is dipyridyl with a yield of 1.25 molecules/100 eV total energy absorbed. Scavenging studies suggest that most, if not all, dipyridyl has a radical precursor, but only about 10% of that is due to the pyridyl radical. The remainder of the dipyridyl may be due to reaction of the parent radical cation with pyridine. Iodine scavenging and quantum chemical

calculations both show that the ortho-pyridyl radical (2-pyridyl) is far more stable than the other two isomers.

Future Plans

Major questions remain about the physical, physico-chemical and chemical processes that occur in a radiation track on the sub-picosecond time scale. (5) The poorly understood energetics and fragmentation patterns of the molecular cation, H_2O^+, in water will be studied with electronic structure methods. To model the situation in the liquid phase, small water clusters will be explicitly treated together with implicit solvation models (6) that describe bulk effects by surrounding the clusters with dielectric continuum. All the available dissociation channels in low-lying states of the cation will be investigated, particularly focusing on the ultrafast deprotonation that produces OH and H_3O^+. It has recently been shown (7) that about 70% of the total molecular hydrogen ultimately produced in the gamma-radiolysis of water originates from a previously unrecognized ultrafast process. Possible explanations involving dissociative electron recombination with H_2O^+ will be studied along with alternatives such as dissociative electron recombination with H_3O^+. (8) The information obtained from *ab initio* theoretical studies will guide stochastic simulations employing simulated fast electron and heavy ion track structures to study the ultra-fast reaction of the molecular cation of water with an adjacent water molecule to give H_3O^+ and OH radical, which is the dominant source of OH in liquid water radiolysis. There is no definitive observation of H_2O^+ in liquid water. The rate coefficient of the proton transfer reaction in the gas phase suggests a lifetime of ~18 fs at the density of liquid water. (9) Furthermore, theoretical calculations for the water dimer give a lifetime of 30-80 fs. (10) Monte Carlo track chemistry simulations will be made employing a range of lifetimes from 10–100 fs, and the results analyzed by comparison with experimental studies on the scavenger kinetics of OH radical decay and H_2O_2 formation. Further calculations will consider the scavenging of the molecular cation, looking at the ultra-fast formation of Br_2^- in concentrated Br^- solution and at the effect of concentrated nitrate solutions on the yield of H_2O_2.

Elucidation of the radiolysis of well-defined organic systems is important in understanding radiation damage of polymers and the radiation-induced degradation of organic solvents as these effects are central to matrix degradation and hazardous gas production in the storage and handling of radioactive waste associated with organic materials. Very few hydrocarbon systems have been examined in detail to obtain a mechanistic description including all of the radiation processes from the initial molecular ionization to final product formation. Monte Carlo track models for the radiolytic chemistry of organic media will be developed in conjunction with experimental observations and incorporating the results of quantum chemical computations undertaken to predict the relative amounts of the molecular radicals.

References

1) J.A. LaVerne & H. Yoshida, H. *J Phys. Chem.* **1993**, *97*, 10720.
2) S.M. Pimblott & J.A. LaVerne, *J. Phys. Chem.*, **1992**, *96*, 746-752.
3) S.M. Pimblott & J.A. LaVerne, *J. Phys. Chem. A*, **2002**, *106*, 9420-7.
4) N. G. Petrik and G. A. Kimmel, *Phys. Rev. Lett.* **2003**, *90*, 166102-1-4.
5) *Fundamental Studies on Effects of Ionizing Radiation: Primary Processes*, in "Research Needs and Opportunities in Radiation Chemistry", eds. P.Barbara, S.M. Pimblott, A.D. Trifunac, G. Choppin, C. Creutz, & P.V. Kamat, DOE Report DOE/SC-0003, **1999**.
6) D.M. Chipman, *J. Chem. Phys*. **2004**, *120*, 5566-75; F. Chen & D.M. Chipman, *J. Chem. Phys.* **2003**, *119*, 10289-97; D.M. Camaioni, M. Dupuis & J. Bentley, *J. Phys. Chem. A*, **2003**, *107*, 5778-88; D.M. Chipman, *J. Chem. Phys*. **2003**, *118*, 9937-42;

7) B. Pastina, J. A. LaVerne and S. M. Pimblott *J. Phys. Chem. A*, **1999** *103*, 5841-5846.
8) J. A. LaVerne and S. M. Pimblott *J. Phys. Chem. A*, **2000,** *104*, 9820-9822.
9) B.R. Rowe, F. Vallee, J.L. Queffelec, J.C. Gomet & M. Morlais, *J. Chem. Phys.* **1988**, *88*, 845-50.
10) H. Tachikawa , *J. Phys. Chem. A.* **2002**, *106*, 6915-21.

BES Sponsored Publications in 2003-2005

1) J.A. LaVerne, I. Štefanić, S.M. Pimblott**, "**Hydrated Electron Yields in the Heavy Ion Radiolysis of Water", *J. Phys. Chem. A*, **2005**, in press.
2) J.A. La Verne, I. Carmichael and M.S. Araos "Radical Production in the Radiolysis of Liquid Pyridine", *J. Phys. Chem. A* **2005**, *109*, 461.
3) D.M. Chipman, "Excited electronic states of small water clusters', *J. Chem. Phys.* **2005,** *122*, 044111.
4) B.C. Garrett, D.A. Dixon, D.M. Camaioni, D.M. Chipman, M.A. Johnson, C.D. Jonah, G.A. Kimmel, J.H. Miller, T.N. Rescigno, P.J. Rossky, S.S. Xantheas, S.D. Colson, A.H. Laufer, D. Ray, P.F. Barbara, D.M. Bartels, K.H. Becker, K.H. Bowen, S.E. Bradforth, I. Carmichael, J.V. Coe, L.R.Corrales, J.P. Cowin, M. Dupuis, K.B. Eisenthal, J.A. Franz, M.S.Gutowski, K.D. Jordan, B.D. Kay, J.A. LaVerne, S.V. Lymar, T.E. Madey, C.W. McCurdy, D. Meisel, S. Mukamel, A.R. Nilsson, T.M. Orlando, N.G.Petrik, S.M. Pimblott, J.R. Rustad, G.K. Schenter, S.J. Singer, A. Tokmakoff, L.-W. Wang, C. Wittig, & T.S. Zwier, "The Role of Water on Electron-Initiated Processes and Radical Chemistry: Issues and Scientific Advances", *Chemical Reviews*, **2005**, *105*, 355-89.
5) P. Wisniowski; K. Bobrowski; I.Carmichael; G.L. Hug "Bimolecular homolytic substitution (S(H)2) reactions with hydrogen atoms. Time-resolved electron spin resonance detection in the pulse radiolysis of ±-(methylthio)acetamide", *J. Amer. Chem. Soc.*, **2004**, *126*, 14468-74.
6) N.R. Brinkmann; I. Carmichael "B3LYP investigation of HPO_2, *trans*-HOPO, *cis*-HOPO, and their radical anions", *J. Phys. Chem. A*, **2004**, *108*, 9390-99.
7) G.L.Hug; D.M. Camaioni; I. Carmichael "EPR detection of HNO_2^- in the radiolysis of aqueous nitrite and quantum chemical calculation of its stability and hyperfine parameters", *J. Phys. Chem. A*, **2004**, *108*, 6599-604.
8) R.M. Macrae; I. Carmichael "Comparative theoretical study of Mu addition to the C=O and C=S bonds", *Physica B-Condensed Matter*, **2004**, *326*, 81-84.
9) J.A. La Verne, I. Stefanic, and S.M. Pimblott "Hydrated Electron Yields in the Radiolysis of Water with Protons"; *Proceedings of the Japanese Society for Radiation Chemistry*, **2004**, Hokkaido University, Soporro, Japan.
10) J.A. La Verne "Radiation Chemical Effects of Heavy Ions." in *Charged Particle and Photon Interactions with Matter*; Mozumder, A., Hatano, Y., Eds.; Marcel Dekker, Inc: New York, **2004**; pp 403.
11) S.M. Pimblott & A. Mozumder, "Modelling of Physicochemical and Chemical Processes in the Interaction of Fast Charged Particles with Matter." in *Charged Particle and Photon Interactions with Matter*; Mozumder, A., Hatano, Y., Eds.; Marcel Dekker, Inc: New York, **2004**; pp75-101.
12) A. Alba García, L.D.A. Siebbeles, H. Schut, A. van Veen & S.M. Pimblott, "Positronium formation polyethylene: a computer simulation study", *Radiat. Phys. Chem.*, **2003**, *68*, 623-25.

Molecular Theory & Modeling

Development of Statistical Mechanical Techniques for Complex Condensed-Phase Systems

Gregory K. Schenter
Chemical Sciences Division
Pacific Northwest National Laboratory
902 Battelle Blvd.
Mail Stop K1-83
Richland, WA 99352
greg.schenter@pnl.gov

Program Scope

The long-term objective of this project is to advance the understanding of the relation between detailed descriptions of molecular interaction and the prediction and characterization of macroscopic collective properties. To do this, we seek to better understand the relation between the form and representation of intermolecular interaction potentials and simulation techniques required for statistical mechanical determination of properties of interest. Molecular simulation has the promise to provide insight and predictive capability of complex physical and chemical processes in condensed phases and interfaces. For example, the transport and reactivity of species in aqueous solutions, at designed surfaces, in clusters and in nanostructured materials play significant roles in a wide variety of problems important to the Department of Energy.

We start from the premise that a detailed understanding of the intermolecular interactions of a small collection of molecules, through appropriate modeling and statistical analysis, will enable us to understand the collective behavior and response of a macroscopic system, thus allowing us to predict and characterize thermodynamic, kinetic, material, and electrical properties. Our goal is to improve understanding at the molecular level in order to address increasingly more complex systems ranging from homogeneous bulk systems to multiple phase or inhomogeneous ones, to systems with external constraints or forces. Accomplishing this goal requires understanding and characterization of the limitations and uncertainties in the results, thereby improving confidence in the ability to predict behavior as systems become more complex.

Recent Progress

In developing interaction potentials, we have recently focused on the relation between accurate *ab initio* electronic structure calculations of aqueous ion clusters, x-ray absorption fine structure measurements and empirical potentials used in molecular simulation. Initially we studied the extended x-ray absorption fine structure (EXAFS) of dilute solutions of Ca^{2+} and Sr^{2+} in water and methanol. [6] Using classical molecular dynamics simulation (MD) techniques and polarizable potential models, we provided a detailed study of the solvation structure of dilute Ca^{2+} and Sr^{2+}-water solutions. We developed a set of polarizable ion-solvent interactions that accurately describes the hydration enthalpy, the coordination numbers and the peak locations of the ion-solvent radial distribution functions. Simulated MD-EXAFS spectra were found to be in good agreement with corresponding experimental measurements. Using similar techniques, the analysis was extended to the study of aqueous K^+ solvation. [13] In both of these studies, subtle

differences were observed between the experimental and theoretical structure of the ion-water interactions in solution. (See Figure 1.)

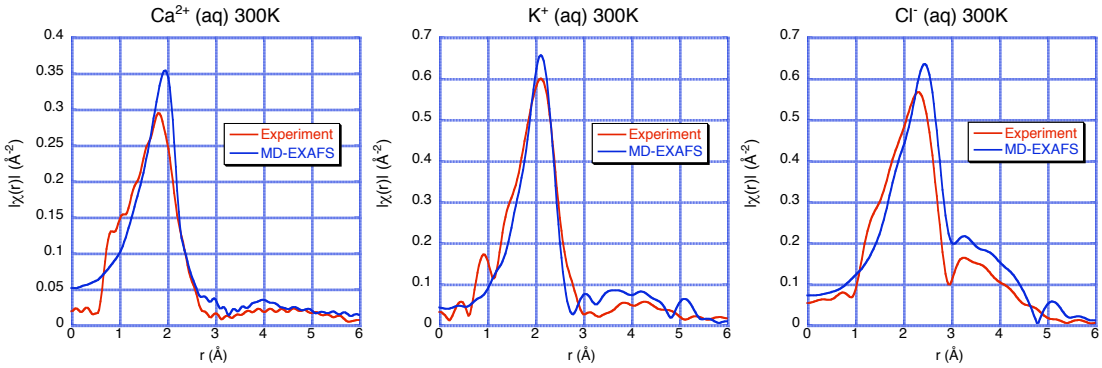

Figure 1. Fourier transform of EXAFS. Comparison of experimental measurement and simulation using an empirical potential at 300K.

The width of the first peak in the ion – oxygen radial distribution function, the Debye-Waller factor (DWF), σ^2, was consistently smaller than that determined from EXAFS measurement. In an attempt to better understand this difference a series of *ab initio* electronic structure calculations of aqueous ion clusters were performed. A harmonic analysis of the DWF was performed for the clusters. Similar analysis was performed for the empirical potential. (See Figure 2(a).) The electronic structure values for the DWF were larger than the values determined from the empirical potential. For practical considerations the electronic structure calculations were limited to a harmonic analysis. Doing simulations using the empirical potential tested the role of anharmonicity. We found that there is a universal relation between the DWF and the ion-oxygen distance that is recovered by the harmonic analysis. (See Figure 2(b).) A procedure was developed that shows that the electronic structure results of the clusters are consistent with experimental measurement of the bulk solvation. Future plans will explore modifications to the empirical potential to improve agreement with experimental measurement.

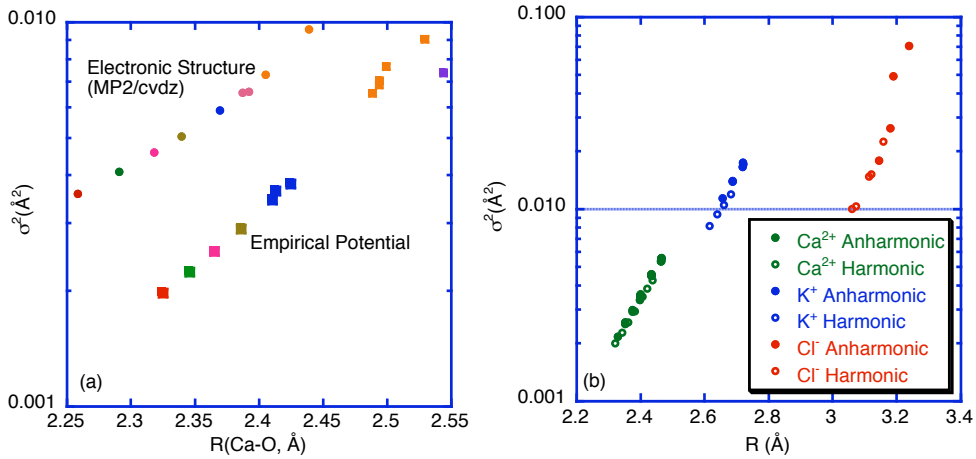

Figure 2 (a). Harmonic DWF versus Ca-O distance for $Ca^{2+}(H_2O)_n$ clusters, n=1-7, at 300K. (b). DWF versus Ion-O distance for $Ca^{2+}(H_2O)_n$, $K^+(H_2O)_n$ and $Cl^-(H_2O)_n$ clusters, comparing anharmonic analysis to harmonic analysis using an empirical potential.

Future Plans

Initial analysis was also carried out on Cl^- solvation using a polarizable ion-solvent interaction that accurately describes the hydration enthalpy, the coordination numbers and the peak locations of the ion-solvent radial distribution functions. The simulated MD-EXAFS spectrum was found to be in good agreement with corresponding experimental measurement. (See Figure 1.) In future studies we will refine our description of ion-solvent interaction in the low concentration limit as we explore the relation between *ab initio* electronic structure calculations of clusters and EXAFS measurement, seeking consistency between the approaches. In the next stage of development we will consider the influence of molecular interaction between ion-pairs. Our challenge is to be able to account for changes in features in EXAFS measurement as a function of solute concentration. Initial simulations of the concentration dependence of HCl EXAFS will allow us to better characterize H_3O^+ Cl^- ion pairing in aqueous solution. Can this interaction be effectively described using an empirical potential? In future studies we will concentrate on $CaCl_2$ and AgCl solutions as electronic structure calculations and experimental EXAFS measurements are being performed.

In an effort to develop more robust representations of intermolecular interaction, we continue to explore the use of semiempirical self-consistent field (SCF) methods. Neglect of differential diatomic overlap (NDDO) methods that include such parameterizations as MNDO, AM1, and PM3, have the ability to treat the formation and breaking of chemical bonds, but have been found to poorly describe hydrogen bonding and weak electrostatic complexes. In contrast, most empirical potentials are not able to describe bond-breaking and formation, but have the ability to add missing elements of hydrogen bonding using classical electrostatic interactions. We continue to develop a method that combines aspects of both NDDO-based SCF techniques and classical descriptions of polarization to describe the diffuse nature of the electronic wavefunction in a self-consistent manner. We have developed the self-consistent polarization NDDO (SCP-NDDO) theory with the additional description of molecular dispersion developed as a second-order perturbation theory expression. Initial efforts using this approach have allowed us to parameterize the model to reproduce the accurate MP2/CBS estimates of small water cluster binding energies of Xantheas *et al*, as well as the intramolecular frequency shifts as a function of cluster size. Initial steps have been made to parameterize protonated and hydroxide water clusters. Future efforts will extend the parameterization to aqueous solvation of more complex ions.

Collaborators on this project include B. C. Garrett, S. M. Kathmann, S. S. Xantheas, and L. X. Dang, V.-A. Glezakou, John Fulton, Yongsheng Chen, T. D. Iordanov and D. T. Chang. Battelle operates Pacific Northwest National Laboratory for the U. S. Department of Energy.

References to publications of DOE sponsored research (2003-present)

1. B. C. Garrett, S. M. Kathmann, and G. K. Schenter, "Thermochemistry and Kinetics of Small Water Clusters," in Water in Confining Geometries, edited by V. Buch and J. P. Devlin, (Springer-Verlag, New York, 2003) p. 25.
2. Y. D. Suh, G. K. Schenter, L. Zhu, and H. P. Lu, "Probing nanoscale surface enhanced Raman-scattering fluctuation dynamics using correlated AFM and confocal ultramicroscopy," *Ultramicroscopy* **97**, 89-102 (2003).

3. L. Zhu, G. K. Schenter, M. Micic, Y. D. Suh, N. Klymyshyn, and H. P. Lu, "Nanosurface-enhanced Raman scattering fluctuation dynamics," in *Proceedings of SPIE*, **4962**, "Manipulation and Analysis of Biomolecules, Cells, and Tissues," edited by D. V. Nicolau, J. Enderlein, R. C. Leif, and D. L. Farkas, (SPIE, Bellingham, WA, 2003) p. 70.
4. M. Dupuis, G. K. Schenter, B. C. Garrett, and E. E. Arcia, "Potentials of mean force with ab initio mixed Hamiltonian models of solvation," *Journal of Molecular Structure (THEOCHEM)* **632**, 173 (2003).
5. G. K. Schenter, B. C. Garrett, and D. G. Truhlar, "Generalized transition state theory in terms of the potential of mean force," *Journal of Chemical Physics* **119**, 5828-5833 (2003).
6. L. X. Dang, G. K. Schenter and J. Fulton, "EXAFS spectra of the dilute solutions of Ca^{2+} and Sr^{2+} in water and methanol," *Journal of Physical Chemistry B* **107**, 14119 (2003).
7. M. P. Hodges, R. J. Wheatley, G. K. Schenter, and A. H. Harvey, "Intermolecular potential and second virial coefficient of the water-hydrogen complex," *Journal of Chemical Physics* **120**, 710 (2004).
8. S. M. Kathmann, G. K. Schenter, and B. C. Garrett, "Multicomponent dynamical nucleation theory and sensitivity analysis," *Journal of Chemical Physics* **120**, 9133-9141 (2004).
9. J. L. Daschbach, G. K. Schenter, P. Ayotte, R. S. Smith, and B. D. Kay, "Helium diffusion through H_2O and D_2O amorphous ice: Observation of a lattice inverse isotope effect," *Physical Review Letters* **92**, 198306 (2004).
10. S. M. Kathmann, G. K. Schenter, and B. C. Garrett, "Dynamical Nucleation Theory: Understanding the Role of Aqueous Contaminants," in Proceedings of the 16th International Conference on Nucleation and Atmospheric Aerosols, edited by M. Kulmala and M. Kasahara (Kyoto University Press, 2004), p. 243-246.
11. S. M. Kathmann, G. K. Schenter, and B. C. Garrett, "Ion-Induced Nucleation: The Importance of Chemistry," *Physical Review Letters* **94**, 116104 (2005).
12. B. C. Garrett, D. A. Dixon, *et al* "The Role of Water on Electron-Initiated Processes and Radical Chemistry: Issues and Scientific Advances," *Chemical Reviews* **105**, 355 (2005).
13. V. -A. Glezakou, Y. C. Chen, J. L. Fulton, G. K. Schenter and L. X. Dang "Electronic Structure, Statistical Mechanical Simulations, and EXAFS Spectroscopy of Aqueous Potassium" Theoretical Chemistry Accounts (in press 2005).
14. T. D. Iordanov, G. K. Schenter, and B. C. Garrett, "Sensitivity Analysis of Thermodynamics Properties of Liquid Water: A General Approach to Improve Empirical Potentials," *Journal of Physical Chemistry* (in press 2005).

Reactive Intermediates in High Energy Chemistry.

Principal Investigators: Ilya A. Shkrob,* Robert A. Crowell, and David Gosztola

Radiation and Photochemistry Group, Chemistry Division, Argonne National Laboratory, Argonne, Illinois 60439; tel.: 630-2529516; FAX: 630-2524993; e-mail: shkrob@anl.gov

1. Program Scope.

Our twofold goal is (i) to study localization, thermalization, and chemical transformations of short-lived reaction intermediates (e.g., electrons and holes) generated by ionization, electron detachment, and other energetic processes in condensed media and (ii) to characterize the structure and dynamics of trapped charges (e.g., excess electrons) in liquids, solids, and oxide nanomaterials. Of special interest are chemical processes initiated by high-power lasers and accelerated particles. The excitation and ionization events in radiolysis are clustered in nanodomains called spurs. We are "dissecting" these spurs and learning about the rapid, concerted processes occurring in the initial phase of their evolution. Presently, the main approach is modeling such processes using ultrashort laser pulses. The methods include pump-probe spectroscopy, pulse radiolysis, time-resolved conductivity, and magnetic resonance. The use of fast and slow techniques, short-pulse lasers and particle accelerators, addressing both the kinetic and structural aspects of the chemistry, and theoretical modeling are the constitutents of our multifaceted approach. Our ability to pursue such comprehensive studies will soon be aided by a 10 TW table-top laser system capable of generating subpicosecond electron pulses (T3 system). Once this T3 system is operational, spurs on the picosecond time scale will be studied. Most of the group effort is currently focused on the development of this T3 system, yet we vigorously pursue the research on the reactive intermediates in radiolysis and photolysis, as summarized below.

2. Progress report.

The studies completed during the previous year were reviewed in the 2004 CPIMS report. These studies focused on rapid, energetic processes in aqueous systems. The aim of our present ultrafast studies on such systems is H-OH dissociation that follows three photon UV excitation of liquid water. Understanding of these dynamics is required for modeling the evolution of radiolytic spurs and water photolysis. So far, there were no experimental or theoretical studies of the dynamics of water photodissociation in liquid phase. We are also completing, in collaboration with S. E. Bradforth of USC, a detailed study of charge transfer to solvent (CTTS) reactions involving photoexcited aqueous anions, including many common polyvalent anions (this research was partially summarized in our 2004 report). This report summarizes our recent progress in understanding of the nature and the dynamics of excess electrons in *nonpolar* media.

2.1. Photo-Stimulated Electron Detrapping and the Two-State Model for Electron Transport in Nonpolar Liquids.

The mechanism for charge conduction and radiation- and field- induced dielectric breakdown in nonpolar liquids and solids (which are common insulating materials) present considerable

practical interest. In such media, there is usually a dynamic equilibrium between trapped (localized) and quasifree (extended) states of the excess electron (the so-called "two-state model"). These equilibria are very rapid and thus difficult to study. The recent time-domain time-resolved THz studies from T. F. Heinz' group at Columbia University suggested that a drastic revision of the two-state models for electron conduction is needed since the properties of quasifree electrons observed using the THz spectroscopy appeared to be very different from those expected from the previous, less direct studies. Our study [1] vindicates the established picture of electron conduction and shows how the unanticipated THz observations can be interpreted within this standard picture. Using time-resolved d.c. conductivity, IR photoexcitation of trapped electrons in saturated hydrocarbons was studied. The light promotes the electron from the trap into the conduction band of the liquid. From the analysis of the two-pulse, two-color photoconductivity data, the life time of the electrons in traps has been estimated as 10 ps. The estimated localization time of the quasifree electron is 20-50 fs; both of these time estimates (for localization and thermal detrapping) are in agreement with the "quasiballistic" model of Mozumder. The localization time is much shorter than 300 fs estimated using THz spectroscopy for the same systems. The properties of trapped electrons in hydrocarbon liquids were accounted for using the simple electron bubble model. The THz signal actually originates from the oscillations of these electron bubbles rather than the oscillations of free-electron plasma; vibrations of these bubbles are responsible for the deviations from the Drude behavior observed below 0.4 THz. Various implications of these results have been analyzed.

2.2. Cluster Chemistry in Dilute Solution: Electron Trapping by Polar Molecules in Alkane Liquids and Electron Encapsulation.

Are there condensed-phase analogs for dipole-bound anions (such as CH_3CN^-) and negatively charged clusters of polar molecules (such as $(H_2O)_n^-$) that occur in the gas phase? Our recent study [2] suggests that both monomers and clusters of polar molecules (such as aliphatic alcohols and acetonitrile) can reversibly trap conduction band electrons in very dilute alkane solutions. The dynamics and energetics of this trapping have been studied using pulse radiolysis and time-resolved photoconductivity. Binding energies, thermal detrapping rates, and absorption spectra of electrons attached to monomer and multimer solute traps were obtained and possible structures for these species suggested. "Dipole coagulation" (stepwise growth of the solute cluster around the cavity electron) predicted in 1972 was observed. Acetonitrile monomer was shown to solvate the electron by its methyl group. The electron is dipole-bound to the CN group; the latter points away from the center of the cavity. The resulting negatively charged species has a binding energy of 0.4 eV and absorbs in the IR. Alcohol molecules cluster in the alkane solution due to the formation of H-bonds between the monomers. These clusters solvate the excess electron by their OH groups; at equilibrium, the predominant electron trap is a trimer or a tetramer; the binding energy of this solute trap is ca. 0.8 eV. Trapping by smaller clusters is opposed by the entropy which drives the equilibrium towards the electron in a *solvent* trap. For alcohol monomers, the trapping does not occur; a slow proton transfer reaction occurs instead. For acetonitrile monomer, the trapping is favored energetically but the thermal detachment is rapid (ca. 1 ns). Our study suggests that a cluster anion consisting of a few polar molecules imbedded in an alkane "matrix" is the closest analog to the core of solvated electron in a *neat* polar liquid. Another conclusion is the possibility of a single-molecule, fixed-geometry supramolecular cage encapsulating the electron in the same fashion that several polar molecules do it in the alkane solution. Such a species would greatly assist the structural and theoretical

studies of solvated/trapped electron, as the solvent flexibility can be eliminated. It would also provide a novel approach to the synthesis of all-organic quantum dots (wells) with uniform properties and long spin decoherence time for the electron. We are actively pursuing this line of research in collaboration with F. T. Williams of UTK and J. F. Wishart of BNL.

2.3. Ammoniated electron as solvent stabilized multimer radical anion

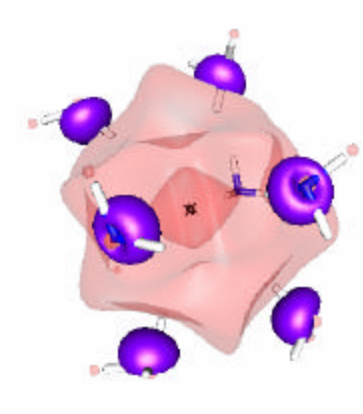

The excess electron in liquid ammonia ("ammoniated electron") is commonly viewed as a cavity electron in which the *s*-type wave function fills the interstitial void between 6-9 ammonia molecules. While this one-electron cavity model accounts for the optical properties of ammoniated electron, it is incompatible with the magnetic resonance and IR-Raman data for this species. Our theoretical study aims to resolve this conflict. An alternative model of ammoniated electron based on many-electron Density Functional Theory (DFT) approach was suggested in which this species is regarded as a solvent stabilized multimer radical anion. In this model, most of the excess electron density resides in the frontier orbitals of *N* atoms in the ammonia molecules forming the solvation cavity; a fraction of this spin density is transferred to the molecules in the second solvation shell. The cavity is formed due to the repulsion between negatively charged solvent molecules. Using DFT calculations for small cluster anions in the gas phase, it is demonstrated that such core anions would account for the observed pattern of Knight shifts for ^{1}H and ^{14}N nuclei as observed by NMR spectroscopy and the downshifted stretching and bending modes as observed by IR-Raman spectroscopies. Our model vindicates the hypothesis of Symons (1976) suggesting just such a picture of the ammoniated electron. Excess electrons in other aprotic solvents (but not in water and alcohols) might be analogous to the ammoniated electron, with substantial transfer of the spin density into the frontier *N* and *C* orbitals of methyl, amino, and amide groups forming the solvation cavity. A revision of the models for electron solvation in medium polarity and nonpolar liquids might be necessary since one-electron models do not capture the essential physics in such liquids. [http://arxiv.org/abs/physics/0509137]

3. Future plans.

We have already began picosecond pulse radiolysis studies of liquid water using the T3 source and we will focus our entire effort on such studies next year. We are particularly interested in the experimental verification of "hot spur" hypothesis formulated in ref. (7) which posits that in radiolysis, the thermalization of the electron occurs on the time scale of 10-30 ps due to the finite time required for the heat to escape the spur. Other priorities are the studies of photoionization in nonaqueous liquids, electron encapsulation and structural characterization, photodynamics of electron during geminate recombination, and the mechanism for photodissociation in liquid water.

Recent publications (2004-2005).

(1) I. A. Shkrob and M. C. Sauer, Jr., *Electron Trapping by Polar Molecules in Alkane Liquids: Cluster Chemistry in Dilute Solution*, J. Phys. Chem. A **109** (2005) 5754;

(2) I. A. Shkrob and M. C. Sauer, Jr., *Photo-Stimulated Electron Detrapping and the Two-State Model for Electron Transport in Nonpolar Liquids*; J. Chem. Phys. **122** (2005) 134503;
(3) R. Lian, R. A. Crowell, and I. A. Shkrob, *Solvation and thermalization of electrons generated by above the gap (12.4 eV) two-photon ionization of liquid H_2O and D_2O*, J. Phys. Chem. A. **109** (2005) 1510;
(4) M. C. Sauer, Jr., I. A. Shkrob, R. Lian, R. A. Crowell, D. M. Bartels, X. Chen, D. Suffern, and S. E. Bradforth, *Electron Photodetachment from Aqueous Anions. II. Ionic Strength Effect on Geminate Recombination Dynamics and Quantum Yield for Hydrated Electron*; J. Phys. Chem. A. **108** (2004) 10414;
(5) R. Lian, D. A. Oulianov, I. A. Shkrob, and R. A. Crowell, *Geminate recombination of electrons generated by above-the-gap (12.4 eV) photoionization of liquid water.* Chem. Phys. Lett. **398** (2004) 102;
(6) M. C. Sauer, Jr., I. A. Shkrob, R. Lian, R. A. Crowell, D. M. Bartels, X. Chen, S. Suffern, and S. E. Bradforth, *Electron Photodetachment from Aqueous Anions. II. Ionic Strength Effect on Geminate Recombination Dynamics and Quantum Yield for Hydrated Electron.* J. Phys. Chem. A. **108** (2004) 10414;
(7) R. A. Crowell, R. Lian, I. A. Shkrob, Jun Qian, D. A. Oulianov, and S. Pommeret, *Light-induced temperature jump causes power-dependent ultrafast kinetics of electrons generated in multiphoton ionization of liquid water*. J. Phys. Chem. A **108** (2004) 9105;
(8) I. A. Shkrob, *Geminate recombination dynamics studied via electron reexcitation: Kinetic analysis for anion CTTS photosystems*, Chem. Phys. Lett. **395** (2004) 264;
(9) I. A. Shkrob and M. C. Sauer, Jr., *Hole Scavenging and Photo-Stimulated Recombination of Electron-Hole Pairs in Aqueous TiO_2 Nanoparticles*. J. Phys. Chem. B **108** (2004) 12497;
(10) M. C. Sauer, Jr., I. A. Shkrob, D. Gosztola, *Efficient, rapid photooxidation of polyatomic alcohols and carbohydrates by aqueous TiO_2 nanoparticles.* J. Phys. Chem. B **108** (2004) 12512;
(11) R. Lian, R. A. Crowell, I. A. Shkrob, D. M. Bartels, X. Chen, and S. E. Bradforth, *Ultrafast Dynamics for the Electron Photodetachment of Aqueous Hydroxide*, J. Chem. Phys. **120** (2004) 11712;
(12) R. Lian, R. A. Crowell, I. A. Shkrob, D. M. Bartels, D. A. Oulianov, and D. Gosztola, *Recombination of Geminate (OH,e_{aq}^-) Pairs in Concentrated Alkaline Solutions: Lack of Evidence For Hydroxyl Radical Deprotonation.* Chem. Phys. Lett. **389** (2004) 379;
(13) R. A. Crowell, R. Lian, M. C. Sauer, Jr., D. A. Oulianov, and I. A. Shkrob, *Geminate recombination of hydroxyl radicals generated in 200 nm photodissociation of aqueous hydrogen peroxide.* Chem. Phys. Lett. **383** (2004) 481;
(14) I. A. Shkrob, D. A. Oulianov, R. A. Crowell, and S. Pommeret, *Frequency-domain "single-shot" (FDSS) ultrafast transient absorption spectroscopy using compressed laser pulses*. J. Appl. Phys. **96** (2004) 25;
(15) M. C. Sauer, Jr., R. A. Crowell, and I. A. Shkrob, *Electron Photodetachment from Aqueous Anions. I. Quantum Yields for Generation of Hydrated Electron by 193 and 248 nm Laser Photoexcitation of Miscellaneous Inorganic Anions*. J. Phys. Chem. A **108** (2004) 5490;
(16) I. A. Shkrob and M. C. Sauer, Jr., *Radical Ions in Liquids*, in *"Charged Particle and Photon Interactions with Matter."*, eds. Y. Hatano and A. Mozumder, Marcel Dekker, New York, **2004**; Ch. 11, pp. 301-331.

Self-Organization and Oxidative Surface Reaction Dynamics of Condensed Phase Systems

Steven J. Sibener
The James Franck Institute and Department of Chemistry
The University of Chicago, 5640 South Ellis Avenue
Chicago, IL 60637 s-sibener@uchicago.edu

I. Program Scope

This research program seeks to examine the heterogeneous reaction kinetics and reaction dynamics of surface chemical processes which are of direct relevance to efficient energy production, condensed phase reactions, and materials growth including nanoscience objectives. We have recently had several notable scientific and technical successes. Illustrative highlights include: (1) a thorough study of how one can efficiently produce synthesis gas (SynGas) at relatively low Rh(111) catalyst temperatures *via* the reaction $CH_4+1/2\ O_2 \rightarrow CO+2H_2$. In these studies methane activation is accomplished utilizing high-kinetic energy reagents generated *via* supersonic molecular beams, (2) experiments which have incisively probed the partial oxidation chemistry of adsorbed 1- and 2- butene on Rh and ice, as well as partial oxidation of propene on Au; (3) investigation of structural changes which occur to the reconstructed $(23x\sqrt{3})$-Au(111) surface upon exposure to atomic oxygen, (4) a combined experimental and theoretical examination of the fundamental atomic-level rules which govern defect minimization during the formation of self-organizing stepped nanostructures, (5) the use of these relatively defect-free nanotemplates for growing silicon nanowires having atomically-dimensioned widths, (6) a combined scanning probe and atomic beam scattering study of how the presence of self-assembling organic overlayers interact with metallic support substrates – this work has led to revision of the currently held view of how such adsorbates reconfigure surface structure at the atomic level, (7) an inelastic He atom scattering study in which we examined the effect of chain length on the low-energy vibrations of alkanethiol striped phase self-assembled monolayers on Au(111), yielding information on the forces that govern interfacial self-assembly, and (8) a study of the activated chemistry and photochemistry of NO on NiO/Ni. Innovative STM and molecular beam instrumentation has been fabricated to enable this program.

II. Recent Progress

1. Molecular Beam Studies of Enhanced Routes to SynGas Production Using Methane

Methane is an abundant natural resource for making larger hydrocarbons through the Fischer-Tropsch process. To do this, it is necessary to partially oxidize CH_4 to synthesis gas (hereafter syngas), CO and H_2, ideally in a 1:2 ratio. One method for accomplishing this is the direct partial oxidation of methane, $CH_4+1/2\ O_2 \rightarrow CO+2H_2$. We have explored, using our multiple-molecular beam reactive scattering techniques, detailed aspects of this reaction on Rh(111). We find that this reaction initially proceeds with the activated direct dissociative chemisorption of methane followed by subsequent oxidative

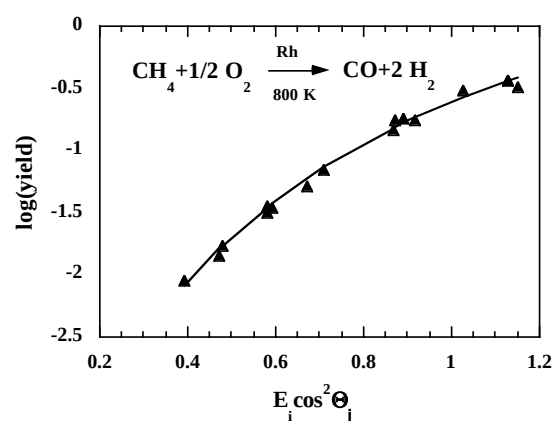

chemistry to yield $CO+2H_2$ from the partial oxidation of CH_4. Concurrent molecular beams of O_2 and CH_4 were used, with both beams having narrow kinetic energy distributions. The reaction is highly activated, with the fraction of CH_4 converted being strongly dependent on normal translational energy, approaching unity for energies greater than ~1.3 eV. No CO_2 was detected under the conditions used, a key observation for reaction efficiency and minimization of greenhouse gases.

2. Reaction of Small Olefins with $O(^3P)$ Adsorbed on Rh, Ice, and Au

Using molecular beams, we have studied the reaction of $O(^3P)$ with 1- and 2-butene on the surface of Rh and ice, and propene on the surface of Au, in vacuum at cryogenic temperatures. For 1-butene, the products are 1,2-epoxybutane, butanal, and a trace of butanone. For the 2-butenes, the reaction products include cis- and trans-2,3 epoxybutane and butanone. The propene reaction yielded a mixture of propylene oxide, propanal, and acetone. These results, taken together, demonstrate that the surface serves as an efficient sink for the excess energy of these highly exoergic reactions, yielding the stabilized adduct products. These investigations have emphasized that significant differences occur in condensed phase reactions as compared to related gas phase oxidative reaction where fragmentation and rearrangement dominate due to the absence of other energy-dissipation channels. Our observations indicate that heterogeneous interfaces provide a mechanism for channeling away excess energy, therefore leading to adduct stabilization. These experiments will, ultimately, provide kinetic data that are needed for the accurate modeling and design of advanced combustion and catalytic reforming systems.

3. O-Atom Induced Reconstruction of the Au(111) Surface

Using He diffraction, we have investigated morphological changes of the reconstructed $(23x\sqrt{3})$-Au(111) surface when small quantities of O atoms are adsorbed. The electronegative oxygen removes charge from the surface, which causes the surface to restructure and ultimately revert to the (111) structure. The extent of this deconstruction is dependent on the initial O coverage and the surface temperature. When the deconstruction is complete, the oxygen can be removed from the terraces by annealing, leaving the surface in the unreconstructed (111) structure. Ultimately, and at a much slower rate, the surface begins to reconstruct. These experiments are important as they demonstrate that catalytic interfaces cannot be viewed as static entities, but rather as having evolving structure upon the adsorption of strongly-interacting reactive gases.

4. Oxygen Induced Restructuring of Stepped Metals: Experiment and Monte Carlo Simulation of Nucleation-Controlled Step Doubling

In order to make effective use of the extreme density of nanoscale elements that form spontaneously in self-assembling architectures, one must address the associated issue of minimizing defect creation during the formation of such structures. In this project we have examined the competing roles that nucleation kinetics and two-dimensional growth processes play in nanostructure formation and defect minimization. We employed oxygen-induced step doubling of vicinal Ni(977) surfaces as our physical system, using elevated temperature scanning tunnelling microscopy and Monte Carlo simulations to extract the desired details of interface evolution. Two interesting topological defect features were observed on the surface after doubling reaches its asymptotic limit: (i) “frustrated ends,” which form when two counter-propagating step-doubling events that have a single step in common intersect, leaving a stable topological defect, and (ii) residual “isolated single steps,” which form when a single step is unable to partner with an adjacent step. Monte Carlo simulations were performed to better

understand these results. These simulations indicate that control of the delicate and competing interplay of nucleation kinetics and two-dimensional growth kinetics is the key to the formation of more perfect interfaces. Such optimized interfaces can act as templates for guiding the hierarchical assembly of nanowires and other nanoscale molecular assemblies (see next section).

5. Reactive Deposition of Silicon Nanowires Templated on a Stepped Nickel Surface

We have employed STM to examine the initial stages of Si nanowire growth by reactive deposition of disilane (Si_2H_6) on Ni(977). At low dosing exposures, Si_2H_6 decomposes on the stepped surface and forms oriented nanoscale wires which decorate the substrate's step edges. This method of gas-phase reactive deposition on a stepped surface, with the substrate acting as both catalyst and nano-template with easily tunable width (by varying the vicinal miscut angle) is a fruitful approach to creating massively-parallel nanoscale arrays of highly aligned structures.

6. Coexistence of the (23x√3)-Au(111) Reconstruction and a Striped Phase SAM

We have studied the effect of adsorption of a low-density alkanethiol monolayer on the state of the Au(111) reconstruction. It is commonly believed that the substrate deconstructs following formation of a thiolate self-assembled monolayer, but our results suggest this is not always the case. He diffraction from 1-decanethiol and 1-octanethiol striped phase monolayers is exploited to establish the surface nearest-neighbor spacing and to illustrate a unit cell corresponding to the long dimension of the 23x√3 reconstruction. Using our observed 0.198 $Å^{-1}$ peak spacing and the 11.5x√3 unit cell reported in the literature, we measure a substrate nearest-neighbor spacing of 2.76 Å along the $[1\bar{1}0]$ direction, which represents the atomic spacing of the uniaxially-compressed, reconstructed gold surface. Moreover, 1/2-order peaks in the diffraction from decanethiol/Au(111) demonstrate a distinction between neighboring thiolate dimers. These peaks are not observed for octanethiol/Au(111). Therefore, the 1/2-order peaks are not an inherent characteristic of alkanethiol SAMs. The most likely explanation is a reconstructed substrate. Complementary STM data indicate persistence of the reconstruction during growth of a decanethiol striped phase monolayer and no evidence for vacancy islands typically associated with deconstruction. Our model involving a still-reconstructed substrate is consistent with all available data, while alternative models fail to explain the results from our laboratory.

7. Surface Vibrations in Alkanethiol Self-Assembled Monolayers of Varying Chain Length

We have performed a series of single-phonon inelastic He atom scattering experiments, complemented by appropriate numerical simulations, in order to dissect the forces driving the self-assembly of alkanthiolate monolayers, including inter-chain and chain-substrate interactions which govern the self-assembly process. The striped phases of 1-decanethiol, 1-octanethiol, and 1-hexanethiol exhibit FT_z phonons at 8.0, 7.3, and 7.3 meV, respectively. Molecular dynamics simulations suggest that the frequencies of the low energy vibrations are relatively constant with respect to chain length, in agreement with experiment. We also suggest that the modestly increased energy of the C10 mode with respect to C8 and C6 comes from increased binding due to the commensurate structure that C10 has with respect to the Au(111) reconstruction. This work represents a step forward in understanding the forces that govern interfacial self-assembly.

8. Activated Chemistry and Photochemistry of NO on NiO/Ni

These activities are exploring the mechanistic details of NO chemistry with NiO(111)/Ni(111). Intense and kinetic energy tunable molecular beams have led to the formation of unusual surface

adsorbate structures exhibiting higher density (new bonding configurations); vibrational and photochemical studies have been performed on these new bonding arrangements. These studies are improving our fundamental understanding of heterogeneous processes which are relevant to controlling NO_x in the environment.

9. Instrumentation Development: During the past grant period we have completed the assembly of a new cryogenically cooled STM ($LiqN_2$ or LiqHe can be used). This facility is giving crucial support to our effort in interface reactivity. We have also recently completed a laser-ignition (7J CO_2 TEA laser) pulsed beam source for the production of $O(^3P)$ atoms spanning the kinetic energy range from sub-eV to multi-eV. This new addition will allow us to examine important dynamical details of condensed phase oxidation reactions.

III. Future Plans

Studies of interfacial oxidation reactions, involving molecular and atomic oxygen, will continue. During the coming year we hope to extend these studies to include our new hyperthermal variable energy (sub-eV to multi-eV) atomic oxygen beam source in order to probe precise dynamical details of adiabatic and non-adiabatic oxidation reactions. SAM overlayers which present spatially-oriented end-groups will also be assessed as a route to probing directly geometry-restricted chemical reaction dynamics at interfaces. STM imaging will be used in support of these scattering experiments, giving an atomic-level view of the reaction systems.

IV. Publications

In Search of Nano-Perfection: Experiment and Monte Carlo Simulation of Nucleation-Controlled Step Doubling, Yi Wang, T. P. Pearl, S. B. Darling, J. L. Gimmell, and S. J. Sibener, J. Applied Physics, 91 (12): 10081-10087 (2002).

Reactive Deposition of Silicon Nanowires Templated on a Stepped Nickel Surface, Yi Wang and S. J. Sibener, J. Phys. Chem. B 106, 12856-12859 (2002).

Coexistence of the (23x√3)-Au(111) Reconstruction and a Striped Phase Self-assembled Monolayer, S.B. Darling, A.W. Rosenbaum, Yi Wang, and S.J. Sibener, Langmuir 18, 7462-7468 (2002).

Surface Vibrations in Alkanethiol Self-Assembled Monolayers of Varying Chain Length, A.W. Rosenbaum, M.A. Freedman, S.B. Darling, I. Popova, and S.J. Sibener, J. Chem. Phys. 120, 3880-3886 (2004).

Applied Reaction Dynamics: Efficient Single Collision Partial Oxidation of Methane to CO on Rh(111), K.D. Gibson, M. Viste, and S. J. Sibener, submitted.

The Reaction of $O(^3P)$ with Condensed Arenes, K.D. Gibson and S. J. Sibener, to be submitted.

The Reaction of 1- and 2-Butene with $O(^3P)$ on the Surface of Rh and Ice, K.D. Gibson and S. J. Sibener, to be submitted.

O-atom Induced Reconstruction of the Au(111) Surface, K. D. Gibson, and S. J. Sibener, to be submitted.

Beam Induced Changes in Adsorption Behavior of NO on NiO(111)/Ni(111), B. D. Zion and S. J. Sibener, to be submitted.

UV-photodesorption of Novel, Beam-Induced NO Layers, B. D. Zion and S. J. Sibener, to be submitted.

Generation, Detection and Characterization of Gas-Phase Transition Metal Containing Molecules

Timothy C. Steimle
Department of Chemistry and Biochemistry
Arizona State University
Tempe, Arizona 85287-1604
E-Mail: Tsteimle@asu.edu

I. Program scope

The reactions of a single metal atom, or possibly a metal dimer, with simple gaseous reagents are reasonable first-order model systems for emulating catalysis. Although the literature abounds with theoretical predictions for the reaction of naked metal atoms or metal clusters with simple hydrocarbons, hydrogen, and other gases, the gap between theoretical predictions and experimental observations is immense. The calculations typically predict structure and relative stability for the pre-reactive complex, insertion products, transition state complexes, and elimination products that occur along plausible reaction paths. The elimination products are small, transient, metal-containing radical molecules which are the focus of our studies. In our case, these molecules are generated in the reaction of a laser ablated metal vapor seeded in an Argon/reagent gas supersonic expansion. Highly quantifiable information about the geometric, and more importantly, electronic structure of these molecules is derived from the analysis of optical spectra recorded at the near natural linewidth limit. These simple molecules are amenable to sophisticated electronic structure calculations, thereby creating the desired symbiosis between theory and experiment.

Experimental determination of the permanent electric dipole moments, μ, has been a major focus because dipole moments: a) are primarily dependent upon the chemically relevant valence electrons; b) are the most fundamental electrostatic property, and c) enter into the description of numerous phenomena. The observed large variation in μ even amongst simple, similar molecules (*e.g.* MoC ($X^3\Sigma^-$) μ = 6.32 D (see below) *vs.* PtC($X^1\Sigma^+$) μ = 1.08D[1]) illustrates its sensitivity to the nature of the chemical bond. A comparison of predicted μ values with experimentally determined values is the primary criteria for assessing the effectiveness of various computational methodologies. This is particularly important for evaluating post-Hartree-Fock treatments, which are essential for obtaining quantitative predictions. A stringent test of computational methods [3,4] is the comparison of predicted values of μ obtained by both a finite field calculation, where $\mu = \left.\frac{\partial \text{Energy}}{\partial \vec{E}}\right|_{\vec{E}\to 0}$, and the expectation value approach, where $\mu = \left\langle \Psi^{el} \left| \sum_i e r_i \right| \Psi^{el} \right\rangle$. The two approaches are related by [2]:

$$\left.\frac{\partial \text{Energy}}{\partial \vec{E}}\right|_{\vec{E}\to 0} = \left\langle \Psi^{el} \left| \sum_i e r_i \right| \Psi^{el} \right\rangle + 2\left\langle \frac{\partial(\Psi^{el})}{\partial \vec{E}} \left| \hat{H}^{el} \right| \Psi^{el} \right\rangle \qquad 1)$$

where $\vec{E}$ is the applied electric field. According to the Hellman-Feynman theorem, the finite field and expectation value prediction will be identical (*i.e.* the 2nd term of Eq. 1 = 0) when Ψ^{el} is either the exact eigenfunction of the Hamiltonian or a predicted wave function

that has been fully optimized in the variational sense. For transition metal containing molecules, *ab initio* generated wave functions require extensive treatment of electron correlation and are not fully optimized in the variational sense. Therefore, if the predicted wavefunction, Ψ^{el}, is an accurate approximation to the true wavefuntion, then the expectation value prediction and the finite field predicted value will agree with the experimentally derived value.

II. Recent accomplishments

a. Dipole moment of transition metal monocarbides

Although the transition metal-carbon bond is of particular importance in catalysis, there is relatively little experimentally derived information for this class of molecules. Previously we reported on the DoE supported experimental studies involving the first row monocabide FeC [5], second row RuC [Publs. 1 &3], and third row IrC[6] and PtC[1]. Our most recent study involves the dipole moment determination for MoC in its $[18.6]^3\Pi_1$ and $X^3\Sigma^-$ states. Previously, the R2PI [7] and dispersed laser induced fluorescence (LIF) [8] spectra have been recorded and analyzed by the Morse group. An example of our high-resolution LIF spectra for the $(0,0)[18.6]^3\Pi_1$ - $X^3\Sigma^-$ band of MoC is presented in Figure 1.

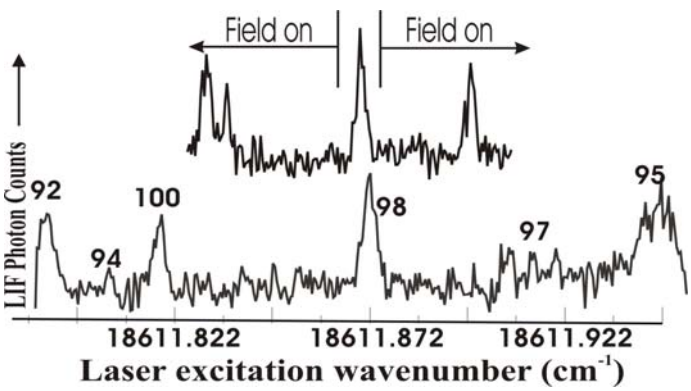

Figure 1. The MoC *Q*(1) transition of the (0,0) band in the $[18.6]^3\Pi_1$-$X^3\Sigma^-$ system recorded field-free (lower panel) and in the presence of a perpendicularly oriented field of 1227 V/cm (upper panel). Note the non-sequential ordering of the different isotopologue and the magnetic hyperfine splitting for ^{95}MoC and ^{97}MoC species.

The measured values for μ and the reduced dipole moment ($\equiv\mu/r_e$), which is a more accurate gauge of the charge distribution, are collected in Table 1. A perusal of Table 1 reveals that the μ/r_e values for molecules having (n+1)*s* metal-centered orbital occupation (*i.e.* FeC, IrC, and PtC) are greatly reduced from those that that do not. Evidently this orbital can readily polarize away from the bond. This polarization effect is difficult to quantitatively predict making the *ab initio* derived μ values for FeC, IrC, and PtC less quantitative than those for MoC and RuC.

Table 1. Measured dipole moments of metal monocarbes.

Parameter	FeC($X^3\Delta_3$)	MoC($X^3\Sigma^-$)	RuC ($X^1\Sigma^+$)	IrC($X^2\Delta$)	PtC ($X^1\Sigma^+$)
Config.	$(3d)\sigma^2\pi^4\delta^3(4s)\sigma^1$	$(4d)\sigma^2\pi^4\delta^2$	$(4d)\sigma^2\pi^4\delta^4$	$(5d)\sigma^2\pi^4\delta^3(6s)\sigma^2$	$(5d)\sigma^2\pi^4\delta^4(6s)\sigma^2$
μ (Debye)	2.36(3)	6.32(20)	4.09(14)	1.60(7)	1.09(5)
μ/r_e (D/Å)	1.47	3.77	2.54	0.952	0.649

b. Stark effect and hyperfine interaction in RuF

Ruthenium-based complexes are important in catalyzing olefin metathesis reactions for, amongst other things, ring catenation, ring closing, and ring-opening. An increasingly important class of ruthenium-based complexes is the first and second generation Grubb's catalysts, the base of which are a chlorinated ruthenium carbene: $Cl_2RuCHPh$. The catalytic action is likely linked to the nature of the Ru-halide bond. One approach to glean insight the electronic contribution, as opposed to the steric effects, is to model the interaction of metal halides and dihalides with simple hydrocarbons [9]. With this in mind, we have recently made the first spectroscopic detection of RuF and the subsequent analysis of the [18.2]5.5 – $X^4\Phi_{9/2}$ band system recorded field-free and in the presence of a static electric field. The determined bond lengths, dipole moments and magnetic hyperfine interactions in the ground and excited states and the vibrational interval in the ground state have been used to provide insight into the bonding. The determined large value μ for the $X^4\Phi_{9/2}$ state (= 5.34(7) D) suggest a $(4d)\sigma\delta^3\pi^3$ dominant configuration, consistent with a ligand-field model and the sole theoretical prediction [10]. It is demonstrated that the $^{19}F(I=1/2)$ magnetic hyperfine interaction is an effective diagnostic of the electronic nature of the ground and excited electronic states.

c. Construction of Mid-infrared Difference Frequency Spectrometer

The metal imides, MNH, amides, MNH_2, hydroxides, MOH, carbenes, MCH_2, and methylidines, MCH, have been, and will continue to be, targets for our high-resolution spectroscopic studies. Many of these molecules are observed in our TOF mass spectra, but detecting them via LIF spectroscopy has been challenging. We have constructed a difference frequency generation (DFG) spectroscopic source, similar to that in used at the Rice University [11,12], to be used for direct absorption measurements. This system incorporates two recent technological advances that greatly facilitate DFG: a) the traditional Ar^+ laser is replaced by a powerful, compact, and low-noise, single frequency, cw, diode-pumped Nd:YAG laser; and b) the mixing media is a periodically poled lithium niobate (PPLN) crystal. The periodic-polling facilitates phase matching eliminating the need for accurate temperature control.

III. Future directions

a. Sensitivity enhancements for the mid-infrared spectrometer.

As a means of improving the sensitivity of the mid-infrared absorption spectrometer we are: a) installing a slit laser ablation source to extend the path length; b) developing a two-tone frequency modulation detection scheme similar to that used at Sandia National Laboratory [13].

b. Discharge sources as an alternative method for molecular production.

The number of polyatomic molecules that we have detected and characterized are far fewer than the number of diatomic molecules. Our current laser ablation/reaction production scheme may favor generation of diatomic fragments because of the associated energetic ablation plasma. In the future, we will also use a dc-discharge supersonic expansion source with volatile organometallic precursors similar to what we used in the study of SiCH [14] and GeCH [15]. Initial studies will use trimethyl (methycyclopetadienyl) platinum, $(CH_3)_3(CH_3C_5H_4)Pt$, seeded in an argon carrier gas.

References

1. S. A. Beaton and T.C. Steimle, *J. Chem. Phys*. **111, 24**, 10876-10882 (1999).
2. *Introduction to Computational Chemistry* F. Jensen (John Wiley & Sons, 1999).
3. M. Medved, M. Urban, and J. Noga, *Theor. Chem. Acc*. **98**, 75 (1997).
4. C. W. Bauschlicher, Jr. S. R. Langhoff, A. Komornicki, *Theor. Chim. Acta* **77** (4), 263 (1990).
5. T.C. Steimle, W. Virgo and David Hostutler, J. Chem. Phys. **117**, 1511 (2002).
6. A.J. Marr, M.E. Flores, and T.C. Steimle, J. Chem. Phys. **104**, 8183 (1996)
7. D. J. Brugh, T,J, Ronningen and M. D. Morse, J. Chem. Phys. **109**, 7851 (1998).
8. R.S. Ball, R.G. Meyer and M.D. Morse, J. Chem. Phys. **114**, 2938 (2000)
9. P.E.M. Siegbahn and M.R.A. Blomberg, Organometallics **13**, 354 (1994).
10. P.E.M. Siegbahn, Theor. Chem. Acta **86**, 219 (1993).
11. Yu. G. Utkin, Jia-Xiang Han, Fuge Sun, Hong-Bing Chen, Graham Scott, and R.F Curl, *J. Chem. Phys* **118**, 10470 (2003).
12. Jia-xiang Han, Yu. G Utkin, Hong-bing Chen, L. A.Burns and R. F Curl, *J. Chem. Phys* **117** 6538 (2002).
13. J.T. Farrel and C.A. Taatjes, J. Phys. Chem. A, **102**, 4846 (1998).
14. T.C. Smith, D.J. Clouthier and T.C. Steimle, *J. Chem. Phys*. **115**, 817 (2001).
15. T.C. Smith, D.J. Clouthier and T.C. Steimle, *J. Chem. Phys*.,**115**, 5047 (2001).

Publications (2003-2004)

1. "The permanent electric dipole moments of ruthenium monocarbide, RuC" T.C. Steimle, W. Virgo and J. M. Brown , *J. Chem. Phys.* 118, 2620-2625 (2003).

2. "The permanent electric dipole moments and magnetic hyperfine interactions of ruthenium mononitride, RuN. Timothy C. Steimle and Wilton Virgo *J. Chem. Phys.* 118, 12965 (2003).

3. "The permanent electric dipole moments of Ruthenium Monocarbide in the $^3\Pi$ and $^3\Delta$ states" Wilton L. Virgo, Timothy C. Steimle, Laura E. Aucoin and J.M. Brown. *Chem. Phys. Lett.* **391**,75-80, (2004).

4. "The permanent electric dipole moments of WN and ReN and nuclear quadrupole interaction in ReN" Timothy C. Steimle and Wilton Virgo J. Chem. Phys. **121** 12411 (2004).

Structural Dynamics in Complex Liquids Studied with Multidimensional Vibrational Spectroscopy

Andrei Tokmakoff

Department of Chemistry, Massachusetts Institute of Technology, Cambridge, MA 02139
E-mail: tokmakof@MIT.edu

Our study of the collective structure and molecular dynamics of liquids has focused on hydrogen bond rearrangements in water, as viewed through infrared spectroscopy. Over the past few years we have used a variety of femtosecond infrared experiments to characterize time-dependent changes in frequency of the OH stretching vibration of HOD in D_2O that result from changing hydrogen bond configuration. This widely studied model system can be used to characterize the vibrational dynamics of an isolated OH stretch vibration within D_2O molecules, whose hydrogen bond dynamics closely mirror those of H_2O. The OH stretch frequency ω is particularly sensitive to the hydrogen bonding environment leading to a broad absorption line in the mid-infrared at 3400 cm^{-1}. Femtosecond IR spectroscopy can be used to characterize spectral diffusion within the OH absorption line, which in turn is determined by the hydrogen bond dynamics and kinetics. These experiments are interpreted with the help of a model for OH vibrational frequency shifts that draws on molecular dynamics simulations.

The physical and chemical properties of water are dictated by hydrogen bond interactions and the reconfiguration of the structure of water during the breaking and forming of hydrogen bonds. Water is a remarkably structured liquid, considering that at any instant it has 80-90% of the hydrogen bonds found in the tetrahedral structure of ice. But the structure imposed by these highly directional hydrogen bonds evolves very quickly. Our earlier studies described how individual hydrogen bonds in water experience configurational fluctuations on femtosecond time-scales preceding a collective reorganization of the liquid.

Our more recent 2D IR experiments seek to reveal mechanisms of hydrogen bond rearrangements, characterize the stability of non-hydrogen bond configurations, and discern different conceptual pictures for the structure and dynamics of hydrogen bonding in liquid water. The theoretical formulations of molecular models for the physical properties of water are often broken into two classes, mixture models and continuum models. Mixture models conceive of the liquid as composed of two or multiple stable species that differ in their hydrogen bonding configurations. Closely associated with the concepts of the mixture models is the language of “broken” or “dangling” hydrogen bonds. Continuum models do not identify different species, but

conceive of the structure as a continuous distribution of geometries or large distortions about an average structure.

2D IR spectroscopy characterizes the evolution of distributions of molecular conformations or local solvent environments. It correlates how molecules initially at one frequency (ω_1) evolve to a final frequency (ω_3) during the course of a waiting period (τ_2). This information is encoded in the details of 2D IR lineshapes, which can be analyzed statistically to describe the variance in structural parameters. For a broad inhomogeneous lineshape consisting of molecules in different environments, the 2D lineshape is diagonally elongated. The interconversion of environments leads to a gradual change to a symmetric (round) lineshape for increased waiting times.

Our 2D IR experiments suggest that non-hydrogen bonded configurations between pairs of molecules in water are not stable, but are transient fluctuations about a hydrogen bonded state or the transition state in a hydrogen switching event. We argue that dangling hydrogen bonds do not exist in water. These conclusions have important implications for the general picture of water structure and how its hydrogen bond network rearranges. Equally important, it has implications for how hydrogen bonds interact with solutes and mediate aqueous chemical processes such as proton transport.

The detailed molecular picture of the processes observed in our experiments has emerged from collaborations, in which theory and molecular dynamics (MD) simulation were used to interpret these IR spectroscopies in terms of hydrogen bonding structure, dynamics, and kinetics. Specifically, our collaboration with Phillip Geissler led to a model for the OH frequency shifts for HOD in D_2O which was used to investigate the relationship between vibrational frequency and hydrogen bonding configurations about the HOD molecule. In a subsequent collaboration with Bruce Berne, this model was used to compare our experiments to simulations of several polarizable models of water. The principles we developed for studying hydrogen bond kinetics in water are broadly applicable, as we have shown with studies of hydrogen bonding of the model peptide N-methylacetamide to a number of polar solvents.

Ongoing work seeks to clarify the mechanistic details about how hydrogen bonds rearrange, and will extend femtosecond infrared experiments to studies of proton transport in water.

DOE Supported Publications (2003-2005)

1. "Coherent 2D IR Spectroscopy: Molecular structure and dynamics in solution," M. Khalil, N. Demirdöven and A. Tokmakoff, *Journal of Physical Chemistry A*, **107** (2003) 5258.
2. "Ultrafast hydrogen bond dynamics in the infrared spectroscopy of water," C. J. Fecko, J. D. Eaves, J. J. Loparo, A. Tokmakoff and P. G. Geissler, *Science*, **301** (2003) 1698.

3. "Dynamics of hydrogen bonds in water: Vibrational echoes and two-dimensional infrared spectroscopy," C. J. Fecko, J. D. Eaves, J. J. Loparo, S. T. Roberts, A. Tokmakoff and P. L. Geissler, in *Ultrafast Phenomena XIV*, ed. by T. Kobayashi, T. Okada, T. Kobayashi, K. A. Nelson, S. DeSilvestri (Springer-Verlag, Berlin).
4. "A unified analysis of ultrafast vibrational and orientational dynamics of HOD in D_2O," J. J. Loparo, C. J. Fecko, J. D. Eaves, S. T. Roberts and A. Tokmakoff, in *Ultrafast Phenomena XIV*, ed. by T. Kobayashi, T. Okada, T. Kobayashi, K. A. Nelson, S. DeSilvestri (Springer-Verlag, Berlin).
5. "Solvation dynamics of N-methylacetamide in D_2O, $CDCl_3$ and DMSO-d_6," M. F. DeCamp, L. P. DeFlores, J. M. McCracken, and A. Tokmakoff, in *Ultrafast Phenomena XIV*, ed. by T. Kobayashi, T. Okada, T. Kobayashi, K. A. Nelson, S. DeSilvestri (Springer-Verlag, Berlin, 2005).
6. "Reorientational and configurational fluctuations in water observed on molecular length scales," J. J. Loparo, C. J. Fecko, J. D. Eaves, S. T. Roberts and A. Tokmakoff, *Physical Review B*, **70** (2004) 180201.
7. "Generation of 45 femtosecond pulses at 3 μm with a $KNbO_3$ optical parametric amplifier," C. J. Fecko, J. J. Loparo and A. Tokmakoff, *Optics Communications*, **241** (2004) 521.
8. "Local hydrogen bonding dynamics and collective reorganization in water: Ultrafast IR spectroscopy of HOD/D_2O," Christopher J. Fecko, Joseph J. Loparo, Sean T. Roberts and Andrei Tokmakoff, *Journal of Chemical Physics*, **122** (2005) 054506.
9. "Amide I vibrational dynamics of N-methylacetamide in polar solvents: The role of electrostatic interactions," Matthew F. DeCamp, Lauren DeFlores, Justine M. McCracken, Andrei Tokmakoff, Kijeong Kwac, and Minhaeng Cho, *Journal of Physical Chemistry B*, **109** (2005) 11016.
10. "Upconversion multichannel infrared spectrometer," Matthew F. DeCamp and Andrei Tokmakoff, *Optics Letters*, **30** (2005) 1818.
11. "Electric field fluctuations drive vibrational dephasing in water," Joel D. Eaves, Andrei Tokmakoff, and Phillip L. Geissler, *Journal of Physical Chemistry B*, in press.
12. "Polarizable molecules in the vibrational spectroscopy of water," Edward Harder, Joel D. Eaves, Andrei Tokmakoff and Bruce J. Berne, *Proceedings of the National Academy of Sciences, USA*, **102** (2005) 11611.
13. "Hydrogen bonds in liquid water are broken only fleetingly," J. D. Eaves, J. J. Loparo, C. J. Fecko, S. T. Roberts, A. Tokmakoff and P. L. Geissler, *Proceedings of the National Academy of Sciences, USA*, **102** (2005) 13019.
14. "A study of phonon-assisted exciton relaxation dynamics for a (6,5) enriched DNA-wrapped single walled carbon nanotubes sample," S. G. Chou, M. F. DeCamp, J. Jiang, Ge. G. Samsonidze, E. B. Barros, F. Plentz, A. Jorio, M. Zheng, G. B. Onoa, E. D. Semke, A. Tokmakoff, R. Saito, G. Dresselhaus, M. S. Dresselhaus, *Physical Review B*, in press.

STRUCTURAL STUDIES OF THE SOLVATION EFFECTS AND CHEMICAL INTERACTIONS IN OPEN-SHELL SYSTEMS

G. N. R. Tripathi

Notre Dame Radiation Laboratory
Notre Dame, IN 46556

Email: Tripathi.1@nd.edu; tel: (574)631 5514; fax: (574)631 8068

This program aims to provide a molecular level description of the nature and role of chemical environment in determining the molecular geometry, bond structure and reactivity of prototype open-shell radical systems. Radical-solvent interactions can involve exchange between the unpaired electron on the radical and electron pairs on the solvent molecules. These interactions are often different in nature, strength and physicochemical effects from those in closely related closed-shell systems, including ions. A variety of experimental techniques, such as the Radiation Laboratory's unique time-resolved Raman, transient absorption and electron spin resonance spectroscopies, complemented by quantum chemical structure calculations, are used to achieve the objectives of the program. The information sought is valuable for gaining insight into the role of the medium in directing the speed and course of reactions and making useful applications to a range of energy related chemical, industrial and biomedical processes. These applications include electron transfer reactions relevant to energy conversion and storage devices. These studies are of utmost importance for the development and testing of appropriate theories for the electronic structure of radicals in condensed phases.

Recently the role of ions in affecting the hydrogen bond network in liquid water has been questioned.[1] It has been believed for a long time that some ions enhance the hydrogen bond structure in water, and that others weaken it.[1-5] However, the concept of structure making and breaking has been based on macroscopic properties, e.g., viscosity and entropy of solvation, and has not been established by structural investigations.[1,3-4] A recent rotational dynamics study of water molecule coordinated with ions and in bulk has led to the startling conclusion that the addition of ions has no influence on hydrogen bonding of water molecules outside the first solvation shells of the ions and does not support the concept of the enhancement or breakdown of the hydrogen-bond network in liquid water by ions.[1] The explanation for the bulk properties of liquid water containing ions, such as viscosity, has been proposed in terms of rigid sphere model of the hydrated ions. Thus far there has been no structural confirmation of this model. Our current studies on solvated radicals are directed towards examining the role of hydrated ions in affecting the hydrogen bond structure of liquid water beyond their hydration shells. Radicals containing hydrogen bonding moieties, such as O and NH_2, are excellent hydrogen bond sensors.[6] Previously well characterized centrosymmetric (e.g., p-benzosemiquinone anion ($O\text{-}C_6H_4\text{-}O^{-\bullet}$), p-phenylenediamine cation ($H_2N\text{-}C_6H_4\text{-}NH_2^{+\bullet}$) and asymmetric radicals (e.g., p-aminophenoxyl ($H_2N\text{-}C_6H_4\text{-}O^{\bullet}$))[6-8] provide sensitive probes for the hydrogen bonding and the potential gradient effects produced by the hydrated cations and anions in solution. Other radical

probes used in these studies are asymmetric benzoate dianion (C_6H_5-CO_2^{2-}·) and N-heterocyclic radicals such as pyridinal (C_5H_5-NH·) radical.

Probe radicals can be inserted in solution at a very low concentration using pulse radiolysis. In these very dilute solutions the mutual interaction between different probe radicals and their hydration shells can be ruled out. The intensity profile and the vibrational frequencies observed in time–resolved resonance Raman spectra contain information on the interaction between the radical and its chemical environment. Because of instantaneous nature of the Raman scattering process, the water molecules coordinated with ions cannot exchange with those in the bulk. Hydrogen bonds are not formed or broken during the scattering process. In the case of ESR experiments, the exchange of water molecules is fast enough that the hydrogen bonding effects are averaged.[5] Therefore, resonance Raman spectroscopy provides information on the space-averaged effects of the hydrogen bonding environment and ESR spectroscopy on the time-averaged effects.

In the rigid sphere model of hydrated ions,[1] a solute molecule with hydrogen-bonding capabilities is expected to interact with the water molecules within the hydration shell spheres. If the ions are incapable of exerting a significant effect beyond the first hydration shell, the structural properties of the solute molecule should not change from that in a pure aqueous solution. In a time-resolved resonance Raman study of an asymmetric (zwitterionic) radical having O and NH_2 end groups (H_2N-C_6H_4-O·), no significant change in vibrational frequencies was observed on addition of very high concentration of Na^+/Li^+ and Cl^- ions to solution.[8] However, the intensity profile of the spectrum changed dramatically, with greatly enhanced dynamic coupling between the NH_2 scissors and the ring stretching motion of the radical, observed in the 1600-1700 cm^{-1} region.[8] It is obvious that the effect of ions beyond their first hydration shell is not strong enough to cause a perceptible shift in the vibrational frequencies, but it is fairly significant in enhancing the intra-molecular vibrational coupling and, as a consequence, the intensity profile of the resonance Raman spectrum.[8]

The clustering of the hydrated anions and cations across the polar ends of a molecule creates a charge gradient. In ESR experiments we have observed the migration of charge under the influence of this potential gradient, using the H_2N-C_6H_4-O· radical as a model probe.[9] The ring proton hyperfine constants provide a measure of the unpaired π-electron distribution on the ring. On addition of 8M LiCl to solution, the proton hyperfine constants of the ring hydrogens adjacent to the amine group increase by 5.2% and decrease by a slightly lesser extent (2.3%) for the hydrogens adjacent to the O atom. The total spin on the aromatic ring is relatively unaffected. This effect of a potential gradient generated by the hydrated anions and counter cations across the length of a polar molecule in solution on intra-molecular charge migration has not been reported previously.

In the absence of a charge gradients, as in the case of centrosymmetric radicals [e.g., $(O\text{-}C_6H_4\text{-}O)^-$· and $(H_2N\text{-}C_6H_4\text{-}H_2N)^+$ ·], no significant change in the ESR hyperfine constants of the ring protons is observed to result from the presence of high concentration of Na^+/Li^+ and Cl^- ions in solution. On the other hand, the resonance Raman spectra of $(H_2N\text{-}C_6H_4\text{-}H_2N)^{+\bullet}$ exhibit a profound change in the dynamic coupling between the NH_2 scissors and the ring stretching vibrations, indicated by the changes in the intensity profile of the corresponding bands in the

1600-1700 cm^{-1} region. This difference arises because of the differences in the time-scales of the Raman scattering and the ESR relaxation processes mentioned earlier.

We have also studied the effects of vibrational excitation on molecular orientation in aqueous metal-molecule systems, using Ag_n-(p-aminothiophenol) as a model.[10] Such molecules adsorb on the metal particles in a radical-like state.[11] It has been found that the surface-bound molecules/radicals that are spontaneously excited into higher vibrational states by Stokes surface-enhanced Raman scattering can reorient in the relaxed vibrational states probed by anti-Stokes surface-enhanced Raman scattering.[10] This phenomenon is identifiable by the anti-Stokes and Stokes intensity ratios of the vibrational bands differing from the Boltzmann factor.

In near future studies, isotopic substitutions in probe radicals will be used for changing the intrinsic coupling strength between the intramolecular vibrations. The relationship between the intrinsic coupling strength and the extent of its enhancement in the presence of ions in solution will be investigated. These studies will also clarify the role of the bending vibration of water molecules in the intramolecular vibrational coupling in the radical probes. Complementary studies in aprotic solvents will distinguish between the hydrogen-bond effects and bulk solvent effects such as viscosity and dielectric constant. In addition to amine radicals, the benzoate dianion (C_6H_5-CO_2^{2-}•) and pyridinal (C_5H_5-NH•) radicals will be used as probes.

We will elucidate the early chemical steps in the radiation chemistry of saline aqueous solutions, relevant to the formation of probe radicals in a strongly ionic environment. Of particular interest is the chemistry induced by the direct and indirect effects of radiation. At high concentrations of hydrated ions, the radiation is likely to interact directly with the ion and cause ionization. The indirect effect involves fragmentation of water molecules into highly reactive radicals (e.g., •OH and e_{aq}^-) which subsequently attack the ion. Initial studies will be performed on neutral aqueous solutions containing high concentrations of chloride ions. Preliminary transient absorption studies have shown the appearance of transient/s absorbing at about 340 nm. The absorbance at this wavelength grows with the Cl^- concentration. We will use the specificity of time resolved resonance Raman spectroscopy to identify the species that contribute towards this absorption at different concentrations of Cl^- and elucidate the mechanism of their formation. These studies will be subsequently extended to the aqueous solutions containing very high concentrations of other halide ions and OH^-.

The radical-water interaction will be studies in hydrated atomic radicals using time-resolved resonance Raman spectroscopy and quantum mechanical structure calculations. We will focus on the systems such as such as $Ag(H_2O)_n^\bullet$ and $ClOH^{-\bullet}/ClOH_2^\bullet$ which are of fundamental importance in a variety of reactions but have been difficult to observe by structure–sensitive techniques. Distinction will be made between a few water molecules associated with the radical centers and the bulk of water molecules and their structural properties will be determined.

Acknowledgement

The research described herein was supported by the Office of Basic Energy Sciences of the Department of Energy.

References

(1) Omta, A. W.; Kropman, M. F.; Woutersen, S.; Bakker, H. J. *Science* **2003**, *301*, 347; *J. Chem. Phys.* **2003**, *119*, 12457.

(2) Krestov, G. A. *Thermodynamics of Solvation* (Ellis Horwood, Chichester, UK, **1991**).

(3) Gurney, R. W. *Ionic Processes in Solution* (McGraw-Hill, New York, **1953**).

(4) Marcus, Y. *Ion Solvation* (Wiley, Chichester, UK, **1985**).

(5) Ohtaki, H.; Radnai, T. *Chem. Rev.* **93**, 1157 (**1993**).

(6) Tripathi, G. N. R. *J. Chem. Phys.* **2003**, *118*, 1378. **2005**, *122*, 071102.

(7) Tripathi, G. N. R. In *Time-resolved Spectroscopy*, Clark, R. J. H., Hester, R. E., Eds.; Advances in Spectroscopy, Vol. 18; Wiley: New York, **1989**; pp 157-218.

(8) Tripathi, G. N. R. *J. Phys. Chem. A* **2004**, *108*, 5139.

(9) Tripathi, G. N. R.; Hug, G. H.; Schuler, R. H. (*to be published).*

(10) Sheehan, D.; Tripathi, G. N. R. (*Submitted for publication).*

(11) Sandroff' J.; Herschbach, D. R. *J. Phys. Chem.* 1982, *86*, 3277.

Publications of DOE sponsored research (2003-2005)

Time resolved resonance Raman observation of the extreme protonation forms of a radical zwitterion in water
G. N. R. Tripathi, J. Chem. Phys. **2005**, *122*, 071102.

Effect of Ionic Modification of the Hydration Shell of a Charge-Neutral Radical on its Resonance Raman Spectrum
G. N. R. Tripathi, J. Phys. Chem. A **2004**, *108*, 5139.

The Origin of Base Catalysis in the OH Oxidation of Phenols in Water
G. N. R. Tripathi & Y. Su, J. Phys. Chem. A **2004,** *108,* 3478-3484

Electronic Structure of para Aminophenoxyl Radical in Water
G. N. R. Tripathi, J. Chem. Phys. **2003**, *118*, 1378.,

p-Benzosemiquinone Radical Anion on Silver Nanoparticles in Water
G. N. R. Tripathi, J. Am. Chem. Soc. **2003**, *125*, 1179.

Adsorption of 2-Mercaptopyrimidine on Silver Nanoparticles in Water
G. N. R. Tripathi & M. Clements, J. Phys. Chem. B **2003**, *107*, 11125.

Molecular Theory & Modeling

Accurate binding energies and structural patterns of water clusters (n=2-21)

Sotiris S. Xantheas
Chemical Sciences Division
Pacific Northwest National Laboratory
902 Battelle Blvd.
Mail Stop K1-83
Richland, WA 99352
sotiris.xantheas@pnl.gov

The objective of this research effort is to provide energetic information regarding the interaction of water molecules in small to medium size clusters (*n*=2-21). This information is essential in order to assess the accuracy of reduced representations of intermolecular interactions for water such as model potentials and/or various density functionals. The parametrization of those reduced representations is commonly performed using available data from a variety of environments ranging from clusters to liquid water and ice. The results for water clusters offer the advantage of probing the fundamental interactions at the molecular level and therefore systematically identifying the physical terms necessary to describe hydrogen bonding. However, no direct experimental measurements have been performed to date for the interaction energies of even small clusters such as the water dimer let alone liquid water and/or ice. All cluster energetic information that is used in the parameterization of interaction potentials comes directly from calculations.

First principles electronic calculations offer the advantage of providing this essential energetic information. The issue of accuracy is of outmost importance since, for instance, numbers within "chemical accuracy" (1 kcal/mol) for the binding energies of small water clusters are needed in order to ensure transferability for larger systems such as bulk water and ice and produce meaningful results. This range typically represents a small (<1%) percentage of the cluster binding energies. However, the computational cost scales theoretically between N^3 to N^5, N being proportional to the size of the system. For the water hexamer, for example, in order to tighten the accuracy of the computed binding energies from 10% to 1% requires a 10,000x increase in the computational cost. These calculations are currently impossible on conventional computers using serial architectures. Recent implementations of electronic structure software methods that exploit the advantages of supercomputers with parallel architectures (NWCHEM) have made these calculations feasible for the first time, thus providing indispensable and currently irreplaceable information needed for the development of accurate interaction potentials.

We are developing a database of accurate binding energies of water clusters up to size *n*=21 from electronic structure calculations that are based on hierarchical approaches in both the correlation and orbital basis set expansions. The correlation part is treated at the second order perturbation (MP2) and coupled cluster with single, double and perturbative estimates of triple replacements [CCSD(T)] levels of theory. The use of the family of augmented correlation-consistent polarized valence basis sets of double to quintuple zeta quality (aug-cc-pV*x*Z, *x*=D, T, Q, 5) allows for estimates of the complete basis set (CBS) limit. These binding energies are becoming the benchmark references for new electronic structure methods describing hydrogen bonding such as the new generation of density functionals (i.e. X3LYP). They are furthermore

being used as the standards in the parametrization of the new generation of interaction potentials for water such as TTM2-R, TTM2-F, AMOEBA, GCPM and MCDHO.

Table 1 shows the comparison between the computed MP2/CBS binding energies and the ones obtained with various potentials for selected clusters.

n	ASP-W	ASP-W4	TTM2-R	TTM2-F	MP2/CBS	|ΔE|/n
2	-4.68	-4.99	-4.98	-5.02	-4.98	0.02
3 cyclic	-14.81	-15.49	-15.59	-15.90	-15.8	0.03
4 cyclic	-24.32	-26.97	-27.03	-27.54	-27.6	0.02
5 cyclic	-30.88	-35.09	-36.05	-36.69	-36.3	0.08
5 cage	-32.65	-35.23	-34.75	-35.22	(-35.1)	0.02
6 prism	-42.54	-47.06	-45.11	-45.86	-45.9	0.01
6 cage	-43.31	-45.86	-45.65	-46.46	-45.8	0.11
6 book	-40.48	-45.00	-45.14	-45.99	-45.6	0.07
6 cyclic	-37.58	-43.36	-44.28	-45.03	-44.8	0.04
8 cube (D_{2d})		-73.15	-71.87	-73.21	-72.7	0.06
8 cube (S_4)				-73.24	-72.7	0.06
20 dodecahedron		-197.1	-198.5	-202.2	-200.1	0.11
20 (5x4mers)		-210.2	-210.9	-214.3	-212.6	0.09
20 (4x5mers)		-210.7	-210.6	-214.0	-215.0	0.05
20 (glob. min)		-210.8	-210.8	-212.6	-217.9	0.08

Table 1. Comparison of the MP2/CBS binding energies of water clusters with the ones obtained with various empirical potentials.

The accurate calculation of the binding energies of various hydrogen bonded networks present in the families of isomers of $(H_2O)_{20}$ has solved a long standing problem regarding their relative stability. For this cluster, based on the arrangement of the oxygen atom network, there are 4 major families of minima (a) *dodecahedron*, (b) *fused cubes*, (c) *face-sharing pentagonal prisms* and (d) *edge-sharing pentagonal prisms*. Interest in the relative stabilities of the various networks of these neutral clusters stems from their importance in understanding the transition from the open 3-fold to the compact 4-fold coordinated structures. The relative energetic order of the most stable isomer of each family is predicted from the *ab-initio* calculations to be: (d) (most stable), (c), (b), (a) (less stable). Their corresponding MP2/CBS binding energies are: -200.1 kcal/mol (*dodecahedron*, 30 hydrogen bonds), -212.6 kcal/mol (*fused cubes*, 36 hydrogen bonds, 36 dangling bonds), -215.0 (*face-sharing pentagonal prisms*, 35 hydrogen bonds, 15 dangling bonds) and –217.9 kcal/mol (*edge-sharing pentagonal prisms*, 34 hydrogen bonds, 10 dangling bonds). Therefore the

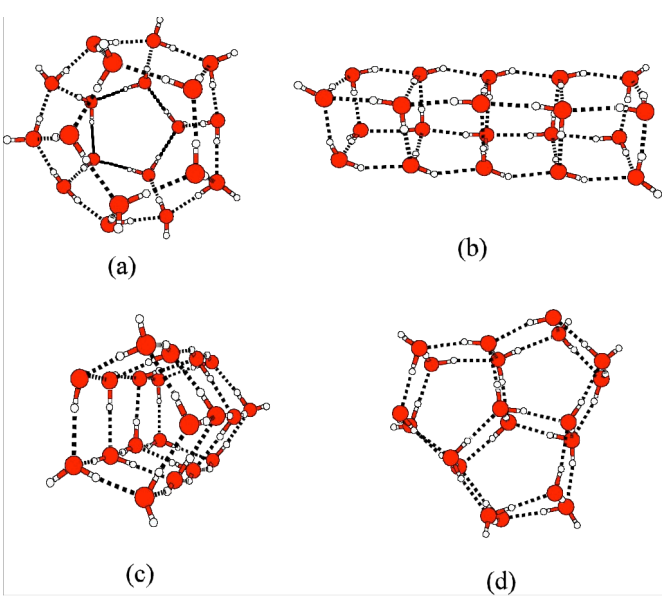

dodecahedron lies ca. 18 kcal/mol higher in energy than the most stable edge-sharing pentagonal prism isomer.

The *ab-initio* investigation of the relative stability of the various hydrogen bonding networks in the *n*=17-21 cluster regime has identified the existence of a transitional size regime where preferential stabilization alternates between "all-surface" (all atoms on the surface of a cluster) and "internally solvated" (one water molecule at the center of the cluster, fully solvated) configurations with the addition or the removal of a single water molecule.

This behavior has been previously suggested based on the results of the TTM2-F interaction potential. It is qualitatively different from the picture that simple, pairwise-additive potentials like TIP4P suggest. The onset of the appearance of the first "interior" configuration in water clusters occurs for *n*=17. The observed structural alternation between "interior" (*n*=17, 19, 21) and "all-surface" (*n*=18, 20) global minima in the *n*=17-21 cluster regime is accompanied by a corresponding spectroscopic signature, namely the undulation in the position of the most red-shifted OH stretching vibrations according to the trend: "interior" configurations exhibit more red-shifted OH stretching vibrations than "all-surface" ones. These most red-shifted OH stretching vibrations form distinct groups in the intramolecular region of the spectra and correspond to localized vibrations of donor OH stretches that are connected to neighbors via "strong" (water dimer-like) hydrogen bonds and belong to a water molecule with a "free" OH stretch.

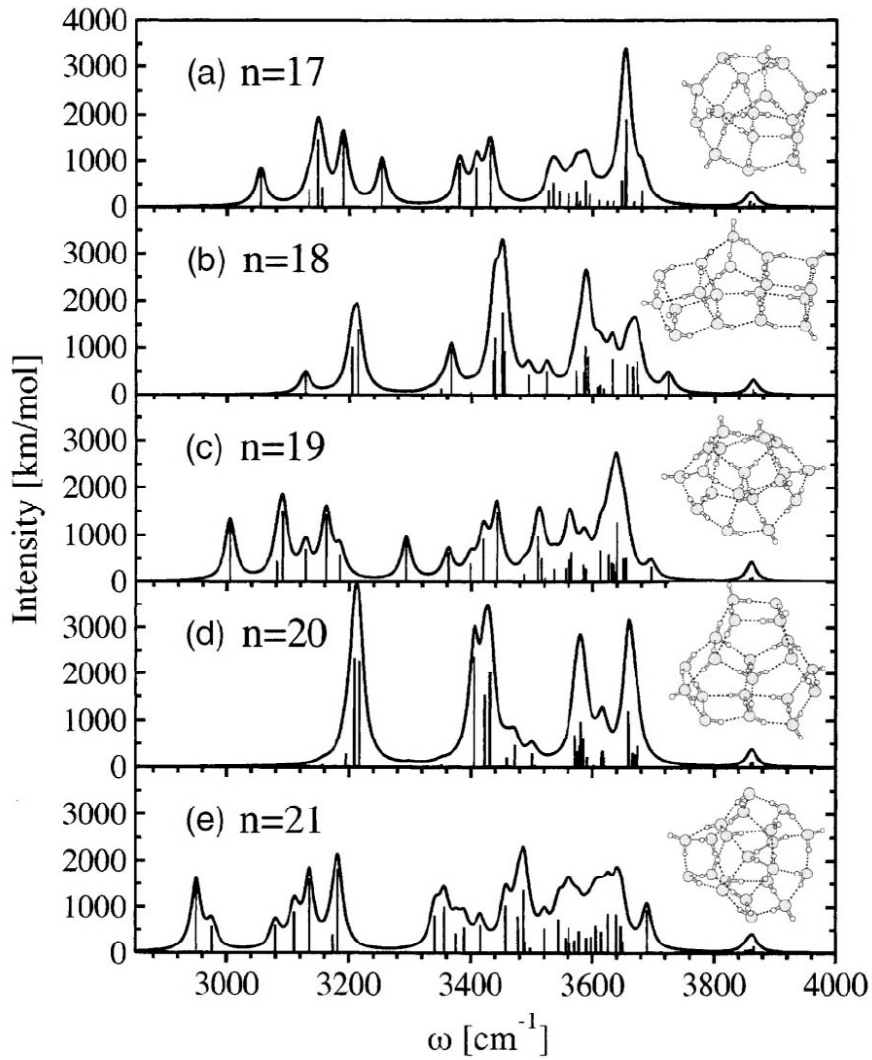

Acknowledgements: This research was performed in part using computational resources in the Molecular Science Computing Facility (MCSF) in the William R. Wiley Environmental Molecular Sciences Laboratory. Battelle operates Pacific Northwest National Laboratory for the U. S. Department of Energy.

Collaborators on this project include A. Lagutschenkov, G. Niedner-Schatteburg, E. Aprà, G. S. Fanourgakis and W. A. de Jong.

References to publications of DOE sponsored research (2003-present)

1. G. M. Chaban, S. S. Xantheas, R. B. Gerber, "Anharmonic Vibrational Spectroscopy of the F^- $(H_2O)_n$ complexes, *n*=1, 2" *Journal of Physical Chemistry A* **107**, 4952 (2003)

2. S. S. Xantheas, E. Aprà, "The binding energies of the D_{2d} and S_4 water octamer isomers: High-level electronic structure and empirical potential results", *Journal of Chemical Physics* **120**, 823 (2004)

3. J. M. Bowman, S. S. Xantheas, "*Morphing* of *ab initio*-based interaction potentials to spectroscopic accuracy: Application to $Cl^-(H_2O)$", *Pure and Applied Chemistry* **76**, 29 (2004)

4. C. J. Burnham and S. S. Xantheas, "On the importance of zero-point effects in molecular level classical simulations of water", *Journal of Molecular Liquids* **110**, 177 (2004)

5. S. S. Xantheas, "Intermolecular Interactions and Cooperative Effects from Electronic Structure Calculations: An Effective Means for Developing Interaction Potentials for Condensed Phase Simulations" in *Novel Approaches to the Structure and Dynamics of Liquids: Experiments, Theories and Simulations*, NATO Science Series II: Mathematics, Physics and Chemistry vol. 133 J. Samios and V. A. Durov (Eds.), pp. 1-15, Kluver Academic Publishers, Dordrecht, The Netherlands (2004)

6. G. S. Fanourgakis, E. Aprà and S. S. Xantheas, "High-level *ab-initio* calculations for the four low-lying families of minima of $(H_2O)_{20}$: I. Estimates of MP2/CBS binding energies and comparison with empirical potentials", *Journal of Chemical Physics* **121**, 2655 (2004)

7. B. C. Garrett, D. A. Dixon, *et al* "The Role of Water on Electron-Initiated Processes and Radical Chemistry: Issues and Scientific Advances", *Chem. Rev.* **106**, 355 (2005)

8. G. S. Fanourgakis, E. Aprà, W. A. de Jong, and S. S. Xantheas, "High-level *ab-initio* calculations for the four low-lying families of minima of $(H_2O)_{20}$: II. Spectroscopic signatures of the dodecahedron, fused cubes, face-sharing and edge-sharing pentagonal prisms hydrogen bonding networks", *Journal of Chemical Physics* **122**, 134304 (2005)

9. A. Lagutschenkov, G. S. Fanourgakis, G. Niedner-Schatteburg and S. S. Xantheas, "The spectroscopic signature of the "all-surface" to "internally solvated" structural transition in water clusters in the *n*=17-21 size regime", *Journal of Chemical Physics* **122**, 194310 (2005)

8. S. Hirata, M. Valiev, M. Dupuis and S. S. Xantheas, S. Sugiki and H. Sekino, "Fast electron correlation methods for molecular clusters in the ground and excited states", *Molecular Physics* (R. J. Bartlett special issue) **103**, 2255 (2005).

9. S. S. Xantheas, "Interaction potentials for water from accurate cluster calculations" in *Structure and Bonding: Intermolecular Forces and Clusters*, Springer Verlag, D. J. Wales (Editor) 2005.

10. S. S. Xantheas, W. Roth, I. Fischer, "Competition between van der Waals and Hydrogen Bonding Interactions: The strucutre of the trans-1-Napthol/N_2 cluster", *Journal of Physical Chemistry A* (in press).

Abstract for DE-FG02-00ER15072
Studies of Protein Conformational Dynamics Via Single-Molecule Electron Transfer

PI: Sunney Xie
Department of Chemistry and Chemical Biology
Harvard University
12 Oxford Street
Cambridge, MA 02138
xie@chemistry.harvard.edu

We investigate protein conformational fluctuations by conducting single-molecule electron transfer experiments. The experimental findings have led to the discovery of a remarkable power law memory kernel spanning from 10^{-3} s to 10 s. The consequence of such a memory kernel for biochemical reactions is studied in the framework of Kramers' theory by stochastic simulations of generalized Langevin dynamics, which accurately accounts for the experimentally observed dynamic disorder in enzymatic reactions. The microscopic origin of multiple timescale fluctuation of protein is also investigated by molecular dynamics simulations. We began a new project on nonequilibrium steady-state thermodynamics of biochemical reactions, developing a methodology of determination of thermodynamic driving force from nonequilibrium turnover time traces of single enzymes.

Recent Progress

1. Power law memory kernel for conformational fluctuation within a single protein molecule (*Wei Min and Guobin Luo, graduate students, Prof. Binny Cherayil, on sabbatical from Indian Institute of Science, Prof. Sam Kou, collaborator at Harvard's Statistics Department*)

The rate of electron transfer (ET) is sensitive to the donor (D) -acceptor (A) distance, which can serve as a probe to monitor protein motion with angstrom resolution. We have investigated the equilibrium fluctuation of DA distance within a single protein molecule. A highly specific monoclonal anti-fluorescein antibody (anti-FL) binds to the fluorescein (FL) and quenches its fluorescence (up to 90%) by excited state ET from a nearby tyrosine residue (Fig.1). The fluorescence lifetime of a single fluorescein anti-fluorescein complex was monitored as a function of time. The autocorrelation function of the DA distance, $C_x(t)$, deduced with high time resolution (Fig. 2a), decays over a broad range of time scales from millisecond to hundreds of seconds.

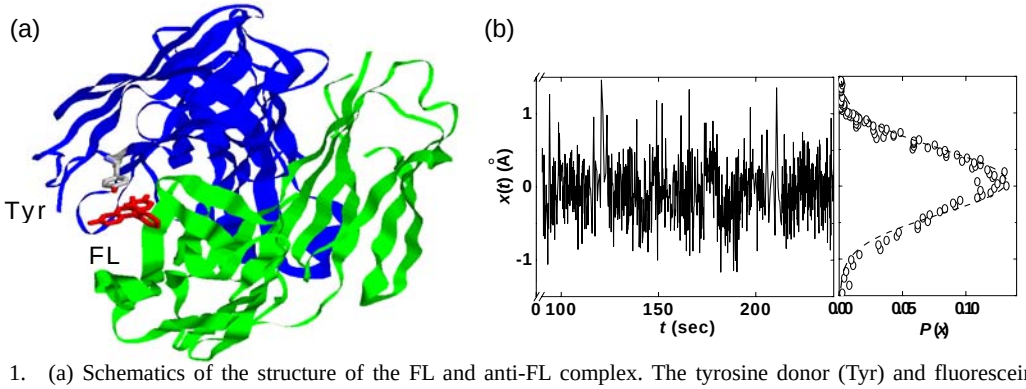

Fig. 1. (a) Schematics of the structure of the FL and anti-FL complex. The tyrosine donor (Tyr) and fluorescein acceptor (FL) for the photo-induced electron transfer reaction are highlighted. (b) An experimental trajectory of the donor acceptor distance, *x*, for a single complex.

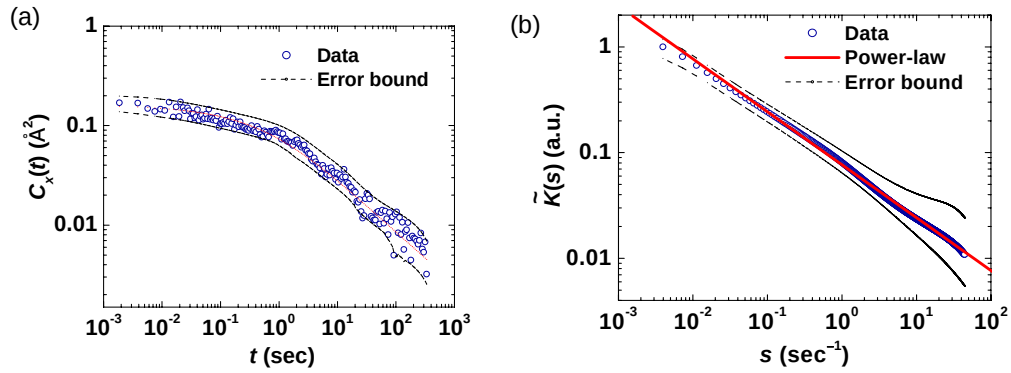

Fig. 2. (a) Autocorrelation function of $x(t)$ is highly stretched multi-exponential decay, indicating fluctuations on a broad range of time scales. (b) Within the frame work of GLE, the memory kernel $\tilde{K}(s)$ is experimentally determined to be a power law.

We model $x(t)$ as the coordinate of a fictitious particle diffusing in a harmonic potential. The generalized Langevin equation (GLE) governs its dynamical evolution:

$$m\frac{d^2x(t)}{dt^2} = -\zeta\int_0^t d\tau K(t-\tau)\frac{dx(\tau)}{d\tau} - \frac{dU(x)}{dx} + F(t)$$

where m is the mass of the particle, $U(x)$ is the harmonic potential, ζ is the friction coefficient, $F(t)$ is the random force with certain memory function $K(t, \tau)$ that is in turn related to $F(t)$ by fluctuation-dissipation theorem, $< F(t)F(\tau) >= k_B T\zeta K(t-\tau)$. In the over-damped limit, where the inertial term can be neglected, we have shown that $\tilde{K}(s)$, the Laplace transform of $K(t)$, exhibits a simple power-law decay, $\tilde{K}(s) \propto s^{\alpha}$, with α=–0.49±0.07 over at least four decades of time (Fig. 2b). The inverse Laplace transform gives $K(t) = t^{-\alpha-1} \propto t^{-1/2}$, which is remarkably simple. This underlies the fact that protein conformational changes take place at broad range of timescales.

2. A unified theory for dynamic disorder of biochemical reactions by incorporating power law memory kernel into the celebrated Kramers' escape theory (*Wei Min, graduate student*)

If a power law memory kernel exists for the distance between any two points within a protein molecule, it must also exist for a 1D reaction coordination of an enzymatic reaction. We have developed a new model to explain dynamic disorder by incorporating power law memory kernel into the Kramers' escape problem. The results were obtained by stochastic simulation of generalized Langevin dynamics in double well.

Fig. 3 shows the first passage time distributions of chemical reactions for three different coupling strengths ζ between the reaction coordinate and the other degrees of motions. Stretched exponential decays was observed for strong coupling condition. This work provides a unified theory for dispersed kinetics in condensed-phase chemical reactions, dynamic disorder in particular, with simple and reasonable assumptions. It reduces to Kramers-Grote-Hynes theory under the condition of timescale separation. Our new model can readily account for the dispersed kinetics of CO binding to myoglobin observed by

Frauenfelder *et al*, as well as our recent observation of fluctuating rate constants of single-molecule enzymatic reactions.

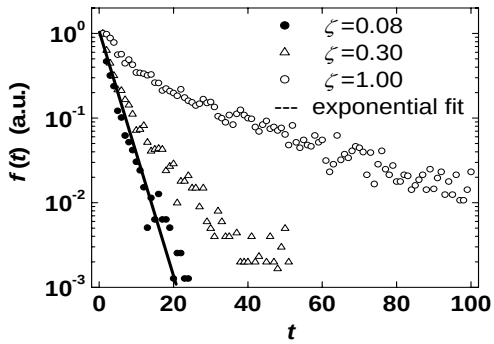

Fig. 3. Stochastic simulation of the first passage time distribution for a particle escaping a barrier with power law memory kernel. The friction constant ζ reflects the coupling strength between the reaction coordinate and the other degrees of motions. The deviation of the decay from single exponential behavior is remarkable when the coupling strength increases.

3. MD simulation of the conformation dynamics of NADH:flavin oxidoreductase *(Guobin Luo, graduate student, and Prof. Martin Karplus, collaborator at Harvard's Chemistry Dept.)*

We further explored the microscopic origin of the stretched-exponential behavior of Fre/FAD complex found in both MD simulations and single molecule experiments.

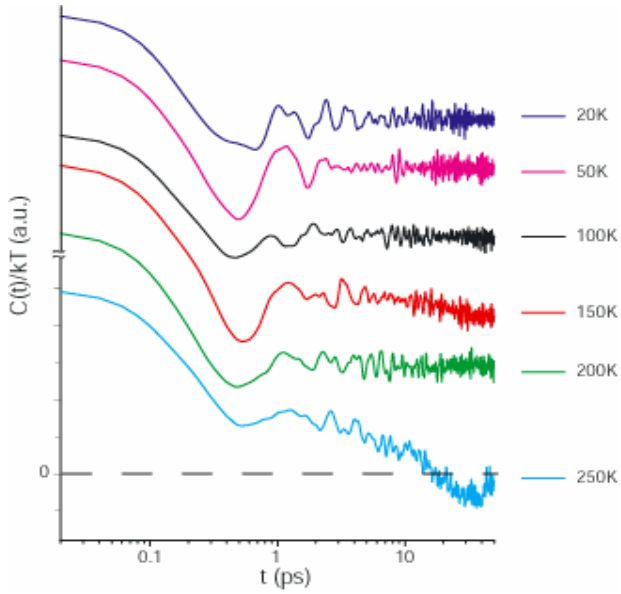

Fig. 4. Distance autocorrelation functions of Tyr[35]-isoalloxazine distance from 100ps simulation trajectories obtained at different temperatures. The correlation functions at 20, 50, 100, 150, and 200 K are offset for clarity. The fast decays from 0.1~1ps are due to the Brownian motion within the local potential well. At low temperatures, the system doesn't have enough thermal energy and the motion is confined within the local potential. Longer time fluctuations occur at higher temperatures as a result of escape from local potential well.

In the previous simulation we have found a transition from the short time Brownian motion to the longer time multi-exponential relaxation at ~1ps. Such behavior originates from the energy barrier crossing process. Now we have done simulations under different temperatures to corroborate it. For a series of simulations of Fre/FAD complex between 20 and 250K, a transition occurred at around 200K where fluctuation amplitude had stronger temperature dependence above that temperature. The distance correlation function has an interesting temperature dependence, shown in Fig. 4. The fast Brownian decay with a similar time scale exists at all different temperatures. Below 200K, only this fast relaxation is present. At 250K, however, a slower

stretched-exponential decay, analogous to that at room temperature, is clearly seen on a longer time scale. Clearly, with the increase in temperature, the system has a higher probability of crossing the barriers between potential wells at a finite simulation time (100ps in our case). This observation provides direct evidence that the complex relaxation dynamics originates from the multi-minimum character of the potential energy surface.

4. Determination of thermodynamic driving force from nonequilibrium turnover time traces of single enzymes (*Wei Min and Liang Jiang, graduate students, Ji Yu, postdoctoral fellow, Prof. Sam Kou, collaborator at Harvard's Statistics Department, Prof. Hong Qian, collaborator at University of Washington's Applied Mathematics Department*)

A single enzyme molecule in a living cell usually undergoes biochemical reactions in a nonequilibrium steady state condition. The thermodynamic driving force is an important quantity that determines the extent to which the reaction is away from equilibrium. Traditionally, this driving force is obtained by measuring substrate and product concentrations and rate constants by ensemble kinetics. In contrast, we have recently shown that this driving force for an enzymatic reaction can be determined from the nonequilibrium time traces of enzymatic turnovers of individual enzyme molecules, which can now be experimentally recorded by single molecule techniques.

Three different thermodynamic driving force estimators are presented from the principles of nonequilirium statistical mechanics, in particular, fluctuation theorem, Kawasaki identity, and fluctuation dissipation theorem. The statistical precisions of these three estimators are analyzed and compared for finite lengths of experimental time traces. These theoretical principles and statistical techniques could provide a general methodology for single-molecule nonequilibrium dynamics.

Publications

[1] S. C. Kou, X. S. Xie. Generalized Langevin Equation with Fractional Gaussian Noise: Subdiffusion of a Single Protein Molecule. *Phys. Rev. Lett. 93*, 180603 (2004).

[2] Wei Min, Guobin Luo, Binny Cherayil, S. C. Kou, X. S. Xie. Observation of a power paw memory kernel for fluctuation within a single protein molecule. *PRL 94*, 198302 (2005).

[3] Wei Min, Brian English, Guobin Luo, Binny Cherayil, S. C. Kou, X. S. Xie. Fluctuating Enzymes: Lessons from Single-Molecule Studies. *Acc. Chem. Res. in press* 2005

[4] Wei Min, X. Sunney Xie. Barrier Crossing with a Power-Law Friction Kernel: Dispersed Kinetics and Dynamic Disorder of Biochemical Reactions. *Phys. Rev. Lett.* submitted.

[5] Wei Min, Liang Jiang, Ji Yu, S. C. Kou, Hong Qian, X. Sunney Xie. Nonequilibrium steady state of biochemical reactions: determination of thermodynamic driving force from single enzyme turnover time traces. *PNAS* submitted.

[6] Guobin Luo, Ioan Andricioaei1, X. S. Xie, Martin Karplus. Distance disorder in proteins is caused by trapping. *Phys. Rev. Lett.* submitted.

[7] J. T. Krug, E. J. Sanchez, X. Sunney Xie. Fluorescence quenching in tip-enhanced nonlinear optical microscopy. *Appl. Phys. Lett. 86*, 233102 (2005).

Author Index

Ahmed, Musahid.....79
Altman, Eric I.....32
Anderson, Scott.....2
Armentrout, Peter.....38
Balasubramanian, Krishnan.....83
Bartels, David 55
Beck, Kenneth M. 13
Beuhler, Robert J. 33
Camillone, Nicholas.....33
Carmichael, Ian.....172, 206
Carter, Emily.....141
Castleman, Jr., A. Welford.....87
Ceyer, Sylvia T. 29
Chandler, David 91
Chang, Bong-Kyu 37
Chelikowsky, James.....141
Chipman, Daniel 55, 206
Cook, Andrew R. 194
Corrales, L. Rene 93
Cowin, James 46
Crowell, Robert.....97, 128, 214
Dang, Liem 67
Daschbach, John L. 164
Dei, Sheng.....37
Dohnalek, Zdenek.....164
Duncan, Michael 101
Dupuis, Michel.....105
Eisenthal, Kenneth 42
Ellison, G. Barney.....108
El-Sayed, Mostafa.....112
Evans, Jim 8
Fayer, Michael 116
Garrett, Bruce.....120
Goldfield, Evelyn.....124
Goodman, Wayne 6
Gordon, Mark.....8
Gosztola, David.....97,128, 214
Gray, Stephen.....131
Harris, Charles 137
Harris, Alex.....33
Harrison, Ian 25
Hase, William L. 124
Head-Gordon, Martin.....141
Head-Gordon, Teresa.....145
Henderson, Michael A. 12
Hess, Wayne 13
Ho, Wilson 149
Jackson, Bret 152
Jackson, Koblar.....131
Jellinek, Julius.....131
Johnson, Mark.....156
Joly, Alan G. 13
Jordan, Kenneth 156
Kathmann, Shawn 160
Kay, Bruce 164
Kimmel, Greg 168
Ladanyi, Branka.....176
Laverne, Jay A. 172, 206
Leone, Stephen R. 79
Levinger, Nancy.....176
Lim, Edward 180
Louie, Steven G. 141
Lu, H. Peter 184
Lymar, Sergei V. 194
Maroncelli, Mark 188
Meisel, Dan 172,191
Miller, John R. 194
Morse, Michael 198
Nørskov, Jens 1
Ogut, Serdar 131
Osgood, Richard 21
Overbury, Steven H. 37
Petek, Hrvoje.....17
Petrik, Nicholas G. 168
Piecuch, Piotr 202
Pimblott, Simon 172, 206
Ratner, Mark S. 131
Sanii, Laurie 112
Saykally, Richard.....72
Schatz, George C. 131
Schenter, Greg.....210
Schlegel, H. Bernhard 124
Shkrob, Ilya.....97,128, 214
Sibener, Steven 218
Smith, R. Scott 164
Stair, Peter C. 7
Steimle, Timothy.....222
Stockman, Mark 131

Thompson, Ward.....63
Tokmakoff, Andrei 226
Tripathi, G. N. R. 229
Tully, John C.....51
Wang, Lai-Sheng 75
Wang, Lin-Wang.....141
White, Michael.....33
Wick, Collin.....67
Wishart, James 59
Wodtke, Alec 50
Xantheas, Sotirs 233
Xie, Sunney.....237
Yan, Wenfu 37

Participants

Musahid Ahmed
Lawrence Berkeley National Laboratory
ms 10-100, 1 Cyclotron road
Berkeley, CA 94720
Phone: 510-486-6355
E-Mail: mahmed@lbl.gov

Eric Altman
Department of Chemical Engineering
Yale University
New Haven, CT 06520
Phone: 203-432-4375
E-Mail: eric.altman@yale.edu

Scott Anderson
Chemistry Department
University of Utah
315 S. 1400 E., Rm 2020
Salt Lake City, UT 84112
Phone: 801-585-7289
E-Mail: anderson@chem.utah.edu

Peter Armentrout
Chemistry Department
University of Utah
315 S 1400 E Rm 2020
Salt Lake City, UT 84112
Phone: 801-581-7885
E-Mail: armentrout@chem.utah.edu

David Bartels
Notre Dame Radiation Laboratory
University of Notre Dame
Notre Dame, Indiana 46556
Phone: 475-631-5561
E-Mail: bartels.5@nd.edu

Nicholas Camillone
Chemistry Department, Bldg 555
Brookhaven National Laboratory
Upton, NY 11973
Phone: 631-344-4412
E-Mail: nicholas@bnl.gov

Ian Carmichael
Notre Dame Radiation Laboratory
University of Notre Dame
Notre Dame, IN 46556
Phone: 574-631-4502
E-Mail: carmichael.1@nd.edu

Michael Casassa
DOE Basic Energy Sciences
SC-22.1/Germantown Bldg.
1000 Independence Ave. SW
Washington, DC 20585
Phone: 301-903-0048
E-Mail: michael.casassa@science.doe.gov

A. Welford Castleman
Pennsylvania State University
104 Chemistry Building
University Park, PA 16802
Phone: 814-865-7242
E-Mail: awc@psu.edu

Sylvia Ceyer
Massachusetts Institute of Technology
6-217 77 Mass Ave
Cambridge, MA 02139
Phone: 617-253-4537
E-Mail: stceyer@mit.edu

David Chandler
Department of Chemistry
University of California, Berkeley
Rm 208 Gilman Hall,
Berkeley, CA 94720
Phone: 510-643-6821
E-Mail: chandler@cchem.berkeley.edu

Daniel Chipman
Notre Dame Radiation Laboratory
University of Notre Dame
Notre Dame, IN 46556
Phone: 574-631-5562
E-Mail: chipman.1@nd.edu

Steven Colson
Pacific Northwest National Laboratory
PO Box 999 - MSN K9-80
Richland, WA 99352
Phone: 509-375-2299
E-Mail: Steve.Colson@pnl.gov

L. Rene Corrales
Pacific Northwest National Laboratory
PO Box 999, MS: K1-83
Richanld, WA 99352
Phone: 509-375-2404
E-Mail: rene.corrales@pnl.gov

James Cowin
Pacific Northwest National Laboratory
Box 999, M/S K8-88, 3335 Q Ave
Richland, WA 99352
Phone: 509 376 6330
E-Mail: jp.cowin@pnl.gov

Robert Crowell
Chemistry Division
Argonne National Laboratory
Argonne, IL 60439
Phone: 630-252-8089
E-Mail: rob_crowell@anl.gov

Liem Dang
Pacific Northwest National Laboratory
PO Box 999, MS: K1-83
Richland, WA 99352
Phone: 509-375-2557
E-Mail: liem.dang@pnl.gov

Michael Duncan
Department of Chemistry
University of Georgia
Athens, Georgia 30602
Phone: 706-542-1998
E-Mail: maduncan@uga.edu

Michel Dupuis
Pacific Northwest National Laboratory
Battelle Blvd
Richland, WA 99352
Phone: 509-375-2617
E-Mail: michel.dupuis@pnl.gov

Kenneth Eisenthal
Columbia University
116th St. and Broadway
N.Y., N.Y. 10027
Phone: 212-854-3175
E-Mail: eisenth@chem.columbia.edu

Barney Ellison
Department of Chemistry
University of Colorado
Boulder, CO 80309
Phone: 303-492-8603
E-Mail: barney@jila.colorado.edu

Mostafa El-Sayed
Georgia Institute of Technology
770 State Street
Atlanta, GA 30332
Phone: 404-894-0292
E-Mail: mostafa.el-sayed@chemistry.gatech.edu

James Evans
Ames Laboratory
315 Wilhelm Hall
Iowa State University
Ames, Iowa 50011
Phone: 515-294-1638
E-Mail: evans@ameslab.gov

Michael Fayer
Department of Chemistry
Stanford University
Stanford, CA 94305
Phone: 650 723-4446
E-Mail: fayer@stanford.edu

Gregory Fiechtner
DOE Basic Energy Sciences
SC-22.1/Germantown Bldg.
1000 Independence Ave. SW
Washington, DC 20585
Phone: 301-903-5809
E-Mail: Gregory.Fiechtner@science.doe.gov

Bruce Garrett
Pacific Northwest National Laboratory
PO Box 999, MS: K1-83
Richland, WA 99352
Phone: 509-372-6344
E-Mail: bruce.garrett@pnl.gov

Evelyn Goldfield
Department of Chemistry
Wayne State University
Detroit, MI 48202
Phone: 313-577-2580
E-Mail: evi@chem.wayne.edu

D. Wayne Goodman
Department of Chemistry
Texas A&M University
College Station, TX 77843
Phone: 979-845-0214
E-Mail: goodman@mail.chem.tamu.edu

Mark Gordon
Ames National Laboratory
201C Spedding Hall
Iowa State University
Ames, IA 50011
Phone: 515-294-0452
E-Mail: mark@si.fi.ameslab.gov

David Gosztola
Argonne National Laboratory
9700 S. Cass Ave.
Argonne, Illinois 60439
Phone: 630-252-3541
E-Mail: gosztola@anl.gov

Stephen Gray
Argonne National Laboratory
Chemistry Division
Argonne, IL 60439
Phone: 630-252-3594
E-Mail: gray@tcg.anl.gov

Mary Gress
DOE Basic Energy Sciences
SC-22.1/Germantown Bldg.
1000 Independence Ave. SW
Washington, DC 20585
Phone: 301-903-5827
E-Mail: mary.gress@science.doe.gov

Alex Harris
Brookhaven National Laboratory
Chemistry Department,
Bldg 555, P.O.Box 5000
Upton, NY 11973
Phone: 631-344-4301
E-Mail: alexh@bnl.gov

Charles Harris
Department of Chemistry
University of California, Berkeley
Berkeley, CA 94720
Phone: 510-642-2814
E-Mail: cbharris@berkeley.edu

Ian Harrison
Department of Chemistry
University of Virginia
Charlottesville, VA 22904
Phone: 434-924-3639
E-Mail: harrison@virginia.edu

Carl Hayden
Sandia National Laboratories
P.O. Box 969, M/S 9055
Livermore, CA 94551
Phone: 925-294-2298
E-Mail: cchayde@sandia.gov

Teresa Head-Gordon
University of California, Berkeley
Calvin 204
Berkeley, California 94720
Phone: 510-486-7365
E-Mail: TLHead-Gordon@lbl.gov

Michael Henderson
Pacific Northwest National Laboratory
3335 Q Avenue, MS K8-93
Richland, WA 99354
Phone: 509-376-2192
E-Mail: ma.henderson@pnl.gov

Wayne Hess
Pacific Northwest National Laboratory
902 Battelle Blvd
Richland, WA 99352
Phone: 509-376-9907
E-Mail: wayne.hess@pnl.gov

Richard Hilderbrandt
DOE Basic Energy Sciences
SC-22.1/Germantown Bldg.
1000 Independence Ave. SW
Washington, DC 20585
Phone: 301-903-0035
E-Mail: Richard.Hilderbrandt@science.doe.gov

Wilson Ho
Department of Physics and Department of Chemistry
University of California, Irvine
Irvine, CA 92697
Phone: 949-824-5234
E-Mail: wilsonho@uci.edu

Koblar Jackson
Physics Department
Central Michigan University
Mt. Pleasant, MI 48859
Phone: 989-774-3310
E-Mail: jackson@phy.cmich.edu

Kenneth Jordan
Department of Chemistry
University of Pittsburgh
Pittsburgh, PA 15260
Phone: 412-624-8690
E-Mail: jordan@pitt.edu

Bruce Kay
Pacific Northwest National Laboratory
PO Box 999 MS K8-88
Richland, WA 99352
Phone: 509-376-0028
E-Mail: bruce.kay@pnl.gov

Branka Ladanyi
Department of Chemistry
Colorado State University
Fort Collins, CO 80523
Phone: 970-491-5196
E-Mail: bl@lamar.colostate.edu

Bret Jackson
Dept. of Chemistry
University. of Massachusetts, Amherst
701 LGRT
Amherst, MA 01003
Phone: 413-545-2583
E-Mail: jackson@chem.umass.edu

Mark Johnson
Department of Chemistry
Yale University
P.O. Box 208107
New Haven, CT 06520
Phone: 203-432-5226
E-Mail: mark.johnson@yale.edu

Shawn Kathmann
Pacific Northwest National Laboratory
P.O. Box 999, MS- K1-83
Richland, WA 99352
Phone: 509-375-2870
E-Mail: Shawn.Kathmann@pnl.gov

Greg Kimmel
Chemical Sciences Division
Pacific Northwest National Laboratory
MSIN K8-88, PO Box 999
Richland, WA 99352
Phone: 509-376-2501
E-Mail: gregory.kimmel@pnl.gov

Jay LaVerne
Notre Dame Radiation Laboratory
University of Notre Dame
314 Radiation Laboratory
Notre Dame, IN 46556
Phone: 574-631-5563
E-Mail: laverne.1@nd.edu

Nancy Levinger
Department of Chemistry
Colorado State University
Fort Collins, CO 80523
Phone: 970 491-1331
E-Mail: levinger@lamar.colostate.edu

Edward Lim
The University of Akron
190 E. Buchtel Commons
Knight Chemical Laboratory
Akron, OH 44325
Phone: 330 972-5297
E-Mail: elim@uakron.edu

H. Peter Lu
Pacific Northwest National Laboratory
P.O.Box 999, MSIN K8-88
Richland, WA 99352
Phone: 509-376-3897
E-Mail: peter.lu@pnl.gov

Diane Marceau
DOE Basic Energy Sciences
SC-22.1/Germantown Bldg.
1000 Independence Ave. SW
Washington, DC 20585
Phone: 301-903-0235
E-Mail: diane.marceau@science.doe.gov

Dan Meisel
Notre Dame Radiation Labortory
University of Notre Dame
Notre Dame, IN 46556
Phone: 574-631-5457
E-Mail: dani@nd.edu

Juan Meza
Lawrence Berkeley National Laboratory
1 Cyclotron Road, MS 50B-2239
Berkeley, CA 94720
Phone: 510-486-7684
E-Mail: JCMeza@lbl.gov

John Miller
Brookhaven National Laboratory
Chemistry 555
Upton, NY 11973
Phone: 631-344-4354
E-Mail: JRMILLER@BNL.GOV

Raul Miranda
DOE Basic Energy Sciences
SC-22.1/Germantown Bldg.
1000 Independence Ave. SW
Washington, DC 20585
Phone: 301-903-8014
E-Mail: Raul.Miranda@science.doe.gov

Jens Nørskov
Technical University of Denmark
Building 307
Lyngby, Denmark DK-2800
Phone: +45 4525 3175
E-Mail: norskov@fysik.dtu.dk

Serdar Ogut
University of Illinois at Chicago
845 West Taylor Street (M/C 273)
Chicago, IL 60607
Phone: 312-413-2786
E-Mail: ogut@uic.edu

Richard Osgood
Columbia University
500 West 120th St.
New York, NY 10027
Phone: 212-854-4462
E-Mail: osgood@columbia.edu

Steven Overbury
Oak Ridge National Laboratory
Bldg. 4500 N/ MS 6201
PO Box 2008
Oak Ridge, TN 37831
Phone: 865-241-5189
E-Mail: overburysh@ornl.gov

Hrvoje Petek
University of Pittsburgh
Department of Physics and Astronomy
3941 O'hara St.
Pittsburgh, PA 15260
Phone: 412-624-3599
E-Mail: Petek@pitt.edu

Simon Pimblott
Notre Dame Radiation Laboratory
University of Notre Dame
304C Radiation Laboratory
Notre Dame, IN 46556
Phone: 574-631-7151
E-Mail: simon.m.pimblott.1@nd.edu

Eric Rohlfing
DOE Basic Energy Sciences
SC-22.1/Germantown Bldg.
1000 Independence Ave. SW
Washington, DC 20585
Phone: 301-903-8165
E-Mail: eric.rohlfing@science.doe.gov

Richard Saykally
Department of Chemistry
University of California, Berkeley
Berkeley, CA 94720
Phone: 510-642-8269
E-Mail: saykally@berkeley.edu

Greg Schenter
Pacific Northwest National Laboratory
PO Box 999, MS: K1-83
Richland, WA 99352
Phone: 509-375-4334
E-Mail: greg.schenter@pnl.gov

Trevor Sears
Chemistry Department
Brookhaven National Laboratory
Upton, NY 11973
Phone: 631-344 4374
E-Mail: sears@bnl.gov

Ilya Shkrob
Chemistry Division
Argonne National Laboratory
9700 South Cass Avenue
Argonne, IL 60439
Phone: 630-252-9516
E-Mail: shkrob@anl.gov

Steven Sibener
University of Chicago
5640 South Ellis Avenue
Chicago, IL 60637
Phone: 773-702-7193
E-Mail: s-sibener@uchicago.edu

Mark Spitler
DOE Basic Energy Sciences
SC-22.1/Germantown Bldg.
1000 Independence Ave. SW
Washington, DC 20585
Phone: 301-903-4568
E-Mail: mark.spitler@science.doe.gov

Peter Stair
Department of Chemistry
Northwestern University
Evanston, IL 60208
Phone: 847-491-5266
E-Mail: pstair@northwestern.edu

Timothy Steimle
Department of Chemistrty and Biochemistry
Arizona State University
Tempe, AZ 85287
Phone: 480-965-3265
E-Mail: TSteimle@asu.edu

Mark Stockman
Department of Physics and Astronomy
Georgia State University
Atlanta, GA 30303
Phone: 678-457-4739
E-Mail: mstockman@gsu.edu

Ward Thompson
Department of Chemistry
University of Kansas
Lawrence, KS 66045
Phone: 785-864-3980
E-Mail: wthompson@ku.edu

Andrei Tokmakoff
Dept. of Chemistry
MIT
77 Massachusetts Ave., Room 6-225
Cambridge, MA 02139
Phone: 617-253-4503
E-Mail: tokmakof@mit.edu

Gorakh Nath Tripathi
Notre Dame Radiation Laboratory
University of Notre Dame
Notre Dame, IN 46556
Phone: 574-631-5514
E-Mail: tripathi.1@nd.edu

Frank Tully
DOE Basic Energy Sciences
SC-22.1/Germantown Bldg.
1000 Independence Ave. SW
Washington, DC 20585
Phone: 301-903-5998
E-Mail: frank.tully@science.doe.gov

John Tully
Department of Chemistry
Yale University
PO Box 208107
New Haven, CT 6520
Phone: 203-432-3934
E-Mail: john.tully@yale.edu

Stefan Vajda
Argonne National Laboratory
9700 South Cass Avenue
Argonne, Illinois 60439
Phone: 630-252-8123
E-Mail: vajda@anl.gov

Albert Wagner
Chemistry Division
Argonne National Laboratory
9700 S. Cass Avenue, Bldg. 200
Argonne, IL 60439
Phone: 630-252-3570
E-Mail: wagner@tcg.anl.gov

Lai-Sheng Wang
Washington State University/PNNL
2710 University Drive
Richland, WA 99354
Phone: 509-376-8709
E-Mail: ls.wang@pnl.gov

Michael White
Chemistry Department
Brookhaven National Laboratory
Upton, NY 11973
Phone: 631-344-4345
E-Mail: mgwhite@bnl.gov

James Wishart
Chemistry Department
Brookhaven National Laboratory
Upton, NY 11973
Phone: 631-344-4327
E-Mail: wishart@bnl.gov

Alec Wodtke
Department of Chemistry and Biochemistry
University of California, Santa Barbara
Santa Barbara, CA California 93106
Phone: 805-893-8085
E-Mail: WODTKE@CHEM.UCSB.EDU

Sotiris Xantheas
Pacific Northwest National Laboratory
PO Box 999, MS: K1-83
Richland, WA 99352
Phone: 509-375-3684
E-Mail: sotiris.xantheas@pnl.gov